wiener klinische wochenschrift

The Central European Journal of Medicine

##. Jahrgang 2026 · Supplement #

Wien Klin Wochenschr
https://doi.org/10.1007/s00508-026-02765-1



ÖKG
Österreichische Kardiologische Gesellschaft

**Abstracts**

# Österreichische Kardiologische Gesellschaft Jahrestagung 2026

## „Herzmedizin der Zukunft“

27.–30. Mai 2026
Salzburg Congress

**Tagungspräsident**
Univ.-Prof. Dr. Daniel Scherr

**Tagungssekretär**
Prof. Priv.-Doz. Mag. Dr. Lukas Fiedler

**Tagunssekretärin und Vorsitzende des Abstract-Wettbewerb**
Ap. Prof. Priv.-Doz. Dipl. Ing. Dr. Noemi Pavo

# BEST ABSTRACTS—CLINICIAL RESEARCH

## Phenotyping by structural and biomarker remodeling in transthyretin amyloid cardiomyopathy: An international multicenter cohort study

**Kronberger C.[1], Hauptmann L.[1], Zlibut A.[2], Zubbrigen L.[3], Hundertmark M.[3], Schwotzer R.[4], Ji-Na Y.[5], Autherith M.[1], Poledniczek M.[1], Schmid L.[1], Rettl R.[1], Duca F.[1], Binder C.[1], Gama F.[6], Manka R.[4], Stämpfli S.[7], Yilmaz A.[2], Beitzke D.[1], Kammerlander A.[1], Gräni C.[3], Nitsche C.[1]**

[1]Universitätsklinik für Innere Medizin II – Abteilung für Kardiologie, Wien, Austria
[2]Universitätsklinikum Münster, Münster, Germany
[3]Inselspital Bern, Bern, Switzerland
[4]Universitätsklinikum Zürich, Zürich, Switzerland
[5]Luzerner Kantonspital, Luzern, Switzerland
[6]Krankenhaus zum Heiligen Kreuz, Lissabon, Portugal
[7]Herzzentrum Luzern, Luzern, Switzerland

**Introduction:** Transthyretin amyloid cardiomyopathy (ATTR-CM) is an infiltrative cardiomyopathy characterized by progressive left ventricular thickening and cardiac biomarker elevation. While structural and biomarker remodeling often progress in parallel, some patients may exhibit a discordance in remodeling patterns. However, the clinical implications of this biomarker-imaging discordance remain unclear.

**Methods:** This multi-center multi-modal international cohort study recruited consecutive patients with ATTR-CM who underwent cardiac magnetic resonance imaging (CMR) and cardiac biomarker assessment at six tertiary referral centers. Receiver operating characteristic curve analysis with Youden index identified optimal mortality thresholds for left ventricular mass index (LVMi; >75 g/m$^2$) and NT-proBNP (>2000 pg/mL) in the derivation cohort. Patients were stratified according to respective thresholds (low [–] vs. high [+]) yielding four groups: [BNP–, LVMi–], [BNP–, LVMi+], [BNP+, LVMi–], [BNP+, LVMi+]. Groups were compared regarding clinical, echo, CMR structural/functional/tissue characteristics, and all-cause mortality.

**Results:** We included 630 patients (derivation: $n=332$, validation: $n=298$) with ATTR-CM (median age 78 years, 86% male, 92% wild-type ATTR, 86% on ATTR-specific treatment). The discordant phenotype of [BNP–, LVMi+] was characterised by lower symptomatic burden, better kidney function, higher left atrial ejection fraction and peak strain, and less pulmonary hypertension and triscuspid regurgitation compared to [BNP+, LVMi–] and [BNP+, LVMi+] (all $p<0.05$) despite high extracellular volume fraction (ECV, 51% [43–60]). Conversely, the discordant phenotype of [BNP+, LVMi–] had worse functional parameters including severely impaired left atrial ejection fraction and peak strain similar to [BNP+, LVMi+] despite lower ECV than [BNP–, LVMi+] of 49% (41–56, $p<0.05$). After a median of 2.6 years (1.2–4.2) 159 patients (25%) died. By multivariate Cox regression with adjustment for known outcome predictors in ATTR-CM (age, sex, TTR mutation status, eGFR, ECV), [BNP-, LVMi+] had similarly favourable outcome to [BNP–, LVMi–] (adjHR 1.24; 95% CI 0.62 to 2.47) and [BNP+, LVMi–] had similarly poor outcome to [BNP+, LVMi+] (adjHR 1.29; 95% CI 0.80 to 2.07) with consistent results in the derivation and validation cohorts. Worse left atrial ejection fraction and peak strain both independently predicted mortality with consistent effects across tertiles of LVMi and ECV (all $p<0.05$).

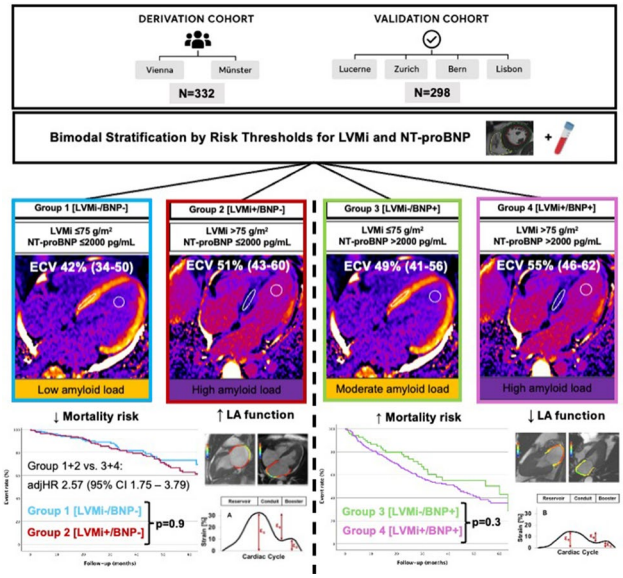


**Fig. 1**

**Conclusion:** In ATTR-CM, bimodal risk stratification by LVMi and NT-proBNP identifies discordant phenotypes regarding structural and biomarker remodelling with distinct functional and prognostic signatures. Left atrial function emerges as a gatekeeper mechanism which determines decompensation into sequential backward failure irrespective of LV amyloid load. Discordant phenotypes may require tailored treatment strategies based on their distinct pathophysiology and prognostic implications.

## Hemodynamic patterns of pacing with digital twins of brainstem circuits

**Hamzaraj K.[1], Riesenhuber M.[1], Pesl M.[2], Wijesinghe P.[3], Lukovic D.[1], Domanig A.[1], Shahi F.[1], Leonhardt M.[3], Abu-Hassan K.[3], Ait Belaid K.[3], Kushwah C.[3], Nogaret A.[3], Gyöngyösi M.[1]**

[1]Medizinische Universität Wien, Wien, Austria
[2]St. Anne's University Hospital in Brno, Brno, Czech Republic
[3]University of Bath, Bath, United Kingdom

**Introduction:** Small neural networks known as central pattern generators (CPG) are being increasingly recognized to re-establish physiological heart rate feedback response in pathologies such as heart failure. This approach restores the natural heart rate variability driven by neuronal autonomic tone that is lost in disease or with age. Our novel 2-lead neuronal-network pacemaker is developed to train and restore the physiologic pacing in adaption to breathing, arterial pO2, and blood pressure. In our first-generation pacemaker we were able to induce a paced respiratory sinus arrhythmia (RSA), mimicking a physiologic pattern. (Fig. 1) We performed large-animal experiments to test the left ventricular hemodynamics in 2-chamber pacing with and without RSA.

**Methods:** A novel 2-chamber pacemaker with a diaphragm respiratory sensor was implanted in healthy pigs ($n=5$), while conventional single-chamber pacemaker was used in pigs with chronic anterior myocardial infarction (AMI) ($n=4$) and reduced ejection fraction (44±2,3%). Echocardiographic measurements were performed in both groups at baseline and during variable pacing mimicking the dynamic heart rate sensor at

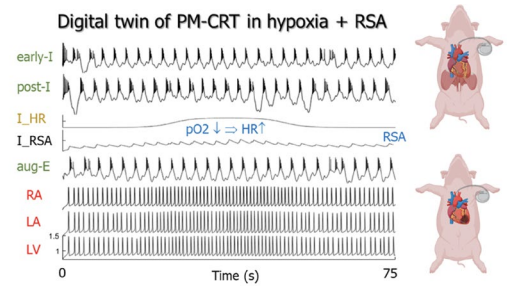


**Figure 1:** Digital twin model of the respiratory central pattern generator (Aug-E, Post-I and Early-I neuron populations of the brainstem) modulating electrical pulses delivered to 3 heart chambers on a beat-to-beat basis by integrating physiological feedback (arterial pO2 and Lung inflation stretch receptors).

**Fig. 1** Digital twin model of the respiratory central pattern generator

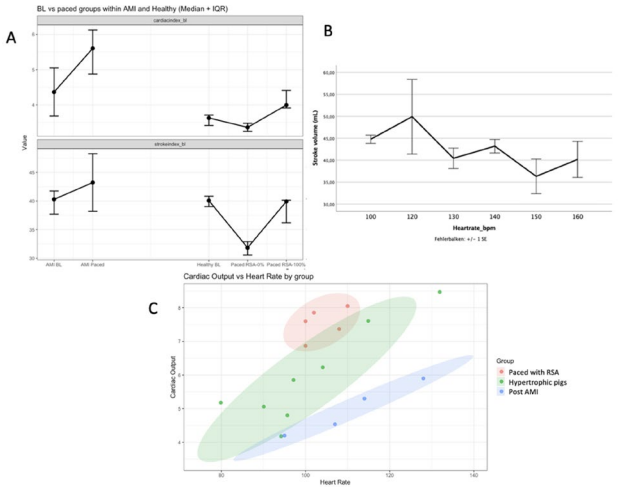


**Figure 2:** (A) Stroke volume among AMI at the baseline and during pacing and healthy pigs at the baseline and pacing mit 0% un 100% RSA (slopes left to right). (B) Stroke volume at variable paced heart rate for AMI pigs. (C) Elliptic clustering in the scatter plot (cardiac output in relation to heart rate) for full RSA paced pigs, hypertrophic pigs and those post-AMI.

**Fig. 2** Stroke volume and cardiac output at healthy, AMI and hypertrophic pigs

the AMI pigs, with/without preserved RSA at the healthy pigs. A control group of pigs with experimentally induced myocardial hypertrophy ($n=7$) and echocardiographic measurements was used for case-control. Cardiac output (CO) and stroke volume (SV) measurements were performed and compared between the groups.

**Results:** Constant pacing of the right ventricle without RSA with variable heart rate sequentially decreased the stroke volume in the AMI pigs from 45.1 (42.8–46.4) mL at the baseline to 42.9 (31.5–46.1) mL at 160 bpm. (Fig. 2) In the healthy pigs pacing without RSA decreased the stroke volume from 72.35 (69.66–74.42) mL to 56.75 (55.71–59.81) mL. By using our novel 2-lead neuronal-network pacemaker, the increasing RSA modulation during pacing sequentially increased the stroke volume (from 56.75 (55.71–59.81) mL to 63.04 (52.57–65.26) mL at 50% RSA and to 68.68 (68.23–73.2) mL at 100% RSA) at the healthy pigs. The elliptic cluster visualization in CO and heart rate scatter plot revealed superior CO progression in RSA paced pigs as compared to hypertrophic and post-AMI pigs.

**Conclusion:** Pacing with dynamic heart rate variability significantly decreased the stoke volume in AMI pigs with reduced left ventricular ejection fraction, presenting an unmet need to optimize hemodynamics in pacing patterns with dynamic heart rate sensor. In healthy pigs, pacing without RSA decreased the SV, while adding the RSA modulation by our neuronal-network pacemaker improved the SV. Pigs with full RSA modulation had a better CO progression with increasing heart rate as compared to hypertrophic and post-AMI pigs.

## Temporal Trends in Cardiovascular Risk Factors and Lifestyle Behaviors in a Community-Based Screening Population: A 20-Year Analysis (2005–2024)

**Mahmoudi M.[1], Kramer B.[2], Huber K.[2,3]**

[1]Sigmund Freud Privatuniversität, Wien, Austria
[2]Österreichischer Herzfonds, Wien, Austria
[3]Medical Private University Burgenland (GmbH), Pinkafeld, Austria

**Introduction:** Background: Cardiovascular disease (CVD) remains the leading cause of global mortality. Understanding temporal trends in cardiovascular risk factors and lifestyle behaviors is crucial for public health planning and prevention strategies. We analyzed 20-year trends in adiposity, lifestyle factors, and estimated CVD risk in a community screening cohort.

**Methods:** Repeated cross-sectional analysis of 16,126 adults from a cardiovascular screening program conducted by the Heart Foundation Austria (2005–2024). We assessed trends in body mass index (BMI), blood pressure (available 2017–2019, 2024), lifestyle factors (smoking, physical activity, stress), and estimated 10-year CVD mortality risk (SCORE; available 2015–2024). Linear and logistic regression models assessed temporal trends and associations between lifestyle factors and high CVD risk, adjusting for age, sex, and year. Analyses were stratified by sex and age groups.

**Results:** Mean BMI increased significantly (0.14 kg/m$^2$/year, $p=0.001$), from 23.6 kg/m$^2$ (2005) to 26.7 kg/m$^2$ (2024). Obesity prevalence increased from 5.3% to 21.2% ($p=0.001$), with the steepest increase in adults <40 years (3.0% to 37.5%). Regular exercise increased from 52.1% to 87.6%, high stress decreased from 51.8% to 20.3%, and smoking modestly decreased from 19.6% to 14.8% ($p=0.582$). Mean SCORE remained stable at 11.0 points (2015–2024). In multivariable models, current smoking—a key component of the SCORE algorithm—showed a strong association with high CVD risk (OR = 12.21, 95% CI: 9.57–15.58), regular exercise was strongly protective (OR = 0.37, 95% CI: 0.32–0.43), high stress increased risk (OR = 2.32, 95% CI: 1.98–2.71),

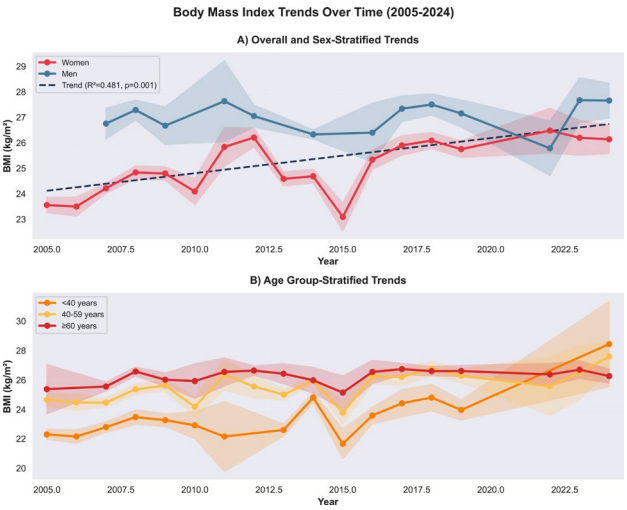


**Fig. 1**

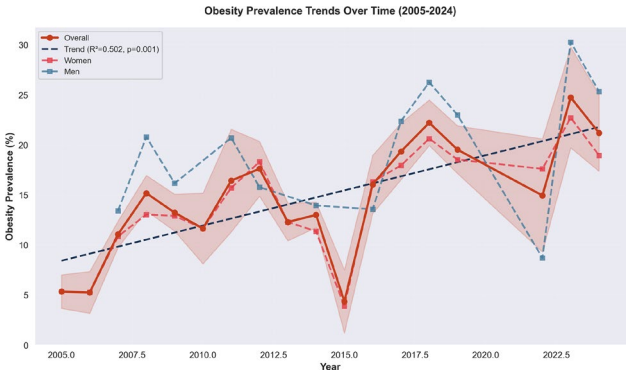


Fig. 2

and obesity was associated with elevated risk (OR = 2.62, 95% CI: 2.22–3.10).

**Conclusion:** Conclusions: Over 20 years, BMI and obesity increased dramatically, particularly among younger adults, alongside improvements in exercise and stress levels. Despite favorable lifestyle trends, smoking remains the strongest modifiable risk factor for high CVD risk. These findings highlight an urgent need for targeted obesity prevention in younger age groups and intensified smoking cessation programs.

## Dapagliflozin in patients hospitalised with newly diagnosed heart failure: an analysis of the randomized DAPA ACT HF-TIMI 68 trial

**Haller P.[1,2,3,4], Patel S.[3,4,2], Palazzolo M.[3,2], Bělohlávek J.[5], Desai A.[3,4], Drożdż J.[6], Inzucchi S.[7], McMurray J.[8], Merkely B.[9], O'Meara E.[10], Verma S.[11], Wiviott S.[12], Sabatine M.[2,3,4], Berg D.[2,3,4]**

[1]Medical University of Vienna, Vienna, Austria
[2]TIMI Study Group, Boston, United States
[3]Brigham and Women's Hospital, Boston, United States
[4]Harvard Medical School, Boston, United States
[5]General University Hospital and First Faculty of Medicine, Charles University, Prague, Prague, Czech Republic
[6]Medical University of Lodz, Lodz, Poland
[7]Yale University School of Medicine, New Haven, United States
[8]British Heart Foundation Cardiovascular Research Centre, University of Glasgow, Glasgow, United Kingdom
[9]Heart and Vascular Center, Semmelweis University, Budapest, Hungary
[10]Montreal Heart Institute, Université de Montréal, Montréal, Canada
[11]Li Ka Shing Knowledge Institute of St. Michael's Hospital, Unity Health Toronto, University of Toronto, Toronto, Canada
[12]AstraZeneca, Boston, United States

**Introduction:** Patients hospitalized for newly diagnosed heart failure (HF) are less well characterized than patients with worsening chronic HF. Clinical trials of novel HF therapies have traditionally excluded patients with newly diagnosed HF.

**Methods:** DAPA ACT HF-TIMI 68 was a randomized, double-blind, placebo-controlled trial of in-hospital initiation of dapagliflozin in patients hospitalized with a primary diagnosis of HF [1,2]. In this prespecified subgroup analysis, we compared the clinical profiles and treatment effects of dapagliflozin vs. placebo in patients with newly diagnosed HF vs worsening chronic HF. The primary efficacy endpoint was the composite of cardiovascular death or first worsening HF (CVD/WHF) event through 2 months; death from any cause was a secondary endpoint. Key safety outcomes included symptomatic hypotension and worsening kidney function.

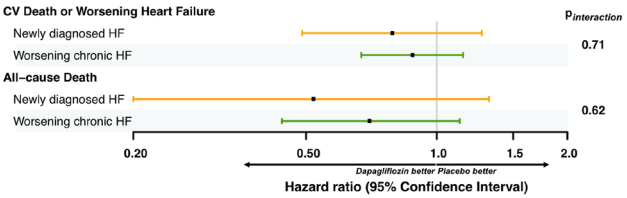


Fig. 1

| | Newly diagnosed heart failure (N=1069) | | | Worsening chronic heart failure (N=1320) | | |
|---|---|---|---|---|---|---|
| Safety Endpoint | Dapagliflozin (N=553) | Placebo (N=516) | p-value | Dapagliflozin (N=657) | Placebo (N=663) | p-value |
| AE leading to study drug discontinuation | 15 (2.7%) | 7 (1.4%) | 0.12 | 43 (6.5%) | 49 (7.4%) | 0.55 |
| Symptomatic hypotension* | 17 (3.1%) | 6 (1.2%) | 0.03 | 26 (4.0%) | 20 (3.0%) | 0.35 |
| Worsening renal function# | 22 (4.0%) | 20 (3.9%) | 0.93 | 49 (7.5%) | 35 (5.3%) | 0.11 |
| Major hypoglycemia§ | 1 (0.2%) | 2 (0.4%) | 0.52 | 2 (0.3%) | 1 (0.2%) | 0.56 |
| Diabetic ketoacidosis | 0 (0.0%) | 0 (0.0%) | | 0 (0.0%) | 0 (0.0%) | |

*leading to hospitalization or study drug discontinuation
# resulting in at least doubling of sCr, hospitalization, study drug discontinuation, dialysis, or renal death
§ resulting in severe impairment in consciousness or behavior, or requiring emergency assistance

Fig. 2

**Results:** Of 2401 randomized patients, 1074 (44.7%) had newly diagnosed HF during the index hospitalization. Compared to patients with worsening chronic HF, newly diagnosed patients were younger (median 64 [Q1–Q3, 54–74] vs. 71 [61–78] years) and had fewer comorbidities, including type 2 diabetes (26.4% vs. 42.8%), hypertension (68.1% vs. 86.4%), chronic kidney disease (34.3% vs. 54.2%), and atrial fibrillation (32.1% vs. 55.4%; all $p < 0.001$). Although patients with newly diagnosed HF were less likely than patients with worsening chronic HF to be treated with neurohormonal antagonists (beta-blockers, renin-angiotensin system inhibitors, mineralocorticoid receptor antagonists) prior to admission (8.6% vs. 21.2% on all three, $p < 0.001$), they were more likely to be treated with these agents by hospital discharge (48.6% vs. 39.6%, $p < 0.001$) and through the remainder of follow-up. Compared to patients with worsening chronic HF, those with newly diagnosed HF had a lower rate of CVD/WHF (6.4% vs. 16.1%, $p < 0.001$) and of death from any cause (1.8% vs. 5.3%, $p < 0.001$) through 2 months. However, hazard ratios of dapagliflozin appeared similar in each group for both outcomes (Fig. 1). Adverse events occurred less frequently in patients with newly diagnosed HF as compared with worsening chronic HF; however, among newly diagnosed HF patients, there was an excess of symptomatic hypotension events in those randomized to dapagliflozin (3.1% vs. 1.2%, $p = 0.03$) (Fig. 2).

**Conclusion:** DAPA ACT HF-TIMI 68 offers contemporary insights into patients hospitalized for newly diagnosed HF. The treatment effect of in-hospital initiation of dapagliflozin on clinical outcomes was generally consistent irrespective of HF chronicity.

## References

1. Berg DD, Patel SM, Haller PM, et al. Nov 18. Circulation. 2025;152(20):1411–22. https://doi.org/10.1161/CIRCULATIONAHA.125.076575.
2. Berg DD, Patel SM, Haller PM, et al. JACC Heart Fail. 2025;13(5):829–39. https://doi.org/10.1016/j.jchf.2025.03.014.

## Extracorporeal membrane oxygenation is associated with increased levels of neuron-specific enolase in the absence of poor neurological outcome and predicts mortality in patients without cardiopulmonary resuscitation

**Hofbauer T., Haider P., Krychtiuk K., Richter B., Zilberszac R., Lenz M.**

Department of Cardiology, Internal Medicine II, Medical University of Vienna, Wien, Austria

**Introduction:** Despite recent advances in treatment of cardiopulmonary resuscitation (CPR) and/or life-threatening disease states using extracorporeal membrane oxygenation (ECMO), outcomes remain poor; specifically, prognostication of neurological outcome remains challenging. Neuron-specific enolase (NSE) is usually measured at 48 h and 72 h, with a cut-off of >60 µg/L suggesting poor neurological outcome. While not used as a sole marker in accordance with international consensus recommending multimodal diagnosis, false positive increases in NSE may lead to discontinuation of life-sustaining treatment even in the absence of poor prognosis. Hemolysis has been shown to interfere with conventional NSE measurements. Whether ECMO itself leads to spurious increases of NSE remains unclear.

**Methods:** In this trial, we aimed to illuminate the influence of ECMO itself on NSE levels measured within 48 h of admission to the ICU. Furthermore, we evaluated whether NSE was prognostic of poor outcome in patients who did not require CPR. This was a prospective, observational cohort study. 215 consecutive patients admitted to a cardiac ICU were screened over the course of one year. Of these, patients without CPR were selected ($n=162$). As a separate cohort, we included patients ($n=49$) treated with ECMO in the setting of CPR, who did not have poor neurological outcome. Patients with active malignancies or traumatic brain injuries were excluded due to a potential modulation of NSE values. Furthermore, samples with hemolysis index >30 units were excluded to guarantee stable measurements. NSE was measured using ECLIA.

**Results:** Median age of the ICU cohort was 65.9 (IQR: 55.0–76.6) years, and 40.0% of the included patients were female. The total 30-day-mortality was calculated to be 27.0%, and 53 patients (24.7%) were admitted following CPR. In the patient cohort treated with ECMO, we observed strikingly increased NSE levels compared to patients not requiring ECMO (Fig. 1). Importantly, both groups did not suffer from poor neurological outcome. In the patient cohort who required neither CPR nor ECMO, patients who died displayed higher NSE levels than patients who survived at 30-day follow-up (Fig. 2). ROC analysis revealed NSE to be positively predictive of 30-day mortality (ROC AUC 0.721, $p<0.001$). No differences in survival were found when stratifying for primary cause of admission. Employing Kaplan-Meier analysis, we found NSE at baseline to predict 30-days mortality ($p<0.001$, Fig. 3).

**Conclusion:** We demonstrate that ECMO support is associated with elevated NSE concentrations despite the absence of poor neurological outcome, suggesting that extracorporeal circulation may confound interpretation of NSE early after ICU admission. Our findings suggest that ECMO-related mechanisms, such as subclinical hemolysis, circuit-induced cellular stress or altered clearance may contribute to spurious NSE elevations. This has important clinical implications since NSE is incorporated into neuroprognostication, with falsely positive elevations potentially influencing the decision to withdraw life-sustaining therapy. Importantly, in patients who required neither CPR nor ECMO, baseline NSE was predictive of 30-days mortality, indicating that NSE might reflect global disease severity beyond hypoxic ischemic brain injury. Our data underscore the need for caution when interpreting early NSE values in ECMO-treated patients and support the need for further mechanistic investigations to define context-adjusted NSE thresholds.

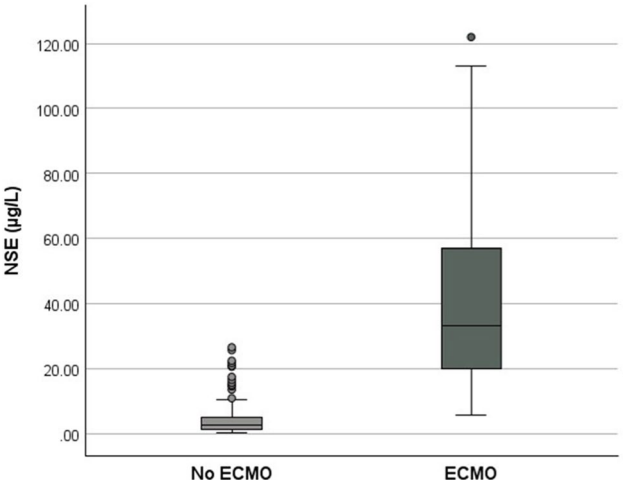


Fig. 1

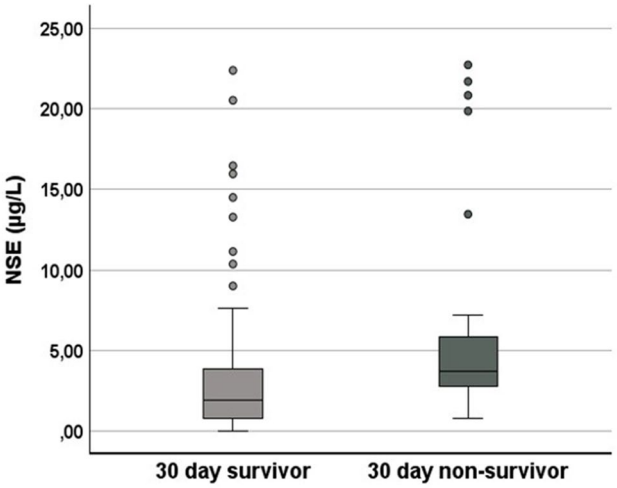


Fig. 2

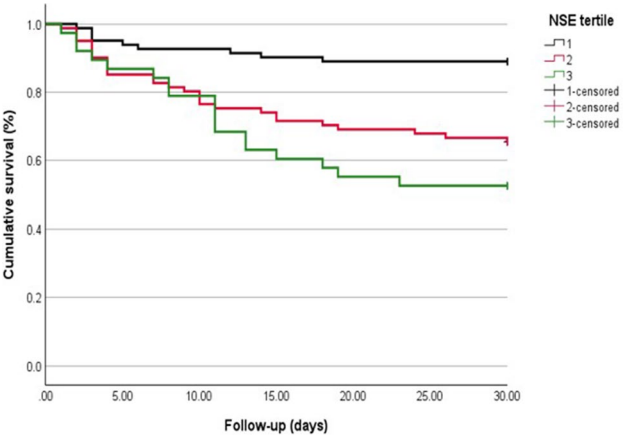


Fig. 3

### Echocardiographic Reference Values in Junior and Adult Elite Athletes: A Retrospective Cross-Sectional Study

**Weber I.[1,2,3], Thamm J.[4], Urhausen A.[4], Meyer T.[4], Kindermann W.[4], Scharhag J.[1,3,2]**

[1]Österreichisches Institut für Sportmedizin, Auf der Schmelz 6, 1150 Wien, Austria
[2]Klinische Abteilung für Kardiologie, Universitätsklinik für Innere Medizin II, Medizinische Universität Wien, Währinger Gürtel 18–20, 1090, Wien, Austria
[3]Abteilung für Sportmedizin, Leistungsphysiologie und Prävention, Zentrum für Sportwissenschaft und Universitätssport, Universität Wien, Auf der Schmelz 6, 1150 Wien, Austria
[4]Institute of Sports and Preventive Medicine, University of Saarland, Saarbrücken, Germany

**Introduction:** The term 'athlete's heart' was first introduced in 1899, when an increased cardiac size observed in cross-country skiers was recognized as a physiological adaptation to exercise. Although initially controversial, this adaptation is now widely accepted as a physiological response to endurance training in athletes, enabling increased cardiac capacity compared with a non-enlarged heart. Nevertheless, several questions concerning cardiac adaptations in athletes remain unresolved. In the clinical setting, the differentiation between pathological hypertrophy, particularly in its early asymptomatic stages, and the physiological adaptations of athlete's heart represents a key challenge in sports cardiology. This study aims to further improve the understanding of these adaptations through a retrospective cross-sectional analysis, with the objective of generating echocardiographic reference values for junior and adult elite athletes. Additionally, echocardiographic parameters were analyzed in relation to maximal oxygen consumption (VO2peak) to identify relevant correlations. Data from screening examinations of healthy German elite athletes examined at the Institute for Sports and Preventive Medicine at the University of Saarland between 1995 and 2005 were used for this study.

**Methods:** This retrospective cross-sectional study consists of a population of 1082 male and 592 female elite athletes, of which 507 and 250 athletes were over the age of 18 years, respectively. The athletes were categorised into endurance sports, team sports, strength sports, and 'other' disciplines. Echocardiograms were carried out according to the American College of Cardiology guidelines and performed or verified by five experienced clinicians. The following parameters were included in the analysis: left ventricular end-diastolic diameter (LV-EDD), interventricular septum thickness (IVS), posterior wall thickness (PW) and heart volume (HV) calculated according to Dickhuth et al. (1996). In addition, LV-EDD was indexed to body surface area (LV-EDD/BSA), relative LV wall thickness (RWT) was calculated, and heart volume (HV) relative to body weight was allometrically scaled to $kg^{2}/^{3}$ and $kg^{3}/^{4}$. The echocardiographic parameters were assessed for statistically significant differences using Kruskal-Wallis ANOVA, Mann-Whitney U tests as well as Bonferroni correction. Maximal oxygen consumption was determined through cycle and treadmill ergometry using the equation $VO_2peak = 11 \times Watts + 700$. Athletes were included in the analysis only if cardiopulmonary exhaustion was reached, defined as reaching at least 95% of the age-predicted maximal heart rate (220—age for treadmill ergometry and 200—age for cycle ergometry).

**Results:** The ranges of upper reference limits (97.5 percentile) across different age groups for males were: LVEDD 52.5–62 mm; LVEDD/BSA 31–38 mm/m2; IVS 10.5–13 mm; PW 10.5–12.5 mm; RWT 43–44%; HV 15–16 ml/kg, 55–67 ml/kg2/3, 40–47 ml/kg3/4; and for females were: LVEDD 50.5–56.5 mm; LVEDD/BSA 31–39 mm/m2; IVS 9.5–11 mm; PW 9.5–11 mm; RWT 40–44%; HV 13–16 ml/kg, 51–57 ml/kg2/3, 37–40 ml/kg3/4. The data confirm previous echocardiographic findings of physiological cardiac hypertrophy in competitive athletes, corresponding to values reported in the literature. The results show that endurance athletes have a larger mean relative heart volume compared to team, strength, and other sports, and that strength athletes present the smallest relative heart volumes. Females had approximately 10% smaller heart volumes compared to males. Additionally, heart volume demonstrated a stronger correlation with maximal oxygen consumption compared to LVEDD, with a correlation coefficient of 0.92.

**Conclusion:** The present study specifies echocardiographic upper reference limits from junior up to adult elite athletes, confirming previous reference values, and extending these by further parameters such as absolute and allometric HV. Taken together, the references values presented in this study provide additional data for the differentiation of physiological adaptations of the athlete's heart versus pathological changes. The data may be helpful for clinical sports cardiology practice and to establish globally standardized reference limits for athlete's heart from children up to master athletes.

## BEST ABSTRACTS—BASIC SCIENCE

### IL4Ralpha signaling delays foam cell formation in atherosclerotic lesions

**Kral-Pointner J.[1,2], Ableitner E.[3], Boccuni L.[1], Salzmann M.[2,1], Haider P.[2], Derler M.[3], Maleiner B.[2], Hengstenberg C.[2], Wojta J.[4], Mussbacher M.[3], Hohensinner P.[5,1]**

[1]Ludwig Boltzmann Institute for Cardiovascular Research, Wien, Austria
[2]Department of Internal Medicine II, Division of Cardiology, Medical University Vienna, Wien, Austria
[3]Department of Pharmacology and Toxicology, University of Graz, Graz, Austria
[4]Ludwig Boltzmann Institute for Cardiovascular Research at the Department of Internal Medicine II, Division of Cardiology, Medical University of Vienna, Wien, Austria
[5]Centre for Biomedical Research, Medical University of Vienna, Wien, Austria

**Introduction:** Lipid uptake by macrophages is a central process in atherosclerotic plaque development. Especially oxidized LDL (oxLDL) shifts macrophages towards foam cell development. We speculate that the cytokines interleukin (IL)4 and IL13 signaling via IL4 receptor alpha (IL4RA) can counteract oxLDL-induced macrophage differentiation and reduce atherosclerotic plaque progression. Here, we aim to clarify the impact of IL-4 and IL-13 on foam cell formation and atherosclerotic development.

**Methods:** Human monocyte-derived macrophages were treated with oxidized low-density lipoprotein (oxLDL) in the presence or absence of IL-4 and IL-13 and foam cell development was examined using RNA sequencing, mass spectrometry and flow cytometry. To identify in vivo consequences wild-type and IL-4Ralpha knockout mice on an LDL receptor (LDLR)-deficient background were fed high-fat diet (HFD) with 21% fat and 0.20% cholesterol for 4 weeks or 14 weeks.

**Results:** Both oxLDL and IL4/IL13 challenge each induced a distinct profile of genes when analyzing a time course set at

2 h, 6 h, and 24 h post stimulation using bulk RNA sequencing. Characteristic for oxLDL was a predominant downregulation of genes whereas IL4/IL13 showed strong induction and downregulation capacity. When combining both stimuli, the induction capability of IL4/IL13 was diminished through the presence of oxLDL. When combining both challenges, we found retaining of oxidative phosphorylation dependent pathway genes and a reduction in genes associated with cholesterol homeostasis. We were able to confirm these RNA observations on altered lipid metabolism using metabolomics demonstrating failing of OXPHOS in oxLDL treated macrophages but an increased capability when treated with IL4/IL13 while challenged with oxLDL. In addition, we observed reduced oxLDL uptake and CD36 expression in macrophages treated with oxLDL and IL4/IL13. Mice deficient for IL4RA showed overall increased atherosclerotic plaque formation together with elevated numbers of GPNMB and TREM2 positive foam cells in established atherosclerotic lesions after 14 weeks of HFD. In addition, we also found an increased proinflammatory phenotype in IL4RA deficient mice with enhanced plasma levels of MCP1, and enhanced accumulation of CD4 T cells within the lesion.

**Conclusion:** Our data emphasize an atheroprotective function of IL-4/IL-13 signaling by combating oxLDL induced proinflammatory protein induction and delaying formation of metabolically inept foam cells. We propose that this mechanism needs to be considered when patients receive treatment for diseases linked to increased IL4/IL13 production as allergies and asthma as chronic inhibition of those cytokines might in turn increase cardiovascular risk.

## Loss of sirtuin 4 confers cardioprotection by lowering succinate oxidation during ischemia-reperfusion

**Byrne N.[1], Koentges C.[2], Pfeil K.[1], Sohn S.[2], Birkle L.[2], Vosko I.[1], Rathner T.[1], Gollmer J.[1], Hoffmann M.[2], Wallner M.[1], Ljubojevic-Holzer S.[1], von Lewinski D.[1], Sedej S.[1], Wende A.[3], Zirlik A.[1], Bugger H.[1]**

[1]Medical University of Graz, Graz, Austria
[2]University of Freiburg, Freiburg, Germany
[3]University of Alabama at Birmingham, Birmingham, United States

**Introduction:** The mitochondrial NAD+-dependent deacylase, sirtuin 4 (SIRT4), regulates energy substrate utilization and ROS homeostasis, mechanisms principally involved in the pathogenesis of myocardial ischemia-reperfusion (I/R) injury. Thus, we hypothesized that targeting SIRT4 may modulate the extent of I/R injury.

**Methods:** We subjected mice with cardiomyocyte-specific overexpression of Sirt4 (cSirt4-Tg) or global deletion of Sirt4 (Sirt4–/–) to transient ligation of the left anterior descending (LAD) coronary artery in vivo, or to I/R in the Langendorff model ex vivo.

**Results:** In vivo or ex vivo I/R injury did not differentially affect cardiac infarct size or recovery of contractile function following ischemia in cSirt4-Tg mice, respectively. In contrast, Sirt4–/– displayed reduced cardiac infarct size and improved recovery of contractile function. Metabolomics revealed decreased ischemic succinate accumulation in Sirt4–/– mice as the most significant contributor to cardioprotection. Inhibition of succinate dehydrogenase (SDH) using dimethylmethoxymalonate improved postischemic recovery of WT hearts to levels of Sirt4–/– hearts, suggesting that SIRT4 deficiency confers cardioprotection by decreasing ischemic succinate accumulation and SDH-driven ROS production. Decreased levels of a-ketoglutarate and glutamate in Sirt4–/– hearts, and equally improved cell survival following hypoxia-reoxygenation in H9C2 cardiomyocytes with siRNA-mediated suppression of SIRT4 or glutamate dehydrogenase suggest that SIRT4 suppression mediates cardioprotection by mitigating glutamate-derived Krebs cycle anaplerosis. In addition, decreased pyruvate and citrate levels and increased pyruvate dehydrogenase kinase 4 expression suggest reduced glycolysis-derived Krebs cycle fueling. Finally, SIRT4 suppression mediated upregulation of antioxidant proteins.

**Conclusion:** Thus, modulation of energy substrate utilization and ROS homeostasis attenuates myocardial I/R injury in SIRT4 deficiency, predominantly by inhibiting Krebs cycle fueling that attenuates accumulation and subsequent oxidation of succinate.

## Macroscopic Myocardial Infarct Size and Area-at-Risk Estimation in a Translational Porcine Model

**Lukovic D., Spannbauer A., Hamzaraj K., Riesenhuber M., Traxler-Weidenauer D., Pavone-Gyöngyösi M.**

Medizinische Universität Wien, Wien, Austria

**Introduction:** Infarct size (IS) and area at risk (AAR) are key endpoints in translational myocardial infarction (MI) studies. Standard approaches such as late-enhancement cardiac magnetic resonance (LE-CMR) and TTC/Evans blue staining can be costly, logistically demanding, or incompatible with rapid myocardial sampling for molecular analyses. We developed macroscopic myocardial infarct size estimation and AAR method for rapid, visual macroscopic quantification of IS/AAR and infarct volume, and validated it by LE-CMR imaging.

**Methods:** In 142 female Landrace pigs, reperfused acute MI was induced by 90-min balloon occlusion of the mid left anterior descending artery followed by reperfusion. Nineteen animals died peri-procedurally; $n = 123$ completed 2-month follow-up with late gadolinium enhancement CMR. After euthanasia, explanted heart underwent further processing before sampling for molecular biology analyses. Infarcted and AAR segments were assigned by visual inspection with photo documentation; partial/non-transmural involvement was weighted proportionally. Macroscopic IS was compared with CMR-derived IS using linear regression (Fig. 1).

**Results:** Across $n = 123$, macroscopic IS was 22.1 ± 7.1% and AAR 28.3%, yielding an IS/AAR ratio of 79.2 ± 6.2%. CMR-derived IS was 23.8 ± 8.5%, with left ventricular ejection fraction 41.1 ± 5.1%. Visual infarct volume was 23.5 ± 3.4 $cm^3$, and total myocardial volume was 71.0 ± 9.0 $cm^3$; CMR-derived LV myocardial mass was 72.8 ± 9.0 g. Macroscopic IS correlated strongly

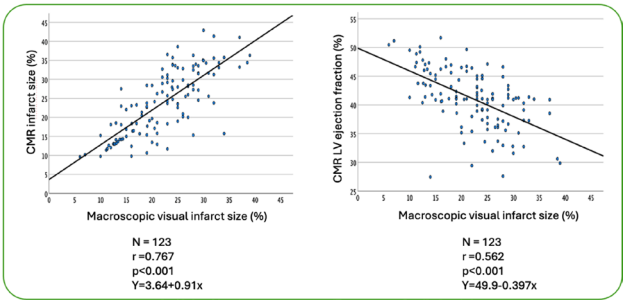


**Fig. 1** Correlation analyses in $n = 123$ animals. Left: Strong correlation between macroscopic visual infarct size and CMR-derived infarct size ($r = 0.767$, $p < 0.001$). Right: Inverse correlation between macroscopic infarct size and CMR-derived left ventricular ejection fraction ($r = 0.562$, $p < 0.001$). Linear regression equations are shown in the plots

with CMR-derived IS (r = 0.767, $p < 0.001$) and moderately with CMR-derived LV ejection fraction (r = 0.562, $p < 0.001$)(Figure B).

**Conclusion:** Our approach provides robust estimates of IS/AAR and infarct volume, demonstrating good concordance with LE-CMR in a large porcine MI cohort. This method avoids toxic staining, supports rapid tissue sampling for downstream molecular/cellular analyses, and serves as a practical alternative when imaging is not feasible.

## Modulating Focal Adhesion Signaling to Prevent Fibrotic Remodeling in Heart Failure

**Ioannou-Nikolaidou M.[1,2], Niedrist V.[1], Eder J.[1], Heim V.[1], Lohmann R.[1], Schmidt S.[1], Hirsch J.[1], Graber M.[1], Nägele F.[1], Engler C.[1], Bonaros N.[1], Grimm M.[1], Gollmann-Tepeköylü C.[1], Winter-Pölzl L.[1]**

[1]Universitätsklinik für Herzchirurgie, Innsbruck, Austria
[2]Institut für klinsch funktionelle Anatomie, Innsbruck, Austria

**Introduction:** Heart failure is frequently driven by progressive cardiac fibrosis and adverse extracellular matrix remodeling. Notably, the right ventricle displays a greater regenerative capacity after injury than the left ventricle, yet the molecular basis for this chamber-specific difference remains poorly understood. Cell adhesions are central regulators of cellular communication, mechanotransduction, and tissue integrity. Dysregulation of adhesion signaling promotes fibroblast activation and pathological matrix deposition, key mechanisms of fibrotic remodeling in heart failure. We recently identified KIAA0408 as a novel antifibrotic mediator selectively active in the right ventricle and associated with enhanced myocardial regeneration. The present study aimed to elucidate the molecular mechanism underlying its protective effects and its role in chamber-specific cardiac repair.

**Methods:** Native co-immunoprecipitation was performed in fibroblasts expressing GFP-tagged KIAA0408 to identify interacting proteins. Subcellular localization was assessed by immunofluorescence microscopy. Functional consequences of gene deletion were evaluated using adhesion assays in KIAA0408 knockout fibroblasts. Extracellular matrix composition was analyzed by secretome profiling. In vivo, right coronary artery ligation was performed in wild type and KIAA0408 knockout mice to induce myocardial injury. Right ventricular scar formation was assessed histologically, and right ventricular function was evaluated by echocardiography.

**Results:** Co-immunoprecipitation identified KIAA0408 as a binding partner of key focal adhesion proteins, and immunofluorescence confirmed its localization at focal adhesions, establishing it as a structural and signaling regulator of cell–matrix interactions. KIAA0408 knockout fibroblasts demonstrated significantly impaired adhesion capacity, indicating a critical role in cellular anchoring and mechanosensing. Secretome profiling revealed profound alterations in extracellular matrix composition in knockout cells, characterized by dysregulated expression of collagens, laminins, integrins, matrix metalloproteinases, tissue inhibitors of metalloproteinases, and tenascins, consistent with a pro-fibrotic remodeling phenotype. In vivo, KIAA0408 knockout mice developed markedly increased right ventricular scar formation following myocardial injury and exhibited reduced right ventricular function on echocardiography. In contrast, wild type mice demonstrated functional recovery and right ventricular regeneration. These findings identify KIAA0408 as an essential regulator of right ventricular repair, whose loss shifts the response to injury from regenerative remodeling toward maladaptive fibrosis and ventricular dysfunction.

**Conclusion:** KIAA0408 is a previously unrecognized regulator of focal adhesion signaling that governs extracellular matrix remodeling and right ventricular regeneration. Its deletion impairs regenerative repair and promotes fibrotic remodeling and ventricular dysfunction following myocardial injury. Importantly, our findings reveal a mechanistic determinant underlying the differential regenerative capacity of the right versus left ventricle. By linking focal adhesion dynamics to chamber-specific myocardial repair, KIAA0408 emerges as a central molecular switch between regeneration and maladaptive scar formation and represents a promising therapeutic target to enhance cardiac repair and prevent heart failure progression.

## Immune Senescence Drives Aortic Valve Calcification via γδ T Cells

**Seeberger D.[1], Maurer T.[2], Dünser C.[3], Muller L.[1], Winter-Pölzl L.[1], Hirsch J.[1], Engler C.[1], Nägele F.[1], Bonaros N.[1], Grimm M.[1], Holfeld J.[1], Tancevski I.[3], Graber M.[1], Salcher S.[2], Gollmann-Tepeköylü C.[1]**

[1]Department of Cardiac Surgery, Medical University Innsbruck, Innsbruck, Austria
[2]Department of Internal Medicine V, Medical University Innsbruck, Innsbruck, Austria
[3]Department of Internal Medicine II, Medical University Innsbruck, Innsbruck, Austria

**Introduction:** Calcific aortic stenosis (AS) is the most common valvular heart disease in the ageing population, yet no medical therapy exists to halt its progression. Chronic inflammation is increasingly recognized as a central driver of AS. Ageing profoundly reshapes the immune system, but how immune senescence contributes to valve calcification remains unclear. We aimed to define age-associated immune alterations within the aortic valve and determine their functional role in calcific remodeling.

**Methods:** Aortic valve function was assessed by transthoracic echocardiography in adult (3 months) and senescent (> 18 months) C57BL/6N mice. Aortic valves were harvested for histological analysis and single-cell RNA sequencing to comprehensively characterize age-associated changes in immune and stromal cell composition. Bioinformatic subclustering and differential expression analyses were performed to define immune cell subsets. Cell–cell communication networks were inferred using ligand–receptor interaction modeling to identify immune–stromal signaling pathways driving valve remodeling. In vitro, primary human valvular interstitial cells (VICs) were stimulated with recombinant IL-17A, followed by quantitative gene expression analysis and functional calcification assays.

**Results:** Senescent mice exhibited early hemodynamic features of aortic stenosis, including reduced valve opening, increased mean transvalvular gradient, and elevated peak velocity. Single-cell RNA sequencing revealed a marked age-associated remodeling of the immune landscape, characterized by significant expansion of γδ T cells. Immunostaining confirmed their accumulation within the aortic valve leaflets. Cell-cell communication analysis identified γδ T cells as the predominant source of IL-17 within the aged valve and revealed preferential signaling toward VICs. IL-17 stimulation of VICs induced robust upregulation of inflammatory mediators (IL-6, IL-1β) and the osteogenic transcription factor Runx2. Functionally, IL-17 directly drove osteogenic differentiation and calcification of VICs in vitro.

**Conclusion:** Ageing reshapes the immune microenvironment of the aortic valve, characterized by expansion of IL-17–producing γδ T cells. These cells drive inflammatory activation and osteogenic reprogramming of VICs, promoting valve calcification. Our findings identify γδ T cells as a previously unrecognized immune driver of calcific AS and position IL-17 signaling as a mechanistically grounded and potentially druggable therapeutic target to slow or prevent disease progression.

## Differential Effects of Simulated Microgravity and Space Radiation on Cardiac Calcium Channel Expression: Implications for Astronaut Cardiovascular Health

**Paar V.[1], Jiang S.[2], Enriquez A.[2], Kim J.[3], Brunetta H.[4,5], Muratani M.[6,7], Kubik A.[8], Blaber E.[8], Allen N.[8], Kaufman B.[2], Mori M.[4,5], Motloch L.[1,9,10], Hoppe U.[1], Mason C.[3], Schisler J.[11], Jirak P.[12,13,14], Beheshti A.[15,16,17]**

[1]Division of Cardiology, Department of Internal Medicine II, Paracelsus Medical University, Salzburg, Austria
[2]Division of Cardiology, Center for Metabolism and Mitochondrial Medicine and Vascular Medicine Institute, School of Medicine, University of Pittsburgh, Pittsburgh, United States
[3]Department of Physiology and Biophysics and WorldQuant Initiative for Quantitative Prediction, Weill Cornell Medicine, New York, United States
[4]Department of Biochemistry and Tissue Biology, Institute of Biology, University of Campinas, Campinas, Brazil
[5]Obesity and Comorbidities Research Center (OCRC), University of Campinas, Campinas, Brazil
[6]Transborder Medical Research Center, University of Tsukuba, Ibaraki, Japan
[7]Department of Genome Biology, Faculty of Medicine, University of Tsukuba, Ibaraki, Japan
[8]Department of Biomedical Engineering, Rensselaer Polytechnic Institute, Troy, United States
[9]Department of Internal Medicine II, Salzkammergut Klinikum, OÖG, Vöcklabruck, Austria
[10]Department of Cardiology, Kepler University Hospital, Medical Faculty, Johannes Kepler University Linz, Linz, Austria
[11]McAllister Heart Institute and Department of Pharmacology, The University of North Carolina at Chapel Hill, Chapel Hill, United States
[12]Paracelsus Medical University, Salzburg, Salzburg, Austria
[13]Rehabilitation Center Moorheilbad Harbach, Moorbad Harbach, Austria
[14]Rehabilitation Center Lebens.Resort Ottenschlag, Ottenschlag, Austria
[15]Stanley Center for Psychiatric Research, Broad Institute of MIT and Harvard, Cambridge, United States
[16]Blue Marble Space Institute of Science, Space Biosciences Division, NASA Ames Research Center, Moffett Field, United States
[17]Center for Space Biomedicine, McGowan Institute for Regenerative Medicine, Department of Surgery, University of Pittsburgh School of Medicine, Pittsburgh, United States

**Introduction:** Space medicine is rapidly evolving as manned missions increase in frequency and duration. Microgravity and cosmic radiation, including Galactic Cosmic Radiation (GCR) and Solar Particle Events (SPE), pose serious health risks, with pathophysiological effects on virtually all organ systems. The cardiovascular system undergoes multiple adaptations to microgravity, including myocardial atrophy, systolic and diastolic dysfunction, vascular impairment, and increased arrhythmogenic substrate. Since calcium (Ca2+) is central to myocardial excitation-contraction coupling, understanding microgravity-associated changes in Ca2+ handling is critical. Hindlimb-unloaded (HU) mice demonstrate spontaneous Ca2+ release events and sarcoplasmic reticulum (SR) Ca2+ leakage. Similarly, radiation impairs SR Ca2+ handling through dysregulation of SR Ca2+-ATPase 2a (SERCA2a). While Ca2+ trafficking through the cell membrane and SR has been studied, mitochondria, major players in cardiomyocyte Ca2+ homeostasis, remain largely unexplored in the context of microgravity and space radiation. Cardiomyocyte Ca2+ homeostasis depends on synergistic trafficking through cell membrane-bound, SR-bound, and mitochondrial Ca2+ channels. This study aims to unveil potential alterations in these channels at the transcriptional and translational levels.

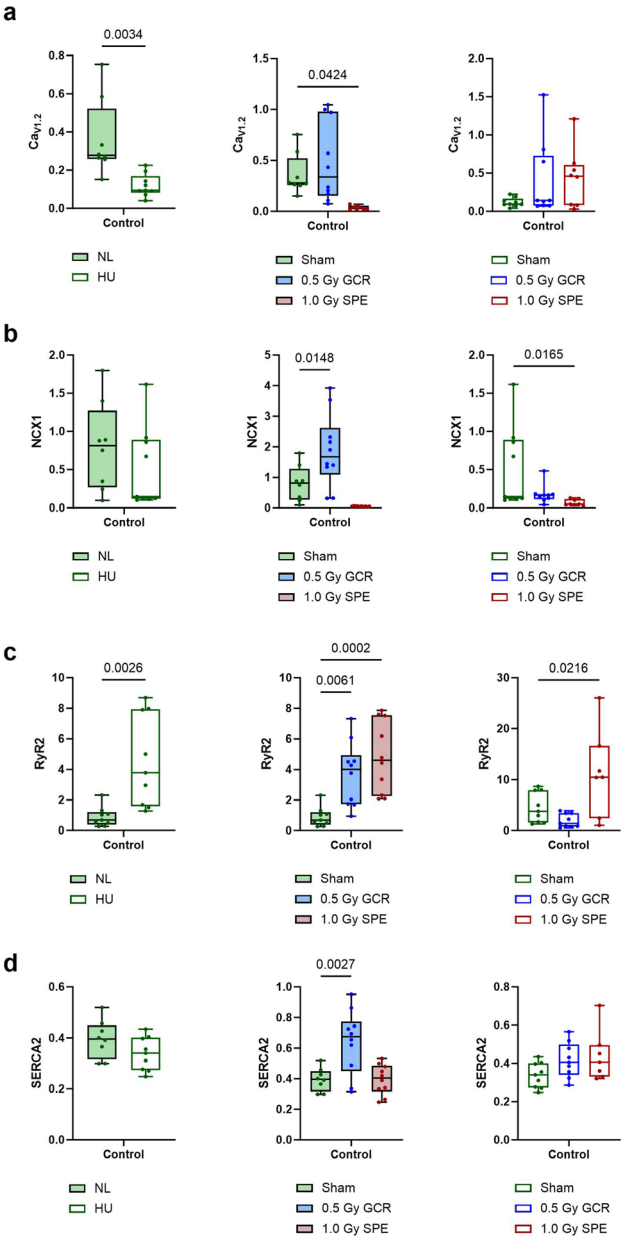


**Fig. 1** Quantification of membrane-bound (a) CaV1.2, (b) NCX1 as well as SR-bound (c) RyR2 and (d) SERCA2 in Sham, 0.5 Gy GCR irradiated and 1.0 Gy SPE irradiated cardiac tissue. Box-and-whisker plots are given with minimum to maximum. CaV1.2: voltage-dependent L-type calcium channel; GCR: galactic cosmic radiation; HU: hindlimb unloaded; NCX1: sodium-calcium exchanger 1; NL: normal loaded; RyR2: ryanodine receptor 2; SERCA2: sarcoplasmic/endoplasmic reticulum calcium ATPase 2; SPE: solar particle event

**Methods:** Fifteen-week-old (± 3 days) C57Bl/6J wild-type female mice ($n = 10$ per group) from Jackson Laboratories underwent either 14 days of HU or normal loading (NL) to simulate microgravity effects. HU was performed using non-invasive traction tape attached to an adjustable pulley system mounted atop a standard rat cage. Mice were positioned head-down (approximately 30° to horizontal), with the pulley free to move along a crossbar spanning the cage length. This allowed mice to navigate freely using forepaws and interact with cagemates while preventing hindlimb ambulation. To study space radiation effects, mice were exposed to GCR or SPE irradiation on day 13. Radiation doses administered were: simplified GCR simulation (0.5 Gy), SPE (1 Gy), and sham control (0 Gy). These doses reflect estimated astronaut exposure, approximately 0.5 Gy total GCR for a Mars round-trip mission and 1 Gy acute proton exposure from solar particle events—and follow established protocols. Mice were euthanized 14 hours post-irradiation by CO2 overdose followed by cervical dislocation. Cardiac tissue was flash-frozen at dissection and stored at –80 °C. To investigate potential alterations in Ca2+-associated ion channel expression, we analyzed protein concentrations of membrane-bound, SR-associated, and mitochondrial Ca2+ channels and their regulatory units.

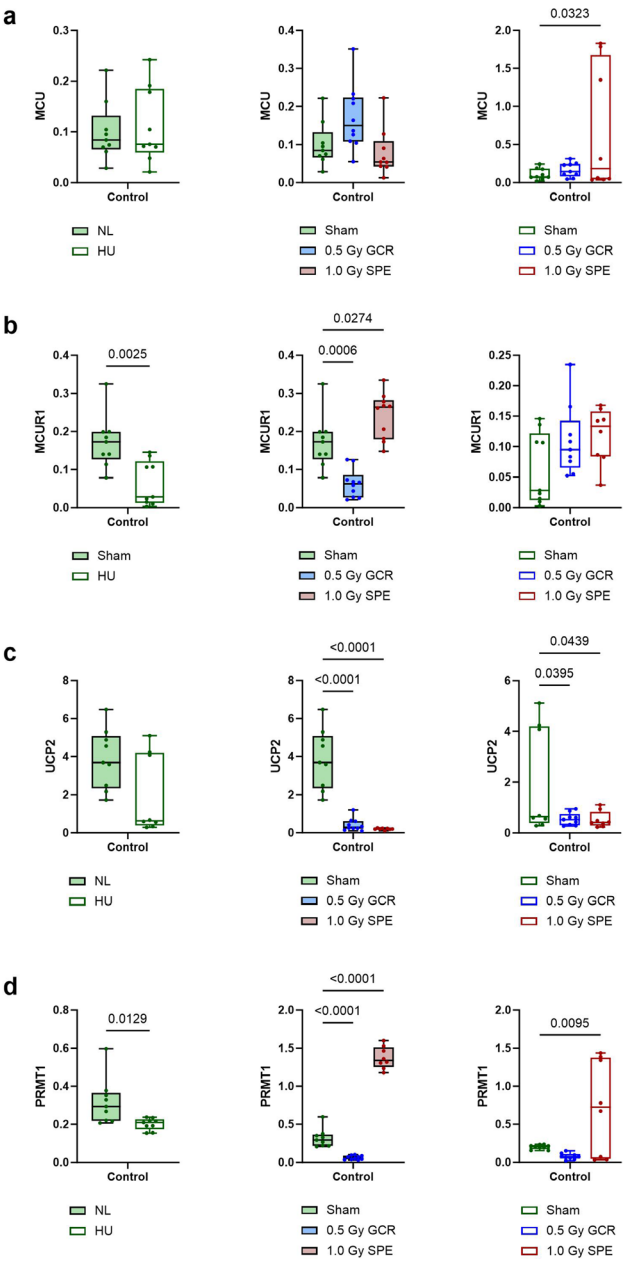


**Fig. 2** Quantification of mitochondrial (a) MCU, (b) MCUR1, (c) UCP2, and PRMT1 in Sham, 0.5 Gy GCR irradiated and 1.0 Gy SPE irradiated cardiac tissue. Box-and-whisker plots are given with minimum to maximum. GCR: galactic cosmic radiation; HU: hindlimb unloaded; MCU: mitochondrial calcium uniporter; MCUR1: mitochondrial calcium uniporter regulator 1; NL: normal loaded; PRMT1: protein arginine *N*-methyltransferase 1; UCP2: uncoupling protein 2; SPE: solar particle event

**Results:** Our analyses showed that HU significantly decreased membrane-bound CaV1.2 expression without affecting its counterpart NCX1. GCR did not impact CaV1.2 but increased NCX1 expression, while SPE decreased both membrane-bound proteins in irradiated cardiac tissue (Fig. 1a and 1b). Regarding SR-associated proteins, HU, GCR, and SPE all increased RyR2 expression. SERCA2 was altered by GCR but not SPE in NL mice, with minimal impact from simulated microgravity alone. CASQ1 and PLN were highly affected by both simulated microgravity and irradiation. HU significantly reduced both proteins in non-irradiated mice. GCR markedly decreased CASQ1 and PLN in NL mice, while SPE reduced only CASQ1. Both proteins remained unaffected by GCR or SPE in HU mice (Fig. 1c and 1d). Mitochondrial Ca2+ channel expression patterns were analyzed for MCU complex-associated proteins (MCU, MCUR1, MICU1, MICU2) and unbound proteins (UCP2, UCP3, PRMT1). HU for 14 days decreased MCUR1 and MICU2 without affecting MCU or MICU1. In NL mice, GCR markedly reduced MCUR1 and MICU2, while SPE differentially altered MCUR1, MICU1, and MICU2. In HU mice, only SPE affected MCU and MICU2 expression. Regarding regulatory proteins, HU markedly reduced UCP3 and PRMT1. GCR decreased UCP2 and PRMT1 in NL mice and partially in HU mice. Notably, SPE increased PRMT1 in both NL and HU mice, contrasting with the suppressive effects of HU and GCR (Fig. 2).

**Conclusion:** This study demonstrates that simulated microgravity and space radiation cause compartment-specific cardiac $Ca^{2+}$ channel changes relevant to astronaut cardiovascular health. Microgravity disrupted membrane-bound CaV1.2 and sarcoplasmic reticulum (SR) proteins CASQ1 and PLN, while mitochondrial channels remained largely unaffected. These alterations may contribute to myocardial atrophy and contractile dysfunction in astronauts. Both galactic cosmic radiation (GCR) and solar particle event (SPE) radiation increased RyR2 expression, potentially promoting SR $Ca^{2+}$ leak and elevating arrhythmogenic risk—critical given limited medical support during missions. SPE produced broader membrane channel effects than GCR, suggesting acute solar particle exposure poses greater immediate cardiovascular risk. Hindlimb unloading appeared to mitigate radiation-induced PLN alterations, indicating complex microgravity-radiation interactions. Mitochondrial $Ca^{2+}$ handling showed radiation sensitivity through altered regulatory proteins (MCUR1, MICU1, MICU2, UCP2, UCP3), despite stable MCU expression, potentially affecting cellular energetics and oxidative stress responses. These findings highlight the importance of cardiovascular monitoring during spaceflight and identify molecular targets for countermeasures. As missions extend toward Mars and beyond, understanding how microgravity and cosmic radiation jointly affect cardiac $Ca^{2+}$ regulation will be critical for safeguarding astronaut heart function.

# BEST ABSTRACTS—CLINICAL CASES

## Association of Postoperative LDL Cholesterol and Statin Therapy With Survival After Coronary Artery Bypass Grafting

**Engler C.[1], Winter-Pölzl L.[1], Lohmann R.[1,2], Graber M.[1], Hirsch J.[1], Nägele F.[1], Ioannou-Nikolaidou M.[1,2], Eder J.[1], Heim V.[1], Schmidt S.[1], Bano S.[1], Hirtenlehner F.[1], Kleineisen H.[1], Lukosch M.[1], Bonaros N.[1], Grimm M.[1], Gollmann-Tepeköylü C.[1]**

[1]Universitätsklinik für Herzchirurgie, Innsbruck, Austria
[2]Institut für Klinisch-Funktionelle Anatomie, Innsbruck, Austria

**Introduction:** Patients undergoing coronary artery bypass grafting (CABG) represent a very high cardiovascular risk population. Current guidelines recommend LDL-cholesterol (LDL-C) targets below 55 mg/dL, yet real-world data on LDL-C target achievement after CABG and its impact on long-term outcomes remain limited. We therefore evaluated LDL-C levels, lipid-lowering therapy patterns, and their association with survival after surgical myocardial revascularization.

**Methods:** We conducted a retrospective cohort study including all patients undergoing CABG at a tertiary cardiac surgery center between 2010 and 2024. Pre- and postoperative LDL-C levels and lipid-lowering therapy were analyzed. Changes in LDL-C were assessed in patients with paired measurements. Long-term survival analyses were performed in patients undergoing isolated CABG to minimize confounding by concomitant procedures. Survival was assessed using Kaplan–Meier analysis, and multivariable Cox regression was used to evaluate the association between lipid-lowering therapy intensity and mortality.

**Results:** A total of 5678 patients underwent CABG, including 3904 isolated procedures. Preoperative LDL-C measurements were available in 4880 patients and postoperative measurements in 4192 patients. Median LDL-C decreased from 99 [72–132] mg/dL preoperatively to 68 [50–92] mg/dL postoperatively. Among patients with paired measurements ($n=3675$), LDL-C declined by –23 mg/dL (–25.8%; $p<0.001$). Achievement of the guideline-recommended LDL-C target <55 mg/dL increased from 11.2% preoperatively to 36.9% postoperatively, yet the majority of patients remained above target. In patients undergoing isolated CABG, postoperative LDL-C levels <55 mg/dL were not associated with improved 5-year survival compared with higher LDL-C levels. In contrast, statin therapy was associated with significantly improved survival (HR 0.44, 95% CI 0.25–0.77, $p=0.004$), with additional benefit observed for high-potency statins (HR 2.70, 95% CI 1.50–4.87, $p=0.001$). In multivariable Cox regression, combination lipid-lowering therapy was independently associated with improved survival compared with monotherapy (HR 0.41, $p=0.025$).

**Conclusion:** Among patients undergoing CABG, LDL-C levels decreased substantially after surgery, yet guideline-recommended lipid targets were achieved in only a minority of patients. While achieved LDL-C levels were not independently associated with long-term survival, the intensity of lipid-lowering therapy was strongly associated with improved outcomes. These findings highlight the potential importance of aggressive lipid-lowering strategies, including combination therapy, to improve long-term survival in patients undergoing surgical myocardial revascularization.

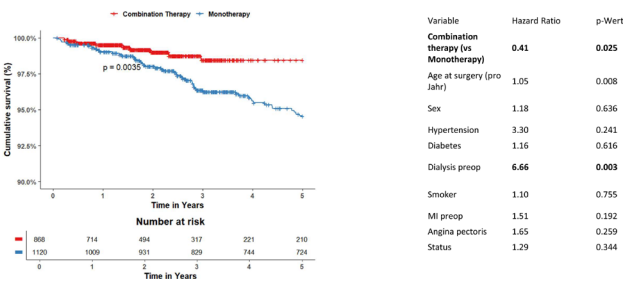


| Variable | Hazard Ratio | p-Wert |
|---|---|---|
| **Combination therapy (vs Monotherapy)** | **0.41** | **0.025** |
| Age at surgery (pro Jahr) | 1.05 | 0.008 |
| Sex | 1.18 | 0.636 |
| Hypertension | 3.30 | 0.241 |
| Diabetes | 1.16 | 0.616 |
| Dialysis preop | **6.66** | **0.003** |
| Smoker | 1.10 | 0.755 |
| MI preop | 1.51 | 0.192 |
| Angina pectoris | 1.65 | 0.259 |
| Status | 1.29 | 0.344 |

**Fig. 1** Mono- vs.combination therapy in isolated CBAG

## Bidirektionale ventrikuläre Tachykardie bei Andersen-Tawil Syndrom

**Fuchs N.**

Universitätsklinik Krems, Krems, Österreich

**Einleitung:** Wir berichten über den Fall einer 17-jährigen Patientin, welche zur weiteren Abklärung Ihrer ventrikulären Extrasystolie zugewiesen wurde. Diese fiel erstmals im Rahmen einer Untersuchung beim Schularzt auf. Im Alltag war die Patientin bisher immer beschwerdefrei. Klinisch auffallend war ein BMI von 16 kg/m² (150 cm, 38 kg). Die Patientin sei in den Wachstumsperzentilenkurven immer unter der Norm geblieben. Laborchemisch zeigte sich ein unauffälliges Blutbild. Herzenzyme, Schilddrüsenparameter, Nierenfunktionswerte und Leberwerte lagen ebenfalls im Normbereich. Das Kalium war hochnormal mit 4,5 mmol/L. Im Ausgangs-EKG zeigte sich ein normfrequenter Sinusrhythmus mit verkürzter PQ-Zeit von 108 ms und prominenten U-Wellen in V2 und V3. In der Telemetrie zeigten sich vermehrt ventrikuläre Arrhythmien in Form von bidirektionalen, ventrikulären Tachykardien und Extrasystolen. Hierunter zeigte sich die Patientin asymptomatisch. Es war jedoch fest zu stellen, dass die ventrikulären Ektopien vor allem bei emotionaler Belastung und Aufregung aufgetreten waren.

**Methoden:** Eine umfangreiche diagnostische Abklärung mittels Labordiagnostik, Elektrokardiographie (EKG), transthorakaler Echokardiographie, kardialer Magnetresonanztomographie und genetischer Testung ist erfolgt.

**Resultate:** Ein 12-Kanal Holter wurde für 24 Stunden angelegt. Hierbei zeigte sich ein durchgehender Sinusrhythmus mit einer signifikant erhöhten Rate an ventrikulären Ektopien (45 %). Ein Fokus lag im Bereich der linken Aortenklappentasche (LCC) und der zweite Fokus im Bereich des posterioren Papillarmuskels (PPM). Die Ratio der zwei Hauptmorphologien lag bei 6:1 (LCC: 30.000, PPM: 5000). Die Lokalisation spricht für eine Beteiligung des Purkinje-Systems. Im transthorakalen Herzultraschall zeigte sich eine niedrig normale Linksventrikelfunktion bei Tachykardie. Strukturell zeigten sich keine Auffälligkeiten. Die Aorta war im Bulbusbereich einsehbar und normal weit. Die Herzhöhlen waren normal groß strukturiert, mit regelrechter Wandstärke. Die Herzklappen ohne Vitien und die Vena cava inferior schlank. Im Herz-MRT ergab sich erneut ein unauffälliger Befund. Late-Enhancement im Bereich der Mitralklappe bzw. der Papillarmuskeln war nicht nachweisbar. Ein Therapieversuch mit Sotalol wurde initiiert und auf bis zu 200 mg/Tag aufdosiert. Hierunter kam es zu keiner Abnahme der VES-Last und einer passageren QTc-Verlängerung. Die Therapie wurde somit wieder beendet. In Zusammenschau der Befunde mit bidirektionalen, ventrikulären Tachykardien bei strukturell normalem Herz, ist eine genetische Testung erfolgt. Hierbei wurde eine pathogene Variante im KCNJ2-Gen in heterozygotem Zustand diagnostiziert. Somit bestätigte sich die Diagnose eines Andersen-Tawil Syndroms.

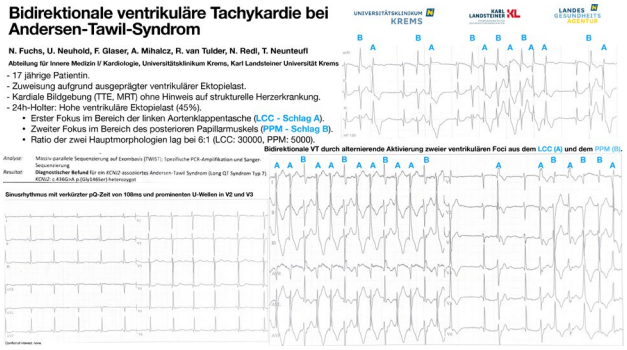


**Abb. 1**

**Schlussfolgerungen:** Der Fokus der ventrikulären Ektopien lag im Bereich des LCC und des PPM. Dies spricht für eine erhöhte Triggeraktivität im Bereich der Purkinje-Fasern. Andersen-Tawil Syndrom ist eine autosomal dominant vererbte, genetische Erkrankung. Das KCNJ2-Gen liegt auf dem 17. Chromosom und kodiert das Kir2.1 Membranprotein. Diese sind in der Zellmembran für den Kaliumeinstrom zuständig (IK1).[1] Somit ist die Pathophysiologie der ventrikulären Ektopien vermutlich ein destabilisiertes Membranpotential, welches die Erregbarkeit der Purkinje-Fasern begünstigt. Durch die Nachdepolarisation kann es somit leichter zu multiplen Foci aus dem Purkinje-System kommen (Delayed Afterdepolarization, DAD).[1] Die emotionalen Trigger steigern womöglich durch eine katecholaminerge Aktivierung das arrhythmogene Potential. Somit ist hier kein Re-entry Kreislauf für die ventrikuläre Tachykardie ursächlich und es gibt kein Ziel für eine Ablation. Von einer ICD-Implantation wurde bei hohem Risiko für inadäquate Schockabgaben abgesehen. Ein Therapieversuch mit Flecainid wäre der nächste Schritt. Durch Blockierung der schnellen Natrium-Kanäle und Reduktion der calcium-abhängigen Nachdepolarisation, könnte die ventrikuläre Ektopie womöglich verringert werden.[1]

## Literatur

1. Smith AH, Fish FA, Kannankeril PJ. Andersen-Tawil syndrome. Indian Pacing Electrophysiol J. 2006 Jan 1;6(1):32–43. PMID: 16943893; PMCID: PMC1501096.

## Caught in Transit: Echocardiographic Visualization of a Thrombus Traversing a Patent Foramen Ovale

**Zsilavecz V.**

LKH Graz II–Standort West, Graz, Austria

**Introduction:** This report describes an 85-year-old patient who initially presented to the neurological emergency department with transient right-sided brachial-dominant hemiparesis accompanied by aphasia. The symptoms began early in the morning and persisted for approximately five minutes before resolving spontaneously. At the time of presentation, the patient was already asymptomatic. He was admitted for inpatient neurological evaluation and further diagnostic workup. Cranial computed tomography revealed no evidence of intracerebral hemorrhage or a recent, demarcated ischemic lesion. However, advanced microangiopathic changes were noted. Carotid duplex ultrasonography demonstrated mild bilateral atherosclerotic changes without hemodynamically significant stenosis. Transthoracic echocardiography revealed cardiac chambers of normal dimensions with preserved left and right ventricular systolic function. A mobile structure was visualized in both atria. Following consultation with the cardiology department, the patient was transferred to the cardiology ward due to high suspicion of intra-atrial thrombi as the cause of the transient ischemic attack.

**Methods:** For further evaluation, venous duplex ultrasound of both lower extremities and CT pulmonary angiography were performed. These investigations revealed a three-segment deep vein thrombosis (DVT) in the left leg and a central pulmonary artery embolism on the right, with evidence of acute right heart strain. Additionally, a mobile thrombus was observed in the descending aorta. Given the extensive findings in an otherwise hemodynamically stable patient, continuous unfractionated heparin infusion was initiated, targeting a 1.5- to 2-fold prolongation of the activated partial thromboplastin time (aPTT). Transesophageal echocardiography further demonstrated a thrombus migrating through a patent foramen ovale (PFO), with mobile portions present in both atria (Fig. 1). Multidisciplinary consultation, including cardiac surgery, angiology, and interventional radiology, was undertaken to evaluate surgical, interventional, or conservative management options. A primarily interventional approach was deemed inappropriate due to the patient's neurologically asymptomatic status and the high risk of peri-procedural thrombus fragmentation and embolization. Surgical thrombectomy was considered feasible but associated with high periprocedural risk.

**Results:** After detailed counseling regarding the procedure and potential complications—including perioperative right- and left-sided embolization and stroke—the patient declined surgical intervention. Consequently, a conservative strategy with continuation of therapeutic anticoagulation via heparin infusion was adopted. Due to limited evidence regarding the management and optimal duration of conservative therapy for a migrating thrombus, a three-week course of unfractionated heparin was selected based on available case reports, followed by transition to oral anticoagulation with apixaban. The patient remained hemodynamically stable throughout hospitalization, without further neurological deficits or sensorimotor abnormalities. Transthoracic echocardiography after 10 days of therapy showed complete resolution of the atrial thrombus. A transesophageal echocardiography performed on day 22 confirmed the absence of any residual or migrating thrombi. After transitioning to apixaban, the patient was discharged home on day 23 post-admission in age-appropriate, good general condition without persistent neurological deficits.

**Conclusion:** An 85-year-old patient presented with a transient ischemic attack. Further evaluation revealed deep vein thrombosis, pulmonary embolism with right heart strain, and a thrombus in transit across a PFO. Due to high procedural risk and patient preference, conservative anticoagulation was initiated, resulting in complete thrombus resolution without recurrent neurological events. Thrombus in transit across a PFO represents a rare but potentially catastrophic condition associated with a high risk of systemic embolization. Therapeutic strategies remain controversial, ranging from urgent surgical thrombectomy1 to interventional removal, thrombolytic strategies2 or anticoagulation alone3. In the absence of robust guideline recommendations, management must be individualized and guided by hemodynamic stability, embolic risk, comorbidities, and patient preference. This case demonstrates that in a hemodynamically stable patient without ongoing neurological deficits a conservative approach with continuous full-dose anticoagulation can lead to complete thrombus resolution and favorable clinical outcome. Close imaging surveillance and interdisciplinary collaboration are crucial to mitigate the risk of thrombus progression or embolic complications. Our report


**Fig. 1** Transesophageal echocardiography showing a thrombus migrating through a patent foramen ovale (PFO), with mobile portions in the left (A) as well as in the right atrium (A).]


**Fig. 2 Video 1** 3D-echocardiography showing a thrombus migrating through a patent foramen ovale (PFO).]

adds to the limited body of evidence suggesting that non-surgical management may be a reasonable alternative in carefully selected patients, particularly when surgical risk is substantial or intervention is declined.

## References

1. Ieva R, et al. Pulmonary Embolism and Thrombus in Transit Through Patent Foramen Ovale. Ann Vasc Surg. 2020 Feb;63:457.e19-457.e21.
2. Pires MIFB, Almeida I, Santos JM, Correia M. Thrombus in transit through a patent foramen ovale: catch it if you can-a case report. Eur Heart J Case Rep. 2021;1;5(10):ytab382. Oct.
3. Li B, Wang H, Cen H, Chen S, Shu S, Peng B, Case Report SP. Embolus in transit vs. in situ PFO thrombus. Front Cardiovasc Med. 2026;12;12:1721995. Jan.

## Electroanatomic voltage-guided endomyocardial biopsy in suspected cardiac sarcoidosis—a case series

**Wörgötter K.[1], Pfeffer M.[2], Fiedler L.[2], Bernreiter T.[2], Zizka J.[2], Roithinger F.[2], Grübler M.[3]**

[1]Sigmund Freud Universität, Wien, Austria
[2]Universitätsklinikum Wiener Neustadt, Wiener Neustadt, Austria
[3]UK Wiener Neustadt, Wiener Neustadt, Austria

**Introduction:** Diagnosis of cardiac sarcoidosis has traditionally relied on imaging modalities such as cardiac magnetic resonance (CMR) and fluorodeoxyglucose positron emission tomography (FDG-PET), given the limited sensitivity of conventional fluoroscopy-guided endomyocardial biopsy (EMB). The recently published 2025 ESC guidelines on myocarditis and pericarditis [1] now acknowledge the role of electroanatomic voltage mapping (EAM)-guided EMB, assigning it a Class IIa recommendation for patients with suspected cardiac sarcoidosis.

**Methods:** Eight patients with suspected cardiac sarcoidosis underwent EAM-guided EMB. All patients received comprehensive pre-procedural evaluation including CMR and FDG-PET. EAM was performed to create three-dimensional ventricular reconstructions and record high-density intracardiac electrograms. Bipolar voltage mapping identified abnormal myocardium, with > 1.5 mV defined as normal and 0.5–1.5 mV as low-voltage areas. Targeted biopsies were obtained from low voltage areas and border zones. Patients were classified in accordance with the HRS guidelines [2] as definite or probable cardiac sarcoidosis (otherwise excluded from the present case series). Additionally Japanese ministry of health diagnostic (JCS) criteria [3] and the ESC criteria were assessed.

**Results:** Among the nine patients, three were classified as definite cardiac sarcoidosis based on the presence of non-caseating epithelioid granulomas on histopathology (one of whom was unguided biopsy). Two patients had negative EMBs, however, their electroanatomic maps closely resembled those observed in histologically confirmed cases. Both patients with negative EAM-EMB had proven extracardiac sarcoidosis and characteristic findings on CMR and FDG-PET, fulfilling both HRS and JCS criteria, and were thus classified as probable cardiac sarcoidosis. Three patients had negative biopsies with inconclusive imaging and clinical findings and were categorized as possible cardiac sarcoidosis. One patient had a negative EMB but was subsequently diagnosed with arrhythmogenic right ventricular cardiomyopathy. Notably, this patient would have fulfilled the JCS criteria for cardiac sarcoidosis.

**Conclusion:** This case series underscores the value of EAM-EMB as an adjunctive tool within a multimodal diagnostic approach to cardiac sarcoidosis. While histological confirmation was achieved in selected patients, non-diagnostic biopsies underscore the need to interpret EMB findings in conjunction with clinical and imaging data. Diagnostic yield appears to depend on appropriate patient selection and integration with complementary imaging modalities, including CMR and FDG-PET, to guide biopsy timing and localization. These findings support incorporating EAM-guided EMB into the overall diagnostic pathway rather than considering it a standalone diagnostic test.

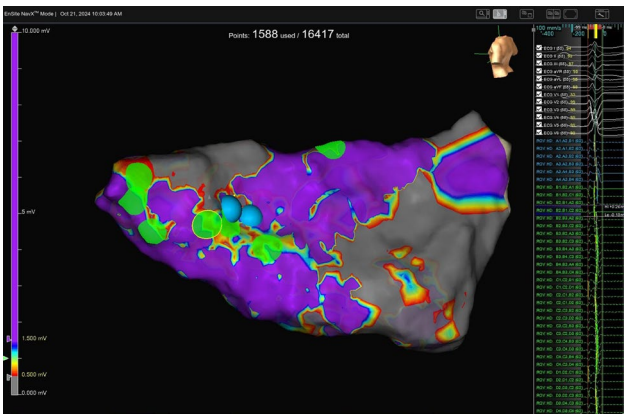


**Fig. 1** Electroanatomic voltage map of the RV demonstrating extensive low-voltage areas involving the basal and apical septum. Although EMB was negative, the voltage pattern was comparable to those observed in biopsy-proven CS]

## References

1. Schulz-Menger J, Collini V, Gröschel J, et al. ESC Guidelines for the management of myocarditis and pericarditis. Eur Heart J. 2025;2025:ehaf192.
2. Birnie DH, Sauer WH, Bogun F, et al. HRS Expert Consensus Statement on the Diagnosis and Management of Arrhythmias Associated With Cardiac Sarcoidosis. Heart Rhythm. 2014;11:1304–23.
3. Terasaki F, Azuma A, Anzai T, et al. JCS 2016 Guideline on Diagnosis and Treatment of Cardiac Sarcoidosis — Digest Version. Circ J. 2019;83:2329–88.


## Parvovirus B19 Cardiomyopathy Masquerading as Drug-Induced Toxicity: Complete Recovery Following Biopsy-Guided Immunomodulation


**Meledeth C., Aigner A., Wichert-Schmitt B., Steinwender C., Reiter C.**

Department of Cardiology, Kepler University Hospital, Medical Faculty, Johannes Kepler University, Linz, Austria


**Introduction:** A 27-year-old woman with a psychiatric history was transferred to our cardiology department with newly diagnosed cardiomyopathy and severely reduced left ventricular ejection fraction (LVEF) of 20%. On admission she presented with acute liver failure, acute kidney injury (creatinine 1.7 mg/dL, estimated glomerular filtration rate (eGFR) 41 mL/min/1.73 $m^2$), and hyperkalaemia. Comorbidities included Crohn's disease with suspected enterocolonic fistula, iron deficiency anaemia, and pneumonia. Echocardiography confirmed LVEF of 20% with a dilated left ventricle. Cardiac magnetic resonance imaging (MRI) revealed no myocardial scarring or oedema. Given the history of high-dose venlafaxine therapy, drug-induced toxic cardiomyopathy was considered the leading differential. Supportive measures led to normalisation of hepatic and renal parameters—notably without haemodynamic compromise at any point, arguing against a cardiogenic cause of the multi-organ dysfunction. Antibiotics were established for the pulmonary infiltrate, neurohormonal therapy initiated, venlafaxine discontinued and replaced with sertraline, and the patient transferred to gastroenterology for Crohn's management.

**Methods:** In ambulatory follow-up, the absence of functional recovery despite venlafaxine cessation and optimised neurohormonal therapy raised significant doubt regarding the toxic hypothesis and prompted endomyocardial biopsy. Histology revealed chronic lymphocytic myocarditis; polymerase chain reaction (PCR) confirmed myocardial parvovirus B19 (PVB19) persistence at 5499 copies/µg myocardial nucleic acid with fewer than 100 copies/µg in peripheral leukocytes, establishing the diagnosis of PVB19-associated inflammatory cardiomyopathy. *N*-terminal pro-brain natriuretic peptide (NT-proBNP) was 19,426 ng/L. Following one cycle of intravenous immunoglobulin (IVIg), LVEF improved to 45–50% and NT-proBNP declined to 4968 ng/L—a meaningful but incomplete response. As partial functional recovery could not confirm resolution of the underlying inflammatory process, and given the risk of corticosteroids impairing viral clearance in active viral myocarditis, repeat endomyocardial biopsy was performed two months later. Reassessment was considered essential to confirm viral load trajectory, document persistent inflammation justifying long-term immunosuppression in a young patient with Crohn's disease, and establish virological status that serum markers alone cannot provide. Repeat biopsy confirmed chronic lymphocytic myocarditis, a reduction in PVB19 copies to 2272/µg, and persistent local immune activation without systemic viral spread.

**Results:** Prednisolone was initiated and the response was striking. NT-proBNP fell to 925 ng/L, then 313 ng/L by January 2026—a cumulative reduction of greater than 98% from the peak of 19,426 ng/L (Graph 1). Symptoms resolved completely and LVEF normalised to 60%, recovering from a nadir of 20%. Serial biomarker tracking provided objective evidence of progressive myocardial recovery at each decision point. This case illustrates that PVB19 inflammatory cardiomyopathy can closely mimic drug-induced disease, and that cardiac MRI may yield false-negative results in chronic low-grade myocarditis—where oedema has resolved and fibrotic remodelling is absent—underscoring the indispensability of biopsy in unexplained cardiomyopathy refractory to standard therapy. The biopsy-guided stepwise strategy was central to safe therapeutic escalation. In virus-positive disease, a declining viral load with persistent immune activation—as demonstrated on repeat biopsy here—may represent a state in which the inflammatory component predominates and immunosuppression is both appropriate and safe.

**Conclusion:** Interferon beta (IFN-β) represents a potential escalation strategy in refractory PVB19 cardiomyopathy. The Betaferon in Chronic Viral Cardiomyopathy (BICC) trial [1] demonstrated viral elimination and LVEF stabilisation in enteroviral and adenoviral disease; however, evidence in PVB19-specific disease remains limited, given its endothelial tropism and non-productive myocardial replication pattern. In this case complete recovery was achieved without IFN-β, but it would represent a logical next step in patients with persistent high viral load and failure to respond to immunomodulation. This case demonstrates that biopsy-guided immunomodulation can achieve full myocardial recovery from severely reduced baseline function in PVB19 inflammatory cardiomyopathy. Repeat endomyocardial biopsy was indispensable in establishing the virological and histological prerequisites for safe corticosteroid escalation. IFN-β warrants consideration in refractory cases, though prospective evidence specific to PVB19 remains limited.


## References

1. Schultheiss HP, Piper C, Sowade O, Waagstein F, Kapp JF, Wegscheider K, Groetzbach G, Pauschinger M, Escher F, Arbustini E, Siedentop H, Kuehl U. Betaferon in chronic viral cardiomyopathy (BICC) trial: Effects of interferon-β treatment in patients with chronic viral cardiomyopathy. Clin Res Cardiol. 2016 Sep;105(9):763–73. https://doi.org/10.1007/s00392-016-0986-9. Epub 2016 Apr 25. PMID: 27112783.


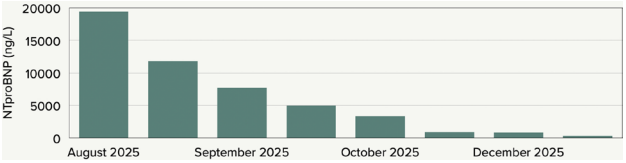


**Fig. 1** NTproBNP Course in Disease Progression

## Rapidly progressive right heart failure

**Alajbegovic L., Heinz G., Burda M., Hofbauer T., Skoro-Sajer N., Gerges C., Lang I.**

Medizinische Universität Wien, Innere Medizin II, Abteilung für Kardiologie, Wien, Austria

**Introduction:** We report on a 46-year old female presenting with acute dyspnea and chronic cough at another emergency department. Patient reported history of robotic-assisted laparoscopic myomectomy. After ruling out pulmonary embolism (PE), patient was discharged with the diagnosis of acute bronchitis. Due to lack of improvement, patient was reevaluated at another peripheral hospital. Transthoracic echocardiography showed severely reduced right ventricular function and systolic pulmonary artery pressure of 60 mmHg. Due to hemodynamic instability and respiratory insufficiency patient was put on vasopressors and non-invasive ventilation.

**Methods:** For further evaluation of possible pulmonary hypertension patient was transferred to cardiology intensive care unit (ICU) at our university clinic. Intravenous (iv) epoprostenol was started because of signs of right heart failure. Abdominal computed tomography showed thickening of the uterine wall. On the second night in the ICU, cardiopulmonary arrest occurred and patient was put on venoarterial (VA)—extracorporeal membrane oxygenation (ECMO). Drop in hemoglobin without bleeding origin led to iv epoprostenol being switched to inhaled iloprost. Patient could be stabilized on ECMO. The gynecological tumorboard diagnosed cystic degeneration of a uterine leiomyoma.

**Results:** Right heart catheterization was performed under VA-ECMO. Under one liter/min flow patient showed a mean pulmonary artery pressure of 40 mmHg and a pulmonary artery wedge pressure of 12 mmHg. Pulmonary angiogram showed vascular lesions resembling pulmonary hemangiomatosis. A wedge aspirate showed large multinucleated cells raising the suspicion of tumor thrombotic microangiopathy (PTTM). Uterine biopsy showed endometrial adenocarcinoma. Patient deteriorated despite ECMO and died 18 days after start of symptoms.

**Conclusion:** Diagnosis postmortem was made of PTTM based on presence of tumor infiltrated lung parenchyma. Pulmonary tumor thrombotic microangiopathy is a rare, rapidly fatal disease characterized by tumor cell emboli in pulmonary arteries, causing intimal proliferation, acute pulmonary hypertension and subsequent right heart failure and death. This case represents a rare disease and highlights the need for early awareness in patients with fulminant right heart failure in the presence of an imminent cancer diagnosis.

# HEART TEAM POSTER SESSION 1

## 1-1

## TAVI Success Is More Than Just the Valve: CT-derived Sarcopenia as a Major Determinant of Long-Term Survival

**Schörghofer N.[1], Clodi N.[2,1], Knapitsch C.[1], Hecke G.[3,4], Hammerer M.[2], Lichtenauer M.[2], Scharinger B.[1], Hergan K.[5], Hoppe U.[2], Boxhammer E.[2]**

[1]Universitätsklinik für Radiologie, Salzburg, Austria
[2]Universitätsklinik für Innere Medizin II, Kardiologie und internistische Intensivmedizin, Salzburg, Austria
[3]Universitätsklinik für Dermatologie, Salzburg, Austria
[4]Department für Radiologie, Radiologische Universitätsklinik, Tübingen, Germany
[5]Universitätsklinik für Radiologie, Universitätsklinikum Salzburg, Salzburg, Austria

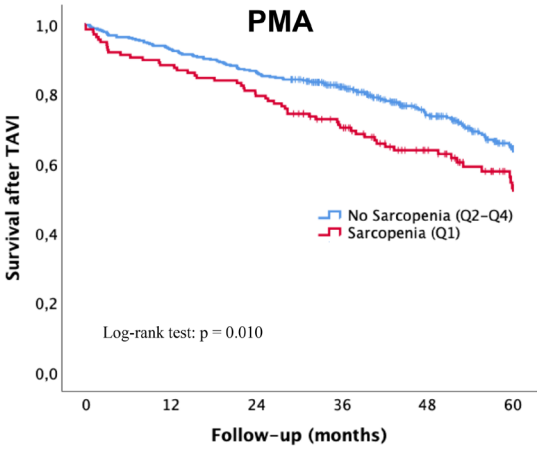


**No. at Risk**

| | | | | | | |
|---|---|---|---|---|---|---|
| Sarcopenia | 136 | 120 | 108 | 85 | 60 | 33 |
| No Sarcopenia. | 403 | 374 | 348 | 287 | 194 | 116 |
| Overall | 539 | 494 | 456 | 372 | 254 | 149 |

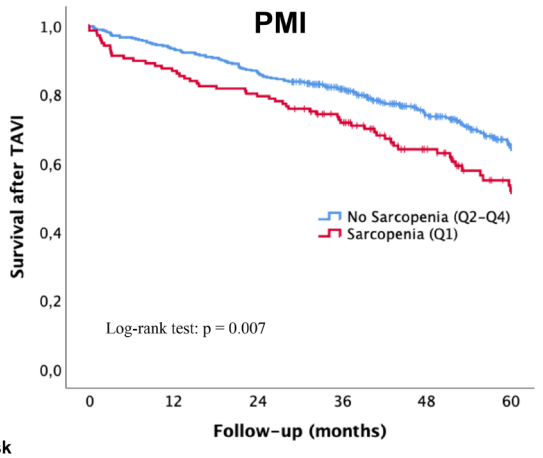


**No. at Risk**

| | | | | | | |
|---|---|---|---|---|---|---|
| Sarcopenia | 136 | 118 | 108 | 86 | 58 | 34 |
| No Sarcopenia. | 403 | 376 | 348 | 286 | 196 | 115 |
| Overall | 539 | 494 | 456 | 372 | 254 | 149 |

**Fig. 1 | 1-1**

**Introduction:** Sarcopenia, characterized by progressive skeletal muscle loss, is a silent yet powerful marker associated with survival, yet its impact on long-term outcomes in transcatheter aortic valve implantation (TAVI) remains underestimated. While frailty has been recognized as a main factor of resilience and recovery, the role of muscle integrity is frequently overlooked. This study explores whether computed tomography (CT)-derived psoas muscle area (PMA) and psoas muscle area index (PMI) are key predictors of post-TAVI survival.

**Methods:** A total of 539 patients (mean age 82.0 ± 5.1 years; 49.9% female) undergoing TAVI were analyzed in this retrospective, single-center study. Sarcopenia was analyzed via sex-specific quartiles of PMA and PMI. Long-term survival was examined using Kaplan-Meier analysis, univariate and multivariate Cox regression analysis. Interaction terms were introduced to assess whether the association between sarcopenia and survival differed by age, sex, renal function and anemia status.

**Results:** Sarcopenia emerged as a predictor of long-term mortality (HR = 1.52, $p = 0.011$ for PMA; HR = 1.55, $p = 0.008$ for PMI) after TAVI. Notably, younger patients (< 80 years) with sarcopenia faced double the mortality risk (HR = 2.48, $p = 0.001$ for PMA; HR = 2.55, $p = 0.001$ for PMI), whereas in older patients, the association was weaker. In women, who typically show a post-TAVI survival advantage, sarcopenia reduced this benefit (HR = 1.75, $p = 0.020$ for PMA; HR = 1.88, $p = 0.008$ for PMI). The most striking finding was the synergistic effect of sarcopenia and chronic kidney disease (CKD), resulting in a threefold increase in mortality risk (HR = 2.82, $p = 0.027$ for PMA; HR 3.14, $p = 0.011$). After multivariate adjustment, sarcopenia remained a strong, independent predictor of long-term mortality (HR = 1.58, $p = 0.009$ for PMA; HR = 1.49, $p = 0.024$ for PMI), reinforcing its clinical relevance in TAVI risk stratification.

**Conclusion:** Our study suggests that sarcopenia is not just a passive bystander, but may serve as a marker associated with long-term mortality in TAVI patients, especially in younger individuals, women, and those with CKD or anemia. Since muscle mass predicts survival and is potentially modifiable, assessing and intervening against sarcopenia before and after TAVI could represent a clinical priority in patients with aortic valve stenosis. This study underscores the importance of a more nuanced approach—not merely focusing on valve replacement, but on strengthening patient-centered care.

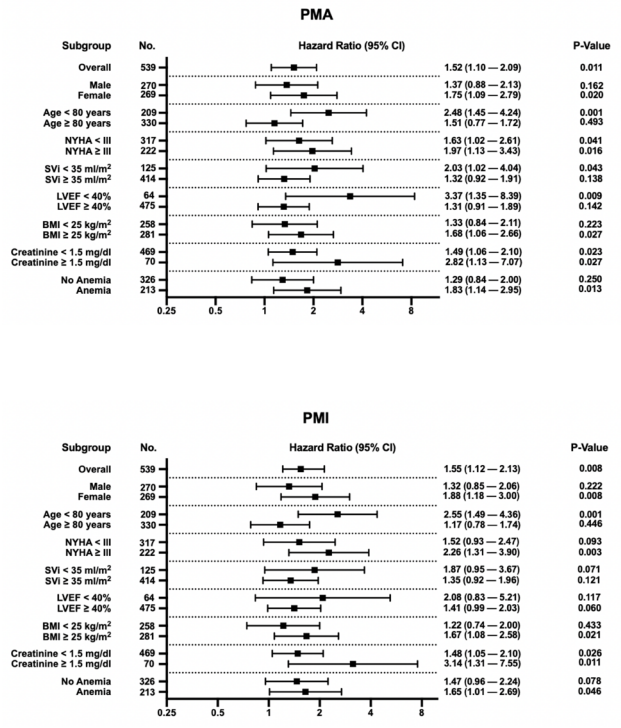


**Fig. 2 | 1-1**

## 1-2

## The value of extended follow-up in early phase device trials: Long-term outcomes of cardiac shockwave therapy beyond the CAST-HF trial

**Nägele F.[1], Graber M.[1], Engler C.[1], Pölzl L.[1], Hirsch J.[1], Schmidt S.[1], Eder J.[1], Heim V.[1], Iannou-Nikolaidou M.[1], Lohmann R.[1], Mayr A.[2], Troger F.[2], Grimm M.[1], Gollmann-Tepeköylü C.[1], Holfeld J.[1]**

[1]Universitätsklinik für Herzchirurgie, Medizinische Universität Innsbruck, Innsbruck, Austria
[2]University Clinic of Radiology, Medical University of Innsbruck, Innsbruck, Austria

**Introduction:** Extending the follow-up of investigator-initiated randomized clinical trials, especially in the field of translational research, offers a unique opportunity to assess long durability of treatment effects and detect late-emerging benefits or harms. Ethically, maximizing information from existing randomized cohorts reduces the need to expose additional patients to early phase therapies without sufficient long-term evidence. This approach, however, is still underutilized in cardiovascular research. In chronic ischaemic heart failure, revascularization strategies such as coronary artery bypass grafting (CABG) alleviate symptoms but have limited regenerative effects on left ventricular function. The CAST-HF trial demonstrated that intraoperative direct cardiac shockwave therapy (SWT) in addition to CABG is safe and improves left ventricular ejection fraction (LVEF), exercise capacity, and quality of life one year post intervention. The present study examines the long-term outcomes of CAST-HF participants, providing both clinical and methodological insights into sustained myocardial recovery after SWT in addition to CABG.

**Methods:** This secondary analysis extends the follow-up of the CAST-HF randomized controlled trial (NCT03859466), in which patients with ischaemic heart failure were assigned 1:1 to receive intraoperative direct cardiac shockwave therapy (SWT) or sham treatment in addition to CABG. The extended observation

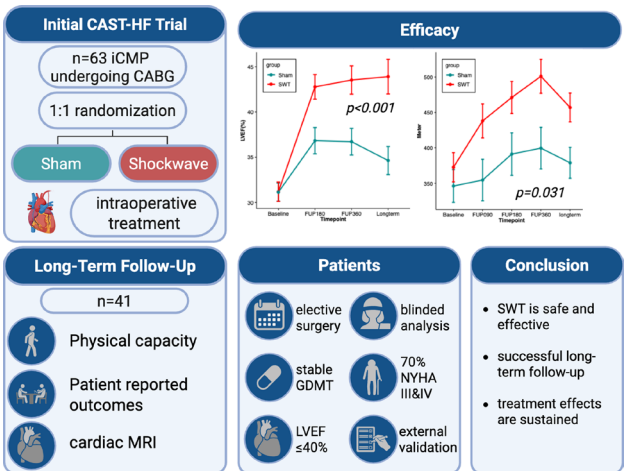


**Fig. 1 | 1-2** Graphical Abstract

aimed to evaluate long-term treatment durability using a different primary endpoint. Left ventricular ejection fraction (LVEF) was quantified by cardiac magnetic resonance imaging (cMRI), exercise capacity by six-minute walk test (6 MWT), and quality of life by the Minnesota Living with Heart Failure Questionnaire (MLHFQ). All imaging and other data were processed and analyzed by investigators blinded to treatment allocation. The original randomization was preserved for all analyses, and safety endpoints were reassessed throughout the observational period.

**Results:** Of the originally 63 randomized patients, a total of 41 patients (SWT $n=22$; Sham $n=19$) completed the extended follow-up period with cMRI. In the intention-to-treat analysis LVEF remained significantly higher in the SWT group, with a mean difference of 9.0% (95% CI 4.0–14.4; $p<0.001$) compared to Sham. Functional capacity also favored SWT (6 MWT: 438 ± 138 m vs. 355 ± 160 m; $p=0.031$), as did quality of life (MLHFQ: 18.9 ± 17.5 vs. 28.5 ± 19.6; $p=0.046$). No differences were observed in the safety outcome measurements including major adverse cardiac events, rehospitalization, or mortality between groups. Further, no device-related or procedural adverse events occurred during long-term follow-up.

**Conclusion:** This long-term follow-up of the CAST-HF trial demonstrates that a single intraoperative application of cardiac shockwave therapy (SWT) in addition to CABG yields sustained improvements in LVEF, exercise capacity, and patient-reported outcomes beyond the one-year horizon. These findings strengthen the evidence that SWT serves as a promising treatment method for the unmet clinical need of myocardial regeneration. Moreover, this analysis also illustrates the feasibility and scientific value of extending follow-ups in early phase medical device trials, an approach that enhances the reliability of safety and efficacy estimates.

## 1-3

### Identical NT-proBNP Levels Correspond to Higher Mortality Risk in Women Undergoing Cardiac Surgery

**Winter-Pölzl L.[1], Lohmann R.[1,2], Engler C.[1], Hirsch J.[1], Graber M.[1], Nägele F.[1], Grimm M.[1], Höfer D.[1], Bonaros N.[1], Gollmann-Tepeköylü C.[1]**

[1]Univ.-Klinik für Herzchirurgie, Innsbruck, Austria
[2]Institut für klinisch-funktionelle Anatomie, Innsbruck, Austria

**Introduction:** Women undergoing cardiac surgery consistently experience higher perioperative mortality than men. NT-proBNP is widely used for perioperative risk stratification, but it remains unclear whether identical biomarker values correspond to the same clinical risk in women and men. We therefore investigated sex differences in preoperative NT-proBNP levels and their relationship with perioperative and mid-term outcomes in a large contemporary cardiac surgical cohort.

**Table 1 | 1-3** Predicted 30-day mortality at defined NT-proBNP levels stratified by sex

| NT-proBNP | Female | Male | Absolute mortality risk difference |
|---|---|---|---|
| 250 | 1.2% (0.8–2.0) | 0.6% (0.4–1.0) | 0.6% |
| 500 | 2.3% (1.7–3.2) | 1.2% (0.9–1.6) | 1.1% |
| 1000 | 3.1% (2.3–4.3) | 1.6% (1.2–2.2) | 1.5% |
| 2000 | 3.2% (2.3–4.4) | 1.7% (1.2–2.4) | 1.5% |
| 4000 | 8.7% (6.2–12.1) | 4.7% (3.3–6.6) | 4.0% |

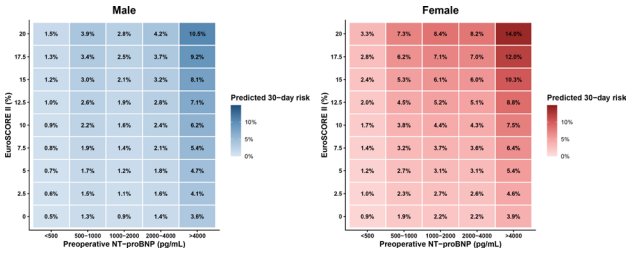


**Fig. 1 | 1-3** Predicted 30-day mortality according to preoperative NT-proBNP and EuroSCORE II stratified by sex

**Methods:** Preoperative NT-proBNP levels were analyzed in consecutive patients undergoing cardiac surgery between 2010 and 2024. Associations with 30-day mortality, 5-year mortality, ECMO support, postoperative dialysis, and prolonged ICU stay were assessed using regression models adjusted for EuroSCORE II. Absolute mortality risk across the NT-proBNP spectrum was modeled separately for women and men. A clinically relevant threshold was defined as the NT-proBNP value at which the absolute difference in predicted 30-day mortality between sexes exceeded 1%.

**Results:** Among 10,458 patients (29% women), women had higher preoperative NT-proBNP levels than men (650 vs 382 ng/L). NT-proBNP showed similar relative prognostic performance in both sexes. After adjustment for EuroSCORE II, female sex remained independently associated with higher 30-day mortality (OR 1.87) and 5-year mortality (HR 1.18). Mortality increased progressively with rising NT-proBNP levels in both sexes, indicating a strong biomarker risk gradient. However, the same NT-proBNP level was associated with higher absolute risk in women. At 1000 ng/L, predicted 30-day mortality was 3.3% in women versus 1.9% in men; at 4000 ng/L, it was 5.2% versus 3.1%. A model-derived threshold of 635 ng/L marked the point at which the absolute mortality difference between sexes exceeded 1%. Above this level, mortality increased substantially and the sex gap became clinically relevant (4.7% vs 2.8%). Among women above this threshold, age, NT-proBNP level, and nonelective surgery further refined risk and identified a subgroup with markedly elevated perioperative and long-term mortality.

**Conclusion:** NT-proBNP predicts outcomes equally well in women and men undergoing cardiac surgery, but identical biomarker levels correspond to higher absolute risk in women. Sex-aware interpretation of NT-proBNP may therefore improve perioperative risk stratification and help identify women at particularly high surgical risk.

## 1-4

### Outcome of patients with Fontan associated protein losing diseases after Norwood palliation

**Sames-Dolzer E.[1], Gierlinger G.[1], Kreuzer M.[1], Mair R.[1], Seeber F.[1], Tulzer A.[2], Zierer A.[3], Mair R.[1]**

[1]Kepler Universitätsklinikum, MC III., Department für Kinderherzchirurgie, Linz, Austria
[2]Kepler Universitätsklinikum, MC IV, Abteilung für Kinderkardiologie, Linz, Austria
[3]Kepler Universitätsklinikum, MC III., Klinik für Herz-, Thorax- und Gefäßchirurgie, Linz, Austria

**Introduction:** Newborns with hypoplastic left heart syndrome and related malformations are usually treated by staged

Norwood palliation leading to Fontan physiology. The occurrence of protein losing diseases during long-term follow up can be associated with severe Fontan failure and may be life limiting. Surgical procedures and lymphatic interventions can positively influence longterm outcome of this critical patient subgroup.

**Methods:** Between 1997 and October 2025 493 Norwood procedures have been performed at a single center using an RVPA conduit in 86% of our patients. 298 Norwood patients received a fenestrated extracardiac Fontan palliation with an on average 20 mm PTFE prosthesis at a median age of 3,6 years (range 0,9–7,7 years). This single center retrospective study investigates the outcome after onset of protein losing diseases as well as intervention strategies in this patient group.

**Results:** 5% of the initial Norwood group developed a protein losing enteropathy (25 pts.) and 2% at least one event of plastic bronchitis (11 pts.) at a median age of 5,9 years (range 3–17 years). Included are two patients showing symptoms of both diseases (total cohort 34 pts.). Residual anatomic problems (mainly at the LPA) have been addressed using catheter interventions or surgery in 23 pts. Furthermore,13 patients received surgical procedures in order to improve Fontan physiology including 10 refenestration procedures and 3 Hraska operations. 8 patients underwent lymphatic interventions. 30% (10/34) died or underwent heart transplantation after median 3,3 years (range 0,4–11,3 years) after diagnosis. The median follow up period of surviving patients without HTX is 6,9 years (range 0,5–18,8 years). The 10 years survival expectancy after diagnosis of PLE is 60% and after plastic bronchitis 74%. 18/34 patients do not show clinical symptoms at last follow up and are in good general condition.

**Conclusion:** Protein losing diseases are still major complications of life threatening dimension leading to death or need for heart transplantation in a relevant percentage of this subgroup. Nevertheless, life expectancy can be improved by successful surgical or lymphatic interventions as is shown by the encouraging median follow up period of 7 years (with a maximum of 19 years in one patient). Besides prevention of anatomic obstacles, enhanced treatment options may alter quality of life of sufferers.

## 1-5

### Targeting Endogenous Retroviruses Prevents Radiation-Induced Aortic Valve Calcification

**Graber M.[1], Hau D.[1], Usko L.[1], Pölzl L.[1], Hirsch J.[1], Engler C.[1], Nägele F.[1], Bonaros N.[1], Grimm M.[1], Holfeld J.[1,2], Gollmann-Tepeköylü C.[1]**

[1]Universitätsklinik für Herzchirurgie, Medizinische Universität Innsbruck, Innsbruck, Austria
[2]Universitätsklinik für Herzchirurgie; Uniklinikum Salzburg, Salzburg, Austria

**Introduction:** Radiation-induced aortic valve calcification is a severe late complication of thoracic radiotherapy and an important cause of secondary calcific aortic stenosis. The underlying molecular mechanisms remain poorly understood. Human endogenous retroviruses (HERVs) are ancient viral elements integrated into the human genome that can be reactivated through epigenetic changes, including radiation exposure. We hypothesized that radiation-induced HERV reactivation promotes inflammation-driven calcification of valvular interstitial cells (VICs), contributing to the development of aortic valve stenosis.

**Methods:** Primary human VICs were exposed to 10 Gy irradiation using a linear accelerator. Radiation-induced transcriptional changes, including HERV activation, inflammatory signaling, and osteogenic gene expression, were analyzed by RNA sequencing and quantitative RT-PCR. Double-stranded RNA (dsRNA) levels were quantified by ELISA, and calcification was assessed using Alizarin Red staining. HERV-K knockdown and overexpression experiments were performed to determine causal involvement. Retrovirus-like particle (RVLP) formation was analyzed by electron microscopy, and reverse transcriptase activity assays were used to assess HERV functionality. Given its ability to inhibit retroviral replication and reduce HERV activity, the nucleoside reverse transcriptase inhibitor Abacavir was investigated as a potential therapeutic strategy to prevent radiation-induced aortic valve calcification. For in vivo validation, mice underwent thoracic irradiation and received Abacavir via drinking water for four months. Aortic valve function was assessed by echocardiography and valve calcification was analyzed histologically.

**Results:** Radiation exposure markedly increased HERV expression in VICs, accompanied by elevated dsRNA levels, indicating activation of innate immune signaling pathways. Irradiated VICs exhibited pronounced calcification, which was HERV-dependent. Knockdown of HERV-K prevented radiation-induced inflammatory and osteogenic responses, whereas HERV overexpression alone induced VIC calcification independent of radiation exposure. Electron microscopy confirmed the presence of retrovirus-like particles in irradiated cells together with increased HERV-K envelope protein expression. Pharmacological inhibition with Abacavir effectively prevented radiation-induced VIC calcification in vitro, supporting the therapeutic potential of antiretroviral therapy in mitigating HERV-driven valvular pathology. In vivo, Abacavir treatment prevented radiation-induced aortic valve stenosis in mice with reduced transvalvular gradients and greater aortic valve opening. Histologically, aortic valves of Abacavir-treated mice showed no sclerotic leaflet changes along with reduced calcification marker expression compared to control.

**Conclusion:** Radiation-induced reactivation of endogenous retroviruses drives inflammatory calcification of valvular interstitial cells and promotes aortic valve stenosis. Antiretroviral therapy with Abacavir effectively prevented radiation-induced valve calcification in vitro and in vivo. These findings identify HERV activation as a previously unrecognized mechanism of radiation-induced valvular disease and suggest antiretroviral therapy as a potential strategy to prevent radiation-associated aortic valve stenosis.

## 1-6

### Zeitliche Trends und Behandlungsergebnisse von Patientinnen und Patienten mit transkatheter-gestützter Aortenklappenimplantation – eine Analyse des SwissTAVI-Registers

**Reichl J.[1], Stolte T.[1], Götzinger F.[1], Wagener M.[1], Jeger R.[2], Roffi M.[3], Stortecky S.[4], Wenaweser P.[5], Huber C.[3], Reuthebuch O.[1], Heg D.[4], Toggweiler S.[6], Nietlispach F.[5], Windecker S.[4], Tueller D.[2], Ferrari E.[7], Mahfoud F.[1], Noble S.[3], Nestelberger T.[1]**

[1]Universitätsspital Basel, Basel, Schweiz
[2]Triemli Hospital Zurich, Zürich, Schweiz
[3]University Hospital Geneva, Genf, Schweiz
[4]Universitätsspital Bern, Bern, Schweiz
[5]Hirslanden Clinic Zurich, Zürich, Schweiz
[6]Cantonal Hospital Lucerne, Luzern, Schweiz
[7]Cardiocentro Ticino Institute, Lugano, Schweiz

**Einleitung:** Die transkathetergestützte Aortenklappenimplantation (TAVI) wird zunehmend auch bei Patientinnen und

Patienten mit niedrigerem Operationsrisiko und jüngerem Alter eingesetzt. Parallel dazu ist das Prozedurvolumen in den letzten Jahren deutlich angestiegen. Ob diese Entwicklung in der klinischen Routine mit einer Veränderung der Behandlungsergebnisse einhergeht oder zu einer potenziellen Verwässerung der Outcomes führt, ist bislang unzureichend untersucht.

**Methoden:** Im SwissTAVI-Register wurden konsekutive Patientinnen und Patienten, die sich in der Schweiz einer TAVI unterzogen, prospektiv erfasst. Basischarakteristika, prozedurale Komplikationen und klinische Endpunkte wurden zwischen drei Zeiträumen verglichen (2011–2015, 2016–2020 und 2021–2024). Der primäre Endpunkt war das Auftreten schwerwiegender kardiovaskulärer Ereignisse (MACE: Gesamtmortalität, nicht-tödlicher Myokardinfarkt und nicht-tödlicher Schlaganfall) nach einem Jahr. Der sekundäre Endpunkt war MACE nach 30 Tagen.

**Resultate:** Unter insgesamt 19.452 Patientinnen und Patienten nahm das TAVI-Volumen um das 11-Fache zu, entsprechend einer jährlichen Wachstumsrate von 27 %. Das mediane Alter (82 Jahre) und die Komorbiditätslast blieben stabil, während der Anteil von Frauen zunahm (51 % auf 58 %) und der mediane STS-Score abnahm (4,5 % auf 3,3 %). Trotz der Ausweitung auf Patientinnen und Patienten mit niedrigerem Risiko sank die 1-Jahres-MACE-Rate signifikant von 16 % über 14 % auf 9,1 % (adjustierte HR 0,69; 95 %-KI 0,62–0,78; $p<0{,}001$). Entsprechend reduzierte sich die 30-Tage-MACE-Rate von 6,9 % über 5,2 % auf 4,0 % (adjustierte HR 0,66; 95 %-KI 0,55–0,78;

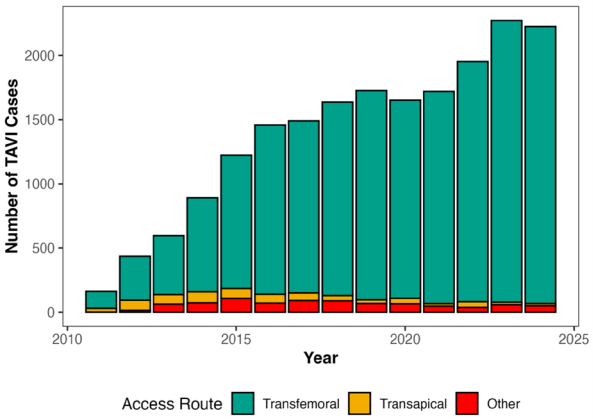


**Figure 1:** Yearly number of transcatheter aortic valve implantation procedures and respective share of transfemoral, transapical and other access routes from 2011 to 2024.

**Abb. 1 | 1-6**

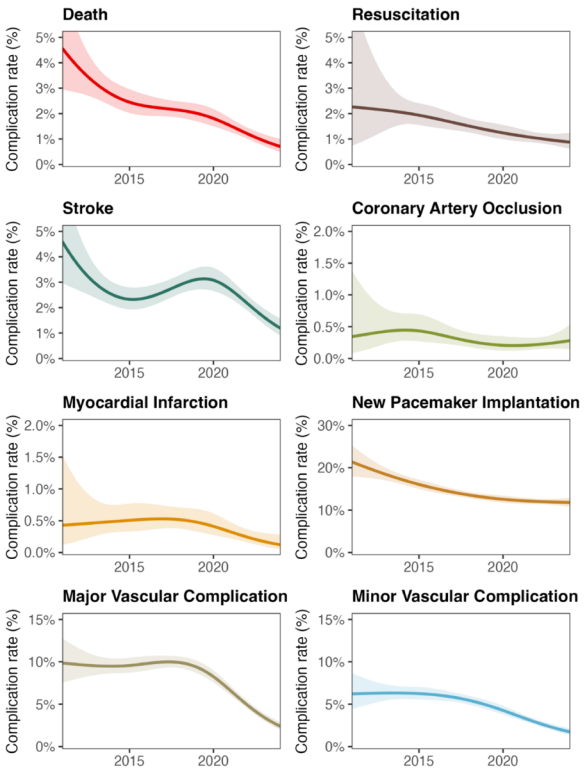


**Figure 2:** The rate of procedural complications of transcatheter aortic valve implantation over time in smoothed line graphs with 95% confidence intervals.

**Abb. 2 | 1-6**

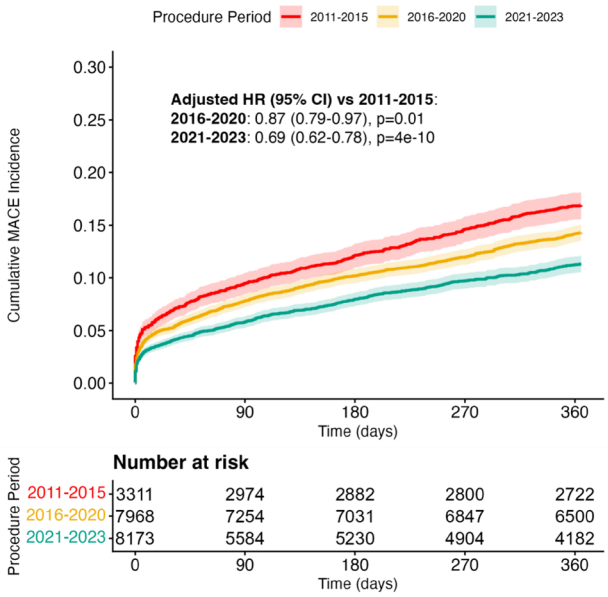


**Figure 3a**: The incidence of major adverse cardiac events (MACE) one year after transcatheter aortic valve implantation (TAVI) between patients undergoing TAVI 2011-2015, 2016-2020 and 2021-2023. HR: hazard ratio

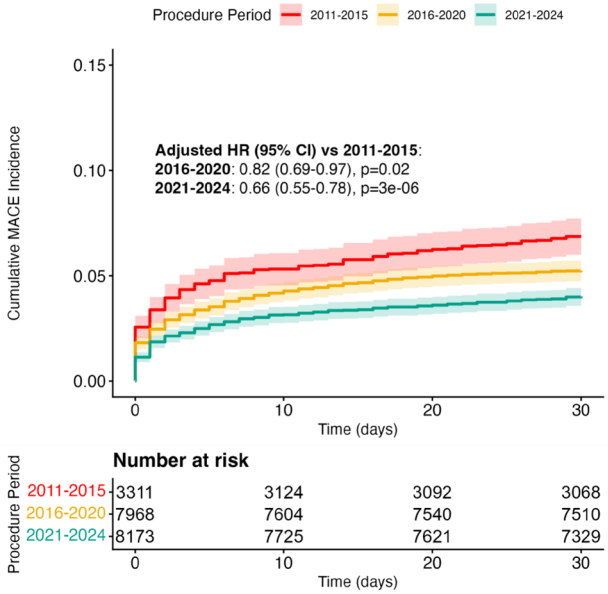


**Figure 3b**: The incidence of major adverse cardiac events (MACE) 30 days after transcatheter aortic valve implantation (TAVI) between patients undergoing TAVI 2011-2015, 2016-2020 and 2021-2024. HR: hazard ratio

**Abb. 3 | 1-6**

$p < 0{,}001$). Die prozedurale Mortalität nahm von 2,9 % auf 1,2 % ab, periprozedurale Myokardinfarkte von 0,4 % auf 0,2 % und Schlaganfälle von 3,2 % auf 2,0 % (alle $p < 0{,}001$).

**Schlussfolgerungen:** Die risikoadjustierten Ergebnisse nach TAVI verbesserten sich kontinuierlich trotz einer 11-fachen Zunahme des Prozedurvolumens. Die beobachteten Verbesserungen überstiegen dabei jene, die allein durch günstigere Risikoprofile der Patientinnen und Patienten zu erwarten gewesen wären.

## 1-7

## Prognostic Value of Right Ventricular–Pulmonary Artery Coupling in Mitral Valve Surgery and Impact of Concomitant Tricuspid Valve Repair

**Kahrovic A., Zilberszac R., Herkner H., Coti I., Kocher A., Andreas M., Zimpfer D., Werner P.**

Medical University of Vienna, Vienna, Austria

**Introduction:** Right ventricular-pulmonary artery (RV-PA) coupling has emerged as a valuable measure for assessing right ventricular contractile performance with pulmonary arterial afterload. In clinical practice, RV-PA coupling is commonly assessed non-invasively using the tricuspid annular plane systolic excursion to systolic pulmonary artery pressure (TAPSE/SPAP) ratio derived from transthoracic echocardiography (TTE). While its prognostic relevance has been investigated in percutaneous mitral interventions, the evidence in the surgical setting is missing. Mitral valve disease frequently leads to secondary TR, which may contribute to right heart failure and adverse outcomes. Current guidelines recommend considering TVr during left-sided valve surgery in patients with moderate TR; however, RV-PA coupling is not routinely included in the decision-making process. This study aimed to evaluate the prognostic significance of preoperative RV-PA coupling in patients undergoing mitral valve surgery and to assess the clinical benefit of concomitant TVr for moderate TR.

**Methods:** A total of 214 patients who underwent mitral valve surgery and presented with moderate tricuspid regurgitation at the index procedure were included. Patients were classified after baseline right ventricular-pulmonary artery coupling (impaired vs. normal). All individuals underwent preoperative TTE assessment at the echocardiography lab in our hospital. Echocardiographic examinations were performed by board-certified cardiologists following a structured standard protocol. Valvular heart disease and its severity were quantified using an integrated approach, in line with current guideline recommendations. In accordance with previously published literature, impaired RV-PA coupling was defined as a TAPSE/SPAP ratio ≤ 0.36. The primary study endpoint was a composite outcome of all-cause mortality and heart failure hospitalization. Secondary study endpoints included all-cause mortality and heart failure hospitalization. Patients were censored at 10 years, at the occurrence of each study endpoint, or April 15, 2025 (the end of follow-up), whichever came first. The mean follow-up duration was 2080 ± 1131 days in patients with normal RV-PA coupling and 2080 ± 1168 days in those with impaired RV-PA coupling ($p = 0.925$).

**Results:** Impaired right ventricular-pulmonary artery coupling was observed in 112 patients (52%), while 102 patients (48%) had normal right ventricular-pulmonary artery coupling. Patients with impaired RV-PA coupling presented with a higher EuroSCORE II value (median 4.7, IQR 2.7–8.8 vs. median 2.6, IQR 1.7–4.2, $p < 0.001$). The rate of concomitant tricuspid valve repair was similar between study groups (50.0% vs. 49.0%, $p = 0.886$). Impaired right ventricular-pulmonary artery coupling was associated with increased risk of attaining the composite outcome (adjusted Hazard Ratio 2.66, 95% Confidence Interval 1.36–5.18, $p = 0.004$), heart failure hospitalization (adjusted Hazard Ratio 3.28, 95% Confidence Interval 1.29–8.37, $p = 0.013$), and all-cause mortality (adjusted Hazard Ratio 2.23, 95% Confidence Interval 1.11–4.48, $p = 0.025$) during follow-up. Additionally, concomitant tricuspid valve repair in patients with

**Table 1 | 1-7** Primary Study Endpoint: Composite outcome (Multivariable Cox proportional hazards regression analysis)

| Variables | HR | 95 % CI | *p*-value |
|---|---|---|---|
| Impaired RV–PA coupling | 2.66 | 1.36–5.18 | *0.004* |
| Concomitant tricuspid valve repair | 0.44 | 0.25–0.77 | *0.004* |
| EuroSCORE II (log-transformed) | 2.00 | 1.44–2.78 | *< 0.001* |
| Atrial fibrillation | 1.31 | 0.75–2.30 | 0.348 |
| Secondary mitral valve disease | 0.75 | 0.41–1.36 | 0.343 |
| Cross-clamp time (min) | 1.01 | 1.00–1.01 | 0.106 |

Bold indicates statistical significance ($p < 0.05$).
CI: Confidence interval, EuroSCORE II: European System for Cardiac Operative Risk Evaluation II, HR: Hazard ratio, RV–PA: Right ventricular–pulmonary artery coupling.

**Table 2 | 1-7** Individual Analyses of Composite Outcome Components

| | Normal RV–PA coupling | Impaired RV–PA coupling | Univariable Relative Effects | | Multivariable Relative Effects | |
|---|---|---|---|---|---|---|
| | 102 (48 %) | 112 (52 %) | 95 % CI | *p*-value | 95 % CI | *p*-value |
| Heart failure hospitalization[a] | 5 (4.9 %) | 23 (20.5 %) | 3.90 (1.59–9.55) | 0.003 | 3.28 (1.29–8.37) | 0.013 |
| All-cause mortality[a] | 11 (10.8 %) | 37 (33 %) | 3.23 (1.65–6.31) | 0.001 | 2.23 (1.11–4.48) | 0.025 |

Bold indicates statistical significance ($p < 0.05$).
[a] Effects calculated as HR based on a multivariable Cox proportional hazards regression model.
CI: confidence interval, HR: hazard ratio, RV–PA: Right ventricular–pulmonary artery coupling.

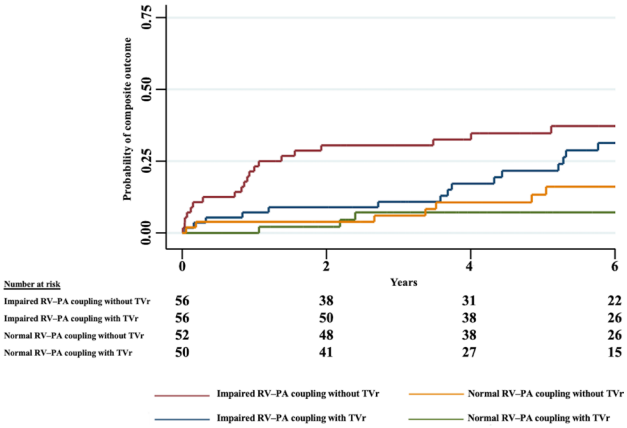


**Fig. 1 | 1-7** Cumulative event curves show the probability of a composite outcome between the study groups, with specific consideration of concomitant TVr. RV–PA: Right ventricular–pulmonary artery coupling, TVr: Tricuspid valve repair

moderate tricuspid regurgitation was associated with a lower risk of experiencing the composite outcome (adjusted Hazard Ratio 0.44, 95% Confidence Interval 0.25–0.77, $p=0.004$). No interaction between right ventricular-pulmonary artery coupling and tricuspid valve repair was observed ($p=0.509$).

**Conclusion:** The findings of this study corroborate the clinical relevance of RV–PA coupling as a prognostic marker in patients undergoing mitral valve surgery and accentuate the benefit of concomitant TVr in the setting of moderate TR. The RV–PA coupling represent an additional tool in the surgeon's armamentarium when considering TVr during mitral valve surgery. Integrating RV–PA coupling assessment into preoperative risk stratification and decision-making might be warranted.

## 1-8

## Heart failure therapy in severe aortic stenosis after surgical or transcatheter aortic valve replacement (The HF-STAR cohort study)

**Autherith M., Hauptmann L., Singer K., Koschatko S., Jantsch C., Halavina K., Torrefranca C., Heitzinger G., Dannenberg V., Hofer F., Demirel C., Coti I., Zimpfer D., Hengstenberg C., Bartko P., Nitsche C.**

Medizinische Universität Wien, Wien, Austria

**Introduction:** In the setting of aortic stenosis (AS), long-standing pressure overload leads to myocardial damage and subjects patients to an increased risk of heart failure (HF) and death even after successful aortic valve replacement (AVR). Conventional HF medications may have the potential to target this residual HF component, but current evidence on the efficacy in severe AS after AVR is limited. The aims of this study were to assess HF medication prescription patterns and their association with outcomes in severe AS after AVR.

**Methods:** Consecutive patients with severe AS undergoing successful AVR between 2013 and 2024 were included. Treatment status with HF medications (Renin-angiotensin-system inhibitors [RASi], Mineralocorticoid receptor antagonists [MRA], beta-blockers [BB], Sodium glucose co-transporter 2 inhibitors [SGLT2i]) at discharge after AVR was recorded. Nearest neighbor propensity score (PS) matching for age, sex, *N*-terminal pro-B-type natriuretic peptide [NT-proBNP], estimated glomerular filtration rate [eGFR], glycated hemoglobin [HbA1c], hypertension and coronary artery disease was performed. All-cause and cardiovascular (CV) mortality at month 60 were assessed in the overall population and prespecified subgroups: a) surgical (SAVR) vs. transcatheter aortic valve replacement (TAVR) b) left ventricular ejection fraction (LVEF) ≥ 50% vs. < 50%.

**Results:** In total, 4882 patients (75.9 years, 56.4% male, 51.8% TAVR, 48.2% SAVR) were included. RASi were prescribed in 35.1%, MRA in 30.5%, SGLT2i in 14.3%, and BB in 10.4%. Patients receiving RASi (LVEF < 50%: 17.2% vs. 10.1%; NT-proBNP: 1238 pg/ml vs. 971 pg/ml), MRA (LVEF < 50%: 18.7% vs. 9.8%; NT-proBNP: 1372 pg/ml vs. 962 pg/ml) and SGLT2i (LVEF < 50%: 20.6 vs. 11.1; NT-proBNP: 1450 pg/ml vs. 1037 pg/ml) were at a more advanced stage of cardiac disease compared to patients not receiving respective medications. Treatment with RASi (HR: 0.68; 95%CI: 0.59–0.78; HR: 0.68; 95%CI: 0.56–0.82), MRA (HR: 0.74; 95%CI: 0.63–0.86; HR: 0.70; 95%CI: 0.57–0.85), and SGLT2i (HR: 0.69; 95%CI: 0.53–0.91; HR: 0.56; 95%CI: 0.38–0.80) was independently associated with a reduced hazard for all-cause and CV mortality, respectively. Treatment bene-

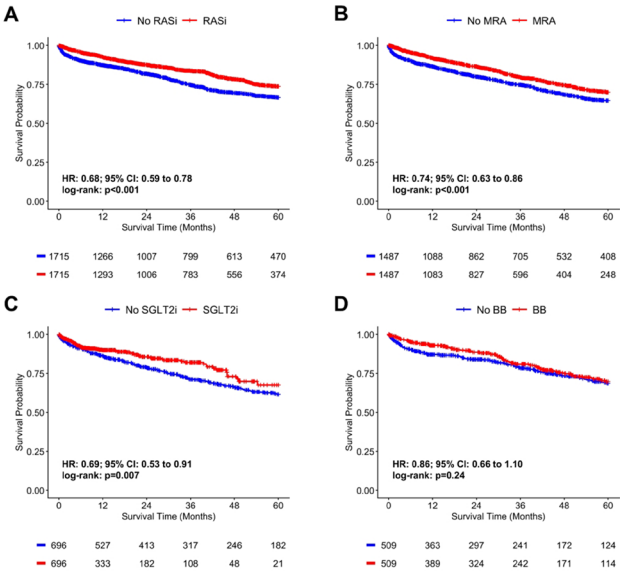


**Fig. 1 | 1-8** Kaplan-Meier curves comparing all-cause mortality in patients with severe AS after AVR treated with RAS inhibitors (Panel A), MRAs (Panel B), SGLT2 inhibitors (Panel C) and beta-blockers (Panel D)

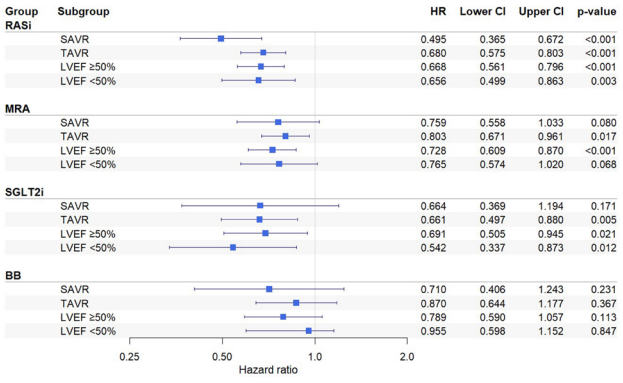


**Abb. 2 | 1-8** Forrest-plots comparing all-cause mortality in patients with severe AS after AVR in the subgroup of patients receiving SAVR and TAVR and in patients with a LVEF ≥50% and a LVEF <50%

fits were confirmed across evaluated subgroups. Conversely, no outcome signals for BB treatment were found.

**Conclusion:** Prescription of HF medications in AS undergoing AVR is impacted by the stage of cardiac disease. Treatment with RASi, MRA and SGLT2i, but not BB, is associated with favourable clinical outcomes, including subgroups of TAVR/SAVR and reduced/preserved LVEF.

# HEART TEAM POSTER SESSION 2

## 2-1

### Definition and Prognosis of Tricuspid Regurgitation in Transthyretin Amyloid Cardiomyopathy: A Multicentre International Cohort Study

**Hauptmann L.[1], Schwarting S.[2], Tomasoni D.[3], Schlender L.[4], Kronberger C.[1], Koschatko S.[1], Jantsch C.[1], Autherith M.[1], Singer K.[1], Heitzinger G.[1], Schwegel N.[5], Serenelli M.[6], Demirel C.[1], Kammerlander A.[1], Duca F.[1], Oerlemans M.[7,8], Verheyen N.[5], Papathanasiou M.[4], Merlo M.[9], Hengstenberg C.[1], Hausleiter J.[2], Adamo M.[3], Bartko P.[1], Nitsche C.[1]**

[1]Department of Internal Medicine II, Clinical Division of Cardiology, Medical University of Vienna, Vienna, Austria
[2]Department of Internal Medicine II, LMU University Hospital, Ludwig Maximilian University of Munich, Munich, Germany
[3]ASST Spedali Civili, Cardiology, Department of Medical and Surgical Specialties, Radiological Sciences, and Public Health, Brescia, Italy
[4]Universitäres Herz- und Gefäßzentrum Frankfurt ZIM – Med. Klinik 3 – Kardiologie, Angiologie Universitätsklinikum Frankfurt, Frankfurt, Germany
[5]Department of Internal Medicine, Division of Cardiology, Medical University of Graz, Graz, Austria
[6]Cardiology Unit, Azienda Ospedaliero Universitaria di Ferrara, Ferrara, Italy
[7]Department of Cardiology, University Medical Center, Utrecht, Netherlands
[8]Department of Cardiology, University Medical Center, Utrecht, Utrecht, Netherlands
[9]Cardiothoracovascular Department, Azienda Sanitaria Universitaria Giuliano-Isontina (ASUGI), European Reference Network for Rare, Low Prevalence and Complex Diseases of the Heart – ERN GUARD-Heart, Trieste, Italy

**Introduction:** In transthyretin amyloid cardiomyopathy (ATTR-CM), tricuspid regurgitation (TR) severity may be underestimated by conventional (semi-)quantitative echocardiographic criteria derived from non-amyloid populations, given restrictive low-flow hemodynamics. We sought to define and validate disease-specific TR risk thresholds and compare their prognostic performance with guideline definitions and the tricuspid valve academic research consortium (TVARC) 5-grade extension.

**Methods:** In this international multicenter cohort study (8 centers, 4 countries; NCT06836011), 1124 patients with newly diagnosed ATTR-CM (derivation: $n=745$, validation: $n=379$) underwent standardized echocardiography with blinded core-laboratory analysis including TR parameters [vena contracta

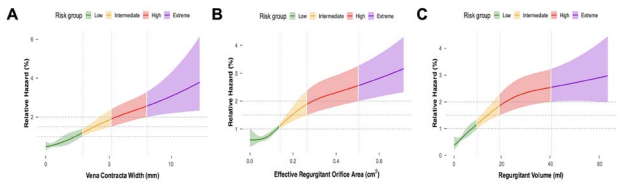


Fig. 1 | 2-1

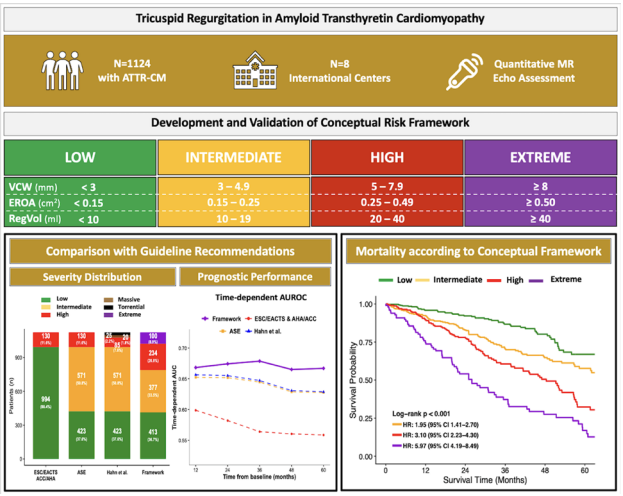


Fig. 2 | 2-1

width (VCW), effective regurgitant orifice area (EROA), and regurgitant volume (RegVol)]. All-cause mortality and time to first heart failure hospitalization (HFH) served as endpoints. Prognostic thresholds were derived from restricted cubic spline analysis, validated externally, and integrated into a multiparametric 4-grade conceptual framework (grade defined by worst-risk category across VCW/EROA/RegVol). Prognostic performance was compared with 2025 ESC/EACTS, 2020 AHA/ACC, 2017 ASE, and TVARC definitions using multivariable Cox regression and time-dependent discrimination analyses.

**Results:** During a median follow-up of 25.2 months (IQR 12.2–43.2), 324 (28.8%) patients died and 251 (22.3%) experienced HFH. Spline-derived thresholds identified stepwise risk strata at VCW 3/5/8 mm, EROA 0.15/0.25/0.50 cm², and RegVol 10/20/40 mL, delineating intermediate-, high-, and extreme-risk ranges (Fig. 1). Integration into the conceptual framework yielded 411 (36.6%) patients classified as low risk, 379 (33.7%) as intermediate risk, 234 (20.8%) as high risk, and 100 (8.9%) as extreme risk, with clear separation of Kaplan–Meier curves in the overall cohort and consistent stepwise separation in both derivation and validation cohorts. Compared with guideline-based and TVARC grading (each 11.6%), the framework classified a significantly higher proportion (29.7%) as ≥severe TR (all comparisons: $p<0.001$) and demonstrated the strongest independent association with outcomes after multivariable adjustment for disease stage and ATTR-specific therapy (mortality: HR 1.45, 95% CI 1.29–1.64; HFH: HR 1.32, 95% CI 1.14–1.52). Time-dependent analyses confirmed superior discrimination of the framework for mortality from 12–60 months in the derivation and validation cohorts (Fig. 2).

**Conclusion:** Quantitative TR thresholds in ATTR-CM are substantially lower than current guideline cut-offs. A validated, risk-based conceptual framework improves prediction of both mortality and HFH, better reflecting restrictive low-flow pathophysiology and supporting disease-specific TR grading in ATTR-CM.

## 2-2

# Right Heart Function Matters: Prognostic Value of sPAP, TAPSE and RV–PA Coupling in a Real-World Cohort of TAVI Patients

**Aglas S.[1], Preuss L.[1], Clodi N.[1,2], Granitz C.[1], Lichtenauer M.[1], Hoppe U.[1], Hammerer M.[1], Boxhammer E.[1]**

[1]Universitätsklinik für Innere Medizin II, Kardiologie und internistische Intensivmedizin, Salzburg, Austria
[2]Universitätsklinik für Radiologie, Salzburg, Austria

**Introduction:** Right ventricular (RV) function is an established prognostic factor in structural heart disease, but is not routinely incorporated into pre-procedural risk assessment in patients undergoing transcatheter aortic valve implantation (TAVI). This study evaluated the prognostic impact of systolic pulmonary artery pressure (sPAP), tricuspid annular plane systolic excursion (TAPSE), and RV-pulmonary artery (PA) coupling (TAPSE/sPAP ratio) in a real-world TAVI population.

**Methods:** This retrospective single-center study included 565 consecutive patients (mean age 82.1 ± 5.1 years; 48.7% male) undergoing transfemoral TAVI between 2016 and 2022. All patients received standardized pre-procedural echocardiographic assessment of sPAP, TAPSE, and TAPSE/sPAP. The primary endpoint was all-cause mortality over a mean follow-up of 47.1 ± 22.8 months.

**Results:** Impaired RV-PA coupling—defined as a TAPSE/sPAP < 0.55 mm/mmHg—was identified in 46.5% of patients, elevated sPAP (≥ 35 mmHg) in 61.2%, and reduced TAPSE (≤ 18 mm) in 22.3%. Both elevated sPAP and reduced TAPSE/sPAP were significantly associated with increased long-term mortality ($p = 0.004$ and $p < 0.001$, respectively), whereas TAPSE alone was not predictive ($p = 0.318$). Subgroup and interaction analyses showed that the prognostic impact of sPAP and TAPSE/sPAP was greatest in patients aged ≥ 80 years, in males, and in those with preserved left ventricular ejection fraction and normal stroke volume index (SVi).

**Conclusion:** RV afterload, as reflected by elevated sPAP and impaired RV-PA coupling, is a key driver of post-TAVI mortality, outperforming isolated RV systolic measurements. The TAPSE/sPAP ratio is a robust, integrative marker whose prognostic value is modulated by age, sex and left heart function. These findings support incorporating RV-PA coupling into routine pre-TAVI assessment to improve risk stratification and identify vulnerable patients before intervention.

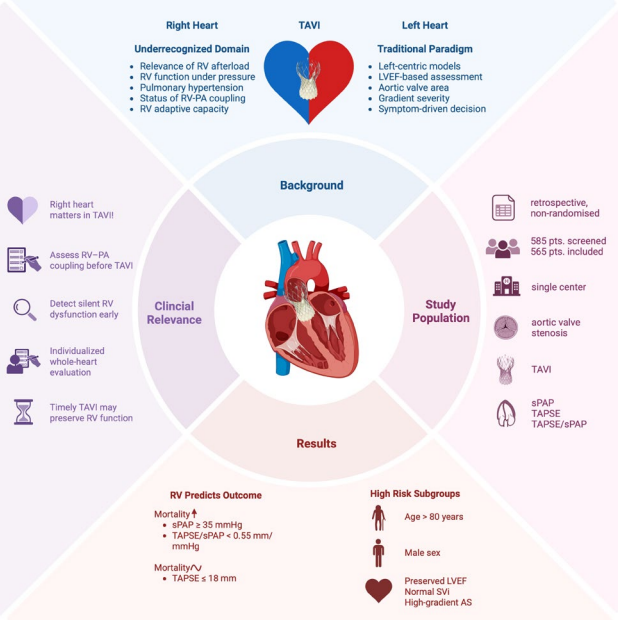


Fig. 1 | 2-2

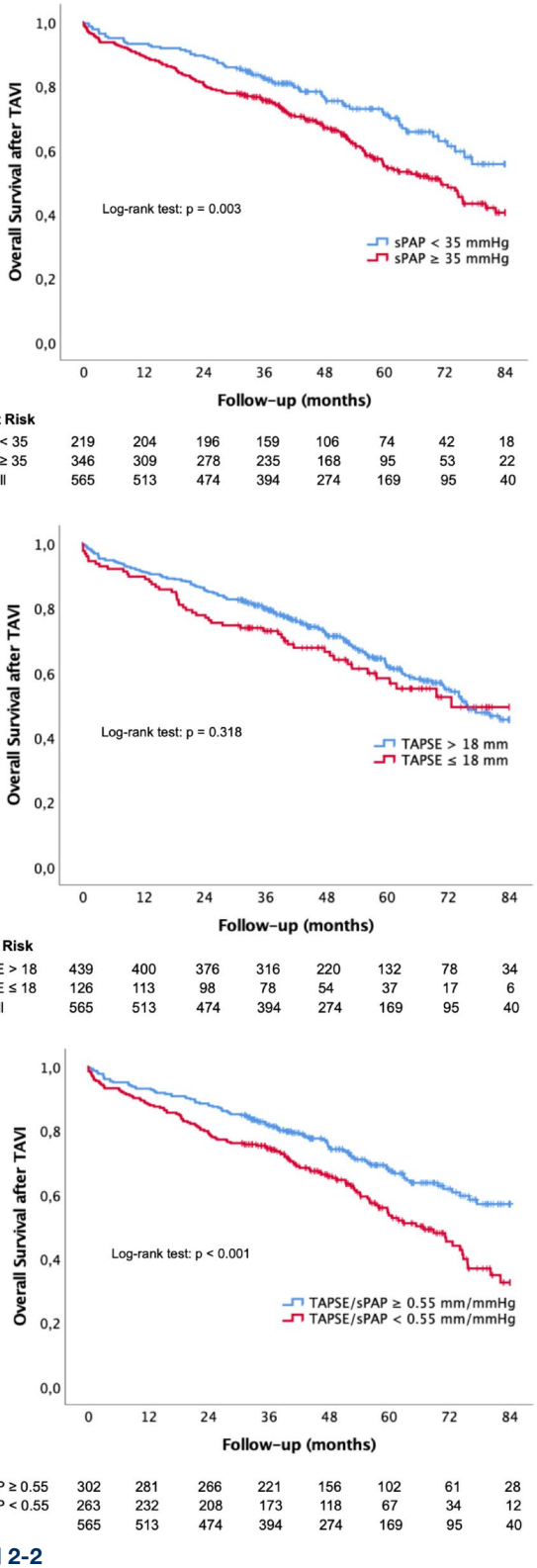


Fig. 2 | 2-2

## 2-3

### Temporal Trends of Transcatheter Aortic Valve Implantation in Austria between 2016 and 2024

**Binder R.[1], Brenner C.[2], Grund M.[3], Schober A.[4], Delle-Karth G.[4], Schmidt A.[5], Neunteufl T.[6], Alber H.[7], Hammerer M.[8], Mascherbauer J.[9], Niessner A.[10], Lamm G.[9]**

[1]Klinikum Wels-Grieskirchen, Wels, Austria
[2]Univ.-Klinik für Innere Medizin III – Kardiologie und Angiologie, Innsbruck, Austria
[3]Kepler Universitätsklinikum, Linz, Austria
[4]Klinik Floridsdorf, Wien, Austria
[5]Medizinische Universität Graz, Graz, Austria
[6]Universitätsklinikum Krems, Krems, Austria
[7]Klinikum Klagenfurt, Klagenfurt, Austria
[8]Paracelsus Medizinische Privatuniversität, Salzburg, Austria
[9]Universitätsklinikum St. Pölten, St. Pölten, Austria
[10]Klinik Landstrasse, Wien, Austria

**Introduction:** Aim: Emerging evidence, changing guidelines, hospital policies and increasing operator experience may impact the practice and outcome of transcatheter aortic valve implantation (TAVI) over time. We hypothesized that within the last decade baseline patients characteristics, procedural aspects and TAVI outcomes changed with distinct temporal trends in Austria.

**Methods:** We assessed yearly aggregated data of the Austrian TAVI registry between 2016 and 2024. Temporal trends over the years were analyzed by the Mann-Kendall test or Spearman's rank correlation.

**Results:** Between 2016 and 2024 a total of 9.505 TAVI procedures were included in this analysis. While the yearly TAVI volume increased curvilinear in the first half of the decade, numbers started to plateau in the second half. Mean age minimally but significantly decreased from 81.7 to 80.4 years ($p=0.006$). While the percentage of male patients increased (45.7% to 53.9%, $p<0.001$), the calculated surgical risk significantly decreased (EURO Score II 5.6% to 4.3%, $p=0.045$). Furthermore, there was a significant decline of pre-procedural mean aortic valve gradient and systolic pulmonary artery pressure. While transfemoral access was almost exclusively used in this cohort (>99%), the indication for valve-in-valve procedures significantly increased (1.2% to 4.4%, $p=0.025$). Although procedural time and fluoroscopy time did not change over the years, there was a substantial decline in the use of contrast medium (164 ml to 111 ml, $p<0.001$) and balloon pre-dilatation (32.9% to 18.2%, $p=0.045$). The use of general anesthesia dropped (5.3% to 0.5%, $p=0.037$) as well as procedural complications (25.0% to 13.6%, $p<0.001$). The mean length of hospital stay significantly decreased over the years (11.6 days to 7.9 days, $p<0.001$) as well as the post-procedural use of dual antiplatelet therapy (47.3% to 7.7%, $p<0.001$) or vitamin-K-antagonists (18.6% to 0.8%, $p<0.001$).

**Conclusion:** There was a numerical but statistical non-significant decline of procedural death (1.3% to 0.6%, $p=$ns), 30-day mortality (3.6% to 2.8%, $p=$ns) and 1-year mortality (7.2% to 5.4%, $p=$ns). Conclusion: A significant change in TAVI practice in Austria was observed over the last decade to younger, lower risk patients while streamlining the procedure with less anesthesia, less pre-dilatation and shortened hospital stays. There was a significant drop in complication rates with a trend towards improved short- and mid-term outcomes.

## 2-4

### Prevalence, morphologic characterization and prognosis of atrial, ventricular and overlap functional tricuspid regurgitation phenotypes

**Jantsch C., Koschatko S., Autherith M., Hauptmann L., Halavina K., Torrefranca C., Koschutnik M., Demirel C., Dannenberg V., Hengstenberg C., Pavo N., Nitsche C., Bartko P., Heitzinger G.**

Medizinische Universität Wien, Wien, Austria

**Introduction:** Functional tricuspid regurgitation (fTR) is associated with symptomatic burden, heart failure (HF) hospitalizations, and increased mortality. Although atrial and ventricular fTR phenotypes have been identified, with important prognostic implications, their characterization is often not entirely possible due to overlapping features. We aimed to investigate the prevalence, morphological characteristics, and outcomes of atrial (AfTR), ventricular (VfTR), and fTR with overlapping features (OfTR).

**Methods:** This retrospective study encompasses patients diagnosed with fTR from 2010 to 2020. Patients with severe fTR were characterized as AfTR, VfTR according to available recommendations.

**Results:** AfTR was present in 144 (11.8%), VfTR in 450 (36.9%), and OfTR in 625 (51.3%) patients. OfTR patients were older and had more atrial fibrillation. This phenotype was characterized by a disproportionate right atrial (RA) to right ventricular (RV) ratio with severe RA dilatation, but preserved RV area. OfTR patients had reduced longitudinal but preserved radial RV function. FTR severity, as indicated by orifice area, was similar between the phenotypes. After eight years, the highest mortality was observed for OfTR (48%), followed by VfTR (38%) and AfTR (33%) ($p<0.001$). OfTR was associated with worse survival (HR 2.55 [2.26–2.88], $p<0.001$), even after adjustment.

**Conclusion:** Distinct phenotypes of fTR present with differential features and outcomes. OfTR is the most prevalent fTR phenotype, associated with the highest mortality, and its hazard increases with increasing fTR severity. Further research is necessary to determine the role of these findings in optimizing fTR treatment.

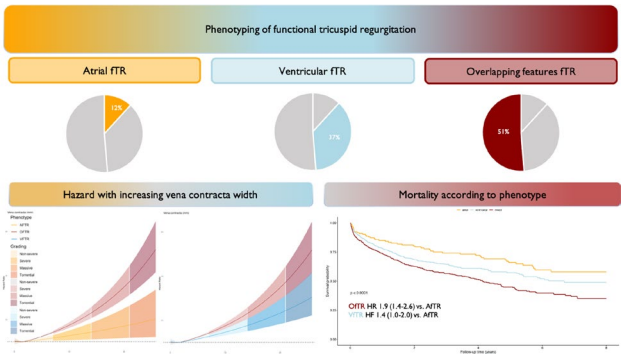


Fig. 1 | 2-4

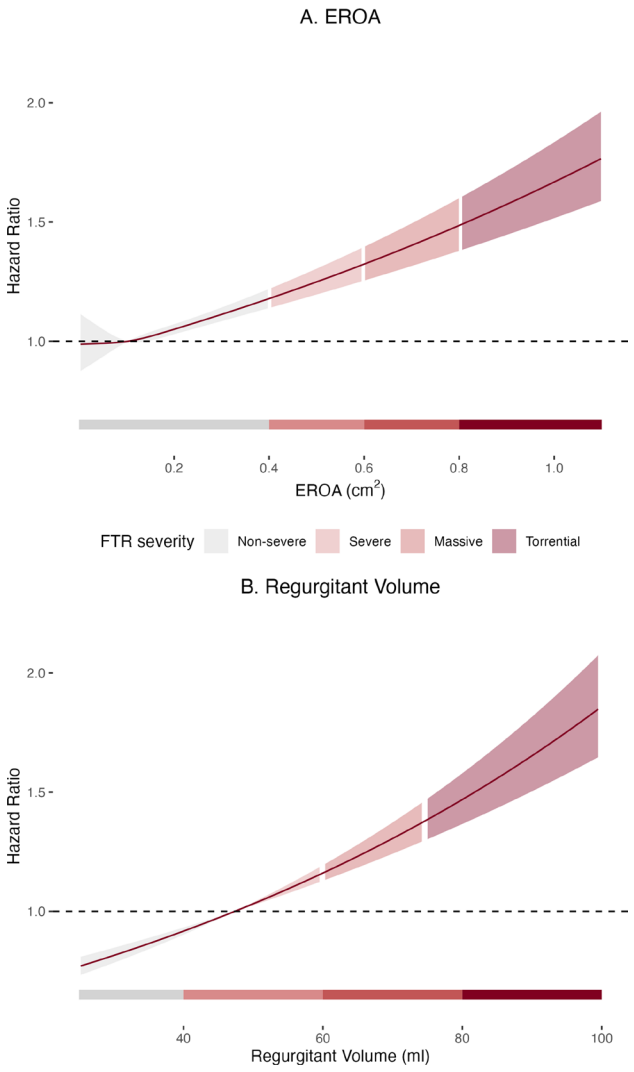


**Fig. 2 | 2-4**

## 2-5

### Colchicine Prevents Intimal Hyperplasia in Venous Bypass Grafts

**Heim V.[1], Weist C.[1], Ioannou-Nikolaidou M.[1,2], Muller L.[1], Eder J.[1], Hirsch J.[1], Winter-Pölzl L.[1], Engler C.[1], Lohmann R.[1,2], Nägele F.[1], Bonaros N.[1], Grimm M.[1], Holfeld J.[1], Gollmann-Tepeköylü C.[1], Graber M.[1]**

[1]Department of Cardiac Surgery, Medical University Innsbruck, Innsbruck, Austria
[2]Department of Clinical and Functional Anatomy, Medical University Innsbruck, Innsbruck, Austria

**Introduction:** Coronary artery bypass grafting (CABG) remains a cornerstone in the treatment of chronic coronary syndrome. However, long-term outcomes are substantially limited by venous graft failure. Intimal hyperplasia is the predominant mechanism driving this process. Endothelial injury following graft implantation triggers leukocyte recruitment and vascular inflammation, leading to migration and proliferation of vascular smooth muscle cells (VSMCs) within the graft wall. These mechanisms closely mirror the inflammatory pathways underlying atherosclerosis. Colchicine has recently emerged as an effective anti-inflammatory therapy for secondary prevention of atherosclerotic cardiovascular disease. Yet, its potential to prevent venous graft remodeling has not been explored. We therefore investigated whether colchicine attenuates endothelial activation, vascular inflammation, and intimal hyperplasia in venous bypass grafts.

**Methods:** Cell culture studies were performed using human endothelial cells and human vascular smooth muscle cells. Dose-response analyses were carried out to assess the effects of colchicine on cell proliferation and apoptosis in both cell types. Endothelial cells were exposed to an inflammatory stimulus, after which Vascular Cell Adhesion Molecule-1 expression was quantified by qPCR. Monocyte adhesion was evaluated using a co-culture system with fluorescently labeled monocytes. VSMC migration and proliferative capacity were examined using scratch and transwell migration assays. For in vivo analysis, a venous bypass model was established in C57Bl/6J mice by grafting a donor inferior vena cava into the carotid artery. The patency of the grafts was assessed with laser Doppler imaging. Mice in the treatment group received colchicine via drinking water for four weeks, after which venous graft intimal hyperplasia was measured by histological analysis.

**Results:** Colchicine suppressed the proliferation of both vascular smooth muscle cells (VSMCs) and endothelial cells (ECs) in a dose-dependent manner. Importantly, even at higher concentrations, colchicine did not induce marked apoptosis. Furthermore, colchicine markedly reduced leukocyte adhesion to ECs following inflammatory stimulation by inhibiting VCAM-1 upregulation. In vitro analyses demonstrated a significant reduction of VSMC proliferation and migration, as evidenced by scratch assays. Transwell migration assays verified a reduction in VSMC motility in vitro after colchicine treatment. In vivo, colchicine treatment led to a significant decrease in venous graft intimal hyperplasia and was associated with a reduced αSMA-positive area compared with untreated controls. Laser Doppler imaging further demonstrated significantly increased graft perfusion in the colchicine-treated group compared with controls.

**Conclusion:** Colchicine effectively suppresses critical mechanisms underlying intimal hyperplasia by limiting endothelial activation, leukocyte adhesion, and vascular smooth muscle cell proliferation and migration. These findings identify colchicine as a promising, readily translatable strategy to preserve venous graft patency and potentially improve long-term outcomes after CABG.

## 2-6

### Routine CT-derived Pulmonary Artery Dimensions Independently Predict Mortality after Surgical Aortic Valve Replacement

**Clodi N.[1,2], Brandstetter L.[2], Steindl J.[3], Gansterer K.[3], Knapitsch C.[2], Schörghofer N.[2], Hammerer M.[1], Scharinger B.[2], Hergan K.[4], Hoppe U.[1], Dinges C.[3], Boxhammer E.[1]**

[1]Universitätsklinik für Innere Medizin II, Kardiologie und internistische Intensivmedizin, Salzburg, Austria
[2]Universitätsklinik für Radiologie, Salzburg, Austria
[3]Universitätsklinik für Herzchirurgie, Salzburg, Austria
[4]Universitätsklinik für Radiologie, Universitätsklinikum Salzburg, Salzburg, Austria

**Introduction:** Risk stratification after surgical aortic valve replacement (SAVR) relies mainly on clinical risk scores, whereas imaging-derived markers are rarely incorporated into prognostic assessment. Pulmonary artery dimensions obtained from routine preoperative computed tomography (CT) may reflect right heart burden and advanced cardiopulmonary remodeling. We investigated their prognostic value for long-term mortality after SAVR.

**Methods:** In this single-center cohort study, 476 patients undergoing isolated SAVR between 2013 and 2023 with available preoperative CT were analyzed. Truncus pulmonalis diameter (TP), TP indexed to body surface area (TP/BSA), and the TP-to-ascending aorta ratio (TP/AA) were assessed. The primary endpoint was all-cause mortality during follow-up of up to 7 years. Cut-offs were derived using receiver operating characteristic (ROC) analysis. Survival was evaluated using Kaplan–Meier estimates. Associations with mortality were assessed using Cox regression and restricted cubic spline analyses. Multivariable models were adjusted for clinical variables (age, sex, eGFR, COPD, AF, NYHA) and alternatively for EuroSCORE II. Incremental prognostic value was evaluated using changes in Harrell's C-index and likelihood ratio testing (LRT).

**Results:** Using ROC-derived cut-offs (TP ≥ 29 mm, TP/BSA ≥ 15.5 mm/m², TP/AA > 0.75), patients with higher pulmonary artery dimensions showed significantly reduced survival (all log-rank $p < 0.001$). ROC analysis demonstrated moderate discrimination for 1-year mortality (AUC: TP 0.782, TP/BSA 0.808, TP/AA 0.746). In clinically adjusted Cox regression models, all parameters were independently associated with mortality (per 1 SD: TP HR 1.26 (1.08–1.47), $p = 0.003$; TP/BSA HR 1.28 (1.08–1.52), $p = 0.005$; TP/AA HR 1.24 (1.05–1.45), $p = 0.009$). Restricted cubic spline analyses demonstrated a continuous increase in risk with increasing pulmonary artery dimensions, with the strongest association observed for TP/BSA (overall $p < 0.01$). Addition of pulmonary artery parameters to the clinical model improved discrimination (C-index 0.647 vs. 0.674 for TP) and significantly improved model fit (all LRT $p \leq 0.011$). Similar incremental prognostic value was observed beyond EuroSCORE II (all LRT $p < 0.001$).

**Conclusion:** CT-derived pulmonary artery dimensions are simple and reproducible markers that independently predict short- and long-term mortality after SAVR and provide incremental prognostic information beyond established clinical risk models. These findings support their potential integration into preoperative risk stratification.

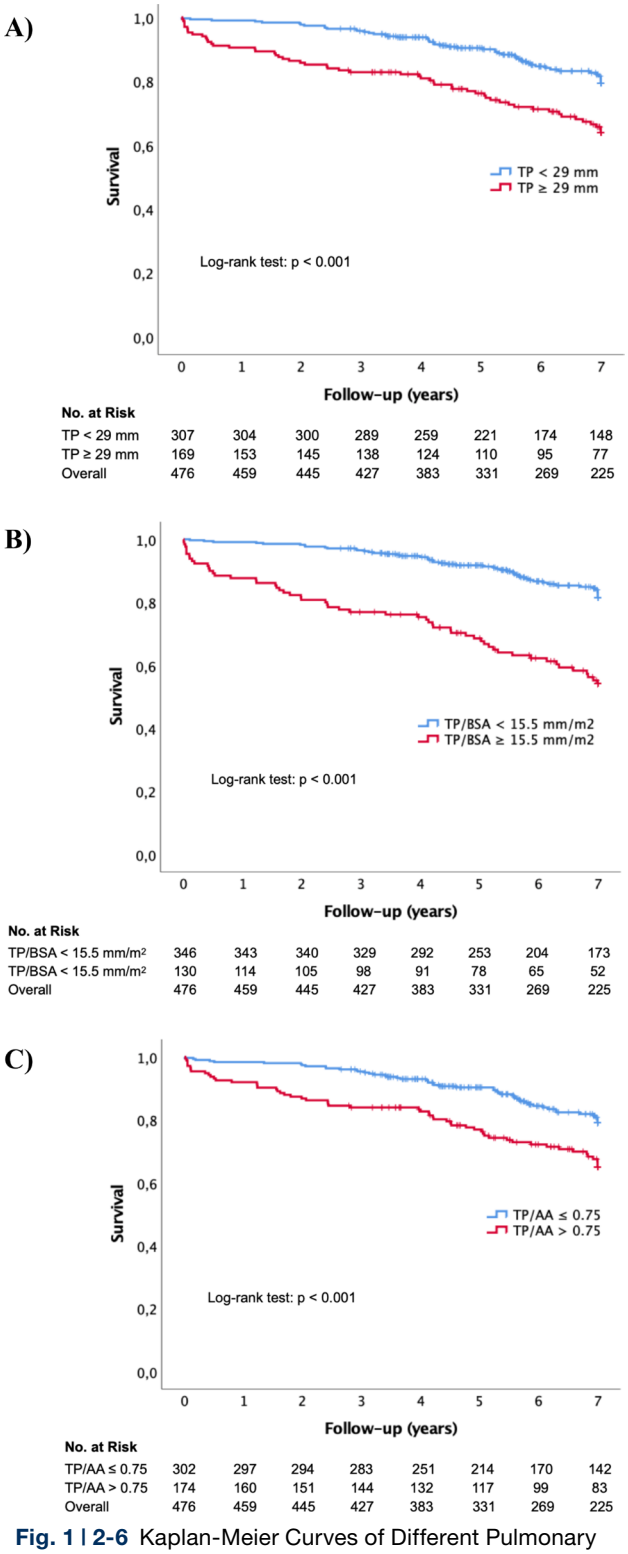


**Fig. 1 | 2-6** Kaplan-Meier Curves of Different Pulmonary Artery Metrics in SAVR

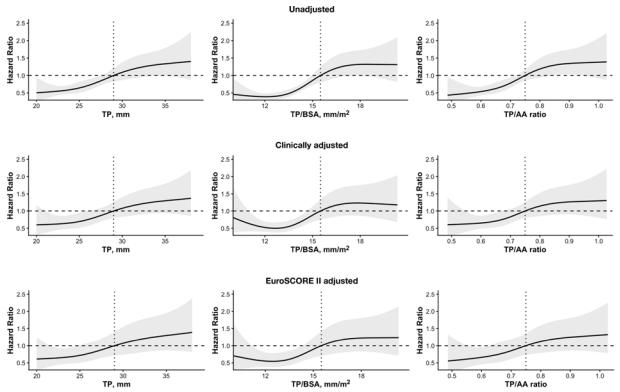


**Fig. 2 | 2-6** Restricted Cubic Spline Analysis regarding Different Pulmonary Artery Metrics (unadjusted and adjusted)

## 2-7

### Phenotype-Driven Risk Stratification in Mitral Valve Surgery: Foundation for a Dedicated Mitral Risk Score

**Lohmann R.[1,2], Ennen V.[1], Fiesel D.[1], Engler C.[1], Hirsch J.[1], Graber M.[1], Nägele F.[1], Grimm M.[1], Höfer D.[1], Bonaros N.[1], Winter-Pölzl L.[1], Gollmann-Tepeköylü C.[1]**

[1]Univ.-Klinik für Herzchirurgie, Innsbruck, Austria
[2]Institut für klinisch-funktionelle Anatomie, Innsbruck, Austria

**Introduction:** Risk stratification in mitral valve (MV) surgery remains largely based on generic cardiac surgery scores that do not reflect the biological and anatomical heterogeneity of mitral valve disease. In contrast, disease-specific risk assessment has recently transformed the field of tricuspid valve surgery through the development of the TriScore. No comparable framework currently exists for MV surgery. We therefore sought to identify disease-specific determinants of early mortality after MV surgery and to evaluate whether these factors could provide the basis for a pragmatic MV-tailored risk stratification approach.

**Methods:** A total of 2287 consecutive patients undergoing MV surgery were analyzed. Thirty-day mortality was evaluated using multivariable logistic regression with multiple imputation for missing data. Model performance was assessed using discrimination and calibration metrics with internal validation. Using a strategy conceptually similar to the methodological framework applied for the development of the TriScore, disease-specific determinants were translated into a pragmatic additive clinical score, and associations with early and long-term outcomes were evaluated. Long-term survival was assessed using Kaplan-Meier analysis.

**Results:** Thirty-day mortality occurred in 65 patients (2.8%). Early mortality was closely linked to the phenotype of mitral valve disease. In multivariable analysis, preoperative atrial fibrillation (OR 2.54, 95% CI 1.46–4.41; $p=0.001$) and mitral valve calcification (OR 3.76, 95% CI 2.04–6.91; $p<0.001$) were independently associated with early death, while secondary mitral regurgitation contributed to risk stratification (OR 1.80, 95% CI 0.99–3.27; $p=0.053$). Translation of these determinants into a simple additive clinical score enabled clear separation of postoperative risk. Patients in the low-risk group (score 0–1, $n=1013$) had a 30-day mortality of 0.5%, compared with 2.8% in the intermediate-risk group (score 2–4, $n=1016$) and 12.4% in the high-risk group (score ≥5, $n=258$). Increasing score categories were also associated with stepwise increases in major postoperative complications, including postoperative dialysis (4.5%, 17.3%, and 32.9%), ECMO support (2.2%, 4.2%, and 12.8%), and prolonged ICU stay (21.7%, 41.0%, and 61.6%) across the three risk strata. Five-year survival differed markedly across risk strata, with progressively worse outcomes in higher score categories ($p<0.0001$).

**Conclusion:** Early mortality after MV surgery follows a disease-specific risk pattern driven by the phenotype of mitral valve disease. Preoperative atrial fibrillation, mitral valve calcification, and MR etiology represent key determinants of outcome and provide the basis for a pragmatic MV-specific risk score. Similar to the transformative impact of the TriScore in tricuspid valve disease, this approach may enable dedicated mitral valve risk stratification and improve clinical decision-making in contemporary MV surgery.

## 2-8

### Surgical Infective Endocarditis: Forty-Five Years of Outcomes and Determinants of Mortality

**Hirsch J.[1], Pölzl L.[2], Nägele F.[1], Engler C.[1], Graber M.[1], Lohmann R.[1], Spilka J.[1], Heim V.[2], Ennen V.[1], Ioannou-Nikolaidou M.[1], Schmidt S.[1], Höfer D.[1], Fisel D.[3], Holfeld J.[1], Grimm M.[1], Ruttmann E.[1], Bonaros N.[1], Gollmann-Tepeköylü C.[1]**

[1]Medical University of Innsbruck, Department of Cardiac Surgery, Innsbruck, Austria
[2]Medical University of Innsbruck, Department of Anatomy, Innsbruck, Austria
[3]Medical University of Innsbruck, Department of Psychiatry, Innsbruck, Austria

**Introduction:** Infective endocarditis (IE) remains one of the most severe conditions encountered in cardiac surgery, characterized by valve destruction, embolic complications, and substantial mortality despite advances in diagnostics, perioperative management, and surgical techniques. Long-term institutional experience may provide valuable insights into the clinical characteristics and determinants of outcome following surgical treatment of IE.

**Methods:** We performed a retrospective single-center analysis of all patients undergoing surgery for infective endocarditis at a tertiary academic cardiac surgery center between 1981 and 2020. Data were derived from a prospectively maintained institutional database, with complete follow-up available for all patients until March 1, 2026. Early mortality was defined as in-hospital and 30-day mortality. Predictors of in-hospital mortality were evaluated using univariate logistic regression, while predictors of mortality during follow-up were assessed using univariate and multivariable Cox proportional hazards regression. Long-term survival was analyzed using Kaplan Meier estimates.

**Baseline Patient Characteristics**

| Variable | Whole cohort (n=478) |
|---|---|
| | *DEMOGRAPHICS* |
| *Age (years)* | 59.3 ± 16.3 |
| *Male gender* | 327.0 (68.4%) |
| | *COMORBIDITIES* |
| *Diabetes (any)* | 55 (11.5%) |
| *Diabetes – oral* | 27 (5.6%) |
| *Diabetes – insulin* | 28 (5.9%) |
| *Renal dysfunction (CKD)* | 151 (31.6%) |
| *COPD* | 92.0 (19.2%) |
| *Hypertension* | 168.0 (35.1%) |
| *Peripheral vascular disease* | 30.0 (6.3%) |
| *Chronic venous insufficiency* | 18.0 (3.8%) |
| *Rheumatic disease* | 36.0 (7.5%) |
| *Pulmonary hypertension* | 151.0 (31.6%) |
| *Status post transplantation* | 26.0 (5.4%) |
| *Smoking* | 106 (22.2%) |
| *Ex-smoker* | 97 (20.3%) |
| | *CARDIAC STATUS* |
| *LV dysfunction* | 224 (46.9%) |
| *Cardiac decompensation* | 235.0 (49.2%) |
| *NYHA I* | 15 (3.1%) |
| *NYHA II* | 131 (27.4%) |
| *NYHA III* | 264 (55.2%) |
| *NYHA IV* | 68 (14.2%) |
| | *PREOPERATIVE SYMPTOMS* |
| *Dyspnea* | 425.0 (88.9%) |
| *Syncope* | 28.0 (5.9%) |
| *Angina pectoris* | 21.0 (4.4%) |

**Fig. 1 | 2-8** Basic Grafics IE

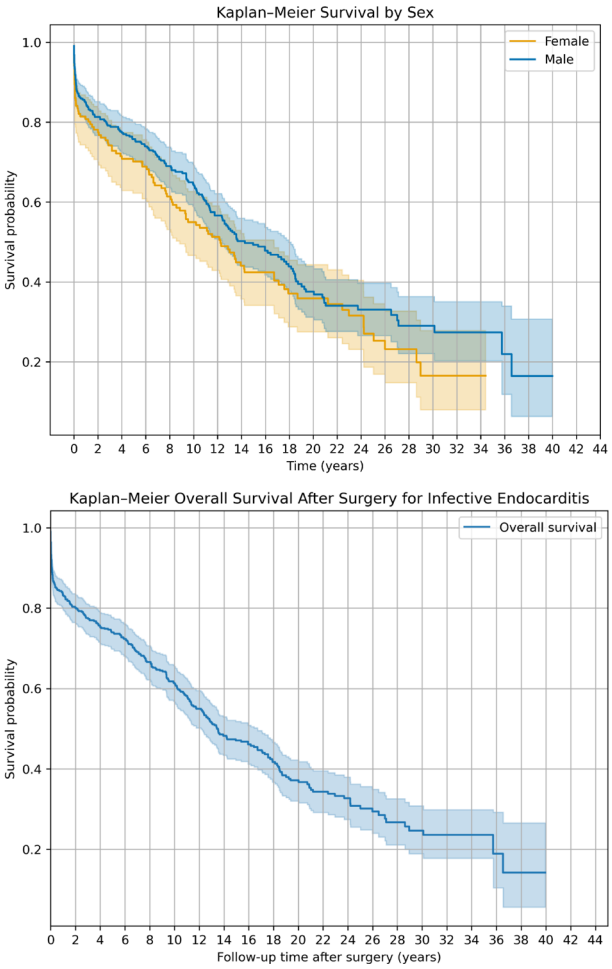


**Fig. 2 | 2-8** Basic Grafics IE

**Results:** A total of 478 patients underwent surgery for infective endocarditis. The mean age was 59.3 ± 16.3 years, and 68.4% were male. Patients frequently presented with advanced disease, including left ventricular dysfunction (46.9%), cardiac decompensation (49.2%), embolic events (39.1%), and perivalvular abscess (29.1%). Left-sided valve involvement predominated, affecting the aortic valve (57.7%) and mitral valve (47.7%), while prosthetic valve endocarditis occurred in 22.4%. Surgical procedures were diverse, including two-valve surgery in 16.1%, additional coronary artery bypass grafting in 9.6%, and aortic root surgery in 13.8%, of patients. Early mortality remained substantial, with in-hospital mortality of 9.2% and 30-day mortality of 9.8%. Major postoperative morbidity included ECMO support in 4.4% and re-exploration for bleeding in 12.3%. During follow-up, 5-year mortality was 25.9%. In multivariable Cox analysis, age (HR 1.03 per year, $p < 0.001$) and renal dysfunction (HR 2.24, $p < 0.001$) were independent predictors of mortality, while cardiopulmonary bypass time remained associated with mortality during follow-up (HR 1.02, $p = 0.044$).

**Conclusion:** In this 45-year single-center experience, surgery for infective endocarditis was performed in a high-risk population with advanced disease and frequent embolic complications. Despite surgical intervention, mortality remained substantial, with nearly one in ten patients dying within 30 days and one quarter within five years. Advanced age, renal dysfunction, and operative complexity emerged as key determinants of outcome and may help refine risk stratification in patients undergoing surgery for infective endocarditis.

# POSTERSITZUNG 1—CLINICAL CASES 1

## 1-1

### Beyond Contamination: Recurrent Non-Purulent Pericardial Effusion With Repeated Cutibacterium acnes Detection

**Zsilavecz V.**

LKH Graz II – Standort West, Graz, Austria

**Introduction:** We report a 36-year-old male with ALK-positive non-small cell lung cancer, diagnosed in 2017 and initially treated with Alectinib. In 2018, a pericardial effusion was detected during routine follow-up. The patient reported progressive exertional dyspnea (NYHA II–III), fatigue, and intermittent thoracic pressure. Pericardiocentesis yielded serous, non-purulent fluid. Cytology was negative for malignancy, Ziehl–Neelsen staining was negative, and bacterial culture grew Cutibacterium acnes, which was considered contamination; no antibiotics were given. No additional comorbidities were known. In January 2024, the patient presented twice to the emergency department with increasing dyspnea, reduced exercise tolerance, and thoracic pain attributed to musculoskeletal causes. He was discharged on both occasions. In February 2024, he presented to the pulmonology clinic with tachycardia, diaphoresis, and borderline hemodynamic stability. Examination revealed heart rate 110 bpm, blood pressure 100/60 mmHg, muffled heart sounds, bilateral basal crackles, and subfebrile temperature. He was admitted for further evaluation.

**Methods:** CT angiography excluded pulmonary embolism but demonstrated a circumferential pericardial effusion up to 5.3 cm with compression of the left main bronchus. A CT scan four weeks earlier had shown no effusion. Laboratory tests revealed CRP >80 mg/L, leukocytosis, and mildly elevated high-sensitivity troponin T. ECG showed diffuse, non-specific ST-segment elevations (V3–V6, II, III, aVF). Echocardiography confirmed a large effusion with beginning right atrial and ventricular compression (Fig. 2). Urgent pericardiocentesis drained approximately 700 mL of sanguineous, non-purulent fluid. Cytology was again negative for malignancy. Bacterial culture again grew C. acnes. The findings were consistent with recurrent, hemodynamically relevant pericardial effusion with repeated detection of C. acnes over six years. Empirical antibiotic therapy with Piperacillin/Tazobactam was initiated due to marked inflammation and subfebrile temperature. Clinical status improved after drainage. Four days later, echocardiography demonstrated recurrent effusion with renewed hemodynamic relevance and increasing orthopnea. Surgical pericardial fenestration with drainage placement was performed.

**Results:** Given persistent inflammatory activity and repeated isolation of C. acnes, antimicrobial therapy was continued. In addition, guideline-based anti-inflammatory therapy with ibuprofen (600 mg three times daily) and colchicine (0.5 mg twice daily) was initiated. Cardiac MRI showed pericardial contrast enhancement consistent with pericarditis (Fig. 1). After five days, the drain was clamped; follow-up echocardiography after 24 hours showed no recurrence. The drain was removed on day six. Inflammatory markers normalized, and clinical condition improved. Echocardiography prior to discharge (approximately 2.5 weeks after admission) showed no residual effusion. Infectious Diseases consultation recommended oral amoxicillin (1 g four times daily) until reassessment two weeks after discharge.

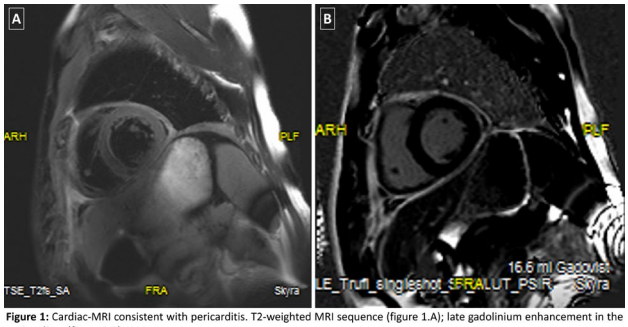


**Figure 1:** Cardiac-MRI consistent with pericarditis. T2-weighted MRI sequence (figure 1.A); late gadolinium enhancement in the pericardium (figure 1.B)

**Fig. 1 | 1-1**

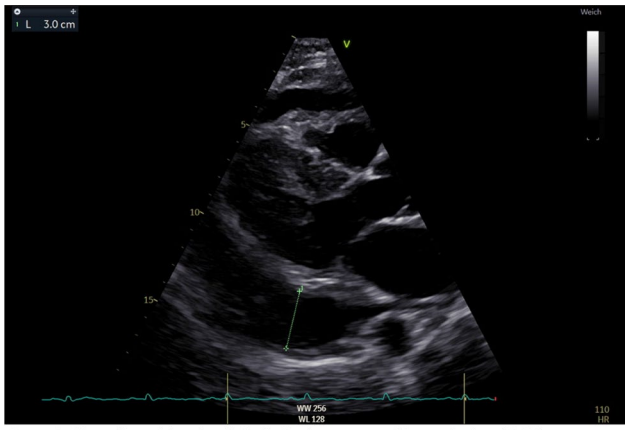


**Figure 2:** Circumferential pericardial effusion in parasternal long axis view (PLAX)

**Fig. 2 | 1-1**

Ibuprofen was tapered. At follow-up, the patient was asymptomatic with normal inflammatory markers and no effusion on echocardiography. Colchicine was discontinued due to diarrhea, and antibiotics were stopped after reevaluation. Subsequent cardiology follow-up remained unremarkable. Oncologic therapy with Lorlatinib and Pemetrexed has continued, with stable disease on restaging imaging.

**Conclusion:** In pericarditis with concomitant pericardial effusion, fluid accumulation is attributed to local inflammation, and pathogen detection in non-purulent effusions is uncommon. Standard treatment consists of anti-inflammatory therapy with NSAIDs and colchicine; antibiotics are not routinely indicated. In this case, antimicrobial therapy was initiated in addition to guideline-directed treatment because Cutibacterium acnes was detected twice in pericardial fluid obtained six years apart, accompanied by markedly elevated inflammatory markers. Although C. acnes has been reported in isolated cases of pericardial infection, these typically involved high fever and purulent or milky effusions.1,2,3 In contrast, our patient presented with subfebrile temperature and serous fluid. The repeated isolation of C. acnes suggests a possible pathogen-related etiology; however, it remains unclear whether the bacterium contributed to the inflammatory process or represented an incidental finding. Accordingly, the specific benefit of antibiotic therapy cannot be determined with certainty and may have primarily addressed concomitant complications, such as suspected congestion pneumonia. A direct association with the underlying malignancy is unlikely given negative cytology, although it cannot be fully excluded. A causal relationship with oncologic therapy also appears improbable, as the episodes occurred under different regimens; nevertheless, immunomodulatory effects cannot be definitively ruled out.

## References

1. Fakhri G, Tayeh C, Dbaibo G, El Sedawy O, Halim AN, Bitar F, Arabi M. Cardiac Tamponade Caused by Cutibacterium acnes: An Updated and Comprehensive Review of the Literature. Can J Infect Dis Med Microbiol. 2020;14;2020:9598210. Jul.
2. Farhat-Sabet A, Hull R, Thomas D. Cardiac Tamponade from Purulent Pericarditis due to Cutibacterium acnes. Case Rep Cardiol. 2018;18;2018:4739830. Nov.
3. Cruz D, Ahmed H, Gandapur Y, Abraham MR. Propionibacterium acnes: A Treatable Cause of Constrictive Pericarditis. Case Rep Med. 2015;2015:193272.

# 1-2

## Sondenloser Herzschrittmacher nach Herztransplantation

**Windhager A., Saleh K., Reiter C., Meledeth C., Steinwender C.**

Klinik für Kardiologie und Internistische Intensivmedizin (Interne I), Med Campus III, Kepler Universitätsklinikum, Linz, Österreich

**Einleitung:** Herztransplantationen stellen bei Patienten mit fortgeschrittener Herzinsuffizienz eine wichtige Therapieoption dar, in Österreich wurden 2025 68 Herztransplantationen durchgeführt [1]. Im Durchschnitt benötigt im Verlauf jeder zehnte Patient einen permanenten Herzschrittmacher nach erfolgter Herztransplantation [2]. Während das allgemeine Risiko für Device assoziierte Infektionen im Langzeitverlauf eher gering einzustufen ist (1,1–4,6 %), steigt das Risiko unter der laufenden Immunsuppression um das 2,5-fache an [3,4]. Die Inzidenz für Blutstrominfektionen nach Herztransplantation wird mit 11 % beziffert [5]. Aufgrund des höheren Infektionsrisikos stellen sondenlose Herzschrittmacher eine potenzielle Alternative dar, zumal die Infektionsrate bei sondenlosen Schrittmachern nahezu 0 % beträgt [6,7].

**Methoden:** Diese Fallserie beinhaltet zwei Patienten mit einem sondenlosen Herzschrittmacher nach erfolgter Herztransplantation. Patient 1: Ein 66-jähriger Patient stellt sich mit einem symptomatischen Bradykardie/Tachykardie-Syndrom bei intermittierender 2:1 blockierter atrialer Tachykardie sowie Pausen von bis zu 5,6 Sekunden bei vorliegendem Sinusarrest vor. Vorbekannt ist eine dilatative Kardiomyopathie mit erfolgter Herztransplantation im Jahr 1988 sowie ein liegendes VVI-System, welches im Verlauf bei Sondenbruch und fehlendem Pacingbedarf stillgelegt wurde. Aufgrund des nun vorliegenden Sick-Sinus-Syndroms und fehlendem ventrikulären Pacingbedarfs wird der Entschluss zur kompletten Systemextraktion und Implantation eines sondenlosen Vorhofschrittmachers (AVEIR AR) gestellt. Patient 2: Eine 78-jährige Patientin stellt sich über die unfallchirurgische Ambulanz aufgrund einer unklaren Synkope mit Verletzungsfolge vor. In der weiterführenden Abklärung zeigt sich als rhythmologisches Korrelat eine 9,6 sekündige Pause bei vorliegendem intermittierendem AV-Block III° ohne junktionalem Ersatzrhythmus. Vorbekannt ist ein Zustand nach Herztransplantation 2013 bei ischämischer/toxischer Kardiomyopathie. Bei erhaltener Linksventrikelfunktion und vorliegendem Sinusrhythmus wurde die Indikation zur Implantation eines sondenlosen Schrittmachers (Medtronic Micra AV 2) gestellt.

**Resultate:** Patient 1: Nach erfolgter Systemextraktion und Neuimplantation des sondenlosen Schrittmachers kann im

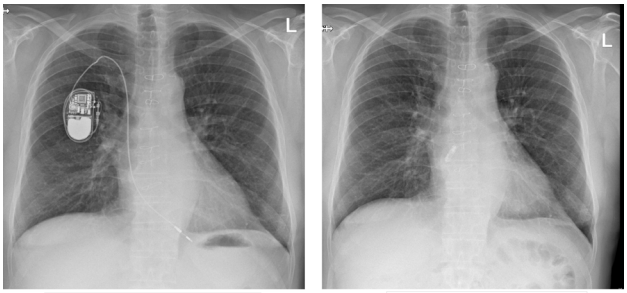


**Abb. 1 | 1-2** Patient 1

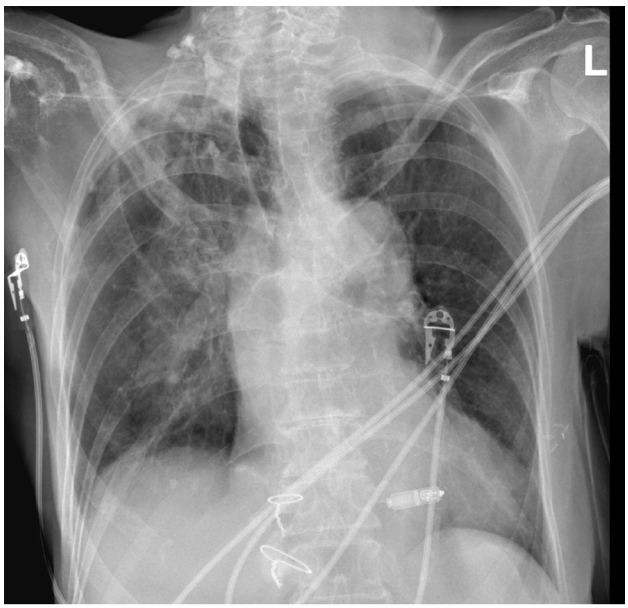


**Abb. 2 | 1-2** Patient 2

Follow-Up eine gute Funktion festgehalten werden. Die Reizschwelle bleibt mit 0,75 V bei 0,2 ms Impulsdauer stabil, ebenso das Sensing mit 3,2 mV. Nach Anpassung des Sensors beträgt der atriale Pacingbedarf 3 % bei unauffälliger Frequenzverteilung im Histogramm. Bei subjektiv guter Belastbarkeit im Alltag kann im Rahmen einer Ergometrie ein adäquater Frequenzanstieg mit einer Herzfrequenz von bis zu 115/min aufgezeichnet werden. Patient 2: Im Follow-Up zeigt sich eine regelrechte Funktion des implantierten Herzschrittmachers mit einer stablien Reizschwelle von 0,38 V bei 0,24 ms Impulsdauer sowie sehr guten Sensing-Werten (12–15 mV). Bei nur geringem ventrikulären Pacingbedarf kann eine überwiegende AV-Synchronität durch die Erkennung der mechanischen Vorhofaktivität gewährleistet werden.

**Schlussfolgerungen:** Die Indikation und das Einsatzspektrum der sondenlosen Herzschrittmacher werden angesichts der fortschreitenden Technologie immer größer. Aufgrund der erhöhten Infektanfälligkeit von Patienten/-innen nach Herztransplantation und laufender Immunsuppression können sondenlose Herzschrittmacher hier eine gute Alternative zu den konventionellen Schrittmachersystemen darstellen. Größere Studien hinsichtlich Langzeitdaten in diesem Patientengut sind allerdings noch ausständig.

## Literatur

1. Eurotransplant. 2052P_Austria_heart: counting recipient transplants [Internet]. Eurotransplant; 2026 [cited 2026 Feb 10]. Available from: https://statistics.eurotransplant.org
2. Cantillon DJ, et al. Long-term outcomes and clinical predictors for pacemaker-requiring bradyarrhythmias after cardiac transplantation: analysis of the UNOS/OPTN cardiac transplant database. Heart Rhythm. 2010;7(11):1567–71.
3. Glikson M, et al. 2021 ESC guidelines on cardiac pacing and cardiac resynchronization therapy: developed by the task force on cardiac pacing and cardiac resynchronization therapy of the European Society of Cardiology (ESC) with the special contribution of the European Heart Rhythm Association (EHRA). Eur Heart J. 2021;42(35):3427–520.
4. Birnie DH, et al. Risk factors for infections involving cardiac implanted electronic devices. J Am Coll Cardiol. 2019;74(23):2845–54.
5. Moreno A, et al. Bloodstream infections among transplant recipients: results of a nationwide surveillance in Spain. Am J Transplant. 2007;7(11):2579–86.
6. Reynolds D, et al. A leadless intracardiac transcatheter pacing system. N Engl J Med. 2016;374:533–41.
7. El-Chami MF, et al. Leadless pacemakers at 5-year follow-up: the Micra transcatheter pacing system post-approval registry. Eur Heart J. 2024;45(14):1241–51.

# 1-3

## Pulmonary embolism with a risk of stroke

**Alajbegovic L.[1], Burda M.[1], Moser B.[2], Haberl T.[3], Hofbauer T.[1], Skoro-Sajer N.[1], Lang I.[1], Gerges C.[1]**

[1]Medizinische Universität Wien, Innere Medizin II, Abteilung für Kardiologie, Wien, Austria
[2]Medizinische Universität Wien, Universitätsklinik für Thoraxchirurgie, Wien, Austria
[3]Medizinische Universität Wien, Universitätsklinik für Herz- und Thorakale Aortenchirurgie, Wien, Austria

**Introduction:** We report the case of a 59-year-old woman with acute pulmonary embolism (PE) who was referred from an external hospital for evaluation by our pulmonary embolism response team (PERT). The patient was normotensive (130/80 mmHg), tachycardic (115 bpm), and had an oxygen saturation of 97% on 4 L/min supplemental oxygen. Laboratory testing showed a lactate of 7.6 mmol/L, which decreased to 1.8 mmol/L, and an elevated troponin I of 640 ng/L. Symptoms consisted of dyspnea for two days and syncope one day prior to presentation. Past medical history was unremarkable.

**Methods:** Computed tomography (CT) demonstrated a central bilateral pulmonary embolism with saddle thrombus, additional thrombus in the right atrium (RA) (Fig. 1, Panel A), and a right ventricular-to-left ventricular diameter ratio of 1.4. After review of the images, PERT suspected the presence of a patent foramen ovale (PFO). Transoesophageal echocardiography (TOE) was therefore recommended prior to treatment decision-making. TOE confirmed the presence of a PFO with the RA thrombus herniating into the left atrium. PERT recommended surgical embolectomy to remove the clots and prevent paradoxical embolism.

**Results:** The patient was transferred to our center, and surgical embolectomy was performed by a multidisciplinary surgical team consisting of a thoracic surgeon and a cardiac surgeon. A median sternotomy was performed, the patient was put on

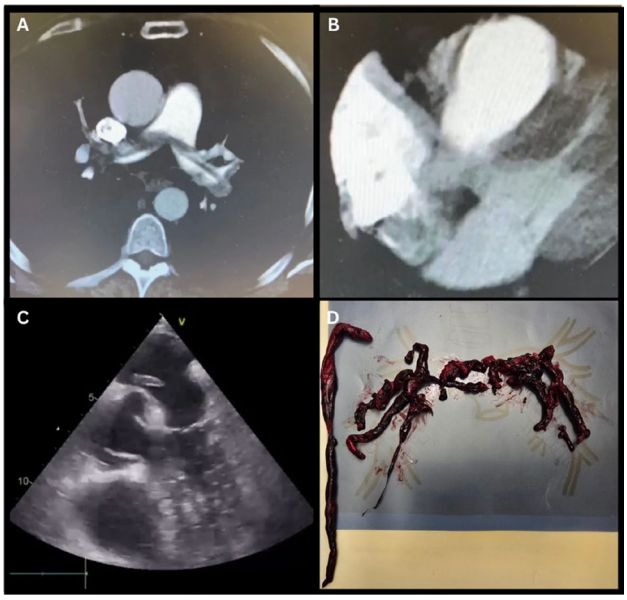


**Fig. 1 | 1-3** Panel A shows the CT image of the saddle thrombus. Panel B shows the CT image of the large RA thrombus that raised suspicion of a PFO, panel C shows the preoperative TOE, and panel D shows the thrombi removed during surgery

cardiopulmonary bypass, and the RA was opened. A large clot extending from the right ventricle to the RA and herniating into the left atrium through the PFO was carefully removed in toto, and the PFO was closed. After closure of the RA, the pulmonary arteries were opened and thrombus was carefully removed by the thoracic surgeon. After removal of all accessible clot, the pulmonary arteries were closed, the patient was weaned off cardiopulmonary bypass, and the surgical site was closed. The patient was transferred in a stable state to the intensive care unit, was extubated the next morning and was discharged from the intensive care unit two days after surgery.

**Conclusion:** This case highlights the importance of PERT assessment in the management of PE and shows that surgical embolectomy remains a valuable treatment modality in selected cases.

## 1-4

### A case of acute-on-chronic pulmonary embolism

**Alajbegovic L., Burda M., Hofbauer T., Skoro-Sajer N., Gerges C., Lang I.**

Medizinische Universität Wien, Innere Medizin II, Abteilung für Kardiologie, Wien, Austria

**Introduction:** A 22-year old female patient with acute pulmonary embolism (PE) was referred for pulmonary embolism response team (PERT) evaluation. Patient presented normotensive, tachycardic, with 99% oxygen saturation on 6L O2 with hs-troponin I of 1107.5 ng/L. She had dyspnea for two weeks, chest pain and a recent syncope, otherwise unremarkable history except for oral anticontraceptives.

**Methods:** Computed tomography showed bilateral central PE and right ventricular (RV) to left ventricular diameter ratio of 1.7. PERT suspected acute PE with underlying chronic disease, "acute-on-chronic PE", because of an unusually thick RV wall,

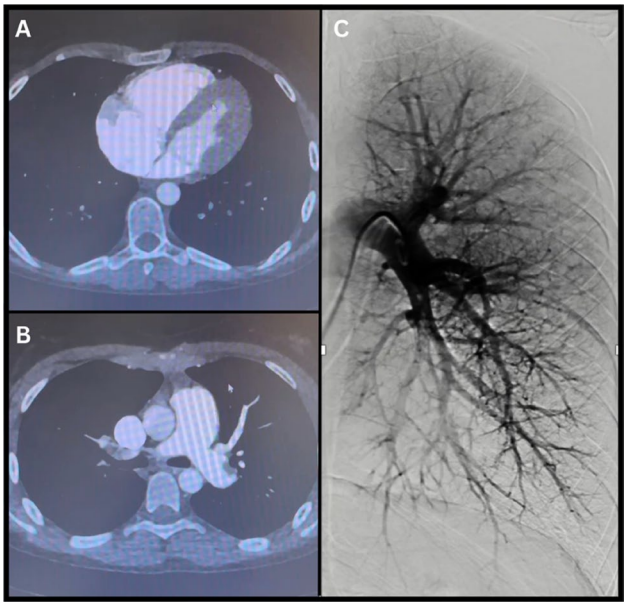


**Fig. 1 | 1–4** Panel A shows the large right ventricular to left ventricular diameter ratio, panel B shows the dilated pulmonary artery and panel C shows the perfusion defect in the left lower lobe

large pulmonary arteries and large right atrium. No mechanical treatment was recommended, but patient was scheduled for follow-up after three months of full anticoagulation.

**Results:** Three months later patient arrived at our clinic in an excellent state. Patient had no dyspnea (WHO FC I), had an *N*-terminal pro-brain natriuretic peptide of 21 pg/ml, walked 611 meters in six minutes, and had a completely normal transthoracic echocardiogram. Scintigraphy showed a large ventilation-perfusion mismatch in the left lower lobe. During right heart catheterization (RHC), mean pulmonary artery pressure was 10 mmHg and pulmonary vascular resistance was normal with 0.5 Wood Units. Pulmonalis angiography revealed a complex web lesion in the left basal artery extending to A10 and A9, completely occluding these two branches. Patient was diagnosed with chronic thromboembolic pulmonary disease (CTEPD). The interdisciplinary CTEPD board elected her for balloon pulmonary angioplasty.

**Conclusion:** This case highlights the importance of PERTs. Awareness of signs of CTEPD (intravascular webs, dilated pulmonary artery, right ventricular hypertrophy) in the setting of acute PE helps avoid the risk of unnecessary and complicated procedures.

## 1-5

### Pulmonary artery stenosis

**Alajbegovic L.[1], Burda M.[1], Bartko P.[1], Kitzmüller E.[2], Hofbauer T.[1], Skoro-Sajer N.[1], Lang I.[1], Gerges C.[1]**

[1]Medizinische Universität Wien, Innere Medizin II, Abteilung für Kardiologie, Wien, Austria
[2]Medizinische Universität Wien, Universitätsklinik für Kinder- und Jugendheilkunde, Abteilung für Pädiatrische Kardiologie, Wien, Austria

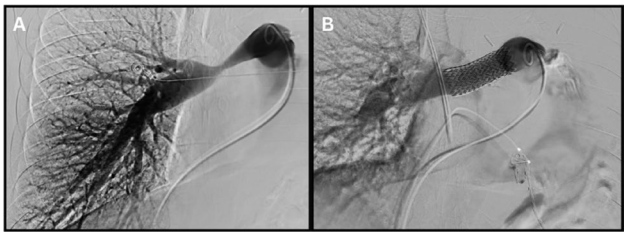


**Fig. 1 | 1-5** Panel A shows a pulmonary angiogram of the unilateral pulmonary artery stenosis. Panel B shows the pulmonary angiogram after implantation of a stent graft

**Introduction:** We report on a 64-year-old male patient presenting to our pulmonary hypertension (PH) clinic with progressive dyspnea on mild exertion (functional class (FC) III-IV), sleep disturbance due to severe orthopnea and an *N*-terminal pro-brain natriuretic peptide (NT-proBNP) of 904 pg/mL. The patient had previously undergone left-sided pneumonectomy for adenocarcinoma ten years earlier and splenectomy for suspected metastasis and had a history of pulmonary embolism twenty and ten years prior.

**Methods:** Transthoracic echocardiography demonstrated preserved right ventricular function, a D-shaped left ventricle, and a torrential tricuspid regurgitation, with an estimated systolic pulmonary artery pressure of 58 mmHg, although this value may have been underestimated. Ventilation perfusion scintigraphy and computed tomography (CT) were performed to evaluate for chronic thromboembolic pulmonary hypertension (CTEPH). Scintigraphy showed a large ventilation-perfusion mismatch in the right upper lobe, while CT revealed a unilateral stenosis of the right pulmonary artery with a minimum lumen diameter of 5 mm caused by a perifocal soft tissue cuff.

**Results:** Right heart catheterization with pulmonary angiography confirmed severe stenosis of the right pulmonary artery (Fig. 1, Panel A) without evidence of intraluminal chronic thromboembolic material. Mean pulmonary artery pressures distal and proximal to the lesion were 14 and 42 mmHg, respectively, corresponding to a mean pressure gradient of 28 mmHg. The peak-to-peak gradient across the lesion was 77 mmHg. The patient was subsequently scheduled for percutaneous treatment. Predilatation was performed followed by implantation of a stent graft (BeGraft 20 mm x 48 mm) (Fig. 1, Panel B). The patient reported immediate symptomatic improvement in dyspnea and was discharged the following day.

**Conclusion:** In this case pulmonary artery stenosis mimicked CTEPH and highlights the importance of comprehensive diagnostic work-up in cases of unexplained dyspnea and suspected pulmonary hypertension.

## 1-6

## Heart-wrenching dyspnea: Pericardial Effusion as the First Sign of an Occult Malignancy

**Pahr S.[1], Füreder T.[2], Gangl C.[1], Bergler-Klein J.[1], Badr-Eslam R.[1], Seilinger L.[1]**

[1]Kardiologie, Wien, Austria
[2]Onkologie, Wien, Austria

**Introduction:** Pericardial effusion may represent an early manifestation of malignancy. In this case, an isolated pericardial effusion was the initial manifestation of adenocarcinoma. This case emphasizes prompt evaluation and multidisciplinary management of unexplained pericardial effusion, as it carries a poor prognosis. (1)

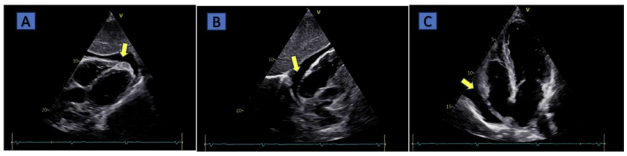


**Fig. 1 | 1-6** A. Subcostal view of the pericardial effusion; Figure B. Subcostal view showing pericardial effusion posterior to the right atrium; Figure C Four-chamber view showing pericardial effusion posterior to the right atrium

**Methods:** Case Presentation: In December 2024, an otherwise healthy 61-year-old woman was admitted to the emergency department with progressively worsening dyspnea and symptoms of angina-like chest pain. Due to an elevated D-dimer level, a CT pulmonary angiography (CTPA) was performed to exclude pulmonary embolism. Incidentally, the imaging revealed a pericardial effusion. Transthoracic Echocardiography (TTE) demonstrated a circumferential pericardial effusion (as shown in the accompanying images) measuring up to 1.5 cm in maximum width, corresponding to a moderate effusion, without hemodynamic significance and an LVEF of 55%. Therefore, a PET-CT was conducted and low-grade FDG-avid lymphadenopathy was present in multiple regions. Despite comprehensive oncological evaluation no primary malignancy could be identified. Of particular concern was a markedly elevated CA 19-9 level 1200 U/ml and a mildly elevated C-reactive protein level of 2.2 mg/dl, yet gastrointestinal histology tests were non-malignant. Eight weeks later, the patient noticed a cervical lymph node, which was diagnosed as adenocarcinoma by biopsy, establishing the diagnosis of occult cancer. Systemic chemotherapy with FOLFOX was initiated. During a lymph node biopsy, an incidental large thrombus was detected in the left internal jugular vein, correlating with cancer associated hypercoagulability. (2)

**Results:** In addition, bevacizumab was added to the treatment regimen. During therapy in March NT-proBNP increased to 790 pg/ml, which could be attributable to chemotherapy-associated cardiotoxicity, while the pericardial effusion showed slight regression. (3) A reduction of left ventricular ejection fraction (LVEF, 45%) as a sign for cancer therapy-related cardiac dysfunction was noted under FOLFOX and bevacizumab therapy regimen. The diagnosis HFmrEF was established and therefore the heart failure therapy was initiated, including an Angiotensin-converting-enzyme (ACE) inhibitor, a beta-blocker, a mineralocorticoid receptor antagonist (MRA) and a SGLT2-inhibitor. After five months the patient reported a stable clinical condition, NT-proBNP decreased to 315 pg/ml. Echocardiography showed minimal improvement, with preserved systolic function. LVEF increased from 45% to 50%.

**Conclusion:** Pericardial effusion should be considered a clinically significant finding even in the absence of hemodynamic compromise, warranting close follow-up and a multidisciplinary management approach. Notably, cancer therapy-related cardiac dysfunction shows a good response to heart failure treatment.

### References

1. Schulz-Menger J, et al. Oct 22. Eur Heart J. 2025;46(40):3952–4041.
2. Falanga A, et al. J Thromb Haemost. 2023;21(6):1397–408.
3. Lyon AR, et al. Nov 1. Eur Heart J. 2022;43(41):4229–361.

## 1-7

### Management of aortic root thrombosis after continuous-flow left ventricular assist device implantation

**Reiter C., Schachner B., Meledeth C., Rechberger S., Steinwender C., Zierer A.**

Kepler Universitätsklinikum Linz, Linz, Austria

**Introduction:** Aortic root thrombosis (ART) is a hazardous, not uncommon complication after continuous-flow LVAD implantation with an incidence of 5–10% [1,2]. It is associated with significant mortality and morbidity, e. g. an increased risk of thromboembolic stroke. The risk of coronary artery occlusion can lead to deleterious consequences, especially in case of myocardial infarction of the unsupported right ventricle or occurrence of ventricular arrhythmias. Intermittent opening of the aortic valve is important to reduce the risk of ART as shown in a patient-derived computed tomography image-based model in a study by Mahr et al. Their study demonstrated that intermittent aortic valve opening, even partially and at low frequency, results in hemodynamic benefits and improved biocompatibility by promoting platelet washout, reducing stasis and decreasing thrombogenicity [3]. Early antithrombotic therapy and early detection of blood stasis or sludge formation are critical. Once ART occurs, there is no well-described management strategy.

**Methods:** A 58-year-old male patient was transferred to our ICU after he had suffered from anterior myocardial infarction which had been managed with systemic thrombolysis at a hospital in Bosnia and Herzegovina. At the time of arrival, he presented with cardiogenic shock necessitating the use of low-dose inotropes and vasopressors as well as high-dose diuretics. Echocardiography showed ischemic cardiomyopathy with severely impaired left ventricular contractility with an EF of 20% due to akinesia extending from the midventricular anteroseptal and anterior walls to the apical inferior wall. The right ventricular contractility was slightly decreased. Coronary angiography revealed multi-vessel disease with chronic total occlusion of the right coronary artery and significant stenosis of the circumflex artery and left anterior descending artery. Percutaneous coronary intervention was performed on each significant stenosis. Over the subsequent days the patient was successfully weaned off catecholamine support, and treatment was adjusted to an SGLT2-inhibitor and a low-dose beta-blocker. However, due to persistent hypotension, further therapeutic escalation was not feasible. Cardiac MRI showed extensive myocardial scars. Since there were no signs of improvement and the patient was still highly symptomatic with necessity of intensive combined diuretic therapy (furosemid and hydrochlorothiazide), he underwent implantation of a permanent LVAD (Fig. 1) as bridge-to-candidacy for heart transplant.

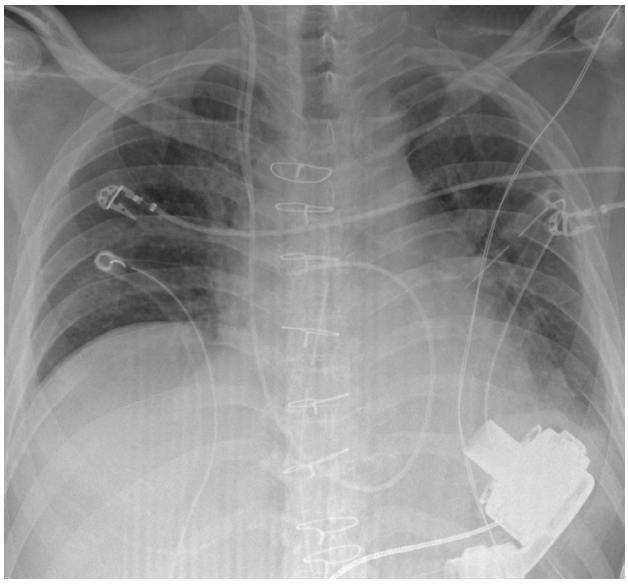

Fig. 1 | 1-7

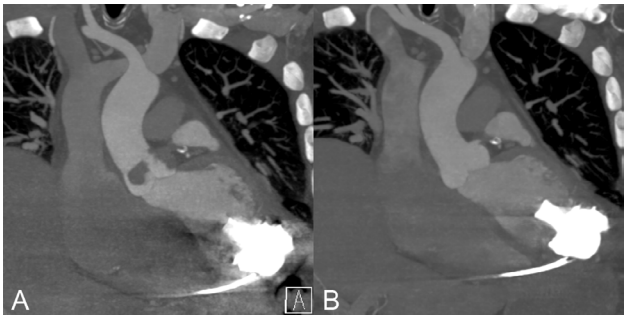


Fig. 2 | 1-7

**Results:** In the early postoperative phase, the patient was rapidly weaned from inotropes and vasopressors. Echocardiography showed adequate programming of the LVAD speed with balanced interventricular septum, slightly decreased RV contractility and intermittent opening of the aortic valve. Heparin was established in addition to aspirin. On the 10th postoperative day heparin was discontinued after reaching an INR value of 2,4 with phenprocoumon and the patient was transferred to the regular ward. In the following days, despite INR values between 2–2.5, the patient reported episodes of angina. Echocardiography showed almost permanent closure of the aortic valve with suspected thrombus formation in the aortic root. CT-angiography (Fig. 2A) confirmed extensive ART with occlusion of the left main coronary artery. To manage this complication, high-dose heparin therapy was established and LVAD speed was increased to hinder the aortic valve from opening and reduce the risk of cerebrovascular thromboembolic stroke. A CT-scan 12 days after the initiation of intensified anticoagulation demonstrated complete resolution of the ART (Fig. 2B). LVAD speed was then decreased to reestablish opening of the aortic valve to optimize blood flow in the aortic root and reduce the risk of recurrent ART in addition to an increased INR target value of 3.0. In the current follow-up, 16 months after LVAD implantation the patient remains stable on therapy with no recurrence of thrombotic masses in the aortic root.

**Conclusion:** Aortic root thrombosis occurs with an incidence of 5–10% after continuous-flow LVAD implantation and is associated with increased mortality and morbidity due to risk of thromboembolic stroke, myocardial infarction or ventricular arrhythmias. Careful programming of LVAD speed settings to allow at least intermittent opening of the aortic valve with regular echocardiographic surveillance as well as adequate anticoagulation is critical to prevent clot formation.

### References

1. Carey RM, Marshall D, Clerkin K, et al. J Heart Lung Transplant. 2024;43(6):866–75. https://doi.org/10.1016/j.healun.2023.08.023.
2. Fried J, Garan AR, Shames S, et al. J Heart Lung Transplant. 2018;37(12):1425–32. https://doi.org/10.1016/j.healun.2018.07.012.

3. Mahr C, Chivukula VK, McGah P, et al. Jul/Aug. ASAIO J. 2017;63(4):425–32. https://doi.org/10.1097/MAT.0000000000000512.

## 1-8

### Erfolgreiche cardiale Resynchronisationstherapie mittels Conduction System Pacing bei einem Patienten mit Coronarsinus-Reducer

**Burkart-Küttner D., Mauerhofer E., Meissner M., Sipötz J., Mitteregger M., Engel H.**

Hanusch-Krankenhaus, Wien, Österreich

**Einleitung:** Fallbeschreibung: Im Jänner 2026 wurde ein 74-jähriger Patient in unsere Device-Ambulanz mit der Bitte um eine CRT-D-Implantation überwiesen. Im April 2025 hatte der Patient aufgrund seiner hochgradig reduzierten EF bei ischämischer Cardiomyopathie und Linksschenkelblock (LSB) in einem anderen Krankenhaus als Primärprophylaxe eine LifeVest erhalten. Zu diesem Zeitpunkt hatte der Patient noch ein Ulcus am Bein, weshalb man ursprünglich mit einer Device-Implantation abwarten wollte, bis dieses ausgeheilt ist. Das Ulcus war nun seit Monaten abgeheilt. Kardiale Anamnese: Ischämische Cardiomyopathie mit hochgradig eingeschränkter LV-Funktion (30–35 %) und apical rocking bei LSB. Chronisches Coronarsyndrom Z. n. 3-fach ACBP (LIMA ad LAD, Vene ad CX, Vene ad PDA) 23.04.2013 Z. n. PTCA und Stent prox. LAD und mid CX 2001 Z. n. PTCA und Stent einer Instent-Restenose LAD 2002 Z. n. Brachytherapie LAD 2002 Z. n. PTCA und Stent der CX 2009 Z. n. PTCA und Stent der CX 2010 Z. n. PTCA und Stent der CX 2020 Z. n. CS-Reducer-Implantation am 08.03.2024 Trotz optimaler medikamentöser antianginöser und Herzinsuffizienz-Therapie hatte der Patient ein NT-proBNP von 2384 ng/l (12/2025) bei NYHA II-III und im EKG einen SR, 79/min, kompl. LSB (QRS: 180 ms).


**Abb. 1 | 1-8** EKG 1) intraoperativ: V6RWPT auf 60 ms; V1V6-Interpeak Intervall: 52 ms; QRS-Breite unipolar: 130 ms

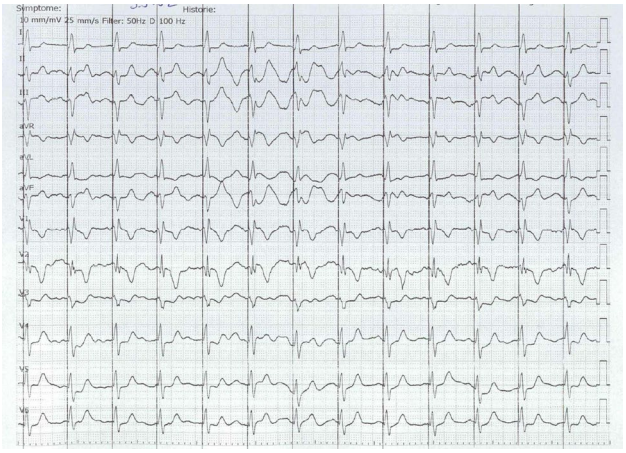

**Abb. 2 | 1-8** EKG 2) Follow Up

**Methoden:** Coronarsinus-Reducer (CSR): Für Patienten, die trotz Ausschöpfung aller medikamentösen und mechanischen Revaskularisierungsmethoden weiterhin an therapierefraktärer Angina pectoris leiden, stellt der CSR nach den 2024 ESC-Guidelines für das Management des chronischen Koronarsyndroms eine alternative Behandlungsoption (Klasse II b) dar. Der CSR ist ein sanduhrförmiger expandierbarer Edelstahlstent, der durch die kontrollierte Verengung des Koronarsinus zu einem erhöhten Druck im venösen System und damit zu einer Verbesserung der koronaren Kollateralzirkulation führen soll. Cardiale Resynchronisationstherapie (CRT) mittels LV-Sonde: Die CRT mittels LV-Sonde ist eine etablierte Behandlungsmethode bei hochgradig reduzierter LV-Funktion, LSB und damit verbundener Dyssynchronie. Nach den 2021 ESC-Guidelines on Cardiac Pacing besteht bei einer Herzinsuffizienz mit einer EF < 35 % und einem LSB mit einer QRS-Dauer > 150 ms eine Klasse I A Indikation zur CRT. In der Literatur sind nur vereinzelt Fälle einer erfolgreichen CRT mit LV-Sonde trotz CSR beschrieben. Cardiale Resynchronisationstherapie (CRT) mittels Conduction System Pacing (CSP): Bei CRT-Kandidaten, bei denen die Implantation einer Coronarsinussonde erfolglos ist, wird laut dem 2025 ESC-Consensus Statement for Conduction System Pacing (CSP) die Implantation einer CSP-Sonde zur Resynchronisation, also ein CSP-CRT, empfohlen.

**Resultate:** Wir haben den Patienten sowohl für eine klassische CRT-D-Implantation als auch für eine CSP-CRT-D-Implantation aufgeklärt, die Entscheidung sollte intraoperativ fallen. CRT-OP am 17.02.2026: In Narkose wurde über eine V. cephalica-Präparation und zusätzlich eine V. axillaris-Punktion links der Venenzugang gelegt. Nach der Implantation der ICD-Sonde (Biotronik Pamira S65) in den rechten Ventrikel versuchten wir mit einem langen Führungsdraht den Coronarsinus zu sondieren, was aber nur bis kurz nach dem CS-Eingang gelang, da offensichtlich der Draht durch den CSR behindert wurde. Daher fiel der Entschluss auf einen CSP-Katheter (Biotronik Selectra 3D-55-42) umzusteigen und statt einer LV-Sonde eine CSP-Sonde (Biotronik Solia CSP S 60) ins Septum zu schrauben. Mittels left bundle branch area pacing (LBBAP) konnten wir folgend Werte erzielen: Verkürzung der V6RWPT auf 60 ms; V1V6-Interpeak Intervall: 52 ms; QRS-Breite unipolar: 130 ms. (EKG 1) Die OP wurde noch durch eine Vorhofsonde (Biotronik Solia S53) ergänzt und alle Sonden an ein CRT-D-Aggregat (Biotronik Rivacor 7 HF-T, DF4/IS-1) angeschlossen. Der schmale Kammerkomplex blieb bestehen (EKG 2), das apical rocking verschwand, die EF besserte sich deutlich und bereits wenige Tage postoperativ konnte sich der Patient besser belasten: NYHA I-II.

**Schlussfolgerungen:** Conclusio: In diesem Fall konnten wir zeigen, dass bei Patient*Innen mit einem Coronarsinus-Reducer (CSR) und der Notwendigkeit einer cardialen Resynchroni-

sationstherapie (CRT) das Implantieren einer für Conduction System Pacing (CSP) zugelassenen Sonde eine gute Alternative zur konventionellen LV-Sonde darstellt. Ideal wäre natürlich eine für CSP zugelassene ICD-Sonde. Damit würde sich das komplette CRT-System um eine Sonde reduzieren und die damit verbundenen Risiken wie etwa Trikuspidalklappeninsuffizienz, Venenthrombose oder Infektionen minimieren.

### Literatur


1. Grebmer C, Bossard M, Attinger-Toller A, Kobza R, Hilfiker G, Berte B, et al. Cardiac resynchronization therapy in patients with a coronary sinus reducer: a case series. Eur Heart J Case Rep. 2023;7:ytad455.
2. Bontempi L, Vassanelli F, Cerini M, Inama L, Salghetti F, Giacopelli D, et al. Can we implant left ventricle pacing lead in a patient with coronary sinus reducer? J Interv Card Electrophysiol. 2018;51:87–8.
3. Constantino J., Zuccaro L., Romani B., Rotolo F., Porcelli D., Successful implantation of cardiac resynchronization therapy in a patient with coronary sinus reducer using proximal coronary sinus branches: a case report: European Heart Journal – Case Reports (2024) 8,
4. Burri H, Jastrzebski M, Cano Ó, Čurila K, de Pooter J, Huang W, et al. EHRA clinical consensus statement on conduction system pacing implantation: endorsed by the Asia Pacific Heart Rhythm Society (APHRS), Canadian Heart Rhythm Society (CHRS), and Latin American Heart Rhythm Society (LAHRS). Europace. 2023;25:1208–36.
5. Mrak M, Pvašič N, Štublar J, Bunc M, Zizek D. Resynchronization therapy with His bundle pacing in a patient after coronary sinus reducer implantation. J Cardiol Cases. 2020;22:226–9.
6. Knuuti J, Wijns W, Saraste A, Capodanno D, Barbato E, Funck-Brentano C, et al. 2019 ESC Guidelines for the diagnosis and management of chronic coronary syndromes. Eur Heart J. 2020;41(6):407–77.
7. Vrints C, Andreotti F, et al. ESC Guidelines for the management of chronic coronary syndromes; Eur Heart. Journal. 2024;2024(45):3415–537.
8. Glikson M, Burri H, et al. ESC Consensus Statement on indications for CSP. Europace. 2025;202(5). 27, euaf050.


## 1-9

### Lipoprotein(a) Levels and Intensification of Lipid-Lowering Therapy After Cardiac Surgery


**Engler C.[1], Winter-Pölzl L.[1], Lohmann R.[1,2], Graber M.[1], Hirsch J.[1], Nägele F.[1], Ioannou-Nikolaidou M.[1,2], Eder J.[1], Heim V.[1], Schmidt S.[1], Bano S.[1], Hirtenlehner F.[1], Kleineisen H.[1], Lukosch M.[1], Bonaros N.[1], Grimm M.[1], Gollmann-Tepeköylü C.[1]**

[1]Universitätsklinik für Herzchirurgie, Innsbruck, Austria
[2]Institut für Klinisch-Funktionelle Anatomie, Innsbruck, Austria



**Introduction:** Elevated lipoprotein(a) [Lp(a)] is an established cardiovascular risk factor that is largely genetically determined and only partially influenced by conventional lipid-lowering therapy. Patients undergoing cardiac surgery often represent a population with advanced atherosclerotic disease and high cardiovascular risk. However, data on the distribution of Lp(a) levels and the implementation of lipid-lowering therapy in routine clinical practice among cardiac surgery patients remain limited. In particular, it is unclear to what extent elevated Lp(a) levels are associated with escalation of postoperative lipid-lowering therapy. The aim of this study was therefore to describe Lp(a) levels and to evaluate patterns of postoperative lipid-lowering treatment across different Lp(a) risk categories in a contemporary cardiac surgery cohort.

**Methods:** We retrospectively analyzed patients undergoing cardiac surgery at a tertiary academic center between 2010 and 2024. Among 11,074 surgical procedures, 3457 patients had at least one available Lp(a) measurement and were included in the analysis. Lp(a) values were categorized into four predefined risk groups: <75 nmol/L, 75–125 nmol/L, 125–430 nmol/L, and >430 nmol/L. Postoperative lipid-lowering therapy was assessed, including statin potency, ezetimibe use, PCSK9 inhibitor therapy, and the use of combination lipid-lowering therapy. Lipid parameters and treatment patterns were compared across Lp(a) categories using descriptive statistics.

**Results:** Among 3457 patients with available Lp(a) measurements, median Lp(a) was 21.0 nmol/L (interquartile range 14.1–93.6). Postoperative LDL-cholesterol levels were broadly comparable across Lp(a) risk groups. High-potency statin therapy was commonly prescribed in all groups, ranging from approximately 67% to 70%, without a clear gradient according to Lp(a) level. In contrast, additional lipid-lowering therapies were more frequently used in patients with higher Lp(a). Ezetimibe use increased from 33.1% in patients with Lp(a) <75 nmol/L to 43.0% in those with Lp(a) 125–430 nmol/L and to 72.2% in patients with Lp(a) >430 nmol/L. PCSK9 inhibitor therapy remained infrequent overall but was more commonly used in patients with very high Lp(a) levels. Similarly, the use of combination lipid-lowering therapy increased across Lp(a) categories, reaching 76.5% in patients with Lp(a) >430 nmol/L.

**Conclusion:** In this contemporary cardiac surgery cohort, higher Lp(a) levels were associated with more intensive postoperative lipid-lowering treatment, particularly regarding the use of ezetimibe, PCSK9 inhibitors, and combination therapy. Despite this treatment escalation, postoperative LDL-cholesterol levels remained broadly similar across Lp(a) categories. These findings suggest that elevated Lp(a) is recognized in clinical practice and may influence therapeutic decisions, although its impact on lipid targets and long-term outcomes requires further investigation.


# POSTERSITZUNG 2— HERZCHIRURGIE 1

## 2-1

### Longterm Outcome after Repair of Interrupted Aortic Arch in a Single Center


**Kreuzer M.[1], Sames-Dolzer E.[1], Tulzer A.[2], Klapper M.[1], Mair R.[1], Gierlinger G.[1], Seeber F.[1], Mair R.[1]**

[1]Department für Kinderherzchirurgie, Kepler Universitätsklinikum, Linz, Austria
[2]Klinik für Kinderkardiologie, Kepler Universitätsklinikum, Linz, Austria



**Introduction:** Mortality in patients with interrupted aortic arch rates among the highest in congenital heart surgery [1,2]. Various techniques for aortic arch repair are described, reintervention rates remain substantially [3]. The aim of this retrospec-

tive single center study: To evaluate the long-term outcome in a biventricular series with a preferably performed direct anastomosis and one-stage repair.

**Methods:** Between 1999 and 2023, 58 biventricular patients with interrupted aortic arch were operated at our center. Median age at operation was 10 [7; 15] days, weight 3.3 [3; 3.7] kg. In the 24 children with VSDs only, the arch was repaired by a direct anastomosis. 34 had complex concomitant heart defects, the arch reconstruction was performed by direct anastomosis (20), direct anastomosis + patch (10), reverse subclavian flap + patch (3), aortic autograft + patch (1).

**Results:** Median cardiopulmonary bypass time was 222 [159; 315] min, aortic cross clamp time 94 [75; 143] min. 2 patients died during the hospital stay (4%), 2 patients after discharge (4%), 4 (7%) required an arch reintervention during a follow-up period of median 9.3 [6.2;17.2] years. There was no death or arch reintervention in the VSD group.

**Conclusion:** All-cause mortality in biventricular patients with interrupted aortic arch was 7%, arch reintervention rate 8%. Direct aortic anastomosis in patients with VSD only can be performed with excellent outcomes, with no deaths or arch reinterventions being observed after a follow-up up to 24 years.

## References


1. Andrianova EI, Naimo PS, Fricke TA, et al. Outcomes of Interrupted Aortic Arch Repair in Children With Biventricular Circulation. Ann Thorac Surg. 2021;111(6):2050–8. Jun.
2. Uzzaman MM, Khan NE, Davies B, et al. Long-term outcome of interrupted arch repair with direct anastomosis and homograft augmentation patch. Ann Thorac Surg. 2018;105:1819–26.
3. McCrindle BW, Tchervenkov CI, Konstantinov IE, et al. Risk factors associated with mortality and interventions in 472 neonates with interrupted aortic arch: A Congenital Heart Surgeons Society study. J Thorac Cardiovasc Surg. 2005;129(1):343–350.e1.


# 2-2

## Outcomes and surgical considerations of Aorto-Carotid and Aorto-Innominate Bypass in Upper Hemisternotomy for Innominate Artery Disease


**Szalkiewicz P., Müller H., Ratschiller T., Gökler J., Benedikt P., Zierer A.**

Department of Cardio-Vascular and Thoracic Surgery, Kepler University Hospital – Medical Faculty of the Johannes Kepler University, Linz, Austria


**Introduction:** As published data on bypass procedures for innominate artery (IA) disease with alternative minimally invasive access approaches are scarce, given procedures were analyzed in this study.

**Methods:** Between 10/2010–12/2024, thirteen patients (male: $n=5$; [38.5%], age: 68 [46.5–76] years) underwent fourteen aorto-carotid (AC) bypass ($n=9$; [69.2%]) and aorto-innominate (AI) bypass ($n=5$; [38.5%]) procedures for IA disease (atherosclerosis: $n=12$; [92.3%]), including 1 (7.7%) patient with concomitant AC and AI bypass, as well as 1 (7.7%) patient with concomitant AC and aorto-right subclavian artery bypass. All procedures were conducted by upper hemisternotomy (UHS). The given analysis is a retrospective single-center study.

**Results:** Two (15.4%) patients underwent acute surgery, while 9 (69.2%) presented with symptoms, including 1 (7.7%) with stroke, three (23.1%) with transient ischemic attack and 3 (23.1%) with arm claudication. During a median follow-up time of 26 (10.5–58.5) months, no restenosis and no neurologic complications, including stroke, transient ischemic attacks or nerve lesions were documented. Two (15.4%) patients underwent reoperations due to pericardial effusion and one (7.7%) experienced myocardial infarction. Overall, three (23.1%) patients died with two (15.4%) patients within thirty days after surgery, including one (7.7%) due to multiorgan failure and one (7.7%) due to respiratory failure, as well as one (7.7%) patient due to chronic heart failure eight months after surgery.

**Conclusion:** Aorto-carotid and AI bypass conducted by UHS are safe and feasible for complex IA disease, with excellent graft patency, low rates of neurologic complications and procedural related mortality.

# 2-3

## Minimally invasive aortic valve replacement by the novel transaxillary approach: considerations and first patient outcomes


**Szalkiewicz P., Gökler J., Huber F., Pawlowska M., Damian I., Benedikt P., Zierer A.**

Department of Cardio-Vascular and Thoracic Surgery, Kepler University Hospital – Medical Faculty of the Johannes Kepler University, Linz, Austria


**Introduction:** Despite rising popularity of the novel right transaxillary access (rTX) for aortic valve surgery, data on its corresponding results remain scarce. The given analysis reports on first outcomes at the start of an established program.

**Methods:** Between 06/2023 and 02/2026 overall 22 patients underwent aortic valve surgery via the rTX approach. The majority were female ($n=14$; [63.6%]), with a median age of 64.5 years (60.0–70.0) and a EuroSCORE II of 0.9 (0.6–1.1). The predominant indication for surgery was aortic valve stenosis ($n=17$; [77.3%]). In most cases, cardiopulmonary bypass (CPB) was established through cannulation of the right groin ($n=21$; [95.5%]).

**Results:** The median aortic cross-clamp time was 78.5 minutes (74.8–90.3), while the median duration of extracorporeal circulation was 143.0 minutes (134.8–178.3). The median length of stay in the intensive care unit was 1.0 days (1.0–2.3). One patient (4.5%) required emergent reoperation via sternotomy because of bleeding at the aortotomy site, with aortic root replacement being successfully carried out consecutively. A stroke occurred in one patient (4.5%). In another case (4.5%), permanent pacemaker implantation became necessary due to the development of a high-grade atrioventricular block. Concerning complications related to cardiopulmonary bypass (CPB) and the surgical access site, one patient (4.5%) developed a postoperative hematoma in the right groin, while another (4.5%) underwent surgical revision for thoracic hematoma. During a median follow-up period of 11.0 months (3.0–16.5), no deaths were recorded.

**Conclusion:** Aortic Valve replacement by rTX is feasible for a variety of valve pathologies, revealing good clinical outcomes at experienced centers, with its safety and low learning curves encouraging its establishment as potential standard in aortic valve surgery.

## 2-4

### Präoperative Frailty bei Patient:innen mit Transkatheter- versus chirurgischem Aortenklappenersatz: Eine retrospektive vergleichende Analyse ernährungs- und muskelspezifischer Frailty-Marker

**Benedikt P.[1,2], Illek J.[1], Huber F.[1,2], Schachner B.[1], Mamunchak O.[1], Damian I.[1], Szalkiewicz P.[1], Riedlsperger I.[1], Lukas J.[1], Zierer A.[1,2]**

[1]Department of Thoracic and Cardiovascular Surgery, Kepler University Hospital, JKU, Linz, Österreich
[2]Clinical Research Institute for Cardiovascular and Metabolic Diseases, Medical Faculty, Johannes Kepler University, Linz, Österreich

**Einleitung:** Frailty ist ein multidimensionales geriatrisches Syndrom, das durch reduzierte physiologische Reserven und eine erhöhte Vulnerabilität gegenüber Stressoren gekennzeichnet ist. Sie gilt zunehmend als wichtiger Prädiktor für das Outcome nach kardialen Interventionen. Ziel dieser Studie war es, die präoperative Frailty bei Patient:innen mit Transkatheter-Aortenklappenimplantation (TAVI) und chirurgischem Aortenklappenersatz (SAVR) zu vergleichen und deren Einfluss auf postoperative Erholungsparameter zu untersuchen.

**Methoden:** In einer retrospektiven Analyse wurden 80 konsekutive Patient:innen eingeschlossen (40 TAVI, 40 SAVR), die zwischen 2021 und 2022 einen isolierten Aortenklappenersatz an unserer Institution erhielten. Frailty wurde mittels Geriatric Nutritional Risk Index (GNRI) und Psoas Area Index (PAI) bewertet. Primäre Endpunkte waren die postoperative Krankenhausverweildauer (Length of Stay, LOS), die Aufenthaltsdauer auf der Intensivstation (ICU-LOS) sowie die Entlassungsmodalität. Die statistische Auswertung erfolgte mittels deskriptiver Statistik, Mann-Whitney-U-Tests und multivariater linearer Regressionsanalysen.

**Resultate:** TAVI-Patient:innen waren signifikant älter als SAVR-Patient:innen (Medianalter 84 vs. 69 Jahre; $p<0{,}001$) und wiesen niedrigere GNRI-Werte auf (112,06 vs. 119,1; $p=0{,}006$), was auf eine höhere Prävalenz ernährungsbedingter Frailty hinweist. Im PAI zeigte sich kein signifikanter Unterschied zwischen den Gruppen (Männer $p=0{,}117$; Frauen $p=0{,}270$). Trotz höherer Frailty-Belastung hatten TAVI-Patient:innen eine kürzere Krankenhausverweildauer (Median 7 vs. 10 Tage; $p<0{,}001$) sowie eine kürzere ICU-Verweildauer (Median 0 vs. 1 Tag; $p<0{,}001$). Ein niedriger PAI war unabhängig mit einer verlängerten Krankenhausverweildauer assoziiert (+12,1 Tage; $p=0{,}002$; adjustiertes $p=0{,}004$). Fraile Patient:innen hatten zudem längere ICU-Aufenthalte (Median 3 vs. 1 Tage; $p=0{,}012$) und wurden häufiger in Übergangs- oder Rehabilitationseinrichtungen entlassen ($p=0{,}018$). Während der GNRI stärker mit intensivstationsbezogenen Outcomes korrelierte, erwies sich der PAI als besserer Prädiktor für die gesamte Krankenhausverweildauer.

**Schlussfolgerungen:** Präoperative Frailty, insbesondere ernährungsbezogene Risiken gemessen mittels GNRI, ist bei TAVI-Patient:innen häufiger ausgeprägt und beeinflusst die postoperative Erholung signifikant. Die routinemäßige Integration von Frailty-Assessments in die präoperative Evaluation könnte die Risikostratifizierung verbessern, die Therapieentscheidung unterstützen und postoperative Versorgungsstrategien optimieren.

## 2-5

### Establishing Modal Analysis of Arterial Hemodynamics as an Innovative Diagnostic Concept in Vascular Medicine

**Benedikt P.[1,2], Mamunchak O.[1], Szalkiewicz P.[1], Huber F.[1,2], Schachner B.[1], Illek J.[1], Hagleitner G.[3,4], Brunnmayr F.[5], Mikota G.[5], Zierer A.[1,2]**

[1]Department of Thoracic and Cardiovascular Surgery, Kepler University Hospital, JKU, Linz, Austria
[2]Clinical Research Institute for Cardiovascular and Metabolic Diseases, Medical Faculty, Johannes Kepler University, Linz, Austria
[3]Central Radiology Institute, Kepler University Hospital, Linz, Austria
[4]Department of Virtual Morphology, Johannes Kepler University, Linz, Austria
[5]Institute of Machine Design and Fluid Power, Johannes Kepler University, Linz, Austria

**Introduction:** This study evaluates whether modal analysis—a technique that examines the natural vibration patterns of a structure to detect changes in its mechanical properties—can provide a clinically applicable, indirect method of detecting and characterising aneurysms and stenoses.

**Methods:** The arterial tree was conceptualised as a dynamic system driven by pulsatile cardiac pressure. Modal analysis was applied to identify the natural frequencies and mode shapes of arterial blood flow. In vivo validation was performed using ultrasound-based blood velocity measurements acquired at 23 predefined anatomical locations. Data were obtained from sixteen subjects, including healthy volunteers and patients with aortic aneurysms. Velocity-time signals were transformed into frequency spectra using Fourier analysis. Spatial distributions of frequency amplitudes were visualised using normalised heatmaps to enable comparison between individuals and pathological conditions..

**Results:** Distinct and reproducible eigenmodes of the cardiovascular system were identified. The fundamental vibration mode occurred at a frequency of approximately 2 Hz. A total of 19 subjects were examined, including seven patients with diagnosed aortic aneurysms and 12 individuals without aneurysmal disease, spanning a range of ages and genders. In patients with aneurysmal disease, characteristic alterations were observed, including the displacement of vibration nodes and the emergence of additional shapes in the flow pattern. In the presence of stenotic lesions, splitting of single vibration modes into multiple frequency components was detected. Heatmap visualisation (Fig. 1 = Proband 3 is a healthy subject; Proband 6 has an aneurysm of the ascending aotta) enabled the immediate visual differentiation of healthy subjects from patients with vascular pathology using routine ultrasound data.

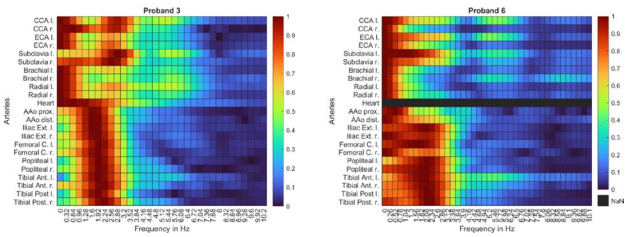


**Fig. 1 | 2-5**

**Conclusion:** Modal analysis of arterial blood flow has not previously been investigated as a diagnostic approach in the cardiovascular system. Given the complex geometry, viscoelastic vessel wall properties, and pulsatile hemodynamics, it was unclear whether distinct and physiologically meaningful eigenmodes could be identified in vivo. In the present study, we demonstrate that eigenmodes can indeed be detected and systematically characterized in the human arterial circulation. This proof-of-concept establishes a novel functional diagnostic modality, the broader clinical implications of which remain to be defined. Importantly, aneurysms were identified indirectly and non-invasively through characteristic alterations in modal patterns, highlighting the potential of modal analysis as an innovative extension of vascular ultrasound and a future tool for screening and decision support in cardiovascular medicine.

## 2-6

### A presentation-outcome paradox in women with acute type A aortic dissection

**Gottsberger J., Huber F., Schachner B., Szalkiewicz P., Zierer A.**

Department of Thoracic and Cardiovascular Surgery, Kepler University Hospital, JKU, Linz, Austria, Linz, Austria

**Introduction:** Sex-specific differences are recognized in cardiovascular medicine, but their relevance in cardiac surgery—particularly in acute aortic syndromes—remains unclear. This study analyzes the impact of sex on outcomes after surgery for acute type A aortic dissection.

**Methods:** We analyzed 336 consecutive patients (33.9% women) treated between January 2017 and December 2025. Baseline characteristics, dissection morphology, operative strategies, and follow-up outcomes were compared between women and men. Endpoints included early and mid-term survival, reoperation, and reintervention. Kaplan–Meier analyses and multivariable regression models were used to assess the impact of sex and perioperative variables on outcomes.

**Results:** Women were significantly older at presentation (66 ± 12 vs. 59 ± 11 years, $p < 0.01$). They required more frequently adrenergic support at presentation (45.6% vs. 32.9%, $p = 0.02$) and had a higher incidence of pericardial tamponade (41.2% vs. 25.7%, $p = 0.003$). Preoperative neurologic symptoms (22.8% vs. 16.7%, $p = 0.17$) and supra-aortic vessel involvement (55.3% vs. 47.1%, $p = 0.15$) were also more common in women. Male patients underwent more often complex reconstructions (aortic arch replacement using the frozen elephant trunk technique: male 23 pts. vs. women 11 pts.; $p < 0.037$). Thirty-day mortality was similar between women and men (16.7% vs. 15.3%, $p = 0.74$). Overall survival at the end of follow-up was comparable (82.5% vs. 80.8%, $p = 0.68$). Rates of reintervention (7.0% vs. 11.7%, $p = 0.61$) and reoperation (7.0% vs. 8.6%, $p = 0.61$) were also comparable.

**Conclusion:** Despite presenting at an older age and in a more critical clinical condition, women achieve postoperative and mid-term outcomes comparable to those of men. These findings suggest that female sex itself does not adversely influence surgical outcomes in this high-risk population. The observed differences in clinical presentation highlight an important knowledge gap. A better understanding of these sex-specific patterns may improve early recognition and optimize management strategies for women with acute aortic dissection.

## 2-7

### Durability of Coronary Bypass Grafts after Ascending Aortic Replacement

**Schmidt S., Renz L., Lohmann R., Nägele F., Hirsch J., Engler C., Grimm M., Bonaros N., Gollmann-Tepeköylü C., Winter-Pölzl L., Graber M.**

Universitätsklinik für Herzchirurgie, innsbruck, Austria

**Introduction:** Coronary artery bypass grafting (CABG) performed during ascending aortic replacement requires proximal graft anastomosis to a prosthetic aortic graft. Whether this configuration affects graft durability remains unclear, as data on mid-term patency in this setting are scarce. We therefore evaluated graft patency after CABG during ascending aortic replacement and examined predictors of graft failure.

**Methods:** Between 2010 and 2024, 270 patients underwent ascending aortic replacement with concomitant CABG at our institution. Graft patency was assessed 12 months postoperatively using contrast-enhanced computed tomography angiography. Imaging follow-up within the predefined interval was available in 118 patients, encompassing 195 bypass grafts, which constituted the study cohort for patency analysis. To account for the hierarchical data structure arising from multiple grafts per patient, associations with graft occlusion were evaluated using mixed-effects logistic regression models with a patient-specific random intercept.

**Results:** At 12 months, 39 grafts were occluded, corresponding to an overall patency rate of 80%. Graft occlusion occurred more frequently in patients with pre-existing coronary artery disease (CAD) than in those without CAD (22.2% vs. 6.7%). Planned procedures were likewise associated with higher graft failure compared with unplanned procedures (22.3% vs. 6.1%), reflecting the greater burden of underlying coronary pathology in this cohort. In contrast, unplanned CABG, most commonly performed in the context of acute aortic dissection, was associated with substantially lower graft occlusion rates than procedures performed in non-dissection cases (3.7% vs. 22.9%). Female sex was also associated with a higher incidence of graft occlusion compared with male patients (25.6% vs. 18.6%).

**Conclusion:** CABG with proximal anastomosis to an ascending aortic prosthesis demonstrates favorable mid-term patency. Pre-existing coronary artery disease and female sex were associated with higher rates of graft occlusion. Notably, unplanned procedures, most frequently performed for acute aortic dissection, exhibited lower graft occlusion rates. These findings suggest that graft durability in this setting is influenced primarily by the underlying coronary pathology rather than procedural urgency.

## 2-8

### Clinical and Morphological Predictors of Outcome After Surgery for Acute Type A Aortic Dissection: A Single-Centre Study of 336 Patients

**Huber F., Gottsberger J., Szalkiewicz P., Schöberl A., Schachner B., Zierer A.**

Department of Thoracic and Cardiovascular Surgery, Kepler University Hospital, JKU, Linz, Austria, Linz, Austria

**Introduction:** Acute type A aortic dissection (ATAAD) is a highly lethal cardiovascular emergency, with mortality increasing by 1–2% per hour if untreated and reaching 15–20% despite emergency surgery. While clinical predictors of poor outcome are well established, the prognostic value of dissection morphology remains unclear. This study aimed to identify independent predictors of early mortality by integrating clinical, intraoperative, and morphological parameters.

**Methods:** All patients who underwent surgical repair for acute type A aortic dissection at our institution between January 2017 and December 2025 were retrospectively analysed. Demographic data, clinical presentation, CT derived morphological characteristics, intraoperative variables, and postoperative outcomes were collected. Independent predictors of early mortality (30 day and in hospital) were identified using multivariable logistic regression. Dissection related morphological risk profiles were further assessed according to the TEM classification.

**Results:** A total of 336 patients (mean age 62 ± 13 years; 33.9% female) underwent surgical repair for acute type A aortic dissection, with a 30 day mortality of 15.8%. Supra aortic vessel involvement was observed in 49.9% of patients. Multivariable analysis identified advanced age (OR 1.04 per year, $p = 0.015$), preoperative intubation (OR 2.86, $p = 0.037$), malperfusion (OR 2.47, $p = 0.016$), and longer cardiopulmonary bypass time (OR 1.01 per minute, $p = 0.044$) as independent predictors of 30 day mortality. Among morphological variables, supra aortic vessel involvement was independently associated with postoperative neurological dysfunction (adjusted OR 1.84, $p = 0.046$), whereas primary entry tear location and overall dissection extent were not associated with early mortality.

**Conclusion:** Early mortality after ATAAD repair is determined by physiological and operative factors, whereas anatomical features—particularly supra aortic vessel involvement—primarily influence neurological complications.

# POSTERSITZUNG 3—HERZCHIRURGIE 2

## 3-1

### CT-Derived Thoracic Muscle Attenuation Predicts Sex-Specific Mid- And Long-Term Mortality After Coronary Artery Bypass Grafting—Sex-Specific Insights Into Risk Stratification and Frailty Assessment

**Krombholz-Reindl P.[1,2], Pilz M.[2], Rassam S.[2], Linni K.[2], Hecht S.[3], Hammerer M.[4], Gottardi R.[5], Boxhammer E.[4], Dinges C.[6], Vötsch A.[7]**

[1]Universitätsklinik für Herzchirurgie, Universitätsklinikum Salzburg, Salzburg, Austria
[2]Universitätsklinik für Gefäßchirurgie und endovaskuläre Chirurgie, Salzburg, Austria
[3]Universitätsklinik für Radiologie, Universitätsklinikum Salzburg, Salzburg, Austria
[4]Universitätsklinik für Innere Medizin II, Kardiologie und internistische Intensivmedizin, Salzburg, Austria
[5]Abteilung für Herz-, Thorax- und Gefäßchirurgie, Kaiserslautern, Germany
[6]Universitätsklinik für Herzchirurgie, Salzburg, Austria
[7]Universitätsklinik für Herzchirurgie, St. Pölten, Austria

**Introduction:** Frailty and impaired muscle quality are strong determinants of adverse outcomes after coronary artery bypass grafting (CABG), yet conventional risk scores overlook this biological dimension. The Hounsfield Unit Average Calculation (HUAC) obtained from routine preoperative computed tomography (CT) quantifies skeletal muscle attenuation, reflecting intramuscular fat infiltration and metabolic reserve. This study evaluated the prognostic value of HUAC measured at two thoracic levels and explored sex-specific differences in its predictive performance.

**Methods:** In this retrospective single-center study, 479 patients (382 men, 97 women) undergoing isolated CABG with available preoperative CT scans were analyzed. Mean HUAC was measured bilaterally at the fourth (TH4) and twelfth (TH12) thoracic vertebral levels. Sex-specific quartiles were generated, with the lowest quartile defining sarcopenia. Associations with 1-, 3-, and 5-year mortality were assessed by Kaplan–Meier analysis, receiver-operating-characteristic (ROC) curves, and sex-stratified Cox regression models incorporating inverse probability weighting (IPW).

**Results:** Patients with low HUAC showed reduced survival at all time points. HUAC measured at TH4 demonstrated superior discriminative ability compared with TH12. In women, TH4 achieved solid predictive accuracy (AUC 0.773 and 0.807 for 1- and 3-year survival), outperforming men (AUC 0.670 and 0.640). In sex-specific Cox analyses, women in the lowest HUAC-TH4 quartile had markedly increased mortality risk (unweighted

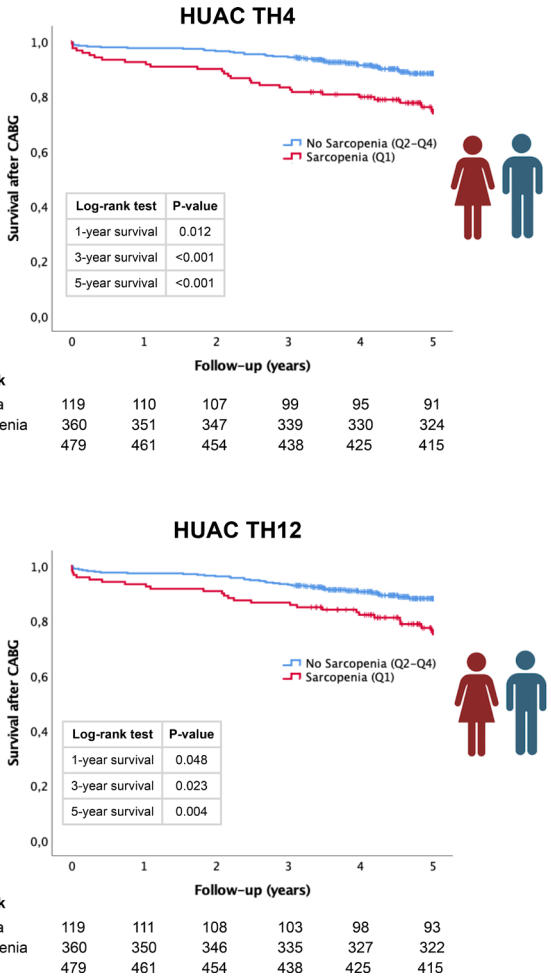


**Fig. 1 | 3-1** Overall Kaplan–Meier Survival According to HUAC at TH4 and TH12

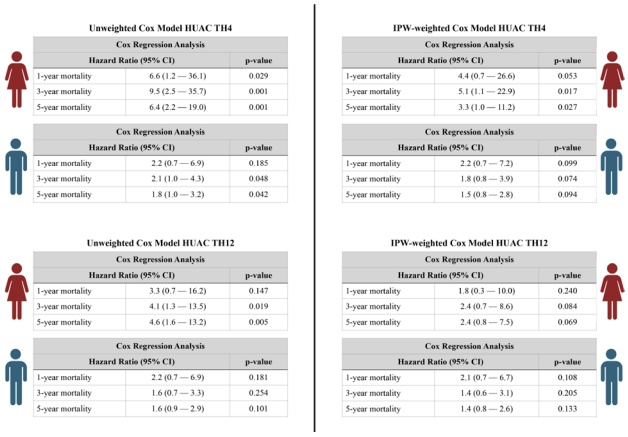


**Fig. 2 | 3-1** Sex-Specific Cox Regression Models for Mid- and Long-Term Mortality After CABG

HRs 6.6, 9.5, and 6.4 for 1-, 3-, and 5-year follow-up; all $p \leq 0.03$), which remained significant after IPW adjustment. In men, the association was weaker and lost significance after weighting.

**Conclusion:** Low thoracic muscle attenuation, particularly HUAC at TH4, independently predicts long-term mortality after CABG, with a stronger and more consistent effect in women. HUAC represents a simple, objective biomarker of physiological reserve that can be derived from existing preoperative CT scans and may enhance individualized risk stratification in contemporary cardiac surgery.

## 3-2

## Bioprosthetic Aortic Valve Replacement Before 60: Acceptable Strategy or Risky Choice?

**Arnold Z.[1,2], Stabernak J.[3,2], Kainz F.[4], Lenz V.[1,2], Moidl R.[2,1], Aschacher T.[1,2], Tauber S.[1,2], Weiss G.[1,2], Grabenwöger M.[1,2]**

[1]Department of Cardiovascular Surgery, Clinic Floridsdorf, Wien, Austria
[2]Institute of Cardiovascular Research, Karl Landsteiner Society, Wien, Austria
[3]Department of Cardiology, Clinic Floridsdorf Vienna, Wien, Austria
[4]Klinische Abteilung für Herzchirurgie, St. Pölten, Austria

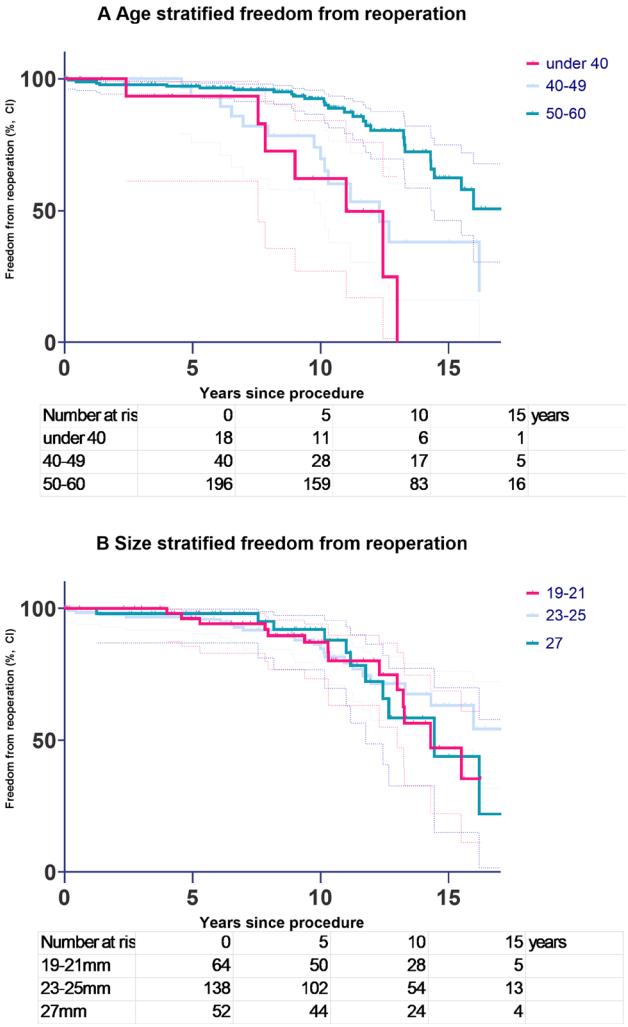


**Fig. 1 | 3-2** Age- and valve size–stratified freedom from reoperation after biological surgical aortic valve replacement

**Introduction:** The use of biological prostheses for surgical aortic valve replacement (SAVR) in younger patients has increased despite guideline recommendations favoring mechanical valves. This study evaluated long-term outcomes, durability, and hemodynamic performance of biological aortic valve prostheses in patients younger than 60 years.

**Methods:** Between January 2005 and December 2016, 256 consecutive patients younger than 60 years underwent biological SAVR. Early and long-term outcomes were analyzed retrospectively. Survival and freedom from reoperation were assessed using the Kaplan–Meier method. Age- and vale size-stratified analyses were performed using the log-rank test. Echocardiographic follow-up was evaluated to assess hemodynamic performance.

**Results:** Mean age was 52.9 ± 7.2 years, and 24.6% of patients were female. Surgery was performed electively in 219 patients (85.5%), urgently in 28 (10.9%), and emergently in 9 (3.5%); infective endocarditis was present in 30 patients (11.7%). Thirty-day mortality was 4.7% overall and 1.9% for isolated procedures. Clinical follow-up was 99.2% complete, with a median duration of 9.6 years (2305 patient-years, maximum 20.6 years). Overall survival was 85.6% and 79.8% at 5 and 10 years, respectively. Freedom from valve-related death was 94.4% at 5 years and 92.4% at 10 years. Freedom from reoperation was 96.4%, 86.8%, and 54.3% at 5, 10, and 15 years, respectively, with a median reoperation-free survival of 15.97 years. Reoperation occurred significantly earlier in younger patients (log-rank $p < 0.0001$). In multivariable Cox regression analysis, younger age independently predicted reoperation, whereas gender, infective endocarditis, prosthesis–patient mismatch, and prosthesis size were not significant predictors. Smaller prostheses showed higher transvalvular gradients, but prosthesis size was not associated with reoperation risk.

**Conclusion:** Biological surgical aortic valve replacement in patients younger than 60 years provided favorable long-term survival and acceptable durability. Younger age at the time of surgery was strongly associated with earlier need for reoperation. Although smaller prosthesis sizes were associated with less favorable hemodynamic performance, this did not translate into a higher rate of reoperation.

## 3-3

### Minimally Invasive Mitral Valve Repair for Bileaflet Prolapse: Technical Success, Safety, and Long-Term Outcomes

**Spilka J.[1], Lehmann R.[1], Winter-Pölzl L.[1], Stastny L.[1], Nägele F.[1], Theurl M.[2], Grimm M.[1], Höfer D.[1], Gollmann-Tepeköylü C.[1], Bonaros N.[1]**

[1]Universitätsklinik für Herzchirurgie, Medizinische Universität, Innsbruck, Austria
[2]Universitätsklinik für Kardiologie und Angiologie, Medizinische Universität, Innsbruck, Austria

**Introduction:** Degenerative mitral regurgitation is the most common underlying pathology in patients undergoing minimally invasive and endoscopic mitral valve repair. In contrast to isolated posterior leaflet disease, bileaflet prolapse represents a more complex degenerative phenotype frequently associated with extensive myxomatous degeneration. While contemporary repair techniques allow reproducible results in endoscopic surgery, perioperative safety, technical success, and long-term durability of repair in bileaflet prolapse remain uncertain.

**Methods:** We performed a retrospective single-high-volume centre study including all patients undergoing minimally invasive surgery for bileaflet mitral valve prolapse at our centre between 2001 and 2025. Long-term outcome analysis was restricted to patients with a mitral valve repair. Follow-up was obtained through systematic review of available medical records, serial echocardiographic studies and correspondence with referring physicians. Survival status was verified through linkage with the national death registry. Time-to-event outcomes were analysed using Kaplan–Meier estimates for overall survival, freedom from mitral valve reoperation, and freedom from recurrent severe mitral regurgitation.

**Results:** A total of 180 patients with bileaflet prolapse underwent video-assisted or totally endoscopic surgery. Nineteen patients received a primary mitral valve replacement, whereas 161 patients underwent attempted mitral valve repair. Conversion to sternotomy occurred in 4 patients (2.5%), and failed repair resulting in a replacement occurred in 4 patients, resulting in a final repair rate of 97.5%. Technical success, defined as successful repair without intraoperative complications such as systolic anterior motion, circumflex artery compromise, or the need for re-clamping, was achieved in 91.3% of cases. Perioperative safety, defined as freedom from major adverse events within 30 days according to MVARC-based criteria was 87,3%. Four patients were lost to follow-up, leaving 153 patients available for long-term analysis. Mean age was 58.7 ± 12.2 years, 67.5% were male, 28% had preoperative atrial fibrillation, mean left ventricular ejection fraction was 60 ± 7%, and median EuroSCORE II 0.89% (IQR 0.5–1.7). Median follow-up was 7.2 years (IQR 4.0–12.5) with a maximum follow-up of 20.3 years. Estimated overall survival after mitral valve repair was 92.9% at 5 years, 83.6% at 10 years, and 71.7% at 15 years. Freedom from mitral valve reoperation was 97.2% at 5 years and 92.6% at 10 years. Freedom from recurrent severe mitral regurgitation was 98.9% at 5 years and 90.9% at 10 years.

**Conclusion:** Minimally invasive and endoscopic mitral valve repair for bileaflet prolapse provides excellent long-term results and repair durability. Perioperative safety and technical success are high even for complex pathologies.

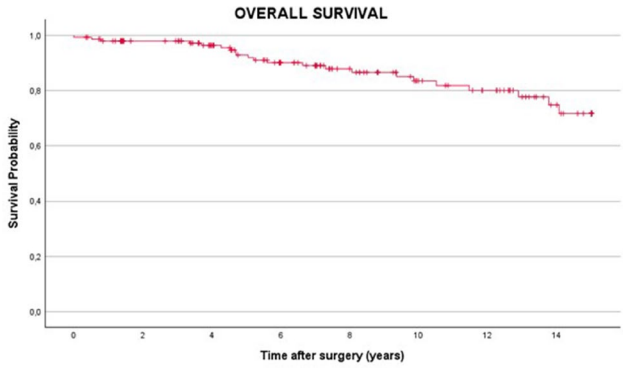


**Fig. 1 | 3-3** Kaplan-Meier estimator for overall survival

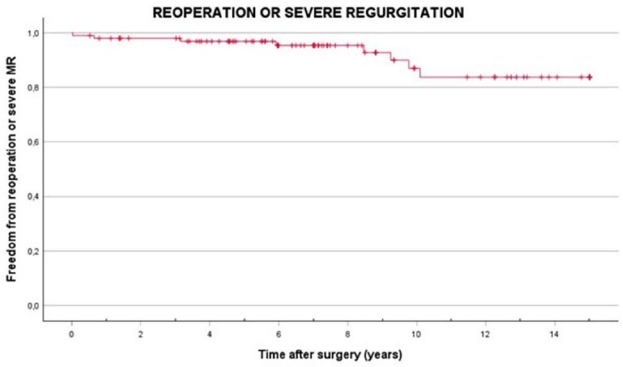


**Fig. 2 | 3-3** Kaplan-Meier estimator for reoperation or recurrent severe mitral regurgitation

## 3-4

### Evaluating the Feasibility of a Novel Device for Enhanced Control of ePTFE Chordal Length Assessment in Mitral Valve Surgery: A Porcine Model Study

**Poschner T.[1], Dimonte G.[2], Mach M.[1], Caracioni A.[1], Putz T.[1], Tasdelen S.[2], Saidian S.[3], Bartz R.[3], Sauer J.[3,4], Andreas M.[1]**

[1]Division of Cardiac Surgery, Medical University of Graz, Graz, Austria
[2]Christian Doppler Laboratory for Microinvasive Heart Surgery, Division of Cardiac Surgery, Medical University of Graz, Graz, Austria
[3]LSI SOLUTIONS®, Victor, NY, United States
[4]Division of Cardiac Surgery, University of Rochester Medical Center, New York, United States

**Introduction:** Chordal length assessment is a key step in mitral valve repair. Using conventional techniques, suture length alterations may occur during knot fixation, potentially compromising outcomes. A novel chordal holder was evaluated in an ex vivo porcine model to temporarily secure expanded polytetrafluoroethylene (ePTFE) sutures during pressurized saline testing, enabling adjustments of chordal length prior to permanent fixation.

**Methods:** Three surgeons performed mitral valve repair in 20 ex vivo porcine hearts with induced Carpentier type II mitral regurgitation. An automated suturing device was used to implant ePTFE sutures. The novel device temporarily secured ePTFE sutures at a chosen length during pressurized saline test-

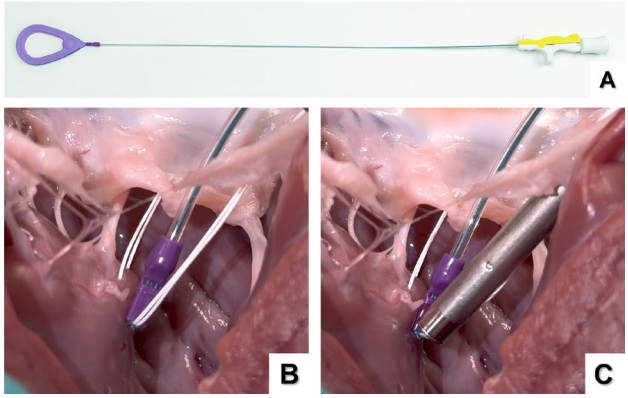


Fig. 1 | 3-4

ing. Sutures were then secured with a customized titanium fastener. Procedural times and valve competency were evaluated.

**Results:** A total of 37 ePTFE chordae were placed. The novel device maintained precise suture length during saline testing. The median time per chord was 3 min and 20 sec (IQR 2:21;5:14). Typically, 1 to 2 chordae were placed for isolated P2 prolapse, and up to 4 for non-isolated P2 lesions. Residual mitral regurgitation greater than trace was absent in all cases.

**Conclusion:** The novel device offers secure temporary fixation and facilitates readjustments of chordal length. This technology has the potential to improve the consistency of MVr and warrants further investigation in animal and clinical trials.

## 3-5

## Human Myocardial Transcriptomics Reveal Biglycan as a Central Angiogenic Mediator of Cardiac Shock Wave Therapy

**Nägele F.[1], Plattner C.[2], Pölzl L.[1], Schmidt S.[1], Hirsch J.[1], Engler C.[1], Iannou-Nikolaidou M.[1], Heim V.[1], Eder J.[1], Lohmann R.[1], Troger F.[3], Mayr A.[3], Trajanoski Z.[2], Bonaros N.[1], Grimm M.[1], Graber M.[1], Gollmann-Tepeköylü C.[1], Holfeld J.[1]**

[1]Universitätsklinik für Herzchirurgie, Medizinische Universität Innsbruck, Innsbruck, Austria
[2]Division of Bioinformatics, Medizinische Universität Innsbruck, Innsbruck, Austria
[3]University Clinic of Radiology, Medical University of Innsbruck, Innsbruck, Austria

**Introduction:** Revascularization strategies in ischemic heart failure improve symptoms but fail to restore myocardial function. The CAST-HF randomized controlled trial demonstrated that adding intraoperative cardiac shockwave therapy (SWT) to coronary artery bypass grafting (CABG) safely improved left ventricular ejection fraction (LVEF) and physical capacity at one year in patients suffering from ischemic heart failure. However, the molecular mechanisms underlying SWT-induced myocardial recovery remain elucidated. Mechanistic validation is crucial to wider adoption of novel treatment strategies, hence embedding of mechanistic endpoints within randomized frameworks represents an underused yet powerful tool to strengthen translation from bench to bedside. This study aimed to validate transcriptomic findings of human myocardial biopsies obtained during the CAST-HF trial.

**Methods:** This secondary analysis investigates the molecular mechanism underlying the treatment effects observed in the CAST-HF randomized controlled trial (NCT03859466), in which patients with ischemic heart failure were assigned 1:1 to receive intraoperative direct cardiac shockwave therapy (SWT) or sham treatment in addition to CABG. Left ventricular biopsies were collected intraoperatively before and after SWT or Sham treatment. Bulk RNA sequencing was subsequently performed, followed by gene expression and pathway analysis to identify key regulators of SWT response. Relevant cardiac cell types were defined with Single-nucleus RNA sequencing, followed by functional validation of BGN in human endothelial cells and in a murine myocardial infarction model using wild-type and $Bgn^{-/-}$ mice. All laboratory analyses were blinded to treatment allocation, preserving the randomized structure of the parent trial.

**Results:** Of the originally 63 randomized patients, in a total of 30 patients (SWT $n=13$; Sham $n=17$), intraoperative myocardial biopsy samples were taken. In the intention-to-treat analysis LVEF remained significantly higher in the SWT group at 180 days compared with sham (12.2% vs. 6.8%; $p=0.05$). Transcriptomic profiling revealed 87 differentially expressed genes, with biglycan (BGN) emerging as a top upregulated target. Single-nucleus RNA-seq reveled endothelial cells, fibroblasts and smooth muscle cells as the main mediators. In vitro, functional assays confirmed that SWT enhanced endothelial proliferation, migration, and tube formation, all of which were abolished by BGN silencing. In $Bgn^{-/-}$ mice, SWT failed to improve LVEF or reduce myocardial fibrosis, but enhanced recovery in wild-type mice, establishing BGN as an essential mediator of SWT-induced cardiac regeneration.

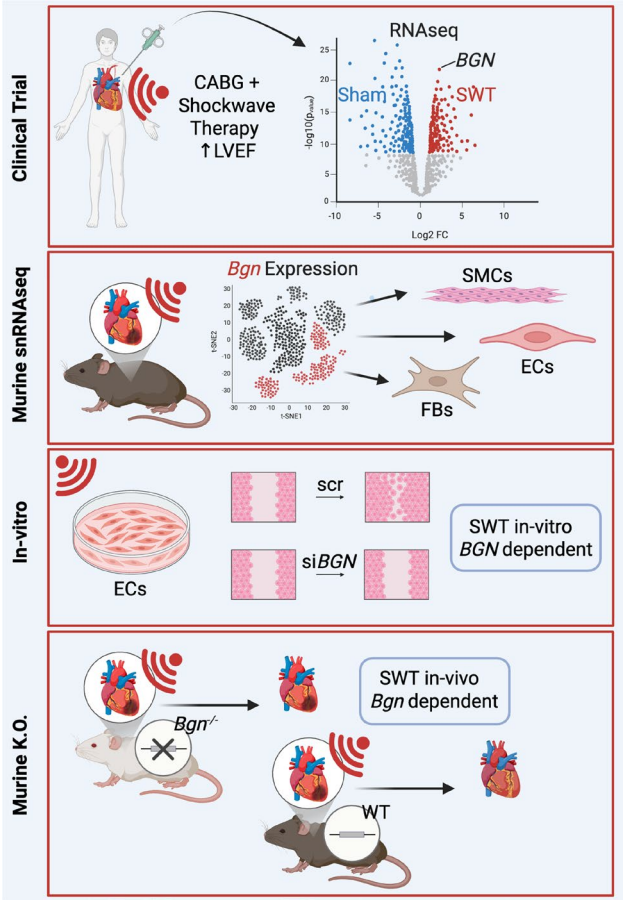


Fig. 1 | 3-5 Graphical Abstract

**Conclusion:** This integrative mechanistic analysis of the CAST-HF randomized trial identifies biglycan as a central effector of the SWT response and validates its role in promoting angiogenesis and functional recovery. Beyond its biological insights, this study exemplifies the methodological potential of including molecular analysis into early-phase to bridge the gap between bench and bedside. Thereby, the translational credibility gets enhanced, and the use of existing patient cohorts is maximized.

## 3-6

### Five-year outcomes from the IMPACT registry

**Damian I.[1], Bakhtiary F.[2], Bonaros N.[3], Benedikt P.[1], Gökler J.[1], Illek J.[1], Zierer A.[1]**

[1]Kepler Universitätsklinikum, Linz, Austria
[2]Herzzentrum Bonn, Bonn, Germany
[3]Meduni Innsbruck, Innsbruck, Austria

**Introduction:** An early overview of midterm safety, haemodynamic performance, and valve durability is provided for patients undergoing surgical aortic valve replacement (SAVR) with a novel bioprosthetic valve in the real-world IMPACT cohort of patients with diverse comorbidities.

**Methods:** IMPACT is a prospective, open-label, multicentre, international study that enrolled consecutive patients undergoing SAVR with a bioprosthetic valve between December 2019 and June 2021 at 21 sites. Here we report preliminary 5-year outcomes for the total cohort, focusing on clinical outcomes as well as haemodynamic performance. This analysis represents an early look at closing-phase data ahead of final study completion in 2026.

**Results:** 556 patients were enrolled with a mean age of 63.4±8.5 years, EuroSCORE II of 2.2±2.5% and STS score of 1.7±2.2%; 29.0% were female. 5-year event rates for all-cause mortality, cardiovascular mortality, stroke, reintervention, and haemodynamic valve deterioration were reported (Table 1). Left ventricular mass index decreased post-discharge and remained low through 5 years (128.5 at baseline, 107.1 at 1 year, and 105.2 g/m2 at 5 years). Haemodynamic performance likewise improved early and sustained levels until 5 years: mean aortic valve gradient was 42.7 at baseline, decreasing to 11.3 at 1 year and 11.9 mmHg at 5 years, while baseline indexed effective orifice area increased from 0.5 at baseline to 0.9 and 0.8 cm2 at 1 and 5 years, respectively. Preliminary findings indicate stable haemodynamic performance, with preserved gradients and effective orifice areas at 5 years.

**Conclusion:** Bioprosthetic surgical aortic valve replacement showed sustained haemodynamic performance and good overall outcomes at 5 years in a real-world population. Final results, including complete follow-up, will be reported after study close-out.

## 3-7

### Drei Dekaden MIDCAB: Retrospektive Analyse eines Single-Center-Erfolgsmodells

**Gadelkarim I.[1,2], de Waha S.[3], Ahmadli A.[1], Schroeter T.[1], Kiefer P.[1], Daschkevich A.[1], Holzhey D.[1], Verevkin A.[1], Davierwala P.[4,5], Borger M.[1]**

[1]Universitätsklinik für Herzchirurgie, Herzzentrum Leipzig, Leipzig, Deutschland
[22] Universitätsklinik für Herz-, Gefäß- und Thoraxchirurgie, Johannes Kepler Universität Linz, Kepler Universitätsklinikum, Linz, Österreich
[3]Abteilung für Rhythmologie, Schleswig-Holstein Uniklinikum, Lübeck“ Deutschland
[4]Abteilung für Herz- und Gefäßchirurgie, Peter Munk Cardiac Center, Toronto General Hospital, University Health Network, University of Toronto, Toronto, Kanada
[5]Abteilung für Chirurgie, University of Toronto, Toronto, Kanada

**Einleitung:** Die minimalinvasive direkte koronare Bypass-Operation (MIDCAB) ermöglicht eine Revaskularisation der Arteria mammaria interna sinistra (LIMA) auf den Ramus interventrikularis anterior (Left anterior descendig artery) (LAD) über eine anterolaterale Minithorakotomie, wodurch eine Sternotomie und der Einsatz einer Herz-Lungen-Maschine vermieden werden. Während bereits über günstige mittel- und langfristige Ergebnisse berichtet wurde, liegen nur begrenzte Daten für Zeiträume von über 20 Jahren vor. Diese Studie untersuchte

**Figure 1. Study Flowchart**

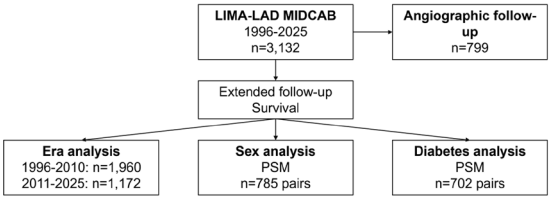


LAD= left anterior descending artery, LIMA=left internal mammary artery, PSM= propensity score matching

**Abb. 1 | 3-7**

**Figure 2. Kaplan-Meier-Schätzung des Langzeitüberlebens in der Gesamtkohorte.**

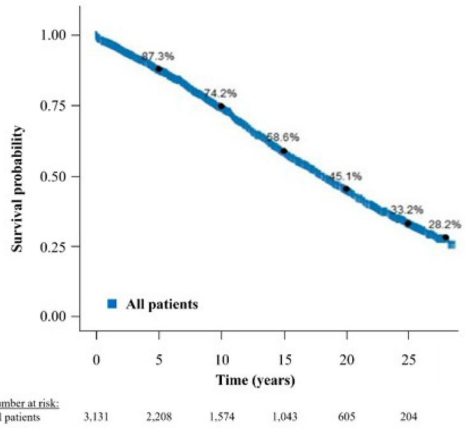


**Abb. 2 | 3-7**

**Tab. 1 | 3-7** Baseline patient characteristics

| | Overall (*n*=3,132) | 1996–2010 (*n*=1,960) | 2011–2025 (*n*=1,172) | *p*-value |
|---|---|---|---|---|
| Age - years, median (IQR) | 65.3 (57.5;72.8) | 64.1 (56.1;71.1) | 67 (60;72.8) | <0.001 |
| Female sex, n (%) | 793 (25.3) | 535 (27.3) | 258 (22.0) | 0.001 |
| Body mass index - kg/m², median (IQR) | 27.7 (25.1;30.5) | 27.4 (25;30.1) | 27.8 (25.1;30.9) | 0.007 |
| EuroSCORE II, median (IQR) | 2.07 (1.22;3.77) | 1.85 (1.22;3.47) | 2.54 (1.51;4.79) | <0.001 |
| *Comorbidities* | | | | |
| Systemic hypertension, n (%) | 2,635 (84.1) | 1,532 (78.1) | 1,103 (84.1) | <0.001 |
| Diabetes mellitus, n (%) | 702 (22.4) | 285 (14.5) | 417 (35.6) | <0.001 |
| COPD, n (%) | 144 (4.6) | 78 (4) | 66 (5.6) | 0.041 |
| Peripheral vascular disease, n (%) | 478 (15.2) | 287 (14.6) | 191(16.2) | 0.21 |
| Prior PCI, n (%) | 719 (23) | 344 (17.6) | 375 (32) | <0.001 |
| Preoperative CVA, n (%) | 102 (3.3) | 61 (3.1) | 41 (3.5) | 0.63 |
| Preoperative dialysis, n (%) | 34 (1.1) | 21 (1.1) | 13 (1.1) | 0.92 |
| Preoperative atrial fibrillation, n (%) | 261 (8.3) | 80 (4.1) | 181 (15.4) | <0.001 |
| *Left ventricular function* | | | | |
| LVEF - %, median (IQR) | 60 (50;67) | 62 (53;70) | 56 (48;62) | <0.001 |
| LVEF ≥50%, n (%) | 2,409 (76.9) | 1,613 (82.2) | 797 (67.9) | <0.001 |
| HFmrEF, n (%) | 402 (12.8) | 154 (7.8) | 248 (21.1) | <0.001 |
| HFrEF, n (%) | 321 (10.2) | 193 (9.8) | 128 (10.9) | 0.33 |
| *Extent of coronary artery disease* | | | | |
| Left main disease, n (%) | 125 (3.9) | 25 (1.2 ) | 100 (8.5) | <0.001 |
| 1-vessel disease, n (%) | 1,617 (51.6) | 1,182 (60.3) | 435 (37.1) | <0.001 |
| 2-vessel disease, n (%) | 865 (27.6) | 497 (25.4) | 368 (31.4) | <0.001 |
| 3-vessel disease, n (%) | 645 (20.5) | 277 (14.1) | 368 (31.4) | <0.001 |

Categorical variables expressed as number (percentage), continuous variables expressed as median (interquartile range).
*COPD* chronic obstructive pulmonary disease; *CVA* cerebrovascular accident; *HFmrEF* heart failure with mildly reduced ejection fraction (LVEF 41%-49%); *HFrEF* heart failure with reduced ejection fraction (LVEF ≤40%) *IQR* interquartile range; *LVEF* left ventricular ejection fraction; PCI percutaneous coronary intervention.

**Tab. 2 | 3-7** Intra- and postoperative characteristics

| | Overall (*n*=3,132) | 1996–2010 (*n*=1,960) | 2011–2025 (*n*=1,172) | *p*-value |
|---|---|---|---|---|
| *Intraoperative parameters* | | | | |
| Length of surgery - min, median (IQR) | 113 (90;139) | 107 (88;135) | 122 (98;145) | <0.001 |
| Conversion to on-pump, n (%) | 50 (1.6) | 49 (0.025) | 1 (0.001) | <0.001 |
| Conversion to sternotomy, n (%) | 31 (0.9) | 31 (1.6) | 0 (0) | <0.001 |
| *Postoperative parameters* | | | | |
| Low cardiac output, n (%) | 32 (1) | 30 (1.5) | 2 (0.2) | 0.02 |
| IABP, n (%) | 12 (0.4) | 11 (0.6) | 1 (0.1) | 0.31 |
| ECMO, n (%) | 4 (0.1) | 1 (0.05) | 3 (0.3) | 0.30 |
| Revision for bleeding, n (%) | 54 (1.7) | 26 (1.3) | 28 (2.4) | 0.04 |
| Cardiac arrhythmias, n (%) | 556 (17.8) | 290 (14.8) | 266 (22.7) | <0.001 |
| Postoperative CVA, n (%) | 7 (0.2) | 3 (0.2) | 4 (0.3) | 0.49 |
| Postoperative wound infection, n (%) | 6 (0.2) | 5 (0.3) | 1 (0.1) | 0.53 |
| Postoperative dialysis, n (%) | 30 (1) | 18 (0.9) | 12 (1) | 0.92 |
| LIMA-LAD revision, n (%) | 71 (2.3) | 65 (3.3) | 6 (0.5) | <0.001 |
| Length of hospital stay - days, median (IQR) | 8 (7;10) | 8 (7;10) | 7 (6;9) | <0.001 |
| In-hospital mortality, n (%) | 23 (0.7) | 17 (0.9) | 6 (0.6) | 0.36 |

Categorical variables expressed as number (percentage), continuous variables expressed as median (interquartile range).
*CVA* cerebrovascular accident; *ECMO* extracorporeal membrane oxygenation; *IABP* intraaortic balloon pump; *IQR* Interquartile range; *LAD* left anterior descending; *LIMA* left internal mammary artery.

**Tab. 3 | 3-7** Multivariable cox-regression predictors for long-term survival

| | Hazard ratio | 95% confidence interval | *p*-value |
|---|---|---|---|
| Age | 1.06 | 1.06–1.07 | <0.001 |
| Female sex | 0.71 | 0.62–0.80 | <0.001 |
| Systemic hypertension | 1.07 | 0.92–1.25 | 0.37 |
| Diabetes mellitus | 1.57 | 1.36–1.81 | <0.001 |
| COPD | 1.73 | 1.38–2.17 | <0.001 |
| Peripheral vascular disease | 1.59 | 1.37–1.83 | <0.001 |
| Preoperative CVA | 1.30 | 1.00–1.67 | 0.047 |
| Preoperative dialysis | 2.66 | 1.77–3.98 | <0.001 |
| Left main disease | 1.12 | 0.82–1.52 | 0.47 |
| 2-vessel disease | 1.24 | 1.09–1.42 | 0.001 |
| 3-vessel disease | 1.52 | 1.31–1.77 | <0.001 |

*COPD* chronic obstructive pulmonary disease; *CVA* cerebrovascular acc

die postoperativen Ergebnisse, die Offenheitsrate der LIMA-Grafts sowie das langfristige Überleben in einer großen Single-Center-Kohorte über einen Zeitraum von drei Jahrzehnten.

**Methoden:** Zwischen Januar 1996 und Januar 2025 unterzogen sich 3132 konsekutive Patienten an einem Zentrum der Maximalversorgung einer MIDCAB-Operation mit LIMA-Anastomose auf den LAD. Die klinischen Daten wurden prospektiv erhoben und retrospektiv analysiert. Mittels Propensity-Score-Matching wurden Analysen nach Ära (1996–2010: $n=1960$; 2011–2025: $n=1172$), Geschlecht ($n=785$ Paare) und Diabetes mellitus ($n=702$ Paare) durchgeführt. Die Offenheitsrate der LIMA-Grafts wurde bei Patienten evaluiert, die sich einer klinisch indizierten koronare Angiographie unterzogen ($n=797$).

**Resultate:** Das mediane Alter lag bei 65,3 Jahren (Interquartilsabstand [IQR] 57,5–72,8) und 25,3 % der Patienten waren weiblich. Die Krankenhausmortalität betrug 0,7 %. Das geschätzte Überleben nach 5, 10, 15, 20, 25 und 28 Jahren lag

**Figure 3.A Kaplan-Meier-Schätzung des long-term LIMA-LAD Graft Offenheitsrate**

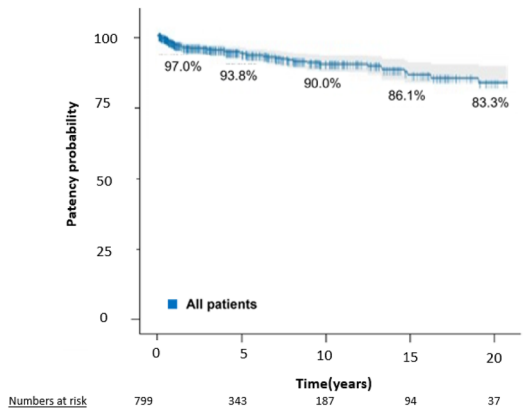


LAD= left anterior descending, LIMA= left internal mammary artery

**Figure 3 B. Cox-Regressionsanalyse zur Identifizierung von Prädiktoren für ein LIMA-LAD-Graft Versagen**

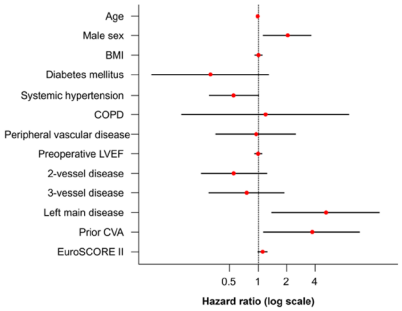


**BMI** body mass index; **COPD** chronic obstructive pulmonary disease; **CVA** cerebrovascular accident; **LAD** left anterior descending artery; **LIMA** left internal mammary artery; **LVEF** left ventricular ejection fraction.

**Abb. 3 | 3-7**

**Figure 4.A Kaplan-Meier-Schätzung des Langzeitüberlebens in der Propensity-Score-gematchten Ären-Analyse.**

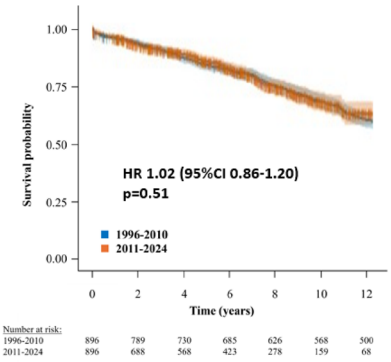


**CI=** confidence interval, **HR=** Hazard ration

**Figure 4.B Kaplan-Meier-Schätzung des Langzeitüberlebens in der Propensity-Score-gematchten Diabetes-Analyse.**

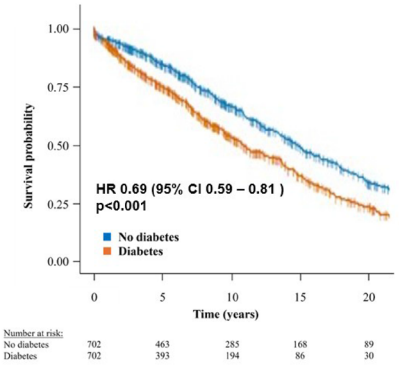


**CI=** confidence interval, **HR=** hazard ratio

**Figure 4 C. Kaplan-Meier-Schätzung des Langzeitüberlebens in der Propensity-Score-gematchten Geschlechter-Analyse.**

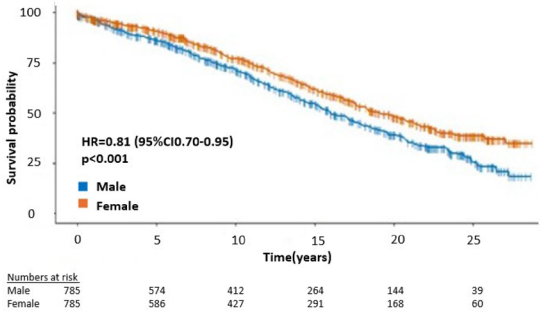


**CI=** confidence interval, **HR=** hazard ratio

**Abb. 4 | 3-7**

bei jeweils 87,3 %, 74,2 %, 58,6 %, 45,1 %, 33,2 % und 28,2 %. Nach dem Propensity-Score-Matching war das Langzeitüberleben zwischen der frühen und der aktuellen Operationsära vergleichbar ($p=0,51$), während das Überleben bei Nicht-Diabetikern (49,7 % vs. 23,7 %, $p<0,001$) und weiblichen Patienten (38,5 % vs. 25,3 %, $p<0,001$) signifikant besser war. Die Offenheitsrate der LIMA-Grafts nach 1, 5, 10, 15 und 20 Jahren betrug entsprechend 97,0 %, 93,8 %, 90,0 %, 86,1 % und 83,3 %.

**Schlussfolgerungen:** In dieser fast drei Jahrzehnte umfassenden Single-Center-Erfahrung war die MIDCAB mit einem günstigen Langzeitüberleben und einer dauerhaften Offenheit des LIMA-LAD-Grafts assoziiert. Diese Ergebnisse bestätigen die MIDCAB als robuste Revaskularisationsstrategie bei Erkrankungen des LAD für entsprechend selektierter Patienten.

## 3-8

## Behandlung der In-Stent-Restenose im Ramus interventricularis Anterior: Minimalinvasive Chirurgie im Vergleich zur perkutanen Intervention

**Gadelkarim I.[1,2], Urbschat M.[1], Elrabai M.[1], Kiefer P.[1], Holzhey D.[1], Daschkevich A.[1], Noack T.[1], Verevkin A.[1], Borger M.[1]**

[1]Universitätsklinik für Herzchirurgie, Herzzentrum Leipzig, Leipzig, Deutschland
[22] Universitätsklinik für Herz-, Gefäß- und Thoraxchirurgie, Johannes Kepler Universität Linz, Kepler Universitätsklinikum, Linz, Österreich

**Einleitung:** Trotz Fortschritten im Stent-Design und bei Angioplastie-Techniken bleibt die In-Stent-Restenose (ISR) mit einer Inzidenz von bis zu 10 % eine wesentliche Limitation der perkutanen Koronarintervention (PCI). Die minimalinvasive chirurgische Revaskularisation (MIDCAB) des Ramus interventricularis anterior (LAD) unter Verwendung der Arteria mammaria interna sinistra (LIMA) stellt eine attraktive, jedoch bisher wenig untersuchte Option für Patienten mit In-Stent-Restenose dar. Ziel unserer Studie war es daher, die MIDCAB mit den besten verfügbaren PCI-Techniken im Management der ISR zu vergleichen.

**Methoden:** Zwischen 2007 und 2024 wurden die Daten von Patienten mit einer ISR des LAD prospektiv erhoben und retrospektiv analysiert. Die Patienten wurden entweder mit einer erneuten PCI ($n=407$) oder einer MIDCAB ($n=153$) behandelt. Die PCI wurde ausschließlich mit Drug-Eluting-Stents (DES) der zweiten Generation durchgeführt, mit oder ohne Einsatz von medikamentenbeschichteten (DEB) oder nicht-medikamentenbeschichteten Ballons. Ein 1:1 Propensity-Score-Matching (PSM) wurde angewandt, um Baseline-Confounder bereinzigen. Der primäre Endpunkt war ein kombinierter Endpunkt aus Langzeitüberleben und Freiheit von einer erneuten Revaskularisation; sekundäre Endpunkte waren das Überleben sowie Sicherheitsoutcomes.

**Resultate:** Die meisten Fälle von LAD-ISR traten sehr spät auf (68,9 %), mit einem Median von 4,6 Jahren zwischen der ursprünglichen Stentimplantierung (Index-Stenting) und der Re-Intervention. Die 30-Tage-Mortalität war zwischen einer erneuten PCI (2,0 %) und der MIDCAB (0,7 %, $p=0,47$) vergleichbar. Ein frühes Stentversagen trat in 1,4 % der Fälle nach PCI auf, ein frühes Graft Versagen in 0,6 % nach MIDCAB ($p=0,44$), was auch nach dem Matching nicht signifikant blieb. Die Krankenhausaufenthaltsdauer war bei der PCI kürzer (Median 1 Tag [IQR 1–3]) im Vergleich zur MIDCAB (9 Tage [IQR 8–14], $p<0,001$). Über einen medianen Nachbeobachtungszeitraum von 7,3 Jahren zeigte die Propensity-Score-gematchte Analyse ein überlegenes 15-Jahres-Überleben ohne erneute Revaskularisation bei der MIDCAB (53,8 %, 95 % Konfidenzintervall [KI] 43,3–66,9) im Vergleich zur PCI (41,0 %, 95 % KI 30,9–54,4; $p=0,004$).

**Schlussfolgerungen:** MIDCAB- und Re-PCI-Ansätze sind gleichermaßen sicher. MIDCAB bietet jedoch eine effektivere Option für Patienten mit einer ISR, was sich im kombinierten Langzeitendpunkt aus Überleben und Freiheit von einer erneuten Revaskularisation widerspiegelt.

**Figure 1 Love plot of matching variables with standardized mean differences (SMD)**

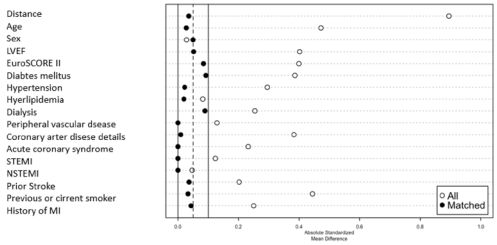


LVEF= left ventricular ejection fraction, STEMI= ST-elevation myocardial infarction, NSTEMI= non ST-elevation myocardial infarction, MI= myocardial infarction

**Abb. 1 | 3-8** Love plot of matching variables with standardized mean differences (SMD)

**Figure 2. Kaplan-Meier estimated long-term survival in the matched cohort.**

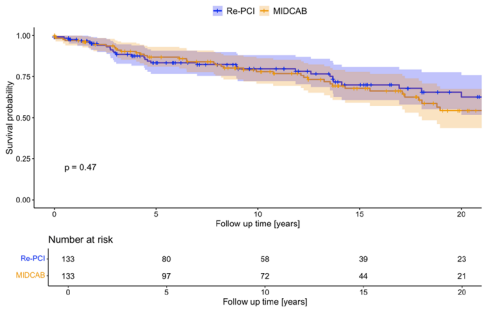


Survival at 20 years: Re-PCI 62.6% (95%-CI 51.7;75.9), MIDCAB 54.3% (95%-CI 43.7;67.5)
Re-PCI= repeat percutaneous coronary intervention, MIDCAB= minimally invasive direct coronary artery bypass grafting

**Abb. 2 | 3-8** Kaplan-Meier estimated long-term survival in the matched cohort

**Figure 3. Kaplan-Meier estimated long-term freedom from the combined endpoint of death and repeat LAD revascularization in the matched cohort.**

MATCHED

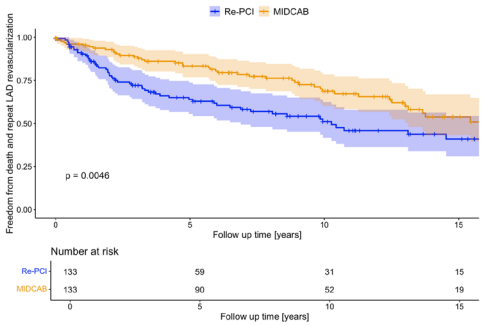


Repeat revascularization free survival at 15 years: Re-PCI 41% (95%-CI 30.9;54.4), MIDCAB 53.8% (95%-CI 43.3;66.9)
Re-PCI= repeat percutaneous coronary intervention, MIDCAB= minimally invasive direct coronary artery bypass grafting

**Abb. 3 | 3-8** Kaplan-Meier estimated long-term freedom from the combined endpoint of death and repeat LAD revascularization in the matched cohort

**Tab. 1 | 3-8** MATCHING VARIABLES BEFORE AND AFTER 1:1 PROPENSITY SCORE MATCHING

| | BEFORE MATCHING | | | POST 1:1 MATCHING | | |
|---|---|---|---|---|---|---|
| | Re-PCI *n* = 407 | MIDCAB *n* = 153 | SMD | Re-PCI *n* = 133 | MIDCAB *n* = 133 | SMD |
| Age [y] | 71 (61.5,77) | 65 (57,73) | *0.473* | 65 (57,73.5) | 66 (58.5,73) | 0.028 |
| Female sex | 96 (23.6) | 38 (24.8) | 0.029 | 36 (27.1) | 32 (24.1) | 0.05 |
| Preop LVEF [%] | 55 (45,60) | 58 (49,63) | *0.402* | 57 (50,61.5) | 58 (47,63) | 0.052 |
| EuroSCORE II [%] | 2.75 (1.47,6.4) | 2.28 (1.33,3.59) | *0.4* | 1.8 (0.95,3.14) | 2.36 (1.59,3.7) | 0.084 |
| Diabetes | 204 (50.1) | 49 (32) | *0.387* | 52 (39.1) | 48 (36.1) | 0.092 |
| Hypertension | 398 (97.8) | 135 (88.2) | *0.296* | 127 (95.5) | 127 (95.5) | 0.022 |
| Dyslipidemia | 331 (81.3) | 129 (84.3) | 0.082 | 116 (87.2) | 114 (85.7) | 0.02 |
| Preop dialysis | 11 (2.7) | 1 (0.7) | *0.254* | 2 (1.5) | 1 (0.8) | 0.089 |
| Peripheral arterial disease | 73 (17.9) | 21 (13.7) | *0.129* | 20 (15) | 20 (15) | 0 |
| Extent of CAD | | | *0.383* | | | 0.009 |
| 1-vessel | 103 (25.3) | 71 (46.4) | | 46 (34.6) | 61 (45.9) | |
| 2-vessel | 164 (40.3) | 49 (32) | | 61 (45.9) | 40 (30.1) | |
| 3-vessel | 153 (37.6) | 33 (21.6) | | 24 (18) | 32 (24.1) | |
| ACS at admission | 143 (35.1) | 39 (25.5) | *0.232* | 31 (23.3) | 30 (22.6) | 0 |
| STEMI at admission | 1 (0.2) | 3 (2) | *0.124* | 1 (0.8) | 0 (0) | 0 |
| NSTEMI at admission | 68 (16.7) | 23 (15) | 0.047 | 19 (14.3) | 19 (14.3) | 0 |
| Prior stroke | 30 (7.4) | 6 (3.9) | *0.202* | 60 (45.1) | 59 (44.4) | 0.037 |
| Previous or current smoker | 253 (62.1) | 64 (41.8) | *0.444* | 60 (45.1) | 59 (44.4) | 0.034 |
| History of MI | 237 (58.2) | 70 (45.7) | *0.251* | 64 (48.1) | 62 (46.6) | 0.043 |

ACS = acute coronary syndrome, CAD = coronary artery disease, LVEF = left ventricular ejection fraction, MI = myocardial infarction, NSTEMI = non ST elevation myocardial infarction, STEMI = ST elevation myocardial infarction

**Tab. 2 | 3-8** Preoperative variables after Propensity score matching

| | Total cohort *n* = 266 | Re-PCI *n* = 133 | MIDCAB *n* = 133 | *p*-value |
|---|---|---|---|---|
| Age [y], median IQR | 65.5 (57,73) | 65 (57,73.5) | 66 (58.5,73) | 0.975 |
| Female sex, n (%) | 68 (25.6) | 36 (27.1) | 32 (24.1) | 0.716 |
| Preop LVEF [%], median (IQR) | 57 (50,62) | 57 (50,61.5) | 58 (47,63) | 0.977 |
| EuroSCORE II [%], median (IQR) | 2.1 (1.3,3.5) | 1.8 (0.95,3.14) | 2.36 (1.59,3.7) | *0.008* |
| Diabetes, n (%) | 100 (37.6) | 52 (39.1) | 48 (36.1) | 0.816 |
| Hypertension, n (%) | 254 (95.5) | 127 (95.5) | 127 (95.5) | >0.99 |
| Dyslipidemia, n (%) | 230 (86.5) | 116 (87.2) | 114 (85.7) | 0.947 |
| Preop dialysis, n (%) | 3 (1.1) | 2 (1.5) | 1 (0.8) | >0.99 |
| Peripheral arterial disease, n (%) | 40 (15) | 20 (15) | 20 (15) | >0.99 |
| COPD, n (%) | 28 (10.5) | 19 (14.3) | 9 (6.8) | 0.089 |
| Extent of CAD, n (%) | | | | |
| 1-vessel | 107 (40.2) | 46 (34.6) | 61 (45.9) | 0.176 |

**Tab. 2 | 3-8** Preoperative variables after Propensity score matching (Fortsetzung)

| | Total cohort *n* = 266 | Re-PCI *n* = 133 | MIDCAB *n* = 133 | *p*-value |
|---|---|---|---|---|
| 2-vessel | 101 (38) | 61 (45.9) | 40 (30.1) | >0.99 |
| 3-vessel | 56 (21.1) | 24 (18) | 32 (24.1) | 0.35 |
| ACS at admission, n (%) | 61 (22.9) | 31 (23.3) | 30 (22.6) | >0.99 |
| STEMI at admission, n (%) | 1 (0.4) | 1 (0.8) | 0 (0) | >0.99 |
| NSTEMI at admission, n (%) | 38 (14.3) | 19 (14.3) | 19 (14.3) | >0.99 |
| Prior stroke, n (%) | 20 (7.5) | 4 (3) | 6 (4.5) | 0.752 |
| Previous or current smoker, n (%) | 119 (44.7) | 60 (45.1) | 59 (44.4) | >0.99 |
| History of MI, n (%) | 126 (47.4) | 64 (48.1) | 62 (46.6) | 0.929 |
| Time since first PCI [days] (IQR) | 914 (236,3911) | 1641 (231,4118) | 639 (239,3467) | 0.131 |
| Stent type first PCI, n (%) | | | | |
| 1st gen DES | 40 (15) | 24 (18) | 16 (12) | 0.268 |
| 2nd gen DES | 182 (68.4) | 88 (66.2) | 94 (70.7) | 0.711 |
| BMS | 37 (13.9) | 19 (14.3) | 18 (13.5) | >0.99 |
| SCAI definition of ISR, n (%) | | | | |
| 1 | 10 (3.8) | 4 (3) | 6 (4.5) | 0.752 |
| 2 | 84 (31.6) | 41 (30.8) | 43 (32.3) | 0.913 |
| 3 | 165 (62) | 86 (64.7) | 79 (59.4) | 0.64 |
| CCS class, n (%) | | | | |
| 1 | 65 (24.4) | 19 (14.3) | 46 (34.6) | *0.001* |
| 2 | 94 (35.3) | 48 (36.1) | 46 (34.6) | 0.918 |
| 3 | 46 (17.3) | 19 (14.3) | 27 (20.3) | 0.302 |
| 4 | 36 (13.5) | 23 (17.3) | 13 (9.8) | 0.134 |
| NYHA class, n (%) | | | | |
| I | 65 (24.4) | 25 (18.8) | 40 (30.1) | 0.082 |
| II | 115 (43.2) | 51 (38.3) | 64 (48.1) | 0.263 |
| III | 56 (21.1) | 27 (20.3) | 29 (21.8) | 0.894 |
| IV | 10 (3.8) | 10 (7.5) | 0 (0) | *0.004* |
| BMI [kg/m$^2$] | 28.1 (25.3,31) | 28 (25.7,31.6) | 28.1 (25.1,30.8) | 0.182 |
| Preoperative rhythm, n (%) | | | | |
| Normal SR | 236 (88.7) | 112 (84.2) | 124 (93.2) | 0.474 |
| AFIB | 24 (9) | 15 (11.3) | 9 (6.8) | 0.307 |
| AVB II or III | 5 (1.9) | 5 (3.8) | 0 (0) | 0.073 |
| Urgent or emergent intervention, n (%) | 1 (0.4) | 0 (0) | 1 (0.8) | >0.99 |
| Prior cardiac surgery, n (%) | 3 (1.1) | 0 (0) | 3 (2.3) | 0.248 |

ACS = acute coronary syndrome, AFIB = atrial fibrillation, AVB = atrioventricular block, BMI = body mass index, BMS = bare metal stent, CAD = coronary artery disease, COPD = chronic obstructive pulmonary disease, CCS = canadian society of cardiac surgery, DES = drug eluting stent, LVEF = left ventricular ejection fraction, MI = myocardial infarction, NSTEMI = non ST elevation myocardial infarction, NYHA = New York heart association, PCI = percutaneous coronary intervention, STEMI = ST elevation myocardial infarction, SCAI = society for cardiovascular angiography and Interventions

**Tab. 3 | 3-8** Intraprocedural data for repeat PCI before and after propensity score matching

| | Unmatched *n* = 407 | Matched *n* = 133 |
|---|---|---|
| Number of stents in LAD, n (%) | | |
| 0 | 56 (13.8) | 11 (8.3) |
| 1 | 251 (61.7) | 97 (72.9) |
| 2 | 75 (18.4) | 19 (14.3) |
| 3 | 23 (5.7) | 6 (4.5) |
| 4 | 2 (0.5) | 0 (0) |
| Bare metal stents used, n (%) | 0 (0) | 0 (0) |
| Drug eluting stents 1st generation used, n (%) | 0 (0) | 0 (0) |
| Drug eluting stents 2nd generation used, n (%) | 352 (86.5) | 122 (91.7) |
| Drug eluting balloon, n (%) | 182 (44.7) | 51 (38.3) |
| Non-drug eluting balloon, n (%) | 266 (65.4) | 81 (60.9) |
| ECLS protected PCI, n (%) | 1 (0.2) | 1 (0.8) |

ECLS = extracorporeal life support, LAD = left anterior descending artery, PCI = percutaneous coronary intervention

**Tab. 4 | 3-8** Intraprocedural data for MIDCAB before and after propensity score matching

| | Unmatched *n* = 153 | Matched *n* = 133 |
|---|---|---|
| CPB used n (%) | 0 (0) | 0 (0) |
| Conversion to sternotomy n (%) | 1 (0.7) | 0 (0) |
| Length of surgery n (%) | 118 (100,135) | 117 (100,135) |
| LIMA used, n (%) | 153 (100) | 133 (100) |
| LIMA as free graft, n (%) | 0 (0) | 0 (0) |

CPB = cardiopulmonary bypass, LIMA = left internal mammary artery, MIDCAB = minimally invasive coronary artery bypass

**Tab. 5 | 3-8** Postoperative outcomes after propensity matching

| | Overall *n* = 266 | Re-PCI *n* = 133 | MIDCAB *N* = 133 | *p*-value |
|---|---|---|---|---|
| LCOS, n (%) | 3 (1.1) | 2 (1.5) | 1 (0.8) | >0.99 |
| IABP, n (%) | 1 (0.4) | 0 (0) | 1 (0.8) | >0.99 |
| ECMO, n (%) | 1 (0.4) | 1 (0.8) | 0 (0) | >0.99 |
| Myocardial infarction, n (%) | 1 (0.4) | 0 (0) | 1 (0.8) | >0.99 |
| Resuscitation, n (%) | 1 (0.4) | 1 (0.8) | 0 (0) | >0.99 |
| AFIB, n (%) | 6 (2.3) | – | 6 (4.5) | – |
| Arrhythmia, n (%) | 17 (6.4) | – | 17 (12.8) | – |
| Redo for bypass revision, n (%) | 1 (0.4) | – | 1 (0.8) | – |
| Mediastinal bleeding complications, n (%) | 3 (1.1) | 0 (0) | 3 (2.3) | 0.248 |
| Percutaneous access site complication“ n (%) | 1 (0.4) | 1 (0.8) | 0 (0) | >0.99 |
| Stroke“ n (%) | 0 (0) | – | 0 (0) | – |
| Wound infection, n (%) | 0 (0) | – | 0 (0) | – |
| Sepsis, n (%) | 1 (0.4) | 1 (0.8) | 0 (0) | >0.99 |
| Max Creatinine [mg/dl], n (%) | 0.95 (0.8,1.1) | 0.94 (0.8,1.1) | 0.99 (0.82,1.2) | 0.129 |
| Dialysis, n (%) | 3 (1.1) | 3 (2.3) | 0 (0) | 0.248 |
| Respiratory failure, n (%) | 4 (1.5) | 0 (0) | 4 (3) | 0.134 |
| Tracheostomy, n (%) | 1 (0.4) | 0 (0) | 1 (0.8) | >0.99 |
| New Pacemaker, n (%) | 1 (0.4) | 0 (0) | 1 (0.8) | >0.99 |
| New ICD, n (%) | 0 (0) | 0 (0) | 0 (0) | – |
| Hospital length of stay [d], median (IQR) | 7 (1,11) | 1 (1,3) | 9 (8,14) | *<0.001* |
| Died in house, n (%) | 2 (0.8) | 1 (0.8) | 1 (0.8) | >0.99 |

AFIB = atrial fibrillation, ECMO = extracorporeal membrane oxygenator, IABP = Intraaortic ballon pump, LCOS = low cardiac output syndrome, ICD = implantable cardiac defibrillator, IQR = interquartile range

**Tab. 6 | 3-8** Cox regression analysis for survival

| | adjusted HR | 95 %-CI | *p*-value |
|---|---|---|---|
| MIDCAB performed | 1.15 | 0.8,1.65 | 0.444 |
| Age | 1.05 | 1.03,1.06 | *<0.001* |
| Peripheral arterial disease | 1.3 | 0.86,1.94 | 0.211 |
| CAD affecting >1 vessel | 1.89 | 1.26,2.84 | *0.002* |
| Preop LVEF | 0.97 | 0.96,0.98 | *<0.001* |
| Preop creatinine | 1.87 | 1.56,2.24 | *<0.001* |
| EuroSCORE II | 1 | 0.996,1.01 | 0.316 |
| Female sex | 0.99 | 0.68,1.43 | 0.951 |

CAD = coronary artery disease, CI = confidence interval, HR = hazard ratio LVEF = left ventricular ejection fraction

# POSTERSITZUNG 4— HERZINSUFFIZIENZ & KARDIOMYOPATHIEN 1

## 4-1

### HerzMobil, telemedical disease management program for heart failure is associated with improved outcomes in Styria

**Leibetseder S.[1], Veeranki S.[2], von Lewinski D.[1], Verheyen N.[1], Hatzl S.[1], Knödl K.[1], Gollmer J.[1], Pötz S.[3], Zirlik A.[1], Bugger H.[1], Günter S.[4], Wallner M.[1]**

[1]Medizinische Universität Graz, Graz, Austria
[2]Steiermärkische Krankenanstaltengesellschaft m. b. H., Graz, Austria
[3]LKH Weiz, Weiz, Austria
[4]Technische Universität Graz, Graz, Austria

**Introduction:** Heart failure affects approximately 1–3% of the population, corresponding to nearly 300,000 individuals in Austria, and represents a prevalent chronic condition with substantial impact on quality of life and survival. HerzMobil, a structured telemedical care program for patients with heart failure, was implemented in Styria to improve prognosis and attenuate disease progression.

**Methods:** In this retrospective case-control study, patients enrolled in the HerzMobil program (HM, $n = 752$) were compared with a propensity score-matched cohort (PS, $n = 673$) between January 1, 2020, and June 30, 2023. Data were obtained from the Medical Documentation and Communication Network of Styria (MEDOCS) and Statistics Austria. The primary endpoint was all-cause mortality at 12 months. The secondary endpoint was first hospitalization due to heart failure. Survival analyses were performed using Kaplan–Meier estimates and log-rank testing.

**Results:** Within 365 days of follow-up, 181 patients (12.5%) died. 69 (9.2%) in the HM group and 112 (16.6%) in the PS group. Participation in the HerzMobil program was associated with a significant 48% relative reduction in all-cause mortality compared with the matched cohort (HR 0.52; 95% CI 0.41–0.67; $p \leq 0.0001$). Heart failure-related hospitalization occurred in 113 patients (15%) in the HM group and 83 patients (12.3%) in the PS group.

**Conclusion:** This retrospective analysis demonstrates that management of heart failure within a multimodal telemedical disease management program is associated with a significant reduction in all-cause mortality.

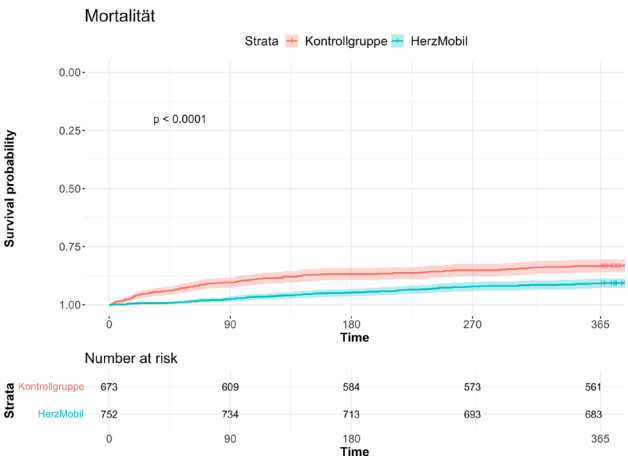


**Fig. 1 | 4-1** Kaplan-Meier curve for overall mortality]

## 4-2

### Veränderung der körperlichen Leistungsfähigkeit unter Antisense Oligonukleotid Therapie bei Patient*innen mit hereditärer ATTR-CM

**Lichtblau L., Badr-Eslam R.**

Medizinische Universität Wien, Wien, Österreich

**Einleitung:** Hereditäre transthyretin-assoziierte Amyloidose (ATTRv) gehört zu den seltenen Erkrankungen mit einer Prävalenz von etwa 1–9/1.000.000 Personen. Klinisch manifestiert sich die ATTRv primär in Form einer Polyneuropathie (PNP). Jedoch gewinnt die ATTRv auch im Bereich der Kardiologie immer mehr an Bedeutung. Hier präsentiert sie sich in Form einer infiltrativen Kardiomyopathie (ATTRv-CM), welche mit reduzierter Leistungsfähigkeit einher geht. Dementsprechende Unterschiede gibt es auch in der Therapie dieser Erkrankung. Mit Eplontersen ist ein neuer Wirkstoff der Gruppe der Antisense Oligonukleotiden (ASO) verfügbar, welcher zur Behandlung der ATTRv mit PNP zugelassen ist. Die Wirkungsweise diese Arzneistoffes auf die ATTR-CM ist derzeit im Fokus der Forschung.

**Methoden:** In diese Beobachtungsstudie werden Patient*innen mit diagnostizierter ATTRv unter Eplontersen Therapie eingeschlossen. Im Fokus steht die Erfassung von Veränderungen der körperlichen Leistungsfähigkeit. Diese wird

| Wert | Baseline | Follow-Up (6 mo) | Change (%) |
|---|---|---|---|
| 6MWT (m) | 331 | 345 | 4% |
| Peak VO2/kg | 11,67 | 12 | 3% |
| Peak O2 Pulse (mL) | 6,5 | 7,27 | 12% |
| VE/VCO2 slope | 48,69 | 41,19 | -15% |
| Peak workload (Watt) | 43,33 | 50 | 15% |
| Peak VE (L/min) | 38,67 | 38 | -2% |

**Abb. 1 | 4-2** Veränderung der Leistungsfähigkeit in CPET sowie 6 MWT der drei Patient*innen nach einem Beobachtungszeitraum von sechs Monaten

mittels 6-Minuten-Gehtests (6 MWT) und kardiopulmonaler Belastungsuntersuchung (CPET) hinsichtlich ihrer Ausgangsbelastbarkeit untersucht. Nach einem Beobachtungszeitraum von sechs Monaten werden sämtliche Untersuchungen erneut durchgeführt, um mögliche Therapieeffekte zu beurteilen.

**Resultate:** Mit Stand Februar 2026 wurden 8 Patient*innen mit ATTRv eingeschlossen. Das Durchschnittsalter beträgt 72,5 Jahre (SD 7,8). Des Weiteren ergab die Baseline Untersuchung einen NTproBNP-Wert von 3295 pg/mL (median) und deutet somit auf eine beträchtliche kardiale Beteiligung hin. Die CPET ergab im Durchschnitt maximale körperliche Belastbarkeit von 43,3 Watt (SD 31,7) sowie im 6 MWT eine durchschnittliche Distanz von 310,5 m (SD 135,1). Drei Patient*innen haben mit Stand Februar 2026 den Beobachtungzeitraum von sechs Monaten absolviert. Es konnte eine durchschnittliche Verlängerung der Gehstrecke im 6 MWT von 14 m festgestellt werden. Die CPET-Untersuchungen im Verlauf ergaben eine Verbesserung der Leistungsfähigkeit auf 50 Watt (SD 34,6), was einer Steigerung um 15 % entspricht. Zusätzlich wurde eine Reduktion der VE/VCO2 Slope um 15 % festgestellt.

**Schlussfolgerungen:** Innerhalb des sechsmonatigen Beobachtungszeitraums zeigte sich bei Patient*innen unter der Therapie mit Eplontersen eine Verbesserung der Gehstrecke, sowie der körperlichen Belastbarkeit gemessen in Watt. In weiterführenden Studien soll dieser beobachtete Effekt nun systematisch überprüft und validiert werden.

## 4-3

### Clinical Effects of Acoramidis Versus Placebo in the ATTRibute-CM Study: Observations from the Intention-To-Treat Population

**Nitsche C.[1], Morbach C.[2], Pfister R.[3], Dintsios C.[4], Thate-Waschke I.[4], Yilmaz A.[5], Störk S.[6]**

[1]Medical University of Vienna–AKH of Vienna–Cardiology Clinic, Wien, Austria
[2]University Hospital Würzburg, Würzburg, Germany
[3]University Hospital Cologne, Cologne, Germany
[4]Bayer, Berlin, Germany
[5]University Hospital Münster, Münster, Germany
[6]Uniklinikum Würzburg, Würzburg, Germany

**Introduction:** Acoramidis is a transthyretin (TTR) stabilizer providing near-complete (≥ 90%) TTR stabilization in vitro and is indicated for the treatment of wild type and variant TTR amyloid cardiomyopathy (ATTR-CM). In the Phase 3 ATTRibute-CM study (NCT03860935) in patients with ATTR-CM, acoramidis significantly improved the 4-step primary hierarchical outcome comprising mortality, morbidity, and physical function vs placebo. The original efficacy analysis considered all randomized patients but excluded those with impaired kidney function (modified intention-to-treat population; $N=611$). The aim of the present analysis was to assess the efficacy of acoramidis in the overall study population (ITT population), including patients with kidney impairment (estimated glomerular filtration rate < 30 ml/min/1.73 m$^2$).

**Methods:** Relative reductions (RRs) in all-cause mortality (ACM), cardiovascular mortality, first all-cause hospitalization, first cardiovascular hospitalization, and first hospitalization for heart failure with acoramidis vs placebo were calculated. Least-squares mean (LSM) differences in 6-minute walk distance (6MWD) and Kansas City Cardiomyopathy Questionnaire–Overall Summary Score (KCCQ-OSS) were evaluated. RRs in achieving a ≥ 5% deterioration and ≥ 5% improvement in KCCQ-OSS with acoramidis vs placebo were assessed; a ≥ 5-point/≥ 5% change was considered as the threshold for a minimal clinically important difference for KCCQ-OSS.

**Results:** In the ITT ($n=421$ acoramidis; $n=211$ placebo), acoramidis significantly improved all evaluated clinical outcomes vs placebo, with RRs (95% confidence interval [CI]) of 0.74 (0.56, 0.98) and 0.57 (0.42, 0.77) for ACM and first hospitalization for heart failure, respectively (Figure). 6MWD and KCCQ-OSS were improved with acoramidis compared with placebo, with LSM differences (95% CI) of 40.81 (22.55, 59.07) and 10.20 (6.30, 14.10), respectively. The RRs (95% CI) in achieving a ≥ 5% deterioration and ≥ 5% improvement in KCCQ-OSS with acoramidis vs placebo were 0.77 (0.68, 0.88) and 1.76 (1.19, 2.59).

**Conclusion:** The present ITT analysis showed consistent favourable results across all endpoints studied, confirming the efficacy of acoramidis on functional status and quality of life.

**Figure. Clinical outcomes with acoramidis versus placebo in the intention-to-treat population (N=632)**

| Outcome description | |
|---|---|
| All-cause mortality, RR (95% CI) | 0.74 (0.56, 0.98); p=0.0390 |
| Cardiovascular mortality, RR (95% CI) | 0.68 (0.49, 0.94); p=0.0198 |
| First all-cause hospitalization, RR (95% CI) | 0.84 (0.72, 0.97); p=0.0190 |
| First cardiovascular hospitalization, RR (95% CI) | 0.64 (0.51, 0.80); p=0.0002 |
| First hospitalization for heart failure, RR (95% CI) | 0.57 (0.42, 0.77); p=0.0003 |
| 6-minute walk distance, least-squares mean difference (95% CI) | 40.81 (22.55, 59.07); p<0.0001 |
| KCCQ-OSS, least-squares mean difference (95% CI) | 10.20 (6.30, 14.10); p<0.0001 |
| ≥5% KCCQ-OSS deterioration, RR (95% CI) | 0.77 (0.68, 0.88); p=0.0001 |
| ≥5% KCCQ-OSS improvement, RR (95% CI) | 1.76 (1.19, 2.59); p=0.0045 |

CI, confidence interval; KCCQ-OSS, Kansas City Cardiomyopathy Questionnaire–Overall Summary Score; RR, relative reduction.

**Fig. 1 | 4-3** Clinical outcomes with acoramidis versus placebo in the ITT population in ATTRibute-CM

## 4-4

### Safety and efficacy of mavacamten compared to alcohol septal ablation in hypertrophic obstructive cardiomyopathy in a retrospective real-world cohort

**Santner V., Pötsch S., Mairhofer H., Höller V., Eber P., Kolesnik E., Ablasser K., Zirlik A., Toth G., Verheyen N., Schwegel N.**

Division of Cardiology, University Heart Center and Department of Internal Medicine, Medical University of Graz, Graz, Austria

**Fig. 1 | 4-4**

**Table 1. Comparison of baseline characteristics of patients treated with Mavacamten or Alcohol septal ablation (n=49)**

| Baseline characteristics | Mavacamten (n=24) | Alcohol septal ablation (n=25) | P-Value* |
|---|---|---|---|
| **Age, yrs** | 59 ± 13 | 60 ± 12 | 0.978 |
| **Women, n (%)** | 11 (49) | 9 (36) | 0.484 |
| **NYHA Class ≥ III, n (5)** | 14 (58) | 12 (52) | 0.671 |
| **NT-proBNP, pg/ml** | 519 [283, 1462] | 729 [329, 2079] | 0.263 |
| **MWTH, mm** | 21 ± 3 | 22 ± 3 | 0.286 |
| **LVEF, %** | 65 ± 5 | 66 ± 7 | 0.463 |
| **Resting LVOT Gradient, mmHg** | 24 [17, 50] | 33 [20, 69] | 0.114 |
| **Provoked LVOT Gradient, mmHg** | 89 [57, 109] | 86 [64, 124] | 0.578 |

Continuous variables are counted as median [25th-75th percentile] or mean ± standard deviation, and count data as absolute frequencies (column%).
* Student´s t-test, Chi square test or Mann-Whitney-U test, as appropriate.

*Abbreviations. LVEF=left ventricular ejection fraction; LVOT=left ventricular outflow tract; NT-proBNP= N-terminal pro-brain natriuretic peptide; NYHA=New York Heart Association.*

**Fig. 2 | 4-4**

**Table 2. Comparison of efficacy outcomes after 12 and 48 weeks between treatment groups.**

| | Mavacamten (n=24) | | | | | Alcohol septal ablation (n=25) | | | | | Differences between treatment groups | |
|---|---|---|---|---|---|---|---|---|---|---|---|---|
| | **Baseline** | **Week 12** | **Week 48** | **Absolute change between BL and W12** | **Absolute change between BL and W48** | **Baseline** | **Week 12** | **Week 48** | **Absolute change between BL and W12** | **Absolute change between BL and W48** | **Baseline and W12** | **Baseline and W48** |
| Resting LVOT Gradient, mmHg | 24 [17, 50] | 17 [10, 23] | 6 [4, 8] | 12 [1, 27] | 15 [7, 49] | 33 [20, 69] | 17 [10, 32] | 12 [5, 17] | 23 [4, 44] | 25 [10, 40] | P=0.265 | P=0.934 |
| Provoked LVOT Gradient, mmHg | 89 [57, 109] | 61 [21, 88] | 8 [5, 15] | 29 [9, 64] | 84 [42, 114] | 86 [64, 124] | 34 [10, 88] | 18 [8, 49] | 37 [10, 96] | 61 [27, 83] | P=0.565 | P=0.548 |
| NT-proBNP, pg/ml | 519 [283, 1462] | 234 [173, 318] | 155 [71, 228] | 232 [82, 688] | 252 [101, 1126] | 729 [329, 2079] | 476 [189, 1487] | 322 [186, 1597] | 240 [15, 818] | 165 [51, 642] | P=0.797 | P=0.326 |

Abbreviations. BL=baseline; *LVOT=left ventricular outflow tract; NT-proBNP= N-terminal pro-brain natriuretic peptide; NYHA=New York Heart Association.*

**Introduction:** In hypertrophic obstructive cardiomyopathy (HOCM), the advent of new treatment options, such as the cardiac myosin-inhibitor mavacamten, on top of established invasive septal reduction therapies has altered guideline recommendations for the treatment of left ventricular outflow tract obstruction (LVOTO). So far, there is limited data comparing safety and efficacy of pharmacological therapy with mavacamten to invasive alcohol septal ablation (ASA). In this retrospective single-center analysis of a real world HOCM cohort, we investigated safety and efficacy of the myosin-inhibitor mavacamten compared to ASA after 12 and 48 weeks.

**Methods:** We performed a single-center cross sectional analysis of patients with HOCM who were either treated with mavacamten or ASA in our University hospital between 2017 and 2025. Baseline characteristics and follow-up data including efficacy outcomes and safety events after 12 and 48 weeks were collected from medical chart review. Echocardiographic analyses were performed using the post-processing software TomTec.

**Results:** In the overall cohort of 49 HOCM patients, 24 were treated with mavacamten and 25 with ASA. Both cohorts were overall comparable in terms of baseline characteristics as gender (49% women in the mavacamten group; 36% in the ASA group), age (59 ± 13 vs. 60 ± 12 years), NT-proBNP (519 [283, 1462] vs. 729 [329, 2079] pg/mL), and LVOT gradients (resting 24 [17, 50] vs. 33 [20, 69]; provocative 89 [57, 109] vs. 86 [64, 124] mmHg) (Table 1). In both treatment groups resting and provoked LVOT gradient and NT-proBNP decreased after 12 and 48 weeks. Absolute changes after 12 and 48 weeks were overall comparable between treatment groups (Table 2). One patient in the ASA group had to undergo a repeat ASA due to persistent LVOTO after the first intervention, and one patient in the mavacamten group was switched to treatment with myectomy due to drug incompliance. In terms of safety, in the ASA cohort five patients suffered from complications (18%) with four patients receiving a pacemaker due to postinterventional complete atrioventricular block and one patient suffering from pulmonary embolism despite anticoagulation. In comparison, in the mavacamten cohort only in one patient (0.4%) treatment had to be stopped due to an LVEF drop below 50% ($p = 0.091$). Additionally during the 48 weeks follow-up, two patients in the ASA group were diagnosed with new onset atrial fibrillation (AF), and two patients in the mavacamten group had to be hospitalized due to tachycardic episodes of AF.

**Conclusion:** In this single-center retrospective analysis, treatment with mavacamten was overall comparable to ASA in terms of efficacy, while there was a trend toward more common treatment-related complications in the ASA group, yet not reaching statistical significance. Future multi-center studies are warranted to confirm our results in larger HOCM cohorts and assess long term follow-up of those patients.

## 4-5

## Soluble transferrin receptor and hepcidin but not standard iron biomarkers are reliable prognostic biomarkers in heart failure

**Lanser L.[1], Pölzl G.[2], Messner M.[2], Ungericht M.[2], Zaruba M.[2], Schütz T.[2], Puelacher C.[2], Haschka D.[1], Ulmer H.[3], Weiss G.[1]**

[1]Univ.-Klinik für Innere Medizin II, Innsbruck, Austria
[2]Univ.-Klinik für Innere Medizin III, Innsbruck, Austria
[3]Institut für Medizinische Statistik und Informatik, Innsbruck, Austria

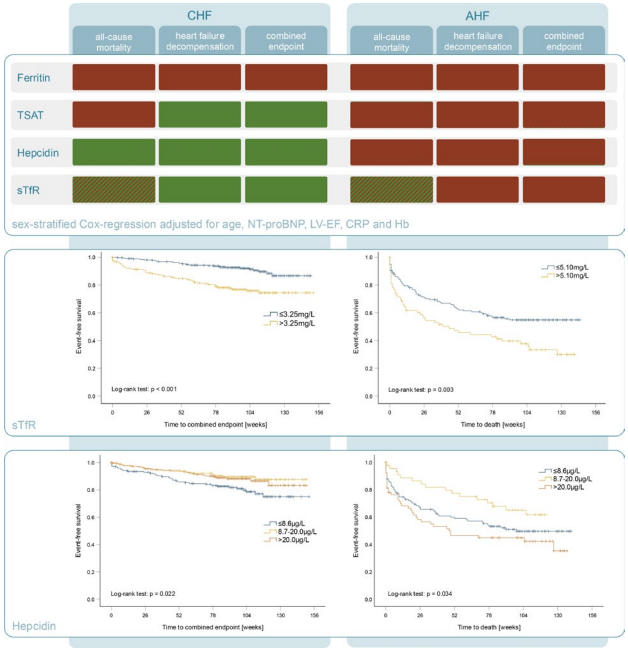


**Fig. 1 | 4-5**

**Introduction:** Definition or iron deficiency (ID) in heart failure (HF) is currently based on serum ferritin and the transferrin saturation (TSAT). In recent years, controverse discussions have emerged about using ferritin, as it is an acute-phase protein that does not always reflect true iron stores. The aim of this analysis was to evaluate the accuracy of standard and alternative iron biomarkers in predicting disease outcome.

**Methods:** We analyzed 238 AHF and 547 CHF patients treated at the Innsbruck University Hospital 11/2020–05/2022 with available iron status at baseline without iron supplementation within the last year, after out-patient visit or hospitalization. Patients were followed until 10/2023. We performed sex-stratified Cox regression analysis adjusted for age, NT-proBNP, LV-EF, CRP and hemoglobin to evaluate the predictive value of iron biomarkers on outcome (all-cause mortality, HF decompensation and combined endpoint of both).

**Results:** Serum ferritin did not predict outcome in AHF and CHF, while a lower ferritin/CRP ratio predicts all-cause mortality and combined endpoint in AHF and CHF. Low TSAT was related to risk of HF decompensation and combined endpoint in CHF but not AHF. High soluble transferrin receptor (sTfR) levels were predicting outcome in CHF and trend to predict all-cause mortality in AHF. Low hepcidin levels were also predicting outcome in CHF, while Cox regression analysis suggested that hepcidin does not predict outcome in AHF. Univariate analysis of hepcidin subgroups showed that both low (≤ 8.6 µg/L) and high (> 20 µg/L) hepcidin levels were related to an elevated all-cause mortality in AHF. When correcting for CRP only hepcidin levels ≤ 8.6 µg/L remained predictive for all-cause mortality in AHF.

**Conclusion:** We could show that serum ferritin levels fail to identify AHF and CHF patients with risk for an adverse outcome thus questioning the suitability of the current ferritin-based ID definition. Introduction of the ferritin/CRP ratio and the alternative iron biomarkers hepcidin and sTfR might help to better identify iron imbalances and patients with poor prognosis in both AHF and CHF.

## 4-6

## Prevalence of iron deficiency in heart failure according to different clinical definitions

**Lanser L.[1], Pölzl G.[2], Messner M.[2], Ungericht M.[2], Zaruba M.[2], Ulmer H.[3], Weiss G.[1]**

[1]Univ.-Klinik für Innere Medizin II, Innsbruck, Austria
[2]Univ.-Klinik für Innere Medizin III, Innsbruck, Austria
[3]Institut für Medizinische Statistik und Informatik, Innsbruck, Austria

**Introduction:** Iron is essential to maintain cellular energy metabolism in the myocardium, thus impaired cellular iron availability negatively affects myocardial physiology and can aggravate acute and chronic heart failure (AHF/CHF). The aim of this analysis was to assess true iron deficiency (ID) prevalence in HF patients based on different ID definitions.

**Methods:** We analyzed 942 continuous HF patients (329 AHF, 613 CHF) treated at the Innsbruck Medical University 02/2021–05/2022. ID was defined according to a general definition, gastroenterology and cardiology guidelines (Figure).

**Results:** ID prevalence was significantly higher in AHF vs. CHF: general definition (74.8% vs. 32.6%, $p < 0.001$), gastroenterology (75.7% vs. 34.7%, $p < 0.001$) and cardiology guidelines (79.9% vs. 47.3%, $p < 0.001$). We found distinctive differences in prevalence of ID types between the three definitions. Absolute ID prevalence was the highest when applying cardiology compared to gastroenterology guidelines and the general definition, while frequency of combined ID was almost equally distributed. Functional ID prevalence was highest when applying the general definition compared to gastroenterology and cardiology guidelines (Figure). Out of 494 patients classified as having absolute or combined ID according to the cardiology guidelines, only 252 patients received the same classification while 107 and 135 patients were classified having no and functional ID when applying the general definition.

**Conclusion:** We show that ID prevalence is higher in AHF vs. CHF in a continuous cohort of patients. There were distinctive differences in ID detection when applying different recommended definitions thus affecting sensitivity and specificity for absolute and functional ID detection. This results in exclusion

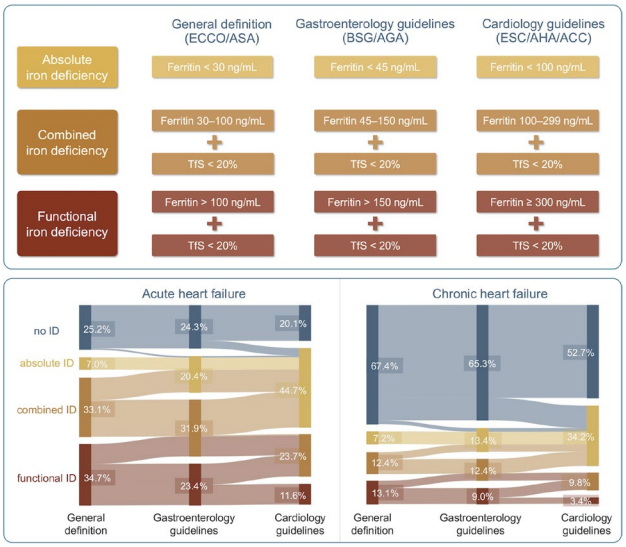


**Fig. 1 | 4-6**

of patients which may benefit from iron supplementation and inclusion of those who may not respond or even anticipate site effects. It is also a question of health economics since extrapolation of our data to the European Union with supplementation of each iron deficient HF patient would cause costs of at least € 754.6 million when applying the general definition and € 1.69 billion when applying the cardiology guidelines. Our study calls for the urgent need of prospective trials for redefinition of ID and identification of biomarkers associated with therapeutic response not only to optimize patient outcomes but also in regard of health economic burden.

## 4-7

## Periodic Repolarization Dynamics and Deceleration Capacity in Heart Transplant Recipients

**Knap B., Messner M., Hofer F., Schreinlechner M., Pavluk D., Bauer A.**

Medizinische Universität Innsbruck, Innsbruck, Austria

**Introduction:** Periodic repolarization dynamics (PRD) is an ECG-based risk marker reflecting sympathetic-activity related modulation of ventricular repolarization. Deceleration capacity of heart rate (DC) represents an integral measure of predominantly vagally mediated heart rate dynamics. Following heart transplantation (HTx), autonomic reinnervation remains incomplete, yet its long-term electrophysiological consequences are poorly understood.

**Methods:** We included 19 stable patients two to five years after orthotopic heart transplantation who underwent standardized 30 min high resolution ECG recordings in Frank lead configuration. PRD and DC were quantified using established algorithms and compared with age-matched controls. Group comparisons were performed using Wilcoxon rank-sum tests and Fisher's exact tests, as appropriate.

**Results:** HTx recipients had a mean age of 59.0 ± 9.6 years and 5 (26.3%) were female compared with mean age of 61.5 ± 7.8 years in the control group ($p = 0.802$), of whom 8 (57.1%) were females ($p = 0.148$). PRD was significantly higher in HTx recipients compared to controls (4.88 [IQR 6.86] vs 1.67 [IQR 2.03] deg²; $p = 0.007$). In contrast, DC did not differ significantly between groups (1.45 [IQR 0.85] vs 1.43 [IQR 1.12] ms; $p = 0.743$).

**Conclusion:** PRD is significantly increased years after HTx, whereas DC remains comparable to age-matched controls. This dissociation suggests enhanced sympathetic modulation of ventricular repolarization, potentially reflecting heterogeneous sympathetic re-innervation without detectable changes in global heart rate deceleration dynamics. Future studies are needed to evaluate the prognostic implications of PRD after HTx.

## References

1. Rizas KD, Nieminen T, Barthel P, Zürn CS, Kähönen M, Viik J, Lehtimäki T, Nikus K, Eick C, Greiner TO, Wendel HP, Seizer P, Schreieck J, Gawaz M, Schmidt G, Bauer A. Sympathetic activity-associated periodic repolarization dynamics predict mortality following myocardial infarction. J Clin Invest. 2014 Apr;124(4):1770–80. https://doi.org/10.1172/JCI70085. Epub 2014 Mar 18. Erratum in: J Clin Invest. 2014 Jun 2;124(6):2808.
2. Bauer A, Kantelhardt JW, Barthel P, Schneider R, Mäkikallio T, Ulm K, Hnatkova K, Schömig A, Huikuri H, Bunde A, Malik M, Schmidt G. Deceleration capacity of heart rate as a predictor of mortality after myocardial infarction: cohort study. Lancet. 2006 May 20;367(9523):1674–81. https://doi.org/10.1016/S0140-6736(06)68735-7.

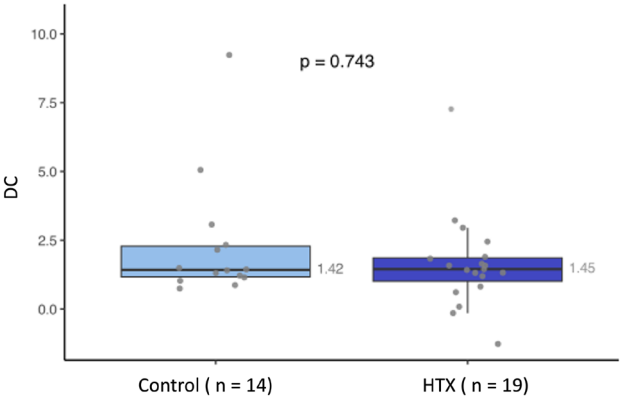


**Figure 1:** Figure Y. Deceleration Capacity (DC) in HTx Recipients and Controls.

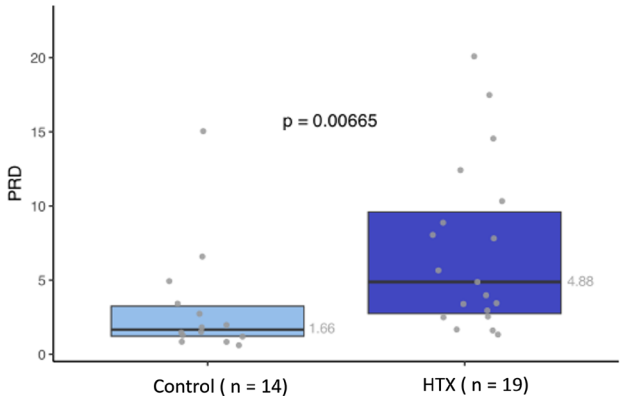


**Fig. 1 | 4-7** Boxplots representing Periodic Repolarization Dynamics (PRD) and Deceleration Capacity (DC) in HTx recipients and matched controls

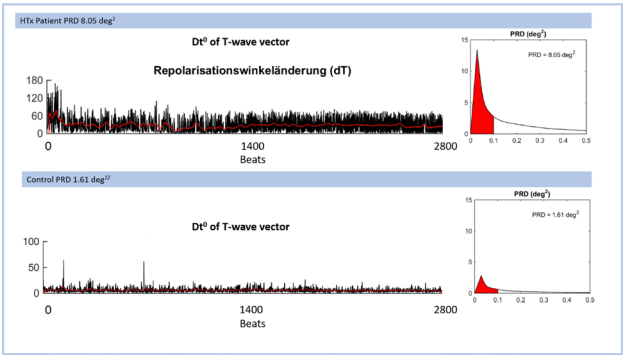


**Fig. 2 | 4-7** Beat-to-beat T-wave vector angle variability and corresponding wavelet spectra in two exemplary cases: one heart transplant (HTX) patient and one subject from the control group, representing low and high periodic repolarization dynamics (PRD)

## 4-8

### Assoziation von Serumharnsäure, Hyperurikämie und Gicht mit subklinischer Atherosklerose der Koronarien und Karotiden—Ergebnisse der Paracelsus-10.000-Studie

**Ausserwinkler M., Paulweber B., Langthaler P., Trinka E., Iglseder B., Aigner E., Wernly B.**

Paracelsus Universität Salzburg, Salzburg, Österreich

**Einleitung:** Serumharnsäure ist konsistent mit einem erhöhten kardiovaskulären Risiko assoziiert; ob dieser Zusammenhang jedoch eine unabhängige vaskuläre Pathologie widerspiegelt oder vielmehr Ausdruck einer Häufung kardiometabolischer Risikofaktoren ist, bleibt bislang ungeklärt. Wir untersuchten daher die Assoziationen von Serumharnsäure, Hyperurikämie und Gicht mit bildgebend definierter subklinischer Atherosklerose der Koronarien und Karotiden in einer großen österreichischen populationsbasierten Kohorte.

**Methoden:** Wir analysierten Daten der Paracelsus-10.000-Studie, einer populationsbasierten Kohorte von Erwachsenen im Alter von 40–77 Jahren, die aus dem österreichischen nationalen Bevölkerungsregister rekrutiert wurden. Die koronare Kalziumlast (CAC) wurde mittels Computertomographie bei 1561 Teilnehmenden mit verfügbarer kardialer Computertomographie und Daten zum polygenen Risikoscore bestimmt; die Plaquebelastung der Karotiden wurde mittels Carotis Doppler Duplex Sonographie bei 8970 Teilnehmenden erhoben. Die Assoziationen wurden mittels ordinaler logistischer Regression untersucht – wobei CAC anhand des Agatston-Scores (0, 1–100, 101–300 und >300) kategorisiert und die karotide Plaquebelastung nach der Gesamtplaquefläche eingeteilt wurde – unter schrittweiser Adjustierung für den kardiovaskulären Risikoscore (SCORE2), das metabolische Syndrom, das polygene kardiovaskuläre Risiko, Lipoprotein(a) sowie systemische Entzündung.

**Resultate:** Höhere Serumharnsäurespiegel waren in unadjustierten Analysen stark mit einer höheren CAC assoziiert (OR 1,60 pro 1 mg/dL; 95 %-KI 1,48–1,74). Nach vollständiger Adjustierung für den kardiovaskulären Risikoscore, das metabolische Syndrom, das polygene Risiko, Lipoprotein(a) sowie Entzündungsmarker war diese Assoziation abgeschwächt, blieb jedoch statistisch signifikant (OR 1,26; 95 %-KI 1,14–1,39). Hyperurikämie war auch nach vollständiger Adjustierung unabhängig mit höheren CAC-Kategorien assoziiert (OR 1,68; 95 %-KI 1,21–2,33). Für die Plaquebelastung der Karotiden zeigte sich eine starke unadjustierte Assoziation mit der Serumharnsäure, die nach vollständiger multivariabler Adjustierung deutlich abgeschwächt war und keine statistische Signifikanz mehr erreichte (OR 1,04; 95 %-KI 0,99–1,08). Analysen bei Patientinnen und Patienten mit ärztlich diagnostizierter Gicht waren aufgrund geringer Fallzahlen limitiert und werden deskriptiv berichtet.

**Schlussfolgerungen:** Serumharnsäure und Hyperurikämie sind unabhängig von etablierten kardiovaskulären Risikofaktoren, genetischer Prädisposition und systemischer Entzündung mit subklinischer koronarer Atherosklerose assoziiert. Die Abschwächung der Assoziationen mit Karotis-Plaques nach vollständiger Adjustierung legt nahe, dass die extrakoronare Plaquebelastung überwiegend durch die Häufung kardiometabolischer Risikofaktoren und weniger durch harnsäurespezifische Mechanismen bestimmt wird. Diese Ergebnisse positionieren Harnsäure als klinisch leicht zugänglichen Marker subklinischer koronarer Atherosklerose und werfen die Frage auf, ob eine systematische Bestimmung der Harnsäure zur kardiovaskulären Risikostratifizierung über etablierte Risikoscores hinaus beitragen sollte. Darüber hinaus stellt sich die Frage, ob eine harnsäuresenkende Therapie auch unabhängig von einer manifesten Gicht künftig als Bestandteil kardiovaskulärer Präventionsstrategien in Betracht gezogen werden sollte.

# POSTERSITZUNG 5— INTERVENTIONELLE & STRUKTURELLE KARDIOLOGIE

## 5-1

### The SALZBURG Score: A Simple Bedside Tool for Long-Term Survival Prediction After TAVI

**Boxhammer E.[1], Clodi N.[1,2], Dinges C.[3], Rezar R.[1], Reiter C.[4], Kellermair J.[4], Wintersteller W.[1], Prinz E.[1], Kammler J.[4], Lichtenauer M.[1], Steinwender C.[5], Hammerer M.[1], Hoppe U.[1]**

[1]Universitätsklinik für Innere Medizin II, Kardiologie und internistische Intensivmedizin, Salzburg, Austria
[2]Universitätsklinik für Radiologie, Salzburg, Austria
[3]Universitätsklinik für Herzchirurgie, Salzburg, Austria
[4]Innere Medizin 1 – Kardiologie und Internistische Intensivmedizin, Linz, Austria
[5]Innere Medizin 1 – Kardiologie und Internistische Intensivmedizin, Universitätsklinikum Linz, Linz, Austria

**Introduction:** Reliable estimation of long-term survival after transcatheter aortic valve implantation (TAVI) remains challenging, and commonly used surgical risk scores such as EuroSCORE II and the STS Score show limited prognostic accuracy in this population. We aimed to identify simple clinical predictors of long-term mortality, develop an intuitive bedside risk score, and evaluate its internal and external validity.

**Methods:** In this multicenter cohort study, a derivation cohort of 585 consecutive patients undergoing transfemoral TAVI was used to develop the score, with an independent external validation cohort of 117 patients. Predictors of 3-year all-cause mortality were identified using LASSO-Cox regression followed by multivariable Cox modeling. A points-based bedside score was derived from the regression coefficients. Model performance was evaluated by discrimination, calibration, decision curve analysis, and net reclassification improvement (NRI). Internal validation was performed using bootstrap resampling, and the final score was applied unchanged in the external validation cohort.

**Results:** Six routinely available variables—age >80 years, male sex, eGFR <60 ml/min, atrial fibrillation, anemia, and diabetes mellitus—were incorporated into the SALZBURG score (range 0–11 points). In the derivation cohort, the score demonstrated moderate discrimination for predicting 3-year mortality (AUC 0.66; 95% CI 0.61–0.71), significantly outperforming EuroSCORE II (AUC 0.56; $p=0.002$) and the STS Score (AUC 0.57; $p=0.005$). Calibration showed good agreement between predicted and observed mortality. Decision curve analysis demonstrated higher net clinical benefit across clinically relevant threshold probabilities compared with both established scores. Risk reclassification was significantly improved, with a categorical NRI of 0.25 (95% CI 0.11–0.40) versus EuroSCORE II and 0.25 (95% CI 0.12–0.39) versus the STS Score. In the external validation cohort, discriminative performance remained stable (C-index 0.62; 95% CI 0.54–0.69).

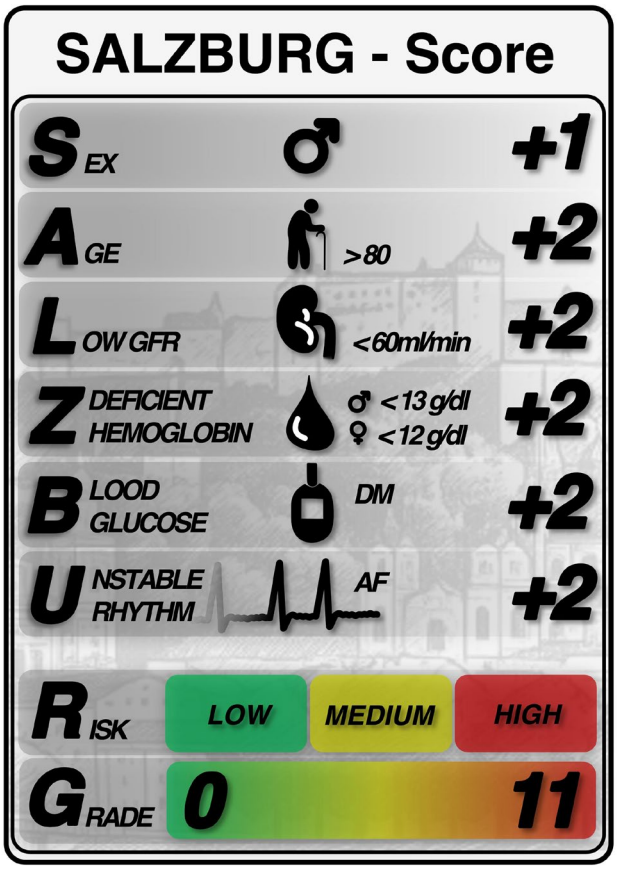


**Fig. 1 | 5-1** SALZBURG Score

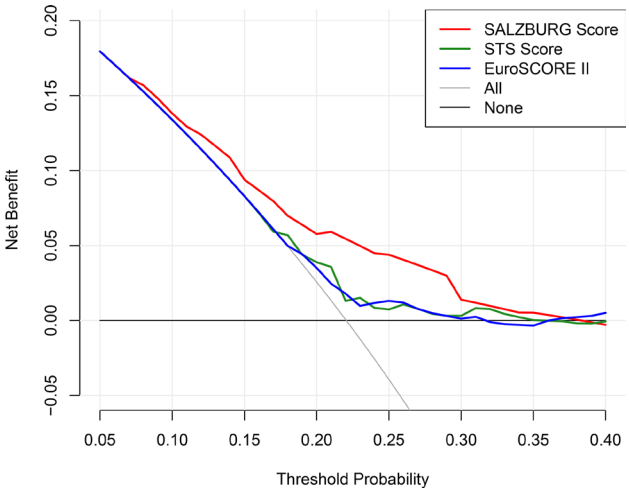


**Fig. 2 | 5-1** Decision Curve Analysis (SALZBURG Score, EuroSCORE II, STS Score)

**Conclusion:** The SALZBURG score is a simple and externally validated clinical tool for predicting long-term mortality after TAVI. Compared with established surgical risk scores, it improves discrimination, clinical utility, and risk classification, supporting its potential use for routine prognostic assessment in TAVI patients.

## 5-2

## Transkatheter paravalvulärer Leckverschluss—eine retrospektive Zentrums-Analyse von 2017 bis 2025

**Danninger K.[1], Alberer M.[1], Geppert A.[2], Porodko M.[1], Tiefenthaller G.[1], Zierer A.[1], Binder R.[1]**

[1]Klinikum Wels-Grieskirchen, Wels, Österreich
[2]Klinik Ottakring, Wien, Österreich

**Einleitung:** Paravalvuläre Leckagen (PVL) stellen eine relevante Komplikation nach chirurgischem oder Transkatheter-Herzklappenersatz dar und können zu Herzinsuffizienz, Hämolyse und eingeschränkter Lebensqualität führen. Der Transkatheter-PVL-Verschluss hat sich als minimalinvasive Therapiealternative zur chirurgischen Reintervention etabliert. Ziel dieser Arbeit war die Darstellung der Erfahrungen mit Transkatheter-PVL-Verschlüssen am Klinikum Wels-Grieskirchen.

**Methoden:** Retrospektiv wurden alle Patientinnen und Patienten erfasst, die zwischen Oktober 2017 und Dezember 2025 einem Transkatheter-PVL-Verschluss unterzogen wurden. Analysiert wurden die Patientencharakteristika, Zahl der paravalvulären Lecks, Anzahl der implantierten Okkluder, anatomische Lokalisation der betroffenen Klappen, Art der zugrunde liegenden Klappenprothese, echokardiographischer Erfolg sowie die prozedurale Mortalität.

**Resultate:** Insgesamt wurden 12 Transkatheter-PVL-Verschlüsse bei 11 Patienten durchgeführt. Ein Patient erhielt zwei separate Eingriffe. Es wurden dabei 17 PVLs behandelt und entsprechend 17 Okkluder implantiert. Die häufigste anatomische Lokalisation war die Mitralklappe ($n=6$), gefolgt von der Aortenklappe ($n=5$) und der Trikuspidalklappe ($n=1$). Bezüglich der Klappenprothesen lagen überwiegend mechanische Klappen vor ($n=8$). In drei Fällen handelte es sich um biologische Klappen, darunter ein Patient nach Transkatheter Aortenklappenimplantation. Mehrere Patient:innen wiesen komplexe kardiochirurgische Voroperationen mit mehrfachen Klappeninterventionen und einem prohibitiven Risiko für eine Re-Operation auf. Die Hauptindikationen für den Eingriff waren klinisch relevante Herzinsuffizienzsymptome bei hochgradigen paravalvulären Insuffizienzen. In alle adressierten PVL konnten perkutan Occluder implantiert werden (Amplatzer Duct Occluder (1x), Amplatzer Muscular VSD Occluder (1x) Amplatzer Vascular Plug II (1) und III (14)). Die Zugangswege waren für aortale PVL transfemoral arteriell retrograd, für das trikuspidale PVL transfemoral venös antegrad und für 4 mitrale PVL transseptal. Eine Patientin mit mitralem PVL wurde transapikal therapiert und eine Patientin mit mitralem PVL transfemoral arteriell retrograd vom linken Ventrikel aus über ein veno-arterielles Loop. Die paravalvuläre Insuffizienz wurde von schwer auf gering reduziert. Die prozedurale Mortalität war null.

**Schlussfolgerungen:** Der Transkatheter paravalvuläre Leckverschluss ist eine sichere und effektive Therapieoption bei komplexen PVL und kann bei sämtlichen Klappenprothesentypen erfolgreich eingesetzt werden.

## 5-3

### Discrepancy between invasive and echocardiographic mean gradients after TAVI in a real-world all-comers cohort

**List L.[1,2], Wallmüller C.[1,2], Stratil P.[1,2], Steinacher A.[1,2], Wilfing R.[2,3], Steiner C.[1,2], Delle-Karth G.[1,2], Schober A.[1,2]**

[1]Department of Cardiology, Klinik Floridsdorf, Wien, Austria
[2]Karl Landsteiner Institute for Cardiovascular and Intensive Care Research, Wien, Austria
[3]Department of Internal Medicine I, Medical University of Vienna, Wien, Austria

**Introduction:** Accurate assessment of transvalvular gradients after TAVI procedures is crucial for early detection of prosthesis dysfunction, as the Valve Academic Research Consortium 3 defines a mean gradient above 20 mmHg indicative of valve dysfunction. While invasive gradients during implantation are considered gold standard, TTE is routinely used for follow-up. We aimed to quantify the discrepancy between invasive and early post-TAVI TTE mean gradients and identify patient- and procedure-related factors associated with larger differences.

**Methods:** We retrospectively analysed 346 patients, undergoing TAVI at our tertiary centre, between June 2019 and July 2024. Demographics, comorbidities, procedural details, echocardiographic parameters and CT findings were collected. Invasive gradients were acquired routinely during intervention, while mean TTE gradients were acquired before discharge or measured retrospectively if missing. The primary endpoint was the discrepancy between invasive and post-TAVI TTE mean gradients. The absolute difference was calculated and patients stratified by the median gradient discrepancy.

**Results:** Overall, 346 patients; 173 females (50%) with a median age of 82 (IQR 78–85), a median EuroSCORE II of 2.7 (IQR 1.8–4.4) and more self-expanding (SEV) then balloon-expanding valves (BEV) (59% vs. 41%) were included. Post-procedural TTE mean gradients overestimated invasive values in 79% of cases (median 9 mmHg [6–12] vs 5 mmHg [3–7], $p<0.001$). The median absolute discrepancy was 5 mmHg (IQR 2–9). Correlation between modalities was weak ($\rho=0.097$, $p=0.073$). Bland-Altman analysis (Fig. 1) demonstrated wide dispersion between measurement methods, frequently outside the limits of agreement. Proportional bias was seen with increasing discrepancy among higher gradients ($p<0.001$). Prosthesis characteristics influenced discrepancy (Fig. 2), with larger discrepancies seen in BEV (median 8 vs 3 mmHg, $p<0.001$) than SEV, peaking in 23 mm sized prostheses (median 9 mmHg [7–14]). When stratified by median discrepancy, peak transvalvular velocity ($p=0.036$), pressure gradient ($p=0.031$) and left ventricular outflow tract mean gradient ($p=0.037$) in pre-procedural TTE were associated with great gradient discrepancy. During the intervention, patients with higher invasive gradients, large prosthesis diameters, SEV and ballon valvuloplasty (all $p<0.001$) showed agreement most often. Twelve patients (3.5%) showed TTE mean gradients >20 mmHg despite low invasive gradients (median 6 mmHg [5–7]). VARC-3 device success was not met in 21 patients (6%), all in the high-discrepancy group (12% vs 0%, $p<0.001$).

**Conclusion:** In this real-world TAVI cohort, early post-procedural TTE mean gradients were consistently higher than invasive measurements. Both methods showed only weak correlation, with increasing discrepancies at higher gradients. A subset of patients exceeded the recommended threshold for prosthesis dysfunction in TTE, all of them showing lower invasive gradients, highlighting the risk of misclassifying prosthesis dysfunction. Procedural and patient-related factors including valve type, valve diameter and pre-procedural TTE showed association with gradient discrepancies. These findings emphasize the need for careful interpretation of TTE mean gradients as a marker for valve dysfunction.

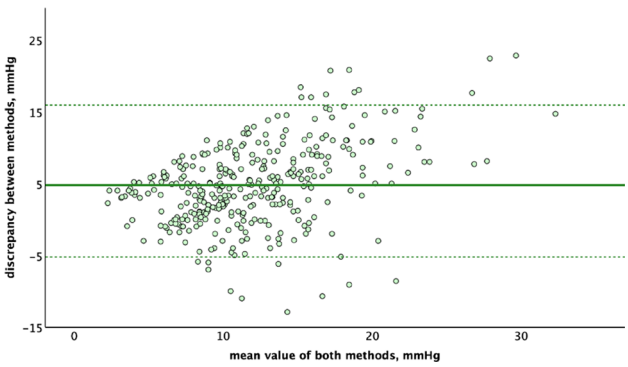


**Fig. 1 | 5-3** Bland-Altman plot of post-TAVI mean transvalvular gradients—absolute discrepancy plotted against mean of both measurements. The solid line indicates mean bias; the dashed lines indicate 95% limits of agreement

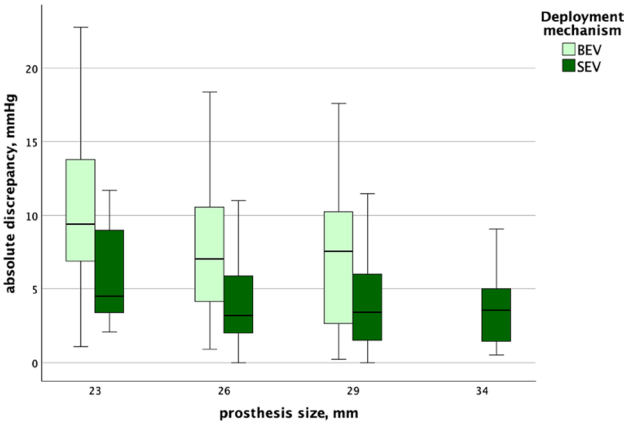


**Fig. 2 | 5-3** Absolute discrepancy between TTE and invasive mean gradients by prosthesis size and deployment mechanism

## 5-4

### Ultra-Low Contrast DCB-Only Strategy in patients with chronic kidney disease—A pilot study

**Abd El-Aal T., Terzi R., Hamzaraj K., Domanig A., Plößner J., Gerges C., Kammerlander A., Frey B., Demirel C., Koller L., Hengstenberg C., Hemetsberger R.**

Medizinische Universität Wien, Wien, Austria

**Introduction:** The aim of this study was to assess the procedural feasibility of an ultra-low contrast, intravascular ultrasound (IVUS) guided percutaneous coronary intervention (PCI) strategy using a drug-coated balloon (DCB)–only approach in

patients with chronic kidney disease at increased risk for contrast-associated acute kidney injury.

**Methods:** Consecutive patients with impaired renal function undergoing ultra-low contrast, DCB-only PCI at a single high-volume centre were included. Patients requiring bailout stenting were not included in this analysis. Baseline coronary angiography was performed using standard projections. After a minimum of 48 h, PCI was planned. Baseline angiography was displayed on the monitor at the time of procedure. Guide catheter intubation and lesion wiring were performed without contras injection. Procedural guidance was performed using high-definition IVUS (HD-IVUS) whenever technically feasible to assess lesion locations, vessel dimensions, and plaque morphology. Lesion preparation included rotational atherectomy and/or dedicated plaque-modifying balloon technologies (cutting balloons or intravascular lithotripsy) at the operator's discretion. Procedural outcomes were evaluated by IVUS, assessing minimal lumen area, the presence of therapeutic dissections or mural hematoma. A final contrast injection was performed for angiographic assessment. Procedural and in-hospital outcomes were descriptively assessed.

**Results:** Eight patients were included. Mean age was 77.6 ± 6.4 years, serum creatinine 2.6 ± 1.8 mg/dL, and estimated glomerular filtration rate 26.3 ± 9.6 mL/min/1.73 $m^2$. All lesions were ACC/AHA type C. All procedures, except one—uncrossable, were performed under IVUS guidance. Rotational atherectomy was used in three cases, cutting balloons in five cases, a high-pressure OPN NC balloon in one case and intravascular lithotripsy in two cases. The procedure was completed in all patients with final TIMI flow 3 using very low contrast (14.4 ± 6.4 mL). Mean procedural duration was 99.4 ± 50.5 minutes, and radiation exposure (dose–area product) was 2974.8 ± 1382.5 cGy·$cm^2$. No major procedural complications, including coronary perforation, acute vessel closure, urgent revascularization, or in-hospital death, were observed.

**Conclusion:** In this small, high-risk patient series, an ultra-low-contrast PCI strategy using a DCB-only approach guided by high-definition IVUS was feasible. Periprocedural dissection assessment using HD-IVUS to guide the intervention was technically feasible. This strategy may represent a potential treatment option for highly selected patients with chronic renal dysfunction.

## 5-5

### Produktprobleme von Herzklappen—Analyse der 2011 bis 2025 vom BfArM veröffentlichten Kundeninformationen

**Siekmeier R.**

Drug Regulatory Affairs, Pharmazeutisches Institut der Universität Bonn, Bonn, Deutschland

**Einleitung:** Vermarktung und Marktüberwachung von Medizinprodukten sind in Europa durch die Verordnung (EU) 2017/745 über Medizinprodukte geregelt. Bei Vorkommnissen und korrektiven Maßnahmen (Field Safety Corrective Action, FSCA) müssen die Hersteller diese den zuständigen nationalen Behörden (Competent Authority (CA); D: Bundesinstitut für Arzneimittel und Medizinprodukte (BfArM), AU: BASG) melden und die Kunden über Kundeninformationen (Field Safety Notice, FSN) informieren, die auch den Behörden zur Verfügung gestellt werden. Die Implantation von Herzklappen mittels chirurgischer/transapikaler oder transfemoraler Verfahren stellt neben Methoden zur Klappenreparatur eine verbreitete Methode zur Behandlung von Patienten mit Klappenvitien dar. Ziel der Studie war die Untersuchung von FSN/FSCA zu Klappenimplantaten in Hinblick auf vorliegende Produktprobleme, damit einhergehende Risiken und Art der FSCA.

**Methoden:** Für die in die Studie eingeschlossenen Medizinprodukte erfolgte eine Analyse der vom BfArM 2011 bis 2025 auf der Homepage (http://www.bfarm.de/DE/Medizinprodukte/riskinfo/kundeninfo/functions/kundeninfo-node.html) publizierten FSCA und FSN.

**Resultate:** Im Untersuchungszeitraum fanden sich 12 (davon 3 mit Folgemeldung) FSCA zu chirurgischen Klappen, 4 FSCA zu transapikalen Klappen und 22 FSCA (davon 2 mit Folgemeldungen) zu Transkatheterklappen (jeweils mit Applikationssystemen), die meist Aortenklappen und im Zeitverlauf zunehmend Transkathetersysteme betrafen. FSCA betrafen, soweit abgrenzbar, häufiger die Klappen als die zugehörigen Applikationssysteme (chirurgische Klappen: 11/1, transapikale Klappen: 2/2, Transkatheterklappen: 12/10). Bei chirurgischen/transapikalen Klappen (einschließlich Applikationssystemen) wurden in 6/1 FSCA Patientenschädigungen berichtet, davon in 1/0 Fällen Todesfälle. Als korrektive Maßnahmen erfolgten (Mehrfachnennungen) ein Rückruf (5/3; Kundeninformation obligat) sowie eine Inquarantänenahme (1/1) und ein Implantations- oder Vertriebsstopp (0/3) (unabhängig vom Rückruf), Anwenderschulungen (1/0), Änderungen der Gebrauchsanweisung (3/0) und Anweisungen zu einer besonderen Patientennachbeobachtung (3/1). Bei Transkatheterklappen (einschließlich Applikationssystemen) wurden in 11 FSCA Patientenschädigungen berichtet, davon in 5 Fällen Todesfälle. Als korrektive Maßnahmen erfolgten (Mehrfachnennungen) ein Rückruf (12; Kundeninformation obligat) sowie eine Inquarantänenahme (1) (unabhängig vom Rückruf), Anwenderschulungen (6) und Änderungen der Gebrauchsanweisung oder der Schulungsunterlagen (10), jedoch keine Anweisungen zu einer besonderen Patientennachbeobachtung.

**Schlussfolgerungen:** Die untersuchten Produkte stellen eine wichtige Produktgruppe mit hohem potentiellem Risiko dar. Produktprobleme, aufgetretene Patientenschädigungen und korrektive Maßnahmen weisen dabei deutliche Unterschiede zwischen den einzelnen Produktgruppen auf. FSCA umfassen bei manifesten Produktmängeln meist Rückrufe, bei prozeduralen Problemen häufiger Anweisungen zur sicheren Handhabung unabhängig von Rückrufen. Aufgrund der darin gegebenen Informationen (Produktproblem, Rückruf, Anweisungen zur sicheren Handhabung und ggf. Patientennachbeobachtung) sind FSN bei FSCA von zentraler Bedeutung für die Verminderung des Risikos durch im Markt befindliche Medizinprodukte.

## 5-6

### Gender-, alters- und indikationsspezifische Unterschiede in der Implantation von subkutanen Defibrillatoren (S-ICDs) einer Schwerpunkt-Einrichtung im Bereich der interventionellen Kardiologie (KARS) im nationalen und internationalen Vergleich. Eine explorative, retrospektive Datenanalyse

**Schütz L.[1], Lemeš C.[2], Martinek M.[2]**

[1]Johannes-Kepler-Universität, Linz, Österreich
[2]Ordensklinikum Linz Elisabethinen, Interne 2 – Kardiologie, Angiologie & Interne Intensivmedizin, Linz, Österreich

**Einleitung:** Der subkutane implantierbare Kardioverter-Defibrillator (S-ICD) ist ein etabliertes System zur Prävention

des plötzlichen Herztodes und stellt eine effektive Alternative zum transvenösen ICD (TV-ICD), vor allem bei Patientinnen und Patienten ohne Bedarf an Bradykardie- oder Resynchronisationstherapie, dar. Trotz zunehmender Evidenz bestehen Hinweise auf geschlechts-, alters- und indikationsspezifische Unterschiede in der Anwendung dieser Technologie. Ziel dieser Arbeit war es, geschlechts-, alters- und indikationsspezifische Unterschiede bei der Implantation von S-ICDs einer Schwerpunkt-Einrichtung im Bereich der interventionellen Kardiologie (KARS) zu analysieren und diese Ergebnisse in einen nationalen (GÖG-Register) sowie internationalen (i-SUSI-Register) Kontext einzuordnen.

**Methoden:** Es wurde eine explorative, retrospektive Datenanalyse durchgeführt. Eingeschlossen wurden 35 erwachsene Patientinnen und Patienten, bei denen im Zeitraum von Jänner 2022 bis Dezember 2024 ein S-ICD implantiert wurde. Erhoben wurden demografische Daten (Alter, Geschlecht) sowie klinische Indikationen. Die Auswertung erfolgte deskriptiv mittels Microsoft Excel und SSPS unter Berechnung von Häufigkeiten, Mittelwerten und 95 %-Konfidenzintervallen. Die Ergebnisse wurden mit nationalen Registerdaten der Gesundheit Österreich GmbH (GÖG) sowie internationalen Daten aus dem i-SUSI-Register verglichen.

**Resultate:** Die S-ICD-Population KARS war im Vergleich zum nationalen Register jünger und wies einen um 6 % höheren Frauenanteil auf. Während Männer sowohl lokal als auch national und international dominierten, zeigte sich am KARS ein geringeres geschlechtsspezifisches Ungleichgewicht. Indikationsspezifisch überwogen im lokalen Kollektiv ventrikuläre Arrhythmien und Kardiomyopathien, während nationale und internationale Register stärker grunderkrankungsbasierte Indikationen, insbesondere strukturelle Kardiomyopathien und genetische Arrhythmiesyndrome, abbildeten. Nationale und internationale Vergleiche verdeutlichten, dass Unterschiede in der Registerstruktur und Klassifikationslogik die Vergleichbarkeit der Daten beeinflussen.

**Schlussfolgerungen:** Die Ergebnisse zeigen, dass die S-ICD-Versorgung am KARS spezifische demografische und klinische Charakteristika aufweist, die sich von nationalen und internationalen Registerdaten unterscheiden. Insbesondere geschlechtsspezifische Unterschiede und die Patientenselektion unterstreichen die Notwendigkeit einer kontextbezogenen Interpretation von Registerdaten. Eine standardisierte Dokumentation könnte die Vergleichbarkeit zukünftiger Analysen verbessern und zur Optimierung der patientenzentrierten S-ICD-Therapie beitragen.

## 5-7

## Length-to-diameter ratio predicts target lesion revascularization in patients undergoing percutaneous coronary intervention

**Radl V.[1], Steinacher E.[1], Baumer U.[1], Hammer A.[1], Hofer F.[1], Kazem N.[1], Lang I.[1], Hengstenberg C.[1], Hemetsberger R.[1], Niessner A.[2], Koller L.[1]**

[1]Medizinische Universität Wien, Wien, Austria
[2]Klinik Landstrasse, Wien, Austria

**Introduction:** The introduction of drug-eluting stents (DES) has substantially improved safety and outcome after percutaneous coronary intervention (PCI), resulting in lower rates of procedure related complications such as target lesion revascularization (TLR) and stent thrombosis (ST). Previous studies have demonstrated associations between TLR and various stent-related characteristics, however, the prognostic performance of these individual parameters remains modest. Therefore we aim to evaluate the predictive performance of basic stent characteristics and introduce a novel length-to-diameter ratio (L/D-Ratio) as a composite metric for the prediction of TLR and ST.

**Methods:** Patients who underwent PCI with second-generation DES implantation between 2010 and 2021 at a tertiary care centre were included in this study. L/D-Ratio was defined as the quotient of maximal stent length divided by minimal stent diameter. The primary endpoint was defined as TLR within a year after the index procedure and the secondary endpoint as 30-day ST.

**Results:** The total study population comprised of 11,910 patients with a median age of 65 (IQR: 55–75) years and 73.8% ($n=8790$) of patients being male. Within one year, TLR occurred in 589 (4.9%) patients. These patients more frequently underwent elective index PCI ($p<0.001$), had a higher prevalence of hypertension, hyperlipidemia, diabetes and chronic kidney disease ($p$ for all $<0.001$) and showed significantly higher mortality rates ($p=0.024$). Patients with TLR had a higher L/D-Ratio (7.5 vs. 7.2, $p=0.001$), greater maximal stent length (23 vs. 22 mm, $p=0.007$), greater total stent length (38.00 vs. 30.00 mm, $p<0.001$) and higher number of stents (2 vs. 1, $p<0.001$) than the ones without. In multivariable regression analysis the L/D-Ratio demonstrated the strongest association with TLR (HR per 1-SD 1.15 [CI: 1.06–1.24], $p<0.001$). Receiver operating characteristic (ROC) demonstrated superior discriminatory performance of the L/D-Ratio for TLR compared to stent diameter (AUC 0.539 vs. 0.465, $p=0.001$) and comparable performance to maximal stent length (AUC 0.539 vs. 0.533, $p=0.139$). In secondary analysis, 30-day ST occurred in a total of 35 patients (0.29%). Patients with higher L/D-Ratios had increased rates of ST (log-rank $p=0.002$). In multivariable logistic regression only L/D-Ratio (adj. HR per 1-SD 1.41 [1.04–1.91], $p=0.026$) and stent length (adj. HR per 1-SD 1.40 [1.01–1.92], $p=0.042$) were associated with a higher risk of 30-day ST.

**Conclusion:** The L/D-Ratio is a suitable predictor of 1-year TLR and 30-day ST after second-generation DES implantation.

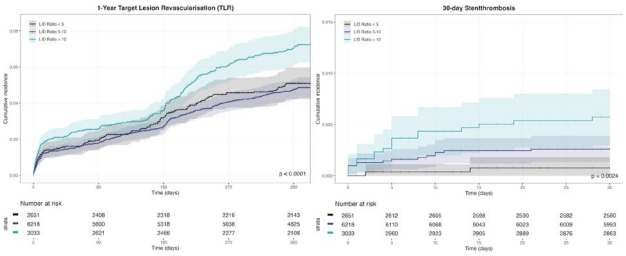


**Fig. 1 | 5-7** KM-Curves for TLR and ST

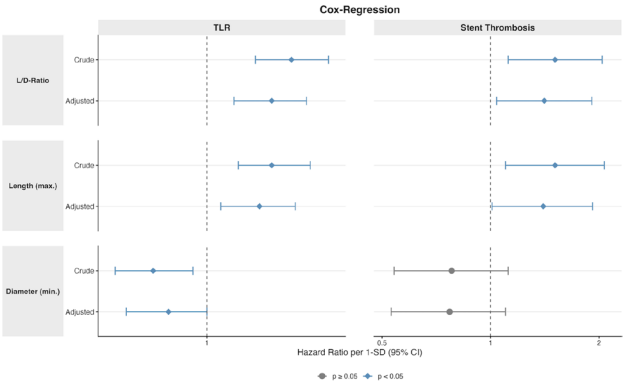


**Fig. 2 | 5-7** HR-Plot TLR and ST

Its predictive value seems to be mainly driven by stent length rather than diameter, highlighting the importance of optimal stent sizing.

# POSTERSITZUNG 6—KARDIALE BILDGEBUNG 1

## 6-1

### Very Severe Aortic Stenosis: Diagnostic Value of Computed Tomography Aortic Valve Calcium Scoring

**Knapitsch C.[1], Schörghofer N.[1], Clodi N.[2,1], Dinges C.[3], Hoppe U.[2], Lichtenauer M.[2], Scharinger B.[1], Hergan K.[4], Hammerer M.[2], Boxhammer E.[2]**

[1]Universitätsklinik für Radiologie, Salzburg, Austria
[2]Universitätsklinik für Innere Medizin II, Kardiologie und internistische Intensivmedizin, Salzburg, Austria
[3]Universitätsklinik für Herzchirurgie, Salzburg, Austria
[4]Universitätsklinik für Radiologie, Universitätsklinikum Salzburg, Salzburg, Austria

**Introduction:** Very severe aortic stenosis (VSAS; Vmax ≥ 5 m/s, MPG ≥ 60 mmHg) is a critical condition with unfavorable clinical outcomes. Guidelines regard VSAS as one criterion for considering valve replacement in asymptomatic patients. Guidelines recommend the use of aortic valve calcium score (AVCS) as an additional parameter to differentiate between moderate AS and severe AS (SAS). The aim of our study is to propose AVCS thresholds for the discrimination between SAS and VSAS.

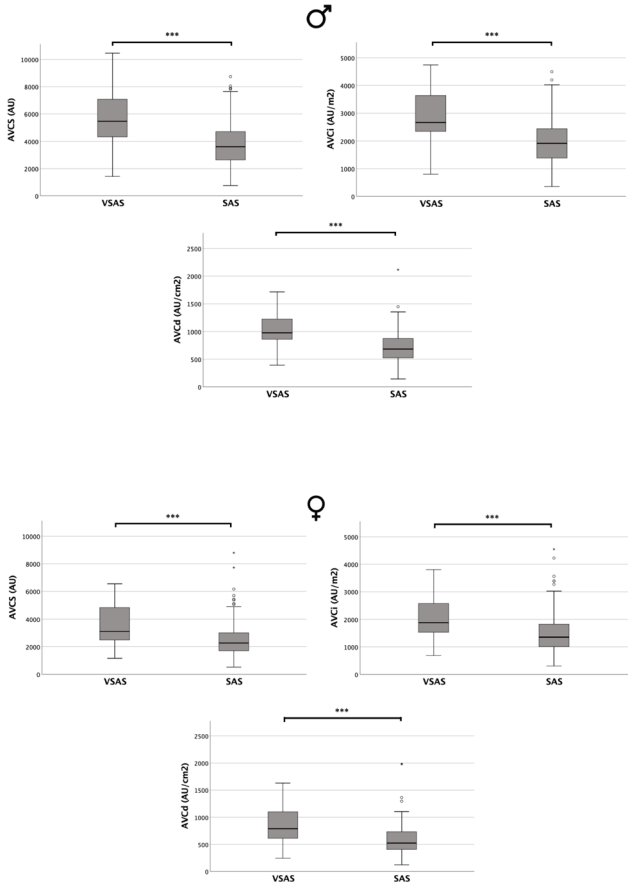


Fig. 1 | 6-1

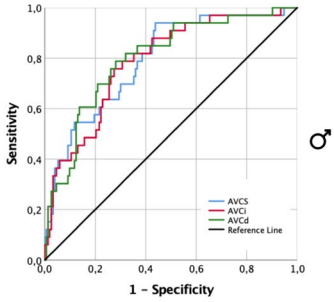


| Value | Prediction | AUC | 95%CI | P-value | Cut-off | Sensitivity | Specificity | Youden Index |
|---|---|---|---|---|---|---|---|---|
| AVCS (AU) | VSAS vs. SAS | 0.794 | 0.711 — 0.876 | < 0.001 | 3706.5 | 0.94 | 0.56 | 0.50 |
| AVCi (AU/m²) | VSAS vs. SAS | 0.787 | 0.705 — 0.870 | < 0.001 | 2324.0 | 0.76 | 0.72 | 0.48 |
| AVCd (AU/cm²) | VSAS vs. SAS | 0.800 | 0.718 — 0.882 | < 0.001 | 810.0 | 0.79 | 0.72 | 0.51 |

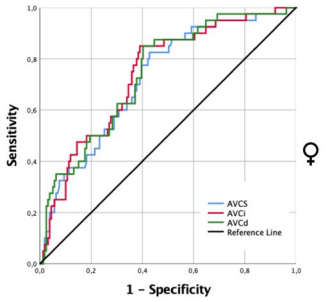


| Value | Prediction | AUC | 95%CI | P-value | Cut-off | Sensitivity | Specificity | Youden Index |
|---|---|---|---|---|---|---|---|---|
| AVCS (AU) | VSAS vs. SAS | 0.725 | 0.642 — 0.808 | < 0.001 | 2374.5 | 0.83 | 0.57 | 0.39 |
| AVCi (AU/m²) | VSAS vs. SAS | 0.741 | 0.659 — 0.823 | < 0.001 | 1478.7 | 0.85 | 0.61 | 0.46 |
| AVCd (AU/cm²) | VSAS vs. SAS | 0.743 | 0.661 — 0.824 | < 0.001 | 580.0 | 0.85 | 0.60 | 0.45 |

Fig. 2 | 6-1

**Methods:** Data of patients from a single center who underwent transcatheter aortic valve implantation ($n = 523$) were retrospectively analyzed. Patients with concordant AS ($n = 430$) were divided into SAS ($n = 344$) and VSAS ($n = 86$) groups and compared in terms of absolute AVCS and indexed AVCS (body surface area; aortic valve annulus area).

**Results:** Mean AVCS was significantly higher in men (m) than in women (w), and significantly higher in VSAS than in SAS (m: SAS 3572.0 AU; VSAS 5465.0 AU; w: SAS 2252.5 AU; VSAS 3064.5 AU; all $p < 0.001$). ROC curve analyses showed AVCS to be a predictor of VSAS in both sexes (m: AUC 0.794; $p < 0.001$; w: AUC 0.725; $p < 0.001$), with optimal cut-off values of 3706.5 AU (m) and 2374.5 (w). Some indexed AVCS had a slightly, but not relevantly, better predictive value.

**Conclusion:** The proposed AVCS thresholds —approximately 3700 AU (m) and 2400 AU (w)—showed significant predictive power to differentiate SAS from VSAS in the study cohort.

## 6-2

### Diagnostische Genauigkeit der Photon-Counting-CT-basierten fraktionellen Flussreserve bei chronischem Koronarsyndrom mit ausgeprägter Koronarkalzifikation

**Steinböck M.[1], Schuchlenz H.[1], Genger M.[1], Kullnig P.[2]**

[1]LKH Graz II, Standort West – Abteilung für Innere Medizin 2, Kardiologie und Intensivmedizin, Graz, Österreich
[2]Diagnostikzentrum Graz, Graz, Österreich

**Einleitung:** Die koronare Computertomographie-Angiographie (CCTA) ist in klinischen Leitlinien zur Diagnostik des chronischen Koronarsyndroms (CCS) etabliert. Die neue Photon-Counting-CT-Technologie bietet eine deutlich höhere räumliche Auflösung und verbessert insbesondere die Darstellung des Koronarlumens bei stark verkalkten Läsionen. Die computergestützte fraktionelle Flussreserve (cFFR) ermöglicht eine nicht-invasive funktionelle Beurteilung hämodynamisch relevanter Stenosen und kann potenziell unnötige invasive Koronarangiographien reduzieren.

**Methoden:** In diese retrospektive monozentrische Analyse wurden konsekutive Patient*innen mit chronischem Koronarsyndrom eingeschlossen, die zwischen Januar 2024 und Januar 2025 sowohl eine Dual-Source-Photon-Counting-CCTA am Diagnostikzentrum Graz als auch eine invasive Koronarangiographie am LKH Graz II, Standort West, erhielten. Die cFFR-Analyse erfolgte verblindet unter Verwendung spezialisierter wissenschaftlicher Software. Hämodynamisch relevante Stenosen wurden definiert als FFR ≤0,80 oder angiographische Stenose >90 %. Die diagnostische Leistungsfähigkeit (Sensitivität, Spezifität, Genauigkeit, positiver prädiktiver Wert [PPV], negativer prädiktiver Wert [NPV]) wurde mit 95 %-Konfidenzintervallen (KI) berechnet. Die Übereinstimmung wurde mittels Cohen-Kappa (κ) nach Landis & Koch beurteilt, systematische Unterschiede mittels McNemar-Test (p).

**Resultate:** Insgesamt wurden 145 Koronargefäße von 87 Patient*innen analysiert (77 % männlich, mittleres Alter 70 Jahre, Spannweit 40–92). Für 64 Patient*innen (108 Gefäße) lag ein Koronararterien-Kalziumscore vor (mittlerer Agatston-Score 1181). In der Gesamtpopulation ($n$=145 Gefäße) zeigte sich eine Sensitivität von 89,3 % (95 %-KI: 82,2–93,8 %), eine Spezifität von 69,7 % (95 %-KI: 52,7–82,6 %), eine Genauigkeit von 84,8 % (95 %-KI: 79,0–90,7 %), ein PPV von 90,9 % (95 %-KI: 84,1–94,9 %) sowie ein NPV von 65,7 % (95 %-KI: 49,2–79,2 %). Die Übereinstimmung war moderat (κ=0,577) ohne Hinweis auf einen systematischen Bias ($p$=0,832). In der Hochrisiko Subgruppe mit schwerer Kalzifikation (Agatston-Score >1000; $n$=53 Gefäße von 29 Patient*innen) zeigte die cFFR eine exzellente diagnostische Performance mit einer Sensitivität von 90,4 % (95 %-KI: 78,3–97,5 %), einer Spezifität von 88,9 % (95 %-KI: 51,8–99,7 %) und einer Genauigkeit von 90,6 % (95 % KI: 82,7–98,4 %). Der PPV betrug 97,6 % (95 %-KI: 87,1–99,9 %), der NPV 66,7 % (95 %-KI: 34,9–90,1 %). Die Übereinstimmung war substantiell (κ=0,705; $p$=0,375).

**Schlussfolgerungen:** Die Photon-Counting-CT-basierte cFFR ermöglicht eine präzise Identifikation hämodynamisch signifikanter Koronarstenosen auch bei Patient*innen mit ausgeprägter Koronarkalzifikation und zeigt eine hohe Übereinstimmung mit der invasiven FFR ohne systematischen Bias. Insbesondere die hohen PPV unterstützen den Einsatz der Methode als zuverlässigen nicht-invasiven Gatekeeper vor invasiver Koronarangiographie.

## 6-3

### [68Ga]Ga-FAPI PET to detect early myocardial fibrotic activity in patients with severe aortic stenosis undergoing TAVR

**Hamzaraj K.[1], Lazarevic A.[1], Sciagra R.[2], Nitsche C.[1], Donà C.[1], Binder P.[1], Nakuz T.[1], Abd El-Aal T.[1], Demirel C.[1], Hemetsberger R.[1], Bartko P.[1], Nejabat M.[1], Kretschmer-Chott E.[1], Hengstenberg C.[1], Hacker M.[1], Calabretta R.[1]**

[1]Medizinische Universität Wien, Wien, Austria
[2]University of Florence, Florence, Italy, Florence, Italy

**Introduction:** Aortic stenosis (AS) causes ongoing pressure overload on the left ventricle and leads to progressive myocardial remodeling. Early diffuse interstitial fibrosis often remains difficult to detect with conventional imaging techniques. Fibroblast activation protein (FAP)–targeted positron emission tomography (PET) can visualize activated fibroblasts and profibrotic activity. However, the usefulness of [$^{68}$Ga]Ga-FAPI PET in evaluating myocardial remodeling in patients with severe AS has not yet been determined.

**Methods:** This post-hoc analysis involved 18 patients with severe aortic stenosis who underwent [$^{68}$Ga]Ga-FAPI PET/CT scans before transcatheter aortic valve replacement. Myocardial tracer uptake was measured as the tracer retention fraction through dynamic PET imaging, evaluated both globally and segmentally. The study also examined correlations between tracer retention and clinical data, cardiac magnetic resonance parameters, and invasive hemodynamics using correlation and receiver operating characteristic analyses.

**Results:** All patients showed widespread myocardial [$^{68}$Ga]Ga-FAPI uptake throughout the heart without focal hotspots, indicating diffuse tracer retention (6.27 ± 2.23 at 60 minutes and 2.88 ± 1.07 at 120 minutes). Segmental retention was inversely related to age at both, 60 and 120 minutes post-injection, especially in basal, mid-ventricular, and apical regions at 120 minutes. Uptake in the mid-septal segments (segments 9 and 14) correlated inversely with the invasively measured mean transaortic gradient (r=–0.61 to –0.62, $p$=0.03–0.04). No rele-

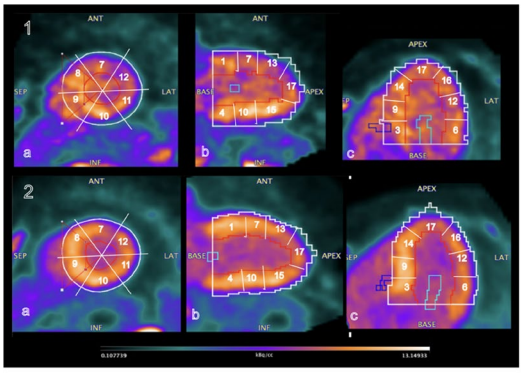


**Figure 1. Representative images of the LV [$^{68}$Ga]Ga-FAPI uptake´s measurement as tracer retention fraction.** ROIs were automatically designed on the LV myocardial wall, identifying the epicardial (white) and the endocardial (red) borders, and on the LV (light blue) cavity. In addition, we manually identified the LV-segments based on the AHA-17-segment model. **Section 1** (upper panels) represents the tracer retention fraction signal at 60 minutes post-injection, and **Section 2** (lower panels) illustrates the tracer retention fraction signal at 120 minutes post-injection.
AHA - American Heart Association; CMR - cardiac magnetic resonance; [$^{68}$Ga]Ga-FAPI- [$^{68}$Ga] - labeled fibroblast activation protein inhibitor; LV - left ventricular; ROIs - regions of interest

**Fig. 1 | 6-3** Tracer uptake patterns

| Variable | Total N=18 |
|---|---|
| Mean transvalvular gradient pre-TAVR (mmHg) | 53.0 (15.0) |
| Mean transvalvular gradient post-TAVR (mmHg) | 2.79 (3.26) |
| LVEDP pre-TAVR (mmHg) | 21.8 (8.32) |
| LVEDP post-TAVR (mmHg) | 22.2 (6.54) |
| LVESP pre-TAVR (mmHg) | 208 (21.7) |
| LVESP post-TAVR (mmHg) | 159 (28.9) |
| Age (y) | 78.6 (3.67) |
| BMI | 9.50 (5.34) |
| Male sex | 14 (77.8%) |
| Diabetes mellitus | 7 (38.9%) |
| Hyperlipidemia | 15 (83.3%) |
| Aterial hypertension | 16 (88.9%) |
| Prior myocardial infarction | 0 (0%) |
| Angina pectoris | 7 (38.9%) |
| NYHA | |
| I | 2 (11.1%) |
| II | 4 (22.2%) |
| III | 8 (44.4%) |
| IV | 1 (5.56%) |
| Septal thickness (mm) | 13.2 (2.60) |
| Left ventricular ejection fraction (%) | 60 (13) |
| Left ventricular end diastolic volume (ml) | 148 (45.2) |
| Left ventricular end systolic volume (ml) | 61.6 (33.9) |
| T1 relaxation time (ms) | 1018 (34.1) |
| Extracellular volume (%) | 25 (2) |

**Abbreviations:** BMI - body mass index; LVEDP - left ventricular end-diastolic pressure; LVESP - left ventricular left systolic pressure; NYHA - New York Heart Association; TAVR - transaortic valve replacement

**Fig. 2 | 6-3** Baseline characteristics

vant associations were found between PET tracer-uptake and LVEF, T1, or ECV values. ROC analysis showed the tracer could effectively distinguish hemodynamic severity in mid-septal segments, with AUC values up to 0.89.

**Conclusion:** In patients with severe aortic stenosis, [$^{68}$Ga] Ga-FAPI PET/CT demonstrated diffuse left ventricular fibroblast activation, with higher tracer retention in mid-septal segments and in younger individuals. These findings suggest that FAPI-PET may serve as a non-invasive biomarker of early myocardial fibrotic remodeling prior to transcatheter aortic valve replacement.

## 6-4

## Epicardial Surface Area of Infarction And Prognosis After STEMI

**Kaser A., Lechner I., Oberhollenzer F., Tiller C., Holzknecht M., Fischer P., Sandor A., Troger F., Mayr A., Schwab M., Gollmann-Tepeköylü C., Bauer A., Metzler B., Reinstadler S., Reindl M.**

Medizinische Universität Innsbruck, Innsbruck, Austria

**Introduction:** Background: The epicardial surface area (EpiSA) of infarction is a novel quantitative measure of transmural extent in ST-elevation myocardial infarction (STEMI). Objectives: To assess the value of EpiSA among other morphological indices of ischemic injury for the prediction of MACE following STEMI.

**Methods:** STEMI patients treated with primary percutaneous coronary intervention and enrolled in the prospective Magnetic Resonance Imaging in Acute ST-Elevation Myocardial Infarction study (MARINA-STEMI, NCT04113356) were included. EpiSA was defined as infarcted epicardial surface determined by cardiac magnetic resonance (CMR). Infarcted endocardial surface area (EnoSA), transmurality, infarct size, microvascular obstruction (MVO) and intramyocardial haemorrhage (IMH) were also assessed. Primary endpoint was the

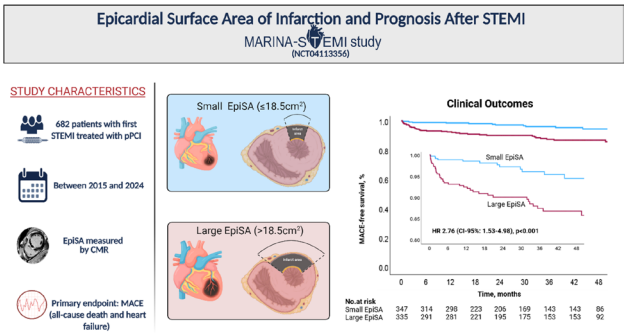


**Fig. 1 | 6-4**

incidence of major adverse cardiac events (MACE), a composite of all-cause mortality and heart failure.

**Results:** In total, 682 patients (median age 59 years, 18% female) were included. MACE was observed in 56 (8%) patients during a follow-up period of 27 [IQR: 12–45] months. Median EpiSA was significantly higher in patients with MACE than in those without MACE (28 [IQR: 14–41] cm$^2$ vs. 17 [IQR: 6–30] cm$^2$, $p=0.002$). The association between EpiSA and MACE remained significant after adjustment for EnoSA, transmurality, infarct size, MVO and IMH (hazard ratio (HR) 1.04, [95%-confidence Interval (95%-CI): 1.01–1.07], $p=0.019$). Adding EpiSA to IMH significantly improved MACE prediction (categorical net reclassification improvement (NRI): 0.34 [95%-CI: 0.21–0.47], $p<0.001$; continuous NRI: 0.53 [95%-CI: 0.28–0.77], $p<0.001$).

**Conclusion:** In patients with acute STEMI, EpiSA emerged as independent and incremental predictor of MACE. These findings support EpiSA as a novel imaging marker for risk stratification.

## 6-5

## Association of mitral annular disjunction on magnetic resonance imaging with cardiovascular outcomes

**Mascherbauer K., Nantschev N., Kronberger C., Donà C., Koschutnik M., Dannenberg V., Poledniczek M., Schmid L., Singer K., Lunzer L., Koschatko S., Jantsch C., Heitzinger G., Halavina K., Nitsche C., Duca F., Beitzke D., Loewe C., Waldmann E., Bartko P., Mascherbauer J., Hengstenberg C., Kammerlander A.**

AKH, Wien, Austria

**Introduction:** Mitral annular disjunction (MAD) is increasingly recognized on cardiac magnetic resonance (CMR) imaging, yet its clinical significance remains debated. We aimed to determine the prevalence, clinical correlates, and prognostic impact of MAD in a large all-comer tertiary care CMR cohort.

**Methods:** We analyzed data from 1969 patients enrolled in a prospective CMR registry at the Vienna General Hospital between 2013 and 2023. MAD was assessed in two-, three-, and four-chamber cine views in both end-systole and end-diastole and defined as a ≥ 1 mm separation between the left atrial wall at the mitral valve hinge point and the adjacent left ventricular myocardium. Additionally, we measured native myocardial T1 relaxation times at the mitral annulus to assess for subclinical tissue remodeling. The primary endpoint was all-cause mortality, analyzed by Cox proportional hazards regression.

**Results:** Overall systolic MAD was present in 509 patients (25.9%), while diastolic MAD was present in 366 patients (18.6%). MAD patients were younger (59.6 ± 18.5 vs. 65.2 ± 17.9 years, $p < 0.001$), had fewer comorbidities (diabetes 9.8% vs. 17.2%, CKD 6.7% vs. 12.6%; both $p < 0.001$), higher left ventricular (LV) ejection fraction (58.8 ± 10.4% vs. 56.8 ± 14.4%, $p = 0.009$), and lower LV mass (123.3 ± 47.2 vs. 148.6 ± 56.1 g, $p < 0.001$). Mitral valve prolapse (MVP) was more common with MAD (8.4% vs. 2.6%, $p < 0.001$). MAD distance correlated positively with native myocardial T1 times (r = 0.24, $p < 0.001$), and patients with MAD ≥ 5 mm showed higher T1 values than those with MAD < 5 mm (1041 ± 148 vs. 1010 ± 72 ms, $p = 0.028$). During a 63.7-month median follow-up time, 485 deaths occurred. After adjustment for age, sex, diabetes, and atrial fibrillation, diastolic MAD was not independently associated with mortality (HR 0.95, 95% CI 0.74–1.23, $p = 0.712$). However, patients with MAD ≥ 5 mm showed a non-significant trend toward higher mortality (HR 1.27, 95% CI 0.77–2.10, $p = 0.345$).

**Conclusion:** Diastolic MAD is common and prognostically neutral. Among MAD-positive patients, larger disjunction distances are associated with higher native myocardial T1 values, suggesting subclinical myocardial remodeling. These findings support that mild MAD represents a benign anatomical variant, whereas larger disjunctions may indicate an evolving pathological substrate warranting closer evaluation.

## 6-6

### Comprehensive Assessment of Remote Myocardium Extracellular Volume Metrics in patients with ST-elevation myocardial infarction

**Oberhollenzer F.[1], Lechner I.[1], Tiller C.[1], Holzknecht M.[1], Kaser A.[1], Fischer P.[1], Sandor A.[1], Mayr A.[2], Bauer A.[1], Metzler B.[1], Reindl M.[1], Reinstadler S.[1]**

[1]Universitätsklinik für Innere Medizin III, Kardiologie und Angiologie, Innsbruck, Austria
[2]Universitätsklinik für Radiologie, Innsbruck, Austria

**Introduction:** Non-invasive markers of myocardium tissue alterations assessed by cardiovascular magnetic resonance (CMR) T1 mapping provide significant prognostic information. Extracellular volume (ECV) in the remote myocardium was found to be an independent predictor of adverse outcome in patients following ST-elevation myocardial infarction (STEMI). Recently, indexed ECV (iECV) has been suggested to outperform conventional ECV in predicting adverse outcome in patients with valvular heart disease. However, the prognostic significance of iECV in patients after STEMI remains unclear. Therefore, we aimed to investigate the prognostic value of iECV in the remote myocardium and to compare its performance with conventional remote ECV in patients with acute STEMI.

**Methods:** This study analyzed 624 STEMI patients treated with primary percutaneous coronary intervention (PCI) that were included in the prospective MARINA-STEMI study (NCT04113356). CMR imaging was performed 4 ([Interquartile range (IQR): 3–5]) days after PCI. CMR images were analyzed for left ventricular (LV) function, standard infarct characteristics including microvascular injury parameters as well as conventional remote ECV and remote iECV determined by T1 mapping. Remote iECV was calculated by incorporating LV ventricular mass and body surface area. The primary clinical endpoint was the composite of all-cause mortality, re-infarction and new congestive heart failure (Major adverse cardiovascular events, MACE).

**Results:** Median age of the cohort was 58 ([IQR: 52–67]) years, 17% ($n = 106$) of patients were female. Median remote ECV was 26.19 ([IQR: 23.94–28.71]) %, median iECV in the remote myocardium was 15.43 ([IQR: 13.32–18.25]) ml/m2. Over a median follow-up of 2.1 ([IQR: 1.0–3.6]) years after STEMI, 69 MACE outcomes occurred. Remote ECV (OR: 1.45 [95% confidence interval (CI): 1.15–1.84], $p = 0.002$) as well as remote iECV (OR: 1.50 [95% confidence interval (CI): 1.19–1.88], $p < 0.001$) were significantly associated with MACE. In receiver operating characteristic analysis, iECV demonstrated a comparable performance to ECV (area under the curve: 0.625 vs. 0.595, $p = 0.295$).

**Conclusion:** In patients following STEMI, both remote ECV and remote iECV were associated with MACE showing comparable prognostic performance. These findings indicate no incremental predictive value of iECV over ECV in patients with STEMI.

## 6-7

### Pulmonary Artery Diameter as a Differential Prognostic Marker in Aortic Valve Replacement: Divergent Impact in SAVR and TAVR

**Brandstetter L.[1], Schörghofer N.[1], Knapitsch C.[1], Clodi N.[2,1], Gansterer K.[3], Steindl J.[3], Scharinger B.[1], Hammerer M.[2], Hoppe U.[2], Hergan K.[4], Dinges C.[3], Boxhammer E.[2]**

[1]Universitätsklinik für Radiologie, Salzburg, Austria
[2]Universitätsklinik für Innere Medizin II, Kardiologie und internistische Intensivmedizin, Salzburg, Austria
[3]Universitätsklinik für Herzchirurgie, Salzburg, Austria
[4]Universitätsklinik für Radiologie, Universitätsklinikum Salzburg, Salzburg, Austria

**Introduction:** Risk stratification in aortic stenosis is predominantly based on left-sided cardiac parameters, whereas the right heart–pulmonary circulation axis remains insufficiently characterized. The diameter of the truncus pulmonalis (TP) reflects chronic pressure overload and pulmonary vascular remodeling, yet its prognostic relevance in patients undergoing isolated aortic valve replacement is unknown. The aim of the study was to determine the association of TP and body surface area–indexed TP (TP/BSA) with long-term mortality and to assess their incremental prognostic value beyond established clinical risk factors in patients undergoing isolated surgical (SAVR) or transcatheter (TAVR) aortic valve replacement.

**Methods:** A total of 1002 consecutive patients undergoing isolated aortic valve replacement at a single tertiary care center between 2013 and 2022 were included (SAVR: $n = 476$; TAVR: $n = 526$). Mean age was 69.3 ± 9.2 years in SAVR and 82.0 ± 5.2 years in TAVR; 200 (42%) and 264 (50%) were female, respectively. TP was quantified on pre-procedural imaging using an orthogonal (double-oblique) measurement approach and analyzed as a continuous variable as well as indexed to body surface area. The primary endpoint was all-cause mortality. Multivariable Cox proportional hazards models were adjusted for age, sex, coronary artery disease, chronic obstructive pulmonary disease, peripheral artery disease, estimated glomerular filtration rate, atrial fibrillation, prior myocardial infarction, NYHA functional class, and moderate-to-severe mitral regurgitation. Model performance was evaluated using bootstrap-corrected Harrell's C-index and time-dependent AUC analyses.

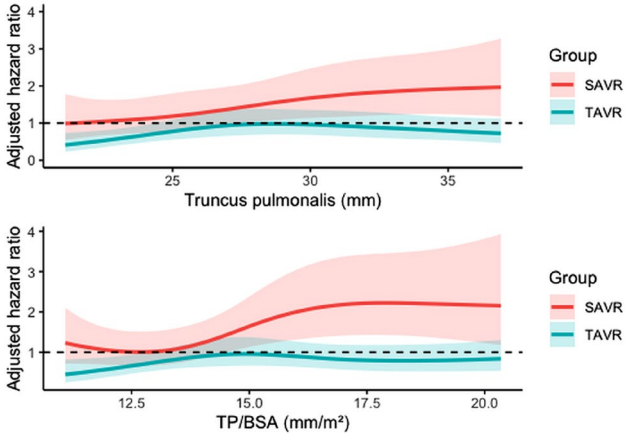


**Fig. 1 | 6-7** Increasing pulmonary artery diameter is associated with higher mortality in SAVR, but not in TAVR

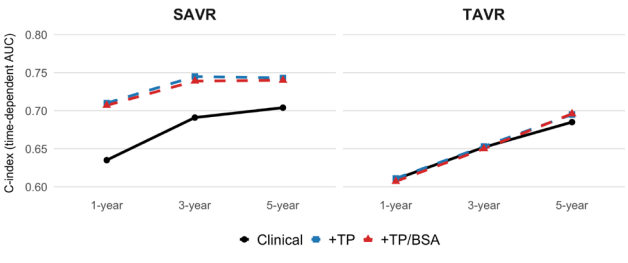


| Group | Time | Clinical AUC (95% CI) | +TP AUC (95% CI) | ΔAUC (+TP) (95% CI) | p | +TP/BSA AUC (95% CI) | ΔAUC (+TP/BSA) (95% CI) | p |
|---|---|---|---|---|---|---|---|---|
| SAVR | 1 year | 63.5 (49.9–77.1) | 71.0 (58.8–83.3) | +7.5 (3.3–11.8) | <0.001 | 70.7 (58.2–83.3) | +7.3 (3.1–11.4) | <0.001 |
| | 3 years | 69.1 (60.8–77.3) | 74.5 (66.8–82.1) | +5.4 (2.4–8.4) | <0.001 | 73.9 (66.1–81.7) | +4.8 (1.7–8.0) | 0.003 |
| | 5 years | 70.4 (63.6–77.2) | 74.3 (67.8–80.7) | +3.9 (1.3–6.5) | 0.003 | 74.0 (67.5–80.6) | +3.7 (1.0–6.4) | 0.007 |
| TAVR | 1 year | 61.0 (51.6–70.3) | 61.1 (52.0–70.2) | +0.1 (−1.5–1.7) | 0.88 | 60.7 (51.6–69.8) | −0.3 (−2.3–1.8) | 0.79 |
| | 3 years | 65.2 (59.0–71.3) | 65.3 (59.3–71.4) | +0.2 (−0.8–1.2) | 0.76 | 65.0 (59.0–71.1) | −0.1 (−1.4–1.2) | 0.87 |
| | 5 years | 68.5 (62.5–74.5) | 69.5 (63.6–75.4) | +1.0 (0.0–1.9) | 0.04 | 69.6 (63.8–75.5) | +1.2 (−0.1–2.4) | 0.06 |

**Fig. 2 | 6-7** Pulmonary artery diameter provides incremental prognostic value in SAVR, but not in TAVR

**Results:** During follow-up of up to 7 years, TP was independently associated with mortality in SAVR, but not in TAVR. In SAVR, each standard deviation increase in TP and TP/BSA was associated with a significantly higher risk of death (TP: HR 1.23, 95% CI 1.04–1.46, $p = 0.018$; TP/BSA: HR 1.29, 95% CI 1.05–1.58, $p = 0.017$), whereas no significant associations were observed in TAVR. Patients with enlarged TP (≥ 29 mm) demonstrated significantly reduced survival, with persistent separation of Kaplan–Meier curves. Addition of TP improved risk discrimination in SAVR (C-index 0.649 to 0.671), but not in TAVR. Time-dependent analyses confirmed significant improvements in predictive accuracy in SAVR (ΔAUC up to +7.5% at 1 year), whereas only minimal effects were observed in TAVR.

**Conclusion:** TP emerges as a powerful, imaging-derived predictor of long-term mortality in isolated SAVR, providing incremental prognostic value beyond established risk models. In contrast, its lack of prognostic relevance in TAVR suggests fundamentally different disease phenotypes. These findings shift the focus toward the right heart–pulmonary circulation axis as a key, yet underrecognized determinant of outcome and support the integration of TP into contemporary surgical risk stratification.

# POSTERSITZUNG 7—KORONARE HERZKRANKHEIT & AKUTES KORONARSYNDROM 1

## 7-1

### Periodic repolarization dynamics in patients undergoing primary PCI for acute myocardial infarction

**Kindl B., Hofer F., Pavluk D., Schreinlechner M., Dolejsi T., van der Merwe C., Klimovskis N., Reinstadler S., Bauer A.**

University Clinic of Internal Medicine III/Cardiology and Angiology, Innsbruck, Austria

**Introduction:** Periodic repolarization dynamics (PRD) quantify low-frequency oscillations of ventricular repolarization and reflect phasic sympathetic modulation of myocardial electrophysiology. Increased PRD has been associated with heightened arrhythmic risk in ischemic heart disease, likely mediated by enhanced repolarization instability under sympathetic drive. During acute ST-elevation myocardial infarction (STEMI), ischemia-induced electrical heterogeneity and autonomic imbalance may further amplify PRD. However, the immediate mechanistic response of PRD to coronary reperfusion remains poorly characterized. We therefore investigated the dynamic changes of PRD before and after primary percutaneous coronary intervention (PCI) in first STEMI.

**Methods:** Patients aged ≥ 18 years presenting with first acute STEMI were prospectively included. High-resolution (1000 Hz) ECG recordings in Frank lead configuration were initiated prior to primary PCI. PRD was quantified during the pre-interventional ischemic phase and continuously for 24 hours following reperfusion. Temporal changes in PRD were analyzed with particular focus on the early reperfusion phase.

**Results:** Twenty-three patients were analyzed (median age 62 years [IQR 55–70]; 26% female). Pre-interventional TIMI flow was 0 in 10 patients, 1 in 7, 2 in 4, and 3 in 2 patients. Post-PCI, TIMI 3 flow was achieved in 20 patients and TIMI 2 flow in 3 patients. Baseline PRD was markedly elevated prior to PCI (median 7.80 deg$^2$ [IQR 6.2–10.6]). Within the first 6 hours after successful reperfusion, PRD significantly decreased to 4.06 deg$^2$ (IQR 2.7–6.9; $p = 0.0039$ vs. pre-PCI). Between 6 and 24 hours post-PCI, PRD remained stable (median 4.6 deg$^2$ [IQR 2.3–7.5]; $p = 0.65$ vs. PRD at 6 hours post reperfusion). When stratified by infarct-related artery, PRD was significantly higher in patients with left anterior descending artery infarction ($n = 9$; median 10.4 deg$^2$ [IQR 9.2–10.9]) compared with non-LAD infarctions (right coronary artery and circumflex artery combined, $n = 14$; median 7.1 deg$^2$ [IQR 4.1–8.8]; $p = 0.035$). No significant association was observed between PRD and pre-interventional TIMI flow.

**Conclusion:** Primary PCI in STEMI is associated with a rapid and significant reduction of PRD within the first hours after reperfusion. This observation supports the concept that acute myocardial ischemia enhances sympathetic-driven oscillations of ventricular repolarization, contributing to electrical instability, and that restoration of coronary blood flow attenuates this autonomic-electrophysiological coupling. PRD may serve as a dynamic, non-invasive biomarker reflecting reversible ischemia-related repolarization instability during the early reperfusion phase. The higher PRD observed in LAD infarctions

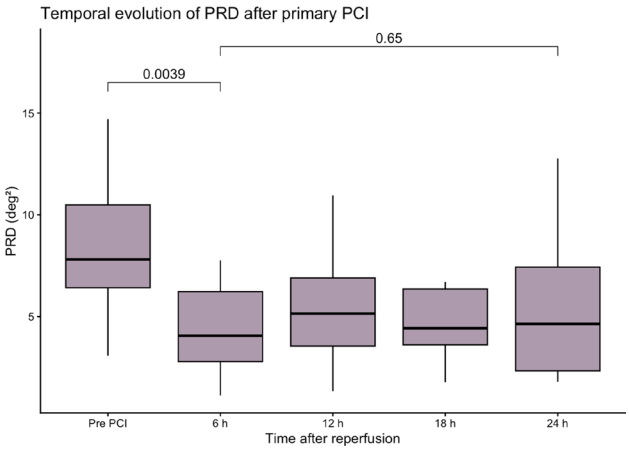


**Fig. 1 | 7-1** Boxplot diagram for PRD change

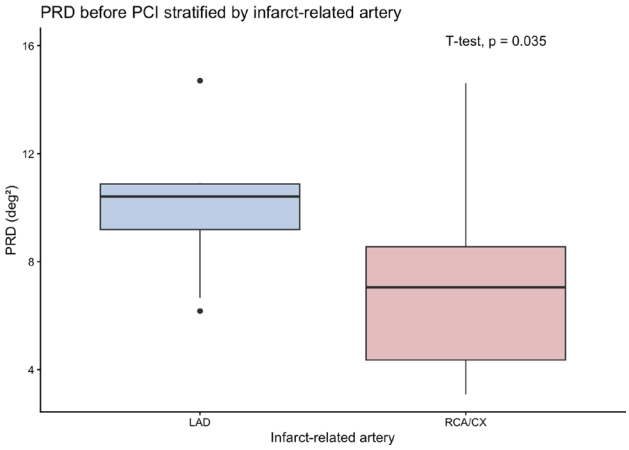


**Fig. 2 | 7-1** PRD compared by affected vessel

compared with non-LAD infarctions suggests that infarct location and the extent of affected myocardium may influence sympathetic-mediated repolarization dynamics. Larger studies are warranted to clarify the relationship between PRD dynamics, autonomic recovery, and arrhythmic outcomes after STEMI.

## 7-2

## Ergotherapeutische Interventionen nach Myokardinfarkt bei Menschen im erwerbsfähigen Alter

**Mühlegger V.[1], Nagiller I.[2]**

[1]Reha Zentrum Münster, Münster, Österreich
[2]fhg – Zentrum für Gesundheitsberufe Tirol GmbH (Fachhochschule), Innsbruck, Österreich

**Einleitung:** Herz-Kreislauf-Erkrankungen zählen weltweit zu den häufigsten Todesursachen. Besonders im erwerbsfähigen Alter können die daraus resultierenden körperlichen und psychischen Einschränkungen die Berufsfähigkeit und Alltagsbewältigung erheblich beeinträchtigen. Im Alltag zeigen sich häufig reduzierte Belastbarkeit und Fatigue, Schmerzen in den oberen Extremitäten, psychische Begleiterscheinungen wie Depressionen und Ängste, Folgeerkrankungen (z. B. Herzinsuffizienz und Herzrhythmusstörungen), hypoxische Hirnschäden und dadurch ein deutlicher Verlust an Lebensqualität. Die kardiologische Rehabilitation ist zentral für die Wiederherstellung sozialer und beruflicher Teilhabe. In Österreich orientiert sie sich am biopsychosozialen Modell der ICF, wobei die Ergotherapie einen wichtigen Beitrag durch individuell angepasste Interventionen leistet.

**Methoden:** Zwischen Juli und Dezember 2024 wurde eine systematische Literaturrecherche durchgeführt, orientiert an den Merkmalen eines Scoping Reviews unter Einbezug grauer Literatur. Die Recherche erfolgte in den Datenbanken PubMed®, Cochrane Library, Oxford Academic, OT Seeker, Google Scholar und EBSCO (fhg) sowie in den Bibliotheken der fhg Innsbruck und der ULB Tirol. Zusätzlich wurden relevante Fachzeitschriften, unter anderem das European Heart Journal, berücksichtigt und weitere Literatur mithilfe des Schneeballprinzips identifiziert. Die Einordnung der Ergebnisse erfolgte anhand der Internationalen Klassifikation der Funktionsfähigkeit, Behinderung und Gesundheit (ICF).

**Resultate:** Körperfunktionen und Körperstrukturen: Kognitives Training; alltagsorientiertes Training; Stressbewältigung und Coping-Strategien; Entspannungsverfahren (z. B. progressive Muskelentspannung, Meditation, Atemübungen, Achtsamkeitstraining); Förderung der Selbstwahrnehmung; Narbenbehandlung Aktivitäten: Energie- und Pausenmanagement; Alltagstraining; Betätigungsprofil; Anpassung von Aktivitäten/Alltagstätigkeiten; Förderung von Selbstwirksamkeit; Erlernen von Problemlösungsstrategien; Assessments (z. B. OSA, FSS, Energietagebuch, Energieprofil) Partizipation: Vorbereitung und Begleitung der beruflichen Wiedereingliederung; Beratung zu stufenweisen Wiedereingliederungsmodellen; arbeitsbezogene Assessments (z. B. COPM, OSA, WRI, WSS, IMBA, EFL), Edukation; Berufs- und Arbeitsplatzanamnese Umweltfaktoren: Anpassungen am Arbeitsplatz; Hilfsmittelberatung; Anpassung von Arbeitsbedingungen; Edukation des sozialen Umfelds; Evaluation der Arbeitsumgebung (z. B. WEIS); Umweltanpassung Personbezogene Faktoren: Edukation zum Krankheitsbild; Unterstützung bei Lebensstiländerungen; Reduzierung von Risikofaktoren; Edukation; Förderung der Teilnahme an kardiologischer Rehabilitation.

**Schlussfolgerungen:** Aufgrund der begrenzten Evidenz zur Ergotherapie nach Myokardinfarkt wurde im Rahmen der Literaturrecherche auch graue Literatur sowie Evidenz angrenzender Fachbereiche einbezogen, was die eingeschränkte Studienlage verdeutlicht. Die ICF diente als strukturierender Bezugsrahmen, wobei Interventionen häufig mehrere Bereiche gleichzeitig adressieren. Dennoch lassen sich zentrale ergotherapeutische Handlungsfelder identifizieren, insbesondere zur Unterstützung der beruflichen Wiedereingliederung und Alltagsbewältigung. Die Ergebnisse betonen die Notwendigkeit eines individuell angepassten, klient:innenzentrierten, alltagsorientierten und handlungsrelevanten Vorgehens. Aus handlungswissenschaftlicher Perspektive zeigen sich nach Myokardinfarkt häufig Betätigungsunterbrechungen und Rollenveränderungen im Sinne von „occupational disruption“ und „occupational loss“, die langfristig „occupational injustice“ begünstigen können. Die Ergotherapie wirkt diesen Ver-

| ICF-Bereich | Ergotherapeutische Interventionen |
|---|---|
| **Körperfunktionen & -strukturen** | Kognitives Training; alltagsorientiertes Training; Stressbewältigung und Coping-Strategien; Entspannungsverfahren (z. B. progressive Muskelentspannung, Meditation, Atemübungen, Achtsamkeitstraining); Förderung der Selbstwahrnehmung; Narbenbehandlung |
| **Aktivitäten** | Energie- und Pausenmanagement; Alltagstraining; Betätigungsprofil; Anpassung von Aktivitäten/Alltagstätigkeiten; Förderung von Selbstwirksamkeit; Erlernen von Problemlösungsstrategien; Assessments (z.B. OSA, FSS, Energietagebuch, Energieprofil) |
| **Partizipation** | Vorbereitung und Begleitung der beruflichen Wiedereingliederung; Beratung zu stufenweisen Wiedereingliederungsmodellen; arbeitsbezogene Assessments (z. B. COPM, OSA, WRI, WSS, IMBA, EFL), Edukation; Berufs- und Arbeitsplatzanamnese |
| **Umweltfaktoren** | Anpassungen am Arbeitsplatz; Hilfsmittelberatung; Anpassung von Arbeitsbedingungen; Edukation des sozialen Umfelds; Evaluation der Arbeitsumgebung (z. B. WEIS); Umweltanpassung |
| **Personbezogene Faktoren** | Edukation zum Krankheitsbild; Unterstützung bei Lebensstiländerungen; Reduzierung von Risikofaktoren; Edukation; Förderung der Teilnahme an kardiologischer Rehabilitation |

**Abb. 1 | 7-2** Darstellung der Ergebnisse

änderungen gezielt entgegen, indem sie Handlungskompetenz, Handlungsrollen und Teilhabe fördert. Durch individuelle, handlungsorientierte Interventionen trägt die Ergotherapie maßgeblich zur kardiologischen Rehabilitation und zur beruflichen Wiedereingliederung bei. Eine stärkere strukturelle und interdisziplinäre Verankerung sowie weitere Forschung zur Wirksamkeit spezifischer ergotherapeutischer Maßnahmen sind erforderlich, um ihre Rolle in diesem Fachbereich langfristig zu sichern und weiter zu etablieren.

## 7-3

### Systemic Progression of Atherosclerosis After STEMI: A Prospective Cohort Analysis

**Pavluk D.[1], Schreinlechner M.[1], Reindl M.[1], Lechner I.[1], Hofer F.[1], Marschang P.[2], Noflatscher M.[1], Tiller C.[1], Metzler B.[1], Bauer A.[1], Reinstadler S.[1]**

[1]Universitätsklinik für Innere Medizin III – Kardiologie und Angiologie – Medizinische Universität Innsbruck, Innsbruck, Austria
[2]Krankenhaus Bozen – Abteilung für Innere Medizin, Bozen, Italy

**Introduction:** ST-elevation myocardial infarction (STEMI) typically reflects an acute event within chronic systemic atherosclerosis. (1) It remains unclear whether STEMI is associated with accelerated progression of atherosclerosis in extracoronary vascular beds, whether such progression carries prognostic relevance, and whether it is related to infarct severity at the tissue level. (2) We therefore investigated 1-year extracoronary plaque progression in patients with STEMI compared with chronic coronary syndrome (CCS), examined its association with long-term outcomes, and evaluated the relationship between infarct severity and subsequent plaque progression.

**Methods:** In this prospective cohort study, 173 patients (CCS $n=84$, STEMI $n=98$) underwent three-dimensional ultrasound quantification of carotid and femoral plaque volume at baseline and 12 months. Plaque progression was defined as absolute change in cumulative plaque volume. Determinants of progression were assessed using multivariable linear regression. In STEMI patients, myocardial infarct severity was assessed by cardiac magnetic resonance (CMR) and tested for association with plaque progression. Major adverse cardiovascular and cerebrovascular events (MACCE) and its association with plaque progression were evaluated using Cox proportional hazards models.

**Results:** Baseline cumulative plaque volume was higher in CCS (mean age: 65.0 years, 26.2% female) than STEMI patients (mean age: 58.6 years, 21.11% female) (161.00 ± 325.75 mm3 vs 66.50 ± 114.75 mm3, respectively, $p<0.001$). Over 12 months, cumulative plaque volume increased more in STEMI than in CCS (median 61.5 (± 90.25) vs 37.5 (± 76.25) $mm^3$, $p=0.001$ (Fig. 1)). In multivariable regression, STEMI presentation was independently associated with greater plaque progression (β 54.6 $mm^3$, 95% CI 27.9 to 81.2, $p<0.001$.) During a median follow up of 6.6 years, high plaque progression was independently associated with MACCE (hazard ratio 5.50, 95% CI 1.59 to 19.05, $p=0.007$) with good model discrimination (C-index 0.758). Unsupervised clustering revealed three distinct systemic progression phenotypes within the STEMI cohort, showing markedly different plaque progression levels, $p=0.003$, and characterized by divergent metabolic and inflammatory risk constellations. CMR-derived Infarct size and presence of microvascular obstruction was not associated with plaque progression ($p=0.713$).

**Conclusion:** STEMI is associated with accelerated extracoronary atherosclerotic plaque progression compared with CCS. Extracoronary plaque progression independently predicts long-term adverse cardiovascular outcomes and exhibits marked heterogeneity across biologically distinct phenotypes, whereas no association with tissue-level infarct severity was observed.

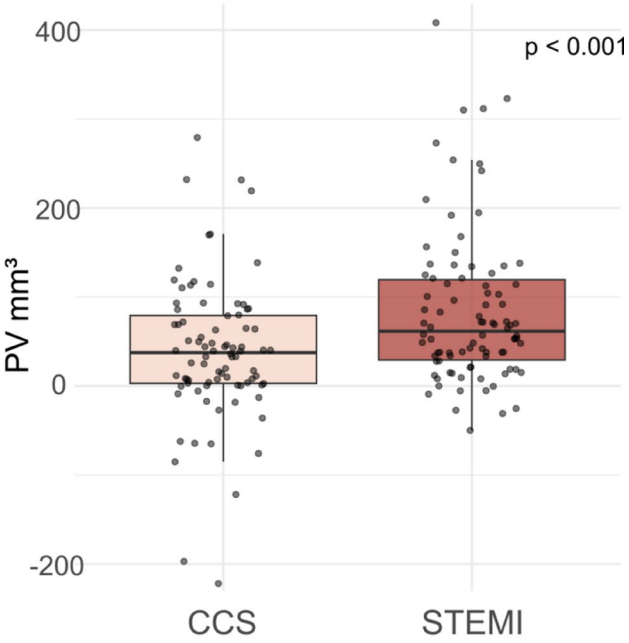


**Fig. 1 | 7-3** Progression of Atherosclerotic Plaque Volume in Patients with CCS and STEMI

### References

1. Bergmark BA, Mathenge N, Merlini PA, Lawrence-Wright MB, Giugliano RP. Acute coronary syndromes. Lancet. 2022;399(10332):1347–58.
2. Falk E. Pathogenesis of atherosclerosis. J Am Coll Cardiol. 2006;47(8 Suppl):C7-12.

## 7-4

### Akute Angstsymptome als Prädiktor depressiver Chronifizierung im Langzeitverlauf nach Myokardinfarkt

**Braun C.[1], Baranyi A.[1], Kolesnik E.[2], Schmidt A.[2]**

[1]Department of Psychiatry and Psychotherapeutic Medicine, Medical University of Graz, Graz, Österreich
[2]Division of Cardiology, Department of Internal Medicine, Medical University of Graz, Graz, Österreich

**Einleitung:** Ein Myokardinfarkt (MCI) stellt für Betroffene ein potenziell lebensbedrohliches Ereignis dar und geht neben den somatischen Akutfolgen häufig mit ausgeprägten emotionalen Reaktionen einher. Insbesondere akute Angstsymptome treten im Kontext des Ereignisses häufig auf, werden jedoch im klinischen Akutsetting meist nur unzureichend berücksichtigt. Dabei legen bisherige Befunde nahe, dass frühe psychische

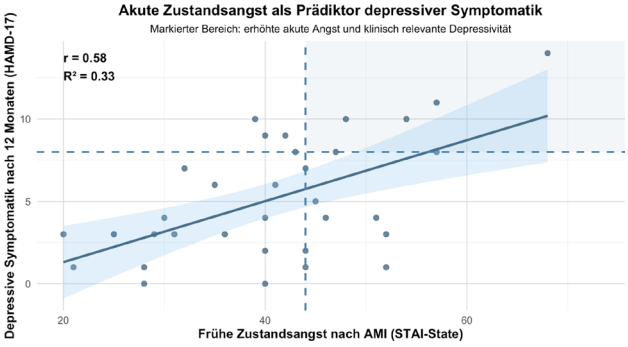


**Abb. 1 | 7-4** Zusammenhang zwischen frühzeitiger Zustandsangst und depressiver Symptomatik bei der Nachuntersuchung nach einem Jahr

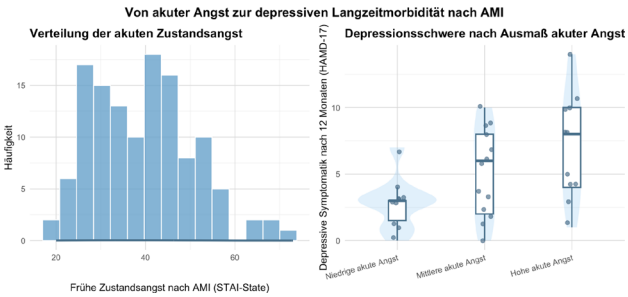


**Abb. 2 | 7-4** Verteilung der frühen Zustandsangst und depressiver Symptomatik im 1-Jahres-Follow-Up nach Angstgruppen

Belastungsreaktionen die Entwicklung und Chronifizierung depressiver Symptome im weiteren Verlauf begünstigen können. Ziel der vorliegenden Studie war es daher zu untersuchen, inwieweit akute Angstsymptome nach MCI als Risikofaktor für eine depressive Chronifizierung im Langzeitverlauf fungieren.

**Methoden:** In die prospektive Studie wurden 128 Patient:innen mit akutem Myokardinfarkt aufgenommen, die an der Abteilung für Kardiologie des Universitätsklinikums Graz rekrutiert wurden. Unmittelbar nach klinischer Stabilisierung wurde die situationsbezogene Angst mit dem State-Trait Anxiety Inventory (STAI; [1]) als Selbstbeurteilungsverfahren erhoben. Zwölf Monate nach dem Indexereignis wurde ein strukturiertes telefonisches Follow-up durchgeführt, bei dem depressive Symptome anhand der Hamilton Depression Rating Scale (HAMD-17; [2]) erfasst wurden. Insgesamt konnten 34 Patient:innen in die Langzeituntersuchung eingeschlossen werden. Zur Prüfung des Zusammenhangs zwischen früher Zustandsangst und depressiver Symptomatik im Langzeitverlauf wurden Pearson-Korrelationen berechnet.

**Resultate:** Es zeigten sich signifikante Zusammenhänge zwischen der unmittelbar nach MCI erfassten situationsbezogenen Angst und depressiven Symptomen im Langzeitverlauf ($r = 0{,}58$, $p < 0{,}001$, $R2 = 0{,}33$, siehe Abb. 1 & 2). Die Befunde sprechen für eine prognostische Relevanz akuter Angstsymptome im Hinblick auf die Entwicklung persistierender depressiver Beschwerden.

**Schlussfolgerungen:** Der stark positive Zusammenhang unterstreicht die klinische Bedeutung einer frühzeitigen standardisierten Erfassung von Angstsymptomen im Akutsetting. Die Implementierung schriftlicher Screeningverfahren könnte als praktikables Instrument zur psychologischen Risikostratifizierung beitragen, Hochrisikopatient:innen frühzeitig zu identifizieren und präventive psychosoziale Interventionen zeitnah einzuleiten.

## Literatur

1. Laux L, Glanzmann P, Schaffner P, Das State-Trait-Angstinventar SCD. (STAI): Theoretische Grundlagen und Handanweisung. Weinheim: Beltz; 1981.
2. Hamilton, M. (1960). A rating scale for depression. Journal of Neurology, Neurosurgery, and Psychiatry. 1960;23(1):56–62. https://doi.org/10.1136/jnnp.23.1.56

# 7-5

## Telemedical cardiac risk assessment by implantable cardiac monitors in patients after myocardial infarction with autonomic dysfunction (SMART-MI-DZHK9): Assessment of MI type in arrhythmic event detection and subsequent cardiovascular complications

**Dolejsi T.[1], Schreinlechner M.[1], Pavluk D.[1], Klimovskis N.[1], Reinstadler S.[1], Rizas K.[2], Massberg S.[2], Bauer A.[1]**

[1]Universitätsklinik für Innere Medizin III, Innsbruck, Austria
[2]LMU Klinikum, Medizinische Klinik und Poliklinik I, München, Germany

**Introduction:** Cardiac autonomic dysfunction assessed by digital ECG-based markers identifies patients at increased risk after myocardial infarction (MI) especially in a patient cohort whose left ventricular ejection fraction (LVEF) is not particularly impaired. Implantable cardiac monitors (ICM) with telemedical surveillance enable early detection of subclinical but prognostically relevant serious arrhythmic events (SArE). The aim of this analysis is to assess the impact of infarct type (STEMI vs NSTEMI) on SArE detection with ICM-based monitoring and subsequent cardiovascular complications.

**Methods:** SMART-MI was a prospective, randomized trial enrolling survivors of acute MI with left-ventricular ejection fraction 36–50% and evidence of autonomic dysfunction, defined by abnormal periodic repolarization dynamics (≥ 5.75 deg²) and/or reduced deceleration capacity (≤ 2.5 ms). Participants were randomized to ICM-based telemedical monitoring or conventional follow-up. The primary endpoint was time to first serious arrhythmic event (SArE), defined as atrial fibrillation lasting ≥ 6 minutes, atrioventricular block ≥IIb, or fast non-sustained ventricular tachycardia (> 187 bpm and ≥ 40 beats) and/or sustained ventricular tachycardia/ventricular fibrillation. Cardiovascular complications comprised all-cause mortality, stroke, systemic arterial thromboembolism, or hospitalization for decompensated heart failure. Treatment effects on SArE detection were analyzed using Cox proportional hazards models, and the prognostic impact of SArE on subsequent com-

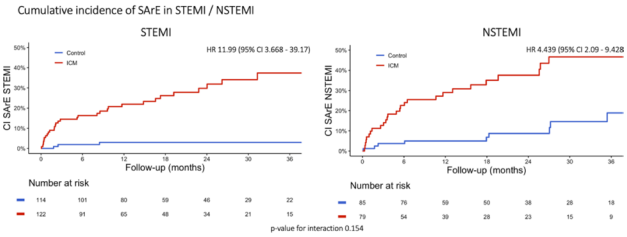


**Fig. 1 | 7-5** CI SArE STEMI/NSTEMI

plications was examined by modeling SArE as a time-dependent covariate.

**Results:** 1305 individuals were screened, and 400 patients were randomized to ICM implantation ($n=201$, 122 STEMI patients) or conventional follow-up ($n=199$, 114 STEMI patients). During follow-up, ICM implantation significantly increased SArE detection in both infarct type patients (HR 11.99, 95% CI 3.668–39.17, $p<0.001$ in STEMI; HR 4.439, 95% CI 2.09–9.428, $p<0.001$ in NSTEMI; $p$ value for interaction 0.154). In both STEMI and NSTEMI patients, detection of SArE was associated with a higher risk of subsequent cardiovascular complications (HR 9.065, 95% CI 4.155–19.78, $p<0.001$ in STEMI, HR 3.312, 95% CI 1.386–7.912, $p<0.01$ in NSTEMI; $p$ value for interaction 0.09).

**Conclusion:** ICM-based telemedical monitoring markedly increased early detection of prognostically relevant SArE, identifying patients at substantially increased risk of subsequent cardiovascular complication in both infarct types.

## 7-6

## Oral Anticoagulant Monotherapy Versus Combination Therapy in Patients With Chronic Coronary Syndrome: A Systematic Review and Meta-analysis

**Tsarouchas A.[1], Mutschlechner D.[1], Tscharre M.[2,3,4], Gremmel T.[5,1,6]**

[1]Innere Medizin I, Abteilung für Kardiologie und internistische Intensivmedizin, Landesklinikum Mistelbach-Gänsendorf, Mistelbach, Austria
[2]Klinische Abteilung für Innere Medizin II, Kardiologie, Nephrologie und internistische Intensivmedizin, UK W. Neustadt, Wiener Neustadt, Austria
[3]Danube Private University, Krems, Austria
[4]Institut für Angiologie und kardiale Elektrophysiologie, Karl Landsteiner Gesellschaft, St. Pölten, Austria
[5]Karl Landsteiner Privatuniversität für Gesundheitswissenschaften, Krems, Austria
[6]Institut für kardiovaskuläre und intensivmedizinische Forschung, Karl Landsteiner Gesellschaft, St. Pölten, Austria

**Introduction:** In patients with chronic coronary syndrome (CCS) who also require long-term oral anticoagulation (OAC) optimal long-term antithrombotic strategy after percutaneous coronary intervention (PCI) remains unclear, particularly with regard to balancing ischemic protection against bleeding risk. We performed an updated systematic review and meta-analysis of randomized trials comparing OAC monotherapy versus OAC plus single antiplatelet therapy (SAPT).

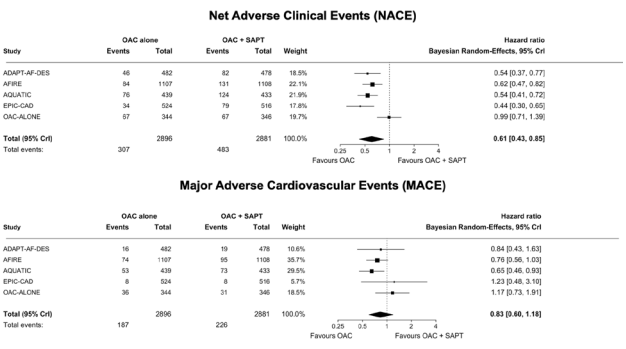


Fig. 1 | 7-6

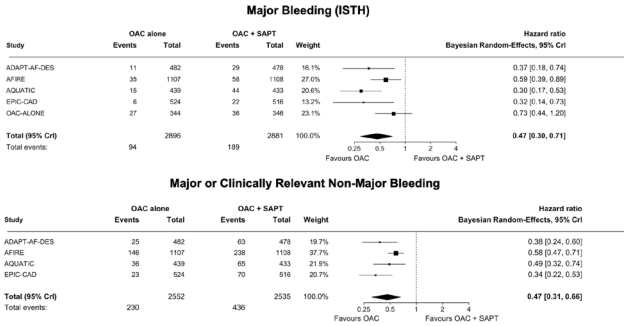


Fig. 2 | 7-6

**Methods:** We systematically searched PubMed/MEDLINE and Embase databases through February 2026 to identify randomized controlled trials enrolling patients with CCS and an indication for for long-term OAC randomized to OAC monotherapy versus OAC+SAPT. The primary outcome was net adverse clinical events (NACE). Key secondary outcomes included major adverse cardiovascular events (MACE), major bleeding, major or clinically relevant non-major bleeding, cardiovascular death, all-cause death, unplanned revascularization, myocardial infarction, stent thrombosis and ischemic stroke. Hazard ratios (HRs) were pooled using Bayesian random-effects models. Certainty of evidence was assessed with the GRADE framework.

**Results:** Six randomized trials met inclusion criteria and were included in the qualitative synthesis; five of them contributed to quantitative synthesis of outcome measures (5777 participants) [1–3]. OAC monotherapy significantly reduced the rate of NACE (HR 0.61, 95% CrI 0.43–0.95; moderate certainty—Fig. 1), major bleeding (HR 0.47, 95% CrI 0.30–0.71; high certainty—Fig. 2) and major or clinically relevant non-major bleeding (HR 0.47, 95% CrI 0.31–0.66; high certainty) compared to OAC+SAPT. No between-group differences were observed for MACE (HR 0.83, 95% CrI 0.60–1.18; moderate certainty—Fig. 1), cardiovascular death (HR 0.70, 95% CrI 0.44–1.33; moderate certainty), all-cause death, unplanned revascularization, myocardial infraction and ischemic stroke. Leave-one-out sensitivity analyses did not materially alter the results. Prespecified subgroup analyses for NACE and MACE outcomes revealed lower risk of MACE with direct anticoagulant monotherapy compared to monotherapy with vitamin K antagonists ($p=0.02$).

**Conclusion:** Among patients with CCS on long-term OAC therapy, OAC monotherapy reduced NACE through fewer bleeding events, without an apparent increase in ischemic risk.

## References

1. Matsumura-Nakano Y, Shizuta S, Komasa A, et al. Open-Label Randomized Trial Comparing Oral Anticoagulation With and Without Single Antiplatelet Therapy in Patients With Atrial Fibrillation and Stable Coronary Artery Disease Beyond 1 Year After Coronary Stent Implantation: OAC-ALONE Study. Circulation. 2019;139(5):604–616. https://doi.org/10.1161/CIRCULATIONAHA.118.036768
2. Cho MS, Kang DY, Ahn JM, et al. Edoxaban Antithrombotic Therapy for Atrial Fibrillation and Stable Coronary Artery Disease. N Engl J Med. 2024;391(22):2075–86. https://doi.org/10.1056/NEJMoa2407362.
3. Lemesle G, Didier R, Steg PG, et al. Aspirin in Patients with Chronic Coronary Syndrome Receiving Oral Anticoagulation. N Engl J Med. 2025;393(16):1578–88. https://doi.org/10.1056/NEJMoa2507532.

# POSTERSITZUNG 8— RHYTHMOLOGIE 1

## 8-1

### Caffeine and the Young Heart: Arrhythmogenic Risks in Children and Adolescents

**Öffl N., Köstenberger M., Sallmon H., Kurath – Koller S.**

Division of Pediatric Cardiology, Department of Pediatrics, Medical University Graz, Graz, Austria

**Introduction:** Caffeine consumption, particularly from energy drinks, is prevalent among adolescents, but official intake recommendations vary and awareness of potential risks is limited. Caffeine can trigger cardiovascular adverse effects through sympathetic stimulation and direct cardiac cellular effects. Literature suggests that symptoms of intoxication can occur at about 1–2 g of caffeine and caffeine amounts above 100–200 mg/kg are viewed as potentially lethal. This systematic review aimed to evaluate the existing literature on the arrhythmogenic effects of caffeine consumption in children and adolescents.

**Methods:** A systematic literature search was performed in Medline, EMBASE and the Cochrane Central Register of Controlled Trials in accordance with PRISMA 2020 guidelines, up to October 2025. We included peer-reviewed articles (case reports, case series, observational studies) reporting on arrhythmogenic or electrophysiological cardiac outcomes in patients younger than 19 years who consumed caffeine containing products. Exclusion criteria included animal studies, non arrhythmic outcomes and abstracts only.

**Results:** Of 126 screened articles, 12 met inclusion criteria (10 case reports, 1 prospective study, 1 retrospective study). These reported on 39 patients with caffeine-associated arrhythmias or electrocardiographic abnormalities. Arrhythmias included sinus tachycardia, premature supraventricular and ventricular contractions, and supraventricular and ventricular tachycardias. ECG changes comprised QTc prolongation, ST-segment elevation and terminal repolarization abnormalities. One patient developed refractory ventricular fibrillation and died. Most patients were healthy, some had underlying conditions like long QT syndrome or myocarditis that were unmasked or worsened. Treatments ranged from supportive care and antiarrhythmics to extracorporeal membrane oxygenation in severe cases.

**Conclusion:** This systematic review confirms that high-dose caffeine from various sources can cause heart rhythm disturbances and electrical abnormalities in children and adolescents, including life-threatening cases. The findings highlight the need for greater awareness, public health education and guidelines on safe caffeine intake in this age group.

## 8-2

### Ten-Year Outcomes of Leadless Pacing with the Micra VR1: Complete Cohort Follow-Up Beyond a Decade

**Puschmann C., Blessberger H., Lacher J., Schwarz S., Reiter C., Gundendorfer M., Saleh K.**

Kepler Universitätsklinikum, Linz, Austria

**Introduction:** Background: Leadless pacemakers (LP) such as the Micra™ VR1 (Medtronic) were introduced to reduce pocket- and lead-related complications of transvenous systems. While projected battery longevity is up to 14 years, real-world data from complete implantation cohorts that have surpassed a full decade of implantation are scarce, and late battery behavior is insufficiently characterized. Objective: To report survival beyond 10 years, causes of death, long-term electrical performance, and device-related outcomes in a complete consecutive cohort of Micra recipients with confirmed long-term implantation.

**Methods:** This retrospective single-center study included all 66 consecutive patients who received a Micra™ VR1 (Medtronic) at our center between 05.12.2013 and 25.09.2015. Baseline R-wave amplitude, pacing impedance, and pacing threshold recorded at implantation were compared with measurements obtained after more than 10 years of continuous device function in surviving patients. Battery voltage and estimated remaining longevity were assessed at the ≥ 10-year follow-up. Survival status and causes of death were collected for the entire cohort.

**Results:** Among the 66 patients implanted with a Micra VR1 device, 52 died during follow-up. Of the deaths with known cause, none were device-related: cardiovascular ($n=18$), malignancy ($n=6$), renal ($n=4$), gastrointestinal ($n=4$), pulmonary ($n=4$), neurological ($n=3$), and diabetes-related ($n=3$); causes of death were unknown in the remaining patients. Device interrogation beyond 10 years after implantation was available in 14 patients (21%). In these 14 patients with confirmed >10-year Micra implantation, electrical performance remained effective and within safe pacing thresholds. Mean R-wave amplitude increased from 10.05 ± 3.43 mV at implantation to 13.64 ± 4.77 mV at >10 years. Mean pacing threshold modestly increased from 0.46 ± 0.25 V to 0.66 ± 0.23 V, while mean pacing impedance decreased from 673.57 ± 115.1 Ω to 522.86 ± 74.36 Ω. No device failures, systemic infections, or device extractions occurred. Battery voltage at >10 years showed substantial interindividual variability (median 2.79 V, Q1 2.62 V, Q3 2.92 V), with estimated remaining battery longevity ranging from 0.25 to 7 years.

**Conclusion:** In this early Micra VR1 cohort with confirmed device function exceeding 10 years, leadless pacing demonstrated sustained long-term safety and electrical reliability without device-related complications. Overall mortality was high, reflecting the advanced age and comorbidity burden of this population rather than adverse device performance. After a decade of implantation, marked variability in remaining battery longevity was observed, highlighting the strong influence of pacing burden, pacing threshold, and individualized device programming on cumulative energy consumption. Compared with longitudinal studies with follow-up up to 7–8 years showing gradual voltage decline, our findings suggest an accelerated, non-linear battery voltage drop in the late phase of device life, which likely reflects intrinsic lithium battery discharge characteristics. Together, these observations emphasize that late battery dynamics cannot be extrapolated from mid-term data and underscore the need for individualized, close long-term monitoring to anticipate timely device replacement and maintain uninterrupted pacing therapy.

## 8-3

### Angiopoietin-2 and Growth Differentiation Factor-15 as Predictors of Device-Detected Atrial Fibrillation Burden

**Bilgeri V.[1], Spitaler P.[1], Gavranovic-Novakovic J.[1], Dolejsi T.[1], Rockenschaub P.[1], Messner M.[1], Zaruba M.[1], Barbieri F.[2], Adukauskaite A.[1], Stühlinger M.[1], Pfeifer B.[3], Lacaita P.[1], Feuchtner G.[1], Willeit P.[1], Bauer A.[1], Dichtl W.[1]**

[1]Medizinische Universität Innsbruck, Innsbruck, Austria
[2]Deutsches Herzzentrum der Charite, Berlin, Germany
[3]UMIT Tirol, Innsbruck, Austria

**Introduction:** In patients with dual-chamber pacemakers enabling continuous rhythm surveillance, device-detected atrial fibrillation (DDAF) burden and progression to persistent AF can be quantified with high precision. We investigated whether circulating biomarkers reflecting endothelial dysfunction, inflammation, and myocardial stress predict (i) progression to persistent AF and (ii) overall DDAF burden.

**Methods:** We analyzed participants of the prospective ACaSA study (NCT05127720) implanted with Microport® BOREA DR or TEO DR dual-chamber pacemakers and monitored weekly via SMARTVIEW®. Patients with permanent AF at baseline or single-chamber systems were excluded. Baseline plasma concentrations of angiopoietin-2 (ANGPT2), growth differentiation factor-15 (GDF-15), fibroblast growth factor-23 (FGF-23), bone morphogenetic protein-10 (BMP10), and TRAIL receptor-2 (TRAIL-R2) were measured by ELISA; NT-proBNP was measured by electrochemiluminescence immunoassay. Biomarkers were log2-transformed (values below detection limits imputed at half the lower limit). After a 30-day blanking period, two endpoints were assessed: (1) progression to persistent AF, defined as ≥7 consecutive days with >99% daily AF burden (Cox regression; multivariable adjustment for age, sex, and heart failure); and (2) DDAF burden, calculated as cumulative AF time normalized to monitored days and categorized as <25%, 25–75%, or >75% (multinomial logistic regression; adjusted for age, sex, heart failure, diabetes, and prior myocardial infarction).

**Results:** A total of 223 patients were included (median age 75 years; 37.2% women). During follow-up, 28 patients (13.3%) progressed to persistent AF. Higher baseline ANGPT2 was the strongest predictor of progression (HR per doubling 1.83, 95% CI 1.27–2.66; $p=0.001$), followed by GDF-15 (HR 1.52, 95% CI 1.03–2.24; $p=0.036$). For burden phenotyping, ANGPT2 showed a marked graded association with arrhythmic load, with substantially higher odds of high (>75%) DDAF burden (OR 8.31, 95% CI 2.63–26.26; $p<0.001$). GDF-15 independently predicted both medium (25–75%) burden (OR 2.05; $p=0.025$) and high burden (OR 2.32; $p=0.037$). NT-proBNP displayed only borderline association with high burden (OR 2.02; $p=0.061$). No significant associations were observed for FGF-23, BMP10, or TRAIL-R2.

**Conclusion:** In continuously monitored pacemaker patients, ANGPT2 and GDF-15 emerged as key biomarkers of AF disease severity. ANGPT2 was strongly associated with both progression to persistent AF and very high DDAF burden, while GDF-15 consistently predicted higher burden and also contributed to progression risk. These results support endothelial and inflammatory/stress-related pathways as clinically relevant markers for AF progression in device-monitored populations and may help identify individuals at risk for high-burden or persistent AF.

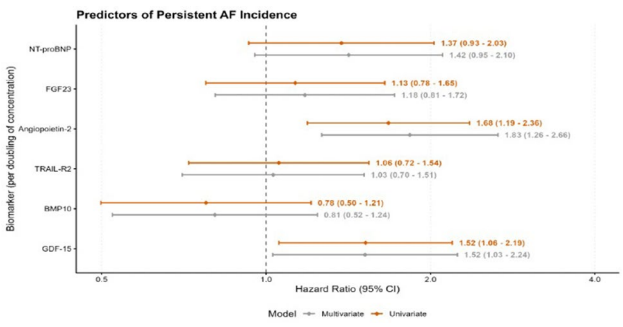


**Fig. 1 | 8-3** Forest plot displaying adjusted hazard ratios (HRs) with 95% confidence intervals for developing persistent AF per 1 SD increase in log2-transformed biomarker levels

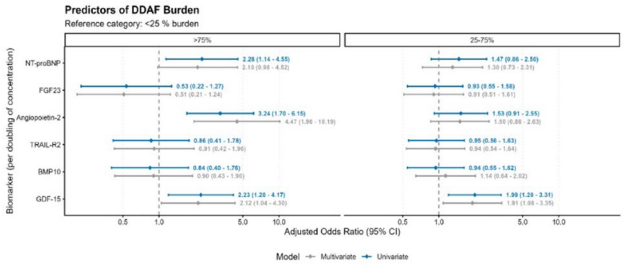


**Fig. 2 | 8-3** Forest plot showing adjusted odds ratios (ORs) with 95% confidence intervals for DDAF burden categories, comparing moderate (25–75%) and high (>75%) burden groups to the low burden group (<25%) across all biomarkers

## 8-4

### Artificial Intelligence in ECG Analysis: Current Practice and Future Directions from the International SAIMO Physician Survey

**Zweiker D.[1], Triantafyllou K.[2], Spartalis M.[3], Engel H.[4], Kaufmann C.[5], Kurath-Koller S.[1], Nakajima K.[6], McIntyre W.[7], Johnson L.[8], Linz D.[9], Vassilikos V.[2], Scherr D.[1], Manninger-Wünscher M.[1]**

[1]Division of Cardiology, Medical University of Graz, Graz, Austria
[2]Aristotle University of Thessaloniki, Division of Cardiology, Thessaloniki, Greece
[3]National & Kapodistrian University of Athens, 3rd Department of Cardiology, Athens, Greece
[4]Hanusch Hospital, Division of Cardiology, Vienna, Austria
[5]3rd Medical Department for Cardiology and Intensive Care, Klinik Ottakring, Wien, Austria
[6]Department of Cardiac Electrophysiology and Arrhythmology, IRCCS San Raffaele Scientific Institute, Vita-Salute University and San Raffaele Hospital, Milan, Italy
[7]McMaster University, Cardiac Electrophysiology and Peri-Operative Medicine, Hamilton, Canada
[8]Lund University, Cardiovascular Research – Epidemiology, Lund, Sweden
[9]Cardiovascular Research Institute Maastricht (CARIM), Department of Cardiology, Maastricht, Netherlands

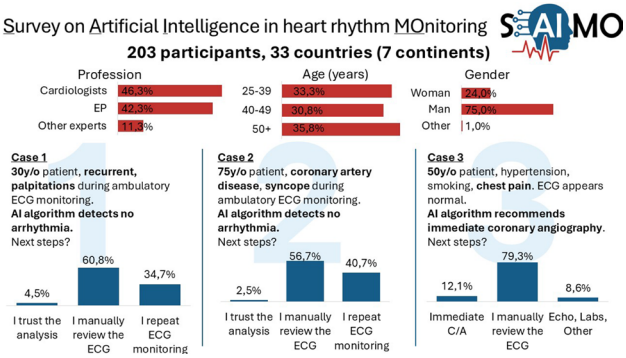


**Fig. 1 | 8-4**

**Introduction:** While many artificial intelligence (AI) algorithms are already available for the analysis and interpretation of electrocardiogram (ECG) signals, it is unclear if these tools have earned the trust of healthcare personnel. We therefore assessed the use and level of trust in AI algorithms for ECG analysis in routine clinical practice.

**Methods:** This is the preliminary analysis of the "Survey on Artificial Intelligence in heart rhythm Monitoring" project, an online survey that assesses healthcare professional's attitude toward the use of AI in ECG signal interpretation. Respondents' trust in AI algorithms was tested in three cases: Case 1 described a young patient with palpitations suggestive of supraventricular tachycardia during 14-day ECG recording and a negative result from AI-based ECG signal analysis. Case 2 described a patient with coronary artery disease, previous syncope who experienced symptoms during 14-day ECG recording, again with a negative AI result. Case 3 described a patient with acute coronary syndrome, without criteria for ST-segment elevation myocardial infarction but with an AI alert suggesting obstructive myocardial infarction.

**Results:** A total of 203 experts (46.3% cardiologists, 42.3% cardiac electrophysiologists, 11.3% other specialists; 24% women; median age 40–49 years) from 33 countries and 7 continents participated in the survey to date. The majority of respondents stated that a prospective randomized trial (46.5%) or a prospective multi-center cohort study (37.0%) should be conducted before approving an AI algorithm for clinical use. Respondents found AI assistance appropriate in the analysis of 14-day ECG (73.0%), wearable-detected ECG (71.5%) and 12-lead ECG (73.5%). AI-only analysis without the possibility to manually review the ECG signal was deemed suitable in only the minority of cases. In case of an AI algorithm missing a critical arrhythmia, respondents recommended that both the physician using the algorithm (44.0%), the manufacturer of the algorithm (36.5%) or the healthcare provider (15.0%) should be held accountable. In Case 1, 95.5% of experts would not trust the AI algorithm and either analyze the ECG signal manually (60.8%) or perform further rhythm monitoring (34.7%). In case 2, 97.5% would not trust the ECG analysis, most would analyze the ECG signal again manually (56.7%). In case 3, 12.1% of experts followed the AI algorithm's suggestion of immediate cath lab activation, the majority (79.3%) recommended transfer to the emergency department for individual evaluation.

**Conclusion:** This survey shows that experts in ECG analysis have only limited trust in currently available AI algorithms, especially in case of results that diverge from clinical suspicion.

## 8-5

## Less complications despite higher risk—temporal trends in patients undergoing left atrial appendage closure in Austria

**Zweiker D.[1], Toth G.[1], Stix G.[2], Vock P.[3,4], Schratter A.[5], Fiedler L.[6], Martinek M.[7], Steinwender C.[8], Binder R.[9], Adukauskaite A.[10], Ablasser K.[1], Verheyen N.[1], Zirlik A.[1], Scherr D.[1]**

[1]Division of Cardiology, Medical University of Graz, Graz, Austria
[2]Division of Cardiology, Medical University of Vienna, Wien, Austria
[3]Department of Internal Medicine III, Karl Landsteiner University Hospital St. Pölten, St. Pölten, Austria
[4]Department of Internal Medicine, Hospital Oberwart, Oberwart, Austria
[5]Department of Cardiology, Hospital North (Klinikum Floridsdorf), Wien, Austria
[6]Department of Internal Medicine, Hospital Wiener Neustadt, Wien, Austria
[7]2nd Medical Department, Cardiology, Angiology and Intensive Care Unit, Hospital Elisabethinen, Linz, Austria
[8]Division of Cardiology, Kepler University Hospital Linz, Linz, Austria
[9]Department of Internal Medicine 2, Hospital Wels-Grieskirchen, Wels, Austria
[10]Division of Internal Medicine III, Medical University of Innsbruck, Innsbruck, Austria

**Introduction:** Left atrial appendage closure (LAAC) is an alternative treatment option in patients with contraindication, intolerance or inefficacy of oral anticoagulation (OAC) in patients with atrial fibrillation (AF). In the last years, the development of LAAC devices progressed, leading to reduced complication rates and higher effectiveness. However, it is unclear how the risk profile and outcome in patients undergoing LAAC in daily clinical practice shifted in the last years.

**Methods:** A retrospective analysis from a multicentre registry including consecutive patients undergoing LAAC was performed, comparing baseline and outcome differences of the last 50% of patients (receiving LAAC after 19 September 2019 until end 2025) and remaining patients (receiving LAAC between 2010 until 19 September 2019). Major short-term complications were defined as any complication necessitating an invasive intervention, or death.

**Results:** A total of 599 patients from 9 centres were included. Median age was 76 (interquartile range 70–80) years and 35.6% were female. Recent patients ($n=299$) were older (median 77 vs. 75 years, $p=0.011$) and had a substantially higher risk profile with a higher prevalence of hypertension (96.0% vs. 87.7%, $p<0.001$), abnormal renal function (32.1% vs. 15.7%, $p<0.001$), previous stroke (44.8% vs. 35.7%, $p=0.025$), and dialysis (3.0% vs. 0.3%, $p=0.021$) compared to remaining patients ($n=300$). As a result, CHA2DS2-VA (mean 4.3 vs. 4.0) and HAS-BLED (mean 3.6 vs. 3.0) score were significantly higher ($p<0.001$). In recent patients, bleeding (71.9% vs. 63.0%) and stroke (13.0% vs. 9.0%) as primary indication for LAAC was more common than in remaining patients, who more often had other indications (such as patient preference, 28.0% vs. 15.1%, $p<0.001$). The choice of device was similar in both groups (Amplatzer, 53.6%; Watchman, 45.7%, $p=0.951$). The rate of successful implantation was similar in both patient groups (95.0% vs. 97.7%, $p=0.253$). Major

complications were numerically lower in recent patients (3.0% vs. 6.0%, $p=0.114$).

**Conclusion:** Recent patients receiving LAAC in Austria have a higher risk profile and still a preferable outcome.

## 8-6

## Vergleiche lokaler und systemischer Konzentrationsveränderungen neuartiger Biomarker (GDF-15, H-FABP, sST2 und suPAR) bei PatientInnen mit Pulmonalvenenisolation mittels Radiofrequenzablation und Pulsed Field Ablation (PFA)

**Petric F.[1], Matejka M.[2], Paar V.[3], Pfeffer M.[4], Tinhofer F.[5], Zechowicz M.[6], Blessberger H.[7], Hoppe U.[3], Roithinger F.[4], Motloch L.[2], Fiedler L.[4]**

[1]Klinik Landstraße, 1030, Österreich
[2]Klinik Salzkammergut, Vöcklabruck, Österreich
[3]Paracelsus Private Medical University, Salzburg, Österreich
[4]Universitätsklinikum Wiener Neustadt, Wiener Neustadt, Österreich
[5]Klinik Ottakring, 1160, Österreich
[6]University of Warmia and Mazury in Olsztyn, Olsztyn, Polen
[7]Kepler Universtitätsklinikum, Linz, Österreich

| Characteristic | PFA N = 15[1] | RFA N = 73[1] | p-value[2] |
|---|---|---|---|
| **Gender** | | | 0.4 |
| female | 4/15 (27%) | 29/73 (40%) | |
| male | 11/15 (73%) | 44/73 (60%) | |
| **Age (years)** | 61.7 ± 7.6 | 63.5 ± 9.0 | 0.4 |
| **LA Volume (ml)** | NA ± NA | 129.9 ± 41.3 | |
| **Creatinine (mg/dl)** | 1.0 ± 0.2 | 1.0 ± 0.2 | >0.9 |
| **NTproBNP (ng/L)** | 478.2 ± 562.4 | 1,016.8 ± 3,259.5 | 0.3 |
| **hsCRP (mg/dl)** | 0.6 ± 0.8 | 1.2 ± 2.9 | 0.14 |
| **EHRA** | | | 0.2 |
| 2A | 1/14 (7.1%) | 1/71 (1.4%) | |
| 2B | 0/14 (0%) | 6/71 (8.5%) | |
| 3 | 13/14 (93%) | 64/71 (90%) | |
| **NYHA** | | | 0.6 |
| 2 | 2/8 (25%) | 6/43 (14%) | |
| 3 | 6/8 (75%) | 37/43 (86%) | |
| **CHA2DS2-Vasc Category** | | | >0.9 |
| 0 | 0/12 (0%) | 0/62 (0%) | |
| 1 | 0/12 (0%) | 0/62 (0%) | |
| ≥2 | 12/12 (100%) | 62/62 (100%) | |
| **HAS-BLED** | | | 0.5 |
| 0 | 4/12 (33%) | 9/64 (14%) | |
| 1 | 2/12 (17%) | 19/64 (30%) | |
| 2 | 4/12 (33%) | 22/64 (34%) | |
| 3 | 1/12 (8.3%) | 11/64 (17%) | |
| 4 | 1/12 (8.3%) | 3/64 (4.7%) | |
| **LVEF in %** | 59.9 ± 7.7 | 55.2 ± 8.4 | 0.059 |
| **Procedure related complications** | | | >0.9 |
| no | 12/12 (100%) | 63/64 (98%) | |
| yes | 0/12 (0%) | 1/64 (1.6%) | |
| **Fluoroscopy Time (min)** | 15.9 ± 7.0 | 9.1 ± 4.3 | **0.006** |
| **Procedure Time (min)** | 44.7 ± 10.1 | 95.7 ± 28.3 | **<0.001** |
| **Heart Failure** | | | 0.7 |
| no | 1/12 (8.3%) | 11/64 (17%) | |
| yes | 11/12 (92%) | 53/64 (83%) | |
| **Hypertension** | | | 0.8 |
| no | 6/12 (50%) | 37/64 (58%) | |
| yes | 6/12 (50%) | 27/64 (42%) | |
| **Diabetes mellitus** | | | >0.9 |
| no | 2/12 (17%) | 12/64 (19%) | |
| yes | 10/12 (83%) | 52/64 (81%) | |
| **History of stroke or TIA** | | | >0.9 |
| no | 0/12 (0%) | 4/63 (6.3%) | |
| yes | 12/12 (100%) | 59/63 (94%) | |
| **Vessel Disease** | | | 0.6 |
| no | 0/12 (0%) | 6/63 (9.5%) | |
| yes | 12/12 (100%) | 57/63 (90%) | |
| **Statins** | | | 0.3 |
| no | 10/15 (67%) | 33/70 (47%) | |
| yes | 5/15 (33%) | 37/70 (53%) | |
| **Beta Blocker** | | | 0.8 |
| no | 5/15 (33%) | 29/71 (41%) | |
| yes | 10/15 (67%) | 42/71 (59%) | |
| **Amiodaron** | | | >0.9 |
| no | 11/15 (73%) | 51/70 (73%) | |
| yes | 4/15 (27%) | 19/70 (27%) | |
| **Klasse 1C AA** | | | 0.7 |
| no | 11/15 (73%) | 56/70 (80%) | |
| yes | 4/15 (27%) | 14/70 (20%) | |
| **Rhythm before EPU** | | | 0.2 |
| AFib | 1/15 (6.7%) | 18/66 (27%) | |
| SR | 14/15 (93%) | 48/66 (73%) | |

**Table 1: Baseline characteristics of the study population subgroups**

[1]n/N (%); Mean ± SD

| Biomarker | LRI CS (Median [95% CI]) | LRI LA (Median [95% CI]) |
|---|---|---|
| GDF | -9.17 (-41.50, 25.40) | -16.54 (-45.89, 17.48) |
| HFABP | -0.06 (-0.20, 0.28) | **-0.32 (-0.42, -0.16)** |
| sST2 | 299.92 (-143.03, 849.95) | 60.87 (-736.69, 421.99) |
| suPAR | **145.77 (24.47, 254.49)** | **287.65 (203.60, 419.99)** |

Bold values indicate confidence intervals not crossing zero; Median with 95% CI

**Table 2:** Local Response Index Effect Size

**Abb. 1 | 8–6**

**Einleitung:** Vorhofflimmern ist die häufigste Rhythmusstörung weltweit und bedarf aufgrund erhöhter Mortalität, erhöhtem Risiko für Hospitalisationen und gehäuftem Auftreten teils schwerer Erkrankungen, besondere Beachtung1. Mittels Pulmonalvenenisolation wurde eine effektive Methode zur Behandlung dieser Erkrankung etabliert1. Durch stetige Forschung wurden neue Ablationsverfahren entwickelt, darunter die Pulsed Field Ablation (PFA), welche wesentlich kardioselektiver wirkt und umliegende Gewebeschäden minimiert2. Biomarker wie GDF-15, suPAR, sST2 und H-FABP zeigten in Studien mögliche Assoziationen mit myokardialem Schaden3, die Effekte der Ablation auf diese Biomarker wurde aber bisher nicht näher untersucht.

**Methoden:** Um der Fragestellung nachzugehen, wurden 88 PatientInnen mit Pulmonalvenenisolation eingeschlossen. Prä- und postprozedural wurden an drei Abnahmestellen (femoral, linkes Atrium sowie Sinus coronarius) Blutproben entnommen. Angabe metrischer Variablen mittels Mittelwert ±SD, kategorische/nominale Variablen mittels Absolutwerten/Prozenten. Biomarkermessungen wurden mit Median und Interquartilabstand angegeben. Vergleiche wurden mittels Wilcoxonrangsummentest berechnet, bei multiplen Vergleichen wurde das Benjamini-Hochberg Verfahren angewendet. Es wurde ein Local Response Index (LRI) berechnet, um lokale sowie systemische Konzentrationsunterschiede zu beschreiben. Alle Tests wurden zweiseitig durchgeführt. Statistisch signifikant wurde ein $P$-Wert ≤ 0,05 festgelegt. Die statistische Auswertung erfolgte mit dem Programm R.

**Resultate:** Die Baseline-Charakteristika zeigten zwischen beiden Gruppen (PFA $n=15$ und RFA $n=73$) bei der PFA-Methode signifikant kürzere Prozedurdauern sowie höhere Durchleuchtungszeiten, ansonsten keine wesentlichen Unterschiede. Die Berechnung des LRI der gesamten Kohorte ($n=88$) zeigte einen systemischen Anstieg für H-FABP sowie lokale

| Biomarker | Δ Femoral (Median [IQR]) | Δ CS (Median [IQR]) | Δ LA (Median [IQR]) | LRI_CS (Median [IQR]) | LRI_LA (Median [IQR]) | n (LRI_CS) | n (LRI_LA) |
|---|---|---|---|---|---|---|---|
| GDF | -2.71 (-47.27, 69.49) | -7.53 (-90.73, 62.23) | -9.10 (-92.75, 49.48) | -9.17 (-115.19, 82.83) | -16.54 (-111.61, 57.55) | 90 | 90 |
| HFABP | 0.51 (0.15, 0.90) | 0.45 (-0.01, 0.93) | 0.27 (-0.09, 0.80) | -0.06 (-0.42, 0.45) | -0.32 (-0.70, 0.06) | 90 | 89 |
| sST2 | -193.10 (-1430.11, 673.75) | -37.90 (-1419.58, 1005.43) | -437.42 (-1429.54, 701.50) | 299.92 (-1013.55, 1798.50) | 60.87 (-1419.76, 1590.86) | 88 | 87 |
| suPAR | -353.00 (-760.34, -34.05) | -222.32 (-525.48, 138.64) | -7.79 (-289.65, 169.51) | 145.77 (-145.53, 547.81) | 287.65 (32.38, 650.36) | 88 | 88 |

[1]Median and corresponding interquartile ranges

**Table 3:** Local Response Index (LRI) per biomarker

| Characteristic | PFA N = 15[1] | RFA N = 73[1] | p | p (FDR) |
|---|---|---|---|---|
| **GDF — Coronary sinus — Post** | 532.84 (249.56, 615.87) | 420.55 (292.12, 630.20) | 0.773 | 0.937 |
| **GDF — Coronary sinus — Pre** | 546.74 (285.34, 712.58) | 434.69 (288.64, 656.56) | 0.594 | 0.937 |
| **GDF — Femoral — Post** | 562.66 (366.41, 659.36) | 438.76 (319.75, 645.23) | 0.437 | 0.937 |
| **GDF — Femoral — Pre** | 416.25 (344.63, 686.19) | 428.57 (295.07, 671.44) | 0.694 | 0.937 |
| **GDF — Left atrium — Post** | 493.90 (253.04, 597.33) | 407.25 (304.19, 608.58) | 0.727 | 0.937 |
| **GDF — Left atrium — Pre** | 453.88 (310.50, 781.61) | 439.38 (317.72, 657.97) | 0.637 | 0.937 |
| **HFABP — Coronary sinus — Post** | 3.35 (2.13, 4.98) | 1.66 (1.28, 1.93) | <0.001 | **<0.001** |
| **HFABP — Coronary sinus — Pre** | 1.27 (0.84, 1.57) | 1.29 (1.05, 1.59) | 0.587 | 0.937 |
| **HFABP — Femoral — Post** | 2.65 (1.95, 4.14) | 1.68 (1.28, 2.08) | <0.001 | **<0.001** |
| **HFABP — Femoral — Pre** | 1.31 (0.94, 1.51) | 1.31 (0.87, 1.67) | 0.799 | 0.937 |
| **HFABP — Left atrium — Post** | 2.98 (2.11, 4.31) | 1.61 (1.30, 1.94) | <0.001 | **<0.001** |
| **HFABP — Left atrium — Pre** | 1.36 (1.17, 2.30) | 1.52 (1.14, 1.84) | 0.799 | 0.937 |
| **sST2 — Coronary sinus — Post** | 6,167.08 (3,375.87, 7,141.81) | 6,937.65 (4,903.72, 10,051.08) | 0.099 | 0.325 |
| **sST2 — Coronary sinus — Pre** | 5,273.83 (2,442.37, 8,158.19) | 6,976.46 (4,979.67, 10,164.53) | 0.043 | 0.226 |
| **sST2 — Femoral — Post** | 6,044.58 (4,492.84, 8,235.81) | 7,291.24 (5,555.28, 9,634.31) | 0.108 | 0.325 |
| **sST2 — Femoral — Pre** | 5,633.98 (3,138.63, 8,508.61) | 7,752.69 (5,718.03, 10,385.94) | 0.047 | 0.226 |
| **sST2 — Left atrium — Post** | 5,747.08 (3,839.46, 7,096.27) | 6,627.22 (4,615.81, 9,047.58) | 0.137 | 0.364 |
| **sST2 — Left atrium — Pre** | 6,312.50 (3,138.63, 8,009.35) | 7,015.27 (5,263.86, 9,962.10) | 0.075 | 0.300 |
| **suPAR — Coronary sinus — Post** | 1,639.94 (1,148.95, 2,058.00) | 1,583.70 (1,403.80, 2,037.81) | 0.859 | 0.937 |
| **suPAR — Coronary sinus — Pre** | 1,987.43 (1,291.44, 2,608.00) | 1,835.30 (1,438.22, 2,223.88) | 0.534 | 0.937 |
| **suPAR — Femoral — Post** | 1,685.58 (1,240.66, 2,176.39) | 1,704.76 (1,340.40, 2,160.45) | 0.822 | 0.937 |
| **suPAR — Femoral — Pre** | 2,227.60 (1,275.30, 3,164.20) | 2,285.39 (1,681.89, 2,656.59) | 0.912 | 0.951 |
| **suPAR — Left atrium — Post** | 1,645.60 (1,123.26, 2,053.76) | 1,560.90 (1,272.05, 1,990.84) | 0.973 | 0.973 |
| **suPAR — Left atrium — Pre** | 1,555.03 (1,263.67, 2,283.93) | 1,642.60 (1,305.96, 2,099.35) | 0.786 | 0.937 |

**Table 4: biomarker concentrations before and after ablation with PFA vs RF catheter ablation**

[1]Median (Q1, Q3)

| Characteristic - femoral | RFA N = 73[1] | PFA N = 15[1] | p | p (FDR) |
|---|---|---|---|---|
| **GDF** | -18.43 (-49.44, 53.29) | 60.36 (-40.80, 166.71) | 0.092 | 0.183 |
| **HFABP** | 0.41 (0.08, 0.65) | 1.56 (1.08, 2.41) | <0.001 | **<0.001** |
| **sST2** | -368.96 (-1,474.60, 896.00) | 8.53 (-267.85, 565.45) | 0.402 | 0.536 |
| **suPAR** | -343.97 (-818.07, -39.22) | -467.36 (-599.35, 23.93) | 0.760 | 0.760 |

[1]Median (Q1, Q3)

| Characteristic - atrium | RFA N = 73[1] | PFA N = 15[1] | p | p (FDR) |
|---|---|---|---|---|
| **GDF** | -5.88 (-87.26, 62.98) | -20.48 (-96.71, 115.75) | 0.756 | 0.756 |
| **HFABP** | 0.32 (-0.04, 0.68) | 2.08 (1.43, 2.98) | <0.001 | **<0.001** |
| **sST2** | -208.89 (-1,461.27, 1,005.92) | 423.69 (-76.39, 1,281.69) | 0.146 | 0.292 |
| **suPAR** | -181.70 (-483.05, 159.15) | -442.59 (-637.48, 8.74) | 0.239 | 0.319 |

[1]Median (Q1, Q3)

| Characteristic – coronary sinus | RFA N = 73[1] | PFA N = 15[1] | p | p (FDR) |
|---|---|---|---|---|
| **GDF** | 0.00 (-89.59, 63.38) | -45.94 (-93.81, -1.77) | 0.194 | 0.259 |
| **HFABP** | 0.03 (-0.16, 0.48) | 1.21 (0.87, 2.70) | <0.001 | **<0.001** |
| **sST2** | -485.41 (-1,466.68, 723.39) | -193.95 (-565.42, 732.73) | 0.320 | 0.320 |
| **suPAR** | 31.10 (-241.77, 184.38) | -100.18 (-379.18, 161.13) | 0.172 | 0.259 |

[1]Median (Q1, Q3)

**Table 5: Measurements for systematic or localized concentration differences of every biomarker in every compartments**

**Abb. 2 | 8–6**

Anstiege bei suPAR (siehe Tab. 2 und 3). Es erfolgte anschließend die Supgruppenanalyse zwischen PFA- und RF-Ablation (siehe Tab. 4). Hier zeigte sich präprozedural kein Unterschied der Biomarkerkonzentrationen, postprozedural zeigten sich in allen Kompartimenten signifikant erhöhte Werte für H-FABP bei PFA. suPAR zeigte lokale Anstiege, insbesondere im linken Atrium (Tab. 1). GDF-15 sowie sST2 zeigten keine signifikanten Auffälligkeiten, sST2 eher ausgeprägte Heterogenität der Konzentrationswerte (Abb. 1). Tab. 5 spiegelt die systemische Erhöhung H-FABP nochmals wider.

**Schlussfolgerungen:** Es zeigte sich die erwartete kürzere Prozedurdauer bei Verwendung der PFA-Methode. Weiters zeigte sich, nicht wie erwartet ein lokaler Anstieg von H-FABP, sondern Hinweise für einen systemischen Anstieg (trotz eigentlich erwarteten lokalen Effekten). Es müssen jedoch weitere größere und randomisierte Studien folgen, um diese Ergebnisse zu verifizieren und die Bedeutung dessen aufzuarbeiten.

## Literatur


1. Van Gelder et al.; ESC Scientific Document Group. 2024 ESC Guidelines for the management of atrial fibrillation developed in collaboration with the European Association for Cardio-Thoracic Surgery (EACTS). Eur Heart J. 2024 Sep 29;45(36):3314–3414. https://doi.org/10.1093/eurheartj/ehae176. Erratum in: Eur Heart J. 2025 Nov 3;46(41):4349. https://doi.org/10.1093/eurheartj/ehaf306. PMID: 39210723.
2. Hunter DW, Kostecki G, Fish JM, Jensen JA, Tandri H. In vitro cell selectivity of reversible and irreversible: electroporation in cardiac tissue. Circ Arrhythm Electrophysiol 2021:14e008817.
3. Ohnewein et al. Dynamics of the Novel Cardiac Biomarkers sST2, H-FABP, GDF-15 and suPAR in HFrEF Patients Undergoing Heart Failure Therapy, a Pilot Study. J Clin Med. 2025 Aug 11;14(16):5668. https://doi.org/10.3390/jcm14165668. PMID: 40869494; PMCID: PMC12386204.


# 8-7

## Evaluierung der Einflüsse des Herzrhythmus und der linksventrikulären Funktion auf die Konzentration neuer kardialer Biomarker GDF-15, H-FABP, sST2 und suPAR bemessen an verschiedenen Abnahmestellen im Rahmen von Pulmonalvenenisolationen


**Petric F.[1], Matejka M.[2], Paar V.[3], Pfeffer M.[4], Zechowicz M.[5], Tinhofer F.[6], Blessberger H.[7], Hoppe U.[3], Roithinger F.[4], Motloch L.[2], Fiedler L.[4]**

[1]Klinik Landstraße, 1030, Österreich
[2]Klinik Salzkammergut, Vöcklabruck, Österreich
[3]Paracelsus Private Medical University, Salzburg, Österreich
[4]Universitätsklinikum Wiener Neustadt, Wiener Neustadt, Österreich
[5]University of Warmia and Mazury in Olsztyn, Olsztyn, Polen
[6]Klinik Ottakring, 1160, Österreich
[7]Kepler Universtitätsklinikum, Linz, Österreich


**Einleitung:** Vorhofflimmern ist die häufigste Rhythmusstörung weltweit [1]. Zudem haben diese PatientInnen ein deutlich erhöhtes Risiko im Verlauf an Herzinsuffizienz zu erkranken (bis zu 50 %) [2]. Die Herzinsuffizienz sowie das Vorhofflimmern haben oft multifaktorielle Genese [2, 3]. Somit könnten einzelne Messwerte das Gesamtausmaß mitunter nicht adäquat abbilden bzw. durch neuere pharmakologische Therapien verfälscht werden [4]. Neuartige kardiale Biomarker (GDF-15, sST2, H-FABP, suPAR) zeigten bereits mögliche Assoziationen mit kardialem Volumenoverload, myokardialen Schaden sowie erhöhter Mortalität bei PatientInnen mit und ohne Herzinsuffizienz4. Bisher wurden keine Studien durchgeführt, um den Einfluss von Herzrhythmus oder der linksventrikulären Funktion auf die Konzentration dieser Biomarker zu untersuchen bei PatientInnen, die eine Pulmonalvenenisolation erhalten.

**Methoden:** Um dieser Fragestellung nachzugehen wurden 83 PatientInnen mit Vorhofflimmern einbezogen, welche eine

| Characteristic | AFib N = 19[1] | SR N = 64[1] | p-value[2] |
|---|---|---|---|
| **Ablation Procedure** | | | 0.2 |
| PFA | 1/19 (5.3%) | 14/62 (23%) | |
| RFA | 18/19 (95%) | 48/62 (77%) | |
| **Gender** | | | 0.3 |
| female | 5/19 (26%) | 26/64 (41%) | |
| male | 14/19 (74%) | 38/64 (59%) | |
| **Age (years)** | 61.7 ± 8.6 | 63.0 ± 8.7 | 0.6 |
| **LA Volume (ml)** | 124.1 ± 35.6 | 130.8 ± 43.9 | 0.7 |
| **Creatinine (mg/dl)** | 1.0 ± 0.2 | 1.1 ± 0.2 | 0.059 |
| **NTproBNP (ng/L)** | 776.9 ± 649.2 | 967.9 ± 3,336.3 | 0.7 |
| **hsCRP (mg/dl)** | 1.7 ± 3.0 | 0.7 ± 1.1 | 0.2 |
| **EHRA** | | | 0.3 |
| 2A | 0/19 (0%) | 2/62 (3.2%) | |
| 2B | 2/19 (11%) | 2/62 (3.2%) | |
| 3 | 17/19 (89%) | 58/62 (94%) | |
| **NYHA** | | | 0.3 |
| 2 | 3/12 (25%) | 4/36 (11%) | |
| 3 | 9/12 (75%) | 32/36 (89%) | |
| **CHA2DS2-Vasc Category** | | | >0.9 |
| 0 | 0/15 (0%) | 0/56 (0%) | |
| 1 | 0/15 (0%) | 0/56 (0%) | |
| ≥2 | 15/15 (100%) | 56/56 (100%) | |
| **HAS-BLED** | | | 0.4 |
| 0 | 1/16 (6.3%) | 12/57 (21%) | |
| 1 | 6/16 (38%) | 14/57 (25%) | |
| 2 | 7/16 (44%) | 18/57 (32%) | |
| 3 | 1/16 (6.3%) | 10/57 (18%) | |
| 4 | 1/16 (6.3%) | 3/57 (5.3%) | |
| **LVEF in %** | 53.5 ± 10.4 | 57.1 ± 7.6 | 0.2 |
| **Procedure related complications** | | | >0.9 |
| no | 16/16 (100%) | 56/57 (98%) | |
| yes | 0/16 (0%) | 1/57 (1.8%) | |
| **Fluoroscopy Time (min)** | 9.1 ± 3.9 | 11.4 ± 6.4 | 0.078 |
| **Procedure Time (min)** | 93.7 ± 29.4 | 86.5 ± 33.5 | 0.4 |
| **Heart Failure** | | | 0.4 |
| no | 3/16 (19%) | 6/57 (11%) | |
| yes | 13/16 (81%) | 51/57 (89%) | |
| **Hypertension** | | | 0.10 |
| no | 12/16 (75%) | 29/57 (51%) | |
| yes | 4/16 (25%) | 28/57 (49%) | |
| **Diabetes mellitus** | | | 0.12 |
| no | 5/16 (31%) | 7/57 (12%) | |
| yes | 11/16 (69%) | 50/57 (88%) | |
| **History of stroke or TIA** | | | 0.6 |
| no | 0/15 (0%) | 4/57 (7.0%) | |
| yes | 15/15 (100%) | 53/57 (93%) | |
| **Vessel Disease** | | | 0.069 |
| no | 3/16 (19%) | 2/56 (3.6%) | |
| yes | 13/16 (81%) | 54/56 (96%) | |
| **Statins** | | | 0.3 |
| no | 7/18 (39%) | 35/64 (55%) | |
| yes | 11/18 (61%) | 29/64 (45%) | |
| **Beta Blocker** | | | 0.8 |
| no | 6/18 (33%) | 26/64 (41%) | |
| yes | 12/18 (67%) | 38/64 (59%) | |
| **Amiodaron** | | | 0.14 |
| no | 16/18 (89%) | 45/64 (70%) | |
| yes | 2/18 (11%) | 19/64 (30%) | |
| **Klasse 1C AA** | | | 0.3 |
| no | 16/18 (89%) | 48/64 (75%) | |
| yes | 2/18 (11%) | 16/64 (25%) | |

[1]n/N (%); Mean ± SD
[2]Fisher's exact test; Welch Two Sample t-test

**Abb. 1 | 8-7** Baseline Charakteristika in der Subgruppenanalyse nach bestehendem Herzrhythmus am Tag der Ablation

| Characteristic | AFib N = 19[1] | SR N = 64[1] | p-value |
|---|---|---|---|
| GDF — Coronary sinus — Pre | 461.52 (325.30, 715.92) | 428.42 (283.36, 650.47) | 0.488 |
| GDF — Femoral — Pre | 640.33 (308.06, 778.34) | 390.94 (297.84, 568.52) | 0.188 |
| GDF — Left atrium — Pre | 487.07 (327.57, 673.01) | 420.08 (299.34, 623.11) | 0.377 |
| HFABP — Coronary sinus — Pre | 1.28 (0.96, 1.51) | 1.32 (1.03, 1.69) | 0.558 |
| HFABP — Femoral — Pre | 1.06 (0.80, 1.62) | 1.32 (0.92, 1.65) | 0.488 |
| HFABP — Left atrium — Pre | 1.32 (0.96, 1.70) | 1.55 (1.16, 1.91) | 0.371 |
| sST2 — Coronary sinus — Pre | 6,754.01 (5,222.10, 10,164.53) | 6,065.84 (3,506.57, 9,002.55) | 0.117 |
| sST2 — Femoral — Pre | 7,869.60 (5,861.92, 9,294.16) | 6,400.70 (4,159.13, 9,745.27) | 0.237 |
| sST2 — Left atrium — Pre | 7,597.65 (6,239.28, 10,202.43) | 6,508.07 (3,849.33, 9,390.10) | 0.071 |
| suPAR — Coronary sinus — Pre | 1,765.23 (1,379.24, 2,150.92) | 1,859.71 (1,354.80, 2,370.07) | 0.700 |
| suPAR — Femoral — Pre | 2,369.95 (1,782.40, 2,722.36) | 2,227.60 (1,665.88, 2,665.89) | 0.502 |
| suPAR — Left atrium — Pre | 1,681.85 (1,190.89, 2,189.24) | 1,546.63 (1,298.70, 2,106.71) | 0.626 |

**Abb. 2 | 8-7** Biomarkermessungen vor der Ablation an vordefinierten Abnahmestellen unterteilt nach linksventrikulärer Funktion

Pulmonalvenenisolation erhielten. Diese wurden in zwei Subgruppen – LVEF (≥ 50 % und < 50 %) sowie Rhythmus (Sinusrhythmus oder Vorhofflimmern) – unterteilt für die weiteren Analysen. Es erfolgte die Blutabnahme an drei spezifischen Punkten (femoral, linksatrial, Sinus coronarius) präprozedural. Metrische Variablen wurden mittels Mittelwertes ± SD angegeben, kategorische/nominale Variablen mittels Absolutwerten oder Prozenten. Um Unterschiede zwischen den Gruppen zu beschreiben, wurden der Fisher Exact test oder der Welch Two Sample t-test verwendet. Die Biomarkermessungen wurden mittels Median sowie deren Interquartilabstand angegeben. Für Vergleiche wurde der Wilcoxonrangsummentest verwendet. Als statistisch signifikant wurde für alle durchgeführten statistischen Methoden ein $P$-Wert ≤ 0,05 festgelegt. Die statistische Auswertung erfolgte mit dem Programm R.

**Resultate:** Subgruppe Rhythmus (Afib $n = 19$, SR $n = 64$) Bei den Baseline-Charakteristika zeigten sich keine signifikanten Unterschiede zwischen Vorhofflimmern und Sinusrhythmus (Tab. 1). Bei den Biomarkeranalysen (Tab. 2) zeigten sich ebenfalls keine signifikanten Unterschiede, jedoch insgesamt leicht höhere Werte an allen Abnahmeorten bei bestehendem Vorhofflimmern bei sST2 und GDF-15. Subgruppe LVEF (≥ 50 % $n = 65$, < 50 % $n = 15$) Die PatientInnen mit reduzierter LVEF erhielten signifikant häufiger Statine. Bezüglich der rhythmuskontrollierenden Medikation wurde bei den PatientInnen mit red. LVEF signifikant häufiger Amiodaron verwendet und umgekehrt signifikant häufiger Klasse Ic AAR (Tab. 3). Die Biomarkeranalysen in Tab. 4 zeigten hier ebenso keine signifikanten Unterschiede, jedoch insgesamt leicht höhere Konzentrationen von GDF-15 sowie suPAR bei reduzierter LVEF.

**Schlussfolgerungen:** Die vorliegende Analyse lässt vermuten, dass sowohl der Herzrhythmus als auch die linskventrikuläre Funktion keinen wesentlichen Einfluss auf die Biomarkerkonzentrationen haben könnte. Die beobachteten leicht höheren Werten von sST2, GDF-15 und suPAR (auch wenn nicht signifikant) könnten mitunter teils beschriebene Assoziationen bzw. Annahmen zuvor durchgeführter Studien widerspiegeln [4, 5, 6]. Weitere größere Studien sind notwendig, um diese Hypothesen zu bestätigen bzw. um fundiertere Aussagen treffen zu können.

| Characteristic | ≥50% N = 65[1] | <50% N = 15[1] | p-value[2] |
|---|---|---|---|
| **Ablation Procedure** | | | 0.3 |
| PFA | 13/64 (20%) | 1/15 (6.7%) | |
| RFA | 51/64 (80%) | 14/15 (93%) | |
| **Gender** | | | 0.8 |
| female | 23/65 (35%) | 6/15 (40%) | |
| male | 42/65 (65%) | 9/15 (60%) | |
| **Age (years)** | 62.9 ± 8.2 | 62.4 ± 12.1 | 0.9 |
| **LA Volume (ml)** | 125.8 ± 33.8 | 132.4 ± 65.6 | 0.8 |
| **Creatinine (mg/dl)** | 1.0 ± 0.2 | 1.1 ± 0.2 | 0.4 |
| **NTproBNP (ng/L)** | 1,038.0 ± 3,453.9 | 772.6 ± 565.1 | 0.6 |
| **hsCRP (mg/dl)** | 1.4 ± 3.0 | 0.6 ± 1.1 | 0.15 |
| **EHRA** | | | 0.7 |
| 2A | 2/63 (3.2%) | 0/15 (0%) | |
| 2B | 5/63 (7.9%) | 0/15 (0%) | |
| 3 | 56/63 (89%) | 15/15 (100%) | |
| **NYHA** | | | >0.9 |
| 2 | 5/37 (14%) | 2/12 (17%) | |
| 3 | 32/37 (86%) | 10/12 (83%) | |
| **CHA2DS2-Vasc Category** | | | >0.9 |
| 0 | 0/55 (0%) | 0/13 (0%) | |
| 1 | 0/55 (0%) | 0/13 (0%) | |
| ≥2 | 55/55 (100%) | 13/13 (100%) | |
| **HAS-BLED** | | | 0.4 |
| 0 | 10/57 (18%) | 3/13 (23%) | |
| 1 | 17/57 (30%) | 3/13 (23%) | |
| 2 | 18/57 (32%) | 6/13 (46%) | |
| 3 | 10/57 (18%) | 0/13 (0%) | |
| 4 | 2/57 (3.5%) | 1/13 (7.7%) | |
| **Procedure related complications** | | | 0.2 |
| no | 57/57 (100%) | 12/13 (92%) | |
| yes | 0/57 (0%) | 1/13 (7.7%) | |
| **Fluoroscopy Time (min)** | 11.2 ± 5.9 | 8.0 ± 4.1 | **0.033** |
| **Procedure Time (min)** | 88.0 ± 33.4 | 91.6 ± 26.3 | 0.7 |
| **Heart Failure** | | | **0.015** |
| no | 5/57 (8.8%) | 5/13 (38%) | |
| yes | 52/57 (91%) | 8/13 (62%) | |
| **Hypertension** | | | >0.9 |
| no | 31/57 (54%) | 7/13 (54%) | |
| yes | 26/57 (46%) | 6/13 (46%) | |
| **Diabetes mellitus** | | | 0.4 |
| no | 8/57 (14%) | 3/13 (23%) | |
| yes | 49/57 (86%) | 10/13 (77%) | |
| **History of stroke or TIA** | | | 0.2 |
| no | 2/56 (3.6%) | 2/13 (15%) | |
| yes | 54/56 (96%) | 11/13 (85%) | |
| **Vessel Disease** | | | >0.9 |
| no | 4/56 (7.1%) | 1/13 (7.7%) | |
| yes | 52/56 (93%) | 12/13 (92%) | |
| **Statins** | | | **0.020** |
| no | 37/65 (57%) | 3/14 (21%) | |
| yes | 28/65 (43%) | 11/14 (79%) | |
| **Beta Blocker** | | | 0.4 |
| no | 30/65 (46%) | 4/14 (29%) | |
| yes | 35/65 (54%) | 10/14 (71%) | |
| **Amiodaron** | | | **0.033** |
| no | 53/65 (82%) | 7/14 (50%) | |
| yes | 12/65 (18%) | 7/14 (50%) | |
| **Klasse 1C AA** | | | **0.031** |
| no | 47/65 (72%) | 14/14 (100%) | |
| yes | 18/65 (28%) | 0/14 (0%) | |
| **Rhythm before EPU** | | | 0.7 |
| AFib | 14/63 (22%) | 4/14 (29%) | |
| SR | 49/63 (78%) | 10/14 (71%) | |

[1]n/N (%); Mean ± SD
[2]Fisher's exact test; Welch Two Sample t-test

**Abb. 3 | 8-7** Baseline Charakteristika in der Subgruppenanalyse nach linksventrikulärer Funktion am Tag der Ablation

## Literatur


1. Hindricks et al. 2020 ESC Guidelines for the diagnosis and management of atrial fibrillation developed in collaboration with the European Association for Cardio-Thoracic Surgery (EACTS): The Task Force for the diagnosis and management of atrial fibrillation of the European Society of Cardiology (ESC) Developed with the special contribution of the European Heart Rhythm Association (EHRA) of the ESC. Eur Heart J. 2021 Feb 1;42(5):373–498. https://doi.org/10.1093/eurheartj/ehaa612. Erratum in: Eur Heart J. 2021 Feb 1;42(5):507. https://doi.org/10.1093/eurheartj/ehaa798.PMID: 32860505
2. Van Gelder et al.; ESC Scientific Document Group. 2024 ESC Guidelines for the management of atrial fibrillation developed in collaboration with the European Association for Cardio-Thoracic Surgery (EACTS). Eur Heart J. 2024 Sep 29;45(36):3314–3414. https://doi.org/10.1093/eurheartj/

| Characteristic | ≥50% N = 65[1] | <50% N = 15[1] | p |
|---|---|---|---|
| GDF — Coronary sinus — Pre | 396.01 (282.79, 620.93) | 469.02 (288.64, 690.61) | 0.613 |
| GDF — Femoral — Pre | 401.26 (300.61, 578.11) | 559.61 (295.07, 826.83) | 0.252 |
| GDF — Left atrium — Pre | 425.27 (298.07, 564.43) | 530.53 (327.57, 744.78) | 0.362 |
| HFABP — Coronary sinus — Pre | 1.28 (1.04, 1.56) | 1.28 (0.90, 1.74) | 0.946 |
| HFABP — Femoral — Pre | 1.31 (0.88, 1.61) | 1.26 (0.91, 1.75) | 0.820 |
| HFABP — Left atrium — Pre | 1.41 (1.09, 1.75) | 1.50 (1.21, 2.19) | 0.398 |
| sST2 — Coronary sinus — Pre | 6,531.21 (4,979.67, 9,231.62) | 6,200.49 (4,136.44, 9,416.13) | 0.467 |
| sST2 — Femoral — Pre | 7,594.34 (5,370.03, 9,904.11) | 6,937.65 (3,556.14, 8,847.04) | 0.518 |
| sST2 — Left atrium — Pre | 6,882.05 (5,105.99, 9,853.07) | 6,856.30 (3,839.46, 8,141.69) | 0.567 |
| suPAR — Coronary sinus — Pre | 1,835.30 (1,321.06, 2,347.32) | 1,952.63 (1,448.38, 2,482.49) | 0.349 |
| suPAR — Femoral — Pre | 2,183.40 (1,688.11, 2,582.23) | 2,656.59 (1,649.86, 2,902.57) | 0.213 |
| suPAR — Left atrium — Pre | 1,585.03 (1,305.96, 2,001.89) | 2,102.33 (1,231.13, 2,606.34) | 0.164 |

**Abb. 4 | 8-7** Biomarkermessungen vor der Ablation an vordefinierten Abnahmestellen unterteilt nach linksventrikulärer Funktion

ehae176. Erratum in: Eur Heart J. 2025 Nov 3;46(41):4349. https://doi.org/10.1093/eurheartj/ehaf306. PMID: 39210723.
3. McDonagh et al.; ESC Scientific Document Group. 2021 ESC Guidelines for the diagnosis and treatment of acute and chronic heart failure. Eur Heart J. 2021 Sep 21;42(36):3599–3726. https://doi.org/10.1093/eurheartj/ehab368. Erratum in: Eur Heart J. 2021 Dec 21;42(48):4901. https://doi.org/10.1093/eurheartj/ehab670. PMID: 34447992.
4. Ohnewein et al. Dynamics of the Novel Cardiac Biomarkers sST2, H-FABP, GDF-15 and suPAR in HFrEF Patients Undergoing Heart Failure Therapy, a Pilot Study. J Clin Med. 2025 Aug 11;14(16):5668. https://doi.org/10.3390/jcm14165668. PMID: 40869494; PMCID: PMC12386204.
5. Yan X, et al. The sST2 level is an independent influencing factor associated with atrial fibrillation in heart failure patients: a case-control study. J Thorac Dis. 2022;14(5):1578–87.
6. Sawalha K, et al. Growth Differentiation Factor 15 (GDF-15), a New Biomarker in Heart Failure Management. Curr Heart Fail Rep. 2023;20(4):287–99.

## 8-8

## Analyse potenzieller Konzentrationsunterschiede kardialer Biomarker (GDF-15, H-FBAP, sST2 und suPAR) bei PatientInnen unmittelbar vor Pulmonalvenenisolation in peripherer Messung, linkem Vorhof sowie Sinus coronarius

**Petric F.[1], Matejka M.[2], Paar V.[3], Pfeffer M.[4], Tinhofer F.[5], Zechowicz M.[6], Blessberger H.[7], Hoppe U.[3], Roithinger F.[4], Motloch L.[2], Fiedler L.[4]**

[1]Klinik Landstraße, 1030, Österreich
[2]Klinik Salzkammergut, Vöcklabruck, Österreich
[3]Paracelsus Private Medical University, Salzburg, Österreich
[4]Universitätsklinikum Wiener Neustadt, Wiener Neustadt, Österreich
[5]Klinik Ottakring, 1160, Österreich
[6]University of Warmia and Mazury in Olsztyn, Olsztyn, Polen
[7]Kepler Universitätsklinikum, Linz, Österreich

**Einleitung:** Die Bestimmung kardialer Biomarker spielen eine zentrale Rolle nicht nur diagnostisch, sondern auch prognostisch bei kardiovaskulären Erkrankungen, so auch bei der Herzinsuffizienz [1]. Die Bestimmung dieser Biomarker ist jedoch fehleranfällig und kann durch bpsw. neuere pharmakologische Therapien in ihrer Aussage verfälscht werden [2]. Neuartige kardiale Biomarker (GDF-15, sST2, H-FABP, suPAR) zeigten bereits mögliche Assoziationen mit kardialem Volumenoverload, myokardialen Schaden sowie erhöhter Mortalität bei Herzinsuffizienz [2, 3]. Aufgrund der gehäuften Assoziation

| Baseline Characteristics | N = 90[1] |
|---|---|
| Age | 63.0 ± 8.8 |
| Gender | |
| female | 35 (39%) |
| male | 55 (61%) |
| Ablation Procedure | |
| PFA | 15 (17%) |
| RFA | 73 (83%) |
| LA Volume (ml) | 129.9 ± 41.3 |
| Creatinine (mg/dl) | 1.0 ± 0.2 |
| NTproBNP (ng/L) | 912.8 ± 2,939.4 |
| hsCRP (mg/dl) | 1.1 ± 2.7 |
| EHRA | |
| 2A | 2 (2.3%) |
| 2B | 6 (7.0%) |
| 3 | 78 (91%) |
| NYHA | |
| 2 | 8 (16%) |
| 3 | 43 (84%) |
| HAS-BLED | |
| 0 | 13 (17%) |
| 1 | 23 (29%) |
| 2 | 26 (33%) |
| 3 | 12 (15%) |
| 4 | 4 (5.1%) |
| HAS_BLED Median (IQR) | 2.0 (1.0, 2.0) |
| CHA2DS2-VASc Median (IQR) | 6.0 (5.0, 7.0) |
| CHA2DS2-Vasc Category | |
| 0 | 0 (0%) |
| 1 | 0 (0%) |
| ≥2 | 76 (100%) |
| LVEF in % | 56.1 ± 8.4 |
| Heart Failure | 66 (85%) |
| Hypertension | 34 (44%) |
| Diabetes mellitus | 64 (82%) |
| History of stroke or TIA | 73 (95%) |
| Vessel Disease | 71 (92%) |
| Procedure related complications | 1 (1.3%) |
| Fluoroscopy Time (min) | 10.6 ± 5.9 |
| Procedure Time (min) | 88.1 ± 32.0 |
| Statins | 42 (48%) |
| Beta Blocker | 53 (60%) |
| Amiodaron | 23 (26%) |
| Klasse 1C AA | 19 (22%) |
| Rhythm before EPU | |
| AFib | 19 (23%) |
| SR | 64 (77%) |

**Tabelle 1: Baseline-Charakteristika der StudienteilnehmerInnen**

[1]Mean ± SD; n (%); Median (Q1, Q3)

**Abb. 1 | 8-8**

| Characteristic | Coronary sinus N = 90[1] | Femoral N = 90[1] | p | p (FDR) |
|---|---|---|---|---|
| GDF | 434.69 (285.34, 679.81) | 419.28 (303.93, 677.37) | 0.081 | 0.108 |
| HFABP | 1.28 (1.02, 1.59) | 1.31 (0.88, 1.62) | 0.542 | 0.542 |
| sST2 | 6,480.67 (4,511.10, 9,416.13) | 7,225.43 (5,230.62, 9,904.11) | <0.001 | **<0.001** |
| suPAR | 1,829.87 (1,383.51, 2,352.70) | 2,243.50 (1,649.86, 2,675.20) | <0.001 | **<0.001** |
| [1]Median (Q1, Q3) | | | | |
| **Characteristic** | **Left atrium N = 90[1]** | **Femoral N = 90[1]** | **p** | **p (FDR)** |
| GDF | 440.09 (310.50, 663.26) | 419.28 (303.93, 677.37) | 0.103 | 0.103 |
| HFABP | 1.50 (1.14, 1.88) | 1.31 (0.88, 1.62) | <0.001 | **<0.001** |
| sST2 | 6,815.67 (4,762.31, 9,743.42) | 7,225.43 (5,230.62, 9,904.11) | 0.009 | **0.012** |
| suPAR | 1,610.21 (1,291.44, 2,102.33) | 2,243.50 (1,649.86, 2,675.20) | <0.001 | **<0.001** |
| [1]Median (Q1, Q3) | | | | |
| **Characteristic** | **Left atrium N = 90[1]** | **Coronary sinus N = 90[1]** | **p** | **p (FDR)** |
| GDF | 440.09 (310.50, 663.26) | 434.69 (285.34, 679.81) | 0.652 | 0.870 |
| HFABP | 1.50 (1.14, 1.88) | 1.28 (1.02, 1.59) | <0.001 | **0.002** |
| sST2 | 6,815.67 (4,762.31, 9,743.42) | 6,480.67 (4,511.10, 9,416.13) | 0.925 | 0.925 |
| suPAR | 1,610.21 (1,291.44, 2,102.33) | 1,829.87 (1,383.51, 2,352.70) | <0.001 | **<0.001** |

**Tabelle 2: Konzentrationen einzelner Biomarker in Abhängigkeit ihres Messortes**

[1]Median (Q1, Q3)

**Abb. 2 | 8-8**

von Vorhofflimmern und Herzinsuffizienz (teils bis zu 50 %) [4] und bisher keinen durchgeführten Studien bezüglich möglicher Messvarianzen je nach Abnahmestelle, führten wir diese Arbeit durch.

**Methoden:** Um der Frage nachzugehen wurden 90 PatientInnen eingeschlossen, die eine Pulmonalvenenisolation erhielten. Präprozedural wurden an drei Abnahmestellen (femoral, linkes Atrium sowie Sinus coronarius) Blutproben entnommen. Metrische Variablen wurden mittels Mittelwertes ± SD angegeben, kategorische/nominale Variablen mittels Absolutwerten oder Prozenten. Die Biomarkermessungen wurden mittels Median sowie Interquartilen-Abstand angegeben, für Vergleiche zwischen wurde der Wilcoxonrangsummentest verwendet. Alle Tests wurden zweiseitig durchgeführt, als statistisch signifikant wurde für alle durchgeführten statistischen Methoden ein *P*-Wert ≤0,05 festgelegt. Die statistische Auswertung erfolgte mit dem Programm R.

**Resultate:** Die Baseline-Charakteristika der Studienteilnehmerinnen sind in Tab. 1 dargestellt. Die PatientInnen hatten ein mittleres Alter von 63 ± 8 Jahren mit einem höheren Anteil männlicher Patienten (61 % vs. 39 %). Bezüglich der abgenommenen Biomarker zeigten sich bei Vergleichen der Abnahmeorte signifikante Unterschiede wie Tab. 2 aufzeigt. H-FABP zeigte signifikant höhere Konzentrationen im linken Atrium verglichen mit der peripheren Messung ($p<0{,}001$, $p=0{,}002$). sST2 zeigte signifikant höhere Messwerte in der peripheren Entnahmestelle ($p<0{,}001$, $p=0{,}012$), selbes gilt für suPAR ($p<0{,}001$ für alle Messungen).

**Schlussfolgerungen:** Diese Arbeit könnte Hinweise darauf zeigen, dass die Abnahmestelle mitunter eine Rolle spielen kann bei Abnahme von H-FABP, sST2 sowie suPAR. Es sind jedoch weitere größere, randomisierte Studien durchzuführen, um diese Hypothesen weiter zu erforschen.

## Literatur


1. McDonagh et al.; ESC Scientific Document Group. 2021 ESC Guidelines for the diagnosis and treatment of acute and chronic heart failure. Eur Heart J. 2021 Sep 21;42(36):3599–3726. https://doi.org/10.1093/eurheartj/ehab368. Erratum in: Eur Heart J. 2021 Dec 21;42(48):4901. https://doi.org/10.1093/eurheartj/ehab670. PMID: 34447992.
2. Ohnewein et al. Dynamics of the Novel Cardiac Biomarkers sST2, H-FABP, GDF-15 and suPAR in HFrEF Patients Undergoing Heart Failure Therapy, a Pilot Study. J Clin Med. 2025 Aug 11;14(16):5668. https://doi.org/10.3390/jcm14165668. PMID: 40869494; PMCID: PMC12386204.
3. Sawalha K, et al. Differentiation Factor 15 (GDF-15), a New Biomarker in Heart Failure Management. Curr Heart Fail Rep. Growth. 2023;20(4):287–99. https://doi.org/10.1007/s11897-023-00610-4. Epub 2023 Jun 8. PMID: 37289373.
4. Van Gelder et al.; ESC Scientific Document Group. 2024 ESC Guidelines for the management of atrial fibrillation developed in collaboration with the European Association for Cardio-Thoracic Surgery (EACTS). Eur Heart J. 2024 Sep 29;45(36):3314–3414. https://doi.org/10.1093/eurheartj/ehae176. Erratum in: Eur Heart J. 2025 Nov 3;46(41):4349. https://doi.org/10.1093/eurheartj/ehaf306. PMID: 39210723.


# POSTERSITZUNG 9—CLINICAL CASES 2

## 9-1

### Transcatheter Edge-to-Edge Repair (MitraClip) in Severe Mitral Regurgitation with Difficult Transesophageal Echocardiographic Access: A Case Report


**Rohringer H., Steinwender C., Kellermair J.**

Kepleruniversitätsklinikum, Linz, Austria


**Introduction:** Mitral valve-TEER is indicated for patients with moderate-to-severe or severe mitral regurgitation (MR), particularly those with primary MR who are at prohibitive surgical risk, as well as select patients with secondary MR. Patient selection relies on echocardiographic assessment to confirm MR severity and aeteology, LVEF, and anatomical suitability, including complex features such as leaflet calcification, bileaflet prolapse, clefts, or commissural jets. Transesophageal echocardiography (TEE) is central to both patient screening and procedural planning. TEE protocols are used to confirm MR severity, assess mitral valve anatomy, and determine eligibility for edge-to-edge repair. Intraprocedural TEE guidance is indispensable for the stepwise execution of the repair. TEE is used to guide the transseptal puncture, ensuring optimal location and height above the mitral valve plane, followed by real-time navigation of the device into the left atrium and across the mitral valve. An 83-year-old male patient was admitted to our clinic due to cardiac decompensation with progressive dyspnea on exertion corresponding to NYHA functional class III. His past medical history included known mitral valve regurgitation, arterial hypertension, and a post-traumatic swallowing disorder following a fall in January 2014 that resulted in a cervical spine fracture requiring surgical stabilization. Additionally, a known posterior bulging of the hypopharynx had previously been documented.

**Methods:** Diagnostic Workup Laboratory testing revealed elevated NT-pro BNP levels (3247 ng/L). Initial transthoracic echocardiography (TTE) demonstrated severe mitral regurgitation with suspected flail leaflet of the posterior mitral leaflet. The left ventricle was dilated and left ventricular systolic function was moderately reduced with an EF of approximately 45%. Right ventricular function was preserved with a TAPSE of 20 mm. Further evaluation with TEE was planned in order to confirm the mechanism of mitral regurgitation and to assess anatomical suitability for interventional therapy. However, the initial attempt at TEE was not possible and difficult probe insertion. The examination was complicated by the patient's known swallowing disorder, the previous cervical spine surgery, and the posterior hypopharyngeal bulging. In order to exclude a

mechanical passage obstruction, gastroscopy was performed. Additionally, computed tomography of the cervical spine was obtained. A repeat transesophageal echocardiographic examination was then performed in an interdisciplinary setting under intensive care conditions with sedation and endotracheal intubation. Using videolaryngoscopic guidance and laryngeal elevation by the otolaryngology team, the probe could be advanced through the right piriform recess without complications. A pediatric transesophageal echocardiography probe was used to facilitate the examination.

**Results:** The repeat examination demonstrated severe excentric mitral regurgitation caused by a flail leaflet of the PMV in the P2 segment. After interdisciplinary heart team discussion, the patient was considered a suitable candidate for transcatheter edge-to-edge repair using the MitraClip system. The procedure was performed under transesophageal echocardiographic guidance using a Philips X11-4T probe, allowing two-dimensional imaging, live xPlane imaging, three-dimensional imaging, and color Doppler assessment. A MitraClip XTW device was successfully implanted at the level of the flail P2 segment. Adequate leaflet grasping and significant reduction of mitral regurgitation were achieved. Outcome The procedure was completed without complications. The patient showed marked clinical improvement following the intervention. At follow-up four weeks after the procedure, the patient reported significant improvement in symptoms with functional status corresponding to NYHA class I–II. Follow-up echocardiography demonstrated a stable clip position with a relevant reduction in mitral regurgitation. Discussion: Beyond patient screening, TEE guidance is indispensable during the procedure itself. Real-time imaging allows accurate transseptal puncture and confirmation of adequate leaflet grasping prior to clip deployment. After implantation, TEE is also essential for assessing residual MR and for identifying complications such as single-leaflet attachment, device embolization or pericardial effusion.

**Conclusion:** After implantation, TEE is essential for assessing residual MR and for identifying complications such as single-leaflet device attachment, device embolization or pericardial effusion. This case highlights the critical importance of TEE imaging access for successful TEER. In our patient, the presence of severe dysphagia, prior cervical spine surgery, and anatomical alterations of the hypopharynx initially prevented adequate probe placement and resulted in insufficient acoustic windows during the initial TEE examination. As adequate TEE imaging is mandatory for procedural guidance, the absence of a sufficient acoustic window would have precluded TEER. However, through a multidisciplinary approach involving cardiology, intensive care medicine, gastroenterology and otolaryngology, adequate imaging conditions were achieved. The use of a new TEE probe allowed safe advancement of the probe via the right piriform recess and enabled sufficient visualization of the MV. This enabled successful MitraClip implantation with significant reduction of MR and clinical improvement. The favorable outcome observed in this case is consistent with previously reported results demonstrating symptomatic improvement and reduction in heart failure symptoms following TEER in appropriately selected patients. Overall, this case emphasizes the pivotal role of TEE pivotal in all stages of TEER therapy and highlights the importance of multidisciplinary collaboration and flexible imaging strategies.

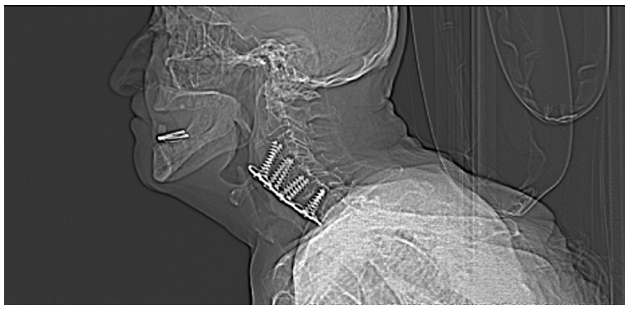

Fig. 1 | 9-1

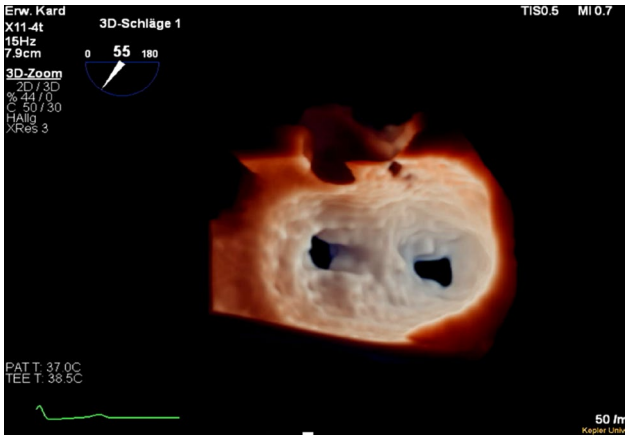


Fig. 2 | 9-1

## References


1. Davidson LJ, Davidson CJ. Transcatheter Treatment of Valvular Heart Disease: A Review. The Journal of the American Medical Association. 2021.
2. Nyman CB, Mackensen GB, Jelacic S, et al. Transcatheter Mitral Valve Repair Using the Edge-to-Edge Clip. Journal of the American Society of Echocardiography: Official Publication of the American Society of Echocardiography. 2018.
3. Hausleiter J, Lim DS, Gillam LD, et al. Transcatheter Edge-to-Edge Repair in Patients With Anatomically Complex Degenerative Mitral Regurgitation. Journal of the American College of Cardiology. 2023.
4. Marcoff L, Koulogiannis K, Aldaia L, et al. Echocardiographic Outcomes With Transcatheter Edge-to-Edge Repair For Degenerative Mitral Regurgitation In Prohibitive Surgical Risk Patients. JACC. Cardiovascular Imaging. 2024.
5. Faletra FF, Berrebi A, Pedrazzini G, et al. 3D Transesophageal Echocardiography: A New Imaging Tool for Assessment of Mitral Regurgitation and for Guiding Percutaneous Edge-to-Edge Mitral Valve Repair. Progress in Cardiovascular Diseases. 2017.
6. Cavalcante JL, Rodriguez LL, Kapadia S, Tuzcu EM, Stewart WJ. Role of Echocardiography in Percutaneous Mitral Valve Interventions. JACC. Cardiovascular Imaging. 2012.
7. Silvestry FE, Kerber RE, Brook MM, et al. Guideline Echocardiography-Guided Interventions. Journal of the American Society of Echocardiography: Official Publication of the American Society of Echocardiography. 2009.
8. Flores G, Mesa D, Ojeda S, et al. Complications of the Percutaneous Mitral Valve Edge-to-Edge Repair: Role of Transesophageal. Echocardiogr J Clin Med. 2022.

## 9-2

### Bland-White-Garland Syndrome Diagnosed in Adulthood After Long-Standing Exertional Symptoms: A Case Report

**Rohringer H., Steinwender C., Wichert-Schmitt B.**

Kepleruniversitätsklinikum, Linz, Austria

**Introduction:** Bland-White-Garland syndrome is a rare congenital coronary anomaly representing less than 1% of all coronary anomalies and occurring in approximately 1 in 300,000 births. In infancy, it typically presents with heart failure due to myocardial ischemia. However, a small proportion of patients survive into adulthood because of extensive collateral circulation from the right coronary artery (RCA) to the left coronary system. This predisposes to chronic myocardial ischemia, left ventricular dysfunction, mitral regurgitation, arrhythmias, and an increased risk of sudden cardiac death. A 25 year female patient was referred for coronary CT angiography. She reported exercise-induced symptoms since the age of ten years, but had never undergone a comprehensive cardiologic evaluation. Her symptoms included dyspnoea on exertion and angina during exertion. Initial transthoracic echocardiography demonstrated preserved left ventricular systolic function with a left ventricular ejection fraction (LVEF) of 55–60%. Global longitudinal strain was mildly reduced (–15%). Mild prolapse of the mitral valve leaflets with minimal mitral regurgitation was observed. TTE also revealed a vascular structure arising from the pulmonary artery, raising suspicion for an anomalous origin of the LAD. In the interventricular septum collateral vessels could be identified. Laboratory testing revealed cardiac enzymes within the normal range. NT-proBNP was mildly elevated at 305 ng/L.

**Methods:** Coronary CT angiography revealed an anomalous origin of the left coronary artery from the main pulmonary artery. The left coronary artery gave rise to the left anterior descending artery and the circumflex artery and appeared ectatically dilated. The right coronary artery was dominant and originated from the right sinus of Valsalva. Prominent collateral vessels from the right coronary artery to the left anterior descending artery were present, resulting in retrograde contrast filling of the left coronary system. Overall, the imaging findings were consistent with Bland–White–Garland syndrome. Therapeutic Strategy After a Heart Team discussion, the indication for surgical correction was established. During surgery, the anomalous origin of the left coronary artery from the main pulmonary artery was confirmed. The left coronary artery followed toward the pulmonary artery and was considered suitable for transfer after adequate mobilization. The coronary ostium was excised and reimplanted into the aortic root using a pericardial patch (trapdoor technique). The patient was transferred to the cardiac surgical ICU and subsequently to the ward. This case illustrates several typical features described in adult ALCAPA patients. The patient reported exertional symptoms since childhood, including exertional dyspnoea and chest pain during physical activity, which is consistent with the typical presentation of exertional angina in ALCAPA adults.

**Results:** Interestingly, despite these long-standing symptoms, the patient had not undergone comprehensive cardiologic evaluation before. This highlights that congenital coronary anomalies may remain undiagnosed for many years, particularly in young females with otherwise preserved functional capacity. ALCAPA in adulthood is rare because untreated patients have a high mortality rate in infancy. Survival into adulthood depends on the development of extensive collateral circulation from the right coronary artery (1). Multimodality imaging plays a crucial role in the diagnosis of ALCAPA. TTE revealed indirect signs such as dilated coronary arteries, collateral vessels within the interventricular septum, or abnormal flow patterns in the pulmonary artery (1). However, coronary CT angiography provides

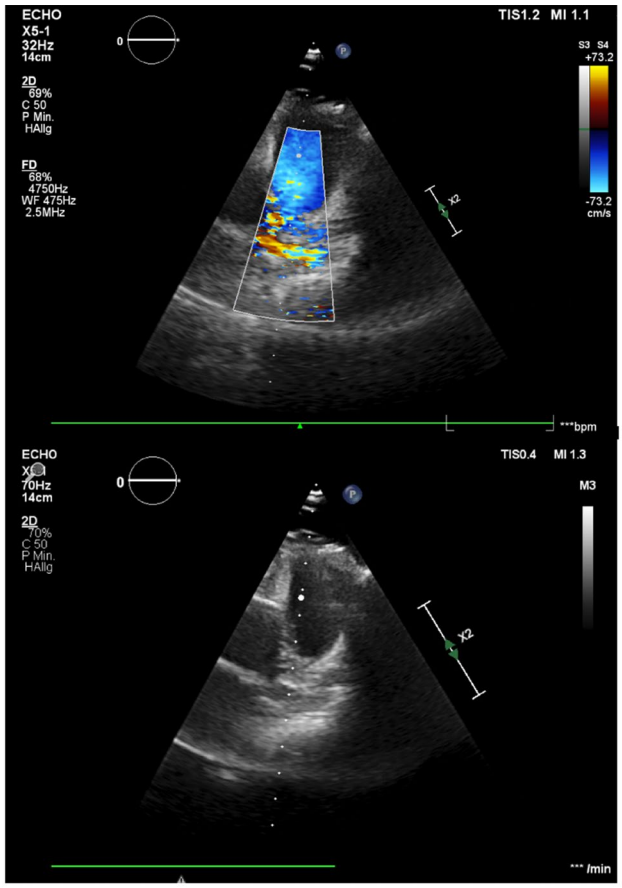


**Fig. 1 | 9-2** Transthoracic echocardiography showing a vessel arising from the pulmonary artery suggestive of ALCAPA

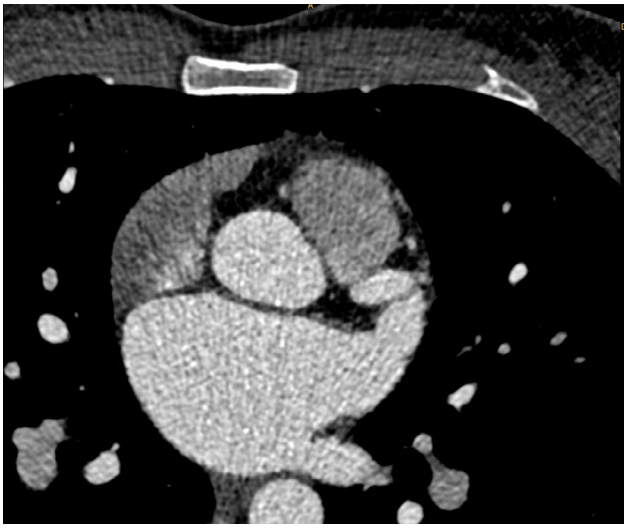

**Fig. 2 | 9-2** Coronary CT angiography demonstrating anomalous origin of the left coronary artery from the main pulmonary artery

ecact visualization of coronary anatomy and was essential in this case to confirm the anomalous origin of the left coronary artery from the pulmonary artery and to demonstrate collateral circulation and retrograde filling of the left coronary system (2,3,6,7). Long-term outcomes after surgical correction of Bland-Garland-White syndrome (ALCAPA) in adults are generally favourable, with most patients achieving normalization of LVEF and significant improvement in MR and symptoms. However, several important considerations persist. Residual myocardial dysfunction is common, particularly in the longitudinal systolic and diastolic function of the LV, even in normalized LVEF.

**Conclusion:** Speckle tracking echocardiography and strain imaging consistently demonstrate persistent subclinical myocardial impairment, especially in the territory supplied by the left coronary artery, likely reflecting irreversible preoperative ischemic injury (8,9). This underscores the need for lifelong surveillance. Arrhythmia risk remains elevated post-repair, due to residual myocardial fibrosis and scarring from prior ischemia. Ventricular arrhythmias and sudden cardiac death have been reported, although the absolute risk is reduced after restoration of a dual coronary system (10). Ongoing monitoring for arrhythmias is advised. Mitral regurgitation typically improves after surgery, but persistent or recurrent regurgitation may require subsequent intervention, especially if structural mitral valve abnormalities are present (11,12). Most patients achieve NYHA class I or II status and have good functional capacity (13,14).

## References


1. Laflamme E, Alonso-Gonzalez R, Roche SL, Wald RM, Swan L, Silversides CK, et al. Anomalous origin of a coronary artery from the pulmonary artery presenting in adulthood: Experience from a tertiary center. Int J Cardiol Congenit Heart Dis. 2021;1:4. https://doi.org/10.1016/j.ijcchd.2021.100169.
2. Wild PS, Stahl F, Gunkel O, Zotz RJ. Atypical Bland-White-Garland Syndrome: A 58-Year-Old Woman with Stenosis of the Pulmonary Origin of the Left Coronary Artery. ECHOCARDIOGRAPHY: A Jrnl. of CV Ultrasound & Allied Tech. 2002. Report.
3. Wang Y, Zheng X, Liu K. Surgical Repair of Bland–White–Garland Syndrome With Giant Right Coronary Artery Aneurysm. Annals of Thoracic Surgery. 2017 Nov 1;104(5):e375–7. https://doi.org/10.1016/j.athoracsur.2017.06.046 PubMed PMID: 29054232.
4. Komócsi A, Simor T, Tóth L, Szabados S, Mágel F, Pintér T, et al. Magnetic resonance studies in management of adult cases with Bland-White-Garland syndrome. Int J Cardiol. 2007 Dec 15;123(1). https://doi.org/10.1016/j.ijcard.2006.11.084 PubMed PMID: 17306388.
5. Maeder M, Vogt PR, Ammann P, Rickli H. Bland-White-Garland syndrome in a 39-year-old mother. Annals of Thoracic Surgery. 2004 Oct;78(4):1451–3. https://doi.org/10.1016/S0003-4975(03)01461-9 PubMed PMID: 15464516.
6. Selmi K, Bergaoui H, Boujnah MR. Echocardiographic marker for bland-white-garland syndrome in adult. Journal of the American Society of Echocardiography. 2011;24(9):1056.e1-1056.e4. https://doi.org/10.1016/j.echo.2011.03.016
7. Parizek P, Haman L, Harrer J, Tauchman M, Rozsival V, Varvarovsky I, et al. Bland-White-Garland syndrome in adults: Sudden cardiac death as a first symptom and long-term follow-up after successful resuscitation and surgery. Europace. 2010 Sep;12(9):1338–40. https://doi.org/10.1093/europace/euq087 PubMed PMID: 20348142.
8. Dabrowska-Kugacka A, Dorniak K, Meyer-Szary J, Rey AH, Lewicka E, Ostrowska K, et al. Myocardial function in patients with anomalous left coronary artery from the pulmonary artery syndrome: A long-term speckle tracking echocardiographic study. PLoS One. 2019 Oct 1;14(10). https://doi.org/10.1371/journal.pone.0223227 PubMed PMID: 31613933.
9. Cabrera AG, Chen DW, Pignatelli RH, Khan MS, Jeewa A, Mery CM, et al. Outcomes of anomalous left coronary artery from pulmonary artery repair: Beyond normal function. Annals of Thoracic Surgery. 2015 Apr 1;99(4):1342–7. https://doi.org/10.1016/j.athoracsur.2014.12.035 PubMed PMID: 25725925.
10. Warnes CA, Williams RG, Bashore TM, Child JS, Connolly HM, Dearani JA, et al. ACC/AHA 2008 Guidelines for the Management of Adults with Congenital Heart Disease: a report of the American College of Cardiology/American Heart Association Task Force on Practice Guidelines (writing committee to develop guidelines on the management of adults with congenital heart disease). Circulation. 2008 Dec 2;118(23). https://doi.org/10.1161/CIRCULATIONAHA.108.190690 PubMed PMID: 18997169.
11. Langen R, Cleuziou J, Krane M, Ewert P, von Ohain JP, Beran E, et al. Long-term outcome after anomalous left coronary artery from the pulmonary artery repair: A 40-year single-centre experience. European Journal of Cardio-thoracic Surgery. 2018 Apr 1;53(4):732–9. https://doi.org/10.1093/ejcts/ezx407 PubMed PMID: 29182759.
12. Lange R, Vogt M, Hörer J, Cleuziou J, Menzel A, Holper K, et al. Long-Term Results of Repair of Anomalous Origin of the Left Coronary Artery From the Pulmonary Artery. Annals of Thoracic Surgery. 2007 Apr;83(4):1463–71. https://doi.org/10.1016/j.athoracsur.2006.11.005 PubMed PMID: 17383358.
13. Yuan X, Li B, Sun H, Yang Y, Meng H, Xu L, et al. Surgical Outcome in Adolescents and Adults With Anomalous Left Coronary Artery From Pulmonary Artery. Ann Thorac Surg. 2018; https://doi.org/10.1016/j.
14. Rajbanshi BG, Burkhart HM, Schaff H V., Daly RC, Phillips SD, Dearani JA. Surgical strategies for anomalous origin of coronary artery from pulmonary artery in adults. Journal of Thoracic and Cardiovascular Surgery. 2014;148(1):220–4. https://doi.org/10.1016/j.jtcvs.2013.08.026 PubMed PMID: 24079879.


## 9-3

## Acoramidis and Functional Capacity in ATTR-CM: A Case Report


**Gregshammer B., Kösters A., Eslami M., Pahr S., Lichtblau L., Ermolaev N., Badr Eslam R.**

Department of Internal Medicine II, Division of Cardiology, Medical University of Vienna, Wien, Austria


**Introduction:** Background: In recent years, substantial resources have been invested in developing disease-modifying therapies for patients with transthyretin amyloid cardiomyopathy (ATTR-CM). Acoramidis (Beyonttra) has been approved in EU since February 2025 after the phase III trial (ATTRibute-CM) showed a significant benefit versus placebo in the four endpoints (all-cause mortality, cardiovascular hospitalizations, NT-proBNP, and 6-minute walk test). This case represents the first patient at our center who received acoramidis and completed CPET both at baseline and at follow-up.

**Methods:** Case presentation: An 80-year-old man was referred following 99mTc-DPD scintigraphy demonstrating

| Changes in Clinical Parameters After 9 Months of Acoramidis | | | | |
|---|---|---|---|---|
| Metric | Baseline | Follow-up (9 mo) | Δ (Follow-up - Baseline) | % Change |
| Peak workload (in W) | 109 | 120 | 11 | 10.1% |
| $VE/VCO_2$ | 33.39 | 30.57 | -2.82 | -8.4% |
| Peak $VO_2$ (in mL/kg/min) | 20.90 | 23.70 | 2.80 | 13.4% |
| RER | 1.05 | 1.00 | -0.05 | -4.8% |
| 6-minute walk test (in m) | 476 | 542 | 66 | 13.9% |
| NT-proBNP (in pg/ml) | 552 | 378 | -174 | -31.5% |
| Troponin T (in ng/L) | 38 | 38 | 0 | 0.0% |

**Table 1. Changes in Clinical Parameters After 9 Months of Acoramidis.**
W, watts; $VE/VCO_2$, ventilatory efficiency (minute ventilation to carbon dioxide output); $VO_2$, oxygen uptake; RER, respiratory exchange ratio ($VCO_2/VO_2$); NT-proBNP, N-terminal pro–B-type natriuretic peptide.

**Fig. 1 | 9-3** Changes in Clinical Parameters After 9 Months of Acoramidis

Perugini grade 3 cardiac uptake. He was still active (skiing and tennis), had never required a cardiac admission, and reported only age-appropriate exertional dyspnea (NYHA class I). NT-proBNP was 552 pg/mL, and he took no regular medication apart from supplements. His relevant comorbidities included arterial hypertension, transient ischemic attacks, and prior foramen ovale closure. The diagnostic work-up confirmed transthyretin wild-type amyloid cardiomyopathy (ATTRwt-CM).

**Results:** Baseline functional assessment: For baseline functional evaluation, cardiopulmonary exercise testing (CPET) demonstrated good age-adjusted exercise capacity: peak workload 109 W (90% predicted), peak $VO_2$ 20.9 mL/kg/min (X% predicted), $VE/VCO_2$ 33.39, and RER 1.05. Six-minute walk distance (6MWD) was 476 m. Treatment: Tafamidis could not be initiated due to lack of insurance approval in the absence of prior cardiac hospitalization. Instead, acoramidis was started, as the patient met the inclusion criteria of the ATTRibute-CM study. In addition, edoxaban was initiated due to paroxysmal atrial fibrillation. Follow-up/outcome: The patient tolerated treatment well and reported no adverse effects. Nine months after treatment initiation, CPET was repeated and showed improvement in exercise parameters. Peak workload increased from 109 W to 120 W (Δ +11 W, +10% relative). Peak $VO_2$ increased from 20.9 to 23.7 mL/kg/min (Δ + 2.8 mL/kg/min, +13% relative). $VE/VCO_2$ decreased from 33.39 to 30.57 (Δ –2.82, –8.4% relative). Notably, RER was lower at follow-up (follow up: 1.00; baseline: 1.05), suggesting less maximal effort and potentially underestimating the true change. In addition the six-minute walk test also improved from 476 m to 542 m (Δ +66 m, +14% relative).

**Conclusion:** On the one hand, this case suggests that initiating disease-modifying therapy in early-stage ATTRwt-CM, even in patients with preserved baseline functional capacity, may be associated with substantial improvements in functional capacity. On the other hand, the improvement in functional capacity supports the potential clinical effectiveness of acoramidis in routine care.

## 9-4

## The suprising diagnosis behind a high degree AV-block

**Petric F.[1], Krutisch G.[1], Niessner A.[1], Pfeffer M.[2], Roithinger F.[2], Grübler M.[2]**

[1]Klinik Landstraße, 1030, Österreich
[2]Universitätsklinikum Wiener Neustadt, Wiener Neustadt, Österreich

**Einleitung:** AV-Block kann durch verschiedene Ursachen bedingt sein, am häufigsten durch degenerative, altersassoziierte oder komorbiditätsbedingte Veränderungen[1]. Seltener liegen entzündliche, infiltrative, genetische oder onkologische Ursachen zugrunde [1].

**Methoden:** Ein 61A Patient stellte sich in der Notaufnahme aufgrund progredienter Dyspnoe vor. Nebenbefundlich zeigte sich ein 2:1 AV-Block (in der telemetrischen Überwachung höhergradiger AV-Block). Anamnestich bestanden keine wesentlichen Vorerkrankungen bis auf einen chronischen Nikotinabusus sowie eine hoch positive Familienanamnese für hypertrophe Kardiomyopathie (Schwester 2008 HTX, Bruder 2014 HTX). Der klinische Status zeigte das Bild einer kardialen Dekompensation mit bibasalen RG's und gestauten Halsvenen. Innerhalb weniger Tage zeigte sich der AV-Block regredient mit wiederum normaler Überleitung. Eine Echokardiographie zeigte eine HFrEF de novo (mit 22 %) bei normalem LV-Volumen. Eine Koronarangiographie zeigte nur Koronarsklerose. Anamnestisch gab es keine Hinweise auf Substanzmissbrauch. Er verneint jemals eine Chemo- oder Immuntherapie erhalten zu habe. ANA, ANCA, dsDNA-AK und ein ENA-AK Screen fielen negativ aus. Serum- und Harnelektrophorese waren ebenfalls negativ. Im weiteren stationären Verlauf zeigte der Patient auch eine nsVT ohne hämodynam. Relevanz, sodass mit einem niedrig dosierten Beta-Blocker begonnen wurde.

**Resultate:** Herz-MRT Hinweise auf Ödem/Entzündung in den T2 gewichteten Sequenzen und das LGE-Muster erlauben eine Reihe von Differentialdiagnosen. Wobei eine kardiale Sarkoidose in Betracht kommt, bei Fehlen einer systemischen Ausprägung (pulmonalen oder nodalen Granulomnachweis) wäre diese eine isolierte Form. Aufgrund des semi-zirkulären LGE-Musters ist, auch aufgrund der Familienamnese, eine Arrhythmogene Kardiomyopathie als wahrscheinlicher eingeschätzt. FDG PET CT Ausgeprägter FDG uptake im LV-Myokard. Dieses homogen und den ganzen LV betreffend. Kein „patchy" oder „septales" Muster wie bei Sarkoidose. A. e. inkomplette Suppression. Voltage guided Endomyokardbiopsie Im voltage map zeigen sich low-voltage areas im RV-Septum, etwas weniger als erfahrungsgemäß bei kardialer Sarkoidose. Histologie Einzelne lymphozyten ohne Nachweis von Granulomen. Keine Riesenzellen, keine eosinophile Myokarditis, keine Nekrosen. Keine HCM oder DCM typische Veränderungen. Genetik Nachweis einer pathogenen (TNNT2, c.304C>T) Mutation im Exon 10 des Troponin T Gen. Am häufigsten im Kontext von HCM beschrieben. Interpretation Beim vorliegenden MRT-Muster sind die diagnostischen „Padua"-Kriterien der Arrhythmogenen (Links-)ventrikulären Kardiomyopathie erfüllt. Die ESC bezeichnet die Entität in den 2023 CMP guidlines als „hypokinetic non-dilated cardiomypathy with pathogenic TNNT2 mutation".

**Schlussfolgerungen:** Dieser Fall unterstreicht die Bedeutung der multimodalen nicht-invasiven Bildgebung bei der Abklärung eines AV-Blocks III°. Eine positive Familienanamnese und eine reduzierte LVEF stellen hierbei wichtige „Red Flags" dar. Keine einzelne diagnostische Methode (Genetik, Endomyokardbiopsie oder kardiale MRT) war für sich allein ausreichend zur Diagnosesicherung. Erst die integrative und sequenzielle Anwendung der diagnostischen Modalitäten ermöglichte die definitive Diagnose.

### Literatur

1. ACC/AHA/HRS Guideline on the Evaluation and. Management. 2018;. of Patients With Bradycardia and Cardiac Conduction Delay.

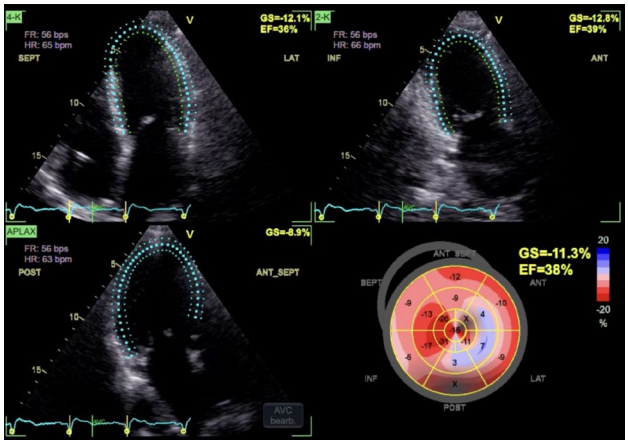


**Abb. 1 | 9-4** TTE mit GL-Strain

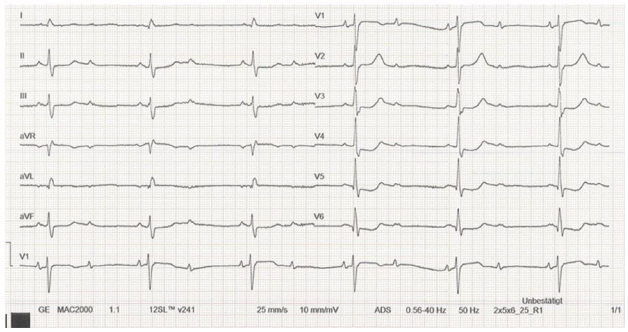


**Abb. 2 | 9-4** EKG bei Aufnahme

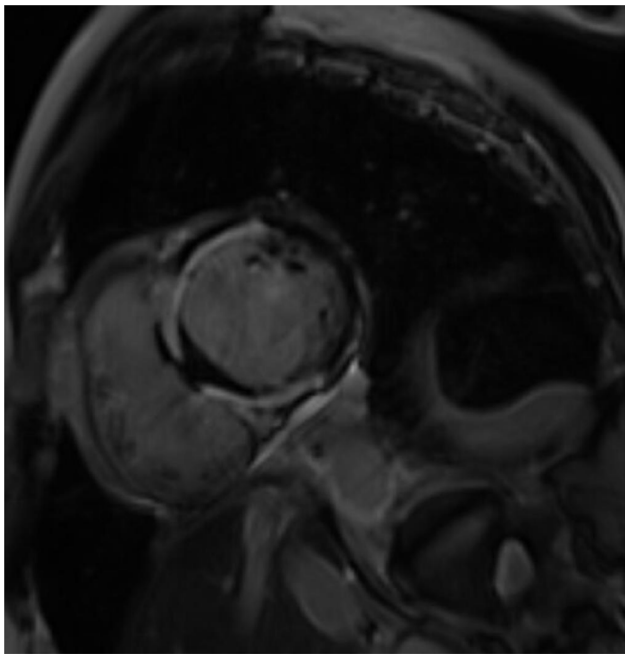

**Abb. 3 | 9-4** Darstellung des teils transmuralen, teils subepikardialen und (weiter anterior) subendokardialen LGE, teils zirkulär

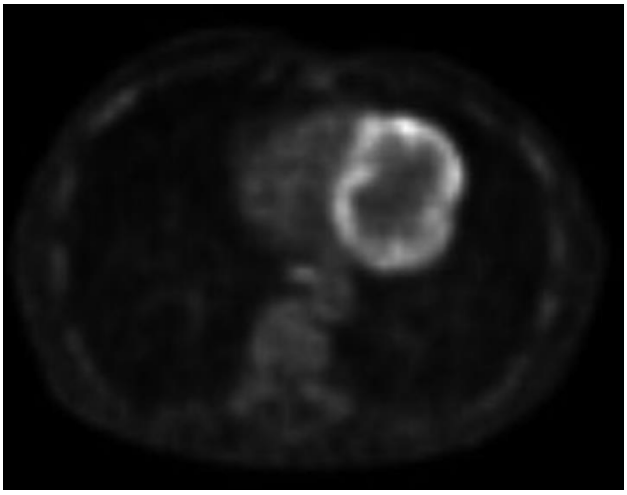

**Abb. 4 | 9-4** PET-CT mit ausgeprägtem Hypermetabolismus des linksventr. Myokards

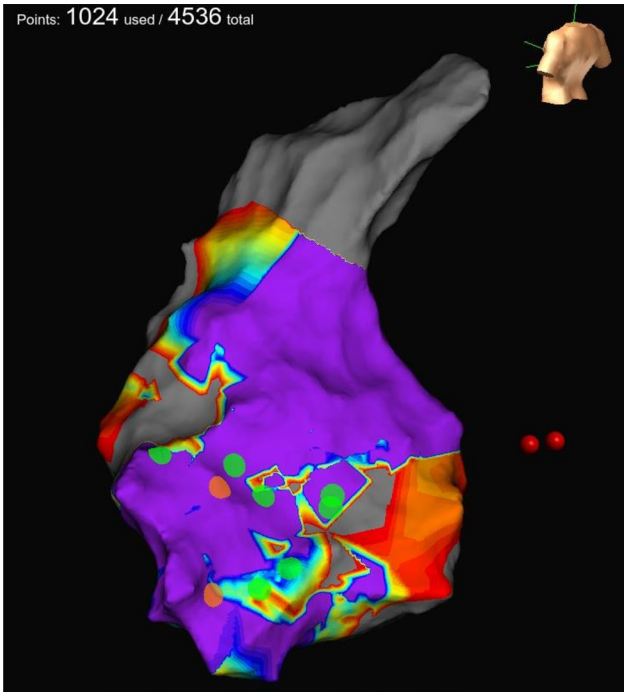


**Abb. 5 | 9-4** high definition voltage map (Abbott, USA) mit low voltage area, vor allem im RV-Septum

## 9-5

### Wenn die PCI an ihre Grenzen stößt: Bailout Fibrinolyse bei Koronaraneurysma

**Schmid D., Wernhart M., Madl-Liebenberger L., Alberer M., Tiefenthaller G., Binder R.**

Klinikum Wels-Grieskirchen, II. Interne, Kardiologie, Intensivmedizin, Wels, Österreich

**Einleitung:** Koronaraneurysmen stellen einen seltenen Befund in der invasiven Koronardiagnostik dar. Als mögliche Ätiologien kommen insbesondere infektiöse sowie autoimmune Erkrankungen in Betracht. Durch ausgeprägte Slow-flow-Phänomene in den peripheren Aneurysmaarealen besteht ein erhöhtes Risiko für intraluminale Thrombenbildung bis hin zum vollständigen Gefäßverschluss. Bei Aneurysmendimensionen, die den Einsatz konventioneller Koronarstents limitieren, kann eine Fibrinolyse als Bailout-Strategie erwogen werden.

**Resultate:** Ein 50-jähriger Patient wurde mit einem inferioren ST-Hebungsinfarkt (STEMI) im kardiogenen Schock sowie komplettem AV-Block III° zugewiesen. Die Koronarangiographie zeigte einen thrombotischen Verschluss eines riesigen Koronaraneurysmas der rechten Koronararterie (RCA). Aufgrund der ausgeprägten Gefäßdilatation war weder eine perkutane Koronarintervention noch eine chirurgische Revaskularisation mittels Bypass als zielführend anzusehen. In dieser Situation wurde eine sekundäre systemische Fibrinolyse durchgeführt. Trotz ini-

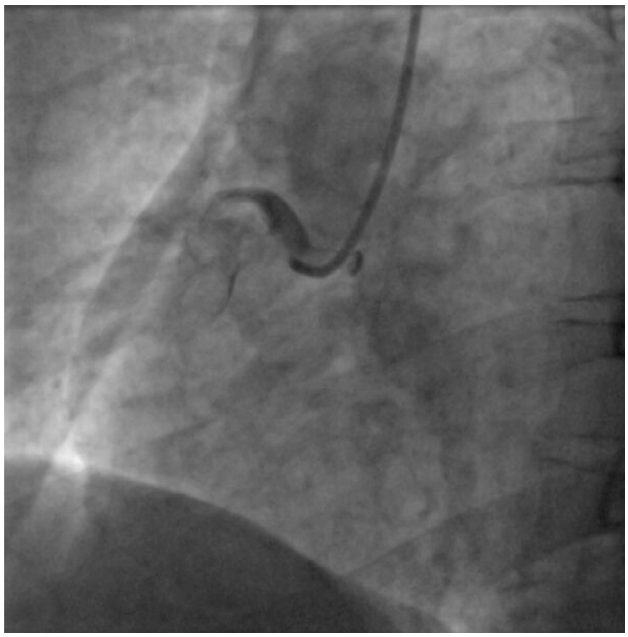

Abb. 1 | 9-5

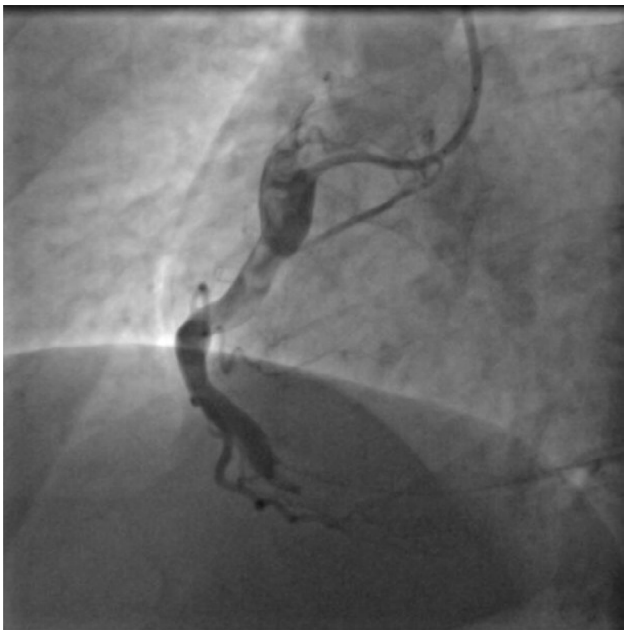

Abb. 3 | 9-5

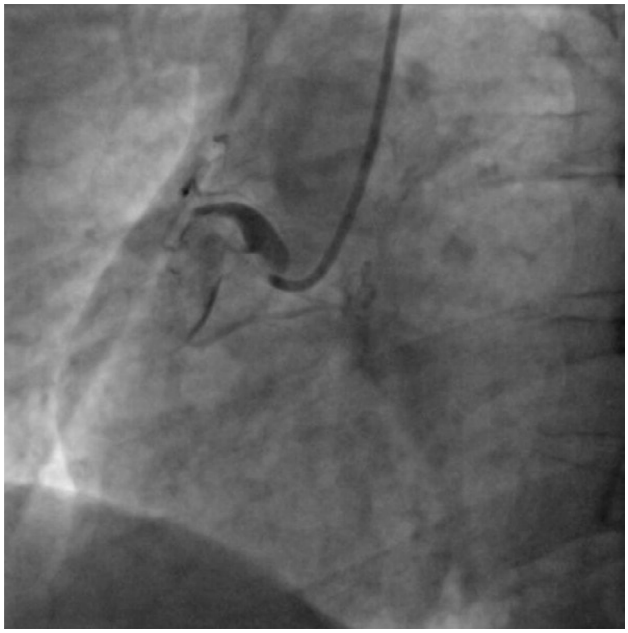

Abb. 2 | 9-5

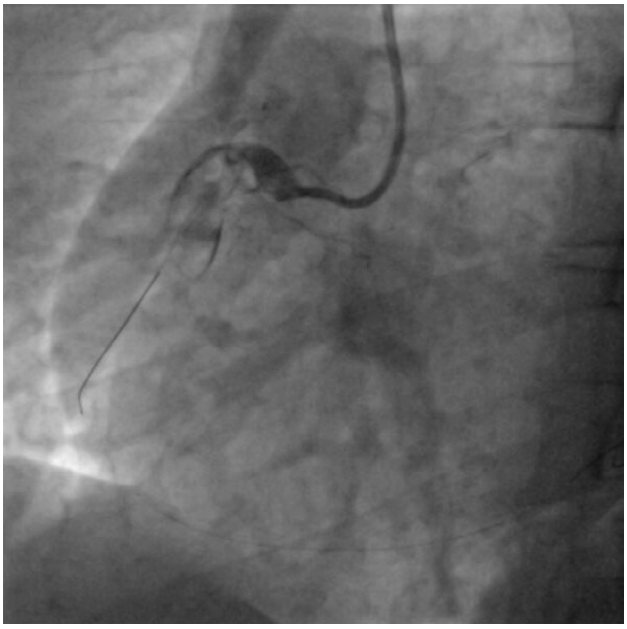

Abb. 4 | 9-5

Abb. 5 | 9-5

tial schwerem kardiogenem Schock und ausgeprägten rhythmologischen Komplikationen bis hin zu einem elektrischen Sturm kam es unter konsequent konservativer Therapie zu einer nahezu vollständigen klinischen Erholung, sodass der Patient wieder uneingeschränkt am Alltagsleben teilnehmen kann.

**Schlussfolgerungen:** In seltenen Fällen begegnen uns im Rahmen eines akuten Koronarsyndroms Läsionen, die mit einer perkutanen oder chirurgischen Revaskularisation nicht beherrschbar sind. Bewährte Therapiekonzepte wie die Fibrinolyse können in ausgewählten Situationen eine therapeutische Alternative darstellen, wenn interventionelle oder operative Verfahren nicht durchführbar sind. Riesige Koronaraneurysmen stellen eine solche besondere Entität dar.

## 9-6

### Mehr als Insuffizienz: der arrhythmogene Mitralklappenprolaps

**Schmid D.[1], Wernhart M.[1], Cojocaru I.[2], Puschmann R.[2], Binder R.[1]**

[1]Klinikum Wels-Grieskirchen, II. Interne, Kardiologie, Intensivmedizin, Wels, Österreich
[2]Herz-, Gefäß- und Thoraxchirurgie, Wels, Österreich

**Einleitung:** Der Mitralklappenprolaps stellt eine häufige Entität in der kardiologischen Praxis dar. In ausgewählten Fällen ist eine operative Rekonstruktion der Mitralklappe erforderlich. Deutlich seltener führt die mechanische Belastung des Klappen- und subvalvulären Apparates zu einer ausgeprägten arrhythmogenen Substratbildung mit dem Auftreten ventrikulärer Arrhythmien.

**Resultate:** Wir berichten über eine 66-jährige Patientin mit progredienter Belastungsdyspnoe und Leistungsabnahme bei schwerer Mitralklappeninsuffizienz infolge eines Bileaflet-Prolaps mit Prädominanz des posterioren Segels. Zusätzlich zeigten sich häufige polymorphe ventrikuläre Extrasystolen sowie nicht-anhaltende ventrikuläre Tachykardien, überwiegend mit Ursprung in der Region des posteromedialen Papillarmuskels.

Abb. 1 | 9-6

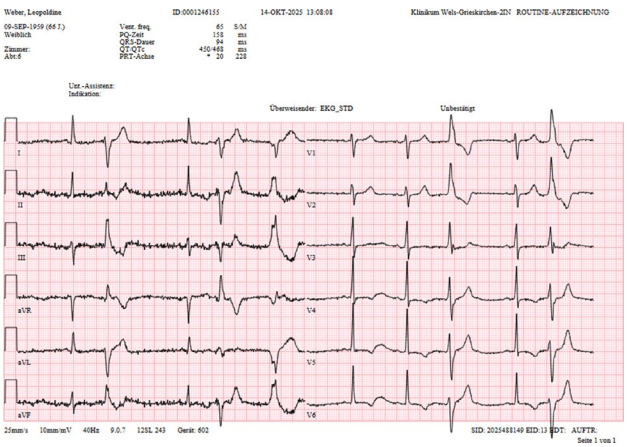

Abb. 2 | 9-6

Korrespondierend hierzu fand sich in der kardialen Magnetresonanztomographie ein Late Gadolinium Enhancement (LGE) im gleichen Areal. Anamnestisch bestanden zudem rezidivierende Synkopen. Vor diesem Hintergrund erfolgte die Ausstattung der Patientin mit einer tragbaren Defibrillatorweste (LifeVest) sowie die Indikationsstellung zur operativen Mitralklappenrekonstruktion. Der operative Eingriff verlief komplikationslos und erfolgreich. Postoperativ zeigte sich eine signifikante Reduktion der ventrikulären Arrhythmielast. Bei fehlenden Hochrisikokriterien konnte auf eine weitere Defibrillatorversorgung verzichtet und die LifeVest abgesetzt werden. Es wurden regelmäßige kardiologische Verlaufskontrollen empfohlen.

**Schlussfolgerungen:** Die operative Sanierung eines Mitralklappenprolaps kann zu einer relevanten Reduktion ventrikulärer Arrhythmien führen, vermutlich durch die Verminderung der mechanischen Zugbelastung auf den papillären und subvalvulären Apparat. Der vorliegende Fall illustriert diesen Zusammenhang in eindrücklicher Weise.

## 9-7

# Nur Muskel oder auch Herz? Myokardiale Beteiligung bei ICI assoziierten Myositiden

**Petric F., Krutisch G., Niessner A.**

Klinik Landstraße, Wien, Österreich

**Einleitung:** Mit der Immuncheckpoint-Inhibitor Therapie wurden „new kids on the block'' geschaffen. Diese greifen in Immunsystem-modulierende Schritte ein, um die durch

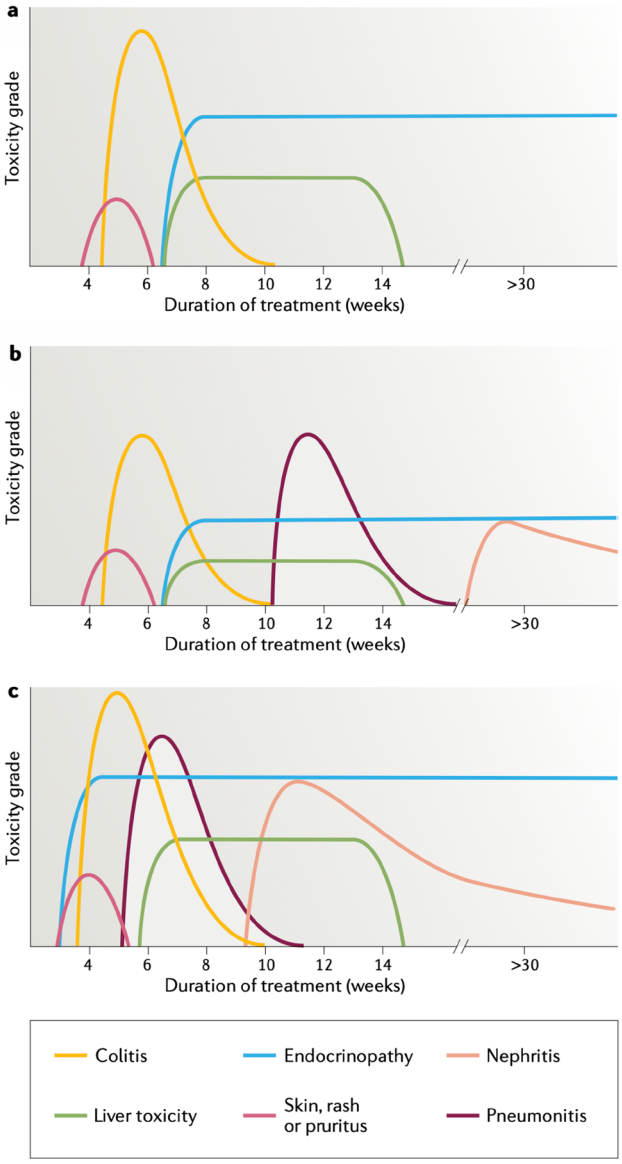


**Abb. 1 | 9-7** Hauptsächliche Nebenwirkungen (irAEs) bei PD-1-AK (a); PDL-1-AK (b) sowie unter Kombinationstherapie mit CTLA-4-AK + PDL-1-AK (c) Quelle: Martins F, Sofiya L, Sykiotis GP, Lamine F, Maillard M, Fraga M, Shabafrouz K, Ribi C, Cairoli A, Guex-Crosier Y, Kuntzer T, Michielin O, Peters S, Coukos G, Spertini F, Thompson JA, Obeid M. Adverse effects of immune- checkpoint inhibitors: epidemiology, management and surveillance. Nat Rev Clin Oncol. 2019 Sep;16(9):563–580. https://doi.org/10.1038/s41571-019-0218-0. PMID: 31092901

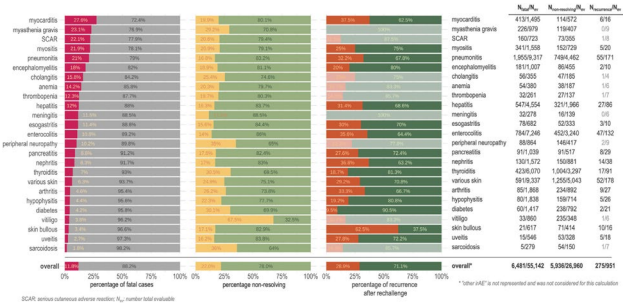

**Abb. 2 | 9-7** Prozentanteil diverser irAEs bezogen auf Letalität (*links*), Ausheilungsrate (*Mitte*) sowie Wiederauftreten (*rechts*) bei Reetablierung der ICI-Therapie Quelle: Gougis P, Jochum F, Abbar B, Dumas E, Bihan K, Lebrun-Vignes B, Moslehi J, Spano JP, Laas E, Hotton J, Reyal F, Hamy AS, Salem JE. Clinical spectrum and evolution of immune-checkpoint inhibitors toxicities over a decade-a worldwide perspective. EClinicalMedicine. 2024 Mar 22;70:102536. https://doi.org/10.1016/j.eclinm.2024.102536. PMID: 38560659; PMCID: PMC10981010

den Tumor gedämpfte autoimmune Antwort wieder zu stärken mit Erfolg in längeren Überlebensraten [1]. Durch die erhöhte Aktivität des Immunsystems zeigen diese jedoch auch toxische Effekte auf unterschiedliste Organsysteme, die es zu erkennen und behandeln gilt [2].

**Methoden:** Ein 63a alter Patient wurde mit der Frage nach myokardialer Beteiligung unter laufender Immuncheckpoint-Inhibitor Therapie vorstellig. Bei dem Patienten bestand ein hochparietal liegendes Melanom Stadium IIIB unter neoadjuvanter Immuncheckpoint-Inhibitor Therapie im Kombinationsschema mit Ipilimumab (CTLA4-AK) + Nivolumab (PD1-AK). Nach erster Gabe kam es zum Aufreten einer ICI-induzierten Myositis mit begleitenden Muskelschmerzen der Extremitäten sowie Diplopie. Daraufhin wurde eine Prednisolonstroßtherapie mit anschließendem Tapering etabliert. Laborchemisch zeigte sich eine zunehmende Auslenkung des Troponin T hs, sodass der Verdacht der myokardialen Beteiligung bestand.

**Resultate:** Der Maximalwert des hsTnT betrug knapp 2850 ng/L (Grenzwert < 14 ng/L). Der Patient verneinte zu jeder Zeit Dyspnoe, Angina pectoris oder thorakale Schmerzen. Unter bereits etablierter Cortisontherapie aufgrund der Myositis zeigte sich das Troponin anschließend bereits rückläufig. Es erfolgte ein kardiales MRT, welches einen unauffälligen Befund zeigte. Ein durchgeführtes Koronar-CT zeigte unauffällige Koronarien (Agatston-Score 0). Zusätzlich erfolgte die Bestimmung von TnI. Dieses zeigte sich initial bei 45,6 ng/L (Grenzwert 45,2 ng/L) und im Verlauf noch fallend auf 26 ng/L.

**Schlussfolgerungen:** Aufgrund der unauffälligen multimodalen Bildgebung, normwertigem TnI sowie fehlender Symptomatik konnte eine myokardiale Beteiligung ausgeschlossen werden. Der Grund der Diskrepanz der Troponinwerte liegt in ihrem Vorkommen. Troponin T hat vier unterschiedliche Isoformen, teils spezifisch für das Herz, teils für die Skelettmuskulatur. Jedoch kann es bei erkrankter Skelettmuskulatur (bspw. Myositis) zu einer Reexpression fetaler TnT Isoformen kommen, die von TnT Assays aufgrund unzureichender Selektivität miterfassst werden, zu deutlichen Erhöhungen dieser führen [3]. Diese TnT Werte zeigten sich auch signifikant erhöht bei PatientInnen mit inflammatorischen Myopathien [4] und es gibt Fälle mit teils deutlich erhöhten TnT Werten (> 1000 ng/L) bei normalen TnI-Werten [5]. Dieser Fall soll die diagnostische Bedeutung der unterschiedlichen Troponin-Biomarker darlegen zur weiteren Differenzierung myokardialer Beteiligung bei bestehenden Myopathien/Myositiden.

## Literatur


1. Gravbrot N, Gilbert-Gard K, Mehta P, Ghotmi Y, Banerjee M, Mazis C, Sundararajan S. Therapeutic Monoclonal Antibodies Targeting Immune Checkpoints for the Treatment of Solid Tumors. Antibodies (Basel). 2019 Oct 21;8(4):51. https://doi.org/10.3390/antib8040051. PMID: 31640266; PMCID:PMC6963985.
2. Martins F, Sofiya L, Sykiotis GP, Lamine F, Maillard M, Fraga M, Shabafrouz K, Ribi C, Cairoli A, Guex-Crosier Y, Kuntzer T, Michielin O, Peters S, Coukos G, Spertini F, Thompson JA, Obeid M. Adverse effects of immune-checkpoint inhibitors: epidemiology, management and surveillance. Nat Rev Clin Oncol. 2019 Sep;16(9):563–580. https://doi.org/10.1038/s41571-019-0218-0. PMID: 31092901
3. Park KC, Gaze DC, Collinson PO, Marber MS. Cardiac troponins: from myocardial infarction to chronic disease. Cardiovasc Res. 2017 Dec 1;113(14):1708–1718. https://doi.org/10.1093/cvr/cvx183. PMID: 29016754; PMCID: PMC5852618.
4. Aggarwal R, Lebiedz-Odrobina D, Sinha A, Manadan A, Case JP. Serum cardiac troponin T, but not troponin I, is elevated in idiopathic inflammatory myopathies. J Rheumatol. 2009;36(12):2711–4. https://doi.org/10.3899/jrheum.090562. Epub 2009 Oct 15. PMID: 19833747.
5. Schmid J, Liesinger L, Birner-Gruenberger R, Stojakovic T, Scharnagl H, Dieplinger B, Asslaber M, Radl R, Beer M, Polacin M, Mair J, Szolar D, Berghold A, Quasthoff S, Binder JS, Rainer PP. Elevated Cardiac Troponin T in Patients With Skeletal Myopathies. J Am Coll Cardiol. 2018 Apr 10;71(14):1540- RESEARCH POSTER PRESENTATIO N DESIG N © 2 01 5 1549. https://doi.org/10.1016/j.jacc.2018.01.070. PMID: 29622161.


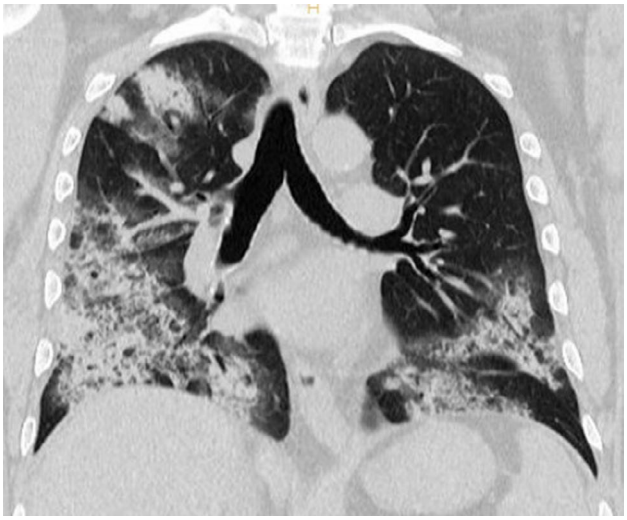

**Abb. 1 | 9-8**

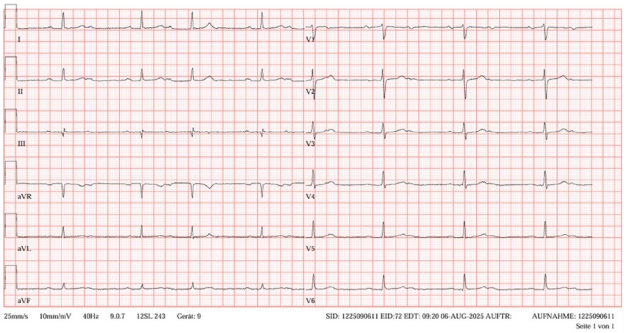

**Abb. 2 | 9-8**

## 9-8

## AV-Block 2. Grades als seltene kardiale Manifestation einer MPO-assoziierten Vaskulitis


**Pöschl C., Strießnig M., Kollias G., Lemes C., Langthaler-Kabicher G., Martinek M.**

Ordensklinikum Elisabethinen, Linz, Österreich


**Einleitung:** AV-Block 2.Grades als seltene kardiale Manifestation einer MPO-assoziierten Vaskulitis Ein 52 Jähriger Patient wird aufgrund einer Synkope und Dyspnoe in unserer Notfallambulanz vorstellig. Zusätzlich gibt er einen Husten seit 10 Tagen an. Vorerkrankungen sind keine bekannt. In der weiteren Abklärung findet sich 1, ein AV Block II mit einer 2:1 Überleitung mit einer Herzfrequenz um 50 Schläge/min bei normaler linksventrikulärer Pumpfunktion 2, eine ausgeprägte normozytäre Anämie mit einem Hb von 7,5 g/dl 3, ein akutes Nierenversagen mit einem Kreatinin von >4 mg/dl 4, eine ausgeprägt rechtsbetont atypisch anmutenden Pneumonie.

**Methoden:** Der Patient wird auf unserer IMCU hospitalisiert. Eine intermittierende High-Flow/CPAP-Therapie ist notwendig, eine antibiotische Abschirmung wird eingeleitet. Ergänzend erfolgt eine Autoimmundiagnostik, wobei sich die MPO-Antikörper hoch positiv zeigen. Bei initial hochgradigem Verdacht auf eine MPO-Vaskulitis (später kann diese biobtisch gesichert werden) erfolgt eine Hochdosis Kortison-Stoßtherapie mit anschließendem Tapering. Weiters erhält der Patient Cyclophosphamid sowie eine intermittierende Plasmapherese, wodurch eine rasche klinische Besserung erzielt werden kann. Nach ca. 6 Tagen kommt es zu einer Rückbildung des AV Blockes 2:1 zu einem Sinusrhythmus.

**Resultate:** Nun stellt sich die Frage hinsichtlich einer Schrittmacher-Indikation. Eine kardiale MRT-Untersuchung zeigt eine Fibrose im Bereich des basalen Septums. In einem durchdurchgeführten Langzeit-EKG findet sich ein durchgehender Sinusrhythmus ohne Pause. Bei 90 %iger Wahrscheinlichkeit einer langfristigen Remission unter Therapie und beschwerdefreiem Patienten entschließt man sich gegen eine Schrittmachertherapie.

**Schlussfolgerungen:** In der Literatur finden sich bislang nur vereinzelte Fallberichte über einen AV-Block im Zusammenhang mit einer MPO-assoziierten Vaskulitis; am ehesten wird eine solche kardiale Manifestation noch im Rahmen einer Granulomatose mit Polyangiitis beschrieben. Laut ESC-Leitlinien besteht ein Schrittmacherindikation bei symptomatischem Patienten mit AV Block 2:1, sofern keine reversible Ursache, wie z. B. eine Myokarditis vorliegt. Für eine Schrittmacherimplantation spricht: 1, In diesem speziellen Fall handelt es sich um eine chronische Erkrankung, die sich unter Therapie zwar gut kontrollieren lässt, die man aber nicht heilen kann. 2, Fibrose im Bereich des basalen Septums Gegen eine Schrittmacherimplantation spricht: 1, AV Block 2:1 mit einer HF um 50, keine weitere Therapie auch während AV Blockierung notwendig gewesen 2, Anhaltender Sinusrhythmus unter Therapie 3, Junger Patient Ein möglicher zu diskutierender Kompromiss bestünde in einer Looprecorder-Implantation.

## 9-9

### Four Valves & One Infection: A Rare Case of Streptococcus bovis Endocarditis

**Gansterer K.[1], Steindl J.[1], Granitz C.[2], Winkler A.[1], Hoppe U.[2], Boxhammer E.[2], Dinges C.[1]**

[1]Universitätsklinik für Herzchirurgie, Salzburg, Austria
[2]Universitätsklinik für Innere Medizin II, Kardiologie und internistische Intensivmedizin, Salzburg, Austria

**Introduction:** Infective endocarditis involving multiple cardiac valves is an uncommon but highly complex clinical condition associated with increased morbidity and mortality. While bi- and tri-valvular endocarditis are well described, true four-valve infective endocarditis remains exceedingly rare. In particular, pulmonary valve involvement is unusual and predominantly reported in intravenous drug users or patients with congenital heart disease. Streptococcus bovis endocarditis is classically linked to gastrointestinal pathology and invasive endoscopic procedures, often presenting with subtle or atypical clinical symptoms. This case highlights the diagnostic and therapeutic challenges of true four-valve endocarditis, including discrepancies between preoperative imaging and intraoperative findings, as well as the surgical management of suspected pulmonary valve involvement.

**Methods:** A 78-year-old male patient was admitted for evaluation of anemia and constitutional symptoms after recent gastroscopy and colonoscopy with polypectomy. Blood cultures revealed Streptococcus bovis bacteremia. Despite a surprisingly mild clinical presentation without overt septic signs, transesophageal echocardiography demonstrated severe infective endocarditis involving all four cardiac valves. Extensive vegetations, valve perforations, and severe regurgitation were present on the aortic, mitral, and tricuspid valves, with additional echogenic structures suspicious for vegetation detected on the pulmonary valve. After interdisciplinary Heart Team discussion, urgent surgical intervention was indicated. Intraoperative findings guided definitive surgical strategy. Antimicrobial therapy consisted of initial intravenous beta-lactam treatment followed by prolonged intravenous ceftriaxone and subsequent oral step-down therapy with amoxicillin in combination with rifampicin, in accordance with current guideline recommendations for Streptococcus bovis infective endocarditis.

**Results:** Surgical exploration confirmed extensive infective destruction of the aortic, mitral, and tricuspid valves, necessitating biological valve replacement of all three valves. In contrast to preoperative echocardiographic findings, no definite macroscopic vegetation or structural destruction was identified on the pulmonary valve. The pulmonary valve was therefore carefully inspected, debrided of suspicious tissue, thoroughly irrigated, and ultimately preserved. Postoperative recovery was complicated by transient atrial arrhythmias, acute kidney injury, and heparin-induced thrombocytopenia type II, all of which resolved under targeted management. Follow-up echocardiography demonstrated excellent prosthetic valve function and preserved pulmonary valve competence. Comprehensive gastrointestinal work-up revealed no evidence of underlying malignancy.

**Conclusion:** This case represents a rare example of true four-valve infective endocarditis caused by Streptococcus bovis with minimal clinical symptomatology. It underscores the potential role of gastrointestinal endoscopy as a source of bacteremia, the limitations of echocardiography in predicting intraoperative findings, and the importance of individualized surgical decision-making. Careful intraoperative assessment allowed preservation of the pulmonary valve after targeted debridement and irrigation, while definitive surgical treatment of the remaining valves was required. Multidisciplinary management and guideline-directed antimicrobial therapy enabled a favorable clinical outcome despite the extraordinary extent of valvular involvement.

# POSTERSITZUNG 10—DIGITAL CARDIOLOGY

## 10-1

### Smartphone-based Digital Screening for Aortic Valve Stenosis: the SMART-VALVE Study

**Pröll S.[1,2], Schreinlechner M.[2], Pavluk D.[2], Kindl B.[2], van der Merwe C.[2], Klimovskis N.[2], Sturm J.[2], Gutwenger T.[2], Haslinger M.[2], Reinstadler S.[2], Dlaska C.[1,2], Bauer A.[2]**

[1]Digital Cardiology Lab, Medical University of Innsbruck, Innsbruck, Austria
[2]University Clinic of Internal Medicine III, Cardiology and Angiology–Medical University of Innsbruck, Innsbruck, Austria

**Introduction:** Aortic stenosis (AS) is the most prevalent valvular heart disease and is associated with substantial morbidity and mortality. Diagnosis relies on resource-intensive imaging modalities that are not universally accessible. Furthermore, AS often progresses asymptomatically, making early detection particularly challenging. Smartphones, which are widely available even among elderly populations, offer a promising platform for low-cost digital screening approaches. The SMART-VALVE study investigates the clinical and practical utility of smartphone-based solutions and examines whether a comprehensive processing pipeline with smartphone-derived biosignals can be established for the early identification of aortic valve disease.

**Methods:** SMART-VALVE is a proof-of-concept study evaluating the feasibility of smartphone-based biosignal acquisition for heart valve assessment. A custom-developed mobile application records acoustic and motion-related signals using

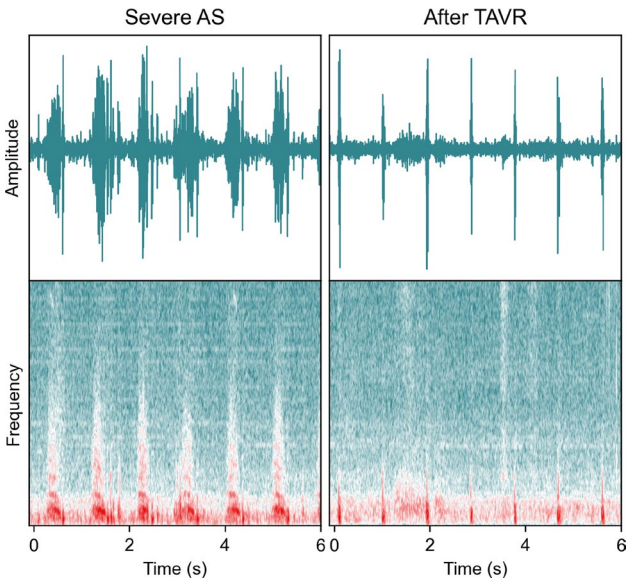


**Fig. 1 | 10-1** Smartphone-based auscultation before and after TAVR

the built-in microphone, accelerometer, and gyroscope of conventional smartphones. The development cohort comprises 150 patients with moderate-to-severe AS and 150 matched controls without AS. For all participants, echocardiography serves as the gold standard. Signal preprocessing, feature extraction, and machine learning-based classification and risk estimation models are optimized in the development phase. Validation is planned in a separate cohort of 200 additional participants.

**Results:** To date, more than 300 participants with concomitant echocardiographic assessment have been enrolled, and corresponding smartphone-based biosignals have been successfully recorded. Preliminary analyses demonstrate the feasibility of detecting individual cardiac cycles and heart sound components from motion-derived signals. Smartphone-based auscultation using the built-in microphone without external hardware is feasible in selected cases but remains susceptible to motion artifacts and user-dependent variability. These findings support the potential for identifying clinically relevant digital biomarkers for AS screening and demonstrate the technical feasibility of establishing a smartphone-based biosignal processing pipeline.

**Conclusion:** The SMART-VALVE study represents an innovative approach to evaluating the feasibility and practical benefit of non-invasive, smartphone-based screening for aortic valve disease and the development of an end-to-end digital biosignal pipeline. Given the widespread availability of mobile devices, this technology has the potential to enable low-cost digital screening strategies for early detection of AS in broad and underserved populations.

## 10-2

### Customizable ECG image generation for deep learning-based ECG digitization

**Pröll S.[1,2], Nicolson A.[1,2], Lunelli R.[1,2], Gruber N.[1,2], Kaser A.[2], Fischer P.[2], Sandor A.[2], Reinstadler S.[2], Bauer A.[2], Dlaska C.[1,2]**

[1]Digital Cardiology Lab, Medical University of Innsbruck, Innsbruck, Austria
[2]University Clinic of Internal Medicine III, Cardiology and Angiology–Medical University of Innsbruck, Innsbruck, Austria

**Introduction:** Extracting waveforms from electrocardiography (ECG) printouts remains a difficult task even today. A recent challenge organized by PhysioNet highlights the need for practical solutions which could give access to billions of ECGs globally stored in image formats. A key limitation of the PhysioNet challenge [1] is its focus on a single fixed layout (3×4 matrix), which does not reflect the variety encountered across devices and health care systems.

**Methods:** To account for variations in ECG layouts and styles, we develop an ECG paper synthesis tool that is capable of generating different layouts (3×4, 6×2, 12×1, optional rhythm strips) with random positioning and styling of visual elements. High-fidelity segmentation masks for each ECG trace are generated. Compared to an ECG image synthesis tool found in literature [2], our method produces more variability and segmentation masks are of better quality. We use this tool to create random images and masks on-the-fly while training a 2D U-Net to segment each pixel into background, 12 leads and rhythm. Post-processing is applied on the segmentation output to extract the 12-lead ECG time-series.

**Results:** Trained on augmented synthetic images, the resulting pipeline is evaluated on internal, real-world ECG images in two ways. First, for a set of 5011 images, extracted signals are visually overlaid with the original image and the signal quality is judged independently by three team members. Through majority voting, we find the quality to be "good but some errors" or "excellent" in 92.9% of cases, while only 2.4% are "bad" extractions (remaining 4.7% are "invalid" or inconclusive images). Second, a subset of 960 high-quality digital PDFs with available ground-truth signals are quantitatively evaluated. We obtain a median signal to noise ratio (SNR) of 41.2 dB (IQR: 34.4 dB). Finally, we apply the extraction pipeline on external test images from the Kaggle challenge "PhysioNet—Digitization of ECG Images" and achieve a SNR of 11.5 dB.

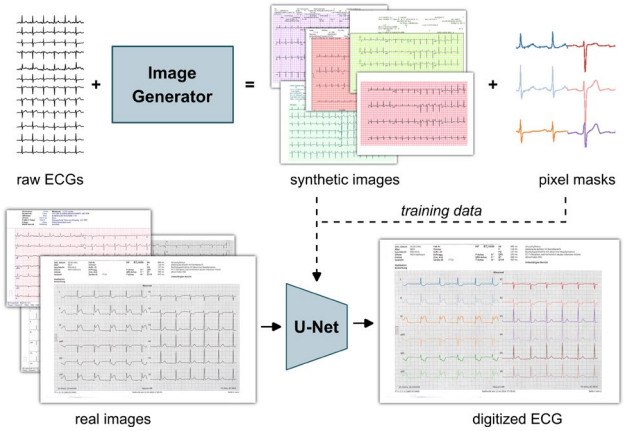


**Fig. 1 | 10-2** Overview: Synthetic images and segmentation masks are used to train a U-Net model which is then applied on real-world data to extract ECG traces

**Conclusion:** The presented workflow allows development of ECG digitization algorithms using fully synthetic data. An extension to other biosignals is feasible with only minor modifications. The derived pipeline achieves qualitatively good ECGs signals for a majority of images. The high SNR highlights strong model performance, paving the way for large-scale biosignal data access from paper-based ECGs.

### References

1. Reyna MA. Deepanshi, Weigle J, Koscova Z, Campbell K, Seyedi S, Elola A, Bahrami Rad A, Shah AJ, Bhatia NK, Clifford GD, Sameni R. Digitization and Classification of ECG Images: The George B. Moody PhysioNet Challenge. Comput Cardiol. 2024;2024(51):1–4.
2. Shivashankara KK, Deepanshi, Mehri Shervedani A, Clifford GD, Reyna MA, Sameni R. ECG-Image-Kit: a synthetic image generation toolbox to facilitate deep learning-based electrocardiogram digitization. Physiological Measurement 2024;45(5):055019. https://doi.org/10.1088/1361-6579/ad4954

## 10-3

### BenchECG and xECG: a benchmark and baseline for ECG foundation models

**Lunelli R.[1], Nicolson A.[1], Reinstadler S.[2], Pröll S.[1], Bauer A.[2], Dlaska C.[1]**

[1]Digital Cardiology Lab, University Clinic of Internal Medicine III, Medical University of Innsbruck, Innsbruck, Austria
[2]University Clinic of Internal Medicine III, Cardiology and Angiology, Medical University Innsbruck, Innsbruck, Austria

**Introduction:** Electrocardiograms (ECGs) are a widely used, inexpensive and standardized modality to assess cardiac functionality. There are approximately 20 million publicly available ECGs but, given the high cost of expert annotations, many have incomplete or unavailable labels. Nevertheless, this data landscape remains highly valuable for the development of self-supervised foundation models that can learn abstract representations without the need for labels. Despite this opportunity, a critical challenge persists in the lack of consistent evaluation: prior work often relies on narrow task selections and inconsistent datasets, making meaningful comparisons of foundation models difficult.

**Methods:** With this work we address this problem by proposing BenchECG, a standardized benchmark comprising a comprehensive suite of publicly available ECG datasets and versatile tasks. These tasks span (1) different signal characteristics (different number of leads and varying signal length), (2) dataset characteristics (clinically different cohorts and geographical diversity) and (3) task characteristics (classification, segmentation, regression, detection and survival analysis tasks). We also propose xECG, a novel recurrent architecture trained in a self-supervised manner on approximately 8 million ECGs.

**Results:** xECG outperformed previous state-of-the art publicly available foundational models, performing strongly on all datasets and tasks. Notably, xECG achieved the highest performance on the sleep apnea task (0.93 AUC). Overall, xECG had an average rank of 1.5 across BenchECG tasks and a BenchECG score of 0.87, whereas the second best model, ST-MEM, had an average rank of 2.6 and a BenchECG score of 0.82.

**Conclusion:** BenchECG enables systematic and rigorous comparison of ECG foundation models, aiming to accelerate progress in ECG representation learning. xECG achieved superior performance over earlier approaches, defining a new state-of-the-art baseline for future ECG foundation models. Moreover, the ease of use of this model will be beneficial in developing new solutions for more specific clinical tasks.

## 10-4

## Artificial Intelligence–Based CT Volumetry of Skeletal Muscle Predicts Long-Term Mortality After Transcatheter Aortic Valve Implantation

**Knapitsch C.[1], Schörghofer N.[1], Clodi N.[2,1], Preuss L.[2], Scharinger B.[1], Hammerer M.[2], Hoppe U.[2], Hergan K.[3], Boxhammer E.[2]**

[1]Universitätsklinik für Radiologie, Salzburg, Austria
[2]Universitätsklinik für Innere Medizin II, Kardiologie und internistische Intensivmedizin, Salzburg, Austria
[3]Universitätsklinik für Radiologie, Universitätsklinikum Salzburg, Salzburg, Austria

**Introduction:** Frailty and sarcopenia are increasingly recognized as important determinants of outcomes in patients undergoing transcatheter aortic valve implantation (TAVI). However, conventional sarcopenia assessment relies on single-slice muscle measurements and does not capture total muscle burden. Artificial intelligence (AI)–based CT segmentation allows automated volumetric quantification of skeletal muscle and intramuscular fat, enabling comprehensive assessment of muscle quantity and quality. We aimed to investigate the prognostic value of AI-derived skeletal muscle volumetry and intramuscular fat in patients undergoing TAVI.

**Methods:** In this retrospective cohort study, preprocedural computed tomography scans of patients undergoing TAVI were analyzed using an AI-based automated whole-body segmen-

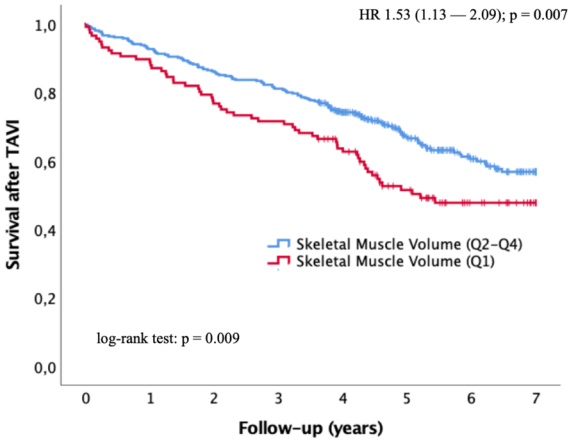


| No. at Risk | | | | | | | | |
|---|---|---|---|---|---|---|---|---|
| Q1 | 116 | 103 | 89 | 83 | 68 | 45 | 25 | 13 |
| Q2-Q4 | 354 | 328 | 304 | 287 | 232 | 144 | 90 | 47 |
| Overall | 470 | 431 | 393 | 370 | 300 | 189 | 115 | 60 |

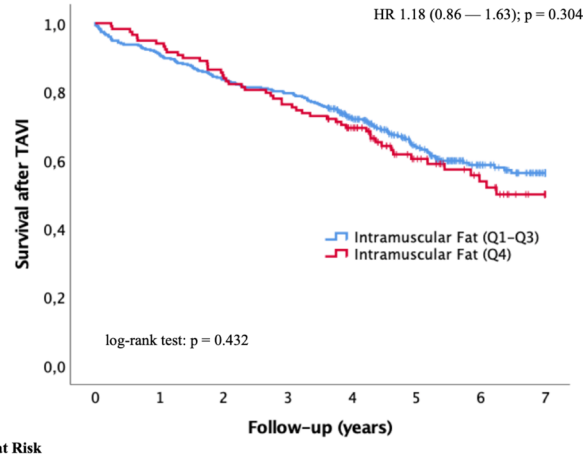


| No. at Risk | | | | | | | | |
|---|---|---|---|---|---|---|---|---|
| Q1 | 118 | 111 | 99 | 90 | 74 | 44 | 30 | 17 |
| Q2-Q4 | 352 | 320 | 294 | 280 | 226 | 145 | 85 | 43 |
| Overall | 470 | 431 | 393 | 370 | 300 | 189 | 115 | 60 |

**Fig. 1 | 10-4** Kaplan Meier Curves

| Variable | Hazard Ratio | 95% CI | p-value |
|---|---|---|---|
| SMV (Q1) | 1.626 | 1.124–2.352 | 0.010 |
| IMF (Q4) | 1.380 | 0.902–2.111 | 0.140 |
| Male sex | 1.261 | 0.823–1.933 | 0.286 |
| Age (per year) | 1.040 | 1.005–1.077 | 0.025 |
| NYHA class | 0.938 | 0.770–1.142 | 0.527 |
| SVi (per ml/m²) | 0.999 | 0.987–1.010 | 0.820 |
| BMI (per kg/m²) | 0.942 | 0.884–1.004 | 0.064 |
| BSA (per m²) | 3.226 | 0.828–12.579 | 0.091 |
| Creatinine (per mg/dl) | 0.996 | 0.975–1.018 | 0.738 |
| Hb (per g/dl) | 0.955 | 0.874–1.043 | 0.303 |
| sPAP (per mmHg) | 1.004 | 0.994–1.014 | 0.456 |

**Fig. 2 | 10-4** Multivariable Cox Regression Including Skeletal Muscle Volume and Intramuscular Fat

tation (TotalSegmentator, Basel, Switzerland) to quantify total skeletal muscle volume (SMV) and intramuscular fat (IMF). Patients were stratified according to sex-specific quartiles. Sarcopenia was defined as the lowest quartile of skeletal muscle volume (SMV Q1), while muscle quality was assessed by the highest quartile of intramuscular fat (IMF Q4). The primary endpoint was all-cause mortality during long-term follow-up.

**Results:** A total of 470 patients with available CT volumetry were included. Patients with low skeletal muscle volume (SMV Q1) were significantly older and had lower body mass index and body surface area, reflecting a frailty phenotype. Kaplan–Meier analysis demonstrated significantly higher mortality in patients with the lowest quartile of SMV compared with higher quartiles (log-rank $p=0.009$). In multivariable Cox regression analysis, low SMV remained independently associated with mortality (HR 1.589, 95% CI 1.101–2.294, $p=0.013$). In contrast, highest quartile of IMF was not significantly associated with mortality (HR 1.326, 95% CI 0.865–2.035, $p=0.196$). When both parameters were included in a combined model, SMV remained an independent predictor of mortality (HR 1.626, 95% CI 1.124–2.352, $p=0.010$), whereas IMF did not.

**Conclusion:** AI-based CT volumetry enables automated quantification of skeletal muscle in patients undergoing TAVI and identifies sarcopenia as an independent predictor of long-term mortality. In contrast to muscle quality parameters such as intramuscular fat, muscle quantity appears to be the dominant prognostic determinant. AI-driven body composition analysis may represent a novel imaging biomarker for risk stratification in TAVI patients.

## References

1. Wasserthal, J., Breit, H.C., Meyer, M.T., Pradella, M., Hinck, D., Sauter, A.W., Heye, T., Boll, D.T., Cyriac, J., Yang, S., Bach, M., & Segeroth, M. (2023). TotalSegmentator: Robust Segmentation of 104 Anatomic Structures in CT Images. Radiology. Artificial intelligence, 5(5), e230024. https://doi.org/10.1148/ryai.230024

# 10-5

## Diagnostische Leistungsfähigkeit von KI-Modellen in der post-Reanimations EKG-Interpretation

**Groche M.[1,2], Silwanis C.[1,2], Maier J.[1,2,3], Huss M.[1,2], Neunteufel A.[1,2], Eder J.[1,2], Lamm L.[1,2], Bamberger M.[1,2], Rechberger S.[1,2], Nahler A.[1,1], Fellner A.[1,2], Steinwender C.[1,2,3], Lambert T.[1,2]**

[1]Kepler Universitätsklinikum Linz, Klinik für Kardiologie und Internistische Intensivmedizin, Medizinische Fakultät, Johannes Kepler Universität Linz, Österreich, Linz, Österreich
[2]Johannes Kepler Universität Linz, Medizinische Fakultät, Altenberger Straße 69, 4040 Linz, Austria, Linz, Österreich
[3]Klinisches Forschungsinstitut für kardiovaskuläre und metabolische Erkrankungen, Medizinische Fakultät, Johannes Kepler Universität, Altenberger Straße 69, 4040 Linz, Österreich, Linz, Österreich

**Einleitung:** Der plötzliche Herzstillstand zählt zu den häufigsten Todesursachen in Europa, wobei das akute Koronarsyndrom (ACS) eine der Hauptursachen darstellt. Die frühzeitige Identifikation von Patienten mit ST-Hebungs-Myokardinfarkt (STEMI) ist essenziell, jedoch können auch in Abwesenheit von ST-Hebungen spezifische EKG-Muster eines okklusiven Myokardinfarkts (OMI) vorliegen. Nach Wiedererlangen eines Spontankreislaufs (ROSC) können metabolische Störungen sowie Reperfusionsschäden und Katecholamine das EKG zusätzlich verfälschen. Dies führt häufig zu transienten ST-Segment-Veränderungen oder unspezifischen Repolarisations- oder Leitungsstörungen, welche eine akute Koronarokklusion imitieren oder maskieren können. Die daraus resultierende diagnostische Unsicherheit kann lebensrettende Maßnahmen, wie eine akute Koronarintervention oder Bypass-Operationen, verzögern. Künstliche Intelligenz (KI) besitzt das Potenzial diese diagnostischen Limitationen zu adressieren. Während die Leistungsfähigkeit von Large Language Models (LLM) in der Textverarbeitung bestätigt ist, ist ihre Eignung zur EKG-Interpretation nur unzureichend untersucht. Parallel haben speziell für die OMI-Erkennung entwickelte Deep Neural Networks (DNN) eine mit menschlichen Experten vergleichbare diagnostische Performance gezeigt. Ziel dieser Studie war, die diagnostische Leistungsfähigkeit von KI-Modellen in der EKG-Interpretation nach kardiopulmonaler Reanimation (CPR) zu untersuchen.

**Methoden:** Für diese Studie wurden Patienten mit ROSC nach durchgeführter CPR analysiert, die von 2020 bis einschließlich 2023 auf der internistischen Intensivstation behandelt wurden. Eingeschlossen wurden Erwachsene mit vorhandenem post-ROSC EKG sowie durchgeführter Koronarangiografie. Für die Analyse wurde das erste nach ROSC angefertigte EKG verwendet. Die EKGs wurden verblindet durch vier Diagnosemethoden ausgewertet: zwei Fachärzte für Kardiologie (FA), eine validierte KI-Lösung zur OMI-Erkennung (Queen of Hearts [QoH]; V. 3.0.1), und zwei KI-gestützte, promptbasierte Chatbots (ChatGPT-4-Turbo und EKG-Analyst). Die Bewertung erfolgte hinsichtlich des Vorliegens eines OMI (ja/nein). Die FA bewerteten zunächst die EKGs unabhängig, anschließend erzielten sie einen Konsens. QoH wurde über die mobile Anwendung PMCardio® eingesetzt, der jeweils höchste OMI-Wahrscheinlichkeitswert pro EKG wurde dokumentiert. Den Chatbots wurden strukturierte Informationen zu den Themen ACS, Nachsorge nach CPR, STEMI und OMI bereitgestellt. Eine standardisierte Eingabeaufforderung mit explizit definiertem Endpunkt wurde für alle Auswertungen verwendet. Die Koronarangiografien wurden von zwei interventionellen Kardiologen beurteilt und anhand des Stenosegrades und der Höhe der Troponinauslenkung in OMI und Nicht-OMI eingeteilt.

**Resultate:** Es wurden 97 Patienten mit post-ROSC EKG und korrespondierender Koronarangiografie eingeschlossen. In 61 Fällen (62,9 %) lag ein OMI vor. Korrekt identifiziert wurden 47 OMI durch FA ($p<0{,}008$), 37 durch QoH ($p<0{,}001$), 60 durch ChatGPT ($p=$ NS) und 60 durch EKG-Analyst ($p=$ NS). ChatGPT und EKG-Analyst erzielten eine Sensitivität von je 98,4 % bei jedoch geringer Spezifität (2,8 % und 0 %) und einem positiven prädiktiven Wert (PPV) von 63,1 % bzw. 62,5 %. Die FA zeigten eine Sensitivität von 77,1 % und eine Spezifität von 50 %, bei einem PPV von 72,3 % und NPV von 56,3 %. QoH zeigte die höchste Spezifität (77,8 %) und den höchsten PPV (82,2 %), bei niedrigerer Sensitivität (60,7 %) und NPV (53,9 %). Für die diagnostische Performance zeigten die AUROC-Werte die besten Ergebnisse für QoH (0.745; [95 % CI 0.647–0.843]), gefolgt von FA (0.635; [95 % CI 0.515–0.755]). Für ChatGPT lag die AUROC bei 0.495 [95 %CI 0.376–0.614] und für EKG-Analyst bei 0.626 [95 %CI 0.508–0.743].

**Schlussfolgerungen:** Die Interpretation von EKGs nach CPR ist eine komplexe Aufgabe, die unter erheblichem Zeitdruck und oft mit unvollständigen Informationen durchgeführt wird. Unter den untersuchten Methoden zeigten FA und QoH die ausgewogenste diagnostische Leistungsfähigkeit zur Identifizierung eines OMI bei Patienten mit ROSC. ChatGPT und

EKG-Analyst konnten keine relevante diagnostische Genauigkeit vorweisen. Domänenspezifische Anwendungen wie QoH können im Rahmen der EKG-Interpretation nach ROSC eine wertvolle diagnostische Ergänzung darstellen, welche Expertenurteile ergänzt und die klinische Entscheidungsfindung unterstützen kann. Angesichts der rasanten Entwicklung im Bereich KI könnten zukünftige Versionen von LLM an diagnostischer Zuverlässigkeit gewinnen und eine Neubewertung ihrer klinischen Einsetzbarkeit rechtfertigen. Dennoch bleibt die menschliche Interpretation der Goldstandard, insbesondere wenn sie durch klinische Intuition und kontextuelles Urteilsvermögen unterstützt wird.

## 10-6

### Smartwatch-based blood pressure measurement: a head to head comparison to the gold standard in cardiovascular patients

**Hofer F., Pavluk D., Kindl B., Tessadri K., Dolejsi T., Schreinlechner M., Bauer A.**

Department of Internal Medicine III, Cardiology and Angiology, Medical University Innsbruck, Innsbruck, Austria

**Introduction:** Smartwatch-based blood pressure (BP) measurement has emerged as a promising tool for continuous and cuffless cardiovascular monitoring. However, evidence comparing different smartwatch technologies against established clinical standards in real-world cardiovascular patients remains limited. This study aimed to perform a head-to-head comparison of two commercially available smartwatches: the Huawei Watch D and the Samsung Galaxy Watch 6, for non-invasive BP measurement, using a validated upper-arm oscillometric blood pressure device as the clinical gold standard.

**Methods:** In this prospective observational study, adult cardiovascular patients receiving either outpatient or inpatient care at a tertiary care cardiology department were enrolled. Blood pressure measurements were obtained using the Huawei Watch D and the Samsung Galaxy Watch 6 according to the manufacturers' instructions. Reference measurements were performed using a clinically validated upper-arm oscillometric blood pressure device routinely used in daily clinical practice. All measurements and device comparisons were conducted in accordance with the applicable international standards for non-invasive blood pressure measurement (ISO guidelines). Measurements were performed under standardized resting conditions, and smartwatch-derived systolic and diastolic blood pressure values were compared with temporally corresponding reference measurements using appropriate statistical methods.

**Results:** A total of 80 patients were included in the analysis. The mean age was 67 ± 11 years, and 60% were male. Comparison of smartwatch-based blood pressure measurements with the reference device showed the following results: for diastolic blood pressure, the Samsung Galaxy Watch 6 demonstrated a bias of 0.3 mmHg with a standard deviation (SD) of 4.4 mmHg and limits of agreement (LoA) ranging from –8.3 to 9.0 mmHg, while the Huawei Watch D showed a bias of 3.5 mmHg, an SD of 8.3 mmHg, and LoA from –12.8 to 19.8 mmHg. For systolic blood pressure, the Samsung Galaxy Watch 6 showed a bias of 2.2 mmHg (SD 7.1 mmHg, LoA –11.7 to 16.1 mmHg), whereas the Huawei Watch D demonstrated a bias of 1.7 mmHg with an SD of 13.1 mmHg and LoA ranging from –23.9 to 27.3 mmHg.

**Conclusion:** In this head-to-head comparison, smartwatch-based blood pressure measurements obtained with the Huawei Watch D and the Samsung Galaxy Watch 6 demonstrated insufficient agreement with a validated upper-arm oscillometric reference device in cardiovascular patients when assessed according to applicable ISO validation criteria. Based on these findings, smartwatch-based blood pressure measurement cannot currently be considered equivalent to standard upper-arm measurements for clinical use in cardiovascular patients. Further dedicated validation studies are required to define the potential clinical role and appropriate use cases of smartwatch-based blood pressure measurement in this patient population.

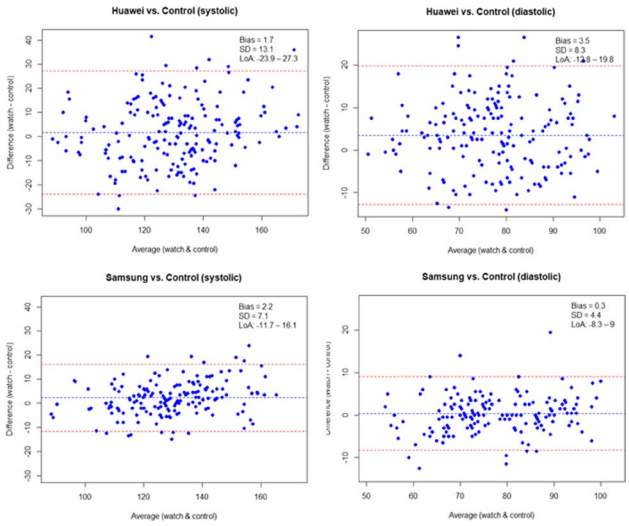


Fig. 1 | 10-6

## 10-7

### Künstliche Intelligenz in der Kardiologie—aktuelle und künftige Entwicklungen

**Siekmeier R.[1], Moissl-Blanke A.[2], März W.[3]**

[1]Drug Regulatory Affairs, Pharmazeutisches Institut der Universität Bonn, Bonn, Deutschland
[2]Department of Medicine I (Cardiology, Hemostaseology, Medical Intensive Care), Medical Faculty Mannheim, Heidelberg University, Mannheim, Deutschland
[3]Synlab Akademie, Mannheim, Deutschland

**Einleitung:** In den letzten Jahren zeigte sich eine rasche Zunahme der Anwendungen der künstlichen Intelligenz (KI) in den verschiedensten Bereichen des allgemeinen Lebens. Dies zeigt sich auch in der klinischen Medizin, in der KI zunehmend Anwendung findet und wo sich deren transformative Bedeutung ebenfalls abzeichnet. So hat die Anzahl der von der US Food and Drug Administration (FDA) zugelassenen Anwendungen in der letzten Dekade exponentiell zugenommen und zwischenzeitlich die Zahl 1357 erreicht (Stand März 2026). Anwendungsgebiete umfassen dabei Bildgebung und Diagnostik, Arzneimittelentwicklung, personalisierte Medizin, prädiktive Analytik, Patientenmonitoring, robotische Chirurgie, Epidemiologie, Telemedizin, medizinische Expertensysteme zur Diagnostik und Chatbots für Patienten. Eine in Bedeutung und Anwendungsbreite herausragende Gruppe stellen dabei Anwendungen aus der Kardiologie dar. Ziel dieser Studie war die Analyse der aktuellen Bedeutung von KI in der Kardiologie, deren derzeitigen und möglichen künftigen Anwendungsindikationen und deren regulatorischen Status.

**Methoden:** Es erfolgte eine Recherche zu Anwendungen von KI in der Medizin in Pubmed und Internet unter Fokussierung auf aktuelle Publikationen und das Gebiet der Kardiologie.

**Resultate:** Die häufigsten von der FDA zugelassenen Anwendungen der KI umfassen die Gebiete Radiologie (1039), Kardiologie (130) und Neurologie (61). Die kardiologischen Anwendungen umfassen dabei vor allem solche zur Arrhythmiediagnostik, koronaren Diagnostik, Echokardiographie, Hämodynamik und endovaskulären Diagnostik. Anwendungen zur Arrhythmiediagnostik umfassen meist solche zur Diagnostik von Vorhofflimmern (auch paroxysmal), aber auch solche zur Diagnostik und Telemonitoring von ventrikulären Arrhythmien und zur Verlaufskontrolle nach Ablationstherapie oder Wiederbelebung sowie zur Klassifizierung von Patienten mit hypertrophen Kardiomyopathien verschiedener Genese mit unterschiedlichem Arrhythmierisiko. In ihrer Bedeutung zunehmend sind Anwendungen zur kardialen Bildgebung, meist basierend auf Echokardiographie, aber auch auf Computertomographie, Magnetresonanztomographie und Single Photon Emission Computed Tomography, die u. a. Aussagen zu Herzstruktur, Kardiomyopathien, Ventrikelfunktion, Myokardperfusion und koronaren Kalkablagerungen und z. T. auch eine Abschätzung des Risikos für das Auftreten kardiovaskulärer Ereignisse erlauben. Als eher experimentell sind jedoch bislang Verfahren zur robotisch unterstützten perkutanen Koronarintervention (R-PCI) anzusehen. Weitere Anwendungen erlauben die Diagnostik und Verlaufsbeurteilung (Risiko von Dekompensation und Hospitalisierung) einer Herzinsuffizienz und die Analyse von Herzgeräuschen.

**Schlussfolgerungen:** KI findet in der Kardiologie zunehmend Verwendung. Sie erlaubt die Erfassung und Verarbeitung großer Datenmengen aus verschiedenen Quellen (z. B. Wearables, EKG, bildgebende Verfahren, elektronische Gesundheitsaufzeichnungen) zur ressourcenschonenden Bearbeitung komplexer diagnostischer und therapeutischer Fragestellungen. Zu berücksichtigen sind jedoch ethische Aspekte, Datensicherheit, Patientenautonomie, Eignung und Verknüpfbarkeit der außerhalb kontrollierter Settings mit verschiedenen Systemen gewonnenen Daten und Akzeptanz KI generierter Befunde bei Ärzten und Patienten sowie unterschiedliche Aspekte des Inverkehrbringens (FDA-Approval (meist 510(k) Clearance) in den USA, CE-Kennzeichnung in Europa).

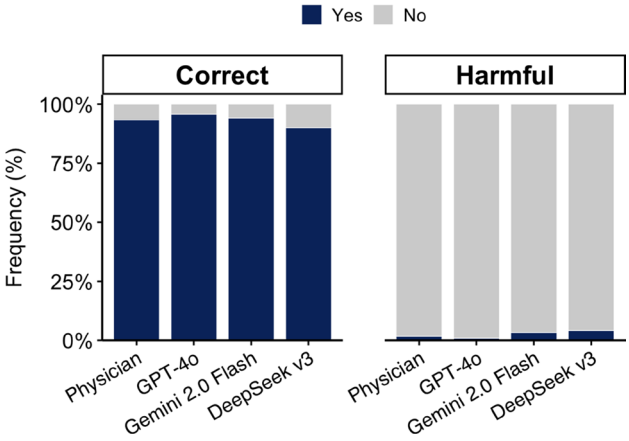


**Fig. 1 | 10-8**

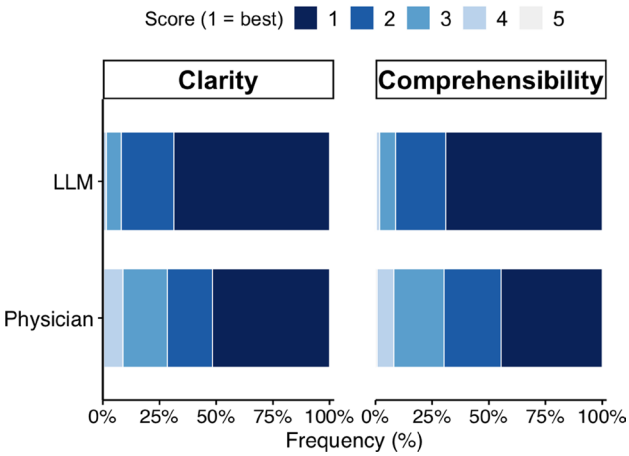


**Fig. 2 | 10-8**

## 10-8

### Evaluating large language models in chronic heart failure—Bridging the Bytes in Heart Failure

**Fugger F.[1], Schütz T.[1], Messner M.[1], Pölzl G.[1], Fischnaller S.[1], Bauer A.[1], Schreier G.[2], Kreiner K.[2], Puelacher C.[1]**

[1]Department of Internal Medicine III, Cardiology & Angiology, Medical University of Innsbruck, Innsbruck, Austria
[2]AIT Austrian Institute for Technology GmbH – Center for Health and Bioresources, Vienna, Austria

**Introduction:** Chronic heart failure (CHF) affects 1–2% of the adult population worldwide and poses a substantial burden on patients and healthcare systems. Improving patient understanding is essential for disease management, yet limited clinical resources often restrict comprehensive education. Large language models (LLMs) may offer scalable, patient-specific information through natural language interaction. However, their safety, appropriateness, and comprehensibility in CHF remain insufficiently evaluated, particularly beyond English-language settings.

**Methods:** This study comprised two subprojects. In Subproject 1, responses to 60 standardized CHF-related patient questions were generated by a cardiologist and multiple LLMs. Answers were independently assessed by two CHF cardiologists for appropriateness and safety. Comparisons across models (GPT-4o, Gemini 2.0 Flash, DeepSeek v3) were performed using Chi-square or Fisher's exact tests as appropriate. In Subproject 2, 100 patients with CHF completed a structured questionnaire assessing digital literacy, technology affinity, and use of digital health tools. Patients additionally rated clarity and comprehensibility of responses provided by the best-performing LLM from Subproject 1 and by a cardiologist, blinded to response origin.

**Results:** Among 100 CHF patients (median age 65.5 years [IQR 56.5–76.5], 29% female), digital literacy (DL) was moderate (median DL score 3.8 [IQR 2.3–4.8], scale 1–7), with intermediate technology affinity (median Austrian technology affinity score 3.6 [IQR 2.7–4.2], scale 1–6). Overall, 68% reported access to a computer and 99% to a mobile phone (smartphone or senior mobile phone). However, regular digital health tool use (27%) and prior AI experience in healthcare (17%) were limited. In Subproject 1, correct response rates across LLMs ranged from 90.0% to 94.9%, while harmful responses were rare (0.0–3.3%). The cardiologist achieved 93.3% correct and 1.7% harmful responses. No statistically significant differences were observed among LLMs or between LLMs and the cardiologist for correctness or harmfulness (all $p > 0.05$). In Subproject 2, LLM-generated responses achieved higher ratings for clarity and comprehensibility compared with cardiologist responses. Distributions differed signif-

icantly between sources for both clarity and comprehensibility (both $p<0.001$), with directional testing favoring LLM responses.

**Conclusion:** LLMs demonstrated high correctness and low harmfulness in CHF-related information, comparable to a physician benchmark. LLM-generated responses were rated better in clarity and comprehensibility by CHF-patients. CHF-patients showed moderate digital literacy, and currently low engagement with digital health tools.

# POSTERSITZUNG 11—HERZCHIRURGIE 3

## 11-1

### PRESAVE Study-validation of graft storage solutions in clinical practice

**Werdenits J.[1,2], Winkler B.[3], Stabernak J.[4], Manville E.[1], Folkmann S.[1], Modi R.[1], Harrer M.[1], Crailsheim I.[1], Gorlitzer M.[3,2], Weiss G.[3], Meinhart J.[3], Aschacher T.[3,2], Grabenwöger M.[3,2]**

[1]Herzchirurgie Klinik Floridsdorf, wien, Austria
[2]Sigmund Freud Universität, Wien, Austria
[3]Herz-Gefässchirurgie Klinik Floridsdorf, Wien, Austria
[4]Klinik Floridsdorf, Wien, Austria

**Introduction:** Damage of the endothelium during graft handling and storage for cardiac surgeries is an important factor contributing to graftfailure and declined long-term patency. Despite already documented evidence of negative effects on human endothelial cell function, Saline still remains the most widely used solution for rinsing and storage of vascular grafts. Therefore, the aim of this study was to assess the effects of three different storage solutions—Natrium chloride (NaCl), Elomel R, and DuraGraft TM—on endothelial integrity using ex vivo and in vitro models.

**Methods:** Human Saphenous vein (HSV) graft segments were collected from 20 patients undergoing aortocoronary bypass surgeries and exposed to the three different preservation solutions. The segments were analyzed histologically and by immunofluorescence using H&E, γ-H2AX, Ki-67, VEGF, and vWF staining. The ex vivo surface morphology of the HSV graft segments was further assessed by scanning electron microscopy (SEM). Additionally, venous endothelial cells (HVEC) were derived from human vein segments, cultured and exposed to the solutions over defined time periods. Standard cell culture medium served as a control.

**Results:** The SEM analysis depicted a trend toward an increase of surface irregularities in NaCl-treated vein segments when compared to Elomel- and DuraGraft-treated segments. The cell culture analysis revealed more distinct results. NaCl-treatment resulted in significant loss of cell numbers when compared to the control at all time points ($p\leq0{,}0062$). In contrast, treatment with Elomel and DuraGraft maintained cell numbers comparable to the control throughout the observation period ($p\leq0{,}05$).

**Conclusion:** The overall results of this study revealed that the storage solutions DuraGraft and Elomel showed good preservation of the endothelial cells and the endothelial barrier, while Saline caused pronounced epithelial damage. These effects were most evident in the cell culture analysis, where the exposure to Saline resulted in extensive reduction of cell numbers. Despite these known shortcomings saline is still widely used in daily clinical practice.

## 11-2

### Clinical Evaluation and Implementation of novel single shot cardioplegia Cardioplexol™

**Winkler B.[1], Gygax E.[2], Folkmann S.[3], Harrer M.[3], Weiss G.[1], Grabenwöger M.[1,4]**

[1]Herz- Gefässchirurgie Klinik Floridsdorf, Wien, Austria
[2]Herzchirurgie Aarau, Aarau, Switzerland
[3]Herzchirurgie Klinik Floridsdorf, wien, Austria
[4]Sigmund Freud Universität, Wien, Austria

**Introduction:** Effective and reliable cardioplegic arrest is essential for optimal myocardial protection during cardiac surgery. Cardioplexol™ is a low-volume (100 mL) single-shot cardioplegic solution designed to simplify cardioplegia delivery while minimizing hemodilution, particularly in minimally invasive extracorporeal circulation (MiECC). Since its introduction, Cardioplexol™ has demonstrated several practical advantages including rapid surgeon-controlled administration, immediate cardiac arrest, and prolonged myocardial protection allowing single-dose strategies in many procedures. This study summarizes evidence from a randomized phase-III trial, a large clinical CABG-MiECC experience, and a multicenter training program evaluating its implementation in routine practice.

**Methods:** Evidence was derived from three complementary studies. A single-centre, randomized, single-blind phase-III non-inferiority trial compared Cardioplexol™ with Buckberg cardioplegia in elective CABG, valve, and aortic root surgery. Peak troponin-T (TnT) within 24 hours after reperfusion served as the primary endpoint. In addition, a single-centre observational analysis assessed outcomes in isolated CABG procedures performed with MiECC using Cardioplexol™. Finally, a prospective multicenter observational study evaluated a standardized training program enabling surgeons without prior experience to adopt Cardioplexol™ strategy safely.

**Results:** In the randomized phase-III trial, 248 patients underwent surgery and 226 (100 Cardioplexol™, 126 Buckberg) were included in the per-protocol analysis. Peak postoperative TnT values during the first 24 hours were comparable between groups (0.77 vs. 0.78 ng/mL), confirming non-inferiority of Cardioplexol™. Cardioplexol™ induced significantly faster cardiac arrest (11 vs. 71 seconds, $p<0.001$) and was associated with shorter aortic cross-clamp time (51.2 vs. 60.7 minutes, $p<0.001$). The rate of electrical defibrillation after reperfusion was markedly lower with Cardioplexol™ (10% vs. 52%, $p<0.001$). Trends toward reduced catecholamine requirements during the first 24 hours (6202 vs. 7170 µg/kg) and shorter ICU stay (38.1 vs. 44.0 hours) were also observed, while overall safety parameters were comparable. In the single-centre CABG-MiECC cohort, 2416 isolated CABG procedures were performed during a 76-month period. Patients were predominantly male (81.3%), with a mean age of $66.2\pm9.7$ years and a median logistic EuroSCORE of 3.2. On average, $3.2\pm0.8$ grafts were performed per patient. Median aortic cross-clamp time was 45 minutes, and more than 75% of patients required only a single 100 mL dose of Cardioplexol™. After reperfusion, over 90% of hearts resumed spontaneous rhythmic activity. Peak troponin-T values were low ($0.9\pm4.5$ ng/mL; median 0.4 ng/mL), and 30-day mortality was 0.9%. The low-volume composition minimizes hemodilution compared with conventional multidose cardio.

**Conclusion:** Cardioplexol™ provides effective myocardial protection with rapid induction of cardiac arrest, reduced reperfusion arrhythmias, reduction of blood transfusion requirements and efficient single-dose administration. Evidence from

randomized trials, large real-world CABG-MiECC data and successful multicenter training implementation supports the safety, reproducibility, and broader adoption of this effective cardioplegic strategy.

## 11-3

### Turning Surgical Waste into Scientific Opportunity: Epicardial Fat as a Reliable Source of Multipotent Adipogenic Stem/Progenitor Cells (ASCs)

**Heuböck E.[1,2], Benedikt P.[3,2], Huber F.[3,2], Mamunchak O.[3], Singh Bhogal C.[1,2], Kotnik M.[1,2], Lugmayr S.[1,2], Charwat V.[1,2], Lipp A.[4], Raml E.[4], Bernhard D.[1,2], Zierer A.[3,2], Mandl M.[1,2]**

[1]Institute for Physiology and Pathophysiology, Department of Pathophysiology, Johannes Kepler University, Linz, Austria
[2]Clinical Research Institute for Cardiovascular and Metabolic Diseases, Medical Faculty, Johannes Kepler University, Linz, Austria
[3]Department of Thoracic and Cardiovascular Surgery, Kepler University Hospital, JKU, Linz, Austria
[4]Core Facility Cytometry, Johannes Kepler University, Linz, Austria

**Introduction:** Epicardial adipose tissue (EAT) is a metabolically active visceral fat depot located in direct anatomical and paracrine continuity with the myocardium. Clinically, increased EAT volume and inflammatory remodeling have been associated with atrial fibrillation, coronary artery disease and heart failure. Despite its recognized involvement in cardiac pathophysiology and its routine accessibility during cardiac surgery, EAT is currently not utilized as a potential resource for in vitro cardiac disease modeling. We hypothesized that human EAT contains ASC populations with a high and unappreciated differential potential and that these cells can be isolated from minimal intraoperative specimens using a novel protocol.

**Methods:** EAT samples were obtained during routine cardiac surgery with informed written consent. We developed a reproducible, semi-automated ASC isolation procedure from EAT samples as low as ~200 mg. Cells were characterized by flow cytometry, histology, and transcriptomic profiling. Directed differentiation assays evaluated adipogenic, chondrogenic, osteogenic and cardiogenic potential.

**Results:** Our novel isolation protocol enabled consistent recovery of viable, proliferative EAT-derived ASCs (EAT-ASCs) from limited surgical material. Cells expressed various stem cell markers on the cell-surface, indicating a defined ASC population within human EAT. Transcriptomic analyses of proliferating EAT-ASCs revealed pro-angiogenic and myogenic gene signatures. Under directed differentiation conditions, EAT-ASCs gave rise to adipocytes, chondrocytes and osteocytes thus indicating multipotency. Intriguingly, EAT-ASCs showed the capability to generate cardiomyocyte-like cells as evidenced by the induction of cardiac-specific markers including cardiac troponin T.

**Conclusion:** We demonstrate that minimal amounts of human epicardial fat are sufficient to isolate stem/progenitor cells with a high differentiation potential. This establishes a reliable autologous cell source for in vitro modeling of adipocyte-myocardial crosstalk—an interaction central to atrial fibrillation, ischemia, and heart failure, yet still mechanistically incompletely understood.

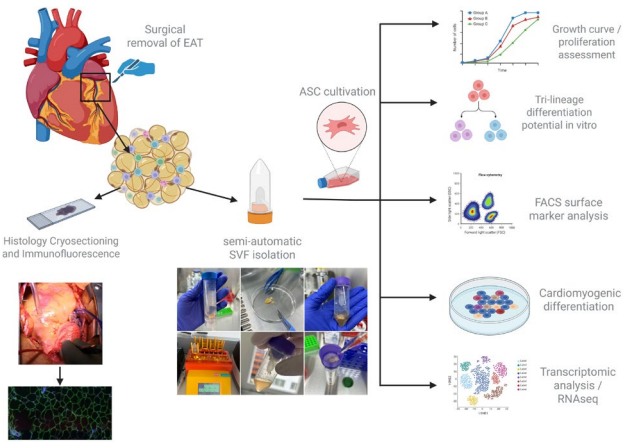


Fig. 1 | 11-3

## 11-4

### Long-term outcomes after mitral valve surgery in women and men

**Kahrovic A.[1], Coti I.[2], Andreeva A.[1], Osipenko K.[1], Bartko P.[3], Kocher A.[4], Andreas M.[4], Sandner S.[1], Zimpfer D.[1], Werner P.[2]**

[1]Department of Cardiac and Thoracic Aortic Surgery, Medical University of Vienna, Vienna, Austria
[2]Department of Cardiac and Thoracic Aortic Surgery, Medical University of Vienna, Wien, Austria
[3]Universitätsklinik für Innere Medizin II, Klinische Abteilung für Kardiologie, Wien, Austria
[4]Medical University of Vienna, Vienna, Austria

**Introduction:** This study aimed to assess long-term clinical outcomes after mitral valve surgery in women and men.

**Methods:** This retrospective, observational study included 2355 patients who underwent mitral valve surgery between November 2008 and November 2024 at the Medical University of Vienna. Patients were grouped based on biological sex (women vs men). The primary endpoint was a hospital readmission for heart failure decompensation; secondary endpoints included mitral valve–related reintervention and all-cause mortality.

**Results:** In this collective, 1021 patients (43%) were female and 1334 (57%) were male. Women were older and presented

**Figure 1. Cumulative incidence curves demonstrating the probability of cardiac readmission in women and men, (Gray's test, p<0.001)**

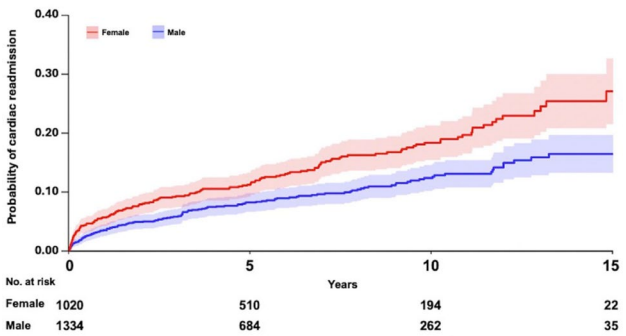


Fig. 1 | 11-4

with a higher European System for Cardiac Operative Risk Evaluation (EuroSCORE) II value (both $p<0.001$). Female sex was associated with a significantly higher risk of cardiac readmission in univariable (sub-hazard ratio (sHR) 1.61, 95% confidence interval (CI) 1.28–2.03, $p<0.001$) and multivariable proportional competing risk regression analyses (adjusted sHR 1.33, 95% CI 1.04–1.71, $p=0.025$). The cumulative incidence of cardiac readmission was 8.2 ± 1.6%, 12.4 ± 2.2%, and 16.5 ± 3.2% at 5, 10, and 15 years in male patients, respectively, compared with 11.2 ± 2.0%, 18.4 ± 2.9%, and 27.1 ± 5.6% in female patients ($p<0.001$). The risk of mitral valve-related reintervention (adjusted sHR 1.25, 95% CI 0.81–1.93, $p=0.320$) and all-cause mortality (adjusted hazard ratio 0.86, 95% CI 0.73–1.01, $p=0.070$) was similar between both groups.

**Conclusion:** Female sex was independently associated with a higher risk of hospital readmission for heart failure decompensation, emphasizing the need for sex-sensitive evaluation of referral timing and systematic postoperative clinical surveillance.

## 11-5

### Higher lipoprotein(a) burden in women undergoing coronary artery bypass grafting

**Abfalterer H., Renz L., Klingler C., Gerlach L., Grimm M., Bonaros N., Ruttmann-Ulmer E.**

Abteilung für Herzchirurgie, Innsbruck, Austria

**Introduction:** Elevated level of lipoprotein (a) is a highly genetically determined, causal risk factor for the development of cardiovascular disease. Furthermore, elevated Lp(a) levels are associated with impaired clinical outcome after coronary artery bypass grafting. Lp(a) lowering medications are currently under investigation in phase 2 and phase 3 clinical trials. We aimed to assess gender-specific differences in the distribution of Lp(a) levels in patients undergoing coronary artery bypass grafting.

**Methods:** This is a prospective, observational trial about secondary prevention in patients undergoing CABG. Lp(a) levels were obtained from preoperative blood sample collection. Lp(a) levels are specified in nmol/l. During the screening period, 413 patients underwent CABG procedure. 300/413 were included after patient informed consent. Analyses were performed in the following cohorts: a) all included cases ($n=300$, 0 missing Lp(a) values) b) all complete cases (with available Lp(a) values) ($n=404$ out of 413) c) all cases ($n=413$ out of 413) using imputation analysis for missing Lp(a) values ($n=9$, 2.18%) with multiple imputations by chained equations (5 imputations used). Median (interquartile range) was obtained for Lp(a) values. Mann-Whitney U Test was used to test for statistical differences between male and female gender. Patients were classified into categorical Lp(a) categories (Lp(a) (nmol/l) ≥125; ≥150; ≥175; ≥200). Cross-tabulations and chi-square test were used to assess for statistical differences in gender-specific distribution of Lp(a) categories. In multivariate setting, binary logistic regression analysis was used.

**Results:** In all included cases ($n=300$), median Lp(a) values were significantly higher in female (45.3 (IQR 217.6) versus 26.9 (IQR 118.2); $p=0.036$). Women were significantly more often represented in Lp(a) categories ≥125 ($p=0.021$); ≥150 ($p=0.009$); ≥175 ($p=0.007$); ≥200 ($p<0.001$). In binary logistic regression analysis, female gender was associated with significantly higher odds to be categorized in Lp(a) categories ≥125, ≥150, ≥175 and ≥200. In all complete cases ($n=404$) and all cases ($n=413$), median Lp(a) values did not differ significantly between male and female ($p$ values ranging from 0.158–0.213). In all complete cases, women were significantly more often distributed in Lp(a) categories ≥125 ($p=0.035$); ≥150 ($p=0.018$); ≥175 ($p=0.027$); ≥200 ($p<0.001$). In all cases, women were significantly more often distributed in Lp(a) categories ≥150; ≥175; ≥200 ($p$-values were significant in all 5 datasets), but not in Lp(a) category ≥125 (only 4 out of 5 datasets were significant). In all complete cases, binary logistic regression analysis revealed that female gender was associated with significantly higher odds to be categorized in Lp(a) categories ≥125, ≥150, ≥175 and ≥200. In all cases, binary logistic regression analysis revealed that female gender was associated with significantly higher odds to be categorized in Lp(a) categories ≥150, ≥175 and ≥200, but not ≥125.

**Conclusion:** The main findings of our trial are the following:—We observed a significantly different gender-specific distribution in Lp(a) in patients undergoing CABG.—Although there was no significant difference in median Lp(a) values,—women were more frequently distributed in higher Lp(a) categories than male patients, especially in Lp(a) categories ≥150 nmol/l, ≥175 nmol/l and ≥200 nmol/l. These findings have various important implications: a) since higher Lp(a) levels are associated with impaired clinical outcome after CABG, we might have found a novel, potential risk factor for impaired outcome of female patients after CABG (more follow-up data necessary). b) Lp(a) lowering medications are currently under investigation with Lp(a) thresholds of ≥150 nmol/l (Pelacarsen), ≥175 nmol/l (Muvalaplin) and ≥200 nmol/l (Lepodisiran, Olpasiran) as inclusion criterion for the participation in these trials. If these medications prove to be effective and receive approval for clinical use, this means, that women undergoing CABG, should receive percentually more of these medication than men.

## 11-6

### Intensive lipid lowering therapies improve LDL-C goal achievement

**Abfalterer H., Gerlach L., Klingler C., Renz L., Corradini V., Grimm M., Bonaros N., Ruttmann-Ulmer E.**

Abteilung für Herzchirurgie, Innsbruck, Austria

**Introduction:** Patients undergoing coronary artery bypass grafting (CABG) count among the very high risk category of total cardiovascular risk according to current guidelines. Class I recommendation is to lower low-density lipoprotein cholesterol (LDL-C) to values <55 mg/dl and reduce LDL-C by ≥50% from baseline. Many previous reports state, that the target goal of <55 mg/dl is not achieved in most of the very high risk patients and lack in lipid-lowering therapy (LLT) leads to worse outcome. Medication-, health care professional- and patient related factors are reasons for non-achievement of LDL-C targets. With this prospective, observational trial, we aimed to find factors associated with the achievement of the LDL-C target goals (<55 mg/dl) in patients under stabile LLT, at the time point of admission for CABG. This knowledge will help to identify ways to improve LDL-C target goal achievement in patients undergoing CABG.

**Methods:** In this analysis, we aimed to find parameters associated with LDL-C goal (<55 mg/dl) achievement at the time-point of admission for CABG surgery, in patients under stabile LLT. A stabile LLT was defined as having a LLT prior to

admission (duration longer than 4 weeks, without any modification within 4 weeks prior to laboratory testing) and not having discontinued any oral LLT (statin, ezetimibe and/or bempedoic acid) ≥1 day prior to preoperative laboratory testing. LLTs were defined as following: 1) Therapies defined by intensity (assumed LDL-C lowering of a: ≤50%, b: >50% and ≤60%, c: >60%) (a: all oral monotherapies, ezetimibe plus bempedoic acid, Inclisiran monotherapy; b: statin plus ezetimibe, statin plus bempedoic acid, PCSK9I monotherapy; c: all other occurring therapies) 2) Therapies defined by number of medications (monotherapy (one agent)/dual therapy (two agents)/triple therapy (3 agents)) 3) Other definition (statin or ezetimibe monotherapy/oral combination therapy/PCSK9I or Inclisiran-based therapies) 4) Monotherapy or combination therapy To assess for independent predictors of LDL-C achievement (<55 mg/dl), multivariate binary logistic regression analyses were performed.

**Results:** 218/300 (72.7%) patients had stabile LLT. 141/218 (64.7%) had achieved the LDL-C goal of <55 mg/dl at admission. 205 (94%) of patients received statins, 173 (79.4%) had ezetimibe, 39 (17.9%) had bempedoic acid, 17 (7.8%) had a PCSK9I and 1 (0.5%) had inclisiran prescribed. Accordingly, 39 (17.9%) patients received low intensity therapy, 134 (61.5%) patients were treated with moderate intensity and 45 (20.6%) were treated with high intensity regime (according to above mentioned definition). 40 (18.3%) had a monotherapy, 139 (63.8%) had dual therapy and 39 (17.9%) had triple therapy. 37 (17%) had statin or ezetimibe monotherapy, 163 (74.8%) had oral combination therapy and 18 (8.3%) had PCSK9I or Inclisiran-based therapies. Overall, 40 (18.3%) had monotherapy and 178 (81.7%) had combination therapy. There were significant differences in the rate of patients achieving LDL-C <55 mg/dl goal within the treatment groups. (Low intensity: 28.2% vs. moderate intensity: 70.9% vs. high intensity: 77.8%; chi-square test: $p<0.001$), (Monotherapy: 25% vs. dual therapy: 73.4% vs. triple therapy: 74.4%; chi-square test: $p<0.001$), (statin/ezetimibe monotherapy: 27% vs. oral combination therapy: 71.8% vs. PCSK9I/Inclisran based therapies: 77.8%; chi-square test: $p<0.001$), (Monotherapy: 25% vs. combination therapy: 73.6%; chi-square test: $p<0.001$). The most important independent factor associated with higher odds of achieving LDL-C <55 mg/dl was the type of LLT (OR ranging from 10.07 up to 20.81).

**Conclusion:** LDL-C goal achievement is still suboptimal in patients transfered for CABG. Most important independent factor associated with higher odds to achieve LDL-C goal was the type of LLT (with monotherapies and low-intensity therapies being worse than combination-therapies or moderate/high-intensity therapies). Therefore, admission for CABG should be seen as an opportunity to optimize secondary prevention (a first step to achieve this goal is to switch from monotherapies or low intensity therapies to combination therapies). It is our responsibility as the treating physicians to improve patients' secondary prevention.

## 11-7

## Failure to Achieve Guideline-Recommended LDL-C Targets After Coronary Artery Bypass Grafting: A Persistent Secondary Prevention Gap

**Abfalterer H., Corradini V., Grill M., Ruttmann-Ulmer E., Bonaros N., Grimm M.**

Department of Cardiac Surgery, Medical University of Innsbruck, Innsbruck, Austria

**Introduction:** According to current ESC/EACTS guidelines, patients undergoing coronary artery bypass grafting (CABG) are classified as very-high cardiovascular risk and should achieve a low-density lipoprotein cholesterol (LDL-C) target of <55 mg/dL. However, real-world attainment of this goal after surgical revascularization remains uncertain. Beyond being a numerical laboratory value, LDL-C represents a measurable surrogate of the overall quality of secondary prevention. Failure to control LDL-C may therefore reflect broader gaps in comprehensive cardiovascular risk management.

**Methods:** We analyzed 350 patients prospectively enrolled in a multicenter study who underwent coronary artery bypass grafting (CABG). For the present investigation, a single-center analysis was conducted including all patients with at least one post-operative LDL-cholesterol (LDL-C) measurement at our institution ($n=331$). For each patient, mean follow-up LDL-C was calculated from all available post-operative values. Target attainment was assessed categorically (<55 vs. ≥55 mg/dL) and continuously. A one-sample t-test examined whether the cohort mean LDL-C differed from the guideline threshold of 55 mg/dL, with effect size quantified using Cohen's d. Statistical significance was defined as $p<0.05$. To explore mechanisms of insufficient LDL-C control, lipid-lowering therapy (LLT) modifications were analyzed during hospitalization and follow-up. Detailed medication data were available for 308 patients; therapy analyses were restricted to this subgroup. Therapy modification was categorized as improvement, no change, or worsening. Improvement was defined as initiation of an additional LLT (ezetimibe, bempedoic acid, or PCSK9 inhibitor) or escalation in statin intensity according to ACC/AHA categories (low, moderate, high). Worsening was defined as discontinuation of LLT or statin de-escalation. Substitution with equivalent potency was classified as no change. Medication changes were assessed (1) during index hospitalization and (2) from discharge to last follow-up.

**Results:** The mean post-operative LDL-C was 64 mg/dL, exceeding the recommended threshold by 9 mg/dL. One-sample testing confirmed that the cohort mean was significantly higher than 55 mg/dL ($p<0.001$), with a moderate standardized effect size (Cohen's $d=0.4$), indicating a clinically meaningful deviation from target. Categorical analysis revealed that the majority of patients did not achieve the LDL-C target of <55 mg/dL. Only 37.2% of patients were below the target. Despite the high proportion of patients failing to achieve guideline-recommended LDL-C targets, lipid-lowering therapy was modified infrequently during the index hospitalization. Among the 308 patients with complete medication data, only 10.1% experienced an improvement in lipid-lowering therapy during their hospital stay, whereas 6.8% had a worsening of therapy and 83.1% were discharged on an unchanged regimen. During post-discharge follow-up, treatment intensification occurred more frequently but remained suboptimal. Therapy was improved in 28.4% of patients, remained unchanged in 66.5%, and worsened in 5.1%.

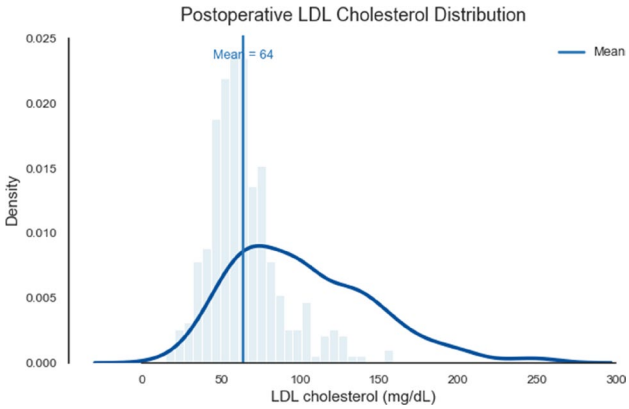


**Fig. 1 | 11-7**

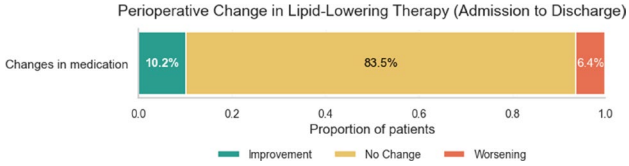


**Fig. 2 | 11-7**

**Conclusion:** In this contemporary CABG cohort, most patients did not reach guideline-recommended LDL-C targets during follow-up. Despite technically successful surgical revascularization, secondary prevention remains insufficiently optimized. Importantly, this gap in secondary prevention was paralleled by a low rate of lipid-lowering therapy intensification, particularly during the index hospitalization. Even among patients with documented hypercholesterolemia and very-high cardiovascular risk, discharge regimens were predominantly unchanged, representing a missed opportunity for early optimization. LDL-C should be viewed not merely as a laboratory parameter but as a surrogate marker of structured secondary prevention. Suboptimal LDL-C control likely reflects broader deficiencies in long-term cardiovascular management, including pharmacological intensification, adherence monitoring, lifestyle intervention, and multidisciplinary follow-up. CABG should not represent the endpoint of care but rather a critical transition toward aggressive and systematic secondary prevention. Strengthening post-operative lipid management may serve as an actionable and measurable entry point to improve overall secondary prevention, graft durability, and long-term survival.

## References

1. Mach F, Baigent C, Catapano AL, Koskinas KC, Casula M, Badimon L, et al. ESC/EAS Task Force for the management of dyslipidaemias. 2019 ESC/EAS Guidelines for the management of dyslipidaemias: lipid modification to reduce cardiovascular risk. Eur Heart J. 2019;41(1):111–88. https://doi.org/10.1093/eurheartj/ehz455.:contentReference[oaicite:0]
2. Mach F, Koskinas KC, Roeters van Lennep JE, Tokgözoğlu L, Badimon L, Baigent C, et al. ESC/EAS Scientific Document Group. 2025 Focused Update of the 2019 ESC/EAS Guidelines for the management of dyslipidaemias: Developed by the task force for the management of dyslipidaemias of the European Society of Cardiology (ESC) and the European Atherosclerosis Society (EAS). Eur Heart J. 2025;46(42):4359–78. https://doi.org/10.1093/eurheartj/ehaf190.:contentReference[oaicite:0]

## 11-8

## Transvenous Transseptal Mitral Valve-in-Valve Implantation for Stenosis of a Transcatheter Mitral Bioprosthesis

**Manville E., Harrer M., Taheri N., Grabenwöger M.**

Klinik Floridsdorf, Wien, Austria

**Introduction:** Stenosis of transcatheter mitral bioprostheses is an emerging clinical challenge. In patients at high surgical risk, transvenous transseptal mitral valve-in-valve (ViV) implantation represents a minimally invasive therapeutic alternative.

**Methods:** A 74-year-old female presented with progressive dyspnea. Three years earlier, she had undergone transapical transcatheter aortic valve replacement with an Edwards Sapien 3 (23 mm) prosthesis due to aortic stenosis and transcatheter mitral valve implantation with an Edwards Sapien 3 (29 mm) prosthesis due to mitral stenosis in MAC disease. Transoesophageal echocardiography showed preserved biventricular function and normal function of the aortic prosthesis. In contrast, stenosis of the mitral bioprosthesis was identified, with restricted leaflet motion and elevated transvalvular gradients (PGmean 12 mmHg, PGmax 26 mmHg). The patient had recently undergone percutaneous coronary intervention with stenting of the left main and proximal right coronary arteries. Given her prohibitive surgical risk, a transvenous transseptal mitral ViV procedure was planned. Pre-procedural planning included multimodality imaging with transoesophageal echocardiography and computed tomography to assess the risk of left ventricular outflow tract (LVOT) obstruction. The predicted neo-LVOT area was considered adequate, allowing safe intervention.

**Results:** Transseptal puncture was performed under fluoroscopic and transoesophageal echocardiographic guidance. Balloon septostomy facilitated delivery of the valve system, and a 26 mm Edwards Sapien 3 prosthesis was successfully implanted. Post-procedural transoesophageal echocardiography demonstrated good leaflet motion, reduced transvalvular gradients (PGmean 4 mmHg, PGmax 12 mmHg), and no paravalvular leak or LVOT obstruction. The patient was extubated on the same day, experienced no neurological complications, and was discharged on post-procedural day seven.

**Conclusion:** Transvenous transseptal mitral valve-in-valve implantation is a safe and effective treatment option for stenotic transcatheter mitral bioprostheses in patients at high surgical risk. Careful pre-procedural planning, particularly LVOT assessment and septal puncture strategy, is essential to optimize outcomes.

# POSTERSITZUNG 12— HERZKLAPPENERKRANKUNGEN 1

## 12-1

### Cardiac Rhythm Determines Prognostic NT-proBNP Thresholds in Mitral Valve Surgery

**Ennen V.[1], Fiesel D.[2], Lohmann R.[1], Engler C.[1], Hirsch J.[1], Graber M.[1], Nägele F.[1], Grimm M.[1], Höfer D.[1], Bonaros N.[1], Winter-Pölzl L.[1], Gollmann-Tepeköylü C.[1]**

[1]Univ.-Klinik für Herzchirurgie, Medizinische Universität Innsbruck, Innsbruck, Austria
[2]Univ.-Klinik für Psychiatrie, Medizinische Universität Innsbruck, Innsbruck, Austria

**Introduction:** *N*-terminal pro-B-type natriuretic peptide (NT-proBNP) is widely used for perioperative risk stratification in cardiac surgery. In patients undergoing mitral valve surgery, however, interpretation of NT-proBNP levels may be confounded by the high prevalence of atrial fibrillation (AF), which independently increases circulating NT-proBNP concentrations. As a result, uniform NT-proBNP thresholds may not accurately reflect perioperative risk. This study aimed to evaluate the prognostic value of preoperative NT-proBNP according to cardiac rhythm and to identify rhythm-specific cut-off values in patients undergoing mitral valve surgery.

**Methods:** This retrospective cohort study included 2320 consecutive patients undergoing mitral valve surgery. Patients were stratified according to cardiac rhythm at admission into sinus rhythm (SR), paroxysmal AF, persistent AF, and permanent AF, and were additionally categorized as SR or AF for rhythm-stratified analyses. Patients receiving chronic dialysis were excluded. Receiver operating characteristic (ROC) analyses were performed to determine optimal NT-proBNP cut-offs for 30-day mortality in the overall cohort and according to rhythm. Multivariable logistic regression models adjusted for EuroSCORE II were used to assess the association between NT-proBNP levels above the rhythm-specific thresholds and adverse perioperative outcomes.

**Results:** Median preoperative NT-proBNP levels differed markedly according to cardiac rhythm, with substantially higher values observed in patients with atrial fibrillation (AF) compared with those in sinus rhythm (SR) (SR: 388 ng/L [IQR 146–111 ng/L] vs. AF: 1828 ng/L [IQR 1216–2875 ng/L]). Cut-offs associated with 30-day mortality varied considerably between rhythm groups, with optimal thresholds of 706 ng/L in the overall cohort, 582 ng/L in patients with SR, and 2516 ng/L in patients with AF. Rhythm-stratified analyses demonstrated moderate discrimination for 30-day mortality, with better prognostic performance in SR patients (AUC 0.762) than in those with AF (AUC 0.678). In multivariable analyses adjusted for EuroSCORE II, NT-proBNP levels above the rhythm-specific thresholds were independently associated with increased risk of adverse outcomes. The association was more pronounced in patients with SR than in those with AF for 30-day mortality (OR 4.8 vs. 3.8), extracorporeal membrane oxygenation (OR 3.6 vs. 2.7), hemofiltration (OR 4.9 vs. 2.5), and prolonged intensive care unit stay (OR 3.0 vs. 2.0).

**Conclusion:** Preoperative NT-proBNP is a powerful predictor of adverse outcomes after mitral valve surgery, but its interpretation is strongly influenced by cardiac rhythm. Patients with atrial fibrillation require substantially higher NT-proBNP thresholds to reflect comparable perioperative risk. Applying rhythm-specific NT-proBNP cut-offs may therefore improve risk stratification and guide perioperative management in mitral valve surgery.

## 12-2

### Societal Definitions of Ventricular Functional Mitral Regurgitation and their Impact on Prevalence, Valve Morphology and Prognosis

**Koschatko S., Heitzinger G., Torrefranca C., Jantsch C., Hauptmann L., Autherith M., Demirel C., Nitsche C., Bartko P.**

Medizinische Universität Wien, Wien, Austria

**Introduction:** Functional mitral regurgitation (fMR) in the setting of heart failure (HF) is a heterogeneous condition. The 2025 ESC Guidelines on Valvular Heart Disease and the 2022 JACC Expert Consensus introduced distinct criteria for ventricular fMR (VfMR). The implications of these definitional differences in patient selection and prognosis remain unclear. The aim of this study was to compare prevalence, baseline characteristics, and long-term prognostic impact of both VfMR definitions in patients with severe fMR.

**Methods:** Both societal VfMR definitions were applied to a comprehensive database of 1163 patients with severe fMR, moderate fMR ($n=7890$) served as reference group. Survival was assessed using Kaplan-Meier analysis and Cox proportional hazards models. Multivariable models were adjusted for common clinical risk-factors. The primary endpoint was all-cause mortality.

**Results:** ESC criteria classified 42.1% of severe cases as VfMR versus 66.2% by JACC (Fig. 1). JACC-defined VfMR patients were slightly older (70 vs. 67 years) and more frequently female (32% vs. 23%), with comparable comorbidities and NT-proBNP levels.

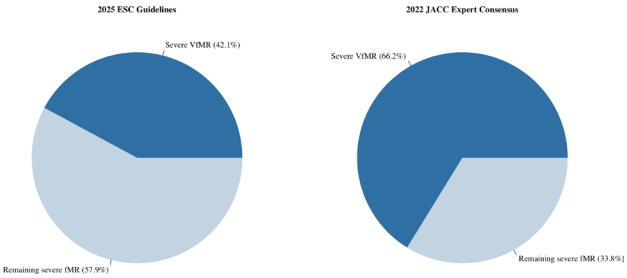


**Fig. 1 | 12-2** Prevalence of VfMR

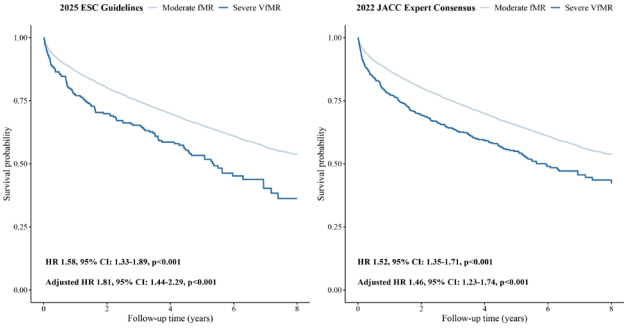


**Fig. 2 | 12-2** Long-term mortality of VfMR

ESC-defined VfMR more often comprised patients with HF with reduced ejection fraction (84% vs. 66%), whereas the JACC definition also included a small proportion with HF with preserved ejection fraction (3% vs. 0%). Cardiac remodeling was more advanced in the ESC cohort with larger indexed LA volumes (52 vs. 42 ml/m$^2$) and LV end-diastolic volumes (109 vs. 86 ml/m$^2$). Furthermore, mitral annular diameters were greater (4-CV: 41.4 vs. 38.2 mm; 3-CV: 36.5 vs. 33.8 mm), as were tenting height (4-CV: 9.3 vs. 8.3 mm; 3-CV: 12.4 vs. 11.2 mm) and tenting area (4-CV: 229 vs. 182 mm$^2$; 3-CV: 261 vs. 222 mm$^2$). Leaflet tethering angles were comparable. Both ESC- and JACC-defined VfMR were associated with increased mortality (Fig. 2) compared with moderate fMR (ESC: HR 1.58, 95% CI 1.33–1.89; JACC: HR 1.52, 95% CI 1.35–1.71; both $p<0.001$). After adjustment, associations remained significant and were more pronounced for ESC-defined VfMR (ESC: adjusted HR 1.81, 95% CI 1.44–2.29; JACC adjusted HR 1.46, 95% CI 1.23–1.74; both $p<0.001$).

**Conclusion:** JACC criteria identify a broader VfMR population, whereas ESC criteria define a smaller but higher-risk subgroup with more advanced remodeling and stronger mortality association. These findings suggest greater prognostic specificity of the ESC definition with potential implications for risk stratification and timing of intervention. Nevertheless, both definitions consistently identify a subgroup of fMR with significantly impaired long-term survival compared with moderate fMR. These findings highlight the prognostic relevance of contemporary VfMR definitions and underscore the need for harmonisation of classification criteria.

## References


1. Praz F, et al. EACTS Guidelines for the management of valvular heart disease.“ European heart journal vol. 46. ESC. 2025;44(2025):4635–736. https://doi.org/10.1093/eurheartj/ehaf194.
2. Zoghbi, William A et al. „Atrial Functional Mitral Regurgitation: A JACC: Cardiovascular Imaging Expert Panel Viewpoint.“ JACC. Cardiovascular imaging vol. 15,11 (2022): 1870–1882. https://doi.org/10.1016/j.jcmg.2022.08.016


## 12-3

## Impact of Phenotype Definition on Prevalence, Valve Morphology, and Prognosis in Atrial Functional Mitral Regurgitation


**Koschatko S., Heitzinger G., Jantsch C., Hauptmann L., Autherith M., Torrefranca C., Demirel C., Goliasch G., Nitsche C., Bartko P.**

Medizinische Universität Wien, Wien, Austria


**Introduction:** Atrial functional mitral regurgitation (AfMR) has emerged as a distinct clinical entity, yet there is no uniformly applied definition. The lack of a unified diagnostic standard creates significant uncertainty regarding its prevalence, valve morphology, patient characteristics, and mortality risk. As the 2025 ESC Valve Guidelines and the 2022 JACC Expert Consensus move toward clinical implementation, it is vital to understand how these definitions impact patient classification and prognosis. The objective was to systematically evaluate all published AfMR definitions, with a specific focus on the JACC and ESC frameworks, and to determine their influence on patient classification, valve morphology, and long-term survival.

**Methods:** A systematic literature review across PubMed, Embase, and Web of Science identified all existing AfMR definitions. These were applied to a real-world database of 581 patients with severe fMR. We performed sensitivity analyses to compare morphological features (mitral annular diameter, tenting indices, leaflet angles) and prognostic outcomes (all-cause mortality) across all definitions. The comparator group consisted of moderate fMR ($n=6755$).

**Results:** The search identified 72 unique AfMR definitions. Their application resulted in a substantial range of prevalence, from 2.1% to 61.8% (Fig. 1). Echocardiographic characteristics showed broad variability: indexed left atrial (LA) volumes ranged from 36 to 62 mL/m2, Carpentier type IIIb motion occurred in 0% to 49% of patients, and mean annulus diameter varied from 31.5 to 37.1 mm. Crude hazard ratios (HR) for all-cause mortality across these definitions ranged from 1.17 to 2.42 (Fig. 2). The JACC and ESC definitions yielded similar overall prevalence rates of 13.1% and 12.0%, respectively (Fig. 1), yet

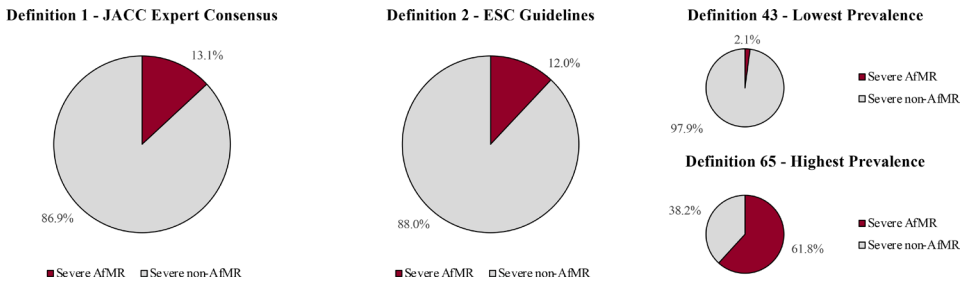


**Fig. 1 | 12-3** Prevalence of AfMR

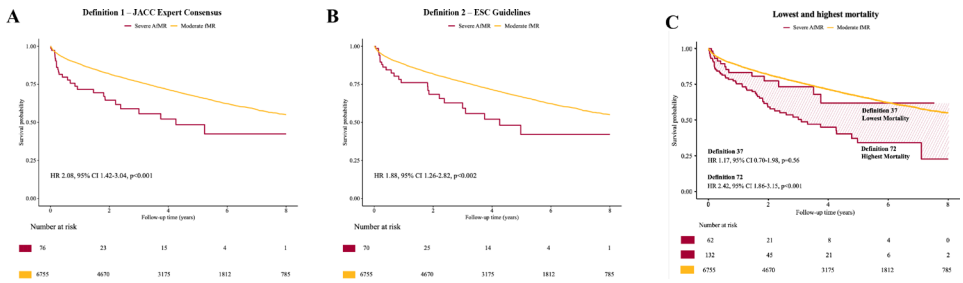


**Fig. 2 | 12-3** Long-term mortality of AfMR

they classified distinct patient subsets with a non-overlap rate of 25–27%. While both were associated with higher mortality compared to moderate fMR in univariate analysis (JACC: HR 2.08, 95% CI:1.42–3.04, $p<0.001$, ESC: HR 1.88, 95% CI:1.26–2.82, $p=0.006$; both Fig. 2), the JACC definition remained a significant predictor of mortality after multivariate adjustment, whereas the ESC definition did not ($p=0.066$). A primary driver of this observed difference was the JACC definition's inclusion of Carpentier IIIb cases and its more stringent LA volume threshold (>40 mL/m2), effectively capturing a broader, more high-risk patient spectrum.

**Conclusion:** AfMR definitions are highly heterogeneous, significantly impacting reported prevalence and morphological features. While both the ESC guidelines and JACC consensus provide clinically relevant frameworks, the JACC definition demonstrates superior prognostic validity and flexibility. By including a wider morphological spectrum (Carpentier Type IIIb), the JACC definition provides a robust foundation for a unified global standard, which is essential for consistent management in clinical practice and future studies.

## 12-4

### Pre-Existing Pacemakers Are Associated With Lower Aortic Valve Calcification in TAVI Candidates

**Veraar C., Lamm G., Will M., Merl L., Granner M., Schwarz K., Mascherbauer J.**

Department of Cardiology, University Hospital Sankt Poelten, St. Poelten, Austria

**Introduction:** Background: Degenerative aortic stenosis (AS) frequently coexists with conduction system disease due to the close anatomical proximity between the aortic valve complex and the atrioventricular conduction system. A subset of patients referred for transcatheter aortic valve implantation (TAVI) already carries a permanent pacemaker PM, indicating pre-existing conduction abnormalities. Whether these patients differ in structural valve characteristics, particularly regarding aortic valve calcification (AVC), remains insufficiently understood. Purpose: To investigate the association between pre-existing PM status and quantitative AVC in patients undergoing TAVI.

**Methods:** Consecutive patients with symptomatic severe AS who underwent transthoracic echocardiography and both contrast-enhanced and non-contrast cardiac computed tomography within four weeks prior to TAVI between January 2020 and April 2023 were included. AVC was quantified using the Agatston score, native volume score, and contrast-enhanced volume score, including leaflet-specific analyses. Patients were stratified according to the presence or absence of a pre-existing PM. Multivariable logistic regression models were adjusted for age, sex, body mass index, diabetes, arterial hypertension, renal function, and left ventricular ejection fraction.

**Results:** Among 868 patients undergoing TAVI, 76 (8.8%) had a pre-existing PM. In multivariable analyses, higher calcification burden was independently associated with lower odds of pre-existing PM: total Agatston score (adjusted OR 0.38, 95% CI 0.21–0.68; $p=0.038$), native volume score (adjusted OR 0.31, 95% CI 0.17–0.56; $p=0.001$), and contrast-enhanced volume score (adjusted OR 0.41, 95% CI 0.24–0.70; $p=0.001$). ROC analyses assessing discrimination for absence of pre-existing PM (i. e., higher calcification in patients without PM) showed modest performance overall (NCC contrast-enhanced volume score AUC 0.608; $p=0.002$), with stronger discrimination in women (NCC Agatston score AUC 0.783; $p<0.001$) than men (NCC contrast-enhanced volume score AUC 0.630; $p=0.001$).

**Conclusion:** Pre-existing PM status is independently associated with lower AVC in patients referred for TAVI, particularly in the non-coronary cusp and in women, suggesting referral at an earlier stage of structural valve degeneration.

**Association Between AVC and pre-PM Status in patients referred to TAVI**

| | Unadjusted Analysis | | Adjusted Analysis | |
|---|---|---|---|---|
| | Pre PM vs. no pre-PM | | Pre- PM vs. no pre- PM | |
| | OR (95% CI) | p-value | OR (95% CI) | p-value |
| Agatson Score | 0.65 (0.3-1.1) | 0.116 | 0.38 (0.21-0.68) | **0.038** |
| Native Volume Score | 0.57 (0.3-0.9) | **0.037** | 0.31 (0.17-0.56) | **0.001** |
| Volume Score | 0.59 (0.36-0.95) | **0.032** | 0.41 (0.24-0.70) | **0.001** |

**Fig. 1 | 12-4**

## 12-5

### Real-World Registry of Transcatheter Tricuspid Valve Edge-to-Edge Repair

**Knap B., Messner M., Pavluk D., Klammer P., Ungericht M., Puelacher C., Bauer A., Brenner C.**

Medizinische Universität Innsbruck, Innsbruck, Austria

**Introduction:** Tricuspid regurgitation (TR) is associated with increased risk of hospitalization and death while therapeutic options for patients at high surgical risk remain limited. Transcatheter tricuspid edge-to-edge repair (T-TEER) has emerged as a minimally invasive treatment to safely reduce TR severity, decrease heart failure related hospitalizations, and improve quality of life in selected patients with TR.

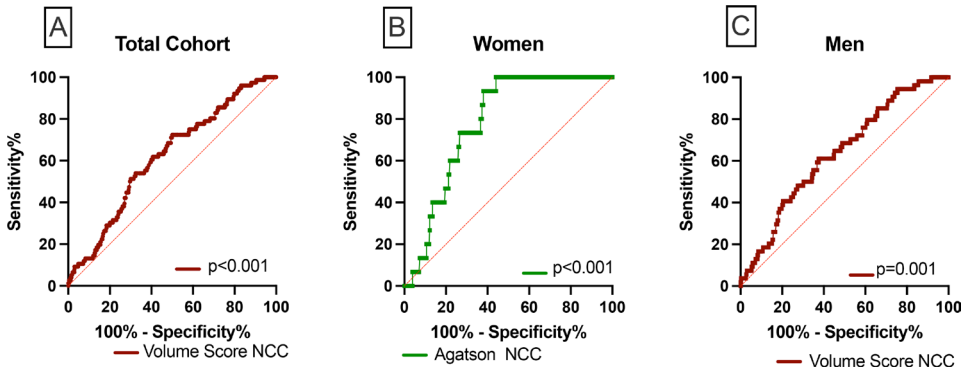


**Fig. 2 | 12-4**

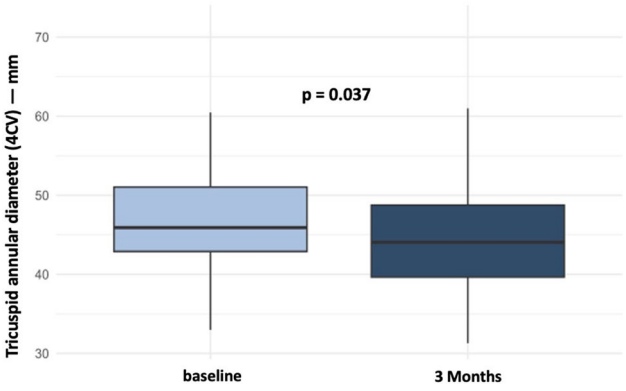


**Fig. 1 | 12-5** Tricuspid annular diameter (mm) at baseline and 3 months postprocedural

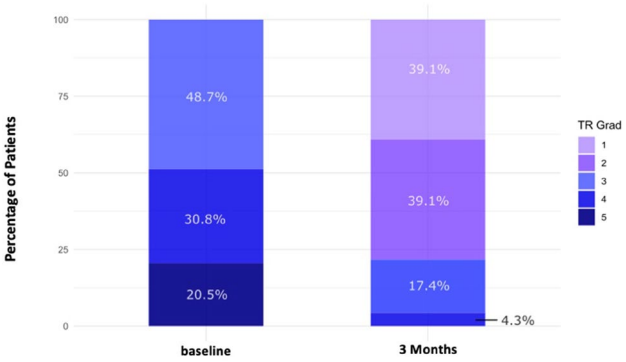


**Fig. 2 | 12-5** Severity of Tricuspid Regurgitation at Baseline and 3 months after T-TEER

**Methods:** We performed a retrospective, single-center registry analysis including all patients who underwent T-TEER in a Real-World Cohort. Follow-up assessments were performed at 3 months and 12 months, including clinical status, echocardiographic assessment, and laboratory parameters.

**Results:** A total of 49 patients were included. At early follow-up (3 months), TR severity decreased significantly (–1.72 ± 0.92 grades; $p < 0.001$) and NYHA class improved (–0.92 ± 0.61; $p < 0.001$). Tricuspid annular diameter decreased numerically (–2.47 ± 6.29 mm; $p = 0.037$), without significant changes in ventricular function or laboratory parameters after correction. At mid-term follow-up, NYHA improvement remained sustained (–0.84 ± 0.81; $p = 0.005$), and tricuspid annular diameter was significantly reduced (–4.49 ± 4.91 mm; $p < 0.001$). LV ejection fraction increased numerically (+3.47 ± 7.69%; $p = 0.020$) but did not remain significant after correction. No relevant changes were observed in right ventricular parameters.

**Conclusion:** This real-world registry suggests that T-TEER is effective in patients with significant TR, resulting in substantial TR reduction and a significant decrease in tricuspid annular diameter, indicating favourable annular remodelling.

## References

1. Sorajja P … Adams DH; TRILUMINATE Pivotal Investigators. Transcatheter Repair for Patients with Tricuspid Regurgitation. N Engl J Med. 2023 May 18;388(20):1833–1842. https://doi.org/10.1056/NEJMoa2300525. Epub 2023 Mar 4.

# 12-6

## Real-World Registry of Transcatheter Mitral Edge-to-Edge Repair

**Knap B., Messner M., Pavluk D., Klammer P., Pölzl G., Ungericht M., Puelacher C., Bauer A., Brenner C.**

Medizinische Universität Innsbruck, Innsbruck, Austria

**Introduction:** Transcatheter edge-to-edge repair (M-TEER) of the mitral valve is a minimally invasive treatment option for patients with significant mitral regurgitation (MR), particularly in individuals with high surgical risk. This study evaluates the effectiveness of M-TEER in a Real-World Cohort and compares outcomes across relevant patient subgroups.

**Methods:** In this retrospective single-center study, patients who underwent M-TEER between October 2010 and October 2024 were analyzed. Demographic, clinical, echocardiographic, and laboratory data was collected before and after intervention. Follow-up examination was performed after 3 months post-procedure. Subgroup analyses were conducted based on age (< 75 vs. ≥ 75 years), MR etiology (functional vs. degenerative), left ventricular ejection fraction (LVEF) and glomerular filtration rate (GFR).

**Results:** A total of 219 patients were included, of whom 47% ($n = 103$) were female. Severe mitral regurgitation (MR) was present in 96.8% ($n = 212$), and 70% ($n = 138$) had advanced heart failure (NYHA ≥ III). At follow-up, M-TEER was associated with a significant reduction in MR severity (median –2 grades, IQR

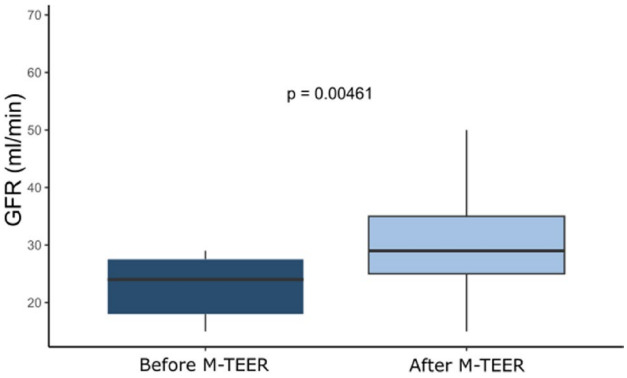


**Fig. 1 | 12-6** Subgroup analysis GFR < 30 ml/min—GFR at baseline and 3 Months after M-TEER

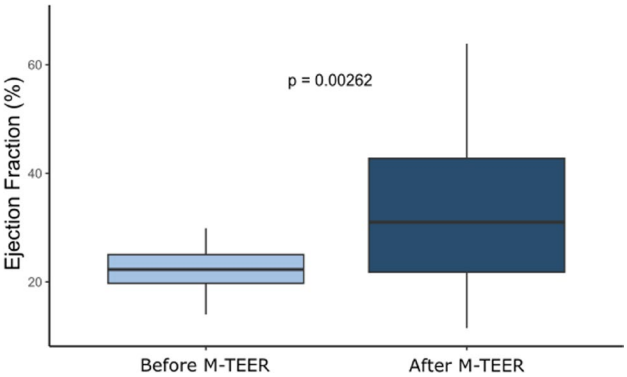


**Fig. 2 | 12-6** Subgroup analysis EF < 30% - EF at baseline and 3 Months after M-TEER

1; $p<0.001$), accompanied by an improvement in NYHA class (median -1, IQR 1; $p<0.001$) and a reduction in systolic pulmonary artery pressure ($p<0.001$). Patients ≤75 years showed greater NYHA improvement compared with older patients ($p=0.008$), while outcomes did not differ by MR aetiology. In subgroup analyses, patients with LVEF <30%, M-TEER resulted in a significant increase in LVEF (+6.7 ± 9.5%; $p=0.001$). Among patients with GFR <30 ml/min, GFR improved significantly (+8.3 ± 12.6 ml/min; $p=0.015$), alongside significant reductions in MR severity and NYHA class, while EF remained unchanged.

**Conclusion:** In our unselected, consecutive patient cohort, M-TEER was associated with significant improvements in both, mitral valve function and clinical symptoms among patients with severe MR and high surgical risk.

### References

1. Feldman T … Mauri L; EVEREST II Investigators. Percutaneous repair or surgery for mitral regurgitation. N Engl J Med. 2011 Apr 14;364(15):1395–406. https://doi.org/10.1056/NEJMoa1009355. Epub 2011 Apr 4. Erratum in: N Engl J Med. 2011 Jul 14;365(2):189.

# POSTERSITZUNG 13—KARDIALE BILDGEBUNG 2

## 13-1

### The neutrophil-lymphocyte ratio is associated with cardiac magnetic resonance imaging-derived myocardial fibrosis and remodelling

**Poledniczek M.[1], Kronberger C.[1], Schmid L.[1], Mascherbauer K.[1], Donà C.[1], Koschutnik M.[1], Lunzer L.[1], Nitsche C.[1], Beitzke D.[2], Loewe C.[2], Hengstenberg C.[1], Kammerlander A.[1]**

[1]Medizinische Universität Wien – Universitätsklinik für Innere Medizin II – Klinische Abteilung für Kardiologie, Wien, Austria
[2]Medizinische Universität Wien – Universitätsklinik für Radiologie und Nuklearmedizin – Klinische Abteilung für Radiologie, Wien, Austria

**Introduction:** Sub-clinical inflammation is considered a key mechanism in cardiovascular disease and myocardial remodelling. We therefore evaluated whether the neutrophil-lymphocyte ratio (NLR), a simple inflammatory marker derived from a routine full blood count, is associated with myocardial fibrosis.

**Methods:** Consecutive patients from a cardiac magnetic resonance imaging (CMR) registry were included and stratified by NLR tertile. The association of the NLR and the levels of C-reactive protein (CRP) with CMR-derived myocardial T1 time and the extracellular volume fraction (ECV) were assessed using linear regression analysis and compared using Z-scores.

**Results:** 1152 patients (72.4 years, 53.1% male) constituted the final cohort. The median NLR was 3.11 [interquartile range (IQR): 2.145–4.67]. Tertiles were based on the cut-off values ≤2.5, >2.5 & <4.0), and ≥4.0. A higher NLR tertile was associated with lower biventricular ejection fraction, hypertrophy, and RV volume. The myocardial native T1 time [tertile 1 vs. 3: 1010 ms (984–1038) vs. 1030 (1001–1059), $p<0.001$] and ECV [tertile 1 vs. 3: 26.3% (24.2–28.6) vs. 28.1% (25.5–31.4), $p<0.001$] also significantly differed between the NLR tertiles. The NLR's and the CRP's association with elevated myocardial T1 time and ECV were comparable, with a β of 6.38 and 0.782, respectively, per standard deviation for the NLR, and 6.39 and 0.862, respectively, per standard deviation of CRP. However, the proportion of variation in the target variables explained by either the NLR or CRP was generally low, with a R-value between 0.17 and 0.26.

**Conclusion:** In our CMR all-comer cohort, NLR and CRP were significantly associated with prolonged myocardial T1 times and increased ECV. However, only a modest variation observed in both parameters was explained by either variables.

## 13-2

### Additive diagnostic value of thoracic SPECT/CT imaging in Perugini grade 1 patients who underwent bone scintigraphy

**Poledniczek M.[1], Rettl R.[1], Kronberger C.[1], Schmid L.[1], Ermolaev N.[1], Duca F.[1], Nitsche C.[1], Binder-Rodriguez C.[1], Camuz Ligios L.[1], Eslami M.[1], Binder P.[2], Spielvogel C.[2], Badr Eslam R.[1], Beitzke D.[3], Kastner J.[1], Bergler-Klein J.[1], Kammerlander A.[1], Hengstenberg C.[1], Hacker M.[2], Calabretta R.[2]**

[1]Medizinische Universität Wien – Universitätsklinik für Innere Medizin II – Klinische Abteilung für Kardiologie, Wien, Austria
[2]Medizinische Universität Wien – Universitätsklinik für Radiologie und Nuklearmedizin – Klinische Abteilung für Nuklearmedizin, Wien, Austria
[3]Medizinische Universität Wien – Universitätsklinik für Radiologie und Nuklearmedizin – Klinische Abteilung für Radiologie, Wien, Austria

**Introduction:** Left ventricular (LV) myocardial uptake of 99mTechnetium-labeled tracers is assessed to diagnose transthyretin amyloid cardiomyopathy (ATTR-CM). The degree of uptake is visually graded using planar images utilising the Perugini score. Today, non-invasive diagnosis of ATTR-CM is broadly established in practice; however, in patients with mild tracer uptake (Perugini grade 1), no definite diagnosis can be made without endomyocardial biopsy.

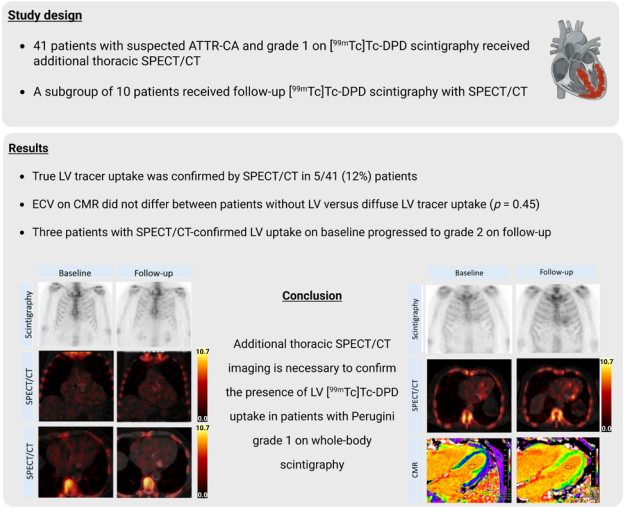


Fig. 1 | 13-2

**Methods:** Within the scope of a prospective cardiac amyloidosis registry at the Medical University of Vienna, all patients who underwent bone scintigraphy graded as Perugini grade 1 with additional SPECT/CT imaging performed between September 2014 and May 2025 were retrospectively analysed.

**Results:** 41 patients (70.8 years, IQR: 64.9–78.8, 41.5% female) were included. The majority ($n = 32$, 78.0%) of scans were ordered for a suspicion of ATTR-CM. On SPECT/CT images, true LV tracer uptake was confirmed in 4 (9.8%) patients, and 1 (2.4%) patient presented with focal myocardial uptake. In all other patients, tracer uptake was not within the myocardial tissue but rather blood-pool uptake. In follow-up [99mTc]-DPD scintigraphy, myocardial tracer uptake eventually progressed to Perugini grade 2 in 3 patients who previously demonstrated mild LV myocardial tracer uptake. In contrast, those with diffuse LV uptake did not show any signs of progression in follow-up SPECT/CT imaging.

**Conclusion:** SPECT/CT is mandatory in patients with mild mediastinal tracer uptake interpreted as Perugini grade 1. Among patients with Perugini grade 1 and confirmed [99mTc]-DPD LV uptake on SPECT/CT images, progression to Perugini grade 2 was observed in all individuals who underwent nuclear medicine imaging follow-up.

## 13-3

### Early Biochemical Prediction of Intramyocardial Hemorrhage in STEMI

**Fischer P.[1], Lechner I.[1], Tiller C.[1], Holzknecht M.[1], Oberhollenzer F.[1], Kaser A.[1], Sandor A.[1], Mayr A.[2], Troger F.[2], Gollmann-Tepeköylü C.[3], Bauer A.[1], Metzler B.[1], Reinstadler S.[1], Reindl M.[1]**

[1]Universitätsklinik für Innere Medizin III – Kardiologie und Angiologie, Innsbruck, Austria
[2]Universitätsklinik für Radiologie, Innsbruck, Austria
[3]Universitätsklinik für Herzchirurgie, Innsbruck, Austria

**Introduction:** Intramyocardial hemorrhage (IMH) is a major determinant of adverse outcomes following ST-elevation myocardial infarction (STEMI), reflecting severe microvascular injury despite epicardial reperfusion. Its presence is strongly associated with adverse left ventricular remodelling, heart failure, and increased mortality. Early identification of patients at risk for IMH is crucial to enable timely risk stratification and to facilitate the development of targeted therapeutic strategies. This study aimed to investigate the value of admission biomarkers for the early prediction of IMH in acute STEMI.

**Methods:** Patients undergoing primary percutaneous coronary intervention (PCI) after first acute STEMI were enrolled in the prospective Magnetic Resonance Imaging in Acute ST-Elevation Myocardial Infarction study (MARINA-STEMI, NCT04113356). At hospital admission, blood samples were obtained for measurement of high-sensitivity cardiac troponin T [hs-cTnT], hematologic indices (hemoglobin [Hb], white blood cell count, platelet count), glucose, lactate dehydrogenase [LDH], lactate, creatinine and alanine aminotransferase [ALT]. The occurence of IMH as the primary endpoint was assessed by cardiac magnetic resonance (CMR) imaging 3 (Interquartile range [IQR]: 2 to 4) days after the index event.

**Results:** In this study 704 STEMI patients (125 women, 17.8%) with a median age of 59 years [IQR: 53–67] were included. IMH was observed in 231 (32.8%) patients. From all admission biomarkers assessed, only hs-cTnT (OR: 1.81, 95% CI 1.30–2.52, $p < 0.001$), Hb (OR: 1.30, 95% CI 1.07–1.58, $p = 0.008$) and LDH (OR: 1.70, 95% CI 1.32–2.19, $p < 0.001$) independently predicted IMH. The addition of Hb and LDH significantly increased the area under the curve (AUC) for the prediction of IMH as compared to hs-cTnT alone (0.74 vs. 0.66, $p < 0.001$). A 3-variable risk score including hs-cTnT, Hb and LDH demonstrated significant predictive value for IMH, allowing stratification into four risk classes (IMH occurred in 14.3% (42/293) of patients in the low-risk group, 30.3% (61/201) in the intermediate-risk group, 59.3% (96/162) in the high-risk group and 66.7% (32/48) in the very high-risk group.

**Conclusion:** An early biomarker approach at hospital admission incorporating hs-cTnT, Hb and LDH significantly improved the prediction of IMH in STEMI patients compared with hs-cTnT alone.

## 13-4

### Quantification of Atrial Fibrillation–Related Imaging Markers Using Spectral Photon-Counting Computed Tomography

**Bilgeri V.[1], Spitaler P.[1], Kindl B.[1], Lacaita P.[1], Barbieri F.[2], Bals L.[3], Tugrul B.[1], Stühlinger M.[1], Widmann G.[1], Dichtl W.[1], Bauer A.[1], Feuchtner G.[1]**

[1]Medizinische Universität Innsbruck, Innsbruck, Austria
[2]Deutsches Herzzentrum der Charite, Berlin, Germany
[3]Tomorrow University of Applied Sciences, Frankfurt am Main, Germany

**Introduction:** Structural remodeling of the cardiac conduction system, including fibrosis and impaired vascular supply, is considered a key contributor to atrial fibrillation (AF). In vivo characterization of these alterations has been limited by the spatial resolution and tissue specificity of conventional imaging techniques. Spectral photon-counting computed tomography (PCCT) enables high-resolution imaging and quantitative tissue characterization, potentially allowing identification of AF-related imaging biomarkers.

**Methods:** This retrospective cohort study included patients referred for clinically indicated PCCT coronary CT angiography (July–December 2025). From 518 screened examinations, 66 patients were analyzed: 33 with documented AF and 33 controls in sinus rhythm (mean age 66.9 ± 12.8 years; 42.4% women). The following PCCT imaging markers were quantified: Sinoatrial (SA)-node artery visibility, origin (right/left/bilateral), and length (score 1–3); cranial interatrial septum (IAS) tissue texture in the SA supply territory using CT attenuation (HU) and spectral iodine concentration (mg/mL); IAS fibrosis, categorized based on CT-density (HU) into a 4-point fibrosis score (fatty to fully fibrous); SA-node density (HU) and iodine concentration; left atrial wall thickness (LAWT) as a marker of remodeling (positive if > 2 mm LAWT). Group comparisons and correlation/regression analyses were performed.

**Results:** Compared with controls, AF patients showed reduced SA-node artery visibility and markedly shorter SA-node arteries (length score lower; $p < 0.001$), while SA-artery origin did not differ ($p = 0.757$). IAS fibrosis was substantially more prevalent in AF: mixed or fibrotic IAS (score 2–4) occurred in 84.8% vs 12.1% of controls ($p < 0.001$), and a fully fibrous IAS in 60.6% vs 3% ($p < 0.001$). IAS attenuation and iodine concentration were higher in AF (median 67 vs –44.8 HU; and 1.8 vs –0.05 mg/mL; both $p < 0.001$). IAS density (HU) strongly correlated with iodine concentration ($r = 0.708$; $p < 0.001$) and was significantly associ-

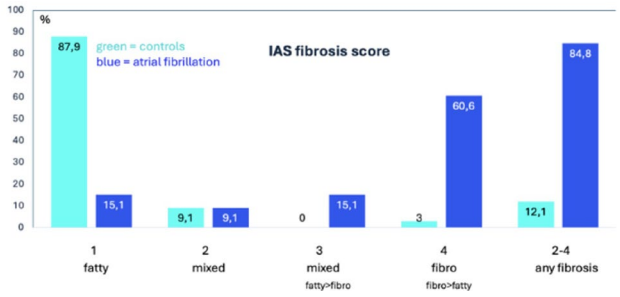


**Fig. 1 | 13-4** Interatrial septum (IAS) fibrosis score in controls vs AF: 1 = fatty (100%) IAS, 2 = mixed (fatty>fibro), 3 = mixed (fibro>fatty) and 4 = fibrous (100%), and group 2–4 (any fibrosis)

ated in linear regression. IAS fibrosis score correlated with SA-node artery length score (r = 0.731; $p < 0.001$). Positive left atrial remodeling (LAWT >2 mm) was linked to higher IAS fibrosis scores, higher IAS HU, and higher IAS iodine concentration (all $p < 0.001$). SA-node density was also higher in AF ($p = 0.014$), with a trend toward higher SA-node iodine concentration.

**Conclusion:** Spectral PCCT enables quantitative assessment of AF-associated imaging markers within the conduction system region. AF was characterized by shorter SA-node arteries and increased IAS density as fibrosis surrogates (higher HU and iodine concentration), supporting an interplay between vascular supply and fibrotic remodeling. These PCCT-derived markers may help identify patients with occult or asymptomatic AF undergoing coronary PCCT angiography for other clinical indications, in whom intensified AF screening may be considered.

## 13-5

### Circadian Dependence of Hemorrhagic Ischemia-Reperfusion Injury in ST-Elevation Myocardial Infarction

**Sandor A.[1], Lechner I.[1], Fischer P.[1], Tiller C.[1], Holzknecht M.[1], Oberhollenzer F.[1], Kaser A.[1], Mayr A.[2], Bauer A.[1], Reindl M.[1], Metzler B.[1], Reinstadler S.[1]**

[1]Universitätsklinik für Innere Medizin III, Kardiologie und Angiologie, Innsbruck, Austria
[2]Universitätsklinik für Radiologie, Innsbruck, Austria

**Introduction:** Circadian regulation of cardiovascular physiology may influence myocardial susceptibility to ischemia-reperfusion injury (IRI) in acute ST-elevation myocardial infarction (STEMI) treated with primary percutaneous coronary intervention (PCI). Patients with a hemorrhagic IRI pattern after PCI face the highest risk of adverse outcome. It remains unknown whether the severity of IRI shows a time-of-day dependence. Aim: To investigate circadian patterns of IRI, based on symptom onset, assessed by cardiac magnetic resonance (CMR), in patients undergoing primary PCI for acute STEMI. Severe IRI was defined by the presence of intramyocardial hemorrhage (IMH) on T2* Mapping.

**Methods:** Patients with first acute STEMI treated with primary PCI at the University Heart Center of Innsbruck between 2015–2024 were included. Symptom onset time was categorized into predefined time-intervals [Model 1: four 6-hour intervals; Model 2: diurnal phase (08:00–15:59) vs nocturnal phase (16:00–07:59); Model 3: on hours (08:00–17:59 on weekdays) vs off hours (18:00–07:59 on weekdays, weekends and holidays)]. CMR for IRI pattern assessment was performed 4 days [Interquartile range (IQR): 3–5] after PCI.

**Results:** A total of 777 patients (140 women, 18%) with a median age of 59 years (IQR: 53–67) were included. IMH was present in 276 (36%) patients. In all three models, symptom onset time was not associated with IMH occurrence [Model 1: ($p = 0.20$); Model 2: 33% vs 37% ($p = 0.25$); Model 3: 34% vs 37% ($p = 0.43$)] or IMH volume (all $p > 0.05$). Furthermore, there was no association between symptom onset time and infarct size (all $p > 0.05$), size of microvascular obstruction (MVO) (all $p > 0.05$) and left ventricular ejection fraction (all $p > 0.05$).

**Conclusion:** Symptom onset was not significantly associated with the presence or severity of IRI in STEMI patients treated with PCI. Our data suggest no evidence for a circadian dependence of hemorrhagic IRI in a contemporary cohort of STEMI patients.

## 13-6

### Sex-Specific Utility of Pulmonary Artery Metrics in Predicting Pulmonary Hypertension and Survival After TAVI: Insights from Advanced CT Imaging

**Schörghofer N.[1], Knapitsch C.[1], Clodi N.[2,1], Hammerer M.[2], Hoppe U.[2], Hergan K.[3], Scharinger B.[1], Boxhammer E.[2]**

[1]Universitätsklinik für Radiologie, Salzburg, Austria
[2]Universitätsklinik für Innere Medizin II, Kardiologie und internistische Intensivmedizin, Salzburg, Austria
[3]Universitätsklinik für Radiologie, Universitätsklinikum Salzburg, Salzburg, Austria

**Introduction:** Pulmonary hypertension (PH) significantly impacts outcomes following transcatheter aortic valve implantation (TAVI), with sex-specific differences suggesting the need for tailored diagnostic and prognostic strategies. This study evaluates the predictive value of computed tomography (CT)-derived main pulmonary artery (MPA) dimensions and their ratios, focusing on their diagnostic accuracy and prognostic relevance in male and female TAVI patients.

**Methods:** A retrospective, single-center analysis of 526 patients (263 male, 263 female) undergoing TAVI was conducted. PH was defined using echocardiographic criteria in accordance

| | MPA | MPA/BSA | MPA/AA |
|---|---|---|---|
| sPAP ≥ 40 mmHg | 29.50 | 16.05 | 0.76 |
| TRVmax ≥ 2.8 m/s | 29.50 | 16.05 | 0.76 |
| TAPSE/sPAP < 0.55 mm/mmHg | 29.50 | 16.05 | 0.77 |

| | MPA | MPA/BSA | MPA/AA |
|---|---|---|---|
| sPAP ≥ 40 mmHg | 29.50 | 18.87 | 0.83 |
| TRVmax ≥ 2.8 m/s | 30.50 | 18.55 | 0.84 |
| TAPSE/sPAP < 0.55 mm/mmHg | 30.50 | 18.55 | 0.91 |

**Fig. 1 | 13-6** Cut-off Values

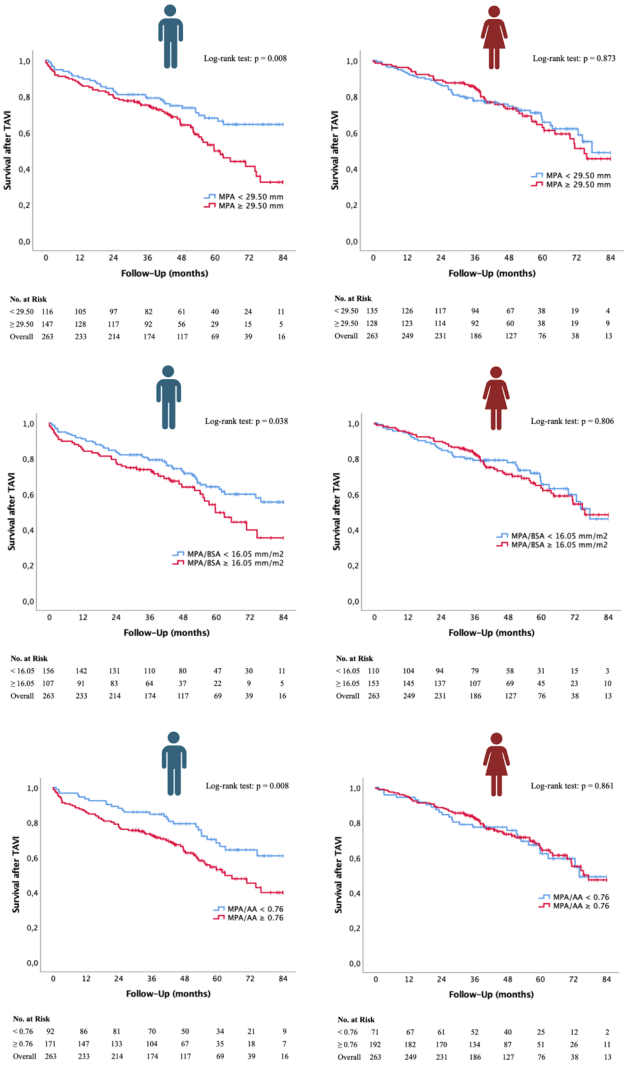


**Fig. 2 | 13-6** Kaplan-Meier Curves

with ESC guidelines. Pre-procedural CT measurements of MPA, ascending aorta (AA), and derived ratios (e. g., MPA/AA) were evaluated. Sex-specific cut-off values were determined using AUROC analyses and validated through Kaplan-Meier survival curves and Cox regression models.

**Results:** MPA and its ratios demonstrated superior diagnostic performance compared to right pulmonary artery (RPA) and left pulmonary artery (LPA) for detecting PH. Non-sex-specific cut-off values were identified as MPA ≥29.50 mm and MPA/AA ≥0.76. Men exhibited stronger associations between elevated MPA or MPA/AA ratios and echocardiographically defined PH. In women, however, the derived cut-off values (MPA ≥30.00 mm and MPA/AA ≥0.86) differed and showed less robust diagnostic utility. Additionally, the MPA/AA ratio was predictive of long-term survival exclusively in males (HR = 1.857, $p = 0.006$), further highlighting the limitations of these parameters in female patients.

**Conclusion:** This study emphasizes the diagnostic value of CT-derived pulmonary artery metrics in predicting PH and survival outcomes in male TAVI patients. Incorporating metrics like the MPA/AA ratio into clinical practice could improve risk stratification in male TAVI candidates, while these parameters showed limited diagnostic utility in women, indicating the need for further research to identify more reliable markers in this group. Tailored approaches should aim to optimize results for both sexes and should be considered for all etiologies of PH.

## 13-7

## Multi-Schallfenster-Doppler-Analyse zur Vermeidung der Unterschätzung des Schweregrades der Aortenklappenstenose

**Stautner B.[1,2,3], Bartholomäus F.[1,2], Merz A.[1,2,3], Ran H.[1,4], Hilgendorf I.[1,2,3], Morris D.[1,2,3], Schneider-Reigbert M.[1,2,3]**

[1]Deutsches Herzzentrum der Charité, Department of Cardiology, Angiology and Intensive Care Medicine, Berlin, Deutschland
[2]Charité – Universitätsmedizin Berlin, corporate member of Freie Universität Berlin and Humboldt-Universität zu Berlin, Berlin, Deutschland
[3]DZHK (German Center for Cardiovascular Research), partner site Berlin, Berlin, Deutschland
[4]Nanjing First Hospital, Nanjing, China, Nanjing, China

**Einleitung:** Die echokardiographische Graduierung der Aortenklappenstenose (AS) beruht wesentlich auf winkelabhängigen Doppler-Parametern wie der maximalen transvalvulären Flussgeschwindigkeit (Vmax) und dem mittleren Druckgradienten (MG). In der klinischen Routine erfolgt die Messung häufig primär aus apikalen Schallfenstern, obwohl Leitlinien die Nutzung mehrerer Fenster empfehlen. Dies birgt das Risiko einer Unterschätzung des Stenosegrades. Ziel dieser prospektiven Studie war es, die Häufigkeit klinisch relevanter Reklassifizierungen durch eine systematische Multi-Schallfenster-Dopplerанalyse zu untersuchen.

**Methoden:** In einer prospektiven Einzelzentrumsstudie wurden konsekutive Patient*innen mit mindestens mittelgradiger AS am Deutschen Herzzentrum der Charité eingeschlossen. Die transthorakale Doppler-Echokardiographie erfolgte systematisch aus apikalen (5-Kammer und 3-Kammer-Blick) und nicht-apikalen Schallfenstern (parasternal, subkostal, suprasternal, per Stiftsonde von rechts-parasternal). Die mittels Continuous-Wave-Doppler gemessene Vmax aus dem apikalen 5-Kammer-Blick wurde mit der maximalen Vmax unter Einbeziehung aller Schallfenster verglichen. Der Vergleich erfolgte mittels Wilcoxon-Vorzeichen-Rang-Test. Zudem wurde der Einfluss auf die Schweregradklassifikation analysiert.

**Resultate:** In der Interimsanalyse von 28 Patient*innen zeigte die Multi-Schallfenster-Analyse signifikant höhere Vmax-Werte als die alleinige apikale Messung ($p = 0{,}011$). In einem Fall (3,6 %) führte dies zu einer Reklassifizierung von mittelgradiger zu hochgradiger AS.

**Schlussfolgerungen:** Die systematische Nutzung mehrerer Schallfenster führt zu höheren gemessenen Vmax-Werten und kann in Einzelfällen eine klinisch relevante Reklassifizierung der AS bewirken. Eine ausschließlich apikale Dopplerakquisition birgt somit das Risiko der Schweregradunterschätzung.

# POSTERSITZUNG 14— RISIKOFAKTOREN, PRÄVENTION, STOFFWECHSEL & LIPIDOLOGIE 1

## 14-1

### Bridging the gap: Real-world eligibility for lipoprotein(a)-targeted therapies in chronic and acute coronary syndrome

**Steinacher E.[1], Bernhard J.[1], Wollmann F.[1], Radl V.[1], Baumer U.[1], Haider P.[1], Hammer A.[1], Hofer F.[1], Kazem N.[1], Lenz M.[1,2], Hemetsberger R.[1], Hengstenberg C.[1], Niessner A.[1,3], Krychtiuk K.[1], Koller L.[1], Speidl W.[1]**

[1]Medizinische Universität Wien, Wien, Austria
[2]Ludwig Bolzmann Institut für Kardiovaskuläre Forschung, Wien, Austria
[3]Klinik Landstraße, Wien, Austria

**Introduction:** Lipoprotein(a) [Lp(a)] is an established causal risk factor for the development and progression of atherosclerotic cardiovascular disease (ASCVD). Multiple phase 3 trials are currently evaluating targeted Lp(a)-lowering therapies using high entry thresholds. However, real-world eligibility in secondary prevention remains limited, and no universally accepted cut-offs exist. The 2025 European Society of Cardiology (ESC) and European Atherosclerosis Society (EAS) guidelines recommend considering Lp(a) ≥ 105 nmol/L as a cardiovascular risk-enhancing factor. [1] The purpose of this study is to evaluate real-world eligibility for emerging Lp(a)-lowering therapies and apheresis in patients with chronic coronary syndrome (CCS) and acute coronary syndrome (ACS), and to determine the association between Lp(a) levels and 5-year cardiovascular outcomes.

**Methods:** Consecutive patients undergoing percutaneous coronary intervention (PCI) at a tertiary care centre between 2010 and 2021 with Lp(a) measured in nmol/L were analysed. Eligibility was assessed according to trial-aligned thresholds (≥ 150, ≥ 175, ≥ 200 nmol/L) and the guideline-recommended risk-enhancing cut-off (≥ 105 nmol/L). Lp(a) apheresis eligibility was evaluated using national Central European criteria (Austria: Lp(a) > 250 nmol/L plus prior revascularization; Germany: Lp(a) > 120 nmol/L plus prior revascularization and LDL cholesterol < 130 mg/dL). Five-year major adverse cardiovascular events (MACE) and target lesion failure (TLF) were endpoints.

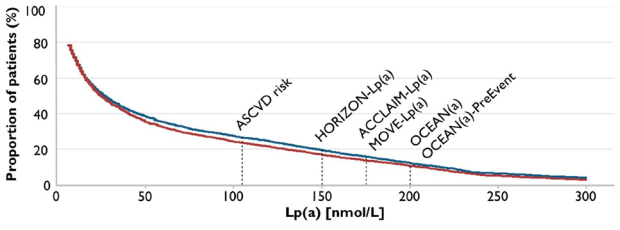


| | Total | CCS | ACS |
|---|---|---|---|
| Lp(a) ≥105 nmol/L [ASCVD risk] | 25.2% | 26.6% | 23.8% |
| Lp(a) ≥150 nmol/L [*HORIZON-Lp(a)*] | 18.4% | 19.7% | 17.1% |
| Lp(a) ≥175 nmol/L [*ACCLAIM-Lp(a), MOVE-Lp(a)*] | 14.8% | 15.9% | 13.7% |
| Lp(a) ≥200 nmol/L [*OCEAN(a), OCEAN(a)-PreEvent*] | 11.6% | 12.4% | 10.7% |
| *Combined apheresis criteria* | | | |
| Lp(a) >250 nmol/L & previous revascularization | 1.8% | 2.4% | 1.3% |
| Lp(a) >120 nmol/L & previous revascularization & LDL cholesterol <130 mg/dL | 6.1% | 9.0% | 3.9% |

Total, CCS, ACS; Eligibility: 0 - 10%, 10 - 15%, 15 - 20%, 20 - 25%

**Fig. 1 | 14-1**

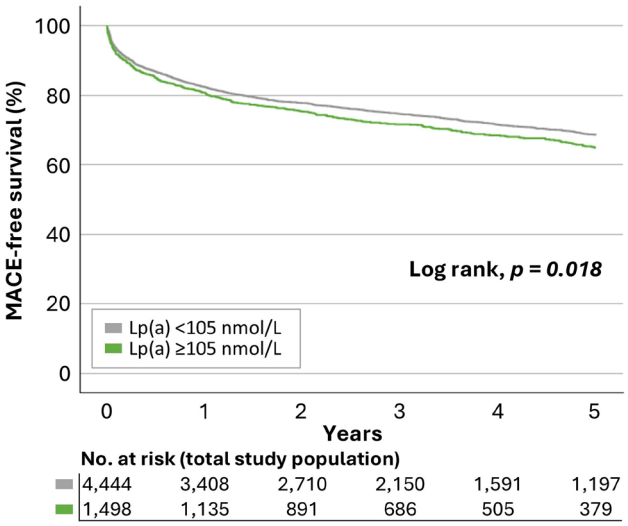


**Fig. 2 | 14-1**

**Results:** Among 5942 PCI patients, median Lp(a) was 26.0 [IQR 9.0–106.0] nmol/L and 1498 (25.2%) patients had Lp(a) levels ≥ 105 nmol/L. Eligibility decreased at higher trial-aligned thresholds: 1094 (18.4%) ≥ 150 nmol/L, 881 (14.8%) ≥ 175 nmol/L, and 688 (11.6%) ≥ 200 nmol/L (Fig. 1). Lp(a) levels were similar in chronic coronary syndrome (CCS; median 28.0 [IQR 9.0–118.5] nmol/L) and acute coronary syndrome (ACS; median 25.0 [IQR 9.0–96.5] nmol/L), with modestly higher values in CCS. National apheresis criteria were fulfilled by 1.8% (Austria) and 6.1% (German) of patients. Over five years, higher Lp(a) was independently associated with an increased risk of MACE (adjusted HR per 1 SD 1.07 [95% CI 1.02–1.12]; $p = 0.008$) and TLF (adjusted HR per 1 SD 1.06 [95% CI 1.01–1.11]; $p = 0.020$), with pronounced associations observed in ACS (Fig. 2).

**Conclusion:** Elevated Lp(a) is highly prevalent in PCI patients and independently associated with adverse 5-year outcomes. While a substantial proportion of patients met thresholds for emerging Lp(a)-lowering therapies, few fulfilled composite apheresis criteria. Systematic Lp(a) testing after PCI may improve risk stratification, identify candidates for emerging therapies, and guide implementation of targeted secondary prevention strategies in routine cardiovascular practice.

## References

1. Mach, F. et al. 2025 Focused Update of the 2019 ESC/EAS Guidelines for the management of dyslipidaemias: Developed by the task force for the management of dyslipidaemias of the European Society of Cardiology (ESC) and the European Atherosclerosis Society (EAS). Eur. Heart J. ehaf190 (2025).

## 14-2

# Therapeutisch relevante Albuminurie im KDIGO Stadium G2: Dokumentations- und Versorgungslücken in einer kardiologischen Kohorte

**Kneist L., Straßmeir M., Voill-Glaninger A., Hasun M., Basic J., Winkler S., Niessner A.**

Klinik Landstraße, 2. Medizinische Abteilung, Wien, Österreich

**Einleitung:** Der demografische Wandel führt zu einer steigenden klinischen Relevanz der altersassoziierten Abnahme der glomerulären Filtrationsrate (eGFR). Während das Kidney Disease: Improving Global Outcomes (KDIGO) Stadium G2 (eGFR 60–89 ml/min/1,73 m²) gerade bei älteren Patient:innen häufig unerkannt bleibt, stellt insbesondere die begleitende Albuminurie (A2/A3) einen unabhängigen Prädiktor für kardiovaskuläre Ereignisse dar. In kardiologischen Patient:innenkollektiven mit hoher Prävalenz von arterieller Hypertonie, Diabetes mellitus und Herzinsuffizienz ist die strukturierte Erfassung früher Stadien der renalen Funktionseinschränkung gemäß KDIGO von besonderer Bedeutung, da sie therapeutische Entscheidungen mit prognostisch relevanten nephroprotektiven Therapien beeinflussen kann. Ziel dieser Analyse war die Evaluierung der Dokumentationsqualität von Nierenfunktion und Albuminurie sowie der leitliniengerechten Umsetzung nephroprotektiver Therapien im KDIGO-Stadium G2, insbesondere bei prognostisch relevanter Albuminurie (A2/A3). [1,2].

*Abbildung 1. Dokumentations- und Versorgungsqualität bei KDIGO Stadium G2A2 und G2A3.*

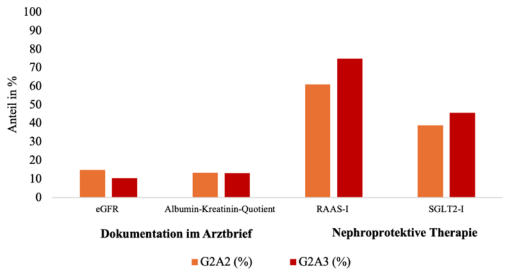


*Anteil der Patient:innen mit dokumentierter eGFR-/UACR-Klassifikation sowie nephroprotektiver Therapie (RAAS-Inhibitoren oder SGLT2-Inhibitoren) bei KDIGO-Stadium G2A2 und G2A3. KDIGO = Kidney Disease: Improving Global Outcomes, eGFR = estimated glomerular filtration rate, RAAS-I = Renin-Angiotensin-Aldosteron-System-Inhibitor, SGLT2-I = Sodium-Glucose Cotransporter-2-Inhibitor, UACR = Albumin-Kreatinin-Quotient.*

**Abb. 1 | 14-2** Dokumentations- und Versorgungsqualität

*Tabelle 1. Baseline-Charakteristika.*

| *Alterskategorien [Jahre]* | Total n=998 | <64 n=345 | 65-74 n=199 | 75-84 n=286 | >84 n=168 |
|---|---|---|---|---|---|
| ***Geschlecht*** | | | | | |
| Männlich, n (%) | 571 (57,2) | 242 (70,1) | 122 (61,3) | 142 (49,7) | 65 (38,7) |
| Weiblich, n (%) | 427 (42,8) | 103 (29,9) | 77 (38,7) | 144 (50,3) | 103 (61,3) |
| ***Laborparameter*** | | | | | |
| eGFR [ml/min/1,73 m²] | 66,3 (41,5 - 88,1) | 86,4 (60,6 - 103,1) | 71,4 (45,9 - 89,2) | 55,1 (37,8 - 75,2) | 45,7 (33,0 - 60,7) |
| UACR [mg/g] | 45,9 (14,7 - 156,0) | 33,0 (9,0 - 147,1) | 45,9 (13,5 - 224,8) | 55,0 (16,7 - 148,7) | 55,4 (19,7 - 185,5) |
| ***Albuminurie-Stadium*** | | | | | |
| A1, n (%) | 410 (41,1) | 162 (47,0) | 80 (40,2) | 114 (39,9) | 64 (38,1) |
| A2, n (%) | 426 (42,7) | 122 (35,4) | 80 (40,2) | 133 (46,5) | 81 (48,2) |
| A3, n (%) | 162 (16,2) | 61 (17,7) | 39 (19,6) | 39 (13,6) | 23 (13,7) |
| ***KDIGO-Klassifikation*** | | | | | |
| G2, n (%) | 302 (30,3) | 95 (27,5) | 73 (36,7) | 98 (34,3) | 36 (21,4) |
| G2A1, n (% von G2) | 144 (47,7) | 47 (49,5) | 40 (54,8) | 42 (42,9) | 15 (41,7) |
| G2A2, n (% von G2) | 120 (39,7) | 31 (32,6) | 25 (34,2) | 45 (45,9) | 19 (52,8) |
| G2A3, n (% von G2) | 38 (12,6) | 17 (17,9) | 8 (11,0) | 11 (11,2) | 2 (5,6) |

*Übersicht über die Baseline-Charakteristika der analysierten Patient:innenkohorte (2025). Insgesamt wurden 998 Patient:innen analysiert, bei denen mindestens eine UACR-Messung bei gleichzeitig bestimmter eGFR vorlag. Die eGFR wurde nach der CKD-EPI-Formel berechnet, die Stadieneinteilung der Nierenfunktion erfolgte gemäß KDIGO-Nomenklatur. Kontinuierliche Variablen werden als Median (Interquartilsabstand, IQR) dargestellt, kategoriale Variablen als Anzahl und Prozentsatz. eGFR = estimated glomerular filtration rate, UACR = Albumin-Kreatinin-Quotient, KDIGO = Kidney Disease: Improving Global Outcomes, CKD-EPI = CHRONIC KIDNEY DISEASE EPIDEMIOLOGY COLLABORATION.*

**Abb. 2 | 14-2** Baseline-Charakteristika

**Methoden:** In dieser retrospektiven, monozentrischen Analyse wurden Patient:innen untersucht, die im Jahr 2025 an unserer Abteilung stationär behandelt wurden. Zur Auswertung wurden 998 Patient:innen herangezogen, bei denen mindestens eine Albumin-Kreatinin-Quotient (UACR)-Messung mit gleichzeitig bestimmter eGFR aus dem standardisierten Aufnahmelabor vorlag. Die eGFR wurde nach der CHRONIC KIDNEY DISEASE EPIDEMIOLOGY COLLABORATION (CKD-EPI)-Formel berechnet; die Stadieneinteilung erfolgte gemäß der KDIGO-Nomenklatur. Bei 302 Patient:innen der Subgruppe mit KDIGO-Stadium G2 wurde die Dokumentation von Diagnosen – insbesondere zur Nierenfunktion und Albuminurie – in den Arztberichten analysiert. Die Auswertung der verordneten nephroprotektiven Therapien mit Renin-Angiotensin-Aldosteron-System-Inhibitoren (RAAS-Inhibitoren) und Sodium-Glucose-Cotransporter-2-Inhibitoren (SGLT2-Inhibitoren) erfolgte ausschließlich auf Grundlage der Entlassungs- bzw. Verlegungsmedikation nach klinischer Stabilisierung ($n = 274$). Zusätzlich wurde in der Subgruppe G2A2/G2A3 der Zusammenhang zwischen begleitender Infektion und nephroprotektiver Entlassungsmedikation deskriptiv analysiert, um potenzielle Verzerrungen durch akute Kontraindikationen („Sick-Day"-Situationen) zu berücksichtigen.

**Resultate:** Die Studienkohorte bestand zu 57,2 % aus Männern; 65,4 % waren älter als 64 Jahre. Die Nierenfunktion nahm über alle Altersgruppen hinweg progressiv ab: Die mediane eGFR sank von 86,4 ml/min/1,73 m² bei Patient:innen unter 64 Jahren auf 45,7 ml/min/1,73 m² bei Patient:innen über 84 Jahren. Gleichzeitig stieg der UACR von 33,0 mg/g auf 55,4 mg/g. 19,7 % der Patient:innen befanden sich im KDIGO-Stadium G1, 30,3 % in G2, 14,7 % in G3a, 13,6 % in G3b, 8,1 % in G4 und 4,3 % in G5. In der Subgruppenanalyse des G2-Stadiums wiesen 52,3 % eine mäßig (G2A2) bis stark erhöhte (G2A3) Albuminurie auf (Tab. 1). Auffällig war ein hoher Anteil an Infektionen unter den Aufnahmediagnosen: Pneumonien wurden bei 19,6 %, COPD-Exazerbationen bei 6,3 % und Harnwegsinfekte bei 1,9 % der Patient:innen beschrieben. In der Subgruppe G2A2/G2A3 erfolgte die Dokumentation der eGFR in 14,6 % und des UACR in 13,3 % der Fälle (Abb. 1); eine vollständige KDIGO-Klassifikation lag bei 10,1 % vor. 72,7 % der Patient:innen dieser Subgruppe erhielten eine nephroprotektive Therapie, davon 63,6 % einen RAAS-Inhibitor und 40,2 % einen SGLT2-Inhibitor (Abb. 1); 27,3 % wurden jedoch weder mit einem RAAS-Inhibitor noch mit einem SGLT2-Inhibitor entlassen oder verlegt. Bei zusätzlich diagnostizierter Infektion erhielten in dieser Subgruppe 64,7 % eine nephroprotektive Therapie, verglichen mit 77,8 % bei Patient:innen ohne Infektion.

**Schlussfolgerungen:** In dieser kardiologischen Studienkohorte zeigte sich bei über der Hälfte der Patient:innen im KDIGO-Stadium G2 eine prognostisch relevante Albuminurie (G2A2/G2A3) mit erhöhtem kardiovaskulärem Risiko. Dennoch war die Dokumentation der Nierenfunktion, insbesondere der Albuminurie, unzureichend; eine vollständige KDIGO-Klassifikation erfolgte nur selten. Obwohl die Mehrheit der Patient:innen eine nephroprotektive Therapie erhielt, verblieb mehr als ein Viertel ohne RAAS- oder SGLT2-Inhibition. Da die Analyse auf der Entlassungs- bzw. Verlegungsmedikation nach klinischer Stabilisierung basierte, lässt sich die Versorgungslücke nicht vollständig durch akute Kontraindikationen erklären. Die Ergebnisse deuten auf eine potenziell relevante Versorgungslücke in einem kardiovaskulären Risikokollektiv hin. Eine standardisierte Integration der KDIGO-Klassifikation in kardiologische Entlassungsprozesse könnte die Risikostratifizierung sowie die Umsetzung leitliniengerechter nephroprotektiver Therapien nachhaltig verbessern.

## Literatur


1. Herrington WG, Judge PK, Grams ME, Wanner C. Chronic kidney disease. Lancet. 2026;407(10523):90–104.
2. Yaqoob K, Naderi H, Thomson RJ, et al. Prognostic impact of albuminuria in early-stage chronic kidney disease on cardiovascular outcomes: a cohort study. Heart. 2025;111(11):506–512.


## 14-3

## Migrationshintergrund und sozioökonomischer Status im Zusammenhang mit KHK Ausprägung bei Patienten mit chronischem Koronarsyndrom


**Straßmeir M., Hasun M., Kneist L., Niessner A.**

Klinik Landstraße, Wien, Österreich



**Einleitung:** Migrationshintergrund und sozioökonomisch benachteiligter Status des Wohnumfelds stehen im Zusammenhang mit Unterschieden in der Morbidität und Mortalität bei koronarer Herzkrankheit (KHK). Es bleibt jedoch unklar, ob dabei der Migrationshintergrund oder der sozioökonomische Status (SES) diese Unterschiede in erster Linie erklärt. (1,2) Ziel dieser Arbeit war es, die unabhängigen Assoziationen von Migrationshintergrund aus einer Region mit hohem und sehr hohem Risiko nach ESC-Klassifikation und dem SES auf Bezirksebene mit (i) prognostisch relevanter Koronaranatomie und (ii) mindestens einer funktionell signifikanten Stenose bei elektiver Koronarangiographie zu untersuchen.

**Methoden:** Die Primäranalysen erfolgten im vordefinierten Primärkollektiv mit elektiver Koronarangiographie. Die Migrationsgruppe wurde definiert als Herkunft aus Regionen, die von der ESC mit hohem und sehr hohem Risiko bewertet wurden. (3) Verglichen wurde mit Österreicher:innen ohne Migrationshintergrund. Aus der Analyse ausgeschlossen wurden demnach Patient:innen mit Migrationshintergrund aus Regionen mit niedrigem oder moderatem Risiko sowie Regionen, die von der ESC nicht klassifiziert wurden. Der SES auf Bezirksebene wurde anhand offizieller Einkommens- und Arbeitslosigkeitsdaten der jeweiligen Bezirke ermittelt und in Tertile eingeteilt. Der primäre Endpunkt war das Vorhandensein einer prognostisch relevanten KHK-Anatomie nach Definition in den ESC-Leitlinien (Stenose des linken Hauptstamms ≥ 50 %, Dreigefäßerkrankung mit ≥ 70 % Stenose in allen drei Hauptgefäßen oder Zwei- bzw. Eingefäßerkrankung mit Stenose der proximalen LAD ≥ 70 %; Seitenäste ausgeschlossen). (4) Der sekundäre Endpunkt war das Vorhandensein mindestens einer funktionell signifikanten Stenose (fraktionelle Flussreserve ≤ 0,80 und/oder visuelle Stenose ≥ 90 % in einem großen epikardialen Gefäß; Seitenäste ausgeschlossen). Logistische Regressionsmodelle wurden a priori adjustiert für Alter, Geschlecht, Diabetes mellitus und arterielle Hypertonie.

**Resultate:** In der Primärkohorte ($n$ = 476) lag bei 47 Patient:innen (9,9 %) eine prognostisch relevante KHK-Anatomie vor, bei 127 Fällen (26,7 %) lag mindestens eine funktionell signifikante Stenose vor. Die Patient:innen in der Migrantengruppe waren mit 63,7 ± 9,9 Jahren jünger als die in der Gruppe ohne Migrationshintergrund (67,8 ± 10,3 Jahre, $p$ < 0,001) und hatten häufiger arterielle Hypertonie (91,5 % vs. 84,0 %, $p$ = 0,034) und häufiger Diabetes mellitus (45,4 % vs. 29,5 %, $p$ = 0,001). Unadjustiert zeigten sich keine signifikanten Unterschiede für die beiden Gruppen: prognostisch relevante KHK-Anatomie 10,4 % in der Gruppe der Österreicher und in 8,5 % der Migranten ($p$ = 0,533) und mindestens eine funktionell signifikante Stenose in 24,3 % der Österreicher und 30,5 % der Migranten ($p$ = 0,171). Nach Bereinigung für Geschlecht, Alter, arterielle Hypertonie und Diabetes mellitus zeigte sich kein unabhängiger Zusammenhang des Migrationshintergrundes für prognostisch relevante KHK-Anatomie (aOR: 0,78 [95 % KI 0,38–1,63; $p$ = 0,516]) oder funktionell signifikante Stenose (aOR: 1,28 [95 % KI 0,79–2,06; $p$ = 0,321]). Bezirks-SES war für $n$ = 382 verfügbar (hohes Tertil $n$ = 26) und zeigte in adjustierten Modellen keinen unabhängigen Zusammenhang mit dem primären (global $p$ = 0,585) oder sekundären Endpunkt (global $p$ = 0,903). Auch in Modellen mit gleichzeitiger Berücksichtigung von Migrationshintergrund und SES zeigten sich keine unabhängigen Assoziationen von Migrationshintergrund oder SES mit beiden Endpunkten.

**Schlussfolgerungen:** In den vorgestellten Analysen zeigte sich kein unabhängiger Zusammenhang zwischen einem Migrationshintergrund aus einer Region mit höherem Risiko als Österreich nach ESC-Klassifikation bzw. dem SES des Wohnbezirks und den anatomischen und funktionellen Endpunkten. Die Interpretation ist jedoch durch die geringe Ereigniszahl, strenge Endpunktdefinition, kleine Subgruppen (insbesondere hohes SES-Tertil) und potenziellen Selektionsbias der Kohorte (u. a. differenzielle Teilnahmewahrscheinlichkeit) eingeschränkt. Es sollte daher eine vollständige Auswertung des Gesamtkollektivs erfolgen, um die Ergebnisse zu bestätigen.


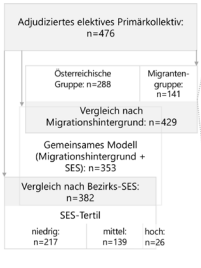


| | Österreicher:innen (n=288) | Migranten (n=141) | p-Wert |
|---|---|---|---|
| Merkmale | | | |
| Alter (Jahre), Mittelwert ± SD (n=287/141) | 67.8 ± 10.3 | 63.7 ± 9.9 | <0.001 |
| Männlich, n (%) | 197 (68.4) | 95 (67.4) | 0.830 |
| Diabetes mellitus, n (%) | 85 (29.5) | 64 (45.4) | 0.001 |
| Arterielle Hypertonie, n (%) | 242 (84.0) | 129 (91.5) | 0.034 |
| Unadjustierte Endpunkte | | | |
| Prognostisch relevante KHK-Anatomie, n (%) | 30 (10.4) | 12 (8.5) | 0.533 |
| Funktionell signifikante Stenose, n (%) | 70 (24.3) | 43 (30.5) | 0.171 |

Abbildung 1: Kohortenfluss und Analysesubgruppen mit Baseline- und unadjustierten Endpunktvergleichen zwischen Österreicher:innen und Patient:innen mit Migrationshintergrund. Angaben als Mittelwert ± Standardabweichung (SD) oder n (%); p-Werte aus Gruppenvergleichen.

**Abb. 1 | 14-3** Kohortenfluss und Analysesubgruppen mit Baseline- und unadjustierten Endpunktvergleichen zwischen Österreicher:innen und Patient:innen mit Migrationshintergrund. Angaben als Mittelwert ± Standardabweichung (SD) oder $n$ (%); $p$-Werte aus Gruppenvergleichen.]

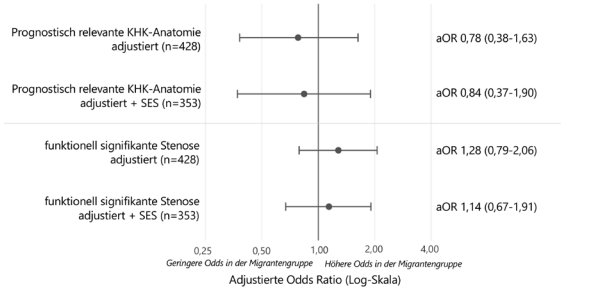


Abbildung 2: Adjustierte Odds Ratios (aOR) mit 95%-Konfidenzintervallen für Migrationsgruppe versus österreichische Referenzgruppe. Adjustiertes Modell: Alter, Geschlecht, Diabetes mellitus, arterielle Hypertonie (N=428); „+ SES" zusätzlich adjustiert für Bezirks-SES-Tertil (N=353). Die vertikale Linie markiert aOR=1 (Log-Skala).

**Abb. 2 | 14-3** Adjustierte Odds Ratios (aOR) mit 95 %-Konfidenzintervallen für Migrationsgruppe versus österreichische Referenzgruppe. Adjustiertes Modell: Alter, Geschlecht, Diabetes mellitus, arterielle Hypertonie ($N$ = 428); "+ SES" zusätzlich adjustiert für Bezirks-SES-Tertil ($N$ = 353). Die vertikale Linie markiert aOR = 1 (Log-Skala)]

## Literatur

1. Nouraei H, Qiu F, Haldenby O, et al. J Am Heart Assoc. 2025;14:e37534. https://doi.org/10.1161/JAHA.124.037534.
2. Sundquist K, Malmström M, Johansson SE. J Epidemiol Community. Health. 2004;58:71–7. https://doi.org/10.1136/jech.58.1.71.
3. Hageman S, Pennells L, Ojeda F, et al. Eur Heart J. 2021;42:2439–54. https://doi.org/10.1093/eurheartj/ehab309.
4. Vrints C, Andreotti F, Koskinas KC, et al. Eur Heart J. 2024;45:3415–537. https://doi.org/10.1093/eurheartj/ehae177.


## 14-4

## The extreme risk category: prevalence, treatment strategies, and real-world attainment of LDL-C < 40 mg/dL in patients with polyvascular disease


**Wollmann F., Bernhard J., Hengstenberg C., Speidl W., Krychtiuk K.**

Medizinische Universität Wien, AKH, Universitätsklinik für Innere Medizin II, Klinische Abteilung für Kardiologie, Wien, Austria


**Introduction:** Patients presenting with atherosclerotic cardiovascular disease (ASCVD) frequently have involvement of multiple vascular beds [1]. Polyvascular arterial disease—atherosclerosis in two or more arterial territories—is consistently associated with an increased risk of major adverse cardiovascular events compared to monovascular disease[2]. Therefore, the 2025 Focused Update of the 2019 ESC/EAS Guidelines for the management of dyslipidaemias introduced an "extreme-risk" category recommending LDL-C targets < 40 mg/dL in such patients [3].

**Methods:** To evaluate prevalence, treatment strategies and real-world attainment of LDL-C < 40 mg/dL in patients with polyvascular ASCVD. Methods: We included all outpatients from a prospective tertiary lipid clinic registry between August 2016 and February 2026. Patients with polyvascular disease were defined as presence of coronary artery disease (CAD) and documented atherosclerotic disease in ≥ 1 additional arterial bed (cerebrovascular and/or peripheral). LDL-C target attainment and lipid-lowering therapy at the time of LDL-C measurement were noted.

**Results:** A total of 193 patients (12.0%) of our cohort ($n = 1605$) had polyvascular disease. 119 patients (61.7%) had cerebrovascular disease, 51 (26.4%) had peripheral arterial disease and 23 (11.9%) had both cerebrovascular and peripheral arterial disease in addition to CAD. Of 156 patients with polyvascular disease with complete LDL-C follow-up, 34.6% ($n = 54$) achieved a target LDL-C < 40 mg/dL. In patients with target goal attainment, the most frequently used treatment regimen was triple therapy consisting of high intensity statin, ezetimibe and a PCSK9 inhibitor (64.8%), followed by dual therapy with statin plus ezetimibe (9.2%). LDL-C levels differed significantly by treatment regimen ($p < 0.001$, partial $\eta^2 = 0.13$), with the lowest levels achieved in triple therapy (statin + ezetimibe + PCSK9 inhibitor: mean 35.8 mg/dL, standard deviation (SD) 31.1 mg/dl overall; mean 25.6 mg/dL, SD 16.5 mg/dl in polyvascular patients). Polyvascular status itself did not influence LDL-C levels ($p = 0.86$) and did not modify treatment response (interaction $p = 0.44$).

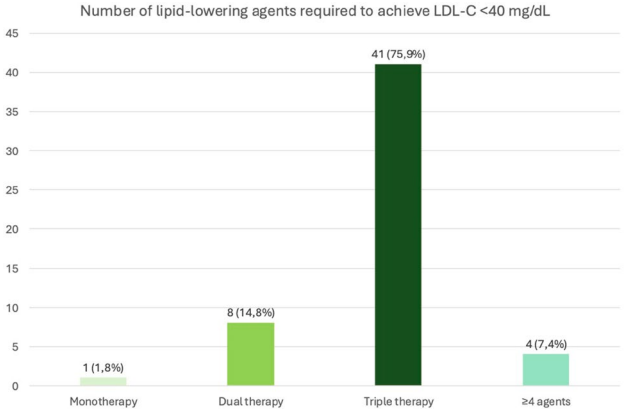


**Fig. 1 | 14-4** Number of agents used for LDL-C target achievement

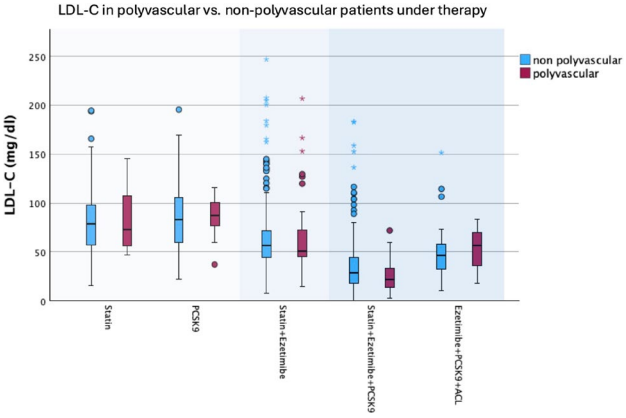


**Fig. 2 | 14-4** LDL-C under lipid lowering therapy

**Conclusion:** In this real-world cohort from a tertiary lipid outpatient clinic, one third of patients with polyvascular atherosclerotic disease achieved the ESC/EAS extreme-risk LDL-C target of < 40 mg/dL. Target attainment required intensive combination therapy in most cases, mainly with high-intensity statin therapy, ezetimibe and a PCSK9 inhibitor. Our results underscore the therapeutic complexity of this extreme-risk population and the need for triple therapy in almost all patients.


## References

1. Steg PhG, Bhatt DL, Wilson PWF, D'Agostino R, Ohman EM, Röther J, u.a. One-Year Cardiovascular Event Rates in Outpatients With Atherothrombosis. JAMA. 21. März 2007;297(11):1197–206. https://doi.org/10.1001/jama.297. Nov. 1197
2. Gutierrez JA, Mulder H, Jones WS, Rockhold FW, Baumgartner I, Berger JS, u.a. Polyvascular Disease and Risk of Major Adverse Cardiovascular Events in Peripheral Artery Disease: A Secondary Analysis of the EUCLID Trial. JAMA Netw Open. 30. November 2018;1(7):e185239. https://doi.org/10.1001/jamanetworkopen.2018.5239
3. Mach F, Koskinas KC, Roeters Van Lennep JE, Tokgözoğlu L, Badimon L, Baigent C, u.a. 2025 Focused Update of the 2019 ESC/EAS Guidelines for the management of dyslipidaemias. European Heart Journal. 7. November 2025;46(42):4359–78. https://doi.org/10.1093/eurheartj/ehaf190

## 14-5

### NT-proBNP vs SCORE2-Diabetes for Cardiovascular Risk Prediction in Type 2 Diabetes

**Prausmüller S., Weidenhammer A., Arfsten H., Spinka G., Bartko P., Hengstenberg C., Pavo N., Hülsmann M.**

Medical University of Vienna, Department of Internal Medicine, Division of Cardiology, Wien, Austria

**Introduction:** Cardiovascular disease (CVD) is the leading cause of morbidity and mortality in patients with type 2 diabetes mellitus (T2 DM). The recently introduced SCORE2-Diabetes model was developed to estimate 10-year cardiovascular risk specifically in diabetic patients. NT-proBNP is an established biomarker with strong prognostic value for cardiovascular outcomes. This study aimed to compare the predictive performance of SCORE2-Diabetes and NT-proBNP for estimating 10-year cardiovascular mortality in patients with T2 DM.

**Methods:** A prospective registry enrolled patients with T2 DM from four diabetes outpatient clinics between December 2005 and January 2010. Patients aged 40–69 years without established CVD and with complete data were included. SCORE2-Diabetes risk estimates were calculated according to the original algorithm. NT-proBNP levels were measured from fasting blood samples. The primary endpoint was 10-year cardiovascular mortality obtained from the Austrian Death Registry. Associations were assessed using Cox regression and Kaplan Meier analysis. Predictive performance was evaluated using C-statistics.

**Results:** A total of 958 patients were included (median age 60 years; 46% female). During the 10-year follow-up, 53 patients (6%) died from cardiovascular causes. Both SCORE2-Diabetes and NT-proBNP were significantly associated with cardiovascular mortality. For SCORE2-Diabetes analyzed as a continuous variable, the hazard ratio (HR) was 1.08 (95% CI 1.05–1.11; $p<0.001$). NT-proBNP (log-transformed) was also strongly associated with cardiovascular mortality (HR 2.91, 95% CI 2.25–3.76; $p<0.001$) (Table 1). Fig. 1 graphically illustrates the association of SCORE2-Diabetes and NT-proBNP risk on cardiovascular mortality for different strata. Discriminatory performance was comparable between NT-proBNP and SCORE2-Diabetes (C-index 0.75 vs. 0.72; $p=0.237$).

**Conclusion:** Both SCORE2-Diabetes and NT-proBNP were significantly associated with 10-year cardiovascular mortality in patients with T2 DM and demonstrated comparable predictive performance. These findings suggest that NT-proBNP, as a simple biomarker-based approach, may provide risk stratification similar to the more complex SCORE2-Diabetes model. Incorporating NT-proBNP into routine clinical assessment may therefore facilitate efficient cardiovascular risk evaluation in patients with T2 DM.

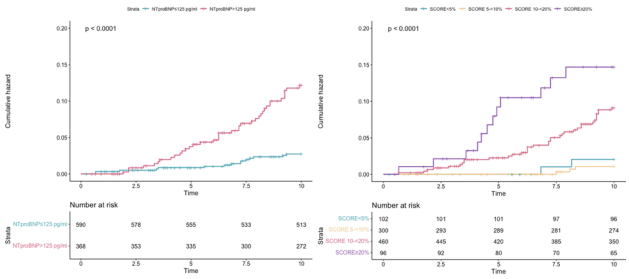


**Fig. 1 | 14-5** Kaplan–Meier curves showing the cumulative incidence of cardiovascular death for NT-proBNP (cut-off: 125 pg/ml) (left), and SCORE2-Diabetes (cut-off: <5%, 5–<10%, 10–<20%, ≥20%) (right)]

**10-y Cardiovascular death**

| | HR [95% CI] | P |
|---|---|---|
| **SCORE2-Diabetes, %** | - | - |
| **<5%** | reference | - |
| **5 - <10%** | 0.52 (0.09 to 3.12) | 0.475 |
| **10 - <20%** | 4.44 (1.07 to 18.43) | 0.040 |
| **≥20%** | 7.71 (1.73 to 34.46) | 0.007 |
| **SCORE2-Diabetes, %** | 1.08 [1.05 to 1.11] | <0.001 |
| **NT-proBNP, pg/ml** | - | - |
| **≤ 125 pg/ml** | reference | - |
| **> 125 pg/ml** | 4.37 [2.41 to 7.95] | <0.001 |
| **NT-proBNP, pg/ml*** | 2.91 [2.25 to 3.76] | <0.001 |

* Refers to log-transformed NT-proBNP

**Fig. 2 | 14-5** Association of 10-Year Cardiovascular Mortality with NT-proBNP and SCORE2-Diabetes, respectively]

## 14-6

### Lipid goal attainment and treatment intensification in oncological versus non-oncological patients undergoing percutaneous coronary intervention

**Pogran E.[1], Peterz P.[2], Hildebrandt T.[2], Zweiker D.[1], Huber K.[3,4,5], Jäger B.[6,2]**

[1]

[3].Medizinische Abteilung für Kardiologie und Intensivmedizin, Klinik Ottakring, Wien, Austria
[2]Sigmund Freud PrivatUniversität Wien, Wien, Austria
[3]Medical Private University Burgenland (MPUB), Pinkafeld/Oberwart, Austria
[4]Austrian Heart Foundation, Wien, Austria
[5]Ludwig Boltzmann Institute for Cardiovascular Research, Wien, Austria
[6]

[3].medizinische Abteilung für Kardiologie und Intensivmedizin, Klinik Ottakring, Wien, Austria

**Introduction:** Patients with malignancy frequently have concurrent cardiovascular risk factors and undergo percutaneous coronary intervention (PCI). Whether oncological history influences lipid-lowering therapy (LLT) practices and achievement of guideline-recommended lipid targets remains insufficiently characterized. European registries have documented substantial treatment gaps in lipid management, but data specifically addressing oncological patients after PCI are lacking (1–3). Aim of this study was to compare lipid profiles, LLT strategies, treatment intensification during hospitalization, and LDL-cholesterol (LDL-C) goal attainment between oncological and non-oncological patients undergoing PCI, stratified by a history of high-risk atherosclerotic cardiovascular disease (prior ASCVD).

**Methods:** In this single-centre retrospective study, consecutive patients undergoing PCI with stent implantation (2022–2023) were stratified by oncological history (active malignancy or history of oncologic diagnosis) and prior ASCVD. LDL-C target was defined as <55 mg/dL per 2019 ESC/EAS guidelines. In the prior ASCVD subgroup, equivalence of lipid target non-achievement was assessed using risk difference (RD) with Newcombe 90% confidence intervals (CI) and a predefined margin of +/–10 percentage points. Baseline LLT was compared within each stratum. As all post-PCI patients qualify as very high-risk ASCVD, LLT intensification and combination therapy at dis-

**Patients with prior ASCVD**

| | Oncological (n=56) | Non-Oncological (n=409) | p-value |
|---|---|---|---|
| Baseline LDL-C, mg/dL, median (IQR) | 63.1 (56.8) | 59.6 (50.2) | ns |
| **LDL-C goal achievement, n (%)** | 19/56 (33.9%) | 118/409 (28.9%) | |
| Adjusted OR | 1.09 (95% CI 0.56–2.12) | | ns |
| **Lipid-Lowering Therapy** | | | |
| High-intensity statin at admission, n (%) | 9/53 (17.0) | 128/359 (35.7) | **0.007** |
| Combination therapy (statine+ezetimibe) at admission, n (%) | 5/55 (9.1) | 61/386 (15.8) | ns |

**Patients without prior ASCVD**

| | Oncological (n=64) | Non-Oncological (n=603) | p-value |
|---|---|---|---|
| Baseline LDL-C, mg/dL, mean (±SD) | 64.2 (±44.4) | 104.6 (±31.6) | **< 0.001** |
| **Lipid-Lowering Therapy** | | | |
| High-intensity statin at admission, n (%) | 10/63 (15.9) | 57/469 (12.2) | ns |
| Combination therapy (statine+ezetimibe) at admission, n (%) | 5/52 (9.6) | 19/432 (4.4) | ns |

**Entire post-PCI cohort**

| Discharge Therapy | Oncological (n=150) | Non-Oncological (n=1145) | p-value |
|---|---|---|---|
| High-intensity statin at discharge, n (%) | 90/142 (63.4) | 796/1121 (71.0) | ns |
| Combination therapy at discharge, n (%) | 31/150 (20.7) | 404/1145 (35.3) | **< 0.001** |
| LLT intensification, n (%) | 105/128 (82.0) | 779/1024 (76.1) | ns |

**Table.** LDL-c values, Lipid Target Non-Achievement and LLT Intensification: Oncological vs Non-Oncological Patients

*LDL-C = low-density lipoprotein cholesterol; LLT = lipid-lowering therapy; ASCVD = atherosclerotic cardiovascular disease; CI = confidence interval; OR = odds ratio; ns = not significant.Adjusted OR from logistic regression including age and high-intensity statin therapy.*

**Fig. 1 | 14-6**

charge were analysed in the entire cohort. Group comparisons used Fisher's exact test. Exploratory logistic regression adjusted for age and high-intensity statin therapy.

**Results:** Among 1314 consecutive patients, 647 had prior ASCVD. In the ASCVD subgroup with available LDL-C ($n=465$), lipid target non-achievement did not differ significantly between oncological (19/56, 33.9%) and non-oncological patients (118/409, 28.9%; RD +5.1 percentage points, Newcombe 90% CI −5.1 to +16.6, $p=0.811$ after adjustment). Oncological patients with prior ASCVD were less frequently treated with high-intensity statins at baseline (9/53, 17.0% vs 128/359, 35.7%; $p=0.007$). Among patients without prior ASCVD, oncological patients had significantly lower baseline LDL-C (64.2 ± 44.4 vs 104.6 ± 31.6 mg/dL, $p<0.001$). In the entire post-PCI cohort, LLT intensification during hospitalization was comparable between oncological and non-oncological patients (105/128, 82.0% vs 779/1024, 76.1%; $p=0.149$). However, oncological patients were discharged with significantly less combination therapy (31/150, 20.7% vs 404/1145, 35.3%; $p<0.001$) and showed a trend toward lower high-intensity statin use at discharge (90/142, 63.4% vs 796/1121, 71.0%; $p=0.065$).

**Conclusion:** Despite comparable rates of LLT intensification during hospitalization, oncological patients undergoing PCI were discharged with significantly less combination lipid-lowering therapy ($p<0.001$). These findings suggest therapeutic inertia specifically regarding combination therapy at the cardio-oncology interface, highlighting an actionable treatment gap in secondary prevention.

## References


1. K.K. Ray et al., „EU-Wide Cross-Sectional Observational Study of Lipid-Modifying Therapy Use in Secondary and Primary Care: the DA VINCI study," Eur. J. Prev. Cardiol., vol. 28, no. 11, pp. 1279–1289, Nov. 2021, https://doi.org/10.1093/EURJPC/ZWAA047.
2. ESC 365 – LDL-C goal achievement and lipid-lowering therapy in patients by atherosclerotic cardiovascular disease subtype: the SANTORINI study https://esc365.escardio.org/presentation/251972?query=santorini%20ray. Zugegriffen: 14. Jan. 2024.
3. M. Arca et al., „LDL-cholesterol goal attainment with ezetimibe and bempedoic acid in patients at high and very-high cardiovascular risk: A simulation study in the Italian cohort of the SANTORINI study: A simulation study in the SANTORINI Italian cohort," European Atherosclerosis Journal, vol. 3, no. 3, pp. 57–66, Dec. 2024, doi: 10.56095/EAJ.V3I3.76.


## 14-7

## Remnant-Cholesterin als Prädiktor für kardiovaskuläre Mortalität bei Patienten mit peripherer arterieller Verschlusskrankheit oder Koronarer Herzkrankheit


**Paul T.**[1,2]

[1]Medizinische Universität Wien, Wien, Österreich
[2]VIVIT Feldkirch, Feldkirch, Österreich


**Einleitung:** Atherosklerotische kardiovaskuläre Erkrankungen (ASCVD) stellen die größte Ursache für Morbidität und Mortalität weltweit dar. Rezente Studien konnten Remnant-Cholesterin (RC) als Indikator für cardiovascular mortality, all-cause mortality und dem Auftreten von major adverse cardiovascular events (MACE) identifizieren. Weiter gibt es Hinweise auf einen kausalen Effekt zwischen RC und dem Risiko der Entwicklung einer peripheren arteriellen Verschlusskrankheit (paVK). Das Ziel dieser Studie war es, Remnant-Cholesterin (RC) als Prädiktor für kardiovaskuläre Mortalität bei Patienten mit peripherer arterieller Verschlusskrankheit (paVK) zu evaluieren und Unterschiede in der prognostischen Relevanz im Vergleich mit Patienten mit Koronarer Herzkrankheit (KHK) aufzuzeigen. Zudem wurde analysiert ob ein Zusammenhang zwischen RC und kardiovaskulärer Mortalität nach Adjustierung für etablierte Risikoparameter atherosklerotisch kardiovaskulärer Erkrankungen (ASCVD) besteht.

**Methoden:** Bei der vorliegenden Studie handelt es sich um eine prospektive Kohortenstudie. Es wurden 1447 Patienten mit angiographisch gesicherter KHK sowie 481 Patienten mit sonographisch gesicherter peripherer arterieller Verschlusskrankheit eingeschlossen. Die Nachbeobachtungsperiode umfasste im Mittel 11 Jahre. Zu Studienbeginn wurden Blutproben unter strikt nüchternen Bedingungen entnommen. Das Lipidprofil umfasste Gesamtcholesterin, Triglyceride, und direkt gemessenes LDL-C und HDL-C. Remnant-Cholesterin wurde berechnet, indem LDL-C und HDL-C vom Gesamtcholesterin subtrahiert wurden.

**Resultate:** Remnant-Cholesterin konnte nach Adjustierung für gängige kardiovaskuläre Risikofaktoren als Prädiktor für kardiovaskuläre Mortalität in der Gesamtkohorte (HR: 1,25 [1,11–1,42], $p<0,001$) und der KHK-Kohorte (HR: 1,26 [1,10–1,44], $p<0,001$) beschrieben werden. In der paVK-Kohorte (HR 1,13 [0,83–1,54], $p=0,450$) ließ sich Remnant-Cholesterin nicht als Prädiktor für kardiovaskuläre Mortalität nachweisen. In den Subgruppenanalysen wurde dieses Ergebnis bestätigt. Bei Männern und Frauen mit KHK wurde ein signifikanter Zusammenhang zwischen Remnant-Cholesterin und kardiovaskulärer Mortalität nachgewiesen, bei den Männern und Frauen mit paVK jedoch nicht.

**Schlussfolgerungen:** Remnant-Cholesterin konnte nach Adjustierung für gängige Risikofaktoren als unabhängiger Prädiktor für kardiovaskuläre Mortalität bei Patienten mit bekannter Koronarer Herzkrankheit bestätigt werden. Eine signifikante Risikoerhöhung der kardiovaskulären Mortalität durch Remnant-Cholesterin konnte bei Patienten mit sonographisch gesicherter paVK nach Adjustierung für geläufige kardiovaskuläre Risikofaktoren, nicht nachgewiesen werden. Remnant-Cholesterin stellte somit in dieser Arbeit keinen Prädiktor für kardiovaskuläre Mortalität bei Patienten mit bekannter paVK dar.

# POSTERSITZUNG 15—SPOTLIGHT TOPICS

## 15-1

### Prescription frequency of heat-vulnerability increasing drugs in Austria

**Abou El-Atta H.[1], Stöllberger C.[2], Lehmann D.[1], Quinton T.[2]**

[1]Klinik Landstrasse, Wien, Austria
[2]Institut Gesünder Leben, Wien, Austria

**Introduction:** Climate change is increasing the frequency, intensity, and duration of heat extremes, putting more individuals, communities, and health systems at risk. Vulnerability to heat-related illnesses may be increased by certain drugs due to various mechanisms. The central thermoregulation may be affected, sweating or dermal circulation may be impaired, water excretion may be increased by diuretics, thus leading to dehydration, thirst may be impaired by drugs, acting on the renin-angiotensin system, elevated ambient temperature increases dermal circulation and thus may elevate serum levels of transdermal or subcutaneously applied drugs. Prescription frequency of these heat-vulnerability increasing drugs (HVID) is largely unknown. Aim of the study was to assess the prescription frequency of HVID in Austria.

**Table 1 | 15-1** Frequently prescribed heat-vulnerability increasing drugs in Austria 2024

| Drug | ATC-Code | Presumed mechanism |
|---|---|---|
| Insulin | A10A | ↑Thermogenesis, ↑Serum level |
| Metformin | A10BA02 | Dehydration |
| Dapagliflozin | A10BK01 | Dehydration |
| Empagliflozin | A10BK03 | Dehydration |
| Amlodipine | C08CA01 | ↓Dermal circulation |
| Candesartan | C09CA06 | ↓Thirst |
| Levothyroxine | H03AA01 | ↑Thermogenesis |
| Dexibuprofen | M01AE14 | ↑Thermogenesis |
| Hydromorphone | N02AA03 | ↓Sweating, Δcentral thermoregulation |
| Prothipendyl | N05AX07 | ΔCentral thermoregulation |
| Triazolam | N05CD05 | ↓Sweating |
| Trazodone | N06AX05 | ΔCentral thermoregulation |
| Escitalopram | N06AB10 | ↓Sweating |

↑ = Increase; ↓ = Decrease; Δ = Change; ATC = Anatomic therapeutic classification

**Methods:** Using data from the literature and the Anatomical Therapeutic Chemical classification-system (ATC), potential HVID were identified. The prescription frequency was assessed for Austria, using data from the national social insurance which covers 9.0 of the 9.2 Austrian inhabitants. A list of the 50 drugs which were most frequently dispensed in 2024 was obtained.

**Results:** Among the 50 most frequently prescribed drugs in 2024 in Austria were 13 potential HVID: insulin, metformin, dapagliflozin, empagliflozin, amlodipine, candesartan, levothyroxine, dexibuprofen, hydromorphone, prothipendyl, triazolam, trazodone and escitalopram (Table). The presumed mechanisms of increasing heat-vulnerability were decreased sweating ($n=3$), affection of central thermoregulation ($n=3$), dehydration ($n=3$), decreased dermal circulation ($n=1$), increased thermogenesis ($n=1$), impairment of thirst ($n=1$) and increased serum levels ($n=1$) for subcutaneously applied insulin.

**Conclusion:** More than a quarter of the 50 most frequently prescribed drugs in Austria are HVID, especially drugs for the nervous, alimentary, cardiovascular and musculoskeletal system. There is an urgent need for research about HVID and their relevance for heat-related morbidity and mortality. Interdisciplinary research involving pharmacologists, physicians of different disciplines, pharmacists and health-care workers is needed to create and evaluate plans about modification of drug-therapy during heatwaves.

## 15-2

### Deciphering therapy-related cardiac damage and late effects in pediatric cancer survivors

**Bojti I.[1], Volk Z.[1], Dietz L.[1], Bacmeister L.[1], Westermann D.[1], Grundmann S.[1], Puzik A.[2]**

[1]Universitäts-Herzzentrum Freiburg-Bad Krozingen, Freiburg-Bad Krozingen, Germany
[2]Pädiatrische Hämatologie und Onkologie, Klinik für Kinder- und Jugendmedizin, Freiburg im Breisgau, Germany

**Introduction:** More than 80% of children and adolescents treated for cancer survive. However, all-cause mortality of childhood cancer survivors remains increased at least 10-fold compared to the general population. Especially, th risk of death is increased by excessive cardiac and pulmonary disease as well as secondary cancers and relapse. Little is known about the individual sensitivity to develop acute cardiac toxicity and organ-specific late effects. This study aims to characterize the most extensive German pediatric cancer survivorship cohort located at a tertiary care center with focus on cardiooncologic complications. Furthermore, we aim to identify potential markers of therapy-related toxicity and late effects by combining clinical data with a planned large-scale proteomics analysis.

**Methods:** Children and adolescents with cancer diagnosis between 01/08 and 12/15, who consented to participation in the local biobank study before the start of anti-neoplastic treatment were screened. Clinical and routine laboratory data were collected from patients' electronic health records. Children were divided according to occurrence of a cardiovascular complication (CV-comp) during or after the anti-neoplastic therapy. CV complications are defined as reduction of the left ventricular ejection fraction >10% compared to the baseline or below 55% and/or one of the following: elevation of cardiac biomarkers (hs-TroponinT and/or proBNP), relevant elongation of the PQ/QRS/cQT-interval, newly diagnosed arterial hypertension,

new T-inversion,new cardiac hypertrophy, pulmonary hypertension.

**Results:** 383 children were screened and 265 children were included in this analysis. Median follow up was 10 years (SD: 3.8). Approx. 60% of the children were male in both groups. 25% of the cohort developed some form of CV-complication during the anti-neoplastic therapy and an additional 25% during the follow up period (e. g.: LVEF reduction: 34%, arterial hypertension: 5.7%, QRS-elongation: 5.3%). Clinically relevant decrease of the LV-EF, defined as LVEF under 55% was observed by 8 patients after anti-neoplastic treatment which only persisted in 3 patients after completion of the follow-up. Children in the CV-complications group were significantly older at cancer diagnosis than patients without CV-complication (mean [SD] 9.6 [5.4] years vs. 7.9 [5.2]). Children in the CV-complication group had more frequently multiple CV-risk factors before cancer-therapy initiation compared to the no complication group ($p < 0.001$) while there was no difference in the frequency of previous CV-disorders ($p = 0.637$). Among the systemically used anti-neoplastic agents, only anthracylines showed a significant dose-dependent association with the occurrence of CV complications.

**Conclusion:** CV-complications are common side effects of the anti-neoplastic therapy in children which needs to be addressed more precisely in the future. CV risk-evaluation and optimal medical therapy before anti-neoplastic therapy may reduce the complication burden.

## 15-3

### Eine prospektive Studie über den Unterschied beim Erreichen der Zielleistung zwischen dem Rampenprotokoll und dem WHO-Stufenschema bei der Ergometrie

**Gloser A., Weiss T., Michael N.**

Sigmund Freud Medizin Universität, Wien, Österreich

**Einleitung:** Die Ergometrie stellt eine zentrale diagnostische Methode zur Beurteilung der körperlichen Leistungsfähigkeit sowie zur Detektion kardialer Funktionsstörungen dar. In der klinischen Praxis kommen überwiegend das Stufenschema und das Rampenprotokoll zur Anwendung. Beim Stufenschema gibt es abrupte Steigerungen in der Wattzahl, im Gegensatz dazu steht die Rampe, bei der die Belastungsinkremente kontinuierlich sind [1]. Das Ziel der Studie war es, die beiden Protokolle hinsichtlich des Erreichens der individuellen Zielleistung zu vergleichen, um in Zukunft eine bessere leistungsdiagnostische Auswertbarkeit zu ermöglichen.

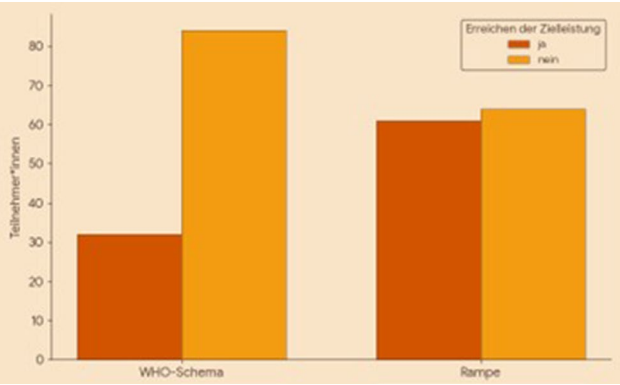


**Abb. 1 | 15-3**

**Methoden:** Für diese prospektive Studie wurden in der Ordination für Kardiologie und Innere Medizin Landstraße 241 Patient*innen, bei denen in einer Periode von 6 Monaten eine Ergometrie durchgeführt werden sollte, mit einem Zufallsgenerator am Tag der Ergometrie in zwei Gruppen (WHO-Stufenschema und Rampenprotokoll) randomisiert. Das Erreichen der Zielleistung wurde erhoben und der Gruppendurchschnitt bestimmt. Anschließend wurden die Ergebnisse mit dem Chi-Quadrat-Test ausgewertet und die einzelnen Variablen mit einer Regressionsanalyse geprüft.

**Resultate:** Es gab einen statistisch signifikanten Unterschied im Erreichen der Zielleistung zwischen Stufen- und Rampenprotokoll. Von den 116 Patient*innen bei denen das WHO-Protokoll durchgeführt wurde, erreichten 32 Patient*innen (28 %) die Zielleistung. Während bei dem Rampenprotokoll 61 (49 %) von 125 Patient*innen die Zielleistung erreichten.

**Schlussfolgerungen:** Das Das Erreichen der Zielleistung wurde häufiger mit dem Rampenprotokoll als mit dem Stufenprotokoll erreicht. Dieser Unterschied könnte damit erklärt werden, dass die kontinuierliche Steigerung des Widerstandes beim Rampenprotokoll für die Patient*innen angenehmer wahrgenommen wird als die abrupten Steigerungen mit dem Stufenprotokoll, welche zu einer schnelleren Beendigung des Belastungstests von Seiten der Patient*innen führen können [2]. Die Wahl des Belastungsprotokolls hat somit Relevanz für die leistungsdiagnostische Aussagekraft.

### Literatur

1. Primus C, Wonisch M, Berent R, Auer J. Praxisleitlinien Ergometrie und Spiroergometrie//Practice guidelines for exercise testing. Journal für Kardiologie. 2022;29(1–2):17–26.
2. Pelliccia A, Sharma S, Gati S, Bäck M, Börjesson M, Caselli S, et al. 2020 ESC guidelines on sports cardiology and exercise in patients with cardiovascular disease. European Heart Journal. 2020 Aug 29;42(1):17–96. https://doi.org/10.1093/eurheartj/ehaa605

## 15-4

### Pregnancy in Patients with Single-Ventricle Physiology: Maternal and Foetal Outcomes

**Gössinger B.[1], Roussel N.[1], Prausmüller S.[1], Karner E.[2], Binder-Rodriguez C.[1], Hengstenberg C.[1], Bartko P.[1], Schrutka L.[1]**

[1]Medizinische Universität Wien, Universitätsklinik Innere Medizin II, Abteilung Kardiologie, Wien, Austria
[2]Medizinische Universität Wien, Universitätsklinik für Frauenheilkunde, Wien, Austria

**Introduction:** Patients born with various single-ventricle physiologies now achieve 20-year survival rates approaching 80%, largely due to advances in surgical techniques, including the Glenn and Fontan procedures. As increasing numbers of these patients survive into adulthood, more women with these complex lesions reach reproductive age. Consequently, managing pregnancy in this population has become more important. However, despite the 2025 European Society of Cardiology guideline update for the management of cardiovascular disease and pregnancy, data remain limited, particularly for single-ventricle physiology. Therefore, the aim of this study was to deter-

mine maternal and foetal outcomes of pregnancies in patients with single-ventricle physiology.

**Methods:** This was a retrospective single-centre cohort study conducted at the Medical University of Vienna's specialized outpatient clinic for adults with congenital heart disease. A total of 390 patients with congenital heart disease were followed during pregnancy between 2000 and 2025.

**Results:** A total of 15 pregnancies were recorded among nine women with single-ventricle physiology. Median age at first pregnancy was 27.1 years (IQR: 25.7–31.2), all patients had systemic left ventricle. Of the patients, five patients (55.6%) underwent Fontan completion, three patients (33.3%) solely received Glenn shunts, and one patient (11.1%) remained surgically unrepaired. Before pregnancy the median oxygen saturation was 95% (IQR: 87.5–96.0) and median left ventricular ejection fraction was 55% (IQR: 45.0–56.5). Out of 15 pregnancies, 11 resulted in miscarriage (68.8%), while four resulted in live birth (26.7%). Miscarriages occurred at a median gestational age of 8 weeks (IQR: 6–13). Live births occurred at a median gestational age of 36 weeks (IQR: 32–37). Two infants (50%) were small for gestational age, defined as birth weight below the 10th percentile, and all infants were monitored at a neonatal intensive care unit. During a median follow-up time of 13 months (IQR: 10–21) no adverse cardiac events or maternal deaths were recorded, and no neonatal adverse events occurred. One child was diagnosed with an atrial septal defect.

**Conclusion:** Women with single-ventricle physiology can become pregnant; however, miscarriage rates are high, and successful pregnancies are often complicated by preterm delivery, small-for-gestational-age neonates, and the need for intensive neonatal care. This highlights the importance of providing care for these patients at a specialised centre with a multidisciplinary team.

## 15-5

### Mitral annular disjunction diagnosed during pregnancy with subsequent survived sudden cardiac death

**Tugrul B., Spitaler P., Mayr A., Theurl M., Stühlinger M., Höfer D., Bonaros N., Bauer A., Dichtl W., Bilgeri V.**

Medizinische Universität Innsbruck, Innsbruck, Austria

**Introduction:** Mitral annular disjunction (MAD) is a structural abnormality involving a separation between the mitral valve and the atrial wall junction with the left ventricular myocardium. MAD can be detected using echocardiography or cardiac magnetic resonance imaging and is increasingly recognized as part of the arrhythmogenic mitral valve disease (AMVD) spectrum.[1] MAD is an independent risk factor for malignant ventricular arrhythmias and sudden cardiac death (SCD). [2, 3] However, risk stratification remains challenging due to a lack of prospective data and validated prognostic scores, particularly in young and asymptomatic patients and especially in pregnant women. [4] There is little data on the clinical course of MAD during pregnancy.

**Methods:** We present the case of a previously healthy 26-year-old pregnant woman who was diagnosed with MAD in her 26th week of pregnancy. An evaluation was initiated due to the presence of premature ventricular complexes in her 12-lead ECG. Holter monitoring revealed frequent premature ventricular beats and non-sustained ventricular tachycardia (13 con-

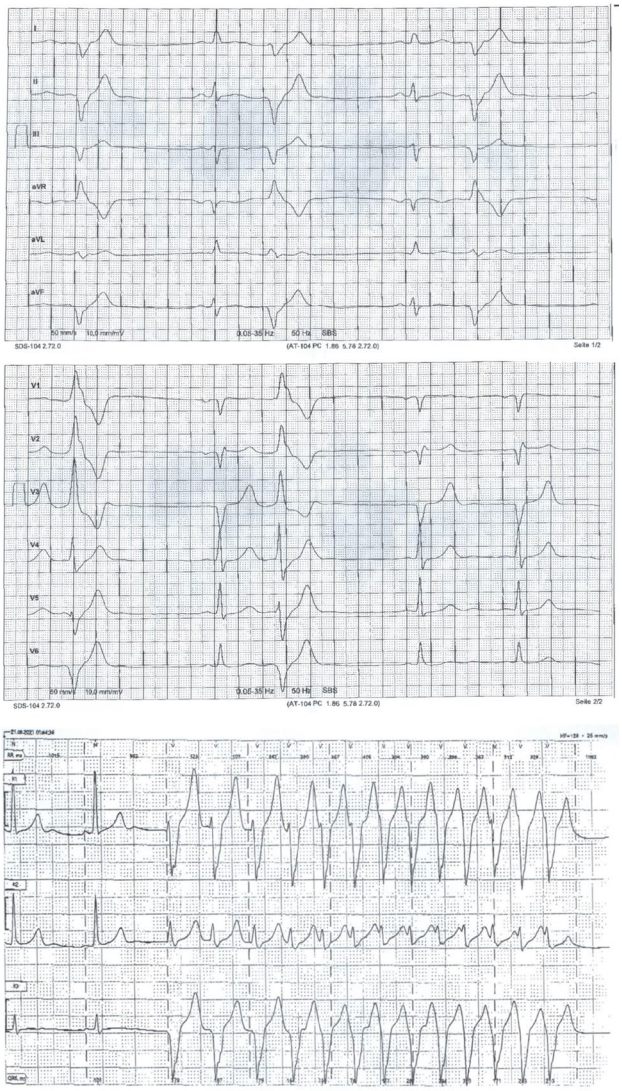


Fig. 1 | 15-5

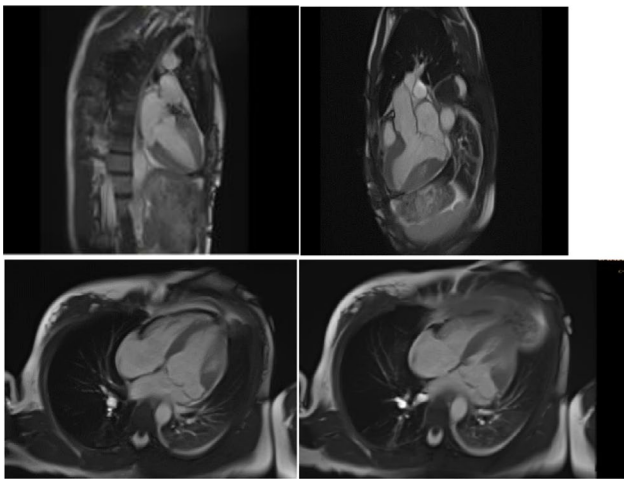

Fig. 2 | 15-5

secutive beats). Transthoracic echocardiography revealed a 12 mm mitral annular disjunction without severe mitral regurgitation or reduced left ventricular ejection fraction. Given the absence of sustained ventricular arrhythmias and considering gestational age, a multidisciplinary team opted for a conservative management strategy involving close clinical and rhythm monitoring after shared decision-making.

**Results:** Pregnancy and delivery were uneventful, and a healthy child was born at term. Six months after giving birth, the patient experienced out-of-hospital cardiac arrest. Immediate bystander cardiopulmonary resuscitation and early defibrillation resulted in a return of spontaneous circulation with no significant neurological impairment. Further evaluation confirmed persistent MAD and complex ventricular ectopy. The patient underwent mitral valve reconstruction surgery and had a subcutaneous implantable cardioverter-defibrillator (ICD) fitted for secondary prevention. At follow-up, no recurrent sustained ventricular arrhythmias were documented.

**Conclusion:** This case highlights the arrhythmogenic potential of AMVD diagnosed during pregnancy and emphasizes the difficulty of risk stratification in young women with the condition. Even when there are no sustained arrhythmias or severe LV dysfunction during pregnancy, there is still a risk of life-threatening ventricular arrhythmias that may persist or manifest after childbirth. Close rhythm surveillance and personalized management within a dedicated multidisciplinary framework are essential. Further research is required to develop evidence-based risk stratification and management strategies for pregnant patients with MAD.

## References


1. Essayagh B, Sabbag A, Antoine C, Benfari G, Batista R, Yang LT, et al. The Mitral Annular Disjunction of Mitral Valve Prolapse: Presentation and Outcome. JACC Cardiovasc Imaging. 2021;14(11:2073–87.
2. Dejgaard LA, Skjolsvik ET, Lie OH, Ribe M, Stokke MK, Hegbom F, et al. The Mitral Annulus Disjunction Arrhythmic Syndrome. J Am Coll Cardiol. 2018;72(14):1600–9.
3. Essayagh B, Sabbag A, El-Am E, Cavalcante JL, Michelena HI, Enriquez-Sarano M. Arrhythmic mitral valve prolapse and mitral annular disjunction: pathophysiology, risk stratification, and management. Eur Heart J. 2023;44(33):3121–35.
4. Van Berendoncks A, McGhie J, Heidbuchel H, Roos-Hesselink JW. Repetitive out of hospital cardiac arrests following pregnancy: a case report of an unfortunate presentation of mitral annular disjunction. Eur Heart J Case Rep. 2020;4(4):1–7.


## 15-6

## Data-Driven Planning of Drone-AED Deployment in Carinthia based on Past Cardiac Arrest Data


**Planka R.[1,2,3], Schuller S.[4,3], Reisinger D.[5], Scharf B.[2,3], Lemesch S.[2], Trampitsch S.[2], Schwegel N.[2], Rohrer U.[2], Alber H.[1], Zirlik A.[2], von Lewinski D.[2], Wankmüller C.[6,3], Kolesnik E.[2,3]**

[1]Department of Internal Medicine and Cardiology, State Hospital Klagenfurt, 9020 Klagenfurt am Wörthersee, Austria
[2]Department of Internal Medicine, Division of Cardiology, Medical University of Graz, 8036 Graz, Austria
[3]Austrian Red Cross, Landesverband Kärnten, 9020 Klagenfurt am Wörthersee, Austria
[4]Department of Environmental Systems Sciences, University of Graz, 8010 Graz, Austria
[5]Institute of Biology, University of Graz, 8010 Graz, Austria
[6]Department of Economics, Analytics, and Operations Research, University of Klagenfurt, 9020 Klagenfurt am Wörthersee, Austria


**Introduction:** Out-of-hospital cardiac arrest (OHCA) is one of the most time-critical medical emergencies. Early defibrillation and the prompt initiation of cardiopulmonary resuscitation (CPR) are critical for patient survival. In rural areas, long travel distances may delay the arrival of emergency medical services and the delivery of the first defibrillation. Drone technology could help address this challenge by rapidly delivering automated external defibrillators (AEDs) to bystanders. This study analyses how drones could be strategically allocated in Carinthia, Austria, to enable coverage of 90% of historical real-world cardiac arrest calls within an 8-minute response time.

**Methods:** All medical emergency operations classified as cardiac arrest in Carinthia, Austria, between 2018 and 2022 were identified and verified using original emergency service reports from air and ground rescue services, resulting in 4518 cases. A k-means clustering approach and a greedy algorithm were applied and compared to determine optimal drone base locations.

**Results:** The analysis indicates that 20 strategically placed drones could achieve the target 8-minute coverage for 90% of cardiac arrest cases. Using a clustering approach to group past cardiac arrest locations, sites were selected iteratively so that each new drone added the most additional coverage, effectively maximising reach with the fewest drones.

**Conclusion:** Strategically deploying drones for AED delivery in Carinthia could reduce response times and improve AED coverage for OHCA. However, practical implementation must consider factors such as terrain, weather, and operational logistics. While a previous study in Carinthia's mountainous regions has demonstrated the feasibility of drone-based AED delivery through simulations, these findings highlight the need for pilot testing to evaluate real-world effectiveness and inform strategic deployment.

## 15-7

### From Early TAVI-Thrombosis to Fatal Shock

**Bernreiter T., Lanzerstorfer J., Roithinger F., Grübler M.**

UK Wiener Neustadt, Wiener Neustadt, Austria

**Introduction:** A 75-year-old male underwent transfemoral transcatheter aortic valve implantation (TAVI) using a 26 mm Edwards Sapien 3 Ultra Resilia prosthesis for symptomatic severe aortic stenosis with concomitant moderate aortic regurgitation. The procedure was uncomplicated, and the patient was discharged two days later in stable cardiorespiratory condition on single antiplatelet therapy with aspirin 100 mg once daily. Eight days after discharge, the patient presented to the emergency department of another hospital with acute chest pain radiating to the left arm. Laboratory testing revealed severe thrombocytopenia (33 G/L) and markedly elevated D-dimer levels. Computed tomography (CT) excluded pulmonary embolism but demonstrated large thrombotic deposits on the prosthetic aortic valve. Shortly thereafter, the patient developed dynamic ST-segment changes accompanied by rising cardiac troponin levels, prompting transfer to our cardiology department for urgent coronary angiography, however no coronary occlusion was identified. The patient was subsequently admitted to the intensive care unit for vasopressor support with norepinephrine that required rapid up-titration. Laboratory evaluation demonstrated acute kidney injury and evolving ischemic hepatic failure. Cardiac biomarkers were markedly elevated (NT-proBNP 622 ng/L, creatine kinase 3773 U/L, troponin 6861 pg/mL). Serial arterial blood gas analyses showed lactate rising from 3 to > 6 mmol/L.

**Methods:** Bedside transthoracic echocardiography revealed severely reduced left ventricular systolic function. Transvalvular gradients across the aortic prosthesis remained within the normal range, however visual inspection showed a virtually immobile TAVI-prosthesis without detectable leaflet motion. A repeat evaluation of the CT images confirmed thrombosis of the TAVI prosthesis. Given the combination of severe thrombocytopenia, markedly prolonged thrombin time (> 120 seconds), and recent exposure to heparin during the TAVI procedure, heparin-induced thrombocytopenia type II (HIT II) was strongly suspected. This suspicion was supported by a positive rapid immunoassay for heparin–PF4 antibodies.

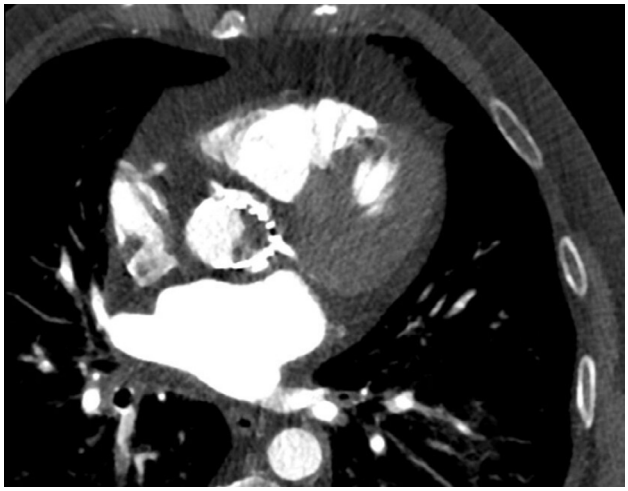

**Fig. 1 | 15-7** CT Scan

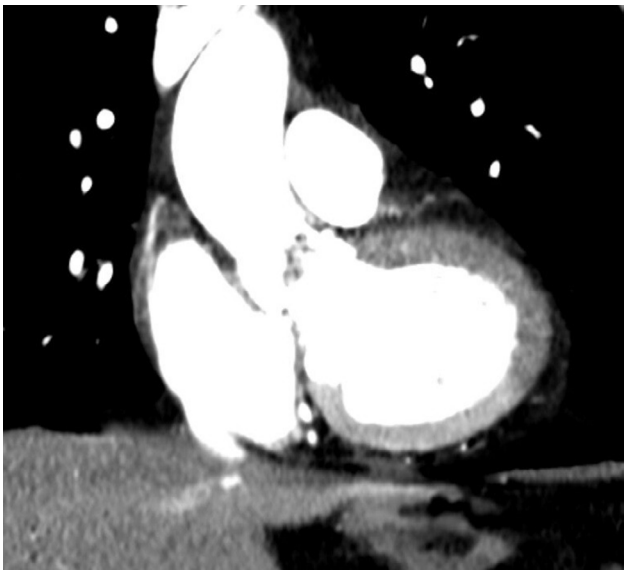

**Fig. 2 | 15-7** CT Scan

**Results:** The patient was diagnosed with acute thrombosis of the TAVI prosthesis leading to cardiogenic shock and progressive multiorgan failure. A multidisciplinary discussion involving cardiologists, cardiac surgeons, and intensive care specialists was conducted to determine the optimal treatment strategy. Due to the patient's rapidly deteriorating clinical condition he was deemed to be at prohibitive surgical risk and TAVI re-intervention was declined by the implanting center. A conservative approach with systemic anticoagulation was therefore pursued. In view of the strong suspicion of HIT II and severe thrombocytopenia, anticoagulation was initiated with the direct thrombin inhibitor argatroban. Despite maximal supportive therapy, vasopressor requirements continued to increase and lactate levels rose further, indicating progressive circulatory failure. Considering co-morbidities and patient's wishes, no mechanical circulatory support was implanted. The patient ultimately diseased despite maximal support 36 h after hospital admission.

**Conclusion:** Clinically apparent bioprosthetic heart valve thrombosis after TAVI is a rare but potentially life-threatening complication, with a reported incidence of 1%. It generally includes a broad spectrum from mild, subclinical cases with hyperattenuated leaflets to cases of fulminant prosthetic valve thrombosis that result in rapid cardiogenic shock, multiorgan failure, and death. Management of acute TAVI thrombosis in critically ill patients remains challenging and is not well standardized. Systemic anticoagulation, re-intervention, surgery or micro-lysis are discussed in small case series, without evidence for any approach being superior to another. In cases of fulminant clinical deterioration where surgical intervention is not feasible, alternative rescue strategies need to be considered. Low-dose, slow-infusion thrombolysis has been proposed as a potential option for obstructive prosthetic valve thrombosis, although evidence in the setting of shock remains limited. This case highlights the devastating course that acute TAVI thrombosis can take and underscores the need for further evidence to guide management in patients presenting with cardiogenic shock when anticoagulation alone fails to be effective. In summary, acute TAVI thrombosis is a life-threatening complication with limited evidence-based treatment pathways in unstable patients. In retrospect, the consideration of micro-thrombolysis and re-intervention can be debated, particularly in the setting of progressive shock.

# POSTERSITZUNG 16—BASIC SCIENCE 1

## 16-1

### Modulating Endothelial Plasticity to Treat Cardiac Fibrosis in Heart Failure

**Eder J.[1], Seeberger D.[1], Ioannou-Nikolaidou M.[1,2], Heim V.[1], Schmidt S.[1], Stranger L.[1], Plattner C.[3], Winter-Pölzl L.[1], Hirsch J.[1], Nägele F.[1,4], Engler C.[1], Lohmann R.[1,2], Trajanoski Z.[3], Bonaros N.[1], Grimm M.[1], Cooke J.[4], Holfeld J.[1], Gollmann-Tepeköylü C.[1], Graber M.[1]**

[1]Department of Cardiac Surgery, Medical University Innsbruck, Innsbruck, Austria
[2]Department of Clinical and Functional Anatomy, Medical University Innsbruck, Innsbruck, Austria
[3]Institute of Bioinformatics, Medical University of Innsbruck, Innsbruck, Austria
[4]Center for Cardiovascular Regeneration, Houston Methodist Research Institute, Houston TX, United States

**Introduction:** Heart failure is a leading cause of morbidity and mortality worldwide and is strongly driven by progressive cardiac fibrosis. Currently, there is no effective antifibrotic therapy available. Endothelial to mesenchymal transition (EndoMT) is a process in which endothelial cells lose their normal vascular characteristics and transform into fibroblast like cells that produce extracellular matrix, thereby promoting fibrosis. Hypoxia inducible factor 2 alpha (HIF 2α) regulates cellular metabolism and phenotype plasticity and may act as a central driver of this process. We therefore investigated whether inhibition of HIF 2α reduces cardiac fibrosis and preserves ventricular function in heart failure.

**Methods:** Heart failure is a leading cause of morbidity and mortality worldwide and is strongly driven by progressive cardiac fibrosis. Currently, there is no effective antifibrotic therapy available. Endothelial to mesenchymal transition (EndoMT) is a process in which endothelial cells lose their normal vascular characteristics and transform into fibroblast like cells that produce extracellular matrix, thereby promoting fibrosis. Hypoxia inducible factor 2 alpha (HIF 2α) regulates cellular metabolism and phenotype plasticity and may act as a central driver of this process. We therefore investigated whether inhibition of HIF 2α reduces cardiac fibrosis and preserves ventricular function in heart failure.

**Results:** Induction of EndoMT in human coronary endothelial cells triggered a marked metabolic shift toward glycolysis and was associated with significant upregulation of HIF 2α. Pharmacological inhibition of HIF 2α with C76 effectively blocked EndoMT, preserved endothelial gene expression, and maintained endothelial functional capacity in vitro. In a murine model of non-ischemic heart failure, HIF 2α inhibition resulted in significant preservation of left ventricular function as assessed by transthoracic echocardiography. Histological analysis demonstrated a robust reduction in myocardial fibrosis, reflected by decreased collagen deposition and reduced myofibroblast accumulation. Importantly, microvascular density was preserved, indicating protection of endothelial integrity. Lineage tracing in Cre:Cdh5/tdTomato mice provided direct in vivo evidence that endothelial cells contribute to fibroblast like cells within the myocardium, confirming true EndoMT. This transition was markedly attenuated by HIF 2α inhibition.

**Conclusion:** HIF 2α emerges as a central driver of EndoMT and cardiac fibrotic remodeling in non-ischemic heart failure. Its pharmacological inhibition prevents endothelial phenotypic transition, reduces myocardial fibrosis, and preserves left ventricular function. Targeting HIF 2α therefore represents a promising and mechanistically grounded therapeutic strategy to address cardiac fibrosis, an unmet need in heart failure treatment, with potential to modify disease progression rather than merely alleviate symptoms.

## 16-2

### Circulating cell-free DNA discriminates resolving from non-resolving thromboembolism

**Artner T.[1], Hofbauer T.[1], Ondracek A.[1], Reil B.[1], Engel L.[1], Valerio L.[2], Konstantinides S.[2], Lang I.[1]**

[1]Medical University of Vienna, Vienna, Austria
[2]Johannes Gutenberg University Mainz, Mainz, Germany

**Introduction:** Acute pulmonary embolism resolves in the majority of cases, but sometimes, chronic thromboembolic pulmonary hypertension (CTEPH) is the consequence, and is usually recognized late. A central unmet need is a non-invasive biomarker capable of distinguishing physiological thrombus resolution from progressive, non-resolving thrombotic disease. Experimental and pathological evidence indicates that unresolved erythrocyte-rich thrombi undergo neutrophil extracellular trap (NET)-driven chronic remodeling and fibrotic transformation rather than resolution. This process may result in sustained release of neutrophil-derived cell-free DNA (cfDNA), providing a mechanism-informed basis for cfDNA as a diagnostic biomarker in CTEPH.

**Methods:** Circulating cfDNA was analyzed in a large, well-characterized cohort comprising healthy volunteers (HV; $n=343$), patients with a history of acute pulmonary embolism without CTEPH at follow-up (PE-FU; $n=274$), and patients with established CTEPH ($n=435$). Total cfDNA concentration and cfDNA fragment length distributions were quantified from plasma. Ex vivo whole-blood thrombosis assays and histological analyses of acute pulmonary emboli and chronic CTEPH thrombotic material were used to link circulating cfDNA profiles to NET-driven thrombus persistence and remodeling. Group differences were assessed using Kruskal–Wallis testing with Dunn's correction for multiple comparisons. Diagnostic performance for discriminating resolving PE from CTEPH was evaluated using receiver operating characteristic (ROC) analyses.

**Results:** Total circulating cfDNA concentrations normalized in patients with resolving pulmonary embolism and did not differ from healthy volunteers, whereas patients with CTEPH showed marked and selective elevation (adjusted $p<0.0001$). In contrast, elongated cfDNA fragments demonstrated a graded increase across clinical states. cfDNA fragments >83 bp and >244 bp increased stepwise from healthy volunteers to PE follow-up patients and were highest in CTEPH, with all pairwise comparisons remaining significant after correction (adjusted $p<0.0001$). In ROC analyses, >83 bp cfDNA achieved the highest diagnostic performance for distinguishing healthy volunteers from CTEPH (AUC = 0.9479), while total cfDNA concentration provided the strongest discrimination between PE-FU patients and CTEPH (AUC = 0.8926). Long cfDNA fragments >244 bp supported disease-associated persistence and impaired cfDNA degradation but showed lower diagnostic performance.

**Conclusion:** Circulating cfDNA integrates key biological processes underlying failed thrombus resolution and chronic thromboembolic remodeling. Total cfDNA concentration distinguishes patients with persistent thromboembolic disease after pulmonary embolism from those with physiological resolution. cfDNA-based plasma measurements may support post-PE risk stratification and guide referral for definitive diagnostic evaluation in patients with suspected CTEPH.

## 16-3

### Neutrophil abundance determines microvascular obstruction in endotoxemia

**Artner T., Ibrahim N., Schmid M., Jilma B., Lang I.**

Medical University of Vienna, Vienna, Austria

**Introduction:** Excessive inflammation is associated with incident and recurrent cardiovascular events. Endotoxin induces stronger systemic inflammation in humans than mice, reflecting granulocyte predominance. We hypothesized that neutrophil abundance and neutrophil extracellular trap (NET) formation determine susceptibility to cardiovascular injury by disrupting extracellular DNA homeostasis.

**Methods:** Neutrophil expansion was induced via CSF3 overexpression prior to sublethal lipopolysaccharide (LPS) challenge in mice. Circulating cell-free DNA (cfDNA), systemic nuclease activity, hematologic parameters, and survival were assessed. Serial plasma samples from healthy volunteers ($n=13$) undergoing controlled endotoxin challenge (2 ng kg$^{-1}$ LPS) were analyzed for NET markers, elongated cfDNA, and circulating nuclease activity. Statistical analyses were performed using mixed-effects models and Kaplan–Meier survival analysis.

**Results:** Neutrophil expansion (38–71% vs 8–18% in controls) converted sublethal LPS exposure into lethal vascular injury, characterized by a marked rise in elongated cfDNA, microvascular DNA-rich occlusions, thrombocytopenia, erythrocyte loss, hypothermia, and 100% mortality within 6 hours (log-rank $\chi^2=12.4$, $P<0.001$; HR 23.9, 95% CI 4.1–139.1). In humans, endotoxin induced a coordinated rise in NET markers and elongated cfDNA (peak at 4 hours, $P<0.001$) together with suppression of nuclease activity ($P<0.05$), consistent with disruption of extracellular DNA homeostasis.

**Conclusion:** We show that endotoxemia impairs extracellular DNA clearance in humans and neutrophil expansion overwhelms this system and drives microvascular obstruction in mice. The balance between NET formation and extracellular DNA clearance is a regulator of inflammatory susceptibility. Our data suggests targeting extracellular DNA clearance to prevent cardiovascular injury and sepsis.

## 16-4

### Conduction Heterogeneity and CXCR4 Expression in MYBPC3-Mutant iPSC-Derived Cardiomyocytes

**Jeyakumar V., Messner M., Puelacher C., Ungericht M., Poelzl G., Bauer A., Zaruba M.**

Medical University of Innsbruck, Innsbruck, Austria

**Introduction:** Mutations in the myosin binding protein C (MYBPC3) gene are a primary cause of hypertrophic cardiomyopathy (HCM), leading to sarcomeric dysfunction and arrhythmias. The lineage-specific effects of these mutations on atrial versus ventricular electrophysiology remains poorly defined. This study utilizes induced pluripotent stem cell-derived cardiomyocytes (iPSC-CMs) to compare the structural, molecular, and functional consequences of MYBPC3 deficiency in atrial and ventricular models.

**Methods:** Healthy (WTSli004-A) and MYBPC3-mutant (Ukki035-B) iPSCs were differentiated into atrial and ventricular cardiomyocytes. Pluripotency was confirmed via qPCR (DPPA5, NANOG) and immunofluorescence (TRA-1-60, SSEA-4). Gene expression profiling at day 21 assessed cardiac markers (MESP1, NKX2.5, TNNT2, MYBPC3, ACTC1, MYH6, MYH7, NPPB) and chemokine receptors CXCR4/CXCR7. RPL0 served as the reference gene due to its stability in this model compared to GAPDH. Structural organization was evaluated through ACTN4 immunostaining. Functional properties, including beat frequency, conduction velocity, and activation heterogeneity, were quantified using optical mapping.

**Results:** RPL0 provided a stable baseline for transcriptomic comparison, whereas GAPDH expression varied significantly. Transcriptional profiling showed significant CXCR4 upregulation in both atrial and ventricular MYBPC3-mutant lines, indicating the activation of inflammatory and survival signaling pathways. Ventricular mutants specifically showed MESP1 upregulation. ACTN4 staining revealed altered cytoskeletal architecture in mutant cells. Functional analysis demonstrated that MYBPC3-mutant ventricular cardiomyocytes displayed a bradycardia phenotype with significantly reduced beat frequency and high variance in conduction velocity compared to healthy controls. These data confirm an increased arrhythmogenic state in the mutant models.

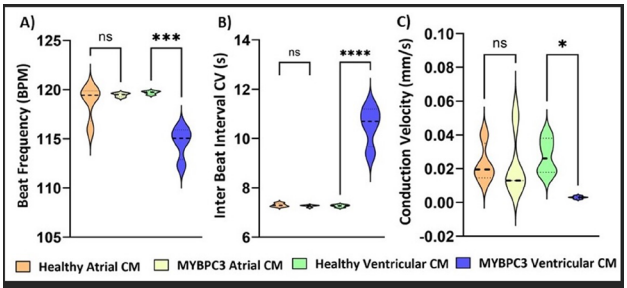


**Figure 1: Longitudinal contractile profiling of MYBPC3-mutant cardiomyocytes via motion analysis.** High-speed video microscopy identifies lineage-specific functional defects in MYBPC3-mutant iPSC-CMs. (A) Beat frequency analysis indicates a reduced spontaneous rate in mutant ventricular lines. (B) Motion vector analysis reveals increased beat-to-beat variability (arrhythmia) via Inter-Beat Interval Coefficient of Variation (CV), and (C) slower conduction velocity compared to healthy controls. Each violin plot represents pooled longitudinal measurements recorded daily from Day 11 to Day 14 post-differentiation.

**Fig. 1 | 16-4**

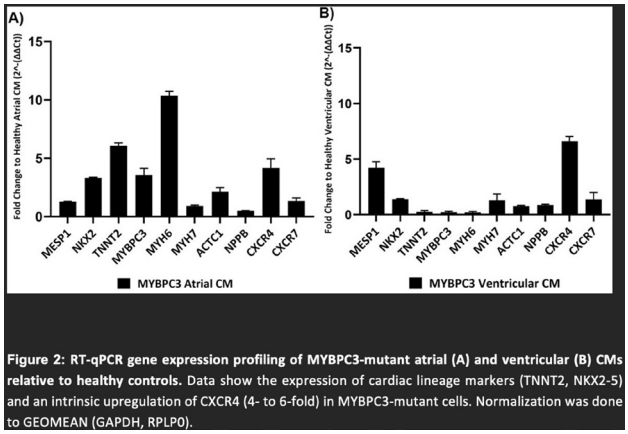


**Figure 2: RT-qPCR gene expression profiling of MYBPC3-mutant atrial (A) and ventricular (B) CMs relative to healthy controls.** Data show the expression of cardiac lineage markers (TNNT2, NKX2-5) and an intrinsic upregulation of CXCR4 (4- to 6-fold) in MYBPC3-mutant cells. Normalization was done to GEOMEAN (GAPDH, RPLP0).

**Fig. 2 | 16-4**

**Conclusion:** The MYBPC3 mutation drives distinct transcriptional and electrophysiological remodeling in atrial and ventricular lineages. The observed conduction heterogeneity and CXCR4 upregulation suggest that non-sarcomeric mechanisms contribute to the HCM phenotype. This iPSC-CM model provides a platform for investigating lineage-specific pathophysiology and testing targeted therapies to stabilize cardiac conduction.

## 16-5

### Humoral Autoimmunity and Cardiac IgG Deposition in Atherosclerotic Disease

**Soukhaklari R.[1], Matzer I.[1], Wolte B.[1], Hopfer A.[1], Gindlhuber J.[1], Vujic N.[1], Kratky D.[1], Zirlik A.[1], Rainer P.[1,2], Sattler S.[1,3]**

[1]Medical University of Graz, Graz, Austria
[2]BKH St. Johann, Tirol, Austria
[3]NHLI, Imperial College London, London, United Kingdom

**Introduction:** Atherosclerosis, the leading underlying cause of cardiovascular disease (CVD), is a chronic inflammatory disorder characterized by the accumulation of immune cells within arterial plaques that predominantly release pro-inflammatory cytokines. A distinctive feature of atherosclerosis is the significant involvement of auto-antibodies targeting epitopes in plaques and vessel walls, and numerous studies have reported an accelerated, early-onset atherosclerosis in individuals with autoimmune diseases. Studies further suggest that autoantibodies may not only promote inflammatory processes but also contribute independently to cardiovascular disease risk. This study aimed to determine whether atherosclerotic disease also triggers the generation of anti-heart auto-antibodies targeting myocardial structures beyond the vasculature.

**Methods:** Male and female Apoe$^{-/-}$ mice were fed a Western-type diet (WTD) for 10 weeks, while control groups were maintained on a chow diet. At the end of the 10-week period, atherosclerotic plaques were quantified in the aortas and aortic roots. ELISA was performed to measure levels of anti-heart, anti-troponin, and anti-myosin IgG antibodies in plasma. In addition, total cholesterol, free cholesterol, and triglyceride levels were measured in plasma. Cryosections of the hearts were stained with anti-mouse IgG, WGA, and DAPI. Images were obtained using widefield microscopy, and mean fluorescence intensity (MFI) was quantified.

**Results:** As expected, atherosclerotic plaques developed in WTD-fed mice. Male mice ($n$=9–13) developed a significant increase in levels of anti-heart IgG ($P$=0.0006), anti-troponin ($P$=0.0003), and anti-myosin ($P$=0.0004) antibodies from 10 weeks after the start of the diet. In these mice, total cholesterol and free cholesterol levels correlated with circulating auto-antibodies. In contrast, female mice ($n$=6–10) showed a less pronounced increase in anti-heart IgG and anti-troponin antibodies, whereas anti-myosin levels ($P$=0.0001) were significantly higher at 10 weeks compared to baseline. Interestingly, IgG deposition in male myocardium was significantly higher ($P$=0.01435) after 10 weeks on diet, and this deposition correlated with circulating auto-antibody levels in male mice.

**Conclusion:** These findings suggest that atherosclerosis triggers the generation of auto-antibodies against the heart that circulate in the blood and accumulate in the myocardium. Anti-heart autoimmune mechanisms may thus play a role in cardiac involvement in atherosclerosis.

## 16-6

### Conversion of Surgical Waste from Open-Heart Surgery into a Model for Investigating the Interaction of Aortic Tissue with TEVAR

**Yusefi M.[1], Ghorbanpour S.[2], Zirngast B.[3], Kolb D.[4], Mächler H.[3], Sommer G.[1], Andreas M.[3], Holzapfel G.[1,5]**

[1]Institute of Biomechanics, Graz University of Technology, Graz, Austria
[2]Institute of Heach Care Engineering, Graz University of Technology, Graz, Austria
[3]Department of Cardiac Surgery, Medical University of Graz, Graz, Austria
[4]Core Facility Ultrastructure, Medical University of Graz, Graz, Austria
[5]Department of Structural Engineering, Norwegian University of Science and Technology, Trondheim, Norway

**Introduction:** Thoracic endovascular aortic repair (TEVAR) is a widely used procedure for treating diseases of the thoracic aorta. However, previous ex vivo studies suggest that implanted stent grafts can induce undesirable biomechanical changes in the aortic wall. To investigate these effects more closely under controlled conditions, a dedicated bioreactor system was developed to study the response of human aortic tissue to simulated, TEVAR-induced mechanical loading.

**Methods:** Tissue samples from the ascending aorta were obtained from patients undergoing elective aortic replacement surgery. A 3 × 3 cm specimen was prepared from each surgical waste specimen and tested in a sterile, custom-built bioreactor. The specimen was subjected to physiological biaxial cyclic loading (60 cycles/min) for 24 hours to simulate pulsatile aortic motion in vivo. Two regions of the same specimen were analyzed. In Group I, biopsies were taken from the region subjected solely to biaxial stretching. In Group II, an additional radial force (~1 MPa) was applied using a structure simulating the imprint of a TEVAR stent. Biopsies were taken from the region exposed to this additional loading. Cellular responses, cytokine release, and structural changes were investigated using biochemical assays and microscopy.

**Results:** Preliminary observations suggest that tissues exposed to simulated stent contact exhibit structural alterations compared to control samples. Differences in tissue mechanics,

extracellular matrix organization, and the release of inflammatory mediators are to be expected.

**Conclusion:** This novel ex vivo bioreactor approach enables the controlled investigation of TEVAR-induced mechanical stress on human aortic tissue. The findings may contribute to a better understanding of tissue-stent interactions and support the development of biomechanically more compatible aortic stent grafts.

## 16-7

### Selective CD11b Blockade Attenuates Immune Checkpoint Inhibitor–Associated Cardiac Dysfunction Without Reducing Anti-Tumor Activity

**Bojti I.[1], Ziegler A.[1], Bojtine Kovacs S.[2], Jung N.[1], Marchini T.[1], Li X.[1], Westermann D.[1], Wolf D.[1]**

[1]Universitäts-Herzzentrum Freiburg-Bad Krozingen, Freiburg-Bad Krozingen, Germany
[2]Innere Medizin I, Universitätsklinkum Freiburg, Freiburg im Breisgau, Germany

**Introduction:** Immune checkpoint inhibitor (ICI) therapy has emerged as a cornerstone of modern oncology but is associated with potentially life-threatening cardiovascular complications, including myocarditis. These adverse events are characterized by inflammatory immune cell infiltration into non-tumor tissues. Current management relies on systemic immunosuppression, which may jeopardize oncologic efficacy. We investigated whether targeted interference with CD11b (Mac-1)-mediated leukocyte adhesion can reduce ICI-associated tissue injury while maintaining anti-tumor immune responses.

**Methods:** ICI-related toxicity was induced in A/J mice by anti–PD-1 administration. Animals received either the activation-specific CD11b inhibitor Neutrophil Inhibitory Factor (NIF) or vehicle control. Cardiac injury was evaluated by serum troponin T levels and serial echocardiography. Immune cell populations in cardiac tissue were analyzed by flow cytometry with focus on inflammatory Ly6C^high monocytes and T-cell subsets. Circulating cytokines were quantified using LEGENDplex multiplex assays. Colonic tissue was examined histologically using H&E staining. CD11b-dependent adhesion was assessed in vitro using ICAM-1–coated plates. Anti-tumor efficacy was tested in a B16.F10 melanoma model under combined anti–PD-1 and NIF treatment.

**Results:** CD11b inhibition significantly attenuated cardiac injury, as reflected by reduced troponin release and preserved left ventricular ejection fraction. Cardiac flow cytometry revealed a pronounced reduction of Ly6C^high inflammatory monocytes in NIF-treated mice, whereas $CD8^+$ T-cell numbers remained unchanged. Colonic histology demonstrated decreased tissue damage and CD11b pos. cell infiltration under CD11b blockade. Serum cytokine profiling indicated distinct modulation of inflammatory mediators during treatment. In vitro assays confirmed concentration-dependent inhibition of CD11b–ICAM-1 interaction by NIF. Importantly, co-treatment with NIF did not alter tumor progression in the melanoma model, indicating preserved anti–PD-1 anti-tumor efficacy.

**Conclusion:** Targeted inhibition of CD11b-mediated leukocyte trafficking reduces ICI-associated cardiac dysfunction and intestinal injury by limiting inflammatory monocyte accumulation while sparing cytotoxic T-cell abundance. Crucially, this strategy does not impair anti-tumor immune activity. Modulation of myeloid adhesion pathways may therefore represent a cardiovascular-protective approach in patients receiving immune checkpoint inhibitors.

# POSTERSITZUNG 17 – CLINICAL CASES 3

## 17-1

### Eine Embolie, drei Verdächtige—Rhythmus, Gerinnung und ein ASD

**Mitteregger M.[1], Mauerhofer E.[1], Gessner M.[1], Sipötz J.[1,2]**

[1]Hanusch Krankenhaus, Wien, Österreich
[2]Karl Landsteiner Institut für Klinische Kardiologie, Wien, Österreich

**Einleitung:** Case Report Ein 69-jähriger Patient stellte sich in der zentralen Notaufnahme (ZNA) mit von radial ausgehenden bis in die Schulter ausstrahlenden Schmerzen der rechten Hand mit begleitendem Kältegefühl vor. Die A. radialis rechts war nicht palpabel. In der Duplex-Sonographie zeigte sich ein echoreicher Thrombus im Bereich der distalen A. brachialis rechts bei gleichzeitig bestehender venöser 3-Etagen Thrombose (TVT) des linken Beins. Nach erfolgreicher Thrombektomie erfolgte eine Durchuntersuchung zur Ursachenklärung.

**Methoden:** In der transthorakalen (TTE) und transösophagealen (TEE) Echokardiographie konnten drei atriale Septumdefekte vom Sekundumtyp (multihole ASD II/MHASD II) mit Links-Rechts Shunt, eine biatriale höhergradige Dilatation, sowie eine Dilatation des rechten Ventrikels (RV) nachgewiesen werden. Die Rechtskontrastmittelstudie (Gelofusin Iso 40 mg/ml) zeigte das Bild eines bidirektionalen Shunts mit geringer Zunahme unter Valsalva-Manöver. Das linke Herzohr präsentierte sich mit einem Flow > 0,5 m/s und thrombusfrei. Zur Beurteilung der hämodynamischen Relevanz des MHASD II erfolgte die Berechnung des Shuntvolumens mittels kardialer Magnetresonanztomographie, welche ein Qp/Qs (Shunt-Fraktion) von 1,47 ergab. Im durchgeführten 72 h-EKG konnten keine Rhythmusstörungen nachgewiesen werden. Jedoch wurde der Patient, nach bereits erfolgter Entlassung, mit einem Vorhofflattern de novo in der ZNA vorstellig, welches mit einer elektrischen Kardioversion erfolgreich terminiert werden konnte.

**Resultate:** Während des stationären Aufenthalts erfolgte ein erstes Thrombophilie-Screening, wobei sich keine Auffälligkeiten zeigten. Zusätzlich berichtete der Patient über eine Hämochromatose mit regelmäßigen ambulanten Kontrollen einschließlich Aderlässen. Es erfolgte eine Überweisung in die Ambulanz für angeborene Herzfehler zur Evaluierung einer operativen Sanierung des MHASD II bei hämodynamischer Relevanz und Verdacht auf eine paradoxe Embolie, sowie die Überweisung in eine Gerinnungsambulanz bei spontaner TVT ohne erhebbaren Risikofaktoren zur Thrombophiliediagnostik. Die Gerinnungsdiagnostik (6 Monate nach Thrombose und unter DOAK-Pausierung) ergab einen Protein-S-Mangel von 40 %. Das Vorliegen einer pathologischen APC-Resistenz, eines Protein-C-Mangels, eines Antithrombin-Mangels sowie eines Antiphospholipid-Syndroms wurde ausgeschlossen. In der Ambulanz für angeborene Herzfehler wurde bei hämodynamisch relevantem MHASD II die Indikation zur operativen Sanierung gestellt. Die Durchführung dieser und eine eventuelle gleichzeitige cavotrikuspidale Isthmusablation ist noch ausständig.

**Schlussfolgerungen:** Hintergrund Hinsichtlich der Ätiologie des Thrombus in der A. brachialis muss von einem multifaktoriellen Geschehen ausgegangen werden. Die bestehende Hyperkoagulabilität bei Protein-C-Mangel erhöht das Risiko für

venöse und arterielle Thromboembolien, der MHASD II ermöglich die paradoxe Embolisation bei bestehender TVT und das neu diagnostizierte VH-Flattern bei hochgradiger LA Dilatation lässt auf eine bereits länger bestehende Rhythmusstörung schließen, welche, ohne therapeutische Antikoagulation, ebenfalls ein hohes Embolierisiko birgt. Die bekannte und durch regelmäßige Aderlässe therapierte Hämochromatose könnte zusätzlich über eine Erhöhung der Blut Viskosität thrombogen wirken. Es besteht die Notwendigkeit einer lebenslangen Antikoagulation.

## 17-2

### Kardiale Raumforderung—Ein Zebra der Kardiologie

**Mitteregger M.[1], Mauerhofer E.[1], Gold T.[1], Gessner M.[1], Burkart-Küttner D.[1], Sipötz J.[1,2]**

[1]Hanusch Krankenhaus, Wien, Österreich
[2]Karl Landsteiner Institut für Klinische Kardiologie, Wien, Österreich

**Einleitung:** Case Report Eine 55-jährige Patientin stellte sich im September 2025 zur Planung einer Pulmonalvenenisolation bei paroxysmalem Vorhofflimmern in der Rhythmusambulanz vor. Präinterventionell wurde zur Darstellung der Anatomie und Anzahl der Pulmonalvenen sowie zur Beurteilung der Koronararterien eine kardiale Computertomographie durchgeführt. Dabei zeigte sich eine Raumforderung des interatrialen Septums mit einer Ausdehnung von 4 × 3,5 × 3 cm, welche solide Dichtewerte und in den KM-verstärkten Sequenzen ein diskret homogenes Enhancement aufwies. Anamnestisch bestand ein Zustand nach Resektion eines Dermatofibrosarkoms, wobei der histologische Originalbefund zur Differenzierung zwischen einem klassischen Dermatofibrosarcoma protuberans (DFSP) und einem fibrosarkomatösen Dermatofibrosarcoma protuberans (FS-DFSP) nicht mehr zu erheben war. Ein FS-DFSP wäre hinsichtlich der höheren Rezidiv- und Metastasierungsrate als prognostisch risikobehafteter zu sehen (1). Die differenzialdiagnostischen Überlegungen bezüglich Dignität schlossen daher neben Myxom und Lymphom, ein Rezidiv des Dermatofibrosarkoms sowie eine Metastase mit ein. Das weitere diagnostische Work up erfolgte mittels transthorakaler Echokardiographie, kardialer Magnetresonanztomographie, und PET-CT.

**Methoden:** In der durchgeführten Echokardiographie stellte sich die Raumforderung des interatrialen Septums heterogen (isoechogene und hypoechogene Anteile) und glatt begrenzt dar, wobei in der Linkskontraststudie keine Kontrastmittelaufnahme vermerkt werden konnte (SonoVue® 1 ml). In der kardialen Magnetresonanztomographie wurde die Raumforderung als scharf begrenzt, homogen und in der STIR-Sequenz mit hyperintensem Signalverhalten (vereinbar mit einem myxoiden Charakter) beschrieben. In der T1-gewichteten Sequenz war ein isointenses Signal vordergründig, in der fettgesättigten T1-Sequenz ein hyperintenses Signalverhalten. Es bestand ein gering ausgeprägtes, homogenes venöses Kontrastmittel-Enhancement ohne Nachweis eines Late-Enhancements. Aufgrund der scharf begrenzten Konfiguration und des nur diskreten Kontrastmittel-Enhancements erschien eine maligne Genese bildmorphologisch unwahrscheinlich. Im FDG-PET/CT konnten keine pathologisch vergrößerten oder hypermetabolen Lymphknoten festgestellt werden und die Raumforderung des interatrialen Septums zeigte kein FDG-Uptake. Aufgrund der DFSP-Anamnese mit fehlendem histologischem Originalbefund und der Größe der Raumforderung wurde im Tumorboard ein chirurgisches Vorgehen beschlossen, da in diesem Kontext eine Malignität mittels Bildgebung nicht ausgeschlossen werden konnte. Über eine mediane Sternotomie wurde der Tumor reseziert und der resultierende Septumdefekt mittels eines bovinen Perikard-Patches verschlossen.

**Resultate:** Das Gewebe wurde zur histopathologischen Untersuchung eingesendet. Aufgrund des paroxysmalen Vorhofflimmerns erfolgte zusätzlich eine Pulmonalvenenisolation beidseits und die Anlage einer Box-Lesion mittels Nanosecond Pulsed Field Ablation (nsPFA), sowie der Verschluss des linken Herzohrs durch einen Penditure-Clip. Während präoperativ MR tomographisch der Verdacht auf ein Vorhofmyxom bestand, lenkte der intraoperative Aspekt eines flüssigen, fettähnlichen Inhalts die Arbeitsdiagnose zunächst in Richtung eines Lipoms. Die anschließende histopathologische Aufarbeitung ergab jedoch durch den Nachweis von Flimmerepithel das Bild einer bronchogenen Zyste (entsprechend einer intrakardialen Foregut-Zyste) ohne Anhalt für Malignität. Hintergrund Bronchogene Zysten sind kongenitale Fehlbildungen, die zu den embryonalen Anomalien des Vorderdarms (Foregut) gezählt werden. Die embryonalen Vorstufen des Herzes befinden sich in unmittelbarer Nähe zum Vorderdarm. Eine abnorme Knospenbildung des primitiven Bronchialbaums mit bronchogener Zystenbildung etwa in der 4. Woche der Embryonalentwicklung kann dazu führen, dass die Zyste während der Bildung der Herzwand in das primitive Herz eingebaut wird und sich anschließend, als intrakardiale bronchogene Zyste manifestiert. Weitere mögliche Lokalisationen einer bronchogenen Zyste sind entlang des embryonalen Vorderdarms, wobei zu den häufigsten die Lunge und das Mediastinum zählt (2).

**Schlussfolgerungen:** Es gibt keine publizierten epidemiologischen Daten zu intrakardialen bronchogenen Zysten, lediglich einzelne Fallberichte. Sie wurden erstmals 1890 bei einer Autopsie beschrieben und über die erste chirurgische Entfernung einer interatrialen bronchogenen Zyste wurde im Jahr 1996, von Soeda et al. berichtet. In der englischsprachigen Literatur finden sich ca. 32 Fallberichte (3). Der überwiegende Teil der Patient:innen mit intrakardialen bronchogenen Zysten präsentiert sich asymptomatisch, jedoch kann es auch zu Palpitationen, Thoraxschmerz, Dyspnoe, Synkopen und Symptomen auf Basis einer Kompression der umliegenden Strukturen kommen (2–4). In Zusammenhang mit intrakardialen bronchogenen Zysten wurde unter anderem über das Auftreten folgender Komplikationen berichtet: Vorhofflimmern, AV-Blockierungen I-III° und Rechtsschenkelblock (3). Darüber hinaus kam es auch in einzelnen Fallberichten zu Komplikationen wie einem akuten Koronarsyndrom (5) und Kammerflimmern (6). Zudem werden auch kongenitale Defekte wie eine persistierende linke obere Hohlvene (PLSVC) und atriale sowie ventrikuläre Septumdefekte beschrieben (3). Patientengruppen, die besonders von der chirurgischen Entfernung einer bronchogenen Zyste profitierten, umfassen neben symptomatischen Patient:innen, auch Patient:innen mit Komplikationen durch die Zyste sowie asymptomatische Patient:innen mit großen oder wachstumsverdächtigen Zysten (7).

### Literatur

1. Liang CA, Jambusaria-Pahlajani A, Karia PS, Elenitsas R, Zhang PD, Schmults CD. A systematic review of outcome data for dermatofibrosarcoma protuberans with and without fibrosarcomatous change. J Am Acad Dermatol. 2014 Oct;71(4):781–6. https://doi.org/10.1016/j.jaad.2014.03.018 PubMed PMID: 24755121.
2. Fukada Y, Endo Y, Nakanowatari H, Kitagawa A, Tsuboi E, Irie Y. Bronchogenic cyst of the interatrial septum. Fuku-

shima J Med Sci. 2020 Apr 22;66(1):41–3. https://doi.org/10.5387/fms.2019-29 PubMed PMID: 32101836.
3. Mingming M, Yana Z, Ran C, Qingqing Z, Bowen Z. Case Report: Multimodality imaging of a bronchogenic cyst in the interatrial septum. Front Cardiovasc Med. 2024;11:1466016. https://doi.org/10.3389/fcvm.2024.1466016 PubMed PMID: 39444549.
4. Phan AT, Hu J, Oganesian B, Williams SO. Symptomatic Bronchogenic Cyst in a Lipomatous Interatrial. Septum Cardiol Res. 2023;14(4):315–8. https://doi.org/10.14740/cr1511. PubMed PMID: 37559710.
5. Azeem F, Finlay M, Rathwell C, Awad WI. A near fatal presentation of a bronchogenic cyst compressing the left main coronary artery. J Thorac Cardiovasc Surg. 2008;135(6):1395–6. https://doi.org/10.1016/j.jtcvs.2007.09.082. PubMed PMID: 18544397.
6. Shiohira S, Sasaki T, Maeda S, Kawabata M, Goya M, Hirao K. Bronchogenic cyst of the atrioventricular septum presenting with ventricular fibrillation. HeartRhythm Case. Rep. 2017;3(8):389–91. https://doi.org/10.1016/j.hrcr.2017.05.005. PubMed PMID: 28840106.
7. Fievet L, Gossot D, de Lesquen H, Calabre C, Merrot T, Thomas P, et al. Resection of Bronchogenic Cysts in Symptomatic Versus Asymptomatic Patients: An Outcome Analysis. Ann Thorac Surg. 2021;112(5):1553–8. https://doi.org/10.1016/j.athoracsur.2020.05.031. PubMed PMID: 32599038.

## 17-3

### Multisystemic Eosinophilic Disorder with Cardiac Involvement: A Complex Case of Eosinophilic Granulomatosis with Polyangiitis

**Meledeth C., Aigner A., Steinwender C., Reiter C.**

Department of Cardiology, Kepler University Hospital, Medical Faculty, Johannes Kepler University, Linz, Austria

**Introduction:** This case report details the presentation of a 58-year-old female patient admitted for inpatient evaluation due to elusive symptoms including painful splinter hemorrhages on fingernails, arm numbness and generalised weakness. A particular diagnostic challenge arose from the interpretation of elevated cardiac enzymes, which initially appeared as an incidental finding, in the absence of corresponding ECG changes or typical symptoms. The patient's pre-existing history included hypereosinophilic bronchial asthma, which was reportedly well-controlled under Dupilumab therapy initiated in January 2024.

**Methods:** The comprehensive diagnostic work-up was conducted interdisciplinarily. Initial laboratory analyses included a detailed differential blood count, showing marked eosinophilia and leukocytosis, and determination of cardiac biomarkers (Troponin T, NT-proBNP). Screening for collagenosis and vasculitis antibodies (e.g., ANA, ANCA) was performed. Various imaging modalities were employed: transthoracic and transesophageal echocardiography, cardiac MRI for detailed myocardial assessment, cerebral MRI with angiography for neurological abnormalities, thoracic CT, abdominal sonography, and hand radiographs for systemic evaluation. Invasive procedures encompassed a left ventricular endomyocardial biopsy with coronary angiography for tissue analysis and a lumbar puncture for cerebrospinal fluid evaluation.

**Results:** Upon admission, laboratory findings were notable for significant leukocytosis and pronounced eosinophilia

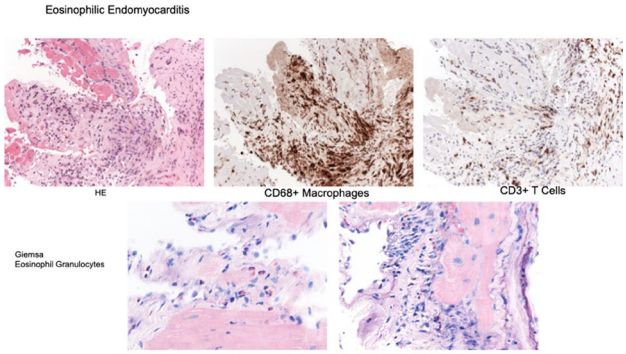


**Fig. 1 | 17-3** Histological Examination of Endomyocardial-biopsy

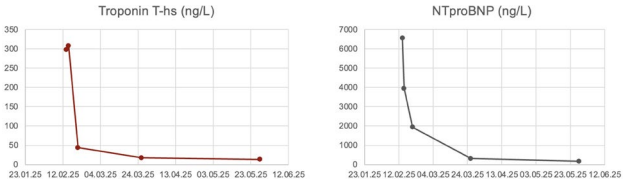


**Fig. 2 | 17-3** Biochemical Markers in the Course of Disease

(absolute eosinophil count 10.62 G/L), alongside elevated cardiac enzymes (Troponin T 298 ng/L, NTproBNP 6573 ng/L). Autoantibody panels (ANA, ANCA, ENA, dsDNA) were negative. Thoracic CT showed minor nodular/micronodular opacities, but no typical interstitial lung disease. Cardiological investigations initially revealed a pericardial effusion lamella, with subsequent cardiac MRI showing signs of perimyocarditis, mild pericardial effusion, and mildly reduced left ventricular contractility (LVEF 45%). Endomyocardial biopsy was done for further clarification, which showed acute eosinophilic endomyocarditis (Löffler endomyocarditis). Neurological assessment identified a central motor deficit of the right hand. Cerebral MRI depicted multifocal cortical/subcortical signal alterations with distinct contrast enhancements, consistent with vasculitis, later interpreted as Posterior Reversible Encephalopathy Syndrome (PRES) in the context of EGPA-associated CNS vasculitis. This complex constellation, including eosinophilia and histologically proven cardiac involvement, led to the interdisciplinary diagnosis of Eosinophilic Granulomatosis with Polyangiitis.

**Conclusion:** This case vividly illustrates the diagnostic challenges posed by non-specific symptoms that may indicate a systemic disease, particularly when primary symptoms are misleading or initially appear isolated. The unique combination of cardiac (eosinophilic myocarditis), neurological (central motor deficit, cerebral vasculitis/PRES), and dermatological manifestations (splinter haemorrhage), coupled with pronounced eosinophilia, ultimately led to the diagnosis of Eosinophilic Granulomatosis with Polyangiitis, a rare and complex vasculitis. The histological confirmation of eosinophilic myocarditis via endomyocardial biopsy was crucial for unequivocally establishing cardiac involvement, distinguishing it from other potential aetiologies. The initiated comprehensive therapy, comprising an initial corticosteroid pulse, was followed by a planned six cycles of cyclophosphamide, administered bi-weekly for the first two doses, then every three weeks. Following the third cyclophosphamide cycle, a transition to Mepolizumab therapy was done for the underlying chronic bronchial asthma. The observed normalisation of left ventricular function highlights the responsiveness of cardiac manifestations to this targeted immunosuppressive regimen.

## 17-4

### A Small Mass with Major Implications: An Unusual Right Atrial Lesion Beyond a Presumed Myxoma

**Mutschlechner D.[1,2,3], Valsky S.[1], Wiedemann D.[4], Gremmel T.[1,3,3]**

[1]LK Mistelbach-Gänserndorf, Mistelbach, Austria
[2]Institute of Cardiovascular Pharmacotherapy and Interventional Cardiology, Karl Landsteiner Society, St. Pölten, Austria
[3]Karl Landsteiner University of Health Sciences, Krems, Austria
[4]Universitätsklinikum St. Pölten, St. Pölten, Austria

**Introduction:** We report the case of a 41-year-old woman who was referred from a peripheral hospital to our echocardiography laboratory for transesophageal echocardiography (TEE). The patient had initially presented to her general practitioner because of precordial pressure following a prolonged respiratory infection with sinusitis and laryngitis and was subsequently referred to the peripheral hospital for further evaluation. She described precordial pressure independent of physical exertion occurring intermittently in an on–off pattern without accompanying dyspnea. However, she reported a more intense retrosternal pressure during forward bending. During the preceding two weeks of respiratory infection, she had not experienced fever or chills. A history of heterozygous factor V Leiden mutation was reported by the patient. No other pre-existing medical conditions were known and she was not taking any regular medication. She was a non-smoker and her family history revealed no clustering of cardiovascular or malignant diseases. Physical examination showed no pathological findings. An electrocardiogram (ECG), transthoracic echocardiography (TTE), and computed tomography (CT) of the aorta performed at the peripheral hospital demonstrated abnormal findings.

**Methods:** A 12-lead ECG demonstrated sinus rhythm with nonspecific ST-segment depressions in leads V1–V3. Laboratory testing, including complete blood count, electrolytes, renal and hepatic parameters, creatine kinase, and high-sensitivity troponin T, was within normal limits. TTE revealed preserved left ventricular ejection fraction without regional wall motion abnormalities or significant valvular disease. However, a hollow mass was visualized in the right atrium with apparent contact to the ascending aorta, while colour Doppler imaging remained inconclusive. Differential diagnoses included an atrial septal defect or a fistulous connection. Therefore, CT of the thoracic aorta was performed. CT demonstrated a hyperdense lesion measuring 1.3 × 1.4 cm at the level of the aortic root with an attenuation of 114 Hounsfield units. Although a hematoma was considered the most likely diagnosis, motion and contrast artifacts limited diagnostic certainty, and a fistulous connection could not be excluded. TEE identified a sharply demarcated, homogeneous mass measuring 1.7 × 1.2 cm in the right atrium adjacent to the aortic root. No interatrial shunt or fistulous communication to the ascending aorta was detected. Multimodality imaging with cardiac magnetic resonance (CMR) localized the lesion within Koch's triangle but did not allow further differentiation.

**Results:** After multidisciplinary review of all imaging studies, the consulted cardiac surgery team recommended minimally invasive resection via right minithoracotomy due to the uncertain nature of the lesion and in accordance with guideline recommendations advocating surgical excision of suspected

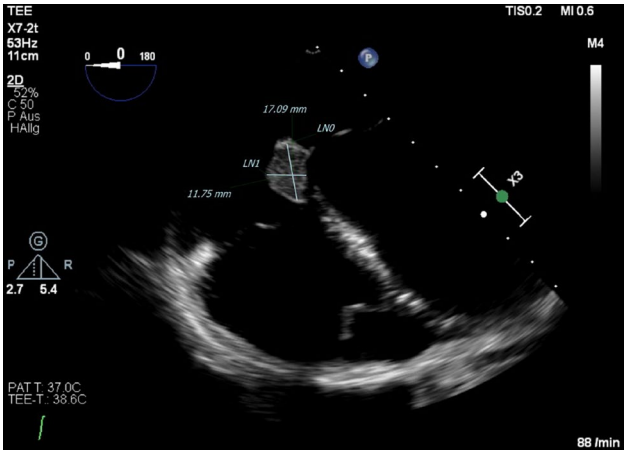


**Fig. 1 | 17–4** Transesophageal echocardiography showing a lesion measuring 1.7 × 1.2 cm within the right atrium, attached to the interatrial septum

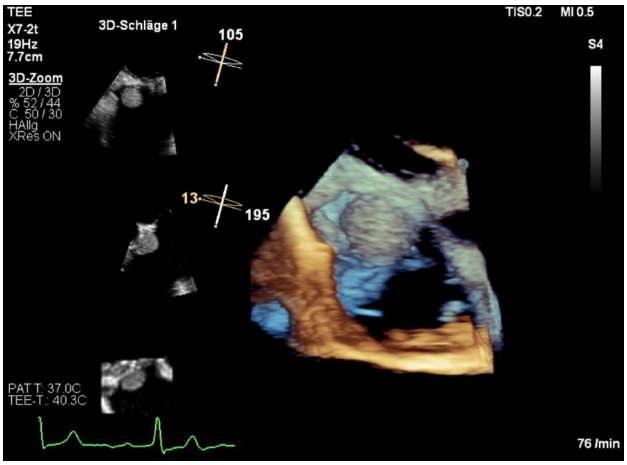


**Fig. 2 | 17–4** Transesophageal echocardiography showing a lesion within the right atrium, attached to the interatrial septum via 3D-modality

primary cardiac tumors when malignancy cannot be excluded. (1) Surgical resection was performed without complications. Intraoperatively, the lesion appeared atypical for a myxoma, presenting as a yellowish, round, solid structure located within Koch's triangle. Minimal manipulation released yellow sebaceous-like material. Microbiological testing of an intraoperative swab showed no microbial growth. Postoperatively, the patient developed intermittent third-degree atrioventricular (AV) block, confirmed on Holter monitoring. As an infectious etiology had not yet been excluded pending histopathological analysis, permanent pacemaker implantation was deferred, and an implantable loop recorder was placed for rhythm surveillance. Histopathology revealed a congenital polycystic tumor of the AV node with squamous and endodermal differentiation and without cytological atypia or mitotic activity, excluding malignancy. Congenital polycystic tumors of the AV node are extremely rare benign cardiac neoplasms with an autopsy incidence of 0.0017–0.03%. They account for approximately 2.7% of primary cardiac tumors and represent the most common primary cardiac tumor associated with sudden cardiac death. (2,3)

**Conclusion:** This case illustrates the diagnostic complexity of right atrial masses in a young patient with nonspecific symptoms. A lesion initially suspected to represent a myxoma on transesophageal echocardiography was ultimately

identified as a congenital polycystic tumor of the AV node, an exceedingly rare but clinically relevant entity. The case highlights the importance of multimodality imaging in the evaluation of intracardiac masses when initial findings are inconclusive. Although histologically benign, congenital polycystic tumors of the AV node have substantial clinical relevance due to their exclusive location within Koch's triangle and their potential to disrupt AV nodal conduction. The occurrence of intermittent third-degree AV block in our patient underscores the close relationship between the tumor, surgical manipulation, and the conduction system. Careful rhythm surveillance allowed a conservative approach and avoided immediate pacemaker implantation. Learning Points: • Not all interatrial masses represent myxomas; lesions within Koch's triangle should raise suspicion for conduction system–related tumors. • Multimodality imaging (TTE, TEE, CT, CMR) is essential for anatomical characterization of cardiac masses. • Congenital polycystic tumors of the AV node, despite benign histology, carry a risk of AV block and sudden cardiac death. • Surgical resection is recommended when malignancy cannot be excluded or clinically relevant arrhythmias occur.

## References


1. Lyon AR, Lopez-Fernandez T, Couch LS, Asteggiano R, Aznar MC, Bergler-Klein J, et al. 2022 ESC Guidelines on cardio-oncology developed in collaboration with the European Hematology Association (EHA), the European Society for Therapeutic Radiology and Oncology (ESTRO) and the International Cardio-Oncology Society (IC-OS). Eur Heart J Cardiovasc Imaging. 2022;23(10):e333–e465.
2. Luc JGY, Phan K, Tchantchaleishvili V. Cystic tumor of the atrioventricular node: a review of the literature. J Thorac Dis. 2017;9(9):3313–8. 3. Butany J, Nair V, Naseemuddin A, Nair GM, Catton C, Yau T. Cardiac tumours: diagnosis and management. Lancet Oncol. 2005;6(4):219–28.


# 17-5

## Fallbeispiel einer sehr seltenen Cardiomyopathie—linksventrikuläre apicale Hypoplasie


**Nimpf J.**

UK Krems, Krems, Österreich


**Einleitung:** Neben den bekannten häufigen Cardiomyopathien gibt es auch seltenere kongenitale Veränderungen des Herzens. Hier wird der Fall einer jungen Patientin mit einer isolierten linksventrikulären apicalen Hypoplasie (truncated left ventricle) vorgestellt. In der Literatur sind nur sehr wenige Fälle dieser unklassifizierten Cardiomyopathie beschrieben.

**Methoden:** Das Fallbeispiel wird anhand von Anamnese, Klinik, EKG sowie echocardiographischen Loops und Bildern vorgestellt.

**Resultate:** Eine 22 jährige, asymptomatische Patientin wurde in Vorbereitung auf eine Gastroskopie und Coloskopie untersucht. Der allgemeine physikalische Status war unauffällig, klinische Zeichen für eine Herzinsuffizienz bestanden nicht. Die Patientin war gut belastbar und berichtete mehrmals pro Woche Ausdauer und Krafttraining zu absolvieren. Bisher war es noch nie zu einer Synkope gekommen, Palpitationen wurden verneint. Die Familienanamnese war negativ. Im EKG zeigte sich ein normofrequenter Sinusrhythmus mit normaler PQ Zeit und ein SI, SII, SIII Lagetyp. Im QRS Komplex war eine Knotung

**Abb. 1 | 17-5** EKG


**Abb. 2 | 17-5** Echocardiographie paratsternale lange Achse

in aVR, sowie V4 und V5 zu erkennen, sowie eine S Persistenz bis V5. Echocardiographisch imponierte ein kugelig deformierter linker Ventrikel, ohne typisch konisch zulaufenden Apex. Es waren 3 Papillarmuskeln zu erkennen. Die LVEF war sehr schwer zu schätzen und dürfte niedrig normal bis leicht reduziert sein. Die 3D Messungen waren schwer zu interpretieren, ergaben ein LVEF von 29 %. Der LV strain lag bei –22,2 %. Der rechte Ventrikel war spitzenbildend und dem abgeschnittenen linksventrikulären Apex aufgelagert, der RV free wall strain ergab –24,9 %, der RV global strain –21,2 %.

**Schlussfolgerungen:** Die isolierte linksventrikuläre apicale Hypoplasie (truncated left ventricle) ist eine sehr seltene Herzerkrankung. In der Literatur sind nur wenige case reports beschrieben. Die erste Pubikation erfolgte im Jahr 2004 durch Fernandez-Valls et al. [1] Von einer isolierten linksventrikulären apicalen Hypoplasie (truncated left ventricle) ist vorwiegend das männliche Geschlecht betroffen, das mittlere Alter bei Diagnose liegt bei 26,1 ± 19,6 Jahren. Meist sind die betroffenen Personen asymptomatisch, Dyspnoe ist jedoch das häufigste Symptom. Im EKG zeigen sich oft T Wellen Veränderungen, fehlende R Progression und Rechtsachsenabweichungen und auch Vorhofflimmer Arrhythmien [2]. Wie die Erkrankung entsteht ist nicht bekannt, ein möglicher Entstehungsmechanismus ist eine inadäquate Dilatation während der Partitionierung der Ventrikel. Die Erkrankung ist auch mit einer Lamin A/C Mutation assoziiert [3]. Es gibt keine Daten, wie die betroffenen Patientinnen und Patienten behandelt werden sollen. Bei klinischen Symptomen kann Herzinsuffizienztherapie angeboten werden, je nach Vorliegen von malignen Arrhythmien kann ein ICD implantiert werden, es wurden auch schon CRT Systeme verwendet.

## Literatur

1. Fernandez-Valls et al. Isolated left ventricular apical hypoplasia: a new congenital anomaly described with cardiac tomography. Heart. 2004.
2. Bassareo PP, et al. Isolated left ventricular apical hypoplasia: Systematic review and analysis of the 37 cases reported so far. World J Clin Cases. 2023.
3. Mutation of the lamin A/C gene associated with left ventricular apical hypoplasia: a new phenotype for laminopathies? G Ital Cardiol. Rome: December; 2014.


## 17-6

### Successful Surgical Tricuspid Valve Repair of Severe Recurrent Tricuspid Regurgitation after Transcatheter Edge-to-edge Repair (TriClip)


**Winkler A.[1], Gansterer K.[1], Boxhammer E.[2], Neuner M.[3], Kirnbauer M.[3], Wuppinger T.[2], Dinges C.[1]**

[1]Universitätsklinik für Herzchirurgie, Salzburg, Austria
[2]Universitätsklinik für Innere Medizin II, Kardiologie und internistische Intensivmedizin, Salzburg, Austria
[3]Universitätsklinik für Anästhesie, perioperative Medizin und anästhesiologische Intensivmedizin, Salzburg, Austria


**Introduction:** Severe tricuspid regurgitation (TR) remains a challenging clinical entity, particularly in elderly patients with advanced right heart failure and multiple comorbidities. Transcatheter edge-to-edge repair (tTEER) using the TriClip system has emerged as a minimally invasive treatment option for patients at high surgical risk, demonstrating favorable short- and mid-term outcomes. However, long-term durability is still uncertain, and recurrent TR represents a clinically relevant problem associated with increased morbidity and mortality. Surgical treatment after failed tTEER remains rarely reported and poses technical challenges. We present a case of severe recurrent TR following initially successful TriClip implantation with subsequent recurrent TR, ultimately requiring surgical valve repair.

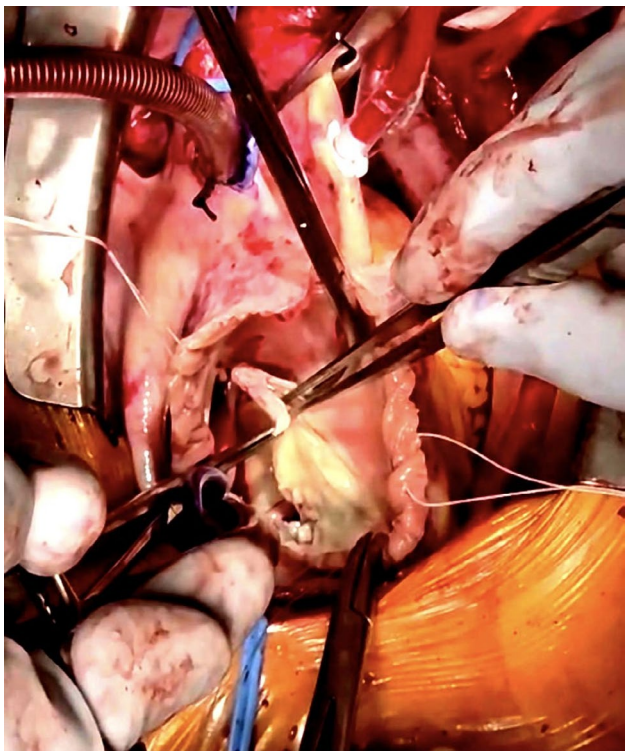

**Fig. 1 | 17-6** TriClip explantation illustrating device–tissue interaction; procedural details are available in video format

**Methods:** A 79-year-old female patient with a history of transcatheter tricuspid valve repair using three TriClips was admitted with progressive dyspnea (NYHA III) and declining functional capacity. Comprehensive diagnostic work-up included transthoracic and transesophageal echocardiography, invasive hemodynamic assessment, and multimodality imaging to evaluate right ventricular function, pulmonary pressures, and associated cardiac pathologies. The case was discussed in a multidisciplinary heart team to assess the feasibility of redo tTEER versus surgical intervention.

**Results:** Imaging revealed severe recurrent tricuspid regurgitation (TR), accompanied by right atrial dilatation, mildly impaired right ventricular function, and holosystolic hepatic vein flow reversal, as well as a chronic pericardial effusion. Redo transcatheter edge-to-edge repair (tTEER) was considered technically not feasible. The patient (EuroSCORE II 1.7; TRI-SCORE low-to-intermediate risk) therefore underwent elective cardiac surgery. Intraoperatively, all three TriClips were found to be securely attached to both valve leaflets, with no evidence of single leaflet device detachment (SLD). Careful inspection revealed that, in addition to leaflet tissue, the clips had partially grasped chordae tendineae. This inadvertent chordal entrapment may have impaired leaflet mobility and coaptation, thereby representing a plausible mechanism for the recurrent valve insufficiency. Following careful explantation of all clips, tricuspid valve repair was performed using ring annuloplasty (Medtronic Contour 3D Annuloplasty Ring, 32 mm) and commissuroplasty. Concomitant procedures included closure of a patent foramen ovale, left atrial appendage occlusion, and creation of a pericardial window. The postoperative course was uneventful. Follow-up echocardiography demonstrated a durable reduction of TR to mild without a significant transvalvular gradient. At three-month follow-up, the patient showed marked symptomatic improvement (NYHA class II) and stable valve function without rehospitalization.

**Conclusion:** This case demonstrates that surgical tricuspid valve repair after failed transcatheter edge-to-edge repair is feasible and can achieve excellent early clinical and echocardiographic outcomes. Careful patient selection, detailed anatomical assessment, and multidisciplinary heart team decision-making are essential for optimizing treatment strategies. With the increasing use of transcatheter therapies, awareness of surgical bailout options will become increasingly important.

## 17-7

### Catastrophic PE


**Burda M.**

Medizinische Universität Wien, Vienna, Austria


**Introduction:** Acute pulmonary embolism (PE) is a major cause of cardiovascular mortality (1, 2). In some patients, acute thromboembolic events may occur on the presence of previously unrecognized chronic thromboembolic disease, resulting in acute-on-chronic pulmonary embolism. The combined acute and chronic increase in pulmonary vascular resistance can precipitate rapid right ventricular failure and hemodynamic col-

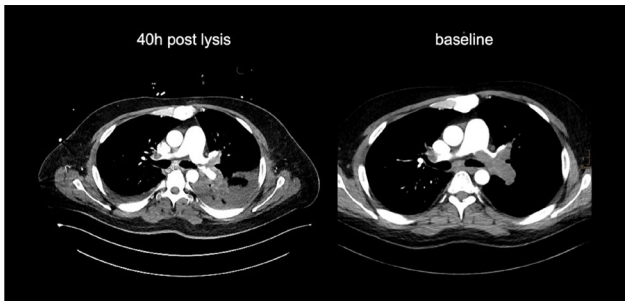


**Fig. 1 | 17-7** Computed tomography pulmonary angiogram pre and 40 h post lysis

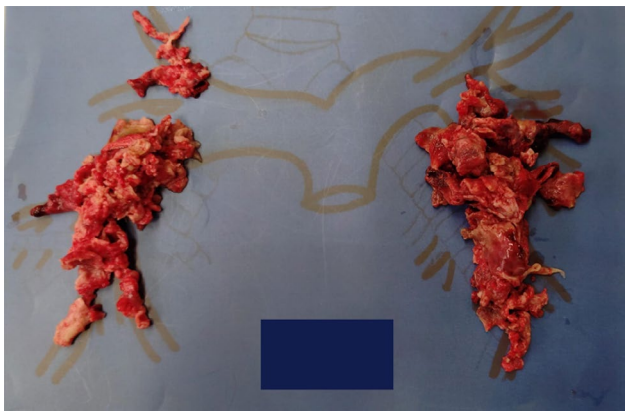

**Fig. 2 | 17-7** Surgical specimen, confirmed chronic thromboembolic disease

lapse, which are major determinants of mortality in PE (3, 4). Early diagnosis is challenging due to overlapping imaging and clinical features with isolated acute PE (1, 3).

**Methods:** This case report describes a catastrophic case of acute-on-chronic PE in a hospitalized patient. Clinical presentation, laboratory findings, imaging studies, surgical intervention and intensive care management were reviewed by the pulmonary embolism response team (PERT) that advised against catheter-directed treatment in this case.

**Results:** A 36-year-old male presented with heavy dyspnea for three days. Vitals: blood pressure 93/55 mmHg, heart rate 122/min, oxygen saturation 90% on 4 L/min of Oxygen. No lactate, but positive high-sensitivity troponin and NTproBNP of 34,983 ng/L. BMI 39.5 kg/m2 and recent Fournier's gangrene with previous month in intensive care. Computed tomography pulmonary angiography (CTPA) showed central PE with right arterial and right ventricle thrombus (Fig. 1), and signs suggestive of chronic thromboembolic pulmonary hypertension (CTEPH). The patient's clinical condition progressively deteriorated, requiring vasopressor support with catecholamines. Referring hospital started systemic lysis. Due to worsening hemodynamic instability, the patient was referred for hemodynamic support via extracorporeal membrane oxygenation (ECMO). During transport the patient suffered a cardiac arrest but was successfully resuscitated and placed on veno-arterial ECMO (VA-ECMO) support. After three days of stabilization on VA-ECMO, the patient underwent pulmonary thrombectomy. Histopathological examination of the surgical specimen confirmed chronic thromboembolic disease (Fig. 2).

**Conclusion:** Acute-on-chronic thromboembolism represents a severe and often underrecognized manifestation of chronic pulmonary thromboembolic disease, with poor prognosis (3). Surgical embolectomy can be considered in acute catastrophic PE (Class I, level c recommendation—according to the 2019 PE Guidelines of the European Society of Cardiology) (1). This approach may be particularly relevant when imaging findings suggest an underlying chronic thromboembolic disease, as pulmonal artery endarterectomy represents the treatment of choice in operable CTEPH. In unstable patients, temporary mechanical circulatory support may serve as a bridge to definitive surgical treatment.

## References

1. Konstantinides, S.V.; Meyer, G.; Becattini, C.; Bueno, H.; Geersing, G.J.; Harjola, V.P. et al. 2019 ESC Guidelines for the diagnosis and management of acute pulmonary embolism developed in collaboration with the European Respiratory Society (ERS): The Task Force for the diagnosis and management of acute pulmonary embolism of the European Society of Cardiology (ESC). Eur Respir J. 2019;54(3). DOI: https://doi.org/10.1183/13993003.01647-2019.
2. Keller, K.; Hobohm, L.; Ebner, M.; Kresoja, K.P.; Munzel, T.; Konstantinides, S.V. et al. Trends in thrombolytic treatment and outcomes of acute pulmonary embolism in Germany. Eur Heart J. 2020;41(4):522–9. DOI: https://doi.org/10.1093/eurheartj/ehz236.
3. Bryce, Y.C.; Perez-Johnston, R.; Bryce, E.B.; Homayoon, B.; Santos-Martin, E.G. Pathophysiology of right ventricular failure in acute pulmonary embolism and chronic thromboembolic pulmonary hypertension: a pictorial essay for the interventional radiologist. Insights Imaging. 2019;10(1):18. DOI: https://doi.org/10.1186/s13244-019-0695-9.
4. Matthews, J.C.; McLaughlin, V. Acute right ventricular failure in the setting of acute pulmonary embolism or chronic pulmonary hypertension: a detailed review of the pathophysiology, diagnosis, and management. Curr Cardiol Rev. 2008;4(1):49–59. DOI: https://doi.org/10.2174/157340308783565384.

# 17-8

## Severe Congenital Aortic Stenosis in Pregnancy Complicated by Postpartum Infective Endocarditis—A Case Report

**Baumer U., Karner E., Gössinger B., Binder C., Yerlinka-Schatten G., Stelzmüller M., Beitzke D., Hengstenberg C., Zilberszac R., Schrutka L., Prausmüller S.**

Medizinische Universität Wien, Wien, Austria

**Introduction:** Severe congenital aortic stenosis during pregnancy is associated with substantial maternal risk. Determining the optimal timing of definitive valve intervention remains challenging.

**Methods:** We report the case of a 26-year-old woman with congenital heart disease involving the aortic and pulmonary valves, who presented at 24 + 2 weeks gestation.

**Results:** Her medical history included balloon valvuloplasty of both valves shortly after birth. Transthoracic echocardiography demonstrated severe aortic stenosis with a mean transvalvular gradient of 68 mmHg, an aortic valve area of 0.7 $cm^2$, mild aortic and moderate pulmonary regurgitation, a left ventricular ejection fraction of 61%, and NT-proBNP levels at 362 pg/mL. Planned delivery was performed at 32 + 6 weeks gestation under general anesthesia with extracorporeal membrane oxy-

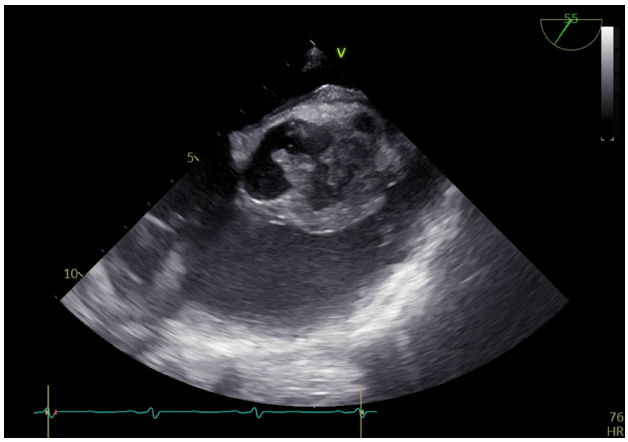

**Fig. 1 | 17-8** Transesophageal echocardiography showing severe destruction of the aortic valve with vegetations

genation standby. The patient was discharged in stable condition with a plan for close outpatient follow-up to allow subsequent planning of definitive aortic valve management. At scheduled follow-up five weeks postpartum, she presented with markedly elevated NT-proBNP levels (3542 pg/mL, at discharge 184 pg/mL) and increased inflammatory markers. Transthoracic echocardiography showed a thickened aortic valve, and on transesophageal echocardiography severe valve destruction with vegetations and suspected annular abscess was identified (Fig. 1). Blood cultures yielded Staphylococcus capitis. Due to extensive valvular and periannular tissue destruction, implantation of a mechanical valve was not feasible, and a biological Bentall conduit was implanted.

**Conclusion:** This case demonstrates that sustained clinical stability throughout pregnancy and the early postpartum period may be followed by severe complications, underscoring the challenge of determining the optimal timing of definitive valve intervention in high-risk patients.

## 17-9

### Diagnosis of type 2 heparin-induced thrombocytopenia via splenic thromboembolism in the absence of decreased platelet count—a case report

**Hofbauer T.[1], Lenz M.[1], Haider P.[1], Zimpfer D.[2], Richter B.[1], Zilberszac R.[1]**

[1]Department of Cardiology, Internal Medicine II, Medical University of Vienna, Wien, Austria
[2]Department of Cardiac and Thoracic Aortic Surgery, Medical University of Vienna, Wien, Austria

**Introduction:** Heparin-induced thrombocytopenia (HIT) type 2 is defined as formation of IgG antibodies against platelet-factor 4 bound to heparin, leading to potentially life-threatening thrombocytopenia and arterial and/or venous thromboses [1]. Both morbidity and mortality are considerable [2]. Diagnosis is commonly made via the 4T score [3], comprising severity of thrombocytopenia, clinical signs of thrombosis, timing of onset after heparin exposure and presence or absence of other causes of thrombocytopenia. Once suspected, discontinuation of heparin and switch to non-heparin-based anticoagulation is indicated.

**Methods:** In this report, we describe a case of a 44-year-old female patient. The patient gave written consent to have this case presented. She was referred to our Department of Cardiac and Thoracic Aortic Surgery due to progressive dyspnea on exertion in the setting of known Ebstein anomaly of the tricuspid valve with severe valvular regurgitation. Other relevant prior diseases included obesity (BMI 31.6), prior smoking and obstructive sleep apnoea. Invasive hemodynamic measurement six months prior to surgery excluded pulmonary hypertension (mean pulmonary arterial pressure 19 mmHg, pulmonary arterial wedge pressure 9 mmHg). The right ventricle was severely dilated, with normal function. There was no history of heparin exposure within the previous 100 days.

**Results:** The patient was operated on October 6th 2025. Since valve reconstruction turned out to be technically unviable, biological valve replacement was performed. Intra-operatively, a cumulative dose of 60,000 Units of unfractionated heparin (UFH) was administered. The patient was transferred to our ICU postoperatively. The trajectory of platelet count is given in Fig. 1. Prior to surgery, the patient had normal platelets of 283 G/L (reference 162–379 G/L). Upon admission at the intensive care unit, platelet count fell to 117 G/L. Prophylactic UFH was started on POD1 (300 Units/h). The lowest measured platelet count occurred on postoperative day (POD)2 (116 G/L), after which platelets rose steadily to 327 G/L on POD14. On POD17, due to extubation failure and protracted respiratory weaning, a CT scan of the lungs and abdomen was conducted, which showed multiple splenic infarctions (affecting ~20% of parenchyma) deemed to be of thromboembolic origin. Importantly, no other organs were affected by thromboembolisms. That day, platelet count was 287 G/L (corresponding to a decline in platelets of ~12% compared to POD 14). Laboratory assessment revealed strongly positive heparin-PF4-induced IgG antibodies (optical density 2.07, lower limit of normal < 0.51). Anticoagulation was switched to the direct thrombin inhibitor argatroban. Upon switch, the patient improved remarkably, making weaning from the respirator possible. After 18 days, apixaban 5 mg b. i. d. was given for three months.

**Conclusion:** While the initial drop in platelets on POD0 would have given two points on the 4T score (decrease of > 50% or nadir ≥ 20 G/L), at that time, reactive thrombocytopenia in response to surgery was deemed more likely (0 points). Furthermore, there were no clinical signs of thrombosis or skin necrosis (0 points). Initial platelet decrease occurred within 4 days without recent exposure (0 points). This resulted in a total 4T score of 2 points, indicating low pretest probability for HIT type 2. Hence, HIT antibodies were initially not assessed. HIT was diagnosed only after detection of splenic thromboembolism. Notably, at that time, platelet count was paradoxically increasing despite continued exposure to UFH. In summary, we report an intriguing case underscoring that HIT type 2 can present with misleading early features and may therefore evade standard risk stratification tools such as the 4T score.

### References

1. Ng JY, D'Souza M, Hutani F, Choi P. Management of Heparin-Induced Thrombocytopenia: A Contemporary Review. JCM. 2024;13.
2. Pishko AM, Lefler DS, Gimotty P, Paydary K, Fardin S, Arepally GM, Crowther M, Rice L, Vega R, Cines DB, Guevara JP, Cuker A. The risk of major bleeding in patients with suspected heparin-induced thrombocytopenia. J Thromb Haemostasis: Jth. 2019;17:1956–65.
3. Lo GK, Juhl D, Warkentin TE, Sigouin CS, Eichler P, Greinacher A. Evaluation of pretest clinical score (4 T's) for the diagnosis of heparin-induced thrombocytopenia in two clinical settings. J Thromb Haemostasis: Jth. 2006;4:759–65.

# POSTERSITZUNG 18 – HERZINSUFFIZIENZ & KARDIOMYOPATHIEN 2

## 18-1

### Hospital at Home (H@H) für Patient*-innen mit Herzinsuffizienz: Evidenzlage, Versorgungslogiken und Implikationen für die kardiologische Praxis

**Grall A.[1], Schulc E.[2], Dieplinger A.[3]**

[1]Paracelsus Medizinische Privatuniversität, Salzburg, Österreich
[2]UMIT Tirol, Hall in Tirol, Österreich
[3]Landespflege und Betreuungszentren des Landes OÖ, Linz, Österreich

**Einleitung:** Gesundheitssysteme stehen angesichts des demografischen Wandels, der steigenden Prävalenz chronischer Erkrankungen und zunehmender Kosten unter zunehmendem Druck. Herz-Kreislauf-Erkrankungen zählen in Österreich zu den häufigsten Ursachen für Hospitalisierungen älterer Menschen und verursachen hohe Belastungen im stationären Setting. Die Anforderungen an die Akutversorgung reichen von ungeplanten Besuchen in der Notaufnahme bis hin zu stationären oder intensivmedizinischen Aufenthalten, was zu erheblichen Kosten für das Gesundheitssystem führt. Internationale Erfahrungen zeigen, dass alternative Versorgungskonzepte wie H@H eine Akutversorgung auf Krankenhausniveau im häuslichen Umfeld ermöglichen können und für ausgewählte Patient*innengruppen sicher, wirksam und ressourcenschonend sein können. Während H@H-Programme in mehreren OECD-Ländern seit Jahren etabliert sind, fehlt es in Österreich bislang an einer systematischen Implementierung.

**Methoden:** Es wurde ein narratives Review mit systematischer Datenbanksuche durchgeführt, um die internationale Evidenz zum Versorgungskonzept H@H im kardiologischen Kontext zusammenzuführen. Die Literaturrecherche erfolgte zwischen April 2024 und Jänner 2026 in den Datenbanken PubMed, CINAHL und Epistemonikos. Berücksichtigt wurden deutsch- und englischsprachige Publikationen. Die Suchstrategie wurde iterativ entwickelt und kombinierte den Begriff „Hospital at Home“ sowie dazugehörige Synonyme mit Freitextbegriffen und MeSH-Terms. Eingeschlossen wurden Publikationen aus dem Zeitraum 2014–2026, die sich mit H@H als Akutversorgung auf Krankenhausniveau im häuslichen Umfeld befassen.

**Resultate:** Die analysierte Literatur zeigt, dass H@H international aus den Modellen „admission avoidance H@H“ und „early supported discharge H@H“ besteht und strukturell in die Krankenhausversorgung eingebunden ist. Studien berichten über vergleichbare Mortalitätsraten bzw. Patient*innensicherheit zum Krankenhaus, niedrige oder vergleichbare Wiederaufnahmeraten sowie eine Reduktion stationärer Behandlungstage. Mehrere Arbeiten belegen zudem relevante Kosteneinsparungen und eine hohe Patient*innenzufriedenheit. Telemedizinische Anwendungen und Telemonitoring werden unterstützend eingesetzt und ermöglichen eine engmaschige häusliche Überwachung. Digitale Transformation im Management und in der Logistik kann die Gesamteffizienz von Gesundheitssystemen erhöhen. H@H stellt bei sorgfältiger Selektion von Patient*-innen eine gleichwertige Versorgung zur stationären Versorgung dar und bietet im Übergang von der Akutbehandlung in die nachfolgende Versorgung Vorteile, deren Umsetzung im Versorgungssystem bislang deutlich unter ihrem Potenzial bleibt.

**Schlussfolgerungen:** Insgesamt zeigt sich, dass H@H für ausgewählte Patient*innengruppen eine sichere, effektive und kosteneffiziente Alternative zur stationären Akutversorgung darstellt. Studien zeigen vermehrt vergleichbare klinische Outcomes zum stationären Aufenthalt, eine hohe Patient*-innenzufriedenheit sowie eine Reduktion der stationären Aufenthaltsdauer und Kosten. Damit ist der Reformansatz H@H nicht nur ein innovatives Einzelprojekt, sondern kann als evidenzbasierte Versorgungsform eingeordnet werden. H@H stellt einen systemischen Reformansatz der Akutversorgung dar, der eine patient*innenzentrierte Versorgung ermöglicht. Weitere Forschung sollte sich verstärkt auf Implementierungsstrategien, langfristige Nachhaltigkeit und die Integration in bestehende Gesundheitssysteme konzentrieren.

## 18-2

### Safety and Efficacy of Mavacamten in the Treatment of Hypertrophic Obstructive Cardiomyopathy in a Prospective Real-World Cohort: A 3 Month Follow-up

**Mairhofer H., Santner V., Höller V., Pötsch S., Eber P., Tuppinger H., Wallner M., Kolesnik E., Zirlik A., Ablasser K., Verheyen N., Schwegel N.**

Medical University of Graz, Graz, Austria

**Introduction:** Mavacamten, a cardiac myosin-inhibitor, was the first non-invasive treatment to improve left ventricular outflow tract obstruction (LVOTO) in symptomatic hypertrophic obstructive cardiomyopathy (oHCM). So far, there is limited follow-up data on the safety and efficacy of mavacamten in the treatment of oHCM. Purpose In this prospective real-world cohort in Austria, we report the 3-month follow-up outcomes of treatment with mavacamten in patients with oHCM.

**Methods:** We included all consecutive patients treated at the outpatient clinic for oHCM at the Medical University of Graz initiated with mavacamten between July 28, 2023, and May 09, 2025. In accordance with prescription guidelines, follow-up examinations were performed every four weeks, with detailed examinations at baseline and after 3 months. Assessments included medical and medication history, laboratory tests, echocardiography with LVOT gradient measurement, cardiopulmonary exercise testing (CPET), and symptom assessment, including patient-recorded quality of life using the Kansas City Cardiomyopathy Questionnaire (KCCQ). Statistical analysis was performed using a linear regression adjusted for the respective baseline value.

**Results:** A total of 27 patients were enrolled. Median (interquartile range (IQR)) age was 54 years (47;68), including 12 (44%) females. Eighteen (67%) patients were started on 2.5 mg of mavacamten and 9 (33%) were started on 5 mg (Table 1). After 12 weeks of treatment, a significant reduction in the cardiac biomarkers *N*-terminal pro-brain natriuretic peptide (NT-proBNP, absolute change [IQR] –198 [1; –952] pg/mL, $p < 0.001$) and high-sensitive troponin T (–4.0 [–2.0; –8.0] pg/mL, $p < 0.001$) was observed. Resting (left ventricular outflow tract (LVOT) gradient showed a significant reduction (–7 [2; –19] mmHg) while parameters for physical capacity derived by CPET showed divergent results (peak oxygen consumption [peak VO2] –0.9 [2.0;

–3.3] mL/kg/min, $p < 0.001$; minute ventilation/carbon dioxide production [VE/VCO2 slope] –0.9 [–2.5; 2.7], $p = 0.043$). Patient-reported quality of life improved but did not meet statistical significance (KCCQ score 10 (–1;23)/100, $p = 0.062$) (Table 2). In terms of safety, one patient developed a left ventricular ejection fraction (LVEF) < 30% on treatment and one patient developed a LVEF < 50%, which led to intermittent discontinuation of the medication. One patient was hospitalized due to new-onset atrial fibrillation.

**Table 1. Baseline characteristics of patients treated with Mavacamten (n=27)**

| Variables | Baseline |
|---|---|
| Age, years | 54 (47;68) |
| Women, n (%) | 12 (44) |
| Myosin-inhibitor Mavacamten, n (%) | 27 (100) |
| Initial Dose 2.5 mg, n (%) | 18 (67) |
| Initial Dose 5 mg, n (%) | 9 (33) |
| NYHA functional class | |
| I, n (%) | 1 (4) |
| II, n (%) | 15 (58) |
| III, n (%) | 10 (39) |
| Angina Pectoris, n (%) | 11 (42) |
| Palpitations, n (%) | 12 (48) |
| Arterial hypertension, n (%) | 17 (65) |
| Fatigue, n (%) | 1 (4) |
| Dizziness, n (%) | 5 (23) |
| History of presyncope, n (%) | 1 (4) |
| History of syncope, n (%) | 1 (4) |
| NT-proBNP, pg/mL | 454 (167;1016) |
| High-sensitive troponin T, pg/mL | 16.5 (10.8;20.5) |
| Creatinine, mg/dL | 0.9 (0.8;1.1) |
| LVEF, % | 64 (59;68) |
| Resting LVOT Gradient, mmHg | 23 (13;45) |
| Valsalva-provoked LVOT Gradient, mmHg | 67 (36;105) |
| Max provoked LVOT Gradient, mmHg | 91 (52;119) |
| Peak $VO_2$, mL/kg/min | 18.4 (15.15;21.9) |
| VE/$VO_2$ slope | 30.7 (28.6;32.9) |
| $O_2$ Pulse max, mL/beat | 12.3 (10.2;16.3) |
| KCCQ Score, /100 | 57 (52;73) |

Variables are reported as median (interquartile range) or frequencies (percentages).

Abbreviations. NYHA, New York Heart Association; NT-proBNP, N-terminal pro-brain natriuretic peptide; LVEF, left ventricular ejection fraction; LVOT, left ventricular outflow tract; peak $VO_2$, maximal oxygen consumption; VE/$CO_2$ slope, minute ventilation/carbon dioxide production, KCCQ, Kansas City Cardiomyopathy Questionnaire.

Fig. 1 | 18-2

**Table 2. Efficacy outcomes after 3 months of follow-up.**

| Variables | Baseline | 3 month follow-up | Absolute change | Percent change | p-value | Available data at baseline, n (%) | Available data at follow-up, n (%) |
|---|---|---|---|---|---|---|---|
| NT-pro BNP, pg/mL | 454 (167;1016) | 236 (122;405) | -198 (1;-952) | -50 (0;-73.7) | **<0.001** | **24 (89)** | **26 (96)** |
| High sensitive troponin T, pg/mL | 16.5 (10.8;20.5) | 10.0 (7.8;16.5) | -4.0 (-2.0;-8.0) | -31 (-18;-46) | **<0.001** | **26 (96)** | **26 (96)** |
| LVEF, % | 64 (59;68) | 61 (60;67) | -3 (2;-6) | -4 (-4;-9) | 0.357 | **26 (96)** | **26 (96)** |
| Resting LVOT Gradient, mmHg | 23 (13;45) | 16 (8;26) | -7 (2;-18.5) | -31 (-19;-59) | **0.017** | **26 (96)** | **26 (96)** |
| Valsalva-provoked LVOT Gradient, mmHg | 67 (36;105) | 48 (17;72) | -5 (6;-67) | -22 (11;-66) | 0.556 | **25 (93)** | **24 (89)** |
| Max provoked LVOT Gradient, mmHg | 91 (52;119) | 59 (34;93) | -16 (-6;-55) | -30 (-13;-48) | 0.296 | **24 (89)** | **7 (26)** |
| Peak $VO_2$, mL/kg/min | 18.4 (15.2;21.9) | 19.5 (15.8;23.6) | -0.9 (3.3;-2.0) | -4 (17;-10) | **<0.001** | **25 (93)** | **21 (78)** |
| VE/$VCO_2$ slope | 30.7 (28.6;32.9) | 30.9 (28.2;33.1) | -0.9 (2.7;-2.5) | -3 (8;-7) | **0.043** | **21 (78)** | **21 (78)** |
| KCCQ Score, /100 | 57 (52;73) | 77 (69;86) | 10 (-1;23) | 12 (-1;37) | 0.062 | 23 (85) | 22 (81) |

Variables are reported as median (interquartile range) or frequencies (percentages). P-values derived from linear regression adapted for the respective baseline value.

Abbreviations. NT-proBNP, N-terminal pro-brain natriuretic peptide; LVEF, left ventricular ejection fraction; LVOT, left ventricular outflow tract; peak $VO_2$, maximal oxygen consumption; VE/$CO_2$ slope, minute ventilation/carbon dioxide production; KCCQ, Kansas City Cardiomyopathy Questionnaire.

Fig. 2 | 18-2

**Conclusion:** After three months, the myosin-inhibitor mavacamten led to a reduction of LVOT gradients and cardiac biomarkers, while trajectories of physical capacity and patient-reported quality of life were neutral. These data indicate that mavacamten-mediated reductions of LVOT gradients and filling pressures do not translate into a significant improvement of physical capacity during the initiation phase of mavacamten.

## 18-3

## Iron deficiency in patients with wild-type transthyretin amyloid cardiomyopathy

**Ungericht M.[1], Lanser L.[2], Fugger F.[1], Puelacher C.[1], Messner M.[1], Zaruba M.[1], Bauer A.[1], Weiss G.[2], Poelzl G.[1]**

[1]Department of Internal Medicine III, Cardiology & Angiology, Medical University of Innsbruck, Innsbruck, Austria
[2]Department of Internal Medicine II, Medical University of Innsbruck, Innsbruck, Austria

**Introduction:** Iron deficiency (ID) is common in heart failure (HF). In contrast, data on the prevalence and clinical relevance of ID in patients with wild-type transthyretin amyloid cardiomyopathy (ATTRwt-CM) are limited. This study aimed to characterize ID and to evaluate its associations with disease severity and functional capacity in ATTRwt-CM.

**Methods:** This retrospective single-center study was conducted at the amyloidosis referral center of the Department of Cardiology, Medical University Innsbruck. ID was defined according to three definitions: (1) ferritin <100 ng/mL irrespective of transferrin saturation (TSAT) (absolute ID), (2) ferritin 100–299 ng/mL with TSAT <20% (combined ID), (3) ferritin ≥300 ng/mL with TSAT <20% (functional ID). Disease severity was assessed using cardiac biomarkers (NT-proBNP, troponin T) and validated risk stratification scores (Mayo score). In a subset of patients, functional capacity was evaluated by six-minute walk distance (6MWD).

**Results:** A total of 167 treatment-naïve patients were included at first diagnosis of ATTRwt-CM. 49.7% of the ATTR cohort had ID, with absolute ID being the most prevalent form (28.7%), followed by combined ID (15%) and functional ID (6%). Of note, TSAT <20% emerged as a marker of disease severity, being associated with higher NT-proBNP ($p=0.023$) and troponin T levels ($p=0.038$), as well as more advanced Mayo stages ($p=0.034$). Further, TSAT<20% was associated with reduced functional capacity, as reflected by a shorter 6MWD ($p=0.042$). Although ATTRwt-CM predominantly affects men (82% male gender in our ATTRwt-CM cohort), women showed more frequently TSAT <20% ($p=0.023$), suggesting a potentially high vulnerability in female patients.

**Conclusion:** ID was highly prevalent in ATTRwt-CM patients. Functional markers of ID, particularly TSAT, were primarily associated with disease severity and reduced functional capacity. Further studies are needed to determine whether ID treatment may favorably influence the clinical course of ATTRwt-CM.

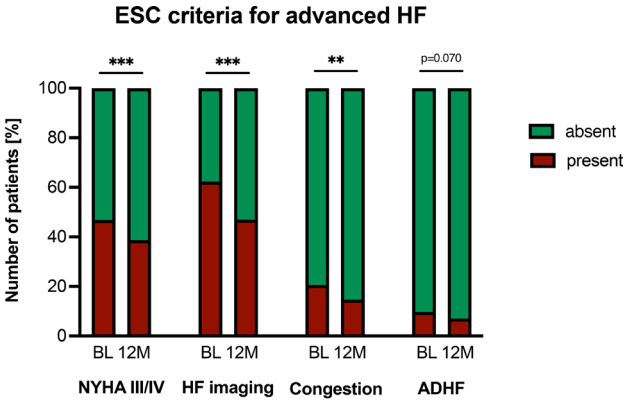


**Figure 1:** Proportion of patients in the cohort fulfilling the ESC criteria for ADHF at BL and 12M. The four ESC criteria for ADHF include: (1) NYHA class III or IV; (2) HF imaging findings defined as one of the following: (a) LVEF <30%, (b) isolated RVF, (c) non-operable severe valvular or congenital heart disease (not recorded), or (d) LVEF ≥40% with elevated NP and significant diastolic dysfunction; (3) congestion defined as either repeated hospitalizations for HF (recorded only for 12M) or need for high-dose diuretics; and (4) severely impaired exercise capacity defined by $pVO_2$ or 6-MWT (not recorded). ADHF is defined by the presence of all four criteria. Modifications: Congestion was definied positive with ≥80mg furosemide daily; exercise capacity was not available in the cohort. ADHF was considered present when all three were fulfilled.

**Abbreviations:** ADHF – advanced heart failure; BL – baseline; ESC – European Society of Cardiology; HF – heart failure; LVEF – left ventricular ejection fraction; NP – natriuretic peptides: NYHA – New York Heart Association; $pVO_2$ – peak oxygen consumption; RVF – right ventricular failure; 6-MWT – six-minute walk test; 12M – 12-month follow-up

**Fig. 1 | 18-4**

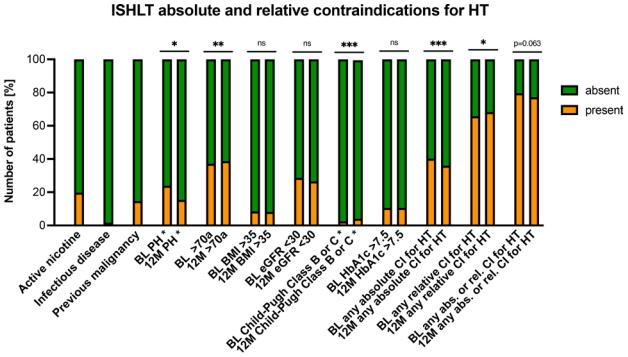


**Figure 2:** Absolute and relative CI for HT according to ISHLT criteria. The proportions of the absolute CI PH and the relative CIs age >70 years, BMI >30 kg/m², eGFR <30 mL/min/1.73 m², Child–Pugh class B or C, and HbA1c >7.5% are shown for BL and 12M. The absolute CIs active nicotine consumption and chronic infectious diseases (HBV, HCV, Tbc, HIV), as well as the relative CI of previous malignancy, were recorded as general patient characteristics and were therefore not assigned to a specific study visit (BL or 12M).

*For parameters with partially missing data, proportions were calculated based on the available observations.

**Abbreviations:**
BMI – body mass index; BL – baseline; CI – contraindication; eGFR – estimated glomerular filtration rate; HBV – hepatitis B virus; HCV – hepatitis C virus; HIV – human immunodeficiency virus; HT – heart transplantation; ISHLT – International Society for Heart and Lung Transplantation; PH – pulmonary hypertension; Tbc – tuberculosis; 12M – 12-month follow-up

**Fig. 2 | 18-4**

## 18-4

## Advanced heart failure definition and eligibility for HT at first presentation and at 12-months FUP: an analysis of the VIENNA-HF registry

**Stix E., Panagiotides N., Prausmüller S., Arfsten H., Spinka G., Heitzinger G., Bartko P., Hengstenberg C., Hülsmann M., Pavo N.**

Medizinische Universität Wien, Wien, Austria

**Introduction:** Advanced heart failure (ADHF) represents a severe stage of heart failure associated with high morbidity and mortality. Therapeutic options for ADHF remain limited, with heart transplantation (HT) being the current gold standard. However, the definitions for ADHF are not exact and vary across cardiologic societies. The aim of this project was to identify the extent to which real-world heart failure populations of a tertiary center fulfill guideline-based ADHF criteria and eligibility for HT at first presentation and at 12-months after GDMT up-titration.

**Methods:** This single-center cohort study analyzed data from the prospective heart failure registry at the Medical University of Vienna VIENNA-HF. Adult patients (≥18 years) with chronic HF and a history of NT-proBNP >1500 pg/ml and LVEF <30% attending routine outpatient visits were included. Patients with both a baseline (BL) visit and a one-year follow-up (12M) visit were selected. ESC guideline-defined ADHF criteria were mapped to the closest available registry variables. Similarly, the presence of absolute and relative contraindications for HT, according to International Society for Heart Lung Transplantation (ISHLT) recommendations, was evaluated. The proportion of patients fulfilling the different criteria were assessed at BL and 12M.

**Results:** A total of 470 patients were included. Median NT-proBNP was 3217 pg/ml (Q1; Q3: 1773; 6454) and 78% were male. The proportion of patients fulfilling each ADHF criterion decreased between BL and 12M upon GDMT implementation [47%, 62% and 21% vs. 39%, 46%, 15% for ADHF criterion 1, 2 and 3, $p<0.001$ for all, respectively] while ADHF definition showed a trend for decrease (9.4% vs 6.6%, $p=0.070$) (Fig. 1). Criterion 3, assessing systemic congestion and HHF, was the most selective for classifying patients as having ADHF. Regarding eligibility for HT, the majority of patients exhibited a relative or absolute contraindication (80% vs. 77%, $p=0.063$), while the distribution of relative and absolute contraindications mostly remained simi-

lar between first presentation and 12 months (Fig. 2). The most common contraindications in the VIENNA-HF cohort were age, impaired renal function, and active nicotine abuse.

**Conclusion:** Only a small proportion of patients with severe HF in this real-world cohort of a tertiary center met ESC-defined criteria for ADHF, while only about 1 in 5 patients was primarily eligible for HT. The most crucial criterion for defining ADHF is congestion, the recognition and management of which will increasingly rely on advances in HF management and the growing outpatient care infrastructure.

## References


1. Kemp CD, Conte JV. The pathophysiology of heart failure. Cardiovasc Pathol. 2012;21(5):365–71. https://doi.org/10.1016/j.carpath.2011.11.007.
2. Tomasoni D, Vishram-Nielsen JKK, Pagnesi M, et al. Advanced heart failure: guideline-directed medical therapy, diuretics, inotropes, and palliative care. Esc Heart Fail. 2022;9(3):1507–23. https://doi.org/10.1002/ehf2.13859.
3. Crespo-Leiro MG, Metra M, Lund LH, et al. Advanced Heart Failure: A Position Statement of the Heart Failure Association of the European Society of Cardiology. European J of Heart Fail. 2018;20(11):1505–35. https://doi.org/10.1002/ejhf.1236.
4. Mehra MR, Canter CE, Hannan MM, et al. The 2016 International Society for Heart Lung Transplantation listing criteria for heart transplantation: A 10-year update. J Heart Lung Transplant. 2016;35(1):1–23. https://doi.org/10.1016/j.healun.2015.10.023.


## 18-5

### Atrial Fibrillation Subtype and Cardiopulmonary Exercise Performance in Transthyretin Amyloid Cardiomyopathy (ATTR-CM)


**Kösters A., Ermolaev N., Gregshammer B., Eslami M., Rettl R., Lichtblau L., Kronberger C., Schmid L., Poledniczek M., Badr Eslam R., Schukro C.**

Medizinische Universität Wien, Wien, Austria


**Introduction:** Atrial fibrillation (AF) is common in transthyretin amyloid cardiomyopathy (ATTR-CM) and may contribute to reduced functional capacity and impaired cardiopulmonary exercise performance. However, the relationship between AF subtype and objective functional and ventilatory parameters in ATTR-CM remains incompletely characterized. We aimed to compare functional capacity and ventilatory efficiency across AF subtypes in patients with ATTR-CM.

**Methods:** This prospective, single-center study included patients with ATTR-CM (wild-type and hereditary) enrolled from 2018 to the present. AF status was categorized as (I) no AF, (II) paroxysmal AF, or (III) permanent AF. Functional capacity and cardiopulmonary exercise parameters were assessed using the 6-minute walk test (6 MWT), maximal workload (W), peak oxygen uptake (peak $VO_2$), and ventilatory efficiency ($VE/VCO_2$ slope). Between-group comparisons were performed using the Kruskal–Wallis test.

**Results:** A total of 169 patients with ATTR-CM were included. Functional capacity differed significantly across AF subtypes. Median 6 MWT distance was 438.5 m (IQR 363–520) in patients without AF, 315 m (IQR 268.5–414.5) in paroxysmal AF, and 372 m (IQR 305–450) in permanent AF ($p=0.0004$). Maximal workload was higher in patients without AF (90 W, IQR 70–110) compared with paroxysmal (65 W, IQR 49–90) and permanent AF (63 W, IQR 49–90) ($p=0.0009$). Peak $VO_2$ was also higher without AF (16.35 $mL \cdot kg^{-1} \cdot min^{-1}$, IQR 12.4–20.0) than with paroxysmal (13.8, IQR 10.6–16.4) or permanent AF (13.7, IQR 11.5–15.8) ($p=0.0044$). Ventilatory efficiency differed across AF subtypes, with $VE/VCO_2$ slope 34.04 (IQR 31.28–40.65) in no AF, 39.41 (IQR 34.06–45.43) in paroxysmal AF, and 39.97 (IQR 36.17–43.15) in permanent AF ($p=0.0008$).

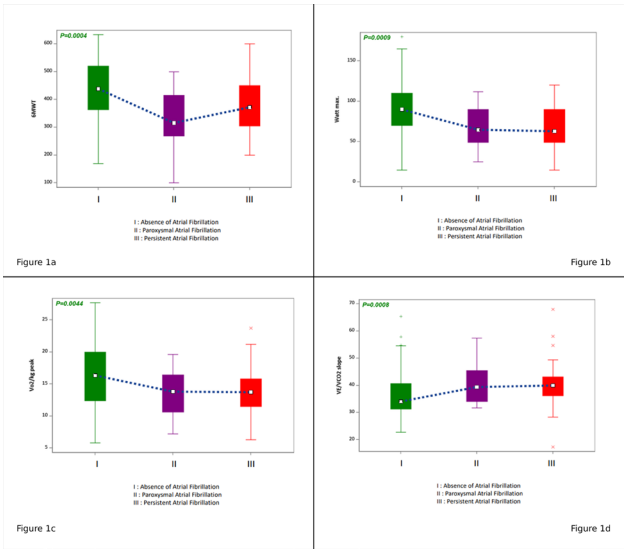


**Fig. 1 | 18-5** Functional capacity and ventilatory efficiency by atrial fibrillation subtype (I: no atrial fibrillation; II: paroxysmal atrial fibrillation; III: permanent atrial fibrillation). (a) 6-minute walk test (6 MWT). (b) Maximal workload (W). (c) Peak oxygen uptake (peak $VO_2$). (d) $VE/VCO_2$ slope

**Conclusion:** In this prospective ATTR-CM cohort, AF subtype was associated with significant differences in functional capacity, exercise performance, and ventilatory efficiency. Compared with patients without AF, those with paroxysmal or permanent AF showed lower 6 MWT distance, reduced maximal workload and peak $VO_2$, and higher $VE/VCO_2$ slope, consistent with greater functional limitation and impaired ventilatory efficiency in ATTR-CM.

## 18-6

### Functional capacity assessment in cardiac wild-type transthyretin amyloidosis with the one-minute sit-to-stand test and the six-minute walk test


**Dhillon M., Pahr S., Lichtblau L., Koesters A., Eslami M., Kronberger C., Schmid L., Poledniczek M., Ermolaev N., Badr Eslam R.**

Universitätsklinik für Innere Medizin II, Klinische Abteilung für Kardiologie, Medizinische Universität Wien, Wien, Austria


**Introduction:** For the evaluation of functional capacity in patients with cardiac wild-type transthyretin amyloidosis (ATTRwt-CM) the 6-minute walk test (6 MWT) is the gold standard, which can be difficult to perform in the clinical setting due to the lack of space, time, and trained staff. Recently, a new test, the one-minute sit-to-stand test (STST) has been proposed as an alternative method, which is easier to perform

due to its minimal time and space requirements. This study will prospectively assess the correlation between the one-minute sit-to-stand test (STST) and the 6-minute walk test (6 MWT) in patients with ATTRwt-CM.

**Methods:** For the STST, patients were required to stand up and sit down from a chair for the duration of one minute. The test used a standard chair (seat height: 46–48 cm) without armrests, positioned securely against a wall. Patients placed their hands on their hips to prevent arm or hand assistance during movement. The goal was to complete as many repetitions as possible within one minute. In the end the number of repetitions was recorded. For the 6 MWT, patients walked back and forth a 50 m corridor for six minutes. The number of completed laps was noted, and any additional distance walked beyond the final lap was measured using 1 m corridor markings.

**Results:** A total of 32 patients were included in this study, with a mean age of 81.3 ± 4.7 years. Of these 28 (87%) were male. The mean BMI was 24.7 ± 3.3. 56% of patients had a Perugini grade 3 uptake. There was a statistically significant positive correlation between the STST and the 6 MWT ($r = 0.68$, $p < 0.05$).

**Conclusion:** The results suggest that performances of the one-minute STST correlate positively with the 6 MWT in ATTRwt-CM patients. It shows potential as a substitute for assessing physical performance in medical practices and gaining knowledge on patients' well-being.

## 18-7

### An Interpretable Machine Learning Approach for Predicting 3-Year Heart Failure–Specific Hospitalization

**Leiherer A.[1,2,3], Schnetzer L.[2], Larcher B.[4,2], Mader A.[4,2], Mink S.[5,6,7], Muendlein A.[2], Bermeitinger B.[8], Hammerer-Lercher A.[3], Drexel H.[2,1,9,10], Saely C.[1,2,4]**

[1]Private University of the Principality of Liechtenstein, Triesen, Liechtenstein
[2]Vorarlberg Institute for Vascular Investigation & Treatment (VIVIT), Feldkirch, Austria
[3]Central Medical Laboratories Feldkirch, Feldkirch, Austria
[4]Department of Medicine I, Academic Teaching Hospital Feldkirch, Feldkirch, Austria
[5]Austrian Red Cross Blood Donation Center in Vorarlberg, Feldkirch, Austria
[6]Department of Laboratory Medicine, Paracelsus Medical University Salzburg, Salzburg, Austria
[7]Department of Medical Sciences, Private University in the Principality of Liechtenstein, Triesen, Liechtenstein
[8]Institute of Computer Science in Vorarlberg, University of St.Gallen (HSG), Dornbirn, Austria
[9]Drexel University College of Medicine, Philadelphia, Philadelphia, United States
[10]Vorarlberger Landeskrankenhausbetriebsgesellschaft, Feldkirch, Austria

**Introduction:** Accurate prediction of heart failure (HF)–specific hospitalization is critical in patients with HF, particularly in the context of type 2 diabetes mellitus (T2 DM). Although machine-learning (ML) approaches show promising predictive performance, their complexity often limits clinical implementation. Interpretable models with robust performance are therefore needed.

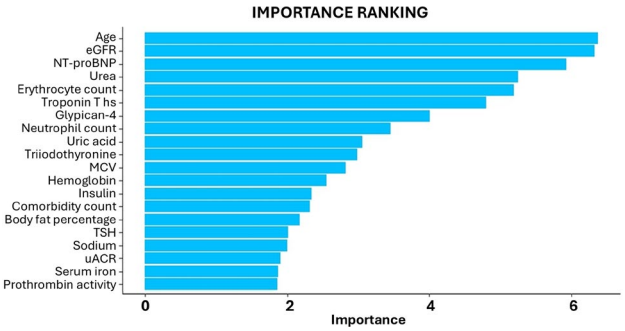


**Fig. 1 | 18-7**

**Methods:** We analyzed HF-specific hospitalization risk over 3 years in 258 heart failure patients with complete, uncensored follow-up, including 41% with T2 DM. We applied AutoScore, an interpretable ML framework designed to derive parsimonious, point-based risk scores. The dataset included 168 candidate variables, covering anthropometric, clinical, laboratory, medication-related, fatigue-related, and psychological factors. Data were randomly split into a training set (75%) and a test set (25%).

**Results:** From the top 20 ranked variables (figure), AutoScore derived a final model comprising four routinely available parameters: age, NT-proBNP, estimated glomerular filtration rate (eGFR), and urea. This parsimonious model showed the best overall performance, with a precision of 83%, sensitivity of 54%, and specificity of 86%.

**Conclusion:** We conclude that AutoScore enables clinically meaningful risk stratification using standard clinical data. Its simplicity and transparency make it well suited for real-world clinical decision support.

## 18-8

### The design and rationale for the dapagliflozin in hemodialysis (DAPA-HD) trial

**Mann C.[1], Paschen C.[1], Eigner M.[2], Hafner-Gießauf H.[3], Klause-Braun R.[4], Lorenz M.[5], Ludvik B.[6], Stulnig T.[7], Waller I.[8], Wezowa J.[9], Hödlmoser S.[1], Hengstenberg C.[1], Oberbauer R.[1], Hecking M.[1], Zelniker T.[1]**

[1]Medizinische Universität Wien, Wien, Austria
[2]Klinik Favoriten, 1. Medizinische Abteilung mit Nephrologie, Intensivmedizin, Psychosomatik und Diabetologie, Wien, Austria
[3]Dialyseinstitut Gießauf GmbH, Elisabethstraße 54, 8010 Graz, Graz, Austria
[4]Klinik Donaustadt, 3. Medizinische Abteilung, Wien, Austria
[5]Wiener Dialysezentrum, Wien, Austria
[6]Klinik Landtraße, 1. Medizinische Abteilung mit Diabetologie, Endokrinologie und Nephrologie, Wien, Austria
[7]Krankenhaus Hietzing, 3. Medizinische Abteilung mit Stoffwechselerkrankungen und Nephrologie, Wien, Austria
[8]Dialyseinstitut Dr. Waller, Feldbach, Austria
[9]Hanusch-Krankenhaus, 1. Medizinische Abteilung, Nephrologie, Wien, Austria

**Introduction:** Sodium-glucose co-transporter 2 inhibitors (SGLT2i) reduce cardiovascular events across a wide range of kidney function up to advanced stages of chronic kidney disease, but their efficacy has not been established in patients with

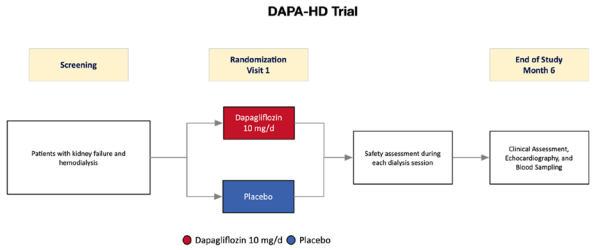


**Primary Endpoint:** Change in left ventricular mass indexed to body surface area using echocardiography.

**Fig. 1 | 18-8** Trial design of the dapagliflozin in hemodialysis (DAPA-HD) trial The DAPA-HD trial is an academic, investigator-initiated, multicenter, randomized, double-blind, placebo-controlled trial evaluating the effect of dapagliflozin (10 mg daily) versus placebo on the left ventricular mass indexed to body surface area using echocardiography over 6 months in patients with kidney failure receiving maintenance hemodialysis

kidney failure on hemodialysis. The underlying mechanisms remain incompletely understood, and whether cardiovascular benefits depend on residual kidney function is unknown.

**Methods:** Research design and methods: The Dapagliflozin in Hemodialysis (DAPA-HD) trial (NCT05179668) is an academic, multicenter, randomized, double-blind, placebo-controlled trial designed to assess the cardiovascular effects of dapagliflozin in 220 patients with kidney failure receiving hemodialysis. The primary endpoint is change in left ventricular mass indexed to body surface area using echocardiography after six months of treatment. Secondary endpoints include additional echocardiographic assessments, changes in biomarker concentrations, quality of life, and clinical events.

**Results:** The trial completed enrollment and randomization of 220 patients with kidney failure with or without residual urine output between October 2022 and January 2025 across 9 sites in Austria. Overall, the median age of the study population is 67 years (Q1–Q3: 57 to 75 years), 26% of participants are women, 42% have type 2 diabetes mellitus, and 39% have established coronary artery disease, and 28% of patients have residual urine output ≤ 200 mL/day. Baseline echocardiography showed a mean LVMI of 136 g/m$^2$ (standard deviation 35 g/m$^2$) and a median LVEF of 59% (Q1–Q3: 54 to 65%) with 10% having an LVEF ≤ 40%; the median NT-proBNP concentration was 2911 pg/mL (Q1–Q3: 1181 to 7602 pg/mL).

**Conclusion:** The DAPA-HD trial is the first trial specifically evaluating the cardiovascular and hemodynamic effects of dapagliflozin in patients with kidney failure on hemodialysis with and without residual urine output.

# POSTERSITZUNG 19 – HERZINSUFFIZIENZ & KARDIOMYOPATHIEN 3

## 19-1

### Vienna Cardiogenetic Registry: Design and first Results on the prevalence of pathogenic variants in cardiomyopathies

**Panagiotides N., Prausmüller S., Arfsten H., Lustig P., Stix E., Hengstenberg C., Stojkovic S., Hülsmann M., Pavo N.**

Division of Cardiology, Department of Internal Medicine II, Medical University of Vienna, Wien, Austria

**Introduction:** In cardiomyopathies (CMP), structured genetic diagnostics improve risk stratification, guide family screening, and enable individualized therapy. Therefore, a dedicated cardiogenetic clinic and registry were established at our institution in 2024.

**Methods:** This prospective, single-center registry includes adults with i) clinical phenotypes suggestive of inherited disease, ii) early-onset heart failure (HF) (<50 years), iii) familial clustering of HF or sudden cardiac death (SCD), iv) peripartum CMP or v) first grade relatives with pathogenic (P) or likely pathogenic (LP) variants irrespective of phenotype or any relatives with a genetic variant with suspected CMP. Whole exome sequencing (WES) is performed in index cases, while targeted carrier testing and cascade screening is offered to relatives in families with a P/LP variant.

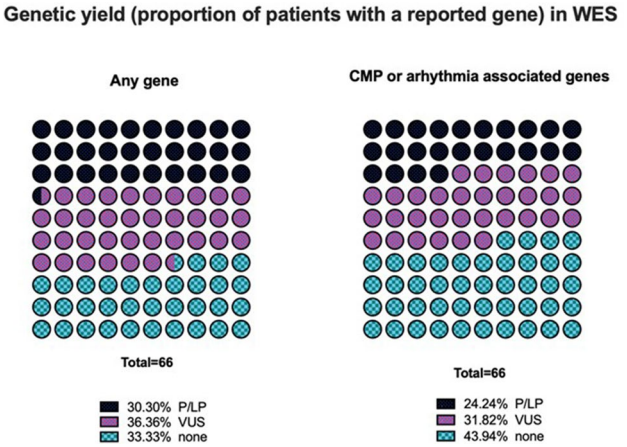


**Fig. 1 | 19-1**

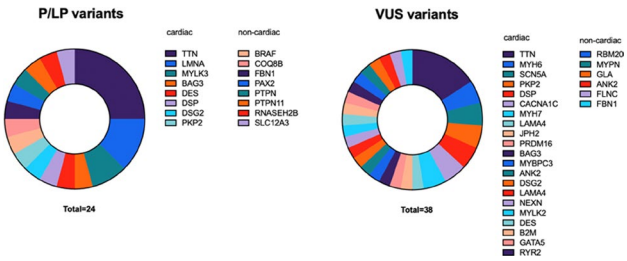


**Fig. 2 | 19-1**

**Results:** By September 2025, 126 (median age 41 [29–50], 64% male, median NT-proBNP was 616 pg/ml [114–2078]) patients had been included (113 index, 13 relatives). 64% had idiopathic CMP, 16% SCD/arrhythmia syndromes, 5% peripartum CMP and 15% other. To time, WES analysis was available for 58% (66/113) of index patients (Fig. 1). Of these, 44 (67%) carried any reported variants [33, 7 and 4 for CMP/arrhythmia, non-cardiac disease or both]. 9 (14%) patients had more than one cardiac variant reported. In total, 21 (32%) patients had variants of uncertain significance (VUS) and 16 (25%) P/LP variants within the CMP/arrhythmia panel. The most common variants were found in the TTN gene.

**Conclusion:** The Cardiogenetic Registry provides structured, real-world data on inherited cardiac diseases in a specialized outpatient setting. First analyses indicate a comparably high diagnostic yield in patients of the Cardiogenetic Registry. The registry will contribute to optimized patient care, individualized therapeutic approaches, and integration into national and international research networks.

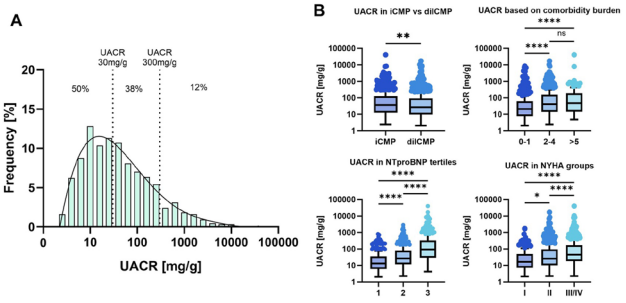


**Figure 1. Distribution and Clinical Correlates of UACR in Patients With HFrEF**
Distribution of urinary albumin-to-creatinine ratio (UACR) in the study cohort (A) and its associations with ischemic vs. dilated cardiomyopathy, NT-proBNP tertiles, NYHA functional class, and comorbidity burden (B). Group comparisons were performed using the Mann–Whitney test (ischemic vs. dilated cardiomyopathy) or the Kruskal-Wallis test with Dunn's post hoc correction for multiple comparisons. ns=not significant; * p<0.05; ** p<0.01; *** p<0.001; **** p<0.0001

**Fig. 1 | 19–2**

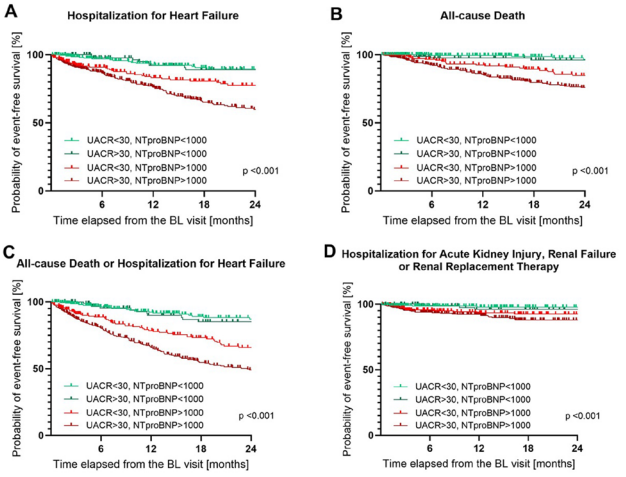


**Figure 2. Clinical endpoints based on NTproBNP and UACR cutoffs in HFrEF.** Kaplan–Meier curves illustrating event rates according to combined UACR and NTproBNP categories: UACR <30 mg/g with NTproBNP <1000 pg/mL; UACR ≥30 mg/g with NTproBNP <1000 pg/mL; UACR <30 mg/g with NTproBNP ≥1000 pg/mL; and UACR ≥30 mg/g with NTproBNP ≥1000 pg/mL. Shown are (A) heart failure hospitalization, (B) all-cause death, (C) the composite of heart failure hospitalization or all-cause death, and (D) the combined renal endpoint (hospitalization for acute kidney injury, progression to kidney failure, or initiation of renal replacement therapy). Group differences were assessed using the log-rank test; corresponding p values are displayed within each panel.

**Fig. 2 | 19–2**

## 19-2

### NT-proBNP and UACR for Outcome Prediction in HFrEF: Analysis from the VIENNA-HF Registry

**Panagiotides N., Prausmüller S., Arfsten H., Stix E., Spinka G., Bartko P., Goliasch G., Hengstenberg C., Hülsmann M., Pavo N.**

Division of Cardiology, Department of Internal Medicine II, Medical University of Vienna, Wien, Austria

**Introduction:** NTproBNP is the central biomarker for risk stratification in heart failure with reduced ejection fraction (HFrEF). The urinary albumin-to-creatinine ratio (UACR) reflects renal and microvascular injury, but its independent and incremental prognostic value beyond NTproBNP remains uncertain. We aimed to evaluate the prognostic relevance of UACR in chronic HFrEF and its additive value beyond NTproBNP.

**Methods:** We analyzed 867 patients with chronic HFrEF with baseline NTproBNP and UACR. Outcomes were heart failure hospitalization (HFH), all-cause death, HFH or death, and a combined renal endpoint (hospitalization for acute kidney injury, progression to kidney failure, or initiation of renal replacement therapy). Cox regression models with interaction terms, ROC/AUC analysis, and Kaplan-Meier analyses were performed.

**Results:** 50% of patients had UACR < 30 mg/g. Higher UACR was associated with ischemic etiology, higher NTproBNP tertiles, and advanced NYHA class (Fig. 1, $p$ for all < 0.05). In univariable Cox models, UACR and NTproBNP were significant predictors across endpoints. For HFH or death, UACR (HR: 1.37 [1.23–1.53]; $p < 0.001$) and NTproBNP (HR: 2.04 [1.77–2.35]; $p < 0.001$) were both associated with risk; in combined models, NTproBNP remained independently predictive (HR: 2.06 [1.75–2.43]; $p < 0.001$), whereas UACR was attenuated (HR: 1.15 [0.98–1.36]; $p = 0.086$). For all-cause death, UACR lost significance after adjustment, while NTproBNP remained associated (adjusted HR: 2.20 [1.70–2.85]; $p < 0.001$). For HFH, NTproBNP remained independently predictive, whereas UACR showed independent association (adjusted HR: 1.22 [1.01–1.47]; $p = 0.038$). For the combined renal endpoint, UACR remained independently associated even in models including NTproBNP (HR: 1.50 [1.07–2.09]; $p = 0.018$). In ROC analyses, NTproBNP consistently outperformed UACR (e. g., death AUC: 0.724 [0.681–0.768] vs. 0.628 [0.578–0.677]; $p < 0.001$). There was significant interaction between UACR and NTproBNP for HFH or death ($p = 0.03$) and for the combined renal endpoint ($p = 0.018$). Kaplan-Meier analyses using clinically defined cutoffs (NTproBNP 1000 pg/mL; UACR 30 mg/g) demonstrated clear separation across all four endpoints, with the highest event rates observed in patients with both elevated biomarkers (Fig. 2, log-rank $p < 0.001$ for all).

**Conclusion:** UACR is associated with adverse HF and renal outcomes in chronic HFrEF but does not provide consistent independent prognostic value beyond NTproBNP. However, UACR seems to refine risk primarily in patients with elevated NTproBNP, but not when NTproBNP is low. A simple dual-threshold approach using NTproBNP 1000 pg/mL and UACR 30 mg/g identifies a distinctly high-risk subgroup across all HF and renal endpoints, supporting a pragmatic and clinically intuitive strategy for risk stratification.

## 19-3

### Real-world clinical experience with acoramidis in patients with wild-type transthyretin amyloid cardiomyopathy

**Öztürk B., Seirer B., Capelle C., Bonderman D.**

Klinik Favoriten, Wien, Austria

**Introduction:** Wild-type transthyretin amyloid cardiomyopathy (wtATTR-CM) is an increasingly recognized cause of heart failure in elderly patients. Acoramidis is a highly selective transthyretin stabilizer designed to achieve near-complete transthyretin stabilization for the treatment of wtATTR-CM in adults. However, real-world clinical data remain limited.

**Methods:** We conducted a single-center observational study of consecutive patients with confirmed wtATTR-CM who were treated with acoramidis. Diagnosis was established according to guideline-based criteria. Baseline characteristics, including prior ATTR-CM-directed therapies and reasons for therapy switch, were collected. National Amyloidosis Centre (NAC) stage, *N*-terminal prohormone of brain natriuretic peptide (NT-proBNP) levels, New York Heart Association (NYHA) functional class, and 6-minute walk distance (6-MWD) were recorded. Treatment duration, time since wtATTR-CM diagnosis, adverse events, and early clinical outcomes were descriptively analyzed. After initiation of acoramidis therapy, patients were monitored via outpatient clinic visits or scheduled phone calls. Follow-up assessments were scheduled every six months.

**Results:** Among 82 patients with wtATTR-CM in our prospective registry, 18 received acoramidis therapy. Nine patients initiated acoramidis as first-line treatment at diagnosis, while the remaining nine were switched from tafamidis. The primary reasons for switching therapy were documented disease progression, including heart failure events, decline in functional capacity, or worsening laboratory parameters. The mean age at treatment initiation was 82.2 ± 3.9 years, and 94.4% were male. At therapy initiation, 66.7% of patients were in NAC stage 1, 16.7% in NAC stage 2, and 16.7% in NAC stage 3. Median NT-proBNP was 1663.5 pg/mL (IQR 900.0–3445.0), 88.9% were in NYHA class I–II, and mean 6-MWD was 386.7 ± 75.7 m. The mean time from wtATTR-CM diagnosis to initiation of acoramidis in patients previously treated with tafamidis was 32 months. At the time of analysis, the mean treatment duration was 4.4 months. Overall, acoramidis was tolerated; however, therapy discontinuation occurred in four patients (22%) due to gastrointestinal adverse events: two cases of diarrhea, one case of constipation, and one case of dysphagia. During follow-up, two patients with impaired systolic function and NAC stage 3 required hospitalization for heart failure. In the remaining patients, early clinical assessment suggested stability or improvement in NYHA functional class without clinical evidence of worsening heart failure.

**Conclusion:** In this small real-world cohort of elderly patients with wtATTR-CM, acoramidis demonstrated acceptable short-term tolerability with preliminary signals of clinical stability. Larger studies with extended follow-up are needed to further assess long-term clinical outcomes.

## 19-4

## A Non-Invasive Hemodynamic-Guided Strategy to Prevent Decompensated Heart Failure: STOP-DHF Trial

**Böhm A.[1,2], Lucka J.[1,2,3], Segev A.[4,1], Pogran E.[5], Hlodakova V.[1], Kollarova M.[1], Jajcay N.[1,6], Jankova J.[1], Sebenova Jerigova V.[1], Spilak M.[1,2], Skorec F.[1,2], Hutnik J.[1,2], Stevkova J.[1,3], Kostekova Z.[1], Karolcik S.[1], Dragunova P.[1], Campbell P.[7], Tschope C.[8], Kohler F.[9], Bezák B.[1,10,11]**

[1]Premedix Academy, Bratislava, Slovakia
[2]Faculty of Medicine, Comenius University, Bratislava, Slovakia
[3]National Institute for Cardiovascular Diseases, Bratislava, Slovakia
[4]Centre for Cardiovascular Innovation, Division of Cardiology, University of British Columbia, Vancouver, Canada
[5]3. Medizinische Abteilung für Kardiologie und Intensivmedizin, Klinik Ottakring, Wien, Austria
[6]Institute of Computer Science, Czech Academy of Sciences, Prag, Czech Republic
[7]Department of Cardiology, Southern Trust, Craigavon Area Hospital, Portadown, United Kingdom
[8]Charité–Universitätsmedizin Berlin; Department of Cardiology, Angiology and Intensive Care Medicine (CVK), Berlin, Germany
[9]German Centre for Cardiovascular Research, Berlin, Germany
[10]Faculty of Medicine, University of Ostrava, Ostrava, Czech Republic
[11]University Hospital Ostrava, Ostrava, Czech Republic

**Introduction:** Heart failure (HF) management based on left ventricular filling pressure (LVFP) monitoring leads to improved quality of life, reduced HF hospitalizations, and enhanced survival. However, the clinical adoption of existing technologies remains limited, largely due to their invasive nature and substantial cost. Seerlinq HeartCore is a novel, CE-certified, non-invasive system for remote monitoring of LVFP, utilizing photoplethysmographic (PPG) signal analysis based on artificial intelligence and hemodynamic principles. The aim of the study was to evaluate the effect of the Seerlinq HeartCore system on outcomes in a real-world HF outpatient population.

**Methods:** STOP-DHF was a multi-centre, prospective, single-arm, open-label trial with a prespecified effectiveness endpoint, conducted at 3 sites in Slovakia. Consecutive HF outpatients, diagnosed according to the latest ESC guidelines, were included regardless of ejection fraction (EF). Patients were instructed to record a PPG signal using a pulse oximeter connected to a smartphone every other day. Data were uploaded remotely and analysed using the Seerlinq HeartCore system (Fig. 1). The primary effectiveness endpoint at 6 months was the composite rate of HF hospitalizations or all-cause mortality,

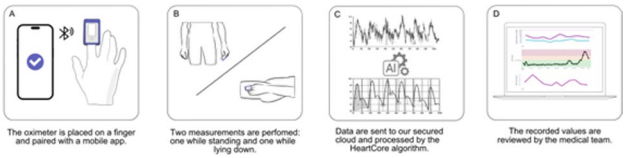


**Fig. 1 | 19-4**

with a predefined performance goal of 9 events per 100 patients, based on local epidemiological data. Safety outcomes included symptomatic hypotension or severe electrolyte disturbances.

**Results:** Total of 330 patients were enrolled (36% female; mean age 67 ± 12 years; HF phenotypes: 40% HFpEF, 16% HFmrEF, 43% HFrEF; NYHA II: 66%, NYHA III: 34%). During a mean follow-up of 6 ± 2 months, 3 HF hospitalizations and 11 deaths occurred. The event rate was 4.2% (95% CI: 2.3–7.0%), significantly lower than the predefined performance goal (9%, $p < 0.001$). There were 7 events of symptomatic hypotension and no severe electrolyte disturbance. On average, the telemedical system prompted 13 medication adjustments, 33 telephone encounters, and 2 in-person visits per 100 patients per month.

**Conclusion:** Non-invasive LVFP monitoring with the telemedical system Seerlinq HeartCore was associated with significantly lower event rates compared to predefined benchmarks, with no safety concerns. These findings support its potential to improve heart failure management in routine care.

## 19-5

### The association of left atrial mechanics and atrial fibrillation in hypertrophic cardiomyopathy

**Masood S.[1], Mann C.[2], Dolas D.[1], Duca F.[2], Binder-Rodriguez C.[2], Hengstenberg C.[2], Zelniker T.[2], Dalos D.[2]**

[1]Medizinische Universität Wien, Wien, Austria
[2]Allgemeines Krankenhaus Wien, Medizinische Universität Wien, Wien, Austria

**Introduction:** Atrial fibrillation (AF) is a frequent complication in hypertrophic cardiomyopathy (HCM) and associated with distinct morbidity and mortality. Various scores, like the HCM-AF score have been established to identify patients at risk. However, this score does not include functional atrial parameters, like left atrial (LA) strain, and, therefore, may not adequately depict patients at early disease stages. Thus, the purpose of the following study was to evaluate the association of LA strain parameters with the occurrence of AF in HCM and to evaluate the potential prognostic accuracy compared to the HCM-AF score.

**Methods:** Between 2018 and 2025, overall, 324 patients were included in a prospective HCM-registry at a tertiary care centre. At initial contact, a complete transthoracic echocardiography was performed. Speckle-tracking analysis was performed offline on stored images to derive LA strain, and the HCM-AF score was calculated. Patients were regularly followed for the occurrence of new-onset AF in an outpatient setting. Regression model was adjusted for age, sex and LA volume index.

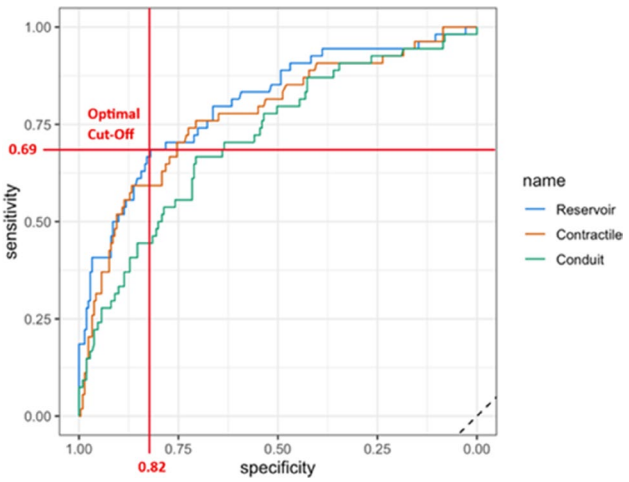


**Fig. 1 | 19-5** Area under the curve comparison of different left atrial strain phases

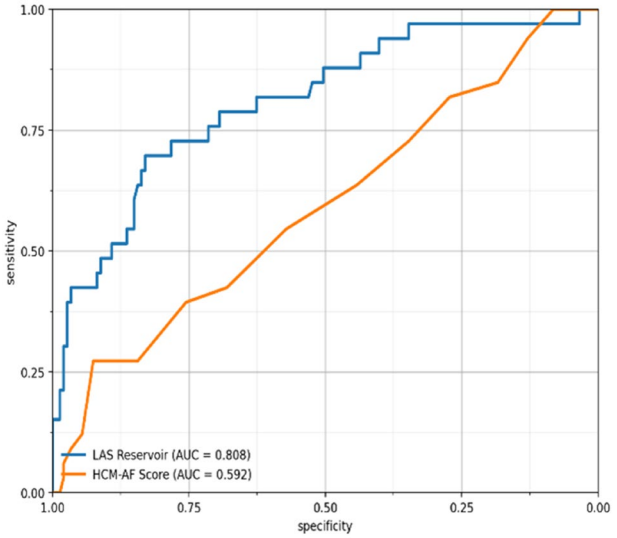


**Fig. 2 | 19-5** Area under the curve comparison between left atrial reservoir strain and HCM-AF

**Results:** Among the 324 patients, 164 patients were excluded due to a prior history of AF ($n = 20$), insufficient image quality or an incomplete dataset ($n = 144$). Out of 180 patients, 33 patients (18.3%) developed AF after a median follow up of 48.9 (Interquartile range: 16.0–59.7) months. Patients with AF were older than those without AF (62.1 vs 52.9 years, $p = 0.0054$), while female sex and obstructive phenotype did not differ significantly between the two groups (42.4% vs 36.5%, $p = 0.661$; 36.4% vs 40.3%, $p = 0.827$, respectively). In multiple logistic regression analysis, LA reservoir strain was significantly associated with AF (adjusted Odds-Ratio: 0.85, 95% confidence interval 0.80–0.91, $p < 0.001$). LA reservoir strain demonstrated substantially higher discrimination for AF than the HCM-AF score (area under the curve 0.81 vs 0.59; DeLong $p < 0.001$). The Youden-derived threshold for reservoir strain was 17.3% (sensitivity 0.69, specificity 0.82).

**Conclusion:** In patients with HCM, LA reservoir strain might be associated with the occurrence of AF. In addition, this atrial functional parameter might outperform the established HCM-AF score, which is mainly based on clinical surrogate parameters. Larger clinical studies are needed to reassure these findings and to potentially redefine rhythm surveillance in a vulnerable patient cohort.

## 19-6

### Association of Beta Blocker Therapy and Functional Parameters in Patients with Transthyretin Amyloid Cardiomyopathy

**Ermolaev N., Willixhofer R., Steiner I., Kronberger C., Poledniczek M., Eslami M., Schmid L., Rettl R., Duca F., Binder C., Kammerlander A., Bergler-Klein J., Kastner J., Badr Eslam R.**

Medizinische Universität Wien, Wien, Austria

**Introduction:** The role of beta-blockers (BB) therapy in transthyretin amyloid cardiomyopathy (ATTR-CM) remains controversial, and its effects on functional capacity in this patient collective have not been systematically evaluated. This study is the first to assess BB therapy in ATTR-CM using cardiopulmonary exercise testing (CPET) to characterize its association with exercise performance and hemodynamic response.

**Methods:** We analysed data from 157 patients with confirmed diagnosis of ATTR-CM who underwent baseline CPET assessment before initiation of disease-specific therapy. Patients were divided into groups according to BB therapy at the time of assessment. Cox regression and Kaplan-Meier analysis were performed to assess the prognostic relevance of CPET-derived parameters. Furthermore, functional, laboratory and imaging parameters were compared exploratively between groups.

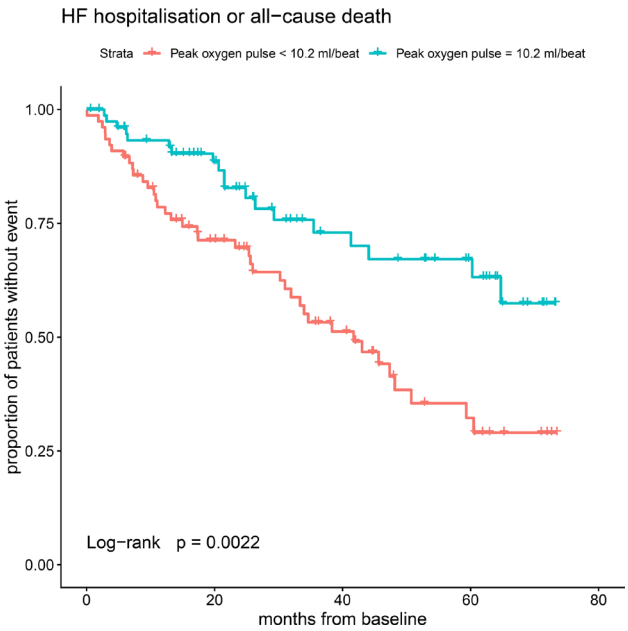


**Fig. 1 | 19-6**

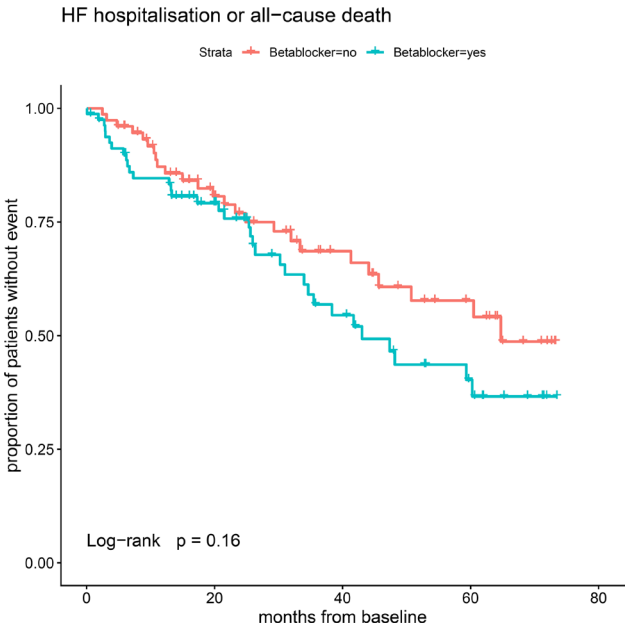


**Fig. 2 | 19-6**

**Results:** Of the total cohort (mean age 77.9 ± 6.8 years, 89% male), 52% received BB therapy. Functional capacity was significantly lower in the BB group, as reflected in reduced peak oxygen uptake (13.7 ± 3.9 vs. 16.2 ± 4.6 ml/min/kg, $p = 0.0005$) and higher VE/VCO2 slope (40.6 ± 8.0 vs. 37.8 ± 9.4, $p = 0.052$). Moreover, patients without BB therapy showed better performance in six-minute walk test (437.8 ± 115.9 vs. 357.2 ± 113.5 m, $p < 0.0001$). BB cohort also demonstrated a blunted chronotropic response in maximal heart rate (118.6 ± 22.2 vs. 133.1 ± 35.8 bpm, $p = 0.0045$), while peak oxygen pulse remained comparable between groups (10.8 ± 3.9 vs. 10.9 ± 3.9 ml/beat, $p = 0.92$). In survival analysis, lower peak oxygen pulse was associated with adverse outcomes (log-rank $p = 0.002$). Cox regression confirmed the prognostic relevance of key CPET-parameters.

**Conclusion:** BB-therapy in ATTR-CM is commonly used but associated with reduced exercise performance and chronotropic response, while stroke volume adaptation appears preserved. Peak oxygen pulse emerged as a prognostic marker, linking impaired outcomes to reduced stroke volume reserve. Our findings suggest that BB use should be individualized particularly when guided by comprehensive assessment using CPET.

## 19-7

## Experience on genetic testing for primary dilated cardiomyopathy in a single Austrian genetic center and the role of myocardial inflammation

**Manzanilla Romero H.[1], Steil A.[1], Santner V.[2], Von der Heidt A.[1], Verheyen N.[2], Pölzl G.[3], Witsch-Baumgartner M.[1], Rudnik-Schöneborn S.[1]**

[1]Medical University of Innsbruck, Institute of Human Genetics, Innsbruck, Austria
[2]Medical University of Graz, Division of Cardiology, Graz, Austria
[3]Innsbruck Medical University, Clinical Division of Cardiology and Angiology, Innsbruck, Austria

**Introduction:** Molecular genetic testing is increasingly offered to patients with dilated cardiomyopathy (DCM). The diagnosis of an inherited cardiomyopathy has major implications for the medical care of patients and their relatives. Here, we report the results of a genotype-phenotype analysis of DCM investigated in Austria.

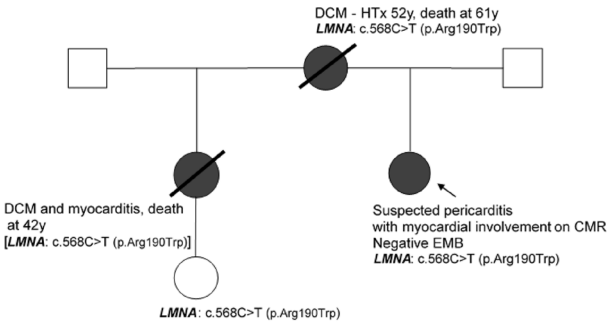


Abbreviations: CMR: cardiac magnetic resonance; DCM: dilated cardiomyopathy; EMB: endomyocardial biopsy; HTx: heart transplant.

**Fig. 1 | 19-7**

**Table 1 | 19-7** Comparison of clinical characteristics between DCM-patients with positive and negative inflammation on EMB

| | EMB | Inflammation positive | Inflammation negative | *p* |
|---|---|---|---|---|
| Total number of patients | N = 32 | N = 20 | N = 12 | |
| female | 10 (31 %) | 7 (35 %) | 3 (25 %) | 0.703 |
| Clinically suspected myocarditis (*N* = 28) | 21 (75 %) | 12 (43 %) | 9 (32 %) | 0.668 |
| Age of onset, years (median +/– SD) | 38.0 +/– 11.4 | 38.5 +/– 12.1 | 36.0 +/– 9.9 | 0.604 |
| NYHA I | 9/31 | 6/20 | 3/11 | 1 |
| NYHA II-IV | 22/31 | 9/20 | 8/11 | |
| Clinical manifestations | | | | |
| Number of patients | N = 27 | N = 17 | N = 10 | |
| Dyspnea | 25 (93 %) | 16 (94 %) | 9 (90 %) | 1 |
| Chest pain | 6 (22 %) | 3 (18 %) | 3 (30 %) | 0.638 |
| Memory of recent infection | 13 (48 %) | 11 (65 %) | 2 (20 %) | *0.041* |
| Number of patients with arrhythmias | N = 19 (60 %) | N = 13 (65 %) | N = 6 (50 %) | |
| VES, VT or VF | 5 (26 %) | 2 (15 %) | 3 (50 %) | 0.262 |
| AT or AF | 3 (16 %) | 2 (15 %) | 1 (17 %) | 1 |
| LBBB | 13 (68 %) | 11 (85 %) | 2 (33 %) | *0.046* |
| AVB | 2 (11 %) | 2 (15 %) | 0 | 1 |
| Premature beats | 2 (11 %) | 1 (8 %) | 1 (17 %) | 1 |
| Valvular heart disease | | | | |
| Number of patients with valvula heart disease | N = 23 (72 %) | N = 16 (80 %) | N = 7 (58 %) | |
| Mitral insufficiency | 20 (87 %) | 16 (100 %) | 4 (57 %) | *0.007* |
| Laboratory | | | | |
| Number of patients | N = 26 | N = 15 | N = 11 | |
| NT-proBNP | 22 (85 %) | 14 (93 %) | 8 (73 %) | 0.625 |
| Troponin T | 16 (62 %) | 11 (73 %) | 5 (45 %) | 0.425 |
| CRP | 12 (46 %) | 9 (60 %) | 3 (27 %) | 0.226 |
| CK-MB | 6 (23 %) | 1 (7 %) | 5 (45 %) | *0.018* |
| Echocardiography | | | | |
| LVEF, % (median +/– SD) | 27.0 +/– 13.1 | 24.5 +/– 11.1 | 33.0 +/– 15.3 | 0.136 |
| LVEDDI, mm/m^2 (median +/– SD) | 31.5 +/– 5.7 (*n* = 28) | 31.4 +/– 5.2 (*n* = 19) | 33.7 +/– 7.0 (*n* = 9) | 0.923 |
| CMR | N = 22 | N = 15 | N = 7 | |
| LVEF, % (Median +/– SD) | 26. 0 +/– 12.5 | 25.5 +/– 11.2 | 32.5 +/– 14.8 | 0.274 |
| Edema | 3 (14 %) | 2 (13 %) | 1 (14 %) | 1 |
| Effusion | 8 (36 %) | 6 (40 %) | 2 (29 %) | 0.657 |
| Fibrosis | 3 (14 %) | 2 (13 %) | 1 (14 %) | 1 |
| LGE positive | 6 (27 %) | 3 (20 %) | 3 (43 %) | 0.621 |
| Endpoints | | | | |
| HTx | 3 (9 %) | 1 (5 %) | 2 (17 %) | 0.54 |
| ROSC | 2 (6 %) | 1 (5 %) | 1 (8 %) | 1 |
| ICD | 11 (34 %) | 7 (35 %) | 4 (33 %) | 1 |
| Genetic background | | | | |
| fDCM | 10 (31 %) | 5 (25 %) | 5 (42 %) | 0.157 |
| pfDCM | 4 (13 %) | 3 (15 %) | 1 (8 %) | |
| sDCM | 14 (44 %) | 12 (60 %) | 2 (17 %) | |
| Number of patients with LP/P variant | 16 (50 %) | 10 (50 %) | 6 (50 %) | 0.642 |

Abbreviations: AF: atrial fibrillation; AT: atrial tachycardia; AVB: atrioventricular block; CK-MB: creatine kinase isoenzyme Muscle-Brain; CMR: cardiac magnetic resonance; CRP: c-reactive protein; EMB: endomyocardial biopsy; fDCM: familial dilated cardiomyopathy; HTx: heart transplant; ICD: implantable cardiac defibrillator; LBBB: left bundle branch block; LGE: late gadolinium enhancement; LP: likely pathogenic; LVEDDI: left ventricular end-diastolic diameter indexed; LVEF: left ventricular ejection fraction; NT-ProBNP: *n*-terminal pro brain natriuretic peptide; P: pathogenic; pfDCM: probably familial dilated cardiomyopathy; ROSC: return of spontaneous circulation; SD: standard deviation; sDCM: sporadic dilated cardiomyopathy; VES: ventricular extrasystole; VF: ventricular fibrillation; VT: ventricular tachycardia.

**Methods:** Over 6 years (January 2015 to December 2021), 194 unrelated patients with DCM underwent genetic testing with a core data set of 12 genes. We performed a genotype-phenotype analysis of 105 DCM patients who showed a genetic variant. In addition, we compared the genetic findings and outcome measures of DCM patients with myocardial inflammation on endomyocardial biopsy (EMB) and those without inflammation.

**Results:** In 51.4% (54/105) patients at least one likely pathogenic or pathogenic genetic variant (LP/P) was detected. 51 of 105 patients (48.6%) showed only variants of unknown significance (VUS). Most LP/P variants (34.3%) were found in the TTN gene. Clinical characteristics of the most prevalent genetic subgroups (TTN, LMNA, MYH7, MYH6, DMD, SCN5A) were not significantly different. DCM patients with inflammation had a significantly higher frequency of memory of infection, left bundle branch block, mitral valve insufficiency, but normal CK-MB levels. We added a case report where two family members initially were considered to have an inflammatory cardiomyopathy before a pathogenic variant in LMNA was found.

**Conclusion:** Cardiac features of DCM were not predictive of a specific genetic subgroup. We recommend applying multigene panels extensively, since a large proportion of patients without a family history or with evidence of myocardial inflammation showed a genetic predisposition for DCM. However, the large number of VUS remains a challenge.

## References


1. Jordan E, Peterson L, Ai T, Asatryan B, Bronicki L, Brown E, et al. Evidence-Based Assessment of Genes in Dilated Cardiomyopathy. Circulation. 2021;144(1):7–19. https://doi.org/10.1161/CIRCULATIONAHA.120.053033 2. Sikking MA, Stroeks SLVM, Henkens MTHM, Venner MFGHM, Li X, Heymans SRB, et al. Cardiac Inflammation in Adult-Onset Genetic Dilated Cardiomyopathy. J Clin Med. 2023;12(12):3937. https://doi.org/10.3390/jcm12123937 3. Verdonschot JAJ, Hazebroek MR, Krapels IPC, Henkens MTHM, Raafs A, Wang P, Merken JJ, et al. Implications of Genetic Testing in Dilated Cardiomyopathy. Circ Genom Precis Med. 2020;13(5):476–487. https://doi.org/10.1161/CIRCGEN.120.003031


# POSTERSITZUNG 20 – INTENSIVMEDIZIN

## 20-1

### Künstliche Intelligenz-gestützte EKG-Auswertung zur Identifizierung okklusiver Myokardinfarkte nach kardiopulmonaler Reanimation


**Silwanis C.[1,2], Groche M.[1,2], Eder J.[1,2], Huss M.[1,2], Neunteufel A.[1,2], Kirchweger B.[1], Nahler A.[1,2], Fellner A.[1,2], Rechberger S.[1,2], Steinwender C.[1,2], Lambert T.[1,2]**

[1]Kepler Universitätsklinikum, Klinik für Kardiologie und Internistische Intensivmedizin, Linz, Österreich
[2]Medizinische Fakultät, Johannes Kepler Universität, Linz, Österreich


**Einleitung:** Der plötzliche Herzstillstand wird häufig durch ein akutes Koronarsyndrom verursacht. Die EKG-Interpretation nach Wiederherstellung des spontanen Kreislaufs (ROSC) ist für die Erkennung eines okklusiven Myokardinfarkts (OMI) entscheidend, jedoch aufgrund metabolischer Störungen und häufig fehlender ST-Hebungen erschwert. Wir führten daher eine prospektive experimentelle Studie durch, um zu evaluieren, ob die KI-basierte Queen of Hearts (QoH)-gestützte EKG-Interpretation die diagnostische Genauigkeit, Reliabilität und Konkordanz bei Ärzt*innen verbessert, die Post-ROSC-EKGs hinsichtlich OMI analysieren.

**Methoden:** In dieser prospektiven experimentellen Studie wurden 69 reale post-ROSC EKGs von 15 Ärzt*innen aus fünf Berufsgruppen zu zwei Zeitpunkten (T1 und T2) unabhängig voneinander ausgewertet, was zu 2070 EKG-Interpretationen führte. Zum Zeitpunkt T1 bewerteten die Auswerter*innen individuell das Vorliegen eines OMI und ihre diagnostische Sicherheit allein auf der Grundlage des EKGs. Zum Zeitpunkt T2 wurden dieselben EKGs mit zusätzlicher Entscheidungsunterstützung durch das neuronale Netzwerk QoH erneut bewertet. Die diagnostische Leistungsfähigkeit, subjektive Diagnose-Sicherheit und Übereinstimmung zwischen den Bewerter*innen wurden zwischen den Zeitpunkten verglichen.

**Resultate:** Zum Zeitpunkt T1 betrug die Gesamtsensitivität 77,97 % (95 % CI: 74,69–81,01), die Spezifität 84,64 % (80,39–88,28), der positive prädiktive Wert (PPV) 91,03 % (88,76–92,88) und der negative prädiktive Wert (NPV) 65,77 % (62,37–69,00). Zum Zeitpunkt T2 erreichten die Auswerter eine Sensitivität von 78,55 % (75,30–81,56), eine Spezifität von 90,43 % (86,83–

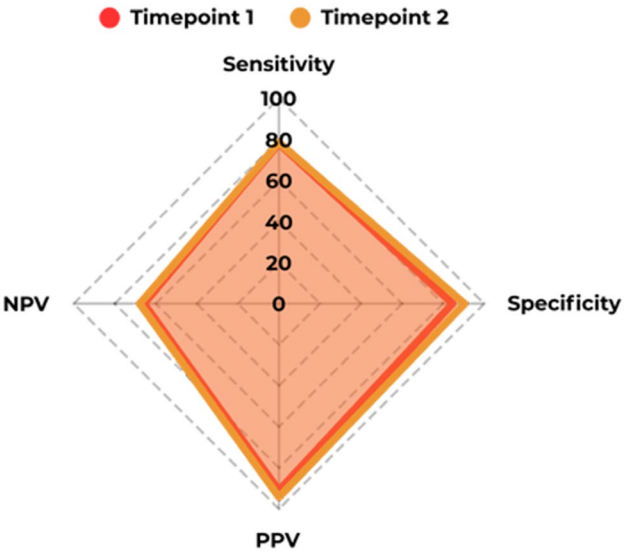


Abb. 1 | 20-1

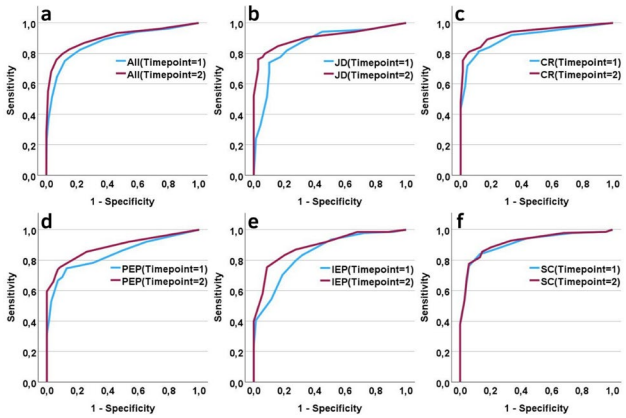


Abb. 2 | 20-1

93,32), einen PPV von 94,26 % (92,22–95,79) und einen NPV von 67,83 % (64,54–70,94). Die AUROC stieg von 0,872 (0,850–0,894, T1) auf 0,903 (0,884–0,921, T2; $p = 0{,}035$). Die QoH-gestützte Interpretation war unabhängig mit einer erhöhten Wahrscheinlichkeit korrekter OMI-Identifizierung assoziiert (aOR 1,16; 95 % CI: 1,05–1,28; $p = 0{,}004$). Die mittlere diagnostische Sicherheit stieg von 78,58 % (T1) auf 82,42 % (T2) an, mit einem signifikanten Anstieg über alle Berufsgruppen hinweg ($\beta = +3{,}84$; 95 % CI: 2,26–5,43; $p < 0{,}001$). Die Interrater-Reliabilität innerhalb der Berufsgruppen stieg von T1 ($\kappa$ zwischen 0,43–0,74) auf T2 ($\kappa$ zwischen 0,53–0,81), wobei Jungärzte ($\Delta\kappa = +0{,}25$) und innerklinische Notfallmediziner ($\Delta\kappa = +0{,}24$) die größten Verbesserungen zeigten (alle $p < 0{,}001$).

**Schlussfolgerungen:** Die KI-gestützte EKG-Interpretation verbesserte die diagnostische Genauigkeit, Reliabilität und Interrater-Konkordanz signifikant, wobei der größte Nutzen bei weniger erfahrenen Ärzten zu beobachten war. Diese Ergebnisse belegen, dass QoH ein wertvolles Instrument zur klinischen Entscheidungsunterstützung darstellt, welches die ärztliche Beurteilung in der zeitkritischen Post-Reanimationsversorgung ergänzt.

## 20-2

### Schockbar vs. Nicht Schockbar: Limitationen einer KI-gestützten Diagnostik des okklusiven Myokardinfarkts nach Herz-Kreislaufstillstand

**Eder J.[1,2], Maier J.[1,2,3], Neunteufel A.[1,2], Groche M.[1,2], Nahler A.[1,2], Fellner A.[1,2], Rechberger S.[1,2], Huss M.[1,2], Silwanis C.[1,2], Lamm L.[1,2], Bamberger M.[1,2], Steinwender C.[1,2,3], Lambert T.[1,2]**

[1]Kepler Universitätsklinikum Linz, Klinik für Kardiologie und Internistische Intensivmedizin, Medizinische Fakultät, Johannes Kepler Universität Linz, Österreich, Linz, Österreich
[2]Johannes Kepler Universität Linz, Medizinische Fakultät, Altenberger Straße 69, 4040 Linz, Austria, Linz, Österreich
[3]Klinisches Forschungsinstitut für kardiovaskuläre und metabolische Erkrankungen, Medizinische Fakultät, Johannes Kepler Universität, Altenberger Straße 69, 4040 Linz, Austria, Linz, Österreich

**Einleitung:** Die Studie untersucht die diagnostische Leistungsfähigkeit eines validierten Deep Neural Networks (Queen of Hearts; QoH) bei der Erkennung eines okklusiven Myokardinfarkts (OMI) nach Rückkehr eines Spontankreislaufs (ROSC) bei Herz-Kreislauf-Stillstand. Ein besonderer Fokus wurde auf den Unterschied von schockbarem zu nicht schockbarem Herzrhythmus während der Reanimation als möglichen Einflussfaktor der Klassifikationsleistung von QoH gelegt.

**Methoden:** In diese retrospektive monozentrische Studie wurden alle Patient*innen eingeschlossen, die zwischen Jänner 2020 und September 2025 nach einer erfolgreichen Wiederbelebung auf der internistischen Intensivstation aufgenommen wurden und bei denen sowohl ein zeitnahes Post-ROSC-EKG als auch eine Koronarangiographie (CAG) durchgeführt wurden. Wurde bei einer Patient*in bei mindestens einer Rhythmuskontrolle ein schockbarer Rhythmus dokumentiert, erhielt die Patient*in das Merkmal „schockbar". Bestand hingegen dauerhaft ein nicht schockbarer Rhythmus, wurde es als „nicht schockbar" klassifiziert. Im Anschluss wurde jeweils das erste Post-ROSC-EKG verwendet und von QoH auf das Bestehen eines OMI analysiert. Als Kontrolle wurden die Ergebnisse der CAG als Goldstandard bei der Diagnostik eines OMI verwendet.

**Resultate:** Von den 139 erfassten Patient*innen waren 36 Frauen und 103 Männer mit einem medianen Alter von 69 Jahren (IQR 59,0–78,3). In dem Patientenkollektiv zeigten 111 Patient*innen einen schockbaren und 28 einen nicht schockbaren Rhythmus während der Reanimation. In der Gesamtkohorte zeigte QoH bei der Diagnose eines OMI nach ROSC eine Sensitivität von 60 % (49,1–70,2 95 % Konfidenzintervall (CI)), eine Spezifität von 74 % (59,7–85,4 CI), mit einer Fläche unter der Receiver-Operating-Characteristic-Kurve (AUROC) von 0,748. Daraus ergibt sich ein positiv prädiktiver Wert (PPV) von 80,6 % (71,7–87,2 CI) und ein negativ prädiktiver Wert (NPV) von 50,7 (43,2–58,2 CI). Separiert man die Patient*innen nun anhand des Herzrhythmus in „schockbar" und „nicht schockbar", so zeigt sich bei einem schockbaren Rhythmus eine Sensitivität von 64,5 % (52,7–75,1 CI) und eine Spezifität von 77,1 % (59,9–89,6 CI) mit einem AUROC von 0,790. Der PPV beträgt 86 % (76,5–92,0 CI), der NPV 50 % (41,3–58,7 CI). Bei Patient*innen mit nicht schockbarem Rhythmus zeigt sich hingegen eine Sensitivität von nur 35,7 % (12,8–64,9 CI), eine Spezifität von 66,7 % (38,4–88,2 CI), ein AUROC von 0,569 mit einem PPV von 50 % (39,6–65,4 CI) und einem NPV von 51,7 % (32,5–70,6 CI).

**Schlussfolgerungen:** Die Ergebnisse dieser Studie zeigen das Vorliegen eines nicht schockbaren Herzrhythmus während der Reanimation als eine mögliche relevante Limitation der diagnostischen Genauigkeit bei der Erkennung eines OMI durch QoH auf.

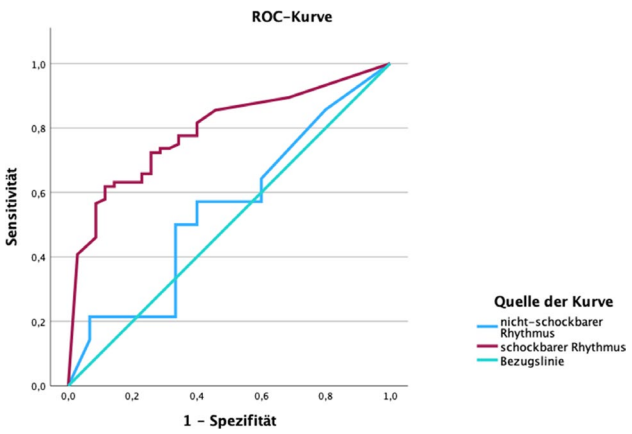


**Abb. 1 | 20-2** ROC-Kurven

## 20-3

### Incidence and survival after out-of-hospital cardiac arrest in Carinthia, Austria

**Planka R.[1,2,3], Scharf B.[2,3], Trampitsch S.[2], Lemesch S.[2], Schuller S.[4,3], Schwegel N.[2], Alber H.[1], Likar R.[5], Peck-Radosavljevic M.[6], Preiß W.[7], Aichinger G.[8,9], Schwarzenberger K.[10], Schwarz M.[3,5], Rohrer U.[2], Zirlik A.[2], von Lewinski D.[2], Wankmüller C.[11,3], Kolesnik E.[2,3]**

[1]Department of Internal Medicine and Cardiology, State Hospital Klagenfurt, 9020 Klagenfurt am Wörthersee, Austria
[2]Department of Internal Medicine, Division of Cardiology, Medical University of Graz, 8036 Graz, Austria
[3]Austrian Red Cross, Landesverband Kärnten, 9020 Klagenfurt am Wörthersee, Austria
[4]Department of Environmental Systems Sciences, University of Graz, 8010 Graz, Austria
[5]Department of Anaesthesia and Intensive Care Medicine, State Hospital Klagenfurt, 9020 Klagenfurt am Wörthersee, Austria
[6]Department of Gastroenterology and Internal Medicine, State Hospital Klagenfurt, 9020 Klagenfurt am Wörthersee, Austria
[7]Department of Internal Medicine, State Hospital Wolfsberg, 9400 Wolfsberg, Austria
[8]Department of Anaesthesia and Intensive Care Medicine, State Hospital Villach, 9500 Villach, Austria
[9]Air Rescue Austria (ARA), 9020 Klagenfurt am Wörthersee, Austria
[10]Christophorus Flugrettungsverein, 1030 Vienna, Austria
[11]Department of Economics, Analytics, and Operations Research, University of Klagenfurt, 9020 Klagenfurt am Wörthersee, Austria

**Introduction:** Out-of-hospital cardiac arrest (OHCA) is associated with poor survival rates. The survival depends on the timing and quality of cardiopulmonary resuscitation (CPR) measures. Some factors associated with a favourable outcome are known, but regional differences do not allow a generalisation. This analysis reflects the situation in Carinthia, Austria.

**Methods:** A retrospective analysis was conducted on all medical emergencies categorised as atraumatic cardiac arrests in the Austrian state of Carinthia from 2018 to 2022. The original protocols of air and ground rescue operations carried out by the emergency medical services were reviewed, and the clinical outcomes of all OHCA survivors were followed up through a retrospective search of the regional clinical information system.

**Results:** 1956 patients with CPR attempt were included in this analysis over 5 years. The annual incidence of OHCA was 696 patients/100,000/year. 586 (30%) achieved a return of spontaneous circulation on site (ROSC). Successful CPR was associated with younger age, shorter duration of CPR, defibrillation, and prompt bystander CPR ($p<0.001$ each). The outcome data of 492 patients post-OHCA was available for analysis. 212 patients survived resulting in an in-hospital survival rate of 43.8%. They were younger ($p<0.001$), received prompt initiation of bystander CPR more often ($p<0.001$), were more frequently defibrillated ($p=0.020$), underwent shorter durations of CPR ($p=0.002$), had a lower rate of in-hospital re-arrests ($p=0.006$), and had lower initial levels of lactate and neuron specific enolase ($p<0.001$ each). In adjusted multivariable regression younger age ($p=0.001$), prompt bystander CPR ($p=0.011$), and lower NSE levels ($p<0.001$) were independently associated with survival. The overall survival was 10.8%.

**Conclusion:** This analysis describes the incidence of OHCA in the Austrian State of Carinthia for the first time. ROSC rates were 30% and overall survival was 10.8%. Younger age, prompt bystander CPR, and lower NSE levels were identified as predictors of survival.

## 20-4

### Distinct Admission Cytokine and Chemokine Profiles in Fulminant versus Acute Myocarditis

**Haider P., Hofbauer T., Richter B., Zilberszac R., Lenz M.**

Innere Medizin II, Abteilung für Kardiologie, Meduni Wien, Wien, Austria

**Introduction:** Fulminant myocarditis (FM) represents the most severe phenotype of myocardial inflammation and is frequently associated with cardiogenic shock, malignant arrhythmias, and the need for mechanical circulatory support. Despite advances in intensive care management, early risk stratifica-

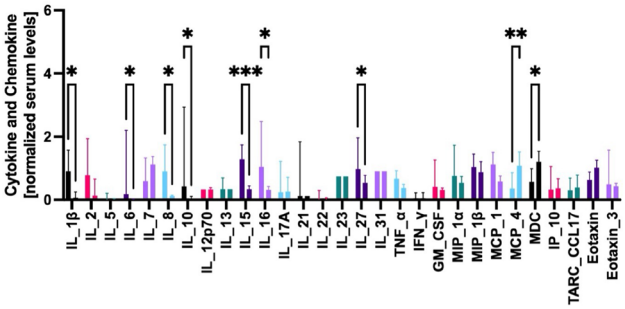


**Fig. 1 | 20-4** Cytokine and chemokine serum levels are shown as normalized levels (averaged to overall amount). The left bars represent FM patients, whereas the right bars represent acute, non-fulminant patient data. Data was analyzed using 2-way ANOVA for repeated measurements. * represents $p<0.05$, ** represents $p<0.01$, *** represents $p<0.001$

| Characteristic | Fulminant Myocarditis (n = 16) | Acute Myocarditis (n = 17) |
|---|---|---|
| Male sex, n (%) | 9 (56.3%) | 16 (94.1%) |
| Female sex, n (%) | 7 (43.7%) | 1 (5.9%) |
| Age, years | 41.5 (31.0–49.0) | 32.0 (26.0–41.0) |
| Body mass index, kg/m² | 23.9 (22.1–28.9) | 24.5 (23.2–28.6) |
| **28-day survival, n (%)** | | |
| Survivors | 12 (75.0%) | 16 (94.1%) |
| Non-survivors | 4 (25.0%) | 1 (5.9%) |
| **Clinical outcome, n (%)** | | |
| Recovery / regeneration | 11 (68.7%) | 16 (94.1%) |
| Heart transplantation | 1 (6.3%) | 0 (0%) |
| Permanent VAD | 0 (0%) | 0 (0%) |
| Death | 4 (25.0%) | 1 (5.9%) |
| **Histology, n (%)** | | |
| Lymphocytic / macrophage dominated myocarditis | 14 (87.5%) | No EMB available |
| Giant cell myocarditis | 2 (12.5%) | No EMB available |
| Eosinophilic myocarditis | 0 (0%) | No EMB available |

**Fig. 2 | 20-4** Data are presented as median (interquartile range) or as counts (percentages), as appropriate. VAD indicates ventricular assist device

tion remains challenging. While immune activation is central to disease pathophysiology, systematic clinical data comparing inflammatory cytokine and chemokine profiles between fulminant and non-fulminant presentations at hospital admission are limited. It remains unclear whether FM differs from acute myocarditis solely by the magnitude of inflammation or by a qualitatively distinct inflammatory signature at disease onset. We therefore aimed to characterize admission cytokine and chemokine profiles in patients with fulminant versus acute, non-fulminant myocarditis.

**Methods:** In this prospective single-center observational study, 16 patients with FM admitted to the intensive care unit were compared with 17 patients with acute, non-fulminant myocarditis treated on the general ward. Blood samples were obtained within 24 hours of hospital admission (ICU admission in FM; ward admission in acute myocarditis). A predefined panel of inflammatory cytokines and chemokines was quantified using multiplex immunoassays (MSD platform). Clinical characteristics and 28-day outcomes were recorded. The objective was to identify differences in inflammatory mediator levels at presentation.

**Results:** At admission, FM patients exhibited a distinct hyperinflammatory profile compared with acute myocarditis. Circulating levels of IL-1β, IL-6, and IL-8 were significantly elevated in FM, indicating accentuated innate immune activation. In parallel, immunoregulatory cytokines IL-10 and IL-27, as well as T-cell–associated mediators IL-15 and IL-16, were also increased, suggesting simultaneous activation of pro-inflammatory and compensatory immune pathways. In contrast, chemokines MCP-4 (CCL13) and MDC (CCL22) were significantly lower in FM, arguing against uniform chemokine upregulation and instead supporting a qualitatively distinct inflammatory activation. Clinically, FM was associated with higher 28-day mortality (25% vs 5.9%) and greater hemodynamic compromise. These findings indicate that fulminant myocarditis is characterized by a specific admission inflammatory signature rather than merely amplified inflammation.

**Conclusion:** FM is associated with a distinct cytokine and chemokine profile already present at hospital admission. The combination of pronounced innate immune activation, concurrent regulatory signaling, and selective alterations in chemotactic mediators suggests a dysregulated immune response underlying severe clinical presentation. Admission immunoprofiling may enhance early phenotypic discrimination and improve risk stratification in acute myocarditis. These data provide a biologically plausible foundation for future longitudinal immune profiling and potential immune-guided therapeutic strategies.

# POSTERSITZUNG 21 – KARDIOLOGISCHE PFLEGE UND MEDIZINISCH-THERAPEUTISCH-DIAGNOSTISCHE GESUNDHEITSBERUFE

## 21-1

### Development and Validation of a Predictive Scoring System for Medical Interventions and ICU Admission in Cardiac Emergency Department Patients

**Schwomma F., Capelle C., Bonderman D.**

Klinik Favoriten, Wien, Österreich

**Einleitung:** Notaufnahmen müssen bei Patientinnen und Patienten mit Verdacht auf akute kardiologische Erkrankungen unter Zeitdruck Entscheidungen zur weiteren Diagnostik und Therapie treffen. Eine frühe Risikostratifizierung ist dabei wesentlich, um eine rasche Eskalation der Versorgung – etwa Intensivüberwachung oder invasive Diagnostik – rechtzeitig einzuleiten. Die Aussagekraft etablierter klinischer Scoringsysteme ist in heterogenen kardiologischen Notaufnahmepopulationen jedoch limitiert. Ziel dieser Arbeit war die Entwicklung und Evaluation eines datengetriebenen, Machine-Learning-basierten Scoringsystems zur frühen Risikoprädiktion bei kardiologischen Notaufnahmepatientinnen und -patienten. Untersucht wurden zwei klinisch relevante Endpunkte innerhalb von 24 Stunden nach Krankenhausaufnahme: (1) Aufnahme auf eine Intensivstation (ICU) und (2) Durchführung einer akuten Herzkatheteruntersuchung.

**Methoden:** Es wurde eine retrospektive, monozentrische Beobachtungsstudie auf Basis anonymisierter Routinedaten von 422 erwachsenen Patientinnen und Patienten (Klinik Favoriten, Wien) durchgeführt. Prädiktoren beschränkten sich auf zum Aufnahmezeitpunkt verfügbare Informationen, darunter demografische Daten, Vitalparameter, klinische Präsentation, Komorbiditäten, frühe therapeutische Maßnahmen, Laborparameter sowie elektrokardiografische Befunde (als erhobene Variable). Für beide Endpunkte wurden separate Random-Forest-Modelle entwickelt. Aufgrund der begrenzten Stichprobengröße erfolgte die Evaluation auf dem vollständigen Datensatz (apparent performance) mittels Accuracy, Sensitivität, Spezifität, Precision, F1-Score und AUC. Zur Interpretierbarkeit wurde eine Feature-Importance-Analyse durchgeführt (Top-10 Variablen je Modell).

**Resultate:** Eine ICU-Aufnahme innerhalb von 24 Stunden trat bei 6 von 422 Patientinnen und Patienten (1,4 %) auf, während bei 100 von 422 Fällen (23,7 %) eine akute Herzkatheteruntersuchung innerhalb von 24 Stunden durchgeführt wurde. Für die Vorhersage einer ICU-Aufnahme zeigte das Random-Forest-Modell eine Accuracy von 0,998, eine Sensitivität von 0,833, eine Spezifität von 1000 sowie eine AUC von 0,940. Für die Vorhersage einer akuten Herzkatheteruntersuchung innerhalb von 24 Stunden erreichte das Modell eine Accuracy von 0,964, eine Sensitivität von 0,860, eine Spezifität von 0,997 und eine AUC von 0,980. Die Feature-Importance-Analyse zeigte für das ICU-Modell als wichtigste Prädiktoren unter anderem Alter (0,119), chronische Einnahme von Acetylsalicylsäure (0,072), systolischen Blutdruck (0,067), geringe Sauerstoffsättigung (0,058), Herzfrequenz (0,055), kardiale Arrhythmien (0,050),

erhöhtes Laktat (0,039) sowie eine vorangegangene Reanimation (0,038). Für die Vorhersage einer akuten Herzkatheteruntersuchung innerhalb von 24 Stunden zählten ein erhöhter Troponin Wert (0,097), eine ACS-Verdachtsdiagnose (0,078), sowie erhöhtes Laktat (0,069) und NT-proBNP (0,064) zu den wichtigsten Variablen. Weitere relevante Prädiktoren innerhalb der Top-10 waren unter anderem Atemfrequenz (0,057), Körpertemperatur (0,049) sowie demografische Variablen.

**Schlussfolgerungen:** Die Ergebnisse dieser Arbeit zeigen, dass routinemäßig erhobene klinische Daten aus der Notaufnahme relevante prognostische Informationen für die frühe Risikostratifizierung kardiologischer Patientinnen und Patienten enthalten. Die entwickelten Machine-Learning-Modelle ermöglichen eine outcome-spezifische Risikoprädiktion für eine ICU-Aufnahme sowie eine akute Herzkatheteruntersuchung innerhalb von 24 Stunden nach Krankenhausaufnahme. Im Vergleich zu in der Literatur berichteten Leistungswerten etablierter klinischer Risikoscores, wie GRACE, HEART, NEWS2 oder qSOFA, die typischerweise AUC-Werte im Bereich von etwa 0,65 bis 0,85 erreichen, zeigten die Random-Forest-Modelle in dieser Studie eine höhere diskriminative Leistungsfähigkeit für die untersuchten Endpunkte. Gleichzeitig zeigte sich, dass die Vorhersage einer akuten Herzkatheteruntersuchung eine höhere Modellleistung aufwies als die Prädiktion einer ICU-Aufnahme. Die Ergebnisse legen nahe, dass datengetriebene Machine-Learning-Ansätze bestehende klinische Risikostratifikationsverfahren sinnvoll ergänzen können. Eine externe Validierung in unabhängigen Patientenkohorten ist jedoch erforderlich, bevor eine klinische Anwendung erfolgen kann.

## 21-2

### Lebensqualität im Herzrhytmus der Technik: Perspektiven von LVAD PatientInnen

**Yildiz E.[1], Zumtobel S.[2]**

[1]Universitätsklinik für Herzchirurgie, Innsbruck, Österreich
[2]fhg – Zentrum für Gesundheitsberufe Tirol GmbH, Innsbruck, Österreich

**Einleitung:** Die Herzinsuffizienz ist eine weltweit zunehmende chronische Erkrankung, die im Endstadium zu erheblichen Einschränkungen der Lebensqualität führt und nur noch durch mechanische Unterstützungssysteme oder eine Herztransplantation behandelbar ist. Linksventrikuläre Unterstützungssysteme (LVADs) der dritten Generation sind eine moderne therapeutische Option für Patient: innen mit schwerer Herzinsuffizienz. Diese Geräte können sowohl die Überlebensrate als auch die Lebensqualität der Betroffenen verbessern. Die Lebensqualität nach LVAD-Implantation ist ein zentraler Faktor für die Patient:innenversorgung, zu dem nach wie vor weiterer Forschungsbedarf besteht. Das Ziel dieser Bachelorarbeit ist es, die Auswirkungen von LVAD-Implantationen auf die Lebensqualität von Patient:innen mit fortgeschrittener Herzinsuffizienz zu untersuchen und dabei insbesondere physische, mentale und soziale Dimensionen zu beleuchten.

**Methoden:** Zur Beantwortung der Fragestellung wurde eine Literaturrecherche durchgeführt. Hierzu wurden die wissenschaftlichen Datenbanken wie PubMed und CINAHL durchsucht. Aus den identifizierten Treffern wurden drei relevante Studien ausgewählt, die unterschiedliche Aspekte der Lebensqualität bei LVAD-Patient: innen untersuchten. Die Qualitätsbewertung der eingeschlossenen Studien erfolgte anhand standardisierter Kriterien, um eine fundierte Synthese der Ergebnisse zu gewährleisten.

**Resultate:** Die drei Studien zeigten eine signifikante Verbesserung der Lebensqualität nach der LVAD-Implantation, insbesondere in den Bereichen körperliche Belastbarkeit, soziale Interaktion und emotionale Stabilität. Durchschnittlich verbesserten sich die Werte in standardisierten Lebensqualitätsmessungen deutlich, und die Patient:innen berichteten über eine zunehmende sozialer Interaktion, Alltagsunabhängigkeit sowie stabilisierte physischen und mentalen Gesundheitsaspekte. Die Gesamtsynthese zeigt, dass LVAD-Patient:nnen sowohl physische als auch psychische Verbesserungen erfahren, jedoch in bestimmten Bereichen wie der physischen Belastbarkeit weiterhin Herausforderungen bestehen.

**Schlussfolgerungen:** Die Auswertung der ausgewählten Studien zeigt, dass LVAD-Implantationen die Lebensqualität von Patient:innen mit schwerer Herzinsuffizienz verbessern können. Besonders Systeme der dritten Generation scheinen eine positive Wirkung auf physische und psychische Stabilität zu haben. Die Ergebnisse verdeutlichen zudem die Notwendigkeit einer langfristigen interdisziplinären Betreuung, um den psychosozialen Herausforderungen und der physischen Begrenzung, die mit der LVAD-Nutzung einher gehen, umfassend gerecht zu werden. Es besteht weiterhin deutlicher Forschungsbedarf, um die physischen, psychischen und sozialen Effekte von LVAD-Implantationen besser zu verstehen.

## 21-3

### “Wenn Sekunden zählen – und Augen zusehen” Auswirkungen des Miterlebens einer Reanimation auf Angehörige

**Thurner B., Neyer S.**

FH Vorarlberg, Dornbirn, Österreich

**Einleitung:** Die Anwesenheit von Angehörigen während der kardiopulmonalen Reanimation, auch als Family-Witnessed Resuscitation (FWR) bezeichnet, wird seit mehreren Jahrzehnten kontrovers diskutiert. Während Befürworter*innen die ethischen Prinzipien von Autonomie, Transparenz und familienzentrierter Versorgung betonen, bestehen auf Seiten des medizinischen Personals häufig Bedenken hinsichtlich möglicher psychischer Belastungen der Angehörigen, einer Beeinträchtigung der Reanimationsqualität sowie einer erhöhten emotionalen Belastung des Behandlungsteams[1]. Internationale Leitlinien äußern sich bislang zurückhaltend und empfehlen FWR meist nur unter bestimmten strukturellen Voraussetzungen[2]. Ziel dieser Arbeit ist es, anhand ausgewählter quantitativer und qualitativer Studien die Auswirkungen des Miterlebens einer Reanimation auf Angehörige darzustellen.

**Methoden:** Zur Beantwortung der Forschungsfrage wurde eine strukturierte Literaturrecherche in den Datenbanken Cochrane Library sowie CINAHL via Ebsco Host und MEDLINE via Pubmed durchgeführt. Für die Recherche wurden vorab geeignete Suchbegriffe identifiziert sowie Ein- und Ausschlusskriterien festgelegt. Die Qualität der inkludierten Studien wurde anschließend mit dem Critical Appraisal Skills Programme (CASP) bewertet.

**Resultate:** Die elf eingeschlossenen Studien zeigen teils unterschiedliche Ergebnisse, stimmen jedoch in zentralen Punkten überein. Randomisierte oder quasi-experimentelle Studien zeigen, dass eine aktiv angebotene und professionell begleitete Anwesenheit mit geringeren Angst-, Depressions- und PTSD-Symptomen verbunden ist[3]. Zudem berichten Angehörige häufiger von besserem Verständnis des Geschehens, erleichterter Akzeptanz und reduzierten Schuldgefüh-

len. Beobachtungsstudien ohne strukturierte Begleitung weisen hingegen darauf hin, dass Anwesenheit ohne Vorbereitung mit erhöhten psychischen Belastungen einhergehen kann. So fanden zwei Studien höhere PTSD-Werte und vermehrt depressive Symptome bei anwesenden Angehörigen, insbesondere bei unzureichender Information und Kommunikation heraus. Qualitative Studien betonen darüber hinaus, dass Angehörige überwiegend die Möglichkeit zur Teilnahme befürworten, sofern diese freiwillig erfolgt und respektvoll begleitet wird.

**Schlussfolgerungen:** Die Evidenz zeigt, dass das Miterleben einer Reanimation sowohl belastende als auch potenziell protektive Effekte haben kann. Eine pauschale Empfehlung oder Ablehnung ist daher nicht gerechtfertigt. Entscheidend sind klare Information, professionelle Begleitung und die freiwillige Entscheidung der Angehörigen. Unter diesen Bedingungen kann das Miterleben die Verarbeitung unterstützen, ohne die medizinische Versorgung negativ zu beeinflussen.

## Literatur


1. Considine J, Eastwood K, Webster H, Smyth M, Nation K, Greif R, Dainty K, Finn J, Bray J. Family presence during adult resuscitation from cardiac arrest: A systematic review. Resuscitation. 2022;180:11–23. https://doi.org/10.1016/j.resuscitation.2022.08.021.
2. Rahmawati I, Page T, Conlon L, Donnelly F. The impact of being present during in-hospital resuscitation on family members: A scoping review. Eur J Cardiovasc Nurs. 2025;24(5):688–97. https://doi.org/10.1093/eurjcn/zvaf054.
3. Soleimanpour H, Tabrizi JS, Rouhi AJ, Golzari SEJ, Mahmoodpoor A, Esfanjani RM, Soleimanpour M. Psychological effects on patient's. Relat Regarding Their Presence Dur Resusc J Cardiovasc & Thorac Res. 2017;9(2):113–7.


# 21-4

## Telemedizinisch unterstützte Trainingstherapie bei Herzinsuffizienz vor herzchirurgischen Eingriffen – Ergebnisse der PREPARE-HF Pilotstudie


**Hagenauer J.[1], Hinterbuchner K.[2], Kleinheinz E.[1], Lohmann R.[2], Winter-Pölzl L.[2], Engler C.[2], Pfeifer B.[1], Neururer S.[3], Gollmann-Tepeköylü C.[2], Puelacher C.[4], Pölzl G.[4]**

[1]Landesinstitut für integrierte Versorgung, Innsbruck, Österreich
[2]Universitätsklinik für Herzchirurgie, Innsbruck, Österreich
[3]Health Data Competence Center, Innsbruck, Österreich
[4]Universitätsklinik für Innere Medizin III – Kardiologie und Angiologie, Innsbruck, Österreich


**Einleitung:** Patient:innen mit Herzinsuffizienz weisen vor elektiver Herzchirurgie ein erhöhtes perioperatives Risiko sowie eine eingeschränkte körperliche Leistungsfähigkeit auf. Präoperative Trainingstherapie (Prehabilitation) gewinnt zunehmend an Bedeutung, ist jedoch in der Hochrisikopopulation bislang wenig erforscht [1, 2]. Die PREPARE-HF Pilotstudie evaluierte die Machbarkeit, Sicherheit und Wirksamkeit eines multidisziplinären, telemedizinisch unterstützten Prehabilitationsprogramms, dessen zentraler Bestandteil eine strukturierte, multimodale Trainingstherapie war [3]. Ziel der vorliegenden Arbeit ist es, die körperliche Leistungsfähigkeit sowie deren Zufriedenheit mit dem Trainingsprogramm der Patient:innen zu untersuchen.

**Methoden:** In dieser prospektiven, einarmigen Pilotstudie wurden Patient:innen mit geplanter Herzchirurgie (Bypass, Herzklappen) und NT-proBNP ≥ 1500 ng/L in ein zehnwöchiges telemedizinisches Prehabilitationsprogramm eingeschlossen. Die leitlinienorientierte und evidenzbasierte Trainingstherapie wurde individuell nach Leistungsniveau (Borg 11–13) gesteuert [4,5,6] und vollständig im häuslichen Umfeld durchgeführt. Die Übungen in Kraft, Beweglichkeit und Koordination wurden mittels videoangeleiteter Einheiten absolviert. Trainingsumfang und -intensität wurden stufenweise an die individuelle Belastbarkeit angepasst. Die Dokumentation erfolgte über Bewegungstagebücher, ergänzt durch regelmäßige telefonische Betreuung durch die Trainingstherapie. Die Patient:innenzufriedenheit wurde anhand eines Fragebogens erhoben. Die körperliche Leistungsfähigkeit wurde mittels 6-Minuten-Gehtest (6 MWT) und 1-Minuten-Sit-to-Stand-Test (STS) zu Beginn und am Ende erhoben. Die statistische Analyse erfolgte mit SPSS, abhängig von der Normalverteilung wurden gepaarte t-Tests oder Wilcoxon-Tests verwendet ($p < 0{,}05$).

**Resultate:** Von 50 eingeschlossenen Patient:innen schlossen 38 das Trainingsprogramm planmäßig ab, von denen sich 36 anschließend der geplanten Herzoperation unterzogen. Sieben Personen befanden sich noch im Programm und fünf wurden als Abbruch gewertet. Für die statistische Auswertung wurden die Daten von 38 Teilnehmenden berücksichtigt. Die funktionelle Leistungsfähigkeit verbesserte sich signifikant. Die Distanz im 6 MWT ($n = 37$) stieg von 361 m (IQR 318–416) zu Beginn auf 420 m (IQR 323–468) nach Abschluss des Programms ($p = 0{,}003$). Auch die Leistung im STS ($n = 38$) nahm signifikant zu und erhöhte sich im Mittel von 20 (SD ± 8) auf 23 (SD ± 10) Wiederholungen ($p = 0{,}004$). Von den 38 Teilnehmenden gaben 33 (86,8 %) ein Bewegungstagebuch ab. Basierend auf diesen Aufzeichnungen absolvierten die Patient:innen im Median 201 (IQR 130–356) Minuten Ausdauertraining pro Woche sowie 3 (IQR 2–6) Einheiten Kraft-, Koordinations- oder Beweglichkeitstraining pro Woche. Das inspiratorische Atemmuskeltraining wurde im Median 2-Mal (IQR 1–2) täglich durchgeführt. Den Fragebogen zur Patient:innenzufriedenheit füllten 37 von 38 Personen (97,4 %) aus. Von diesen berichteten 84,2 % vom Bewegungsprogramm profitiert zu haben und 86,8 % bewerteten das Feedback der Trainingstherapeutin als wichtig. 65,8 % gaben an, sich durch das Programm besser auf die Operation vorbereitet zu fühlen und 73,7 % äußerten die Absicht, auch postoperativ ein weiteres Bewegungsprogramm zu absolvieren.

**Schlussfolgerungen:** Insgesamt zeigen die Ergebnisse, dass ein multimodales, strukturiertes Trainingsprogramm auch in dieser Population wirksam umgesetzt werden kann. Die dokumentierten Trainingsumfänge entsprechen den empfohlenen Bewegungsvorgaben für kardiologische Patient:innen [4]. Insgesamt erreichten 50 % der Patient:innen eine Verbesserung von mindestens 30 m im 6 MWT und 60,5 % verbesserten sich im STS um mindestens zwei Wiederholungen. In der Literatur gelten diese Werte als minimal klinisch relevante Veränderungen [7,8]. Limitation dieser Pilotstudie ist das einarmige Studiendesign, dadurch ist die Aussagekraft der kausalen Wirksamkeit der Intervention eingeschränkt. Aufbauend auf diesen Ergebnissen wird derzeit eine randomisierte-kontrollierte Studie initiiert, um den Effekt des Programms auf klinische Endpunkte sowie perioperative Outcomes zu evaluieren.

## Literatur


1. Steinmetz C, Bjarnason-Wehrens B, Walther T, Schaffland TF, Walther C. Efficacy of Prehabilitation Before Cardiac Surgery. Am J Phys Med Rehabil. 2023;102(4):323–30. Apr.

2. Hurtado-Borrego JC, Bayonas-Ruiz A, Bonacasa B. Exercise-Based Prehabilitation Before Cardiac Surgery: A Systematic Review, Meta-Analysis, Meta-Regression, and Proposal for a Clinical Implementation Model. J Clin Med. 2025;19;14(22):8195. Nov.
3. Hinterbuchner K, Kleinheinz E, Fetz B, Pölzl L, Holfeld J, Pfeifer B, Neururer S, Puelacher C, Gollmann-Tepekoeylue C, Krestan S, Huber A, Pölzl G. HerzMobil Tirol PreOp – A Multidisciplinary Telemonitoring Project for Heart Failure Patients Prior to Cardiac Surgery. Stud Health Technol Inform. 2024;26(313):141–2. Apr.
4. Pelliccia A, Sharma S, Gati S, Bäck M, Börjesson M, Caselli S, et al. 2020 ESC Guidelines on sports cardiology and exercise in patients with cardiovascular disease. Eur Heart J. 2021;42(1):17–96. Jan.
5. Zhang S, Li B, Meng X, Zuo H, Hu D. The Effects of Inspiratory Muscle Training (IMT) on Patients Undergoing Coronary Artery Bypass Graft (CABG) Surgery: A Systematic Review and Meta-Analysis. Rev Cardiovasc Med. 2023;24(1):9.
6. Mans CM, Reeve JC, Elkins MR. Postoperative outcomes following preoperative inspiratory muscle training in patients undergoing cardiothoracic or upper abdominal surgery: a systematic review and meta analysis. Clin Rehabil. 2015;26;29(5):426–38. May.
7. Shoemaker MJ, Curtis AB, Vangsnes E, Dickinson MG. Clinically meaningful change estimates for the six-minute walk test and daily activity in individuals with chronic heart failure. Cardiopulm Phys Ther J. 2013;24(3):21–9. Sep.
8. Nguyen NM, Le HT, Ngo BL, Truong HP, Reychler G, Deboeck G. Validity, test-retest reliability, and learning effect on the 1-minute sit-to-stand test in individuals with heart failure. Arch Phys Med Rehabil. 2025;106:1–7. May.

## 21-5

## Patient*innenakademie—Ein pflegegeleitetes, interprofessionelles Versorgungsangebot zur Stärkung des Selbstmanagements bei Herz-Kreislauf-Erkrankungen

**Qin H.[1], Teichert K.[1], Petz E.[2], Hengstenberg C.[1]**

[1]Klinische Abteilung für Kardiologie, Universitätsklinik für Innere Medizin II, Medizinische Universität Wien, Wien, Österreich
[2]Univ. Klinik für Innere Medizin II, Klinische Abteilung für Kardiologie, Universitätsklinikum AKH Wien, Medizinische Universität Wien, Wien, Österreich

**Einleitung:** Herz-Kreislauf-Erkrankungen zählen zu den häufigsten chronischen Erkrankungen und gehen mit hoher Morbidität, Mortalität sowie erheblichen psychosozialen Belastungen einher. Insbesondere während des Krankenhausaufenthalts und in der Phase nach der Entlassung sowie im Rahmen ambulanter Betreuung besteht bei vielen Patient*innen ein ausgeprägter Informationsbedarf bei gleichzeitig erhöhter emotionaler Vulnerabilität. Im klinischen Alltag stehen jedoch häufig nur begrenzte zeitliche Ressourcen für strukturierte edukative Maßnahmen und Gespräche zur Krankheitsbewältigung zur Verfügung. Vor diesem Hintergrund wurde an der Universitätsklinik die Patient*innenakademie als pflegegeleitetes Versorgungsangebot etabliert. Ziel ist die nachhaltige Förderung der Selbstmanagement-Kompetenz von Patient*innen mit chronischen Herzerkrankungen durch regelmäßige interprofessionelle Informationsveranstaltungen. Die Teilnehmenden erhalten verständlich aufbereitetes krankheitsspezifisches Wissen sowie praxisnahe Strategien zum Umgang mit Symptomen, Therapieanforderungen und psychosozialen Belastungen. Zudem haben die Teilnehmenden die Möglichkeit, sich direkt mit Expert*innen auszutauschen, was die Sicherheit im Umgang mit der Erkrankung stärkt, die Entscheidungsfähigkeit im Alltag verbessert und zur emotionalen Entlastung beiträgt.

**Methoden:** Die Patient*innenakademie ist als praxisnahes Edukationsprogramm konzipiert. Grundlage bildet ein strukturiertes didaktisches Konzept mit Fokus auf verständliche Wissensvermittlung, die Förderung der Selbstmanagement-Kompetenz und die psychokardiologische Begleitung. Die monatlichen Veranstaltungen werden interprofessionell vorbereitet und durchgeführt. Die Inhalte sind krankheitsspezifisch (u. a. Herzinsuffizienz, koronare Herzkrankheit, Herzklappenerkrankungen) und folgen einem ganzheitlichen Ansatz. Zielgruppe sind Patient*innen vor, während und nach dem stationären Aufenthalt sowie ambulant betreute Patient*innen der Klinik und deren Angehörige. Die Evaluation erfolgt mittels standardisierter Feedbackbögen und qualitativer Rückmeldungen. Erfasst werden der subjektive Wissenszuwachs, die wahrgenommene Sicherheit im Umgang mit der Erkrankung sowie die Relevanz psychokardiologischer Themen.

**Resultate:** Seit der Initiierung der Patient*innenakademie im Oktober 2024 wurden insgesamt 15 Veranstaltungen mit 13–30 Teilnehmenden pro Termin durchgeführt. Die Rückmeldungen

**Abb. 1 | 21–5** Veranstaltung der Patient*innenakademie

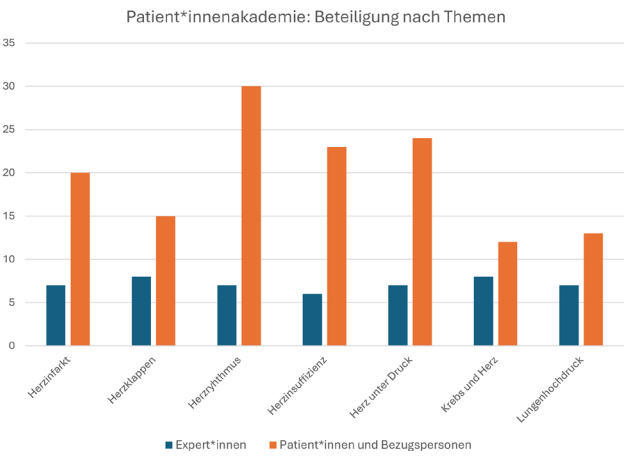


**Abb. 2 | 21–5** Beteiligung nach Themen

der Patient*innen waren durchgehend positiv. Psychokardiologische Themen, insbesondere Strategien zur Stressbewältigung und zum Umgang mit krankheitsbedingten Ängsten, wurden als besonders relevant und hilfreich bewertet. Als wesentliche Erfolgsfaktoren zeigten sich laienverständlich aufbereitete Vorträge, interprofessionelle Zusammenarbeit sowie die Möglichkeit individueller Gespräche. Pro Veranstaltung waren sechs bis acht Expert*innen aus unterschiedlichen Berufsgruppen eingebunden.

**Schlussfolgerungen:** Die Patient*innenakademie zeigt, dass ein praxisnahes Edukationsprogramm eine sinnvolle Ergänzung zur kardiologischen Regelversorgung ist. Durch die Einbindung sowohl stationärer als auch ambulanter Patient*innen trägt das Angebot zu einer kontinuierlichen und sektorenübergreifenden Versorgung bei. Die strukturierte Wissensvermittlung in Kombination mit einer kontinuierlichen APN-basierten Cardio-nursing Begleitung ermöglicht eine gezielte Unterstützung von Patient*innen mit chronischen Herzerkrankungen. Die hohe Akzeptanz unterstreicht die Versorgungsrelevanz des Konzepts. Zur weiteren wissenschaftlichen Fundierung ist eine prospektive Evaluation mittels standardisierter Erhebungsinstrumente geplant, um Effekte auf Selbstmanagement-Kompetenz, wahrgenommene Sicherheit und gesundheitsbezogene Lebensqualität zu untersuchen.

# POSTERSITZUNG 22—RHYTHMOLOGIE 2

## 22-1

### Sex-Specific Prognostic Significance of Telemonitoring-Detected Serious Arrhythmic Events After Myocardial Infarction: A Rhythmology-Focused SMART-MI Analysis

**Dolejsi T.[1], Schreinlechner M.[1], Pavluk D.[1], Klimovskis N.[1], Reinstadler S.[1], Rizas K.[2], Massberg S.[2], Bauer A.[1]**

[1]Universitätsklinik für Innere Medizin III, Innsbruck, Austria
[2]LMU Klinikum, Medizinische Klinik und Poliklinik I, München, Germany

**Introduction:** Post–myocardial infarction (MI) patients without particularly impaired left ventricular function (LV-EF 36–50%) but autonomic dysfunction detected by ECG delineate a subgroup with heightened vulnerability to clinically silent arrhythmias. Continuous rhythm surveillance using an implantable cardiac monitor (ICM) with remote transmission may therefore improve arrhythmia detection and refine prognostic assessment. The aim was to evaluate whether sex influences (1) the incremental diagnostic yield of telemedical implantable cardiac monitoring for serious arrhythmic events (SArE) and (2) the prognostic significance of an identified SArE for subsequent major clinical complications.

**Methods:** In the prospective, randomized SMART-MI trial, acute MI survivors with LVEF 36–50% and autonomic risk markers—periodic repolarization dynamics (PRD) ≥ 5.75°[2] and/or deceleration capacity (DC) ≤ 2.5 ms—were assigned to ICM implantation with telemedical monitoring or conventional follow-up. The primary rhythm endpoint was time to first SArE (atrial fibrillation ≥ 6 min; AV block ≥IIb; fast non-sustained VT > 187 bpm and ≥ 40 beats, or sustained VT/VF). Clinical complications comprised mortality, stroke, systemic arterial thromboembolism, or heart-failure hospitalization. Cox models assessed monitoring effects on SArE detection; SArE was additionally modeled as a time-dependent covariate to quantify its association with later complications.

**Results:** 400 patients were randomized (ICM $n = 201$, including 49 women; control $n = 199$, including 29 women). During a median follow-up of 21 ± 23 months, ICM monitoring detected substantially more SArE than standard care (60/201 [30%; 12 women] vs 12/199 [6%; 1 woman]). The detection benefit was evident in both sexes (men: HR 6, 95% CI 3.113–11.56; $p < 0.001$; women: HR 9.946, 95% CI 1.286–76.89; $p = 0.03$) with no sex-dependent difference in monitoring yield ($p$ for interaction = 0.790). In prognostic terms, occurrence of SArE was associated with a higher risk of subsequent clinical complications in both sexes, with a markedly stronger association in women (men: HR 3.64, 95% CI 1.89–7.02; $p < 0.001$; women: HR 16.19, 95% CI 4.76–55.11; $p < 0.001$; interaction $p = 0.030$).

**Conclusion:** In autonomic high-risk MI survivors, telemedical ICM surveillance substantially improves detection of clinically unapparent atrial fibrillation, atrioventricular conduction, and ventricular tachyarrhythmic events in both women and men. Once a SArE is captured, its linkage to subsequent major clinical complications appears significantly stronger in women, suggesting that arrhythmia detection in female post-MI patients may warrant particularly intensified rhythmology-guided risk stratification and follow-up.

## 22-2

### Characterization of patients with late pacemaker implantation after ablation for AVNRT or septal accessory pathways

**Schuetz T.[1], Adukauskaite A.[1], Schgör W.[1], Dichtl W.[1], Hintringer F.[1], Hangler H.[2], Bauer A.[1], Stühlinger M.[1]**

[1]Department of Internal Medicine III – Cardiology and Angiology, Innsbruck, Austria
[2]Department of Cardiac Surgery, Innsbruck, Austria

**Introduction:** The risk for permanent atrioventricular (AV) block and subsequent pacemaker (PM) implantation after ablation for atrioventricular nodal reentry tachycardia (AVNRT) or atrioventricular reentry tachycardia (AVRT) caused by septal accessory pathways (AP) is increased. This work aims to characterise these patients included in local ablation and PM registries at a tertiary health care centre in Austria.

**Methods:** Data from patients from the local ablation registry who underwent ablation of AVNRT or AVRT between 2015 and 2024, were included in this analysis. Data regarding PM implantations were taken from the local PM implantation registry. Patients, which already had a PM implanted at the time of ablation, were excluded. Data of the two registries were merged using the unique social security number as identifier. Patients with PM implantation were only included, if AV block was the indication for PM implantation. Late PM implantation (LPMI) was defined as PM implantation ≥ 30 days post ablation. Patients were characterised by age at time of ablation, sex, number of ablations delivered, and application of a 3D electroanatomical mapping (EAM) system.

**Results:** Between 2015 and 2024, 868 patients underwent ablation for AVNRT (57.7% female), and 295 patients underwent ablation for AVRT (33.1% female). Median follow up in the AVNRT group was 5.3 years (IQR 2.5–7.7), and 5.6 years (IQR 2.5–7.7) in the AVRT cohort, respectively. Of the AVNRT patients, 8

(1.0%) of 868 underwent PM implantation within the first days after ablation, and 2 (0.2%) after ≥30 days (679 and 1217 days). Four (1.4%) of the 295 AVRT patients needed PM implantation—3 within the first 8 days, 1 at day 52. Importantly the single patient with LPMI developed AV block already at the time of AVRT ablation, but because of an adequate escape rhythm and to allow the possibility for recovery, PM implantation was delayed. EAM was used in 1.76% of AVNRT patients (not in the 2 patients with LPMI), and in 51.76% of AVRT patients, including the one with LPMI. Except for 7 patients of the AVRT group, who were ablated using cryo catheters (CC), RF was the energy form of all the AVNRT and AVRT ablations. CC were used only in patients with a septal AP close to the conduction system. None of the CC patients suffered from AV block and subsequent PM implantation. In the AVNRT group a median of 5 (IQR 3–9), and in the AVRT group a median of 4 (IQR 2–10) ablations were performed.

**Conclusion:** While EAM and CC are commonly employed for ablation in challenging anatomical AP locations, AV block remains a potential complication during procedures targeting both AVRT and AVNRT. In our local registry, all cases of AV block in patients undergoing ablation for an AP occurred during the procedure itself. Additionally, 0.2% of individuals who underwent ablation for AVNRT experienced delayed onset AV blocks necessitating pacemaker implantation.

## 22-3

### Treatment of lead-associated obstruction of the superior venous system—an advanced interventional approach

**Jenner D., Gundendorfer M., Schwarz S., Reiter C., Steinwender C., Saleh K.**

Department of Cardiology, Kepler University Hospital Linz, Medical Faculty Johannes Kepler University Linz, Linz, Austria

**Introduction:** Lead-associated stenosis or complete occlusion of the superior venous system ("obstruction of the superior venous system", OSVS)—that is, the superior vena cava and/or its tributary veins—are observed as not infrequent complications in the context of transvenous cardiac implantable electronic device therapy. The symptoms of OSVS depend significantly on the location of the stenosis/occlusion and the size of the drainage area affected by the impacted vein. In some cases, such as with superior vena cava syndrome, life-threatening complications may occur. The treatment of OSVS and its consequences is generally complex and requires a high level of expertise. This report outlines an interventional strategy derived from a case series involving five patients treated at our institution.

**Methods:** From January 2023 to February 2026, all patients with the diagnosis or symptoms of lead-associated OSVS received individual interventional treatment at our institution.

**Results:** The patient cohort ($n=5$) consisted of three males and two females, with a median age of 66 years (range: 52–75). Four individuals had a dual-chamber pacemaker system in situ, while one had a single-chamber defibrillator system. All patients exhibited highly symptomatic, functional OSVS syndromes despite long-term conservative management including oral anticoagulant therapy. The affected veins, each in different combinations, included the subclavian vein, the brachiocephalic vein—each on the implantation side—as well as the superior vena cava. Three patients showed the full clinical picture of superior vena cava syndrome. In all cases, treatment involved extraction of the existing pacemaker/defibrillator system and subsequent implantation of a leadless pacemaker or extravascular defibrillator. Additionally, all patients, in four out of five cases even during the same session, underwent endovascular stent implantation to revascularize the affected vessels. In all cases, complete resolution of OSVS symptoms was achieved without compromising the functionality of device therapy and without post-interventional complications.

**Conclusion:** Lead-associated OSVS syndromes represent potentially dangerous complications of transvenous pacemaker or defibrillator systems. Interventional treatment of these syndromes by system extraction and reimplantation of leadless or extravascular systems, as well as endovascular stenting of the stenotic/occluded vessels, proved to be a safe and effective therapeutic approach with the majority of procedures being performed in the same session.

## 22-4

### Real-world comparison of bleeding scores in patients with atrial fibrillation receiving DOACs

**Radl V.[1], Baumer U.[1], Hofer F.[1], Hammer A.[1], Steinacher E.[1], Hengstenberg C.[1], Niessner A.[2], Koller L.[1], Kazem N.[1]**

[1]Medizinische Universität Wien, Wien, Austria
[2]Klinik Landstrasse, Wien, Austria

**Introduction:** The prediction of potentially life-threatening major bleeding events in patients with atrial fibrillation (AF) receiving direct oral anticoagulation (DOAC) remains challenging. Several clinical and biomarker-based bleeding risk scores have been developed and validated across broad populations of

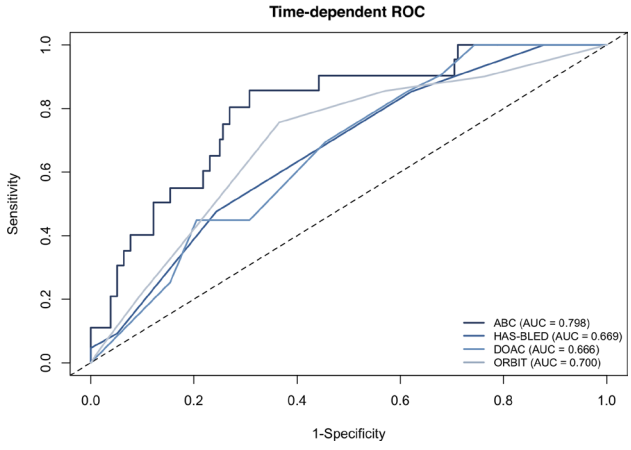


**Fig. 1 | 22-4** ROC-Curves

C-Statistics

| Score | AUC | 95% CI | C-Index | 95% CI | p for ABC |
|---|---|---|---|---|---|
| ABC-Bleeding | 0.80 | 0.7–0.89 | 0.76 | 0.67–0.85 | – |
| HAS-BLED | 0.67 | 0.56–0.78 | 0.67 | 0.57–0.77 | 0.04* |
| DOAC | 0.67 | 0.56–0.77 | 0.64 | 0.54–0.74 | 0.02* |
| ORBIT | 0.70 | 0.58–0.82 | 0.67 | 0.56–0.77 | 0.04* |

p for ABC: p-value for comparison of discriminative performance against the ABC-Bleeding score using DeLong's method.; * p < 0.05

**Fig. 2 | 22-4** C-Statistics

anticoagulated patients. However, the performance of these risk scores varies and a comprehensive comparison in real-world anticoagulated AF patients with long term follow-up has not yet been undertaken. We therefore aimed to evaluate the performance of available clinical and biomarker-based bleeding risk scores for predicting major bleeding events in a real world AF-cohort.

**Methods:** Between August 2020 and June 2024, we prospectively enrolled and followed all-comer patients with AF receiving a DOAC at our institution. Patients had to be eligible for the DOAC agent in accordance with the ESC AF guidelines. For each patient the HAS-BLED, DOAC, ORBIT and ABC-Bleeding scores were calculated at baseline. The primary endpoint was major bleeding as defined by the International Society on Thrombosis and Haemostasis (ISTH).

**Results:** In this analysis 300 patients with AF under DOAC therapy were included and followed for a median time of 3.2 years (IQR 2.5–4.6). The median age was 76 years (IQR 66–81) and 62.3% ($n = 187$) of patients were male. The most frequently used DOACs were Apixaban (33.3%) and Edoxaban (34.3%). At baseline, 110 (36.7%) patients received a reduced DOAC dose, 50 (16.7%) suffered from chronic kidney disease and 83 (27.6%) had a history of bleeding. The median CHADS-VA-Score was 4 (IQR 2–5). A total of 25 (8.3%) patients reached the endpoint of ISTH major bleeding. The most common major bleeding event was gastrointestinal bleeding with 14 (56%) events, followed by haematuria with 4 (16%). The ABC-Bleeding score presented the highest predictive performance with an AUC of 0.798 [0.65–0.83] in the time-dependent ROC-analysis. Its discriminative capacity was superior to the HAS-BLED (AUC 0.669, $p = 0.04$), DOAC (AUC 0.665, $p = 0.02$) and ORBIT (AUC 0.700, $p = 0.04$) score. Additionally, the ABC-Bleeding score showed the highest Harrel's C-Index of 0.761 [0.672–0.85]. Decision curve analysis was performed and demonstrated higher net benefit for the ABC Score across thresholds of 5%–12% compared to HAS-BLED, DOAC and ORBIT. Calibration plots suggested that the DOAC and ORBIT score overestimated bleeding risk in the lower predicted-risk range and underestimated it in higher ones, whereas ABC and HAS-BLED showed good agreement in lower predicted-risk ranges and overestimated it in higher ones.

**Conclusion:** Biomarker-based scores, such as the ABC-Bleeding score, may provide superior predictive performance compared with clinical risk scores in real-world DOAC-treated AF patients.

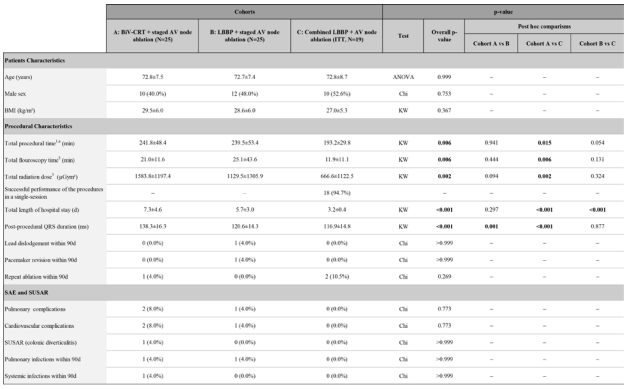

| | Cohorts | | | p-value | | | | |
|---|---|---|---|---|---|---|---|---|
| | A: BiV-CRT + staged AV node ablation (N=25) | B: LBBP + staged AV node ablation (N=25) | C: Combined LBBP + AV node ablation (ITT, N=19) | Test | Overall p-value | Post hoc comparisons | | |
| | | | | | | Cohort A vs B | Cohort A vs C | Cohort B vs C |
| **Patients Characteristics** | | | | | | | | |
| Age (years) | 72.8±7.5 | 72.7±7.4 | 72.8±8.7 | ANOVA | 0.999 | – | – | – |
| Male sex | 10 (40.0%) | 12 (48.0%) | 10 (52.6%) | Chi | 0.753 | – | – | – |
| BMI (kg/m²) | 29.5±6.0 | 28.6±6.0 | 27.0±5.3 | KW | 0.367 | – | – | – |
| **Procedural Characteristics** | | | | | | | | |
| Total procedural time[1,6] (min) | 241.8±48.4 | 239.5±53.4 | 193.2±29.8 | KW | **0.006** | 0.941 | **0.015** | 0.054 |
| Total fluoroscopy time[2] (min) | 21.0±11.6 | 25.1±43.6 | 11.9±11.1 | KW | **0.006** | 0.444 | **0.006** | 0.131 |
| Total radiation dose[3] (µGym²) | 1383.8±1197.4 | 1129.5±1305.9 | 666.6±1122.5 | KW | **0.002** | 0.094 | **0.002** | 0.324 |
| Successful performance of the procedures in a single-session | – | – | 18 (94.7%) | | – | – | – | – |
| Total length of hospital stay (d) | 7.3±4.6 | 5.7±3.0 | 3.2±0.4 | KW | **<0.001** | 0.297 | **<0.001** | **<0.001** |
| Post-procedural QRS duration (ms) | 138.3±16.3 | 120.6±14.3 | 116.9±14.8 | KW | **<0.001** | **0.001** | **<0.001** | 0.877 |
| Lead dislodgement within 90d | 0 (0.0%) | 1 (4.0%) | 0 (0.0%) | Chi | >0.999 | – | – | – |
| Pacemaker revision within 90d | 0 (0.0%) | 1 (4.0%) | 0 (0.0%) | Chi | >0.999 | – | – | – |
| Repeat ablation within 90d | 1 (4.0%) | 0 (0.0%) | 2 (10.5%) | Chi | 0.269 | – | – | – |
| **SAE and SUSAR** | | | | | | | | |
| Pulmonary complications | 2 (8.0%) | 1 (4.0%) | 0 (0.0%) | Chi | 0.773 | – | – | – |
| Cardiovascular complications | 2 (8.0%) | 1 (4.0%) | 0 (0.0%) | Chi | 0.773 | – | – | – |
| SUSAR (colonic diverticulitis) | 1 (4.0%) | 0 (0.0%) | 0 (0.0%) | Chi | >0.999 | – | – | – |
| Pulmonary infections within 90d | 1 (4.0%) | 1 (4.0%) | 0 (0.0%) | Chi | >0.999 | – | – | – |
| Systemic infections within 90d | 1 (4.0%) | 0 (0.0%) | 0 (0.0%) | Chi | >0.999 | – | – | – |

**Table 1: Results of the High-Volume CSP Experience with Combined LBBP and AV Node Ablation. Overall p-values were derived from ANOVA, Chi-square or Kruskal-Wallis tests, as appropriate. Post hoc pairwise comparisons were performed using Nemenyi test following KW analysis. p-values are alpha-adjusted. Note: For some variables a significant overall group effect was observed, whereas pairwise comparisons did not reach significance, potentially due to data characteristics and small group size. Abbreviations: AV=atrioventricular, BiV-CRT=Biventricular Cardiac Resynchronization Therapy, ITT=Intention-to-Treat, KW= Kruskal-Wallis test, LBBP=Left Bundle Branch Pacing, N=Total cohort size, SAE=Serious Adverse Event, SUSAR= Suspected Unexpected Serious Adverse Reaction. [1]Time from patient arrival at procedure room until pickup from procedure room. [2]Available cases: Cohort A n=14, B n=12, C n=18. [3]Available Cases: Cohort A n=23, B n=23, C n=18. [4]Available Cases: Cohort A n=23, B n=25, C n=19.**

**Fig. 1 | 22-5**

**Conclusion:** Biomarker-based scores, such as the ABC-Bleeding score, may provide superior predictive performance compared with clinical risk scores in real-world DOAC-treated AF patients.

## 22-5

## High-Volume CSP Experience with Combined LBBP and AV Node Ablation

**Autz C.[1], Kollias G.[2], Alibegovic-Zaborsky J.[2], Hölzl M.[2], Martinek M.[2], Pürerfellner H.[2], Derndorfer M.[2]**

[1]Johannes Kepler Universität Linz, Medizinische Fakultät, 4020 Linz, Austria
[2]Ordensklinikum Linz Elisabethinen, Interne 2 – Kardiologie, Angiologie & Interne Intensivmedizin, 4020 Linz, Austria

**Introduction:** Pace-and-ablate is a guideline-endorsed strategy for therapy-refractory atrial fibrillation (AF),[1] traditionally performed in two separate procedures due to concerns regarding lead stability.[1,2] With growing expertise in conduction system pacing (CSP), this approach may be reconsidered. At our high-volume CSP center, left bundle branch pacing (LBBP) has been implemented as default physiological pacing strategy and transitioned from staged procedures to a standardized single-session LBBP including atrioventricular (AV) node ablation workflow. We evaluated the feasibility, safety and clinical outcomes of this single-session approach compared to traditional two-staged strategies.

**Methods:** This combined retrospective and prospective non-interventional cohort study with historical control compares three cohorts: • Biventricular cardiac resynchronization therapy (BiV-CRT) + staged AV node ablation ($n = 25$), • LBBP + staged AV node ablation ($n = 25$), • LBBP + AV node ablation in a single session (ITT $n = 19$; PP $n = 17$). Total ITT population: 69 patients (72.8 ± 7.7 yrs; 46.4% male). Primary endpoints: Procedural efficiency, electrical stability (threshold, sensing, impedance at day 1 and 3 months), lead stability and length of hospital stay. Secondary endpoint: Complications. Linear mixed-effects model analyses assessed electrical parameters and repeated measures.

**Results:** Procedure and hospital stay: Performing LBBP in a single session reduced cumulative treatment burden by obviating a second procedure. The total procedural time was shorter compared with staged BiV-CRT and LBBP (193.2 ± 29.8 vs. 241.8 ± 48.4 and 239.5 ± 53.4 min), with concomitant reductions in fluoroscopy time and radiation exposure. The single-session intervention was associated with a shorter hospital stay (3.2 ± 0.4 vs. 7.3 ± 4.6 and 5.7 ± 3.0 days) and was feasible in 94.7% of cases. Physiological advantage: The post-procedural QRS duration was significantly shorter with LBBP (116.9 ± 14.8 and 120.6 ± 14.3 ms) compared with BiV-CRT (138.3 ± 16.3 ms). The linear mixed-effects model analyses did not demonstrate a significant overall time effect on threshold, impedance or sensing over three months. The BiV-CRT cohort showed higher adjusted threshold and impedance values than both LBBP cohorts, whereas sensing amplitude was similar among all groups. Safety signal: Across all groups, 9 serious adverse events (SAE) and 1 suspected unexpected serious adverse reaction (SUSAR) occurred, without excess complications in the single-session cohort. One lead dislodgement requiring operative revision was observed in the staged LBBP cohort. Key results are summarized in the appendix (Fig. 1).

**Conclusion:** In this high-volume CSP center experience, transition from staged to single-session workflow did not compromise safety or electrical performance. A standardized combined LBBP plus AV node ablation strategy was efficient and feasible, suggesting that staged workflows could be safely replaced in experienced centers.

## References

1. Van Gelder IC, Rienstra M, Bunting KV, Casado-Arroyo R, Caso V, Crijns HJGM, et al. 2024 ESC Guidelines for the

management of atrial fibrillation developed in collaboration with the European Association for Cardio-Thoracic Surgery (EACTS). Eur Heart J. 2024;45(36):3314–414. https://doi.org/10.1093/eurheartj/ehae176.
2. Rijks JHJ, Lankveld T, Manusama R, Broers B, Van Stipdonk AMW, et al. Left Bundle Branch Area Pacing and Atrioventricular Node Ablation in a Single-Procedure Approach for Elderly Patients with Symptomatic Atrial Fibrillation. J Clin Med. 2023;12:4028. https://doi.org/10.3390/jcm12124028.

## 22-6

### Stereotactic Arrhythmia Radioablation (STAR) for Therapy-Refractory Ventricular Tachycardia: Clinical Impact and Limitations from a Single-Center Case Series

**Gölly K.[1], Seiß L.[2], Manninger-Wünscher M.[1], Langsenlehner T.[2], Rohrer U.[1], Winkler P.[2], Eberl A.[1], Fuchsjäger M.[3], Zirlik A.[1], Brunner T.[2], Scherr D.[1]**

[1]Klinischen Abteilung für Kardiologie, Universitätsklinik für Innere Medizin, LKH Graz, Graz, Austria
[2]Universitätsklinik für Strahlentherapie-Radioonkologie, LKH Graz, Graz, Austria
[3]Universitätsklinik für Radiologie, LKH Graz, Graz, Austria

**Introduction:** Stereotactic arrhythmia radioablation (STAR) has emerged as a non-invasive bailout therapy for patients with therapy-refractory ventricular tachycardia (VT) who are not amenable to further catheter ablation. Evidence of this method remains limited, and long-term efficacy and safety are uncertain. This single-center case series describes clinical outcomes and key limitations of STAR in patients with treatment-refractory VT.

**Methods:** Four patients with advanced structural heart disease and recurrent electrical storm underwent STAR between 2024 and 2025. All had persistent VT despite maximally tolerated antiarrhythmic drug therapy and multiple prior endocardial and/or epicardial ablations. Target volumes were defined by integrating electroanatomical mapping, multimodal cardiac imaging, and 12-lead ECG morphology. A single fraction of 25 Gy was delivered using stereotactic body radiotherapy, with dose reduction near radiosensitive structures. Follow-up included ICD interrogation and clinical assessment, with a median observation period of approximately 3–4 months (range 2–12 months).

**Results:** STAR was technically feasible in all patients and was not associated with acute procedural complications. VT burden decreased in all cases, but the magnitude and durability of response differed: one patient remained free of recurrent VT for 3.5 months before dying from a non-cardiac cause, whereas the others experienced VT recurrences with a reduced overall episode burden and fewer ICD therapies. Two patients developed radiographic signs of first degree radiation pneumonitis, both asymptomatic and managed conservatively. All four patients died during follow-up, predominantly from progression of advanced cardiomyopathy. No definite treatment-related mortality was observed, and the limited survival limited meaningful assessment of long-term efficacy and late toxicity.

**Conclusion:** In this small case series, STAR was feasible and associated with reduced arrhythmia burden in treatment-refractory VT patient. Complete remission was achieved in one case, whereas the remaining patients showed only partial and transient VT suppression. Durability cannot be reliably assessed because early mortality related to underlying disease limited follow-up. Even though radiation-induced changes were mild, the complexity of target definition supports a cautious clinical approach. Given the advanced disease stage and the high competing risk of death, STAR should currently be regarded as a palliative bailout strategy. Its use should be confined to specialized centers with close collaboration between electrophysiology, cardiac imaging, and radiation oncology teams and further prospective data is needed to better define its role.

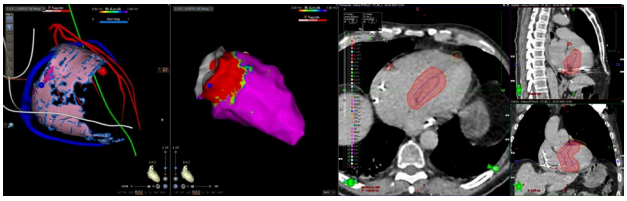

**Fig. 1 | 22-6** Procedure planning with definition of the target volume for STAR

## 22-7

### Effect of atrial stimulation on cardiac function in patients with an atrial leadless pacemaker—a pilot study

**Winkelbauer L.[1], Saleh K.[1], Reiter C.[1], Wichert-Schmitt B.[1], Rohringer H.[1], Lacher J.[1], Maier J.[1,2], Lambert T.[1], Kellermair J.[1,2], Kammler J.[1], Genger M.[3], Steinwender C.[1,2], Blessberger H.[1,2]**

[1]Department of Cardiology, Kepler University Hospital, Linz, Austria
[2]Clinical Research Institute for Cardiovascular and Metabolic Diseases, Johannes Kepler University, Linz, Austria
[3]Department of Cardiology, LKH Graz West, Graz, Austria

**Introduction:** Leadless pacemakers developed as a valid alternative to conventional pacemakers in selected patients. Long-term data on cardiac function have yet to be evaluated.

**Methods:** In this retrospective study, we enrolled patients who had received an atrial leadless pacemaker with or without a ventricular pacemaker capsule (AVEIR®, Abbott Inc., Chicago, US). Pre- and post-implantation echocardiographic studies had to be available for right/left atrial and ventricular strain analyses. Strain measurements after pacemaker implantation were taken in both sinus rhythm and at an atrial pacing rate that was well above the intrinsic heart rate. All echocardiographic studies were performed with commercially available echo machines (GE Vivid E9, Horton, Norway; Philips Epiq 7, Amsterdam, The Netherlands) and corresponding post-processing software. Discrete variables are presented as counts and percentages, continuous variables as median and interquartile ranges. Statistical analyses were computed with SPSS 30 (IBM, New York, US). *P*-values for differences between timepoints were calculated applying a Wilcoxon signed-rank test.

**Results:** Between September 2022 and July 2025, 6 patients (median age of 79 [66;83] years, 2 females) fulfilled the inclusion criteria. The indications for pacemaker implantation were sick sinus syndrome or intermittent high-degree AV block. Median time between implantation and post implantation echocardiography was 11 (8; 37.5) months. Left atrial reservoir strain (LASr) slightly decreased after implantation (34.7% vs 30.9%)

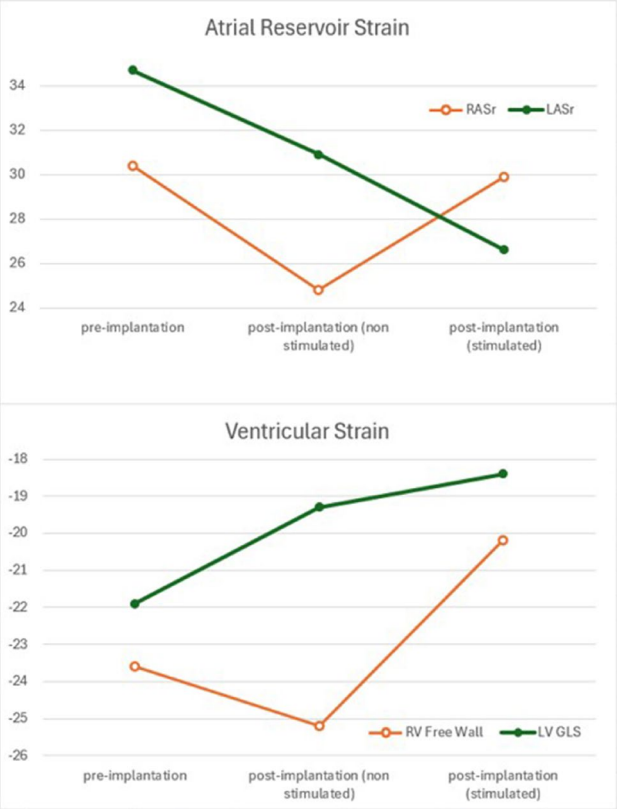


**Fig. 1 | 22-7** Change in atrial reservoir and ventricular strain, pre-, post-stimulation and stimulated

| Table 1: Baseline characteristics | |
|---|---|
| **Parameter** | **N = 6** |
| **Age (years, median, IQR)** | 79 (66; 83) |
| **Sex (N female, %)** | 2 (33%) |
| **NT-proBNP (pg/ml, median, IQR)** | 193.5 (105.4; 431.0) |
| **Troponin T (ng/L, median, IQR)** | 20.4 (11.5; 30.2) |
| **Indication (N, %)** | Sick sinus syndrome: 5 (83%) |
| | Intermittent high-degree AV block: 1 (17%) |
| **Atrial pacemaker capsule only (N, %)** | 4 (67%) |
| **Atrial and ventricular pacemaker capsule (N, %)** | 2 (33%) |

Table 2: Strain parameters pre-, post-implant non- and stimulated

| Parameter | Pre-implant N = 6 | Post-implantat (non-stimulated) N = 6 | P-value (pre- vs. post-implant non stimulated) | Post-implant (stimulated) N = 6 | P-value (stimulated vs. non-stimulated | P-value (pre- vs post-implant stimulated |
|---|---|---|---|---|---|---|
| **RASr (%)** | 30.4 (25.2; 45.4) | 24.8 (16.4; 42.2) | 0.345 | 29.9 (21.8; 40.5) | 0.345 | 0.893 |
| **RAScd (%)** | -25.3 (-33.8; -14.9) | -13.5 (-24.1; -9.3) | 0.5 | -21.2 (-25.6; -12.3) | 0.249 | 0.686 |
| **RASct (%)** | -10.3 (-17.8; -1.5) | -11.2 (-19.2; -6.3) | 0.686 | -12.7 (-18.9; -1.4) | 0.686 | 0.686 |
| **LASr (%)** | 34.7 (30.3; 37.5) | 30.9 (25.0; 37.2) | 0.5 | 26.6 (20.4; 37.1) | 0.249 | 0.345 |
| **LAScd (%)** | -17.5 (-20.8; -16.6) | -14.2 (-20.3; -10.6) | 0.345 | -14.3 (-16.8; -12.3) | 0.600 | 0.138 |
| **LASct (%)** | -17.8 (-18.7; -11.4) | -13.3 (-17.8; -11.0) | 0.225 | -12.3 (-21.8; -8.4) | 0.753 | 0.893 |
| **RV GLS (%)** | -19.4 (-24.5; -8.3) | -19.5 (-23; -16.1) | 0.345 | -17.9 (-21.0; -12.2) | 0.043* | 0.753 |
| **RV FW GLS (%)** | -23.6 (-30; -17.5) | -25.2 (-27.5; -18.9) | 0.500 | -20.2 (-23.3; -15.4) | 0.043* | 0.462 |
| **LV GLS (%)** | -21.9 (-23.8; -21.4) | -19.3 (-22.7; -18.4) | 0.042* | -18.4 (-22.8; -13.9) | 0.463 | 0.116 |

**Fig. 2 | 22-7** Table 1: Baseline characteristics; Table 2: Strain parameters pre-, post-implant non- and stimulated

with a further decline in patients who were actively stimulated (26.6%). A similar pattern—albeit more pronounced—could be observed for right atrial reservoir strain (RASr) that was reduced after implant (30.4% vs 24.8%). However, as opposed to LASr, RASr improved with atrial stimulation (29.9%). Right ventricular free wall global longitudinal strain (GLS) improved after implantation (–23.6% vs –25.2%), but significantly deteriorated when atrial stimulation was present (–20.2%, $p$-value = 0.043). Left ventricular GLS decreased after implantation (–21.9% vs. –19.3%) and continued to decline with atrial stimulation (–18.4%).

**Conclusion:** Atrial contraction patterns, particularly of the right atrium, could be compromised solely due to the weight of the inactive atrial pacemaker capsule and its effect on the atrial geometry. Active atrial stimulation counterbalanced this effect on the RASr but not on the LASr. In addition, atrial pacing led to a deterioration in GLS of the left and right ventricle, which could be explained by altered atrial function, which in turn caused impaired ventricular diastolic filling. Further studies are required to gain more insights into the effects of leadless pacemakers on cardiac function.

## 22-8

## Bidirectional Temporal Association of Device Detected Atrial Fibrillation and Sleep Apnea

**Spitaler P.[1], Bilgeri V.[1], Feuchtner G.[2], Rockenschaub P.[3], Barbieri F.[4], Tugrul B.[1], Adukauskaite A.[1], Stühlinger M.[1], Pfeifer B.[3], Willeit P.[3], Bauer A.[1], Dichtl W.[1]**

[1]Universitätsklinik für Innere Medizin III (Kardiologie), Innsbruck, Austria
[2]Universitätsklinik für Radiologie, Innbruck, Austria
[3]Institut für klinische Epidemiologie, Innsbruck, Austria
[4]Klinik für Kardiologie, Angiologie und Intensivmedizin – Charité, Berlin, Germany

**Introduction:** The relationship between atrial fibrillation (AF) and sleep apnea (SA) is well established, but the temporal direction of this frequently described "chicken-and-egg" association remains uncertain due to the limitations of traditional, episodic diagnostics. Continuous device monitoring was used to examine bidirectional, cross-lagged associations between device-detected AF (DDAF) and severe device-detected sleep apnea (DDSA).

**Methods:** Data were obtained from the prospective ACaSA study in dual-chamber pacemaker patients under continuous remote monitoring. Patients with permanent AF at baseline or < 30 days of follow-up were excluded. Severe DDSA was defined as a respiratory disturbance index (RDI) ≥ 20, and DDAF as ≥ 6 minutes of AF burden. Two multivariable generalized linear mixed-effects models (GLMMs) evaluated day-level temporal associations: Model A (AF → SA) related the previous day's DDAF status to severe DDSA on the subsequent night. Model B (SA → AF) related the current day's nocturnal severe DDSA status to the current day's DDAF status. Both models accounted for the event status from the previous day and adjusted for relevant clinical variables.

**Results:** A total of 93,475 patient-days from 225 patients were analyzed. A DDAF episode on the preceding day was associated with higher odds of severe DDSA on the subsequent night (adjusted OR 2.15; 95% CI 1.96–2.37; $p < 0.001$), independent of the prior day's DDSA status. Conversely, nocturnal severe DDSA

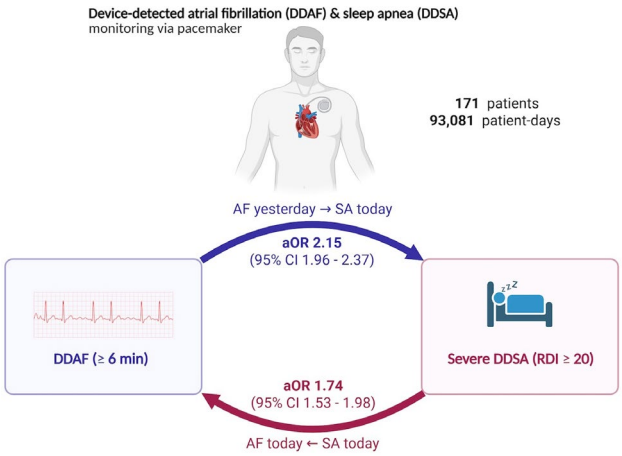


**Fig. 1 | 22-8**

was associated with higher odds of a DDAF episode on the same day (adjusted OR 1.74; 95% CI 1.53–1.98; $p<0.001$), independent of the preceding day's DDAF status.

**Conclusion:** Continuous longitudinal pacemaker monitoring demonstrated bidirectional day-level temporal coupling between DDAF and DDSA. These findings highlight a close dynamic interplay between the two conditions and emphasize the need for integrated, multidisciplinary management.

## 22-9

### Comparison of the Efficacy and Safety of Three Single-Shot Techniques for Atrial Fibrillation Ablation—Retrospective Analysis of 535 Consecutive Patients

**Aboelela A., Simonis G., Scharfe F., Karolyi L., Sayed A., Pu L., Spitzer S., Langbein A.**

Praxisklinik Herz und Gefäße, Dresden, Germany

**Introduction:** Atrial fibrillation (AF) is the most common sustained cardiac arrhythmia and represents a considerable cardiovascular and socioeconomic burden. Pulmonary vein isolation (PVI) using cryoballoon ablation (CBA) is an established therapeutic option. Pulsed field ablation (PFA) is intended to simplify procedures and reduce risks. However, data on its application under real-world clinical conditions remain limited.

**Methods:** Direct comparison of efficacy, safety, and procedural efficiency of three Single-Shot PVI techniques: • CBA (Arctic Front Advance Pro™, Medtronic, Minneapolis, USA) • CBA (POLARx™, Boston Scientific, Massachusetts, USA) • PFA (FARAWAVE™, Boston Scientific, Massachusetts, USA) A total of 535 patients treated consecutively (58.3% male; mean age 68.9 ± 9.4 years) with paroxysmal ($n=231$; 43.2%) or persistent AF ($n=304$; 56.8%) who underwent first-time PVI using CBA or PFA in 2023 were included. Baseline characteristics, procedural parameters (procedure duration, fluoroscopy time, contrast agent use), periprocedural complications, and recurrence rates at 3 and 12 months (24-h Holter ECG) were assessed.

**Results:** Of the 535 patients included in the study, 65.8% underwent ablation using the Arctic Front system, 22.6% with POLARx, and 11.6% with PFA. The median procedure duration was shortest in the PFA group at 51.5 min, which was significantly shorter than in the POLARx group (60.0 min; $p=0.003$) and the Arctic Front group (70.0 min; $p<0.001$). Regarding contrast agent usage, PFA procedures required no contrast, whereas POLARx and Arctic Front used 12 ml and 13 ml, respectively. In terms of safety, no atrioesophageal fistulas or pericardial tamponades were observed in any of the groups. Phrenic nerve palsy occurred exclusively in the cryoballoon groups—3.1% in the Arctic Front group and 4.1% in the POLARx group—while no such complications were seen with PFA. At the 12-month follow-up, there was no significant difference in recurrence-free survival between the three ablation strategies, both in patients with paroxysmal AF (Arctic Front: 82.9%, POLARx: 83.7%, PFA: 80.8%; $p=0.95$) and those with persistent AF (Arctic Front: 60.0%, POLARx: 63.2%, PFA: 61.8%; $p=0.74$).

**Conclusion:** All single-shot PVI techniques investigated demonstrated comparable long-term efficacy and a high safety profile. PFA was associated with shorter procedure times and avoidance of contrast agent. The absence of phrenic nerve palsy in the PFA group highlights the potentially more favorable safety profile of tissue-selective electroporation. The combination of shorter procedure duration and enhanced safety suggests increased procedural efficiency with PFA. Prospective long-term studies are warranted to assess whether these advantages translate into relevant clinical practice implications, such as same-day discharge ablation programs.

# POSTERSITZUNG 23—BASIC SCIENCE 2

## 23-1

### Pressure Overload Drives CaMKIIδC into the Nucleus

**Ajdari A.[1], Matzer I.[1], Kiessling M.[1], Manojlovic V.[2], Masser S.[2], Stelzl U.[2,3], Holzer M.[4], Gindlhuber J.[1], Ljubojevic-Holzer S.[1,3,5]**

[1]Division of Cardiology, Medical University of Graz, Graz, Austria
[2]Institute of Pharmaceutical Sciences, University of Graz, Graz, Austria
[3]BioTechMed-Graz, Graz, Austria
[4]Division of Pharmacology, Otto Loewi Research Center for Vascular Biology, Immunology and Inflammation, Graz, Austria
[5]Gottfried Schatz Research Center, Medical University of Graz, Graz, Austria

**Introduction:** Calcium/calmodulin-dependent protein kinase II δC (CaMKIIδC) is a key regulator of cardiac calcium handling and contractile function. The kinase comprises an *N*-terminal catalytic domain, a regulatory region, and a C-terminal association domain responsible for holoenzyme formation. Although mostly cytoplasmic and lacking a canonical nuclear localization sequence, previous studies have shown that cardiac pressure overload may induce nuclear translocation of CaMKIIδC, contributing to maladaptive cardiac remodeling. This study therefore aims to elucidate the mechanisms regulating CaMKIIδC nuclear import and its contribution to disease progression.

**Methods:** To investigate the mechanisms underlying this translocation, healthy rat hearts were subjected to increased perfusion pressure in a Langendorff perfusion setup. After perfusion, left ventricular tissue was fractionated into subcellular

compartments to assess CaMKIIδ localization under control and pressure overload conditions. To gain deeper insight into the regions critical for CaMKIIδC nuclear translocation, we next performed mass spectrometry on the subcellular fractions. In addition, to explore which part of the enzyme mediates translocation, we generated GFP-tagged full-length and truncated CaMKIIδC constructs (aa 1–316) lacking the C-terminal association domain. These constructs were expressed in H9C2 and HEK293 cells, and fluorescence microscopy was used to analyze their localization under baseline conditions and after ionomycin-induced stress.

**Results:** Analysis of the fractionated tissue revealed a significant pressure overload-dependent nuclear accumulation of CaMKIIδ. Mass spectrometry of the subcellular fractions further identified arginine 260 (R260) as a potential regulatory site involved in nuclear import. Consistent with previous observations, fluorescence microscopy showed that under baseline conditions CaMKIIδC remained predominantly cytoplasmic and translocated to the nucleus only after ionomycin-induced stress. In contrast, under baseline conditions the truncated construct already entered the nucleus, indicating that the critical nuclear import region resides within the *N*-terminal domain and becomes accessible only in the monomeric form.

**Conclusion:** In summary, we have identified that catalytic and/or regulatory regions of CaMKIIδC contain signal for nuclear import which is accessible only in enzyme's monomeric form. This process is stress-dependent, thereby linking nuclear translocation to pathological cardiac remodeling and suggesting CaMKIIδC-nuclear entry as a potential target to limit the progression of adverse cardiac manifestations.

## 23-2

### The Cardiorenal Nexus in ATTR-Amyloidosis: Enhanced Risk Stratification beyond estimated Glomerular filtration ratio(eGFR)

**Eslami M., Ermolaev N., Kösters A., Kronberger C., Schmid L., Poledniczek M., Pahr S., Ahmadi-Fazel D., Rettl R., Kammerlander A., Kastner J., Haslacher H., Badr Eslam R.**

Medical University of Vienna, Vienna, Austria

**Introduction:** Transthyretin amyloid cardiomyopathy (ATTR-CM) staging using the National Amyloidosis Centre (NAC) system relies on NT-proBNP and eGFR levels. However, eGFR is a late marker of renal dysfunction and may miss early structural kidney damage. The heart and kidney form a delicate cardiorenal axis, in which structural damage, as reflected in the urine albumin-to-creatinine ratio (UACR), often precedes a decline in eGFR. Relying solely on eGFR risks misclassifying early-stage ATTR-CM patients as "low risk" despite significant glomerular damage. According to KDIGO 2024 guidelines, comprehensive renal risk assessment requires evaluating both filtration capacity and structural damage.We aimed to evaluate the comprehensive renal burden in an ATTR-CM cohort by assessing the incremental diagnostic value of UACR beyond eGFR in identifying early cardiorenal risk.

**Methods:** A retrospective longitudinal study was conducted in 124 patients with biopsy- or scintigraphy-confirmed transthyretin amyloid cardiomyopathy (ATTR CM). Clinical, biochemical, and renal parameters were collected at baseline and at follow-up visits. Renal structural damage was assessed using the UACR, and renal filtration capacity using the eGFR. The longitudinal cardiorenal correlation between myocardial stress, assessed by NT-proBNP levels, and structural glomerular damage, assessed by UACR, was evaluated. All parameters were assessed at baseline and 12-month follow-up using Spearman's rank correlation, with statistical significance defined as $p < 0.05$.

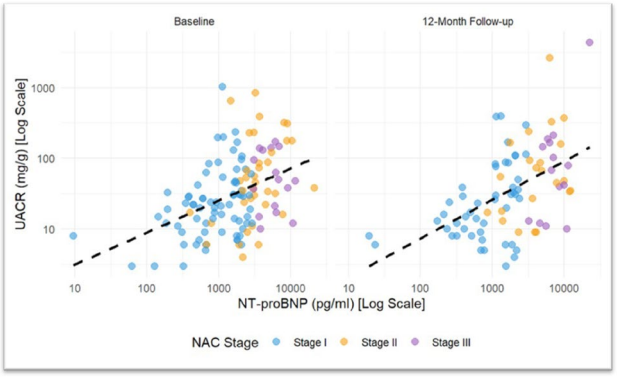


**Fig. 1 | 23-2**

**Results:** The cohort included 124 patients with ATTR-CM (median age 80.2 years, 88.7% male). At baseline, patients had a median eGFR of 61.2 mL/min/1.73 $m^2$ and a median UACR of 18.4 mg/g. The population was distributed across NAC stages I (58%), II (31%), and III (11%), with a median NT-proBNP of 2450 pg/mL. The cross-sectional analysis at baseline demonstrated a continuous, positive correlation between NT-proBNP level and UACR (Spearman's rho = 0.45, $p < 0.001$). As illustrated in Fig. 1, stratification by clinical cardiac severity revealed that while NAC Stage III patients consistently exhibited high UACR, a substantial proportion of clinically "low-risk" NAC Stage I patients also demonstrated significant pathological protein leakage. This visualizes early cardiorenal axis activation, showing that structural kidney compromise often precedes advanced clinical cardiac staging. At 12-month follow-up, the positive longitudinal correlation between NT-proBNP level and UACR remained robust and highly significant (Spearman's rho = 0.50, $p < 0.001$).

**Conclusion:** Relying solely on eGFR in ATTR-CM overlooks early structural kidney damage, which is frequently present even in NAC Stage I patients. These findings highlight the importance of incorporating albuminuria into risk assessment frameworks for ATTR CM.

## 23-3

### αKAP as a potential membrane-anchoring molecule for CaMKIIδ in the heart

**Matzer I.[1], Kiessling M.[1], Gindlhuber J.[1], Ajdari A.[1], Masser S.[2], Stelzl U.[2], Ljubojevic-Holzer S.[3,1,4]**

[1]University Heart Center Graz, Division of Cardiology, Medical University of Graz, Graz, Austria
[2]Institute of Pharmaceutical Sciences, University of Graz, Graz, Austria
[3]BioTechMed-Graz, Graz, Austria
[4]Gottfried Schatz Research Center, Division of Molecular Biology and Biochemistry, Medical University of Graz, Graz, Austria

**Introduction:** Ca2+/Calmodulin-dependent protein kinase II δ (CaMKIIδ) is a key regulator of cardiac excitation-contrac-

tion coupling at membrane sites, but under pathological conditions it relocates into the nucleus, where it promotes maladaptive cardiac remodelling. The molecular mechanisms that anchor CaMKIIδ to cellular membranes—and how these are altered in heart disease—remain poorly understood.

**Methods:** Dahl salt-sensitive rats were fed a high-salt diet (HSD, 8% NaCl) for 5 or 10 weeks to model early and late stages of hypertensive cardiac remodelling. Control animals were fed a low-salt diet (LSD, 0.3% NaCl). To assess the subcellular localisation of CaMKIIδ and identify potential anchoring proteins, we fractionated left-ventricular tissue into cytoplasmic, membrane, nuclear and chromatin fractions and subsequently performed mass spectrometry (TIMS-TOF nano-LC). To validate our data and to get translational insights, we further performed qPCR on rat and human left ventricular tissue.

**Results:** Using the mass-spectrometric analysis, we detected the highest amount of CaMKIIδ in the nuclear fraction of both LSD and HSD-fed animals at the early stage of remodelling. We further detected a substantial amount of the anchoring molecule αKAP, a splice variant of neuronal CaMKIIα, predominantly in the membrane and nuclear fractions. αKAP contains a hydrophobic sequence on the *N*-terminus, which allows stable membrane anchoring. On the C-terminus, it shares the association domain with CaMKIIδ and therefore they are expected to associate in the form of heterododecamers. αKAP has two splice variants, which differ only by the presence or absence of a nuclear localization sequence. An isoform-specific qPCR confirmed the expression of both isoforms in rat and in human hearts. Although we could not detect differences in the expression of αKAP between control and hypertensive animals, we will further test whether post-translational modifications, like CaMKIIδ-phosphorylation, affect the interaction between CaMKIIδ and αKAP.

**Conclusion:** We highlight αKAP as potential CaMKIIδ anchoring mechanism in the heart, which may pave the way for new strategies to prevent CaMKIIδ-mediated maladaptive nuclear signalling in heart disease.

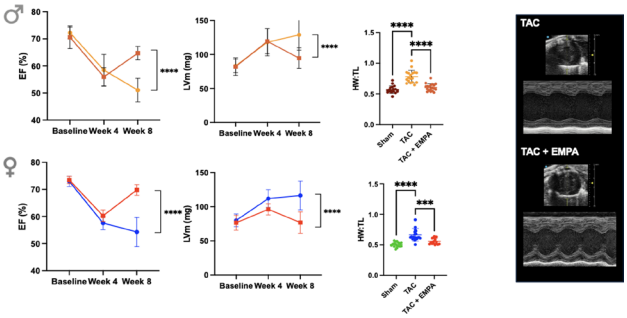


**Fig. 1 | 23-4** LV structure and function

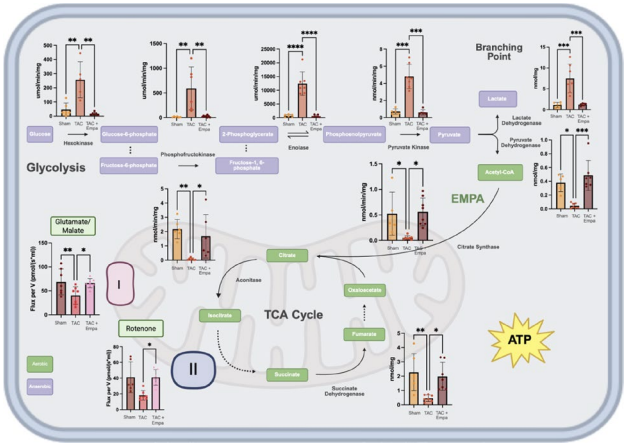


**Fig. 2 | 23-4** Metabolism and mitochondrial respiration

## 23-4

## Empagliflozin promotes reverse remodeling via cardiometabolic reprogramming in established pressure-overload left ventricular hypertrophy

**Ernst M.[1,2], Antunes Gonçalves A.[1], Dostal C.[1], Ye Q.[1,2], Hu C.[1,2], Pokreisz P.[1], Riganti C.[3], Ghigo A.[3], Podesser B.[1,2], Kiss A.[1,2]**

[1]Medizinische Universität Wien, Wien, Austria
[2]Ludwig Boltzmann Institute for Cardiovascular Research, Wien, Austria
[3]University of Turin, Turin, Italy

**Introduction:** Left ventricular hypertrophy (LVH) due to chronic pressure overload is a major precursor of heart failure (HF) and is characterized by metabolic inflexibility and mitochondrial dysfunction. Sodium–glucose cotransporter-2 inhibitors (SGLT2i) improve HF outcomes; however, their myocardial mechanisms in LVH remain incompletely defined. This study investigates whether empagliflozin (EMPA) reverses established LVH and systolic dysfunction delineates the underlying cardiometabolic mechanisms using integrated multi-omics and mitochondrial functional analyses.

**Methods:** Adult male ($n=59$) and female ($n=53$) A/J mice underwent transverse aortic constriction (TAC). Four weeks after surgery—once hypertrophy and systolic dysfunction were established—mice received EMPA (30 mg/kg/day, oral) or vehicle for four weeks. Serial echocardiography and cardiac PET-MRI assessed cardiac structure, function and metabolism. LV-tissue underwent bulk RNA sequencing, untargeted metabolomics, metabolic enzyme activity assays, and high-resolution mitochondrial respirometry. Multi-omics pathway integration identified coordinately regulated metabolic programs.

**Results:** TAC induced marked LVH, increasing LV mass from baseline by 34.8 ± 17.4 mg in males and 31.8 ± 15.9 mg in females (both $p<0.001$), with corresponding reductions in LVEF by 14 ± 5% and 15 ± 2% (both $p<0.001$). This remodeling phenotype was associated with impaired mitochondrial oxidative metabolism and increased glycolytic activity ($p<0.05$). EMPA attenuated hypertrophy versus TAC, reducing heart weight/tibia length in males (0.61 ± 0.06 vs. 0.78 ± 0.10 mg/mm, $p<0.0001$) and females (0.56 ± 0.05 vs. 0.67 ± 0.10 mg/mm, $p<0.001$), and improved LVEF by 9 ± 3% and 10 ± 2%, respectively (both $p<0.0001$). RNA sequencing revealed upregulated oxidative phosphorylation and mitochondrial fatty acid oxidation (both FDR<0.05). Integrated metabolomics and enzyme assays identified fatty acid oxidation as the predominant regulated pathway (FDR<0.05, $p<0.05$), accompanied by increased tricarboxylic acid cycle activity, elevated pyruvate:lactate ratio and reduced glycolytic signatures (all $p<0.05$). High-resolution mitochondrial respirometry confirmed increased complex I- and II-supported respiratory capacity ($p<0.05$), with a more pronounced effect in females despite comparable recovery of systolic function.

**Conclusion:** Empagliflozin promotes reverse remodeling in established pressure-overload LVH by restoring mitochondrial oxidative metabolism through coordinated transcriptional and metabolic reprogramming. These findings provide mechanistic

evidence that SGLT2 inhibition modulates myocardial energetic remodeling and support its role as a disease-modifying strategy in hypertrophic heart disease.

## 23-5

### IL-6 as a Central Mediator of Cardiac and Vascular Complications in Cancer Cachexia

**Antunes Gonçalves A., Qilang Y., Dostal C., Rohdenburg I., Karamali Palangtschi M., Harakaly-Bottka E., Pokreisz P., Podesser B., Koenig X., Kiss A.**

Medical University of Vienna, Vienna, Austria

**Introduction:** Cachexia is a multifactorial metabolic syndrome manifested and driven by substantial loss of lean skeletal muscle mass, often accompanied by adipose tissue depletion that occurs in multiple diseases such as heart failure (HF) and cancer. Elevated circulating levels of pro-inflammatory mediators, including IL 6, IL 1β, TNF α, and GDF 15, play a role driving catabolic pathways in various tissue. Among these, IL-6 has been consistently associated with heart failure severity and poor clinical outcomes; however, its exact role in cancer-related cachexia and its association with cardiac dysfunction remains unknown.

**Methods:** Male BALB/c mice (10–12 weeks old) were inoculated into the right flank with 1×106 cells/100 µL mouse colon-26 carcinoma (C26) or IL6-silenced C26 (C26shIL6) cells, PBS served as control. Cardiac function and body composition (echocardiography and echo-MRI) were assessed at baseline, day 10, and endpoint. At endpoint, organ weights and cardiac tissue wet-to-dry ratios were measured. Vascular endothelial function was evaluated by myography. Multi-organ/tissues molecular fingerprints were assessed by histological, molecular, and biochemical approaches such as proteomic, RNA sequencing, western blot, qPCR and immunofluorescence.

**Results:** C26 tumour-bearing mice developed a cachectic phenotype characterized by loss of fat (4.77 g vs 1.87 g), lean mass (25 g vs 20 g) and marked systemic inflammation, including elevated neutrophil-to-lymphocyte ratio, and increased activated platelets ($p<0.001$) compared to control. Both tumour groups showed trends toward impaired LV systolic and diastolic function at the end-point measurements. Cardiac Bulk RNA sequencing with WebGestal gene enrichment analysis revealed downregulation of mitochondrial function and metabolic processes alongside with upregulation of inflammatory and cell death-related pathways in C26 mice; IL-6 silencing partially normalized these transcriptional alterations. Oroboros respirometry confirmed impaired mitochondrial respiration, with reduced responses to complex I-III stimulation and a significant decrease in OXPHO capacity ($p<0.001$) in cachectic heart. At a protein level, phospho-STAT3, phospho-MLKL, SUMO1, RIPK1, and RIPK3 were significantly ($p<0.001$) increased in C26 hearts. These alterations were partially reversed in the IL-6–silenced group. Endothelial dysfunction was evidenced by a rightward shift in ACh EC50 values (–7.33 vs –6.91, $p<0.001$), increased endothelial activation markers gene expression (*P*-selectin, VCAM-1, ICAM-1) in aorta from C26 mice. Immunofluorescence analysis of CD31 in aortic segments demonstrated a significant reduction in endothelial signal in C26 cachectic mice ($p<0.05$), which was partially restored in C26shIL 6.

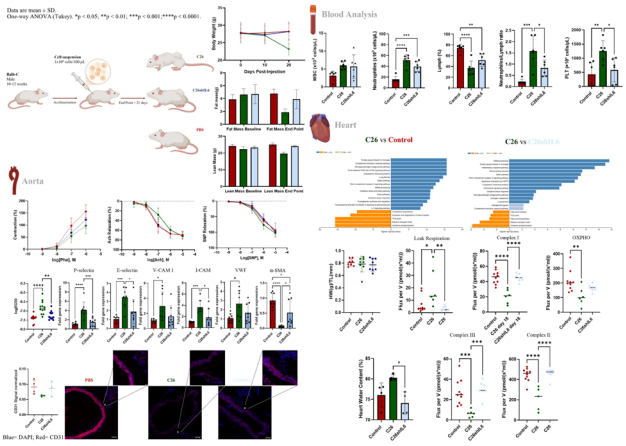


**Fig. 1 | 23-5**

**Conclusion:** Cancer cachexia drives a distinct cardio-oncology phenotype marked by systemic inflammation, peripheral endothelial dysfunction, mitochondrial failure, and necroptotic signalling, culminating in early LV impairment reminiscent of HF. IL-6 links tumour burden to cardiac metabolic remodelling and vascular injury, and its silencing partially reverses transcriptional, bioenergetic, and endothelial alterations, supporting IL-6–targeted strategies in cancer-associated HF.

## 23-6

### Early changes in plasma eicosanoid profiles and oxidized lipids in the course of proprotein convertase subtilisin-kexin type 9 inhibition

**Ondracek A.[1], Hagn G.[2], Galli L.[3], Pöschl A.[1], Seidl V.[1], Resch U.[4], Bileck A.[2], Lang I.[1], Hengstenberg C.[1], Krychtiuk K.[1], Speidl W.[1], Pils D.[5], Gerner C.[2], Distelmaier K.[1], Schrutka L.[1]**

[1]Department of Internal Medicine II, Division of Cardiology, Medical University of Vienna, Wien, Austria
[2]Department of Analytical Chemistry, Faculty of Chemistry, University of Vienna, Wien, Austria
[3]Department of Cardiology, Clinic Landstraße, Vienna Healthcare Group, Wien, Austria
[4]Department of Vascular Biology and Thrombosis Research, Center of Physiology and Pharmacology, Medical University of Vienna, Wien, Austria
[5]Department of General Surgery, Medical University of Vienna, Wien, Austria

**Introduction:** Inhibition of proprotein convertase subtilisin/kexin type 9 (PCSK9) markedly reduces low-density lipoprotein cholesterol (LDL-C) and cardiovascular events; however, residual risk persists. Bioactive lipid mediators derived from polyunsaturated fatty acids, including eicosanoids and oxylipins, regulate inflammation, oxidative stress, and may reflect additional effects of PCSK9 inhibition beyond lipoprotein reduction.

**Methods:** In this prospective, translational single-centre study, plasma samples were collected from 62 patients with atherosclerotic cardiovascular disease and dyslipidaemia before and one and six months after initiation of PCSK9 antibody therapy. Targeted lipidomic profiling was complemented by proteomic, inflammatory and oxidative stress analyses. Longitudinal changes were assessed using paired models with false

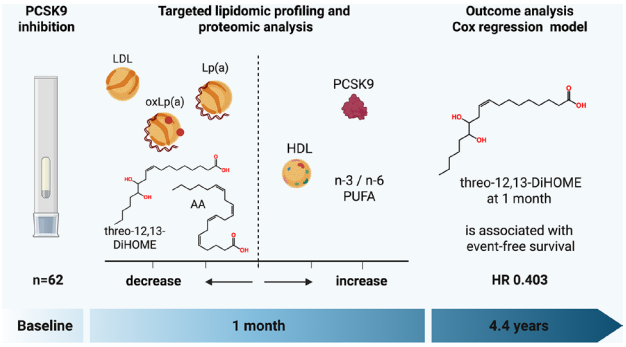


**Fig. 1 | 23-6** Graphical Abstract

discovery rate correction. Lipid mediators demonstrating the largest treatment-induced changes were evaluated for associations with clinical long-term outcomes (all-cause death, acute myocardial infarction, or revascularization) using Cox proportional hazards regression.

**Results:** Targeted lipidomic profiling quantified 62 bioactive fatty acids and eicosanoids. PCSK9 inhibition induced sustained reductions in multiple lipid mediators, including arachidonic acid, hydroperoxyoctadecadienoic acids and the linoleic acid-derived lipokine threo-12,13-dihydroxy-octadecenoic acid (threo-12,13-DiHOME), Changes persisted for up to 6 months and were largely independent of reductions in LDL-C or apolipoprotein B. Markers of lipid peroxidation were significantly reduced, while systemic inflammatory parameters remained low and unchanged. During a median follow-up of 4.4 years, 22% of patients experienced an adverse cardiovascular event. Lower circulating threo-12,13-DiHOME levels at 1 month were independently associated with increased risk of cardiovascular events in multivariable Cox regression models.

**Conclusion:** PCSK9 inhibition is accompanied by coordinated alterations in circulating eicosanoid and oxylipin profiles indicative of modified lipid mediator signaling and reduced oxidative stress. Inter-individual variability in threo-12,13-DiHOME responses may reflect components of residual risk not captured by traditional lipid measures, supporting further investigation of oxylipin profiling for risk stratification in atherosclerotic cardiovascular disease.

## 23-7

### Acute myocardial infarction with low LDL-cholesterol is associated with inflammatory activation of peripheral blood mononuclear cells

**Ondracek A.[1], Hofbauer T.[1], Nechvile J.[1], Kühn S.[1], Seidl V.[1], Häner J.[2], Aszlan A.[1], Artner T.[1], Ueki Y.[2], Losdat S.[3], Spirk D.[4], Hengstenberg C.[1], Koskinas K.[2], Räber L.[2], Lang I.[1]**

[1]Department of Internal Medicine II, Division of Cardiology, Medical University of Vienna, Wien, Austria
[2]Department of Cardiology, Bern University Hospital, University of Bern, Bern, Switzerland
[3]CTU Bern, University of Bern, Bern, Switzerland
[4]Institute of Pharmacology, University of Bern, Bern, Switzerland

**Introduction:** Elevated serum low-density lipoprotein cholesterol (LDL-C) is the most important driver of atherosclerosis and subsequent acute myocardial infarction (AMI). Nevertheless, events occur in individuals without elevated LDL-C, and despite extensive lowering by secondary prevention measures. In recent years, inflammatory mechanisms like inflammasome-driven immune activation have been implicated in plaque progression and destabilization. In this study, we aimed to characterize peripheral blood mononuclear cell (PBMC) activation across different LDL-C concentrations in patients presenting with AMI.

**Methods:** Patients referred to the catheter laboratory for suspected acute myocardial infarction were screened for participation in the PACMAN-AMI trial. Arterial blood was collected from 67 patients from the arterial sheath prior to primary percutaneous coronary intervention (pPCI). Patients were stratified into three groups: statin-naïve patients with LDL-C > 3.2 mmol/L (high LDL-C, $n=34$), statin-naïve patients with LDL-C ≤ 3.2 mmol/L (low LDL-C, $n=23$), and patients receiving chronic statin therapy ($n=10$). PBMCs were isolated for analysis of relative mRNA expression of genes related to pattern recognition (toll-like receptors 4 and 9), inflammasome activation (caspase 1, NLRP3, IL-1b, IL-6), endoplasmatic reticulum stress (X-box protein 1), and clearance (DNase 1-like 3, DNase 1). Data were normalized to a reference gene and presented relative to the mean of all samples.

**Results:** Of 291 screened patients, 241 received pPCI for treatment of AMI. About 58% of patients presented with LDL-C serum concentrations below 3.2 mmol/L, but only 30% of these patients had already been on statins. Isolated PBMCs from statin-naïve patients with low LDL-C serum levels showed significantly higher expression of NLRP3, caspase-1, and IL-6 than PBMCs from patients with high LDL. Moreover, relative expression of DNase 1-like 3 and DNase 1 was about 4-fold higher in the low LDL group as compared to the high LDL group. X-box protein-1 and toll-like receptor 4 transcription were markedly upregulated under low LDL compared to high LDL, while only expression of toll-like receptor 9 was comparable between the groups.

**Conclusion:** Inflammatory activation of circulating monocytes and lymphocytes is more prominent in AMI patients without elevated LDL-C levels highlighting drivers of atherosclerosis beyond LDL-C.

## 23-8

### High LDL-cholesterol is associated with a NET-prone neutrophil phenotype in patients presenting with acute myocardial infarction

**Ondracek A.[1], Hofbauer T.[1], Nechvile J.[1], Kühn S.[1], Seidl V.[1], Häner J.[2], Aszlan A.[1], Artner T.[1], Ueki Y.[2], Losdat S.[3], Spirk D.[4], Hengstenberg C.[1], Koskinas K.[2], Räber L.[2], Lang I.[1]**

[1]Department of Internal Medicine II, Division of Cardiology, Medical University of Vienna, Wien, Austria
[2]Department of Cardiology, Bern University Hospital, University of Bern, Bern, Switzerland
[3]CTU Bern, University of Bern, Bern, Switzerland
[4]Institute of Pharmacology, University of Bern, Bern, Switzerland

**Introduction:** Elevated low-density lipoprotein cholesterol (LDL-C) has been linked to neutrophil activation and impaired DNase activity. Neutrophil extracellular traps (NETs) formed by activated neutrophils have been recognized as drivers of atherosclerosis and atherothrombosis. However, how circulating

LDL-C levels shape leukocyte activation patterns during acute myocardial infarction (AMI) remains incompletely understood.

**Methods:** We studied 67 patients screened for participation in the PACMAN-AMI trial. Arterial blood was collected at the time of infarction from the arterial sheath prior to percutaneous coronary intervention. Patients were stratified into three groups: statin-naïve patients with LDL-C > 3.2 mmol/L (high LDL-C, $n = 34$), statin-naïve patients with LDL-C ≤ 3.2 mmol/L (normal LDL-C, $n = 23$), and patients receiving chronic statin therapy ($n = 10$). Plasma markers of NET formation i. e. double-stranded DNA (dsDNA), citrullinated histone H3 (citH3), neutrophil elastase (NE), and myeloperoxidase (MPO), as well as DNase activity were measured. Neutrophils were isolated for analysis of relative mRNA expression of genes related to inflammation, ER stress, and cholesterol metabolism. Neutrophil CD62L, CXCR4, and lipid receptor expression were assessed by flow cytometry.

**Results:** Patients with LDL-C > 3.2 mmol/L exhibited markedly higher circulating levels of dsDNA, NE, and MPO than those with normal LDL-C. Neutrophil surface expression of the LDL-receptor and the oxidized LDL-receptor LOX-1 were downregulated under high LDL-C levels. Across all groups, LDL-C correlated positively with dsDNA ($rs = 0.434$, $p < 0.001$) and inversely with neutrophil LDL receptor ($rs = -0.498$, $p < 0.001$) and LOX-1 expression ($rs = -0.474$, $p < 0.001$). The homing receptor CXCR4, and CD62L were lower on neutrophils from patients with high LDL-C. Moreover, neutrophils from patients with high LDL-C serum concentrations demonstrated significantly higher expression of genes involved in cholesterol metabolism and NET formation, including proprotein convertase subtilisin/kexin type 9 (PCSK9), 3-hydroxy-3-methylglutaryl-CoA reductase (HMGCR), NLRP3 and peptidyl-arginin deiminase 4 (PAD4), and their expression correlated positivley with LDL-C levels.

**Conclusion:** These results show that elevated LDL-C serum concentrations are associated with upregulation of cholesterol-metabolism pathways in neutrophils potentially enhancing their capacity to undergo NET formation.

# POSTERSITZUNG 24—CLINICAL CASES 4

## 24-1

### Overcoming a Diagnostic Barrier: Right Ventricular Thrombus Aspiration Prior to Endomyocardial Biopsy in Impella-Supported Fulminant Myocarditis

**Haider P., Gerges C., Hengstenberg C., Hofbauer T., Richter B., Hemetsberger R., Zilberszac R., Lenz M.**

Medical University of Vienna, Wien, Austria

**Introduction:** Fulminant myocarditis is a life-threatening presentation of inflammatory myopericardial syndrome (IMPS) with hemodynamic instability requiring inotropes or mechanical circulatory support (MCS). Contemporary ESC guidelines emphasizes rapid risk stratification and early endomyocardial biopsy (EMB) in high-risk cases, including patients on temporary MCS, because histology can identify the subtype and trigger time-critical, targeted therapy. In practice, EMB may be constrained by the configuration of MCS and by intracardiac thrombus burden, which can obstruct access to the biopsy target. We present a patient with fulminant myocarditis supported with left-sided Impella in whom extensive right-ventricular thrombi prevented safe EMB until catheter-based thrombus aspiration enabled tissue sampling.

**Methods:** A 55-year-old man was transferred for hemodynamic support for suspected fulminant myocarditis to our cardiac intensive care unit at a tertiary university hospital. Prior work-up included coronary angiography excluding obstructive coronary artery disease, cardiac MRI showing active myocardial inflammation, and echocardiography with severely reduced biventricular function and two large right-ventricular (RV) thrombi as well as a venous thrombosis of the left jugular vein. Owing to deteriorating perfusion with rising lactate, oligu-anuria and malignant ventricular ectopy, an Impella CP was implanted (left ventricle). Because left-sided tMCS limited biopsy options, EMB was planned from the right heart. Because RV thrombus burden precluded straightforward biopsy, percutaneous catheter-based aspiration of the RV thrombi was performed before EMB using the Penumbra Lightning 12 device. To facilitate complete removal and provide maximum procedural safety, the procedure was performed using transesophageal echocardiographic guiding. ICU management included invasive ventilation/sedation, vasoactive support and later escalation to VA-ECMO with ongoing Impella support (ECMELLA), plus hemofiltration for persistent anuria. Microbiological sampling revealed multiple infections needing broad antimicrobial/antifungal therapy.

**Results:** Despite inotropes, the patient developed progressive shock with lactate levels up to 5.7 mmol/L, low cardiac output and worsening renal failure. After thrombus aspiration, histologic workup of the EMB confirmed lymphocytic myocarditis. He was evaluated for heart transplantation and listed nationally. During the course of stay, a large retroperitoneal hematoma became apparent with peri-arrest requiring massive transfusion and escalation to VA-ECMO. Further, the Impella support continued for left ventricular venting (ECMELLA). Despite maximum of mechanical support, sustained multiorgan failure evolved: persistent anuria requiring hemofiltration, cholestatic liver dysfunction with direct hyperbilirubinemia (peak 13.3 mg/dL), thrombocytopenia and intermittent bleeding at cannulation sites. Inflammatory activity remained high (CRP 30–40 mg/dL; IL-6 up to 4900 pg/mL) despite broad antimicrobial/antifungal therapy. Microbiological samples revealed Proteus spp. in blood culture, Enterococcus faecium from groin and Staphylococcus epidermidis from central access. Subsequently the catecholamine requirements rose again with lactate increase. The patient died at our intensive care unit despite maximal vasoactive support, ECMO and Impella.

**Conclusion:** ESC guidance for IMPS highlights early EMB in high-risk/fulminant myocarditis, even under temporary MCS, to enable subtype-directed management. This case demonstrates that extensive RV thrombus burden can be a practical barrier to EMB when RV sampling is the only feasible route during left-sided tMCS. Catheter-based aspiration thrombectomy enabled subsequent RV biopsy and histological confirmation of lymphocytic myocarditis. Current reports mainly describe vacuum/aspiration systems for therapeutic removal of right-heart thrombi or masses; we found no readily identifiable PubMed-indexed case describing thrombus aspiration performed specifically to enable EMB in fulminant myocarditis. Recognition of such technical obstacles, and multidisciplinary planning of aspiration-assisted EMB, may broaden access to guideline-recommended diagnostics in unstable myocarditis patients.

## 24-2

### Perioperative management of antithrombotic therapy after acute coronary syndrome: competing risks of bleeding and thrombosis

**Gelbenegger G.[1], Heinz G.[2], Zilberszac R.[2]**

[1]Department of Clinical Pharmacology, Medical University of Vienna, Wien, Austria
[2]Department of Medicine II, Division of Cardiology, Medical University of Vienna, Wien, Austria

**Introduction:** Managing antithrombotic therapy in patients with recent drug-eluting stent implantation who require urgent high-risk non-cardiac surgery is clinically challenging, particularly when competing risks of thrombosis and bleeding coexist. Patients who underwent very recent coronary drug-eluting stent implantation require uninterrupted platelet inhibition to prevent early stent thrombosis. Conversely, patients with unstable spinal fractures complicated by paraplegia require urgent surgical stabilization to avert further neurological deterioration, alleviate pain, and reduce complications related to prolonged immobilization. When these competing priorities collide, a profound therapeutic dilemma arises between maintaining ischemic protection and minimizing perioperative bleeding risk. A 74-year-old woman with a history of recurrent venous thromboembolism suffered cardiac arrest shortly after elective knee arthroplasty. Following successful cardiopulmonary resuscitation, percutaneous coronary intervention with drug-eluting stent implantation to the right coronary artery was performed. Triple antithrombotic therapy with aspirin, ticagrelor and unfractionated heparin was initiated. After stabilization, the patient developed paraplegia caused by an unstable lumbar spine fracture, necessitating urgent surgical intervention.

**Methods:** To mitigate bleeding risk while maintaining a sustainable triple antithrombotic treatment regimen, ticagrelor was de-escalated to clopidogrel. Aspirin was discontinued after one week and the patient remained on treatment with clopidogrel and unfractionated heparin. Perioperative antiplatelet bridging was managed with the intravenous P2Y12 inhibitor cangrelor. To guide antiplatelet bridging, platelet function testing was performed using multiple electrode aggregometry. Clopidogrel was discontinued and platelet function testing was performed 12-hourly. Once levels of more than 46 U (suggesting recovered platelet function) were measured, cangrelor was initiated. Cangrelor was given as a continuous infusion with a dosing regimen of 0.75 µg/kg per minute. Cangrelor was discontinued 2 hours before surgery to allow for timely recovery of platelet function. Unfractionated heparin was monitored using activated partial thromboplastin time and anti-factor Xa levels (target anti-factor Xa level of 0.2–0.4 IU/mL) and discontinued 2 hours before surgery. The timeline of antithrombotic treatment prior to surgery is shown in Fig. 1.

**Results:** Intraoperative hemodynamic and respiratory deterioration led to sharply rising ventilatory requirements and high-dose treatment with catecholamines to maintain adequate oxygenation and perfusion. Upon ICU readmission, the patient was in refractory shock, receiving high-dose continuous infusions of epinephrine and norepinephrine. Transthoracic echocardiography revealed a massively dilated right ventricle with severely impaired systolic function and severe tricuspid regurgitation, highly consistent with an acute, hemodynamically relevant pulmonary embolism. Duplex ultrasound demonstrated a long, non-compressible thrombus of the right femoral vein with echogenic material. A computed tomography scan

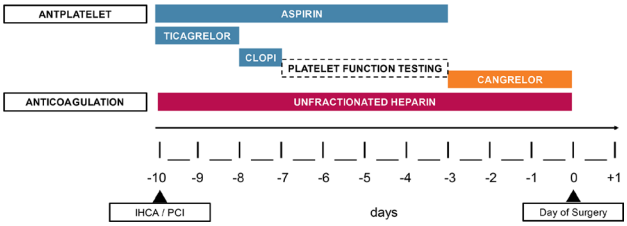


**Fig. 1 | 24-2** Timeline of antithrombotic therapy

was deemed impracticable because of ongoing hemodynamic and respiratory compromise. Diffuse, uncontrollable bleeding ensued—from mouth and nose, catheter insertion sites, and the lumbar surgical site. Disseminated intravascular coagulation (DIC) was suspected, with rising DIC scores of 5 (on ICU readmission), to 8 (at 8 hours after ICU readmission). Despite massive transfusions and hemostatic support, the patient died within 24 hours after surgery.

**Conclusion:** Vertebral fractures and spinal injury are a rare but severe complication of CPR.

Balancing ischemic protection against bleeding risk in the context of urgent non-cardiac surgery after recent PCI remains a major clinical challenge and requires individualized, multidisciplinary decision-making.

While not routinely recommended, cangrelor may be used a bridging strategy in high ischemic risk patients who require continuous, uninterrupted P2Y12 blockade before surgery.

## 24-3

### Impending paradoxical embolism

**Schauperl M.**

3. Medizinische Abteilung mit Kardiologie, Klinik Ottakring, Wien, Austria

**Introduction:** Thrombus in transit is a rare but highly hazardous manifestation in patients with pulmonary embolism. In particular, thrombus entrapment in a patent foramen ovale (PFO), representing an impending paradoxical embolism (IPDE), is associated with an extremely high risk of systemic embolization and increased mortality, constituting a true therapeutic emergency.

**Methods:** Diagnostic work-up included computed tomography pulmonary angiography followed by repeat transthoracic and transesophageal echocardiography for detailed intracardiac thrombus characterization and assessment of right ventricular function. Treatment strategy was determined by an interdisciplinary team based on imaging findings and estimated risk of systemic embolization. Emergent surgical thrombectomy was selected as definitive treatment approach.

**Results:** We report the case of a 59-year-old female admitted via emergency medical services due to acute dyspnea. Computed tomography demonstrated bilateral central pulmonary embolism with a saddle thrombus. Transthoracic echocardiography revealed signs of acute right ventricular strain and raised strong suspicion of a thrombus in transit within the right atrium, which, in retrospect, was also detectable on CT imaging. Subsequent transesophageal echocardiography, performed to evaluate the feasibility of mechanical thrombectomy, demonstrated a large thrombus in transit entrapped within a patent foramen ovale, with a substantial portion protruding into the left atrium, indicating imminent risk of systemic embolization. Given this high-risk finding, immediate interdisciplinary decision-making

was performed, and the patient was transferred for emergent surgical thrombectomy. The intracardiac thrombus was completely removed without thromboembolic complications. Postoperative recovery was uneventful with excellent clinical outcome.

**Conclusion:** This case highlights the pivotal role of early transesophageal echocardiography in suspected thrombus in transit. Detection of thrombus entrapment within a PFO defines an immediately life-threatening condition requiring urgent multidisciplinary therapeutic decision-making. Surgical thrombectomy represents an effective and potentially life-saving treatment strategy in this clinical scenario to prevent catastrophic systemic embolic events.

## 24-4

### Precision Management of Complex Aortic Pathology: Two Cases Demonstrating Individualised Surgical and Endovascular Approaches

**Hannover A., Mahr S., Dumfarth J., Ehrlich M., Funovics M., Zimpfer D., Stelzmüller M.**

Medizinische Universität Wien, Wien, Austria

**Introduction:** Complex aortic diseases require highly individualised therapeutic strategies due to anatomical variability, progressive disease patterns, the presence of Heritable Thoracic Aortic Disease (HTAD), and patient-specific risk profiles. Contemporary treatment approaches increasingly integrate tailored combinations of open surgical and endovascular techniques to achieve durable outcomes in these challenging cases.

**Methods:** We present two cases illustrating individualized management strategies for complex aortic disease. The first case concerns a 28-year-old male with genetically confirmed Loeys-Dietz Syndrome who developed progressive aortic disease over several years. Initial treatment was performed at another hospital, where the patient underwent ascending aortic replacement for acute aortic dissection type A in 2009, followed by total arch replacement with implantation of a frozen elephant trunk prosthesis and supra-aortic vessel transposition in 2010. Due to progression of a chronic aortic dissection type B, endovascular stent-graft extension was performed in 2018, also at another hospital, which was complicated by a stent-induced new entry tear. In 2019, the patient presented to our center with severe thoracic pain and rapid expansion of the false lumen, raising suspicion of a contained rupture and associated visceral malperfusion. The second case describes a 72-year-old female with arterial hypertension in whom a thoracoabdominal aneurysm was incidentally detected during abdominal ultrasound. Subsequent computed tomography angiography revealed a thoracoabdominal aneurysm with a maximum diameter of 6.9 cm (Crawford type II), accompanied by renal artery stenosis and chronic occlusion of the celiac trunk.

**Results:** Both patients were treated using individualized, staged strategies tailored to their anatomy, underlying genetic tissue disorder, and clinical presentation. In the first patient with heritable thoracic aortic disease (HTAD), definitive management required open thoracoabdominal aortic replacement. Emergency thoracoabdominal aortic replacement (Crawford type I) was performed under deep hypothermic circulatory arrest. The procedure was initially successful; however, during the postoperative course the patient developed rupture of the intercostal patch reimplanted into the aortic prosthesis, requiring emergency thoracic endovascular aortic repair (TEVAR). The patient recovered without neurological complications. During subsequent follow-up, progressive dilatation of the native aortic root necessitated mechanical Bentall root replacement in 2025. In contrast, the second patient underwent complete endovascular extension of the frozen elephant trunk to the infrarenal aorta using a branched endograft. A staged hybrid treatment strategy was applied, consisting of total arch replacement with frozen elephant trunk implantation, followed by thoracoabdominal endovascular repair using an off-the-shelf branched endograft with bridging stent grafts to the visceral arteries. Follow-up imaging demonstrated stable aortic reconstruction without significant progression of the treated segments.

**Conclusion:** These cases highlight the importance of personalised treatment strategies in complex aortic disease. Tailored combinations of open surgical and advanced endovascular techniques enable effective management of anatomically challenging aortic pathologies while addressing the individual needs and risks of each patient. They further emphasise the value of multidisciplinary decision-making and staged treatment concepts in achieving stable long-term outcomes.

## 24-5

### Transcatheter Edge-to-edge Repair of the Mitral and Tricuspid Valve Through a 15 Years Prior Implanted Inferior Vena Cava Filter

**Punzengruber G., Danninger K., Alberer M., Binder R.**

Department of Cardiology, Klinikum Wels-Grieskirchen, Wels, Austria

**Introduction:** This case report details the management of an 81-year-old female patient with an implanted inferior vena cava (IVC) filter, who underwent a combined Mitral Transcatheter Edge-to-Edge Repair (M-TEER) and Tricuspid Transcatheter Edge-to-Edge Repair (T-TEER) procedure. The patient, with a history of heart failure with reduced ejection fraction and severe secondary mitral and tricuspid regurgitation, presented

**Fig. 1 | 24-5** Final documention of 2 implanted Tri-Clips und 1 Mitra-Clip

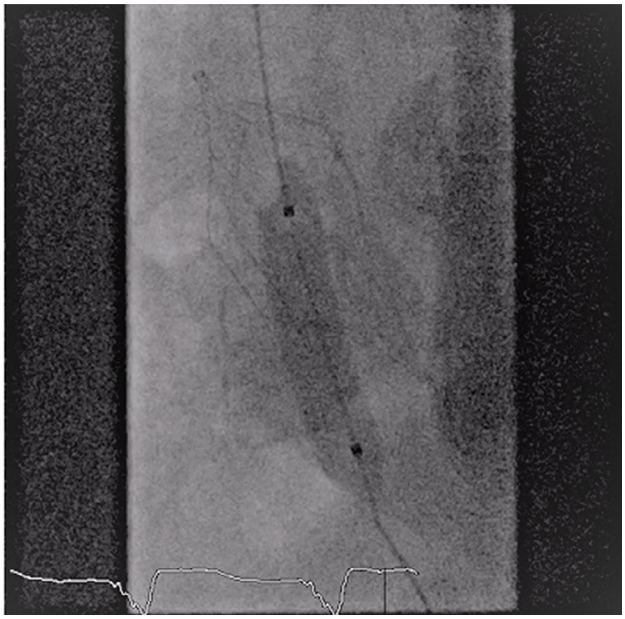

**Fig. 2 | 24-5** Inflated 10 mm PTA Ballon showing correct placement of the wire through the larger IVC orifices

with persistent heart failure symptoms (NYHA II-III) despite maximal tolerated doses of guideline directed medical therapy.

**Methods:** A significant challenge in her case was navigating an IVC filter, implanted more than a decade earlier, prior to a spine surgery after having suffered from 2 pulmonary embolisms, in order to advance the delivery system for both valve interventions. The Cordis OptEase Filter, positioned in the IVC, posed a potential obstruction for the device delivery system required for the transcatheter procedures. Visualized with computed tomography, due to the tilted position of the filter, with the cranial tip positioned anteriorly, it was possible to maneuver the guidewire through the larger orifices of the filter using a Judkins Right catheter.

**Results:** By inflation of a 10 mm PTA balloon in the filter, the correct placement of the wire was ensured and the track dilated. Subsequently, the advancement of the TEER delivery systems posed no challenge with successful placement of 1 Mitra-Clip and 2 Tri-Clip devices.

**Conclusion:** This case highlights the possibility of performing a TEER procedure in patients with an implanted IVC Filter. Through careful planning and advanced imaging techniques, the procedure was successfully carried out without complications and with anticipated procedural success.

## 24-6

## Erstmalige LVAD-Implantation nach Tendyne™-TMVR—Fallbericht

**Schachner B.[1], Reiter C.[2], Meledeth C.[2], Steinwender C.[2], Zierer A.[1]**

[1]Kepler Universitätsklinikum Linz – Universitätsklinik für Herz-, Gefäß- und Thoraxchirurgie – Medizinische Fakultät der JKU Linz, Linz, Österreich
[2]Kepler Universitätsklinikum Linz – Interne 1 – Kardiologie und Internistische Intensivmedizin – Medizinische Fakultät der JKU Linz, Linz, Österreich

**Einleitung:** Einleitung: Der transkatheter Mitralklappenersatz (TMVR) mit dem Tendyne™-System ist eine Therapieoption bei schwerer Mitralinsuffizienz. Daten zur späteren Implantation eines dauerhaften linksventrikulären Unterstützungssystems (LVAD) in dieser Patientengruppe sind bislang nicht vorliegend. Wir berichten über die erste Implantation eines HeartMate 3™ LVAD nach vorangegangenem Tendyne™-TMVR.

**Methoden:** Fallbeschreibung: Ein 68-jähriger Patient mit ischämischer Kardiomyopathie unterzog sich 2020 einer dringlichen Bypassoperation. Bei progredienter Herzinsuffizienz mit stark reduzierter linker Ventrikelfunktion (LVEF) und ausgeprägter Dilatation entwickelte sich eine schwere sekundäre Mitralklappeninsuffizienz. 2021 erfolgte ein TMVR mit dem Tendyne™-System mit klinischer Stabilisierung. 2025 kam es zur erneuten Dekompensation (NYHA IV). Trotz optimaler medikamentöser Therapie bestand eine terminale Herzinsuffizi-

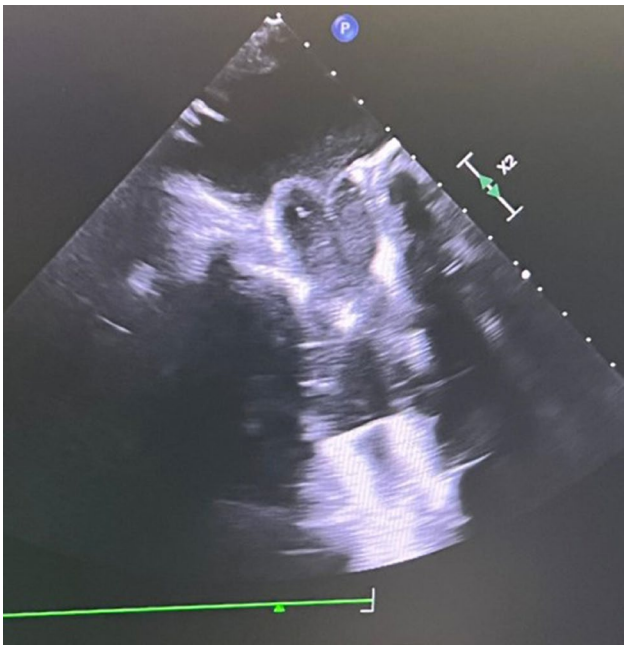

**Abb. 1 | 24-6** Intraoperatives Echo nach LVAD Implantation

**Abb. 2 | 24-6** Postoperatives CT mit Tendyne und HeartMate 3

enz mit LVEF ~10 %. Eine Herztransplantation wurde erwogen, jedoch vom Patienten abgelehnt. Es erfolgte die Indikationsstellung zur LVAD-Implantation als Destination Therapy im interdisziplinären Herzinsuffizienz Team.

**Resultate:** Operatives Vorgehen und perioperativer Verlauf: Nach umfassender präoperativer Bildgebung (TTE, TEE, CT) zur Beurteilung der linksventrikulären Geometrie und der Beziehung zwischen Mitralklappenprothese und geplanter LVAD-Zuflusskanüle erfolgte im Dezember 2025 die Implantation. Nach etablieren des kardiopulmonalem Bypass erfolgte die Resternotomie. Zunächst wurde die Stabilität der Tendyne™-Prothese durch manuelle Kompression des linken Ventrikels unter echokardiographischer Kontrolle geprüft. Nach Bestätigung der sicheren Verankerung wurde das apikale Haltesystem sorgfältig entfernt. Anschließend wurde das HeartMate 3™ regelgerecht am Apex implantiert. Die intraoperative TEE zeigte eine korrekte Lage der Inflow Kanüle und stabile Prothesenfunktion ohne Obstruktion. Postoperativ war eine einmalige Revision bei Blutung erforderlich. Danach stabilisierte sich der Patient rasch mit Verbesserung der Hämodynamik und Endorganfunktion. Die Verlegung auf die Normalstation erfolgte am 7. postoperativen Tag. Am 28. Tag wurde der Patient in stabilem Zustand in eine kardiologische Rehabilitation entlassen.

**Schlussfolgerungen:** Schlussfolgerung Die LVAD-Implantation nach Tendyne™-TMVR ist technisch machbar und bei sorgfältiger Planung sicher durchführbar. Entscheidend sind präzise präoperative Bildgebung, strukturierte intraoperative Evaluation der Prothesenstabilität sowie exakte Positionierung der Zuflusskanüle. Mit zunehmender Anwendung transkatheter Mitralklappentherapien wird die Zahl potenzieller LVAD-Kandidaten nach TMVR steigen. Eine vorausschauende interdisziplinäre Herzteam-Strategie ist essenziell, um zukünftige Therapieoptionen bei terminaler Herzinsuffizienz zu sichern.

## 24-7

## Aortenwurzelabszess nach biologischem Aortenklappenersatz

**Auer J., Schönegger N., Muhr T., Genger M.**

LKH Graz II, Standort West, Graz, Österreich

**Einleitung:** Der Aortenwurzelabszess stellt eine seltene, jedoch lebensbedrohliche Komplikation der infektiösen Endokarditis dar, insbesondere im Kontext einer Prothesenklappenendokarditis. Aktuelle Literatur zeigt, dass das Vorliegen eines Aortenwurzelabszesses die Mortalität bei Prothesenendokarditis etwa verdoppelt. Die perivalvuläre Ausbreitung der Infektion ist Ausdruck eines destruktiven Krankheitsverlaufs und mit einer deutlich ungünstigeren Prognose assoziiert.

**Methoden:** Eine 74-jährige Patientin stellte sich letzten Herbst mit seit mehreren Wochen progredienter Dyspnoe und nächtlichen Schweißausbrüchen in unserer internistischen Notaufnahme vor. Anamnestisch bestand ein Zustand nach chirurgischem biologischen Aortenklappenersatz vor 20 Monaten bei hochgradiger Aortenklappenstenose. Eine in der Notaufnahme durchgeführte PAE-CT verblieb ohne Hinweis Infiltrate, im Aufnahme EKG ließ sich ein neu aufgetretener langer AV-Block I° (PQ 312 ms) objektivieren. Bei Aufnahme präsentierte sich die Patientin in septischem Zustandsbild mit einem Laktat von 3 mmol/l und einer, trotz adäquaten Volumensubstitution, persistierenden Hypotonie (MAP < 65 mmHg), sodass die Patientin auf der ICU aufgenommen wurde. Eine empirische antibiotische Therapie mit Ceftriaxon und Daptomycin wurde etabliert, überdies erfolgte bei persistierender Hypotonie die Gabe von Katecholaminen und periphere Blutkulturen wurden abgenommen. Im Sinne der septischen Herdsuche wurde bei bekanntem AKE eine TEE durchgeführt, in welcher sich der dringende Verdacht auf einen paravalvulären Abszess im Bereich der biologischen Aortenklappenprothese stellte. Es erfolgte die umgehende herzchirurgische Kontaktaufnahme zur Übernahme und dringlichen operativen Sanierung. Im Verlauf kam es zum Auftreten einer Sinusbradykardie mit nachfolgender *p*-Wellen Asystolie, welche in einer Asystolie terminierte. Es erfolgte die umgehende prolongierte kardiopulmonale Reanimation, welche frustran verlief.

**Resultate:** Im Falle dieser Patientin konnte im Rahmen der Obduktion ein ausgedehnter Aortenwurzelabszess als septischer Fokus bei Zustand nach biologischem Aortenklappenersatz verifiziert werden, im Abstrich der Aortenklappenprothese ließen sich post mortem die Keime Escherichia coli und Streptococcus galacticae nachweisen. Besonders die Infektion der Aortenklappe kann zur Bildung eines Aortenwurzelabszesses führen, welcher eine ausgedehnte chirurgische Sanierung bis hin zum kompletten Ersatz der Aortenwurzel notwendig machen kann [1, 2, 3]. Perivalvuläre Abszesse treten bei etwa 7,5 % der Patienten mit nativer und bei 14 % mit prothetischer Aortenklappe auf [2]. Zu den häufigsten Erregern zählen Staphylococcus aureus sowie koagulase-negative Staphylokokken sowie Streptokokken [6]. Diagnostisch sind neben der klinischen Untersuchung und Bakteriämie insbesondere bildgebende Verfahren, vor allem die Echokardiographie (transthorakal/transösophageal) als auch die CT und PET-CT von zentraler Bedeutung [5]. Ein neu aufgetretener AV-Block gilt als klinischer Warnhinweis für eine perivalvuläre Ausbreitung mit möglicher Abszessbildung [7]. Gemäß aktuellen Guidelines stellt die unverzügliche chirurgische Sanierung mit Aortenwurzelersatz den therapeutischen Goldstandard bei perivalvulären Komplikationen dar [3, 4, 8]. Die chirurgische Therapie sollte durch eine keimspezifische sechswöchige intravenöse Antibiotikatherapie ergänzt werden [8].

**Schlussfolgerungen:** Der Aortenwurzelabszess nach biologischem Aortenklappenersatz ist eine prognostisch hochrelevante Komplikation der Prothesenklappenendokarditis. Entsprechend den aktuellen Leitlinien erfordert diese Konstellation eine rasche, interdisziplinär abgestimmte Diagnostik und frühzeitige chirurgische Sanierung in Kombination mit einer prolongierten, gezielten Antibiotikatherapie. Ein neu aufgetretener AV-Block sollte bei V. a. eine infektiöse Endokarditis der Aortenklappe immer als Warnsignal für eine mögliche Abszessbildung angesehen und die frühzeitige Versorgung mittels passagerem Schrittmacher angestrebt werden.

### Literatur

1. Imran A, Quarrell A, Edhem L, Eni G, Ahmed A, Solano J. Prosthetic Valve Endocarditis and Aortic Root Abscess: A Case of High-Risk Infection. Cureus. 2025;11;17(4):e82063. Apr.
2. Yang B, et al. Root abscess in the setting of infectious endocarditis: Short- and long-term outcomes. J Thorac Cardiovasc Surg.162(4):1049–1059.e1.
3. Haidari Z, Knipp S, Turaev I, El Gabry M. Aortic Valve Infective Endocarditis with Root Abscess: Root Repair Versus Root Replacement. Pathogens. 2025;14:626.
4. Elderia A, Wallau A-M, Bennour W, Gerfer S, Gaisendrees C, Krasivskyi I, Djordjevic I, Wahlers T, Weber C. Impact of Aortic Root Abscess on Surgical Outcomes of Infective Endocarditis. Life. 2024;14:92.
5. Erba PA, Lancellotti P, Vilacosta I, Gaemperli O, Rouzet F, Hacker M, Signore A, Slart RHJA, Habib G. Recommendations on nuclear and multimodality imaging in IE and CIED

infections. Eur J Nucl Med Mol Imaging. 2018;45(10):1795–815. Sep.
6. Murdoch DR, Corey GR, Hoen B, Miró JM, Fowler VG Jr, Bayer AS, Karchmer AW, Olaison L, Pappas PA, Moreillon P, Chambers ST, Chu VH, Falcó V, Holland DJ, Jones P, Klein JL, Raymond NJ, Read KM, Tripodi MF, Utili R, Wang A, Woods CW, Cabell CH, International Collaboration on Endocarditis-Prospective Cohort Study (ICE-PCS) Investigators.. Clinical presentation, etiology, and outcome of infective endocarditis in the 21st century: the International Collaboration on Endocarditis-Prospective Cohort Study. Arch Intern Med. 2009;9;169(5):463–73. Mar.
7. Patel M, Grotton C, Ravi S, Benson S, Soni RG. First-Degree Heart Block: The Guiding Light to Discovering an Aortic Root Abscess. Cureus. 2020;18;12(12):e12159. Dec.
8. Victoria Delgado, Nina Ajmone Marsan, Suzanne de Waha, Nikolaos Bonaros, Margarita Brida, Haran Burri, Stefano Caselli, Torsten Doenst, Stephane Ederhy, Paola Anna Erba, Dan Foldager, Emil L Fosbøl, Jan Kovac, Carlos A Mestres, Owen I Miller, Jose M Miro, Michal Pazdernik, Maria Nazarena Pizzi, Eduard Quintana, Trine Bernholdt Rasmussen, Arsen D Ristić, Josep Rodés-Cabau, Alessandro Sionis, Liesl Joanna Zühlke, Michael A Borger, ESC Scientific Document Group, 2023 ESC Guidelines for the management of endocarditis: Developed by the task force on the management of endocarditis of the European Society of Cardiology (ESC) Endorsed by the European Association for Cardio-Thoracic Surgery (EACTS) and the European Association of Nuclear Medicine (EANM), European Heart Journal, Volume 44, Issue 39, 14 October 2023, Pages 3948–4042

## 24-8

## Ein Myosininhibitor, ein Luftballon und Strain-myocardial Work Stressechokardiographie—eine HOCMP-Patientengeschichte

**Altersberger M.[1,2], Krumphuber A.[1], Cho Y.[1], Siebermair J.[1]**

[1]PEK Steyr, Kardiologie, Nephrologie und Intensivmedizin, Steyr, Österreich
[2]Rehabilitationszentrum Hochegg, Hochegg, Österreich

**Einleitung:** Ein 50-jähriger männlicher Patient stellt sich im Krankenhaus mit signifikanter Atemnot und reduzierter Belastbarkeit vor. Die Diagnose einer hypertrophen Kardiomyopathie (HCMP) war vorbekannt. Der Patient wurde mit Bisoprolol 2,5 mg 2 × tgl. behandelt, eine höhere Dosis wurde nicht toleriert. Ein permanentes Vorhofflimmern und eine arterielle Hypertonie waren ebenso vorbekannte Diagnosen (1, 2).

**Methoden:** Im ambulanten Setting wurde beim Patienten eine vollständige Echokardiographie, eine Kontrastmittel (KM) Untersuchung sowie eine Messung mittels Strain mit myokardialer Arbeit durchgeführt. Die Septumdicke wurde im hiesigen Echolabor mit 20 mm im KM-Setting gemessen. Der globale longitudinale Strain (GLS) war mit –9,6 % hochgradig reduziert, die EF hyperdynam (75 %). Die myokardiale Arbeit (Strain-Druck) war, obwohl eine hypertensive Entgleisung vorlag, reduziert (globaler Arbeitsindex (GAI) 1184 mmHg%, ineffiziente Arbeit (GUA) 258 mmHg, Effizienz (GAE) 85 %) (3). In Ruhe konnte kein Gradient im linksventrikulären Ausflusstrakt (LVOT) gemessen werden. Bei einer vorliegenden Bewegung der Mitralklappe in den LVOT (SAM) wurde der Verdacht auf eine HCMP mit Obstruktion gestellt. Der Patient wurde animiert ausgiebig zu frühstücken, Kaffee zu konsumieren und sich erneut zur Echokardiographie vorzustellen. Mit diesen Maßnahmen konnte ein LVOTO-Gradient herausgearbeitet werden (75 mmHg Spitzengradient). Die weitere Therapie gestaltete sich initial als frustran, da das Aufdosieren des Betablockers nur beschwerlich möglich war. Im Verlauf wurde die Therapie um einen Myosininhibitor erweitert. Darunter besserte sich der Gradient (Mavacamten 5 mg/Tag), das NT-proBNP, (initial 3200 ng/l auf 1500 ng/l) und die Symptomatik deutlich (12 Wochen Therapie).

**Resultate:** Im Verlauf zeigten sich der GLS mit –12 %, die myokardiale Arbeit mit GAI 1213 mmHg% GUA mit 104 mmHg% und die GAE mit 92 % gebessert. Um eine Darstellung mit einer körperlichen Belastung zu erhalten, führte der Patient Kniebeugen (ca. 30) durch. Es konnte damit eine Strain-Arbeit-Stressuntersuchung durchgeführt werden. Der GLS blieb konstant, mit einem höheren Blutdruck im Stress zeigte sich der GAI 1420 mmHg% gebessert (die GAE blieb mit 92 % konstant). Im Verlauf war der Patient ca. 2 Jahre stabil, bis es zu einer Zunahme von Beschwerden kam. Das NT-proBNP mit 2202 ng/l stieg deutlich an. In der durchgeführten Echokardiographie war der Strain mit GLS –12 % stabil, jedoch war ein prominenteres SAM darstellbar. Die Ruhegradienten waren nicht erhöht. Im Valsalva- und Handgrip-Stresstest kam es dabei zu keiner Änderung der Gradienten. Mit Kniebeugen konnte kein Gradient nachgewiesen werden (Bildqualität). Es wurde eine neue Modalität, ein Luftballon-Valsalva, zur Evaluierung gewählt. Beim Aufblasen eines Luftballons, wurde ein Gradient von > 50 mmHg provoziert (4, 5). Darunter wurde der Myosininhibitor auf 10 mg erhöht. Im Verlauf kam es zu einer Besserung des GLS (–16 %) und der myokardialen Arbeit und im Verlauf konnte keine LVOTO (Spitzengradient < 30 mmHg) mehr nachgewiesen werden.

**Schlussfolgerungen:** Die Strainechokardiographie bietet viele Vorteile für eine Prognose- und Verlaufsevaluation von Patient/innen mit einer HOCMP (6). Im konkreten Fall konnte mit einer sukzessiven Aufdosierung eines Myosininhibitors eine klare Besserung des GLS dargestellt werden (6). Myokardiale Arbeit ist ein neuer Parameter, welcher Potential hat, als einziger Parameter mit direkter Messung der Nachlast, zusätzlichen Nutzen zu bringen (3). Die Strain-Stress-Work-Echokardiographie als solche bedarf noch viel Diskussion, da die Bildqualität (vor allem bei Tachykardie) nicht immer optimal ist und cut-offs im Stress noch nicht klar definiert sind (3). Für die HOCMP ist es selbstverständlich essentiell, eine optimale Situation für eine Gradientenevaluation zu kreieren. Dies inkludiert ein postprandiales Setting und verschiedene Formen der Provokation, sollte sich kein Ruhegradient finden. In unserem Setting hat sich dabei die Ballon-Valsalva-Untersuchung bewährt und im konkreten Fall, konnte mit dem Aufblasen eines Partyballons ein signifikanter LVOT Gradient provoziert werden (4,5). Auf Basis dieses Ergebnisses, wurde der Myosininhibitor erhöht. Die klinische und die laborchemische Situation des Patienten besserte sich signifikant. Auch der GLS und die myokardiale Arbeit zeigten sich nach Dosiserhöhung deutlich gebessert.

### Literatur

1. Arbelo E, Protonotarios A, Gimeno JR, Arbustini E, Barriales-Villa R, Basso C, et al. 2023 ESC Guidelines for the management of cardiomyopathies: Developed by the task force on the management of cardiomyopathies of the European Society of Cardiology (ESC). Eur Heart J. 2023;1;44(37):3503–626. Jan.
2. Lang RM, Badano LP, Mor-Avi V, Afilalo J, Armstrong A, Ernande L, et al. Recommendations for Cardiac Chamber Quantification by echocardiography in adults. Eur Heart J Cardiovasc Imaging. 2015;2015.

3. Smiseth OA, Rider O, Cvijic M, Valkovič L, Remme EW, Voigt JU. Myocardial Strain Imaging: Theory, Current Practice, and the Future. JACC: Cardiovascular Imaging. Elsevier Inc.; 2025. p. 340–81. https://doi.org/10.1016/j.jcmg.2024.07.011 PubMed PMID: 39269417.
4. Kito K, Okamoto M, Shirakura K, Kobayashi H, Chikuda I, Nishikawa J, et al. Efficacy of the party balloon inflation maneuver comparing with the valsalva maneuver for diagnosis of PFO and HOCM in transthoracic echocardiography [Internet]. Report. Available from: https://academic.oup.com/ehjcimaging/article/26/Supplement_1/jeae333.329/7986585
5. Kito K, Kataoka A, Okamoto M, Nakada S, Shirakura K, Kobayashi H, et al. Feasibility of party balloon inflation manoeuvre for haemodynamic provocation: a pilot study in healthy volunteers. European Heart Journal – Imaging Methods and Practice. 2025 Jan 13;3(1). https://doi.org/10.1093/ehjimp/qyaf071
6. Desai MY, Okushi Y, Gaballa A, Wang Q, Geske JB, Owens AT, et al. Serial Changes in Ventricular Strain in Symptomatic Obstructive Hypertrophic Cardiomyopathy Treated With Mavacamten: Insights From the VALOR-HCM Trial. Circ Cardiovasc Imaging. 2024 Sep 1. https://doi.org/10.1161/CIRCIMAGING.124.017185 PubMed PMID: 39221824.

## 24-9

### A Case of a complete AV-Block with persistent left superior vena cava in a patient with Turner syndrome

**Yoshida T.[1], Lechner C.[2], Niessner A.[1]**

[1]Klinik Landstraße, Wien, Austria
[2]Ordination 1010 Wien, Wien, Austria

**Introduction:** Persistent left superior vena cava (PLSVC) is the most common congenital thoracic venous anomaly and occurs with increased prevalence in patients with congenital heart disease. Although generally considered a benign and often asymptomatic condition, it is frequently detected incidentally during invasive procedures or imaging studies. We report a case of PLSVC identified during urgent pacemaker implantation for advanced atrioventricular (AV) block in a patient with Turner syndrome. Turner syndrome is associated with congenital cardiovascular and thoracic vascular anomalies, including PLSVC. This case emphasizes the need for targeted evaluation of thoracic venous anatomy prior to transvenous pacemaker implantation in patients with Turner syndrome.

**Methods:** A 63-year-old woman with Turner syndrome and a medical history of arterial hypertension, diabetes mellitus, hypothyroidism, and pulmonary hypertension was referred to our hospital for management of complete atrioventricular (AV) block. She had undergone surgical correction of a webbed neck. Otherwise, she was in a good general condition. Over the preceding six weeks, she had experienced progressive exertional dyspnea and peripheral edema. Evaluation by her cardiologist revealed complete AV block. On admission, the 12-lead electrocardiogram confirmed complete AV block, while telemetry monitoring intermittently demonstrated second-degree AV block type II (Mobitz II). An urgent pacemaker implantation was indicated. The procedure was initiated via a left-sided approach with puncture of the left subclavian vein. After venous access was obtained, the guidewire was advanced. Fluoroscopy revealed an unusual course descending along the left cardiac border. A sheath was introduced over the wire, and contrast injection through the sheath demonstrated a persistent left superior vena cava.

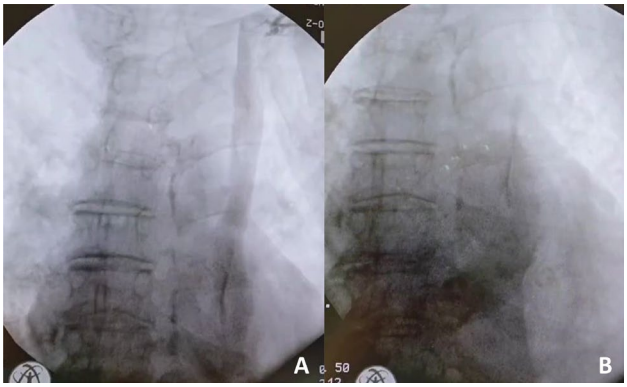


**Fig. 1 | 24–9** Intraoperative contrast injection via the sheath placed in the left subclavian vein (A), demonstrating a persistent left superior vena cava draining into the coronary sinus (B)

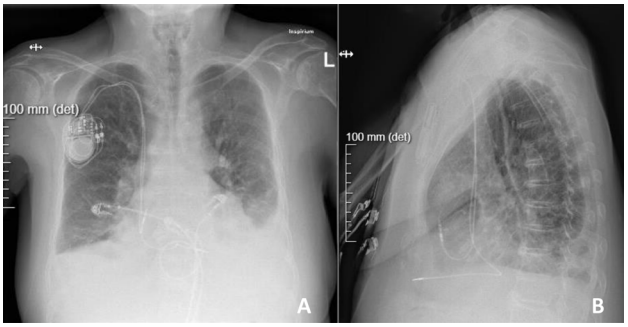


**Fig. 2 | 24–9** Postprocedural chest radiograph after pacemaker implantation showing atrial and ventricular lead positions in posteroanterior view (A) and lateral view (B)

**Results:** Due to the absence of an appropriately long stylet, continuation of the implantation via the left-sided approach was not feasible. Therefore, we decided to switch to a right-sided approach. A right superior vena cava was present, allowing uncomplicated advancement and positioning of both the ventricular and atrial leads. The pacemaker implantation was completed without further difficulty. Subsequent transthoracic echocardiography with agitated saline contrast injection via the left arm confirmed the presence of a persistent left superior vena cava draining into the coronary sinus. The patient was treated with diuretics, resulting in rapid resolution of dyspnea and peripheral edema. She was discharged in stable condition on postoperative day 6. At six-week follow-up, the patient remained clinically well, and device interrogation as well as chest radiography confirmed stable lead position and appropriate pacemaker function.

**Conclusion:** Persistent left superior vena cava (PLSVC) is the most common thoracic venous anomaly, present in 0.3–0.5% of the general population and up to 10% of patients with congenital heart disease [1]. Turner syndrome (TS), affecting 1 in 2500 females, is associated with congenital cardiovascular abnormalities in up to 50% of cases, mainly involving left-sided structures [2]. PLSVC has been reported in up to 13% of patients with TS, and phenotypic features such as neck webbing or increased anterior-posterior thoracic diameter may predict vascular anomalies [3]. Although atrioventricular block is not directly linked to TS, pacemaker implantation can be challenging in the presence of PLSVC. In 80–90% of cases, PLSVC drains

into the right atrium via a dilated coronary sinus, creating an acute angle toward the tricuspid valve and complicating ventricular lead placement [4]. Shaped stylets, active fixation leads, or atrial looping techniques may be required, and the risk of lead instability appears to be increased. A right-sided approach represents a reasonable alternative; however, assessment of the right superior vena cava is essential, as it is absent in 10–20% of patients with PLSVC (isolated PLSVC) [5, 6]. Therefore, targeted evaluation of thoracic venous anatomy prior to device implantation is recommended in patients with TS.

## References


1. Shiekh Eldin G, El-Segaier M, Galal MO. High prevalence rate of left superior vena cava determined by echocardiography in patients with congenital heart disease in Saudi Arabia. Libyan J Med. 2013;8;8(1):21679. Oct.
2. Silberbach M, Roos-Hesselink JW, Andersen NH, Braverman AC, Brown N, Collins RT, De Backer J, Eagle KA, Hiratzka LF, Johnson WH Jr, Kadian-Dodov D, Lopez L, Mortensen KH, Prakash SK, Ratchford EV, Saidi A, van Hagen I, Young LT. American Heart Association Council on Cardiovascular Disease in the Young; Council on Genomic and Precision Medicine; and Council on Peripheral Vascular Disease. Cardiovascular Health in Turner Syndrome: A Scientific Statement From the American Heart Association. Circ Genom Precis Med. 2018;11(10):e48. Oct.
3. Ho VB, Bakalov VK, Cooley M, Van PL, Hood MN, Burklow TR, Bondy CA. Major vascular anomalies in Turner syndrome: prevalence and magnetic resonance angiographic features. Circulation. 2004;21;110(12):1694–700. Sep.
4. Azizova A, Onder O, Arslan S, Ardali S, Hazirolan T. Persistent left superior vena cava: clinical importance and differential diagnoses. Insights Imaging. 2020 Oct 15;11(1):110. https://doi.org/10.1186/s13244-020-00906-2. Erratum in: Insights Imaging. 2021 Apr 16;12(1):49. https://doi.org/10.1186/s13244-021-00983-x.
5. Gøtzsche CO, Krag-Olsen B, Nielsen J, Sørensen KE, Kristensen BO. Prevalence of cardiovascular malformations and association with karyotypes in Turner's syndrome. Arch Dis Child. 1994;71(5):433–6. Nov.
6. Biffi M, Boriani G, Frabetti L, Bronzetti G, Branzi A. Left superior vena cava persistence in patients undergoing pacemaker or cardioverter-defibrillator implantation: a 10-year experience. Chest. 2001 Jul;120(1):139–44. https://doi.org/10.1378/chest.120.1.139.


# POSTERSITZUNG 25— HERZKLAPPENERKRANKUNGEN 2

## 25-1

### Cardiac Magnetic Resonance Imaging Versus Computed Tomography to Guide Transcatheter Aortic Valve Replacement: Long-Term Outcomes of a Randomized Trial


**Lechner I.[1], Reindl M.[1], Tiller C.[1], Oberhollenzer F.[1], Kaser A.[1], Fischer P.[1], Sandor A.[1], Holzknecht M.[1], Binder R.[2], Klug G.[3], Bauer A.[1], Mayr A.[4], Metzler B.[1], Reinstadler S.[1]**

[1]Universitätsklinik für Innere Medizin III – Kardiologie und Angiologie, Medizinische Universität Innsbruck, Innsbruck, Austria
[2]Abteilung für Kardiologie und Intensivmedizin, Wels, Austria
[3]LKH Bruck an der Mur, Bruck, Austria
[4]Universitätsklinik für Radiologie, Medizinische Universität Innsbruck, Innsbruck, Austria



**Introduction:** The TAVR-CMR trial demonstrated that cardiac magnetic resonance (CMR)-guided TAVR planning was noninferior to computed tomography (CT)-guided planning for device implantation success at discharge. Long-term clinical outcomes and valve performance following CMR- versus CT-guided TAVR are unknown. The aim was to compare long-term clinical outcomes and valve performance after CMR- versus CT-guided TAVR planning.

**Methods:** This investigator-initiated, prospective, randomized, open-label, noninferiority trial enrolled 380 patients with severe aortic stenosis at two Austrian centers and randomized them 1:1 to CMR- or CT-guided TAVR planning. A total of 267 patients ultimately underwent TAVR (138 in the CMR group and 129 in the CT group). This analysis evaluated clinical outcomes and valve performance at 2 years and clinical outcomes at 4 years. The primary clinical endpoint was the composite of all-cause mortality, stroke, and rehospitalization at


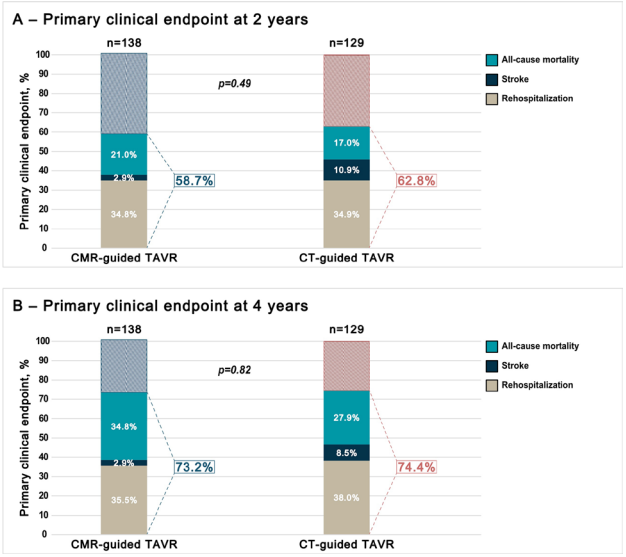


**Fig. 1 | 25-1**

2 years, and echocardiographic valve performance defined as moderate or severe hemodynamic valve deterioration per VARC-3 criteria at 2 years.

**Results:** Among 267 randomized patients (mean age 82 years, 50% women), the primary clinical endpoint occurred in 58.7% vs. 62.8% at 2 years ($p=0.49$) and 73.2% vs. 74.4% at 4 years ($p=0.82$) for CMR-guided and CT-guided TAVR, respectively. The combined endpoint of all-cause death or disabling stroke was likewise similar between groups (2 years: 23.9% vs. 27.9%, $p=0.46$; 4 years: 37.7% vs. 36.4%, $p=0.83$). At 2 years, moderate or severe hemodynamic valve deterioration occurred in 19 of 138 (14%) CMR-guided patients and 15 of 129 (12%) CT-guided patients ($p=0.37$).

**Conclusion:** In patients with severe aortic stenosis undergoing TAVR, CMR-guided and CT-guided TAVR showed no significant differences in echocardiographic valve performance at 2 years or in the composite outcome of all-cause death, stroke, or rehospitalisation at 2 and 4 years.

## 25-2

### Soluble ST2 as a Dynamic Biomarker of Biological Response After Transcatheter Tricuspid Valve Intervention

**Edlinger C.[1], Schlegl J.[2], Lichtenauer M.[3], Paar V.[3], Haase-Fielitz A.[2], Kücken T.[4], Neuss M.[2], Bannehr M.[2], Butter C.[2]**

[1]Herzzentrum Brandenburg; Bernau/Berlin, Berlin, Germany
[2]Herzzentrum Brandenburg, Berlin, Germany
[3]PMU Salzburg, Salzburg, Austria
[4]Herzzentrum Brandenburg, Bernau, Germany

**Introduction:** Biomarker trajectories following transcatheter tricuspid valve intervention (TTVI) remain poorly characterized. Interpretation of natriuretic peptides in this population is often limited by renal dysfunction and cardiorenal syndrome. Soluble ST2 (sST2) provides prognostic information independent of renal function and natriuretic peptides. The aim of this study was to characterize longitudinal changes of sST2 after TTVI and to compare its dynamics with biomarkers reflecting systemic stress, inflammation, and myocardial injury.

**Methods:** In this prospective single-centre cohort study, 135 patients undergoing TTVI were included. Levels of sST2, GDF-15, suPAR, H-FABP, and NT-proANP were measured at baseline, discharge, 3 months, and 12 months. Longitudinal biomarker changes were analysed using paired non-parametric tests.

**Results:** The cohort was elderly (median age 82 years) with a high prevalence of atrial fibrillation and advanced right-sided heart failure. sST2 demonstrated a distinct biphasic trajectory, with a significant increase from baseline to discharge ($n=135$; $p=0.004$), followed by a significant reduction at 3 months ($n=124$; $p=0.003$) and a sustained decrease at 12 months ($n=82$; $p<0.0001$). GDF-15 showed no significant longitudinal changes. suPAR decreased early at discharge ($p<0.001$) and at 3 months ($p=0.004$), but without sustained reduction at 12 months ($p=0.895$). H-FABP decreased only at 12 months ($p=0.007$), whereas NT-proANP showed no consistent dynamic pattern over time. Conclusion:

**Conclusion:** Among the investigated biomarkers, sST2 showed the most consistent longitudinal trajectory following TTVI. These findings suggest that sST2 may be a promising biomarker for monitoring biological response after TTVI and warrant further validation in independent cohorts.

| Variable | Overall (n=135) |
|---|---|
| Device implanted | |
| Pascal | 91 (67.4%) |
| TricValve | 20 (14.8%) |
| TriClip | 15 (11.1%) |
| EVOQUE | 9 (6.7%) |
| | |
| Age, years | 82.0 (78.0–84.0) |
| Female sex | 59 (43.7%) |
| BMI, kg/m² | 25.0 (23.4–28.0) |
| Coronary artery disease | 54 (40.0%) |
| Diabetes mellitus | 37 (27.4%) |
| COPD | 19 (14.1%) |
| Hypertension | 81 (60.0%) |
| Atrial fibrillation | 104 (77.0%) |
| 6MWT, m | 180.0 (69.0–339.0) |
| LVEF, % | 54.0 (45.0–60.0) |
| TAPSE, mm | 16.0 (13.8–18.0) |

**Fig. 1 | 25-2**

Figure 1A
Serial sST2 levels at baseline, discharge, 3 months, and 12 months presented as boxplots (median and interquartile range).

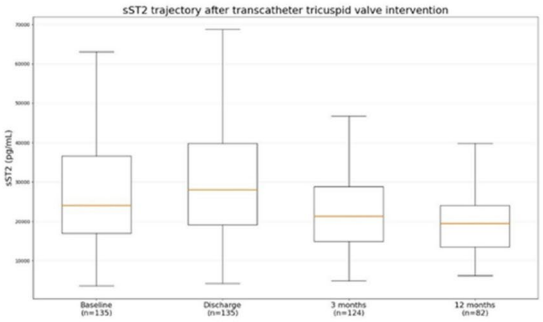


Figure 1B
Relative longitudinal changes (Δ% from baseline median) of sST2, GDF-15, suPAR, H-FABP, and NT-proANP over follow-up.

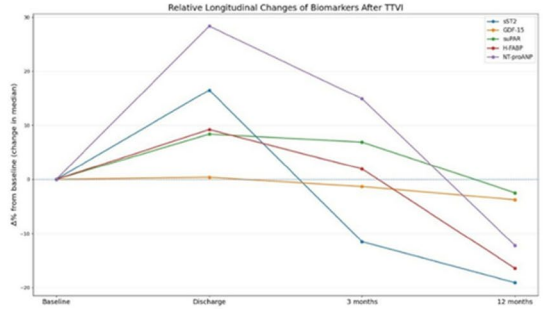


**Fig. 2 | 25-2**

## 25-3

### Global Myocardial Performance and Long-Term Mortality After Transcatheter Aortic Valve Implantation: Prognostic Value of the TEI Index

**Clodi N.[1,2], Granitz C.[1], Hoppe U.[1], Hammerer M.[1], Lichtenauer M.[1], Boxhammer E.[1]**

[1]Universitätsklinik für Innere Medizin II, Kardiologie und internistische Intensivmedizin, Salzburg, Austria

[2]Universitätsklinik für Radiologie, Salzburg, Austria

**Introduction:** Transcatheter aortic valve implantation (TAVI) effectively relieves valvular obstruction in patients with severe aortic stenosis (AS); however, long-term outcomes remain heterogeneous. While procedural success is high, many patients continue to experience excess mortality, suggesting that factors beyond the valve itself may determine prognosis. Global myocardial performance, reflecting integrated systolic and diastolic function, may capture residual heart failure biology after TAVI.

**Methods:** In this retrospective single-center cohort study, consecutive patients undergoing transfemoral TAVI between 2016 and 2022 were screened. Patients with permanent atrial fibrillation (AF) or inadequate echocardiographic data were excluded. Global myocardial performance was assessed pre-procedurally using the myocardial performance (TEI) index. The primary endpoint was all-cause mortality at 3 years. A total of 412 patients (mean age 82.1 ± 5.1 years; 47.1% male) were included.

**Results:** Higher TEI index values were associated with increased 3-year mortality in a graded manner. In multivariable Cox regression, each 0.1-unit increase in the TEI index was independently associated with a higher risk of death (HR 1.49, 95% CI 1.19–1.87; $p < 0.001$). A pre-specified TEI index threshold of 0.45 effectively stratified patients into distinct long-term risk groups, with early and persistent separation of Kaplan–Meier survival curves. The TEI index provided incremental prognostic value beyond established clinical and echocardiographic parameters and demonstrated consistent associations across clinically relevant subgroups. Restricted cubic spline analyses supported an approximately linear relationship between the TEI index and mortality risk.

**Conclusion:** In patients undergoing TAVI, impaired global myocardial performance assessed before intervention is an independent predictor of long-term survival. The TEI index provides incremental prognostic value beyond established parameters, highlighting myocardial dysfunction as an important determinant of outcomes beyond valvular obstruction.

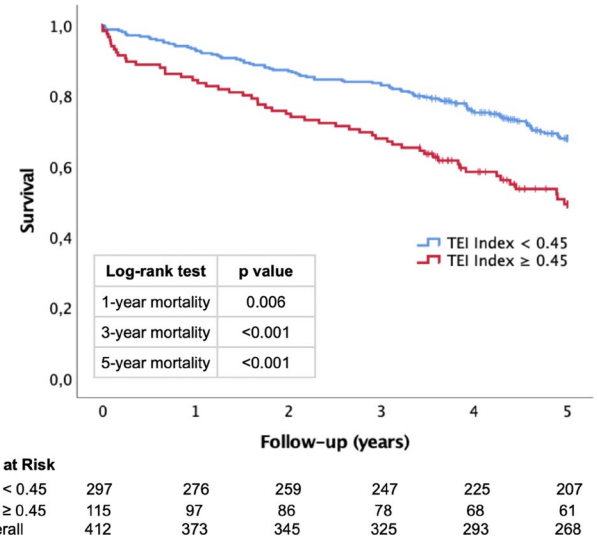


**Fig. 1 | 25-3** Kaplan-Meier Curve

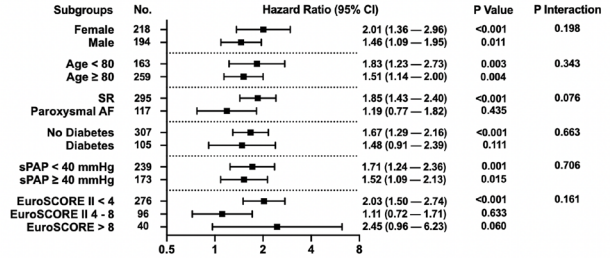


**Fig. 2 | 25-3** Forest-Plot with HR according to Subgroups

## 25-4

## Postoperative Atrial Fibrillation After Mitral Valve Surgery: Incidence, Persistence, and Prognostic Impact

**Fiesel D., Ennen V., Lohmann R., Engler C., Hirsch J., Graber M., Nägele F., Grimm M., Höfer D., Bonaros N., Winter-Pölzl L., Gollmann-Tepeköylü C.**

Universitätsklinik für Herzchirurgie, Medizinische Universität Innsbruck, Innsbruck, Austria

**Introduction:** Postoperative atrial fibrillation (POAF) frequently occurs after mitral valve surgery, yet procedure-specific data quantifying its independent association with perioperative complications remain limited. In addition, the persistence of POAF beyond hospital discharge and the impact of concomitant surgical ablation on rhythm outcomes require further clarification. This study aimed to evaluate the association of POAF with perioperative morbidity, rhythm persistence, and survival after mitral valve surgery for mitral regurgitation.

**Methods:** This single-center cohort study included 2376 patients undergoing mitral valve surgery for mitral regurgitation. Two patient cohorts were analyzed. The first cohort comprised patients without preoperative atrial fibrillation (AF) to evaluate the incidence of POAF and its association with perioperative morbidity. Outcomes included prolonged intensive care unit (ICU) stay (≥ 24 hours), postoperative renal replacement therapy, extracorporeal membrane oxygenation (ECMO) use, and 30-day mortality. Multivariable logistic regression models adjusted for EuroSCORE II were used to assess associations with POAF. The second cohort included patients with preoperative AF to evaluate the impact of concomitant surgical ablation on postoperative rhythm and long-term survival. Data on atrial fibrillation during cardiac rehabilitation (1–6 months postoperatively) were available in 64.6% of patients and used to assess rhythm persistence. Long-term survival was analyzed using Cox regression adjusted for EuroSCORE II.

**Results:** Among 1339 patients without preoperative AF, POAF occurred in 663 patients (49.5%). POAF was independently associated with prolonged ICU stay (35.9% vs. 24.9%; OR 1.51) and renal replacement therapy (12.2% vs. 6.2%; OR 1.85), but not with ECMO use or 30-day mortality. At rehabilitation follow-up, atrial fibrillation persisted in 8.7% of patients with perioperative POAF, while 4.1% of patients without documented perioperative AF developed atrial fibrillation during rehabilitation. Among 760 patients with preoperative AF, concomitant surgical ablation was associated with significantly lower rates of POAF (66.4% vs. 90.0%, $p < 0.001$) and reduced AF prevalence at rehabilitation (27.1% vs. 66.4%, $p < 0.001$). In Cox regression analysis adjusted for EuroSCORE II, patients with preoperative atrial fibrillation without surgical ablation had significantly higher mortality (HR 3.30) than patients without atrial fibrillation before surgery or at rehabilitation. Patients undergoing surgical ablation showed comparable survival.

**Conclusion:** Postoperative atrial fibrillation after mitral valve surgery is independently associated with increased perioperative morbidity and frequently persists beyond hospital discharge. Concomitant surgical ablation improves rhythm control and is associated with long-term survival comparable to patients without atrial fibrillation.

## 25-5

### Diagnostic Criteria for Atrial Functional Tricuspid Regurgitation: Sensitivity Analysis Across Competing Definitions

**Jantsch C., Koschatko S., Hauptmann L., Autherith M., Halavina K., Torrefranca C., Demirel C., Dannenberg V., Hengstenberg C., Pavo N., Nitsche C., Heitzinger G., Bartko P.**

Medizinische Universität Wien, Wien, Austria

**Introduction:** Atrial functional tricuspid regurgitation (AfTR) has emerged as an important clinical entity due to its unique clinical characteristics, morphological features, and implications for outcomes. Despite a relatively clear conceptual framework, the transition to a clear definition shows substantial variability across published studies and state-of-the-art documents. The aims of this study were to develop a systematic and comprehensive overview of available AfTR definitions and to examine resulting differences and variability in clinical characteristics, morphology, and outcomes. Furthermore, it aimed to cluster definitions according to common criteria to provide a potential roadmap towards consensus in the AfTR definition.

**Methods:** Systematic PubMed and Embase search to identify all published definitions for AfTR. All identified definitions were applied to an independent individual-patient data cohort and sensitivity analyses were performed for clinical, morphological, and outcome variables.

**Results:** The systematic search of PubMed and Embase yielded 22 distinct definitions. Stratification according to mandatory features revealed four clusters based on right atrial dilatation, right atrial-to-right ventricular size ratio, atrial fibrillation, and preserved left ventricular function. Considerable variability was observed between definitions for prevalence (0.2–44.8%) and valve features (annulus size 30.3–42.5 mm; tenting area 45–205 mm2). Only 6 of 22 definitions showed a significant prognostic

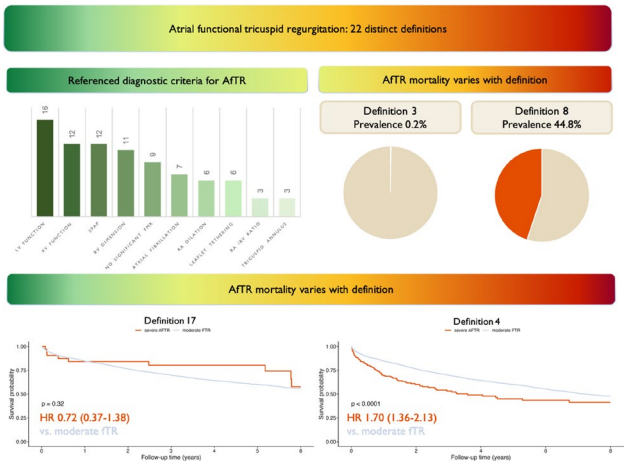


Fig. 1 | 25-5

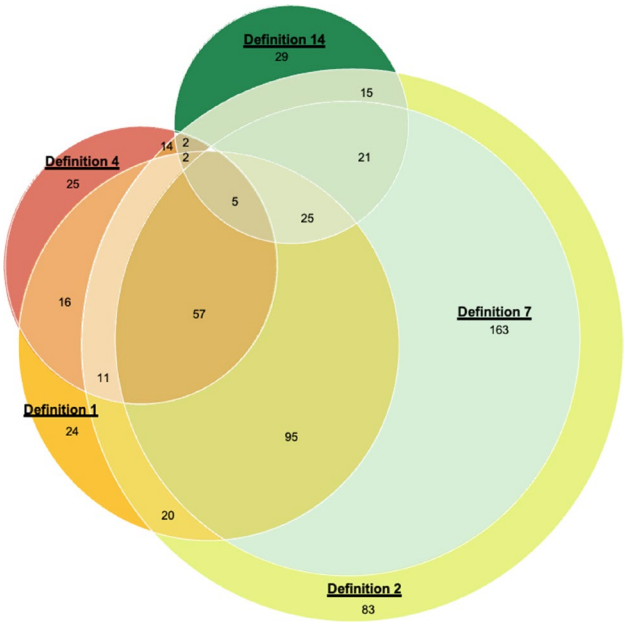


Fig. 2 | 25-5

impact compared to patients with moderate functional tricuspid regurgitation, with hazard ratios ranging from 1.31 to 1.70. Definitions with significant impact on survival were exclusively observed within clusters of right atrial dilatation or right atrial-to-right ventricular size ratio. Recommended definitions from ESC and JACC state-of-the-art publications were identified within the right atrial dilatation cluster and showed comparable, but not identical, patient selection, with a significant non-overlap of 14%/54%.

**Conclusion:** Implementation of the conceptual AfTR framework is subject to substantial variability with 22 distinct definitions that evolved over the past decade. These different definitions show considerable differences in patient selection, with implications regarding valve features and prognosis. Stratification by mandatory features revealed clusters based on right atrial dilatation and right atrial-to-right ventricular size ratio to include definitions with significant impact on survival. Therefore, these clusters might be specifically relevant for providing a roadmap towards consensus in AfTR definitions.

# POSTERSITZUNG 26 – HERZINSUFFIZIENZ & KARDIOMYOPATHIEN 4

## 26-1

### Heart Failure in Transgender Individuals: What Do We Really Know?

**Rech L.[1,2], Siqueira A.[3], Siqueira S.[3], Siepmann T.[4,2], de Abreu-Silva E.[5,2]**

[1]Medizinische Universität Graz, Graz, Austria
[2]Dresden International University, Dresden, Germany
[3]Brigham and Women's Hospital, Boston, United States
[4]TU Dresden, Dresden, Germany
[5]Hcor Research Institut, Hcor (IP-Hcor), Sao Paulo, Brazil

**Introduction:** The number of transgender individuals is increasing worldwide, along with access to gender-affirming hormone therapy (GAHT). While cardiovascular risks associated with GAHT are being increasingly investigated, the impact on the development of heart failure has not been adequately researched. This study aims to summarise the available evidence on heart failure in transgender individuals and to explore potential associations with GAHT.

**Methods:** A systematic literature search was conducted across PubMed, Embase, the Cochrane Library, and Google Scholar until December 2024. Studies and conference abstracts reporting heart failure (HF) in transgender individuals, compared to cisgender men or women, were included. Odds ratios (ORs) were either extracted or calculated and pooled using random-effects meta-analyses for two comparisons: (1) transgender vs. cisgender individuals and (2) transgender men vs. cisgender women. Additionally, data from the 2022 Health and Retirement Study (HRS) were analysed to reassess the prevalence of heart failure in older transgender adults.

**Results:** The systematic review identified seven full-text studies from a total of 477 cited references that investigated heart failure in transgender individuals. However, only one of these studies explicitly evaluated the association between GAHT and heart failure in transgender individuals. An exploratory meta-analysis of three studies (1 full paper, 2 abstracts) comparing 'transgender vs. cisgender individuals' showed no significant association (OR 1.10 [95% CI: 0.60–2.01]). A second exploratory meta-analysis comparing 'transgender men with cisgender women' (2 full paper, 1 abstract) yielded an odds ratio of 1.04 [95% CI: 0.38–2.86]. Both analyses demonstrated a very high heterogeneity ($I^2 > 98\%$). A supplementary exploratory analysis of the 2022 Health and Retirement Study dataset also indicated no significant difference in the prevalence of heart failure between heterosexual individuals and the 'Others' group (OR 1.56 [95% CI: 0.66–3.72]), a heterogeneous category that may partially include transgender individuals but does not permit direct ascertainment of gender identity.

**Conclusion:** Currently, the results show no reliable evidence of a connection between GAHT and heart failure. However, the validity of these findings is limited by methodological differences, a lack of data on GAHT, and insufficient differentiation of heart failure types. These findings likely reflect methodological constraints rather than true cardiovascular neutrality, underscoring the urgent need for targeted, prospective studies to clarify long-term heart failure risk associated with GAHT.

## 26-2

## Neutrophil Extracellular Trap Deposition Drives Adverse Cardiac Remodeling in Transthyretin Amyloid Cardiomyopathy (ATTR-CM)

**Bojti I.[1], Schönig L.[1], Bojtine Kovacs S.[2], Ziegler A.[1], Güler A.[1], Stallmann D.[1], Klingel K.[3], Gauchel N.[1], Häßner J.[1], Selle M.[2], Westermann D.[1], Steenbuck D.[1], Heger L.[1]**

[1]Universitäts-Herzzentrum Freiburg-Bad Krozingen, Freiburg-Bad Krozingen, Germany
[2]Innere Medizin I, Universitätsklinkum Freiburg, Freiburg im Breisgau, Germany
[3]Cardiopathology, Institute for Pathology and Neuropathology, University Hospital Tübingen" Tübingen, Germany

**Introduction:** Transthyretin amyloid cardiomyopathy (ATTR-CM) is a progressive form of restrictive cardiomyopathy caused by the deposition of misfolded transthyretin (TTR) in the myocardium, leading to heart failure. While amyloid deposition is central to disease pathology, the contribution of immune-mediated mechanisms—particularly neutrophil activation and formation of neutrophil extracellular traps (NETs)—remains poorly understood. NETs and NLRP3 inflammasome activation have been implicated in chronic inflammation and tissue remodeling, suggesting a potential role in ATTR-CM pathogenesis. This study aimed to investigate the extent and spatial distribution of neutrophil activation and NET deposition in cardiac tissue of ATTR-CM patients, to evaluate the relationship between neutrophil activation and amyloid accumulation, and to assess the effects of transthyretin stabilization therapy on circulating neutrophil activation and inflammasome activity.

**Methods:** Endomyocardial biopsies from age-matched ATTR-CM patients and healthy controls were analyzed using immunofluorescence microscopy for DNA (DAPI, blue), citrullinated histone H3 (H3Cit, green), and myeloperoxidase (MPO, red). NET deposition was quantified as the percentage of H3Cit-positive area relative to total area per field of view. Spatial analyses were performed to determine the proximity of activated neutrophils to transthyretin (TTR) deposits. In parallel, peripheral blood neutrophils were isolated from ATTR-CM patients before and after initiation of TTR stabilizer therapy, and from healthy controls. NET formation (spontaneous and PMA-stimulated) was assessed by immunofluorescence, and inflammasome activation was evaluated via ASC speck formation.

**Results:** ATTR-CM samples showed markedly increased neutrophil infiltration ($7.1 \pm 1.3\%$ vs. $1.47 \pm 0.4\%$; $p = 0.003$) and NET deposition ($315.8 \pm 292.9$ vs. $51.3 \pm 34.5\ \mu m^2$/FOV; $p = 0.0097$) compared with controls. Spatial analysis revealed that activated neutrophils were significantly closer to TTR deposits ($16.1 \pm 95.8\ \mu m$ vs. $241.6 \pm 368.5\ \mu m$; $p < 0.0001$), suggesting direct interaction between neutrophils and amyloid fibrils. Ex vivo analyses demonstrated increased spontaneous NETosis ($5.7 \pm 4.6\%$ vs. $0.74 \pm 0.19\%$; $p = 0.007$) and enhanced NET formation upon stimulation ($45.1 \pm 14.8\%$ vs. $17.2 \pm 12.4\%$; $p < 0.001$) in ATTR-CM patients compared with healthy controls. Neutrophils also displayed elevated ASC speck formation, indicating augmented inflammasome activation. After six months of TTR stabilizer therapy, both spontaneous and stimulated NETosis were significantly reduced ($44.7 \pm 18.4\%$ vs. $8.0 \pm 8.2\%$; $p = 0.006$).

**Conclusion:** Our findings reveal that neutrophil activation and NET deposition are prominent features of ATTR-CM and spatially associated with amyloid accumulation, implicating NET-driven inflammation in disease progression. Transthyretin stabilization therapy attenuates neutrophil activation and inflammasome activity, highlighting a potential therapeutic avenue targeting innate immune mechanisms to mitigate adverse cardiac remodeling in ATTR-CM.

## 26-3

### Prevalence of Conduction System Disease and AF in Cardiac Transthyretin Amyloidosis: A Single-Center Analysis

**Krumphuber A.[1], Altersberger M.[1], Schlender L.[2], Papathanasiou M.[2], Siebermair J.[1,3]**

[1]Pyhrn-Eisenwurzen Klinikum, Steyr, Austria
[2]Universitätsklinikum Frankfurt am Main, Frankfurt am Main, Germany
[3]Universitätsklinikum Essen, Essen, Germany

**Introduction:** Cardiac transthyretin amyloidosis (ATTR-CA) is a progressive disease causing heart failure and rhythm disorders significantly contributing to morbidity and mortality. Early diagnosis and initiation of disease-specific therapy with transthyretin stabilizers and/or silencers have shown to slow disease progression and improve outcome [1]. Despite advancing therapies, overall prognosis remains poor. Whether these therapies can prevent the development of conduction system diseases remains largely unknown [2,3]. The objective of this study was to evaluate atrioventricular (AV) and intraventricular conduction system disorders and their association with clinical outcomes.

**Methods:** This single-center analysis was conducted within an ongoing observational multicenter registry. We aimed to analyze baseline and most recent follow-up data from patients with ATTR-CA treated at a tertiary referral center for ATTR amyloidosis. Patients receiving transthyretin stabilizers and those without disease-specific therapy were included. Patient characteristics, laboratory data, electrocardiographic (ECG) and echocardiographic parameters were collected and analyzed. Baseline characteristics were analyzed using two tailed Mann-Whitney U test for age, NAC-stage, number of hospitalizations and NYHA class. Binary data were analyzed with McNemar-Test.

**Results:** Twenty patients diagnosed with ATTR-CA at our center were included in this preliminary analysis. Genetic testing results were available in 50% of patients but no pathogenic variants were detected. Baseline characteristics were analyzed according to treatment status. The mean age at diagnosis was 79.9 ± 5.4 years (84 ± 2.9 years off-treatment vs. 78 ± 5.4 years on-treatment, $p = 0.013$), with 80% males. Mean follow-up duration was 20 months. Patients on treatment had a significant lower National Amyloidosis Centre (NAC) stage ($p = 0.0465$). There was no statistically significant difference in NYHA class at baseline ($p = 0.087$). At baseline ECG, $n = 11$ (55%) were in sinus rhythm (SR), and 45% presented with atrial fibrillation (AF). No patient had a pacemaker at baseline, during follow-up (FU) two patients (10%) required pacemaker implantation due to higher grade AV blocks. Low-voltage ECG criteria were met in 10% at baseline and in 25% at follow-up ($p = 0.0526$, ns) wieder qui square). Electrical dyssynchrony (QRS > 130 ms) was observed in 30% at baseline and 40% at follow-up. Among the 11 patients in sinus rhythm at baseline, mean heart rate was 63 ± 8 bpm. AV block was present in 27.3% at baseline and increased to 63.3% at follow up (ns). Mean number of hospitalizations was 2.55 ± 3.2 (5.5 ± 4.6 off-treatment vs. 1.3 ± 0.8 on-treatment, $p = 0.0196$). No deaths were recorded during the observational period. Therapy was discontinued in one patient.

**Conclusion:** Conduction system disorders and AF were highly prevalent in this ATTR-CA cohort and increased over time, underscoring the progressive electrophysiological involvement in the disease course. Notably, a marked increase in AV conduction abnormalities was observed during FU.

| | overall (n =20) | ATTR stabilizer (n = 14) | No treatment (n = 6) |
|---|---|---|---|
| male sex - no. (%) | 16 (80) | 12 (85,7) | 4 (66,7) |
| Age - years | 79,9 ± 5,4 | 78 ± 5,4 | 84 ± 2,9 |
| Sinus rhythm - no. (%) | 11 (55) | 10 (71,4) | 1 (16,7) |
| NAC-Stage - no. (%) | | | |
| NAC-Stage I | 10 (50) | 9 (64,3) | 1 (16,7) |
| NAC-Stage II | 3 (15) | 2 (14,3) | 1 (16,7) |
| NAC-Stage III | 7 (35) | 3 (21,4) | 4 (66,7) |
| NYHA Stage - no. (%) | | | |
| NYHA I | 1 (5) | 1 (7,1) | 0 (0) |
| NYHA II | 11 (55) | 9 (64,3) | 2 (33,3) |
| NYHA III | 7 (35) | 4 (28,6) | 3 (50) |
| NYHA IV | 1 (5) | 0 (0) | 1 (16,7) |

**Fig. 1 | 26-3**

Patients on treatment were statistically significant younger, had a lower NAC stage, and a non-significant trend towards lower NYHA class at baseline. Furthermore, fewer hospitalizations were observed in patients receiving transthyretin stabilizers compared to those who didn't. However, this finding may be confounded by treatment selection bias, as patients with more advanced disease were less likely to receive disease-specific therapy but large randomized clinical trials observed the same effect (3). Larger prospective studies are needed to further evaluate how disease-modifying therapies can influence the progression of conduction system disease.

### References

1. Garcia-Pavia P, Gonzalez-Lopez E, Anderson LJ, Cappelli F, Damy T, Fontana M, et al. Non-amyloid specific treatment for transthyretin cardiac amyloidosis: a clinical consensus statement of the ESC Heart Failure Association. Eur Heart J. 2026 Jan 5;47(1):22–36. https://doi.org/10.1093/eurheartj/ehaf710
2. Ruberg FL, Maurer MS. Cardiac Amyloidosis Due to Transthyretin Protein. JAMA. 2024 Mar 5;331(9):778. https://doi.org/10.1001/jama.2024.0442
3. Miyamoto M, Nakamura K, Nakagawa K, Nishii N, Kawada S, Ueoka A, et al. Prevalence and Treatment of Arrhythmias in Patients With Transthyretin and Light-Chain Cardiac Amyloidosis. Circ Rep. 2023 Jul 10;5(7):CR-23-0022. https://doi.org/10.1253/circrep.CR-23-0022

## 26-4

### Die Rolle des kardialen Lymphsystems bei ischämischer Herzerkrankung: die Identifizierung der Lymphangiogenese-Aktivität bei Patienten nach einem akuten Myokardinfarkt und dessen Bedeutung auf die Entwicklung von Herzinsuffizienz

**Gamper H.:**

Univ. Klinik LKH Salzburg – Kardiologie, internistische Intensivmedizin und Notaufnahme, Salzburg, Österreich

**Einleitung:** Das kardiale Lymphsystem spielt eine zentrale Rolle bei der Aufrechterhaltung der myokardialen Homöostase sowie in der Pathophysiologie kardiovaskulärer Erkrankungen. Es ist wesentlich am Abtransport interstitieller Flüssigkeit, Lipiden, Proteinen und inflammatorischer Mediatoren aus

dem Myokard beteiligt und trägt damit zur Regulation der lokalen Immunantwort und Gewebereparatur bei. Nach akutem Koronarsyndrom, kann die ischämische Schädigung zu ausgeprägtem Gewebeödem und inflammatorischer Aktivierung führen. Eine Dysfunktion des lymphatischen Systems kann in dieser Phase die Clearance dieser Substanzen beeinträchtigen, wodurch Entzündungsprozesse prolongiert, die Heilung verzögert und maladaptives kardiales Remodeling gefördert werden, was wesentlich zur Entwicklung einer Herzinsuffizienz beiträgt [1]. Trotz der zentralen Bedeutung dieser Mechanismen ist bislang nur unzureichend verstanden, wie die Lymphangiogenese in der akuten postinfarktiven Phase reguliert wird und welchen Einfluss sie auf myokardiale Schädigung, Entzündungsaktivität und funktionelle Erholung hat [2,3]. Ein vertieftes Verständnis der frühen lymphatischen Antwort nach Myokardinfarkt könnte neue Einblicke in kardiale Reparaturmechanismen liefern, innovative therapeutische Zielstrukturen identifizieren und die Risikostratifizierung von ACS-Patient:innen verbessern, insbesondere im Hinblick auf die Prävention der Herzinsuffizienz.

**Methoden:** In dieser prospektiven, beobachtenden Studie werden 128 Patient:innen im Alter von ≥ 50 Jahren mit erstmaligem ST-Hebungs-Myokardinfarkt, die mittels perkutaner Koronarintervention behandelt werden, eingeschlossen. Eine initiale transthorakale Echokardiographie innerhalb von 24–48 Stunden ermöglicht die Stratifizierung in eine „High-Risk" Gruppe (H) für Herzinsuffizienz und eine Kontrollgruppe „Low-Risk" (K) für Herzinsuffizienz. Standardisierte Blutabnahmen erfolgen nach 24, 48 und 72 Stunden postinfarkt sowie nach drei Monaten (T1 bis T4). Analysiert werden lymphangiogene Wachstumsfaktoren (VEGF-C, VEGF-A), kardiale Biomarker (Troponin, CK-MB, NT-proBNP), Entzündungsmarker (CRP, IL-6) sowie Nierenfunktionsparameter. Zur Bewertung der relativen lymphangiogenen Aktivität wird der VEGF-C/VEGF-A-Index verwendet. Serielle Echokardiographien während des stationären Aufenthalts sowie nach drei Monaten erfassen links- und rechtsventrikuläre Funktion ebenso wie klinische Parameter. Zum Zeitpunkt der Abstract-Einreichung liegen erste vorläufige Ergebnisse vor. Die vorläufigen Daten von 50 der geplanten 120 Patienten wurden ausgewerten.

**Resultate:** Insgesamt wurden bislang 50 Patienten eingeschlossen (39 Männer, 11 Frauen, mittleres Alter 63,3 Jahre). Die Hauptgruppe umfasste 27 Patienten (darunter 5 Frauen), die Kontrollgruppe 23 Patienten (darunter 6 Frauen). 29 Patienten hatten einen Vorderwandinfarkt, 17 einen Hinterwandinfarkt. Im Vergleich zur Kontrollgruppe zeigte die Herzinsuffizienzgruppe eine veränderte zeitliche Dynamik der VEGF-C-Spiegel mit insgesamt höheren Werten über den Beobachtungszeitraum (T1 416 ± 240 vs 359 ± 325, T2 372 ± 248 vs. 320 ± 205, T3 361 ± 230 vs. 333 ± 240, T4 504 ± 265 vs. 456 ± 317 pg/ml). In der Herzinsuffizienzgruppe zeigte sich insbesondere im späteren Verlauf eine tendenziell höhere Gesamtexposition (AUC), was auf eine prolongierte lymphangiogene Antwort hinweisen könnte. Diese Veränderungen waren mit höheren NT-proBNP-Werten, reduzierter LVEF und höherer klinischer Krankheitslast assoziiert. Patienten mit Vorderwandinfarkt zeigten höhere VEGF-C-Spiegel als Patienten mit Hinterwandinfarkt, möglicherweise im Zusammenhang mit größeren Infarktarealen (höhere CK, Trop-T). Gleichzeitig war in der Herzinsuffizienzgruppe eine stärkere inflammatorische Aktivität nachweisbar (IL-6, CRP), die positiv mit den VEGF-C-Spiegeln korrelierte.

**Schlussfolgerungen:** Die Studie zielt darauf ab, die Rolle der Lymphangiogenese in der frühen postinfarktiven Phase besser zu charakterisieren. Die gewonnenen Erkenntnisse könnten neue prognostische Marker identifizieren und zukünftige therapeutische Strategien zur Prävention der Herzinsuffizienz unterstützen [1]. Die erhöhten VEGF-C-Spiegel bei Patienten mit späterer Entwicklung einer Herzinsuffizienz im Vergleich zur Kontrollgruppe ohne Herzinsuffizienz könnten auf eine prolongierte lymphangiogene Aktivierung nach ACS hinweisen. Dies könnte mit persistierenden inflammatorischen Prozessen und postinfarktivem kardialem Remodeling assoziiert sein und möglicherweise zur Entwicklung/Progress einer Herzinsuffizienz beitragen [2] Diese Beobachtungen stehen im Einklang mit experimentellen Studien [3] die zeigen konnten, dass Myokardschädigungen mit einer vermehrten Expression von VEGF-C und einer daraus resultierenden Expansion des kardialen Lymphgefäßnetzwerks einhergehen.

## Literatur


1. Brakenhielm E, Alitalo K, et al. Cardiac Lymphatics in Health and Disease. Nat Rev Cardiol. 2019.
2. Shimizu Y, Polavarapu R, Eskla KL, et al. Impact of Lymphangiogenesis on Cardiac Remodeling After Ischemia and Reperfusion Injury. JAHA Journal of the American Heart Association. 2018.
3. Klotz L, Norman S, Vieira JM, et al. Cardiac Lymphatics Are Heterogeneous in Origin and Respond to Injury. Nature. 2015.


# 26-5

## Characterization of NT-proBNP Dynamics according to Obesity and Renal Dysfunction in Elderly Patients with Acute Heart Failure


**Kaufmann C.[1,2], Ahmed A.[1], Harbich P.[1], Auer L.[1], Weltler P.[1], Eberl T.[1], Pogran E.[1,2], Huber K.[3], Geppert A.[1], Jäger B.[1,2]**

[1]Klinik Ottakring, Wien, Austria
[2]Sigmund Freud Privatuniversität, Wien, Austria
[3]Austrian Heart Foundation, Vienna, Austria and Medical Private University Burgenland (GmbH), Pinkafeld, Austria, Pinkafeld, Austria


**Introduction:** Acute heart failure (AHF) is a major contributor to cardiovascular morbidity and mortality. While the influence of obesity and renal dysfunction on NT-proBNP levels has been well described in chronic heart failure, data in AHF remain limited.

**Methods:** This single-center, retrospective real-world study included patients aged ≥ 65 years admitted with AHF to a tertiary care hospital in Austria between 2012 and 2019. We assessed the prognostic impact of NT-proBNP at hospital admission across body mass index (BMI) and estimated glomerular filtration rate (eGFR) categories and determined BMI- and eGFR-specific cut-off values.

**Results:** A total of 1624 patients admitted for AHF were included (mean age 81 ± 8 years; 51.8% female). NT-proBNP levels were significantly lower in patients with obesity and increased with worsening renal function. BMI and eGFR were the strongest independent predictors of NT-proBNP levels (BMI: $\beta = -0.334$; $P < 0.001$; eGFR: $\beta = -0.336$; $P < 0.001$). In multivariable Cox regression analysis, NT-proBNP was a significant predictor of 1-year all-cause mortality (aHR 2.25; 95% CI 1.83–2.77; $P < 0.001$), with consistent associations across BMI and eGFR subgroups. Optimal NT-proBNP cutoffs for predicting 1-year mortality differed markedly: the threshold was nearly threefold lower in severely obese patients (obesity class II/III: 3277 vs normal/underweight: 8894 ng/L) and almost twofold

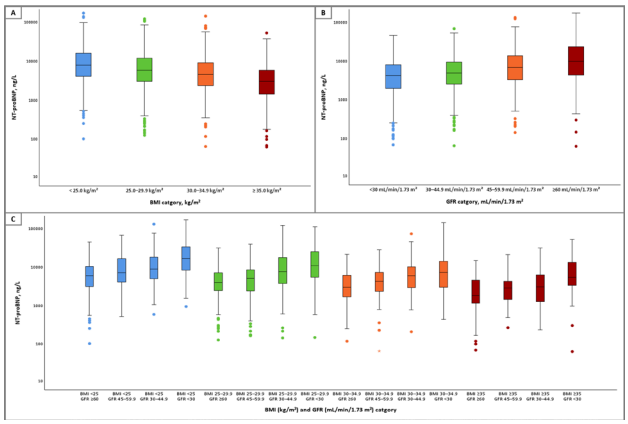

**Fig. 1 | 26-5** NT-proBNP Values Across (A) BMI, (B) GFR and (C) combination of BMI & GFR Categories

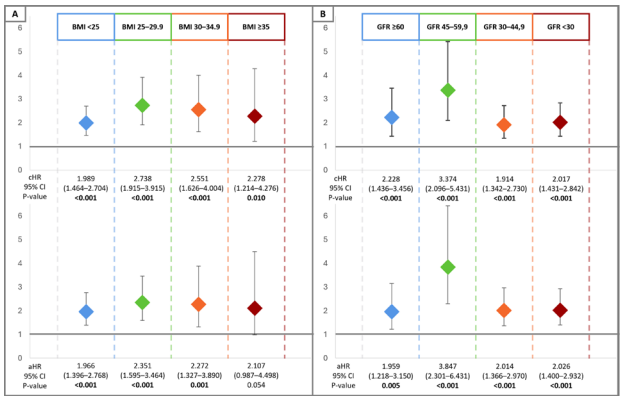


**Fig. 2 | 26-5** Crude and Adjusted Hazard Ratios for 1-Year Mortality according to log-transformed NT-proBNP levels across (A) BMI and (B) GFR Categories

higher in patients with advanced renal dysfunction (CKD G4/G5: 9604 vs CKD G1/2: 5225 ng/L).

**Conclusion:** In elderly patients with AHF, NT-proBNP levels were strongly influenced by both obesity and renal dysfunction. Optimal cutoff values for risk prediction varied substantially according to baseline BMI and eGFR, highlighting the need for BMI- and eGFR-specific thresholds.

## 26-6

### Screening study for early detection of cardiac amyloidosis (Find-CA Study)

**Schmid L., Kronberger C., Poledniczek M., Ermolaev N., Rettl R., Grubmüller A., Binder C., Badr Eslam R., Kammerlander A., Kastner J., Bergler-Klein J., Hengstenberg C., Duca F.**

Universitätsklinik für Innere Medizin II – Abteilung für Kardiologie, Wien, Austria

**Introduction:** Data on the prevalence of cardiac amyloidosis (CA) remain limited. With several effective disease-modifying therapies now available, early detection and timely initiation of treatment are essential for improving patient outcomes. Despite screening recommendations from the European Society of Cardiology (ESC) [1], systematic screening studies remain scarce, highlighting the need for improved screening strategies. This study aimed to prospectively assess the prevalence of CA in at-risk populations according to ESC recommendations and to address potential underdiagnosis while enabling early treatment initiation.

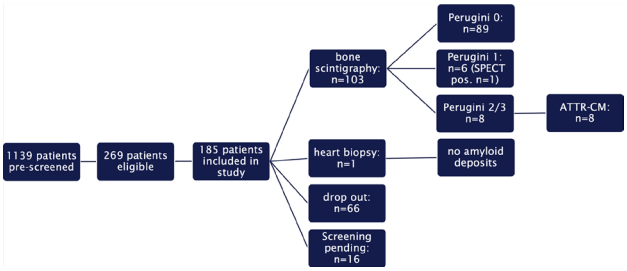


**Fig. 1 | 26-6**

**Methods:** Between November 15th 2024, and March 5th 2026, at-risk patients were enrolled in this prospective, non-interventional, single-center study. Recruitment was conducted in the general cardiology wards as well as in the echocardiography and cardiac magnetic resonance (CMR) imaging laboratories. Eligible patients who provided informed consent underwent CA screening according to current guideline recommendations.

**Results:** Of 1139 pre-screened patients, 269 were classified as at-risk, and 185 were enrolled in the study (64.3% male; median age 78 years) and scheduled for CA screening. Among these, 103 patients (55.7%) completed the full diagnostic workup, while results remain pending for 16 patients (8.6%). The remaining 66 patients (35.7%) were classified as dropouts due to withdrawal of consent or failure to attend scheduled screening examinations. Among patients who completed all screening procedures, transthyretin amyloid cardiomyopathy (ATTR-CM) was diagnosed in 8 cases (7.8%).

**Conclusion:** Prospective systematic screening of at-risk patients revealed a notable prevalence of previously unrecognized ATTR-CM. These findings highlight the potential value and challenges of structured screening strategies in detecting cardiac amyloidosis in clinical practice.

### References

1. Garcia-Pavia P, Rapezzi C, Adler Y, et al. Diagnosis and treatment of cardiac amyloidosis: a position statement of the ESC Working Group on Myocardial and Pericardial Diseases. Eur Heart J 2021;42(16):1554–1568. (In eng). https://doi.org/10.1093/eurheartj/ehab072.

## 26-7

### When Genetic Testing Strikes Twice: Cardiomyopathy in a 43-Year-Old Woman with Lamin A and Filamin C Mutations

**Bernreiter T.[1], Zizka J.[1], Medeiros-Domingo A.[2], Roithinger F.[1], Grübler M.[1]**

[1]UK Wiener Neustadt, Wiener Neustadt, Austria
[2]Swiss DNAlysis, 8600 Dübendorf, Switzerland

**Introduction:** In December 2025 a 45-year-old woman was referred to our heart failure outpatient clinic by her primary care internist for further evaluation. The referral was prompted by symptomatic premature ventricular contractions, reduced

exercise tolerance, and recurrent presyncope. For the past five years, she has experienced recurrent palpitations, which have markedly increased in several months. She now reports almost daily episodes of heart pounding occurring both at rest and during exertion. Until the summer of 2025, she had maintained a high level of physical activity; however, due to recurrent presyncope, she has significantly reduced her activity level. Family history revealed that her father underwent heart transplantation at the age of 48 and died at 62 years. Her uncle had a history of cardiac disease and died at the age of 50, and her grandfather died at 60 years of age. Detailed medical records or specific diagnoses are not available. Her medical history includes thyroidectomy in 2015 for Graves' disease. At the time of presentation, she was taking levothyroxine and a beta-blocker. In 2015, at the age of 32, she had undergone a 24-hour Holter monitoring for the first time, which revealed frequent (12.3%/24 h) premature ventricular and supraventricular beats, as well as short runs of ventricular tachycardia.

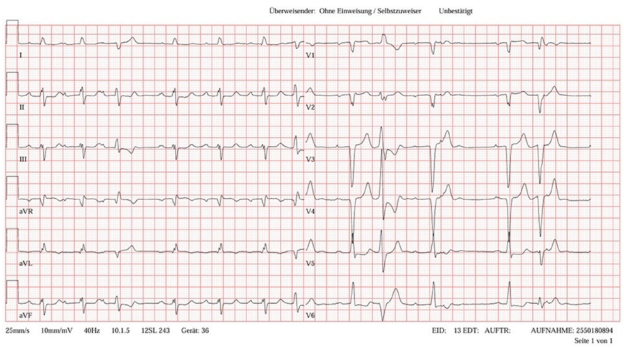


**Fig. 1 | 26-7** ECG


**Fig. 2 | 26-7** Late Enhancement in the basal anteroseptal and inferoseptal segments

**Methods:** The electrocardiogram demonstrated sinus rhythm at normal rate with first-degree atrioventricular block, absent R-wave progression up to V3, marked left axis deviation, and an intraventricular conduction delay. Pronounced left lateral repolarization abnormalities were present. Ventricular premature beats are already observed on the resting ECG. Laboratory testing was largely unremarkable, except for mildly reduced platelet count (142 G/L) and elevated NT-proBNP levels (517 pg/mL). Transthoracic echocardiography showed normal chamber dimensions and wall thickness. Left ventricular systolic function was low normal, with no regional wall motion abnormalities. Apart from mild mitral and tricuspid regurgitation, no valvular abnormalities were detected. Systolic pulmonary artery pressure was within the normal range. In accordance with current guideline recommendation a cardiac magnetic resonance imaging was performed as a next diagnostic step. It showed mild left ventricular dilatation and extensive non-ischemic, band-like subepicardial late gadolinium enhancement in the basal anteroseptal and inferoseptal segments. Left ventricular ejection fraction was 49%.

**Results:** Given the family history and the collected clinical findings, it was decided—after appropriate counseling—to proceed with genetic testing. Remarkably, two mutations were revealed: one in the Lamin A (LMNA) gene and one in the Filamin C (FLNC) gene. The LMNA gene mutation which has been previously reported in literature, is a heterozygous splice-site variant in the intron 6 and is classified as pathogenic according to ACMG criteria, c.1157 + 1G>A. Additionally, a heterozygous missense variant in the FLNC gene c.5426C>T in the exon 33 was detected, which has not been reported yet in the literature. It is classified as a variant of uncertain significance. Mutations in the FLNC gene are also considered highly arrhythmogenic. The clinical impact of concomitant variants in these genes remains insufficiently defined. The variant in the filamin C (FLNC) gene may contribute to the observed phenotype. Genotype–phenotype correlation studies in family members may help to further elucidate the clinical significance and impact of this variant, but unfortunately no residual tissue from diseased family members is available.

**Conclusion:** Due to the highly symptomatic premature ventricular contractions (PVCs), the patient underwent catheter ablation of ventricular ectopy in early March 2026. As LMNA and FLNC mutations are recognized as high-risk genotypes for malignant ventricular arrhythmias, even in the absence of severe left ventricular dysfunction, our Heart Team recommended the implantation of a dual-chamber implantable cardioverter-defibrillator (ICD). Furthermore, genetic testing using buccal swab samples was offered to the patient's sister as well as to her two daughters. Overlap cardiomyopathy associated with concomitant LMNA and FLNC mutations represents a potentially high-risk genetic substrate. Early electrical symptoms should prompt guideline-directed, genotype-informed risk stratification to optimize prevention of sudden cardiac death.

# POSTERSITZUNG 27 – KONGENITALE HERZERKRANKUNGEN & EMHA

## 27-1

### Pregnancy Outcomes in Women With Ebstein Anomaly: A Single-Centre Cohort Study

**Prausmüller S.[1], Gössinger B.[1], Karner E.[2], Binder-Rodriguez C.[1], Schlein J.[3], Hengstenberg C.[1], Bartko P.[1], Schrutka L.[1]**

[1]Medical University of Vienna, Department of Internal Medicine, Division of Cardiology, Wien, Austria
[2]Medizinische Universität Wien, Abteilung für Gynäkologie, Wien, Austria
[3]Medizinische Universität, Abteilung für Herzchirurgie, Wien, Austria

**Introduction:** Ebstein anomaly is a rare congenital heart defect characterised by apical displacement of the tricuspid valve with varying degrees of tricuspid regurgitation (TR) and right ventricular dysfunction. As survival into adulthood improves, increasing numbers of women with Ebstein anomaly reach reproductive age. However, data regarding pregnancy outcomes in this population remain limited. This study aimed to evaluate maternal cardiac outcomes and echocardiographic changes in women with Ebstein anomaly during and after pregnancy.

**Methods:** This retrospective single-centre cohort study was conducted at the Medical University of Vienna's specialised outpatient clinic for adults with congenital heart disease. Women with Ebstein anomaly who experienced pregnancy between 1998 and 2024 were included. Clinical characteristics, maternal cardiac events, and echocardiographic parameters before and after pregnancy were analysed.

**Results:** Among nine women with Ebstein anomaly and a history of pregnancy, complete pregnancy data were available for seven and included in the analysis. Three patients (43%) had previously undergone surgical correction with residual TR, while four (57%) had unrepaired or mild forms of the disease. The median age at first pregnancy was 31 years (IQR 25–36). Functional status remained stable, with six patients (86%) in NYHA class I and one patient (14%) in NYHA class II before and after pregnancy. Left and right ventricular systolic function were preserved in all patients. Before pregnancy, TR ≤ grade II was present in five patients (71%), whereas TR ≥ grade II–III was observed in four patients (57%) after pregnancy (Fig. 1). No major cardiovascular complications occurred during pregnancy or the postpartum period. One patient (14%) experienced an uncomplicated supraventricular tachycardia. Caesarean section was the predominant mode of delivery ($n=6$, 86%), while one patient (14%) delivered vaginally.

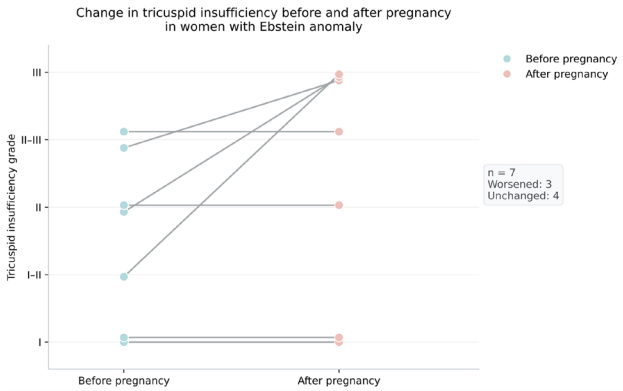


**Fig. 1 | 27-1** Tricuspid regurgitation severity before and after pregnancy in women with Ebstein anomaly. Each line represents an individual patient

**Conclusion:** In this single-centre cohort, pregnancy in women with Ebstein anomaly was associated with favourable maternal cardiac outcomes, with preserved ventricular function and no major cardiovascular complications. Although an increase in tricuspid regurgitation was observed in a subset of patients, overall cardiac status remained stable. These findings suggest that pregnancy can be well tolerated in women with Ebstein anomaly when managed in specialised centres with multidisciplinary care.

## 27-2

### Incidental Findings of Liver Lesions in Cardiac Magnetic Resonance Imaging Examinations in Patients with Congenital Heart Disease: a Pilot Study

**Hecke G.[1,2], Haase B.[3], Clodi N.[4,5], Hauptvogel K.[6], Plajer D.[2], Spogis J.[2], Boxhammer E.[4], Hanser A.[2], Schäfer J.[2], Nikolaou K.[2], Nordmeyer J.[2], Nordmeyer S.[2]**

[1]Universitätsklinik für Dermatologie, Salzburg, Austria
[2]Department für Radiologie, Radiologische Universitätsklinik, Tübingen, Germany
[3]Kreisklinik Reutlingen, Reutlingen, Germany
[4]Universitätsklinik für Innere Medizin II, Kardiologie und internistische Intensivmedizin, Salzburg, Austria
[5]Universitätsklinik für Radiologie, Salzburg, Austria
[6]Paracelsus Medizinisch Privatuniversität, Nürnberg, Germany

**Introduction:** During cardiac magnetic resonance imaging (cMRI) exams in patients with congenital heart disease (CHD) incidental findings of liver lesions are increasingly found. No systematic data, however, exist on the prevalence of liver lesions in patients with different CHD. In order to gain a first overview, we retrospectively analyzed cMRI examinations from the last 10 years at our institution.

**Methods:** CMRI examinations including T2 weighted images covering parts of the liver were performed in 899 patients with CHD at our institution between 2014 and 2024. cMRI exams were analyzed by a medical student, a pediatrician, a radiologist and a pediatric cardiologist. Liver lesions were defined as atypical liver parenchyma showing T2 hyper- or hypointensity compared to the surrounding liver tissue.

**Results:** Liver lesions were found in 9.5% (85/899) of all cMRI studies, were unknown at time of cMRI in 89% (76/85) of cases, T2 hyperintens in 96% (82/85) and larger than 1 cm in 38% (32/85). Patients with liver lesions were older (29 years vs. 22 years, $p<0.0001$), there were no sex differences in the prevalence of liver lesions or differences in right or left ventricular function (LVEF: 57% vs. 58%, $p=0.78$; RVEF: 55% vs. 54%, $p=0.35$). Patients with univentricular hearts, transposition of great arteries after atrial switch operation and atrial septal defects showed the highest prevalence (18%, 17%, 21%, respectively). However, also patients with left heart sided valve disease showed liver lesions in 9%.

**Conclusion:** Incidental findings of liver lesions in cMRI examinations of patients with CHD are reasonably high with almost 10%. In the growing population of adults with CHD, liver monitoring might be helpful to assure overall patient health.

## 27-3

### Shunt-Related Platelet Activation in Patients with Patent Foramen Ovale

**Gössinger B., Aynacioglu E., Salzmann M., Demirel C., Hengstenberg C., Lang I., Bartko P., Gerges C., Hohensinner P., Schrutka L.**

Medizinische Universität Wien, Universitätsklinik Innere Medizin II, Abteilung Kardiologie, Wien, Austria

**Introduction:** Patent foramen ovale (PFO) is present in about one-third of the population, and percutaneous PFO closure is recommended for the secondary prevention of cryptogenic stroke. Evidence suggests that patients with PFOs exhibit a prothrombotic phenotype, which is thought to be associated with an increased incidence of migraines and early-onset dementia. Percutaneous PFO closure has indeed been associated with improvements in migraine symptoms. However, the underlying mechanism remains unclear. Therefore, the study aimed to investigate whether platelets are activated at the site of PFO due to a left-to-right shunt, and if so, whether this activation ceases after PFO closure.

**Methods:** This prospective, single-centre, observational study included patients undergoing percutaneous PFO closure between February 2024 and January 2026. Blood samples were collected from the right atrium before and immediately after closure. We assessed platelet activation by quantifying adenosine diphosphate (ADP)-stimulated CD62P (*P*-selectin) expression using flow cytometry. Migraine was classified according to the International Classification of Diseases (ICD) criteria, and severity was assessed using the Migraine Disability Assessment (MIDAS) questionnaire and the Headache Impact Test (HIT-6).

**Results:** A total of 125 patients were included in the study. Mean age was 51.2 years (± SD 11.9) and 76 patients (60.8%) were male. Of those, 21 patients had migraines (16.8%), 15 (71.4%) of whom were female and six (28.6%) of whom were male. ADP stimulation revealed significantly higher CD62P+ count in samples from the right atrium before device closure, compared to samples collected immediately after closure ($p < 0.001$), with a mean reduction of 6.2% (± SD 5.9; Fig. 1). Further, multivariable linear regression analysis revealed a significant interaction between sex and migraine, indicating that female patients with migraines experienced a greater reduction in platelet activation following PFO closure (estimated effect size $\beta = 7.54$, 95% CI 1.58–13.49, $p = 0.014$).

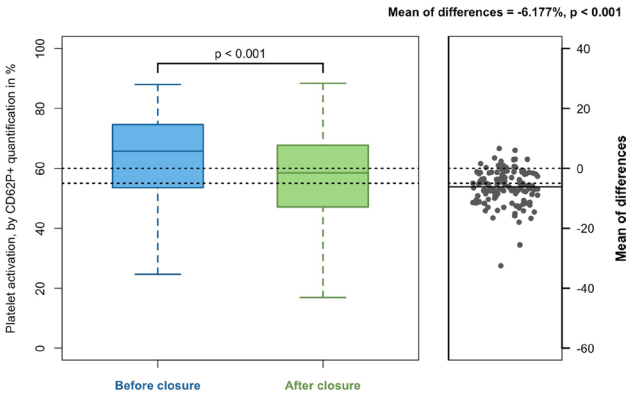


Fig. 1 | 27-3

**Conclusion:** Left-to-right shunt, as occurs in PFO, leads to measurable changes in platelet activation that decrease significantly immediately after PFO closure. These findings are particularly relevant for female patients with migraines, because our data support a sex-specific mechanism in which women with migraines appear to have a greater biological benefit from PFO closure.

## 27-4

### Outcomes after Ross Procedure over the Pediatric Age Spectrum—Autograft and Right-Ventricle-to-Pulmonary-Artery Conduit Durability

**Schlein J.[1], El-Shaer M.[1], Wollmann F.[2], Andreeva A.[1], Edlinger-Stanger M.[3], Binder C.[2], Gössinger B.[2], Vieth V.[4], Atteneder C.[1], Prausmüller S.[2], Werner P.[1], Urganci E.[1], Pees C.[4], Michel-Behnke I.[4], Base E.[3], Schrutka L.[2], Zimpfer D.[1]**

[1]Universitätsklinik für Herz- und Thorakale Aortenchirurgie, Medizinische Universität Wien, Wien, Austria
[2]Universitätsklinik für Innere Medizin II, Abteilung für Kardiologie, Medizinische Universität Wien, Wien, Austria
[3]Universitätsklinik für Anästhesie, Allgemeine Intensivmedizin und Schmerztherapie, Klinische Abteilung für Herz-Thorax-Gefäßchirurgische Anästhesie und Intensivmedizin, Medizinische Universität Wien, Wien, Austria
[4]Universitätsklinik für Kinder- und Jugendheilkunde, Abteilung für Kinderkardiologie, Medizinische Universität Wien, Wien, Austria

**Introduction:** During the Ross procedure the patient's native pulmonary valve is harvested as an autograft and translocated to the aortic position. The continuation from the right ventricle to the pulmonary artery (RV-PA) is restored with implantation of either a homograft or a biological valved conduit (xenograft). Durability of RV-PA conduits might be limited in younger patients due to patient-prosthesis-mismatch, especially in infants. There is a paucity of literature comparing the durability of the autograft between different pediatric age groups. Further insight on outcomes after Ross procedure in different pediatric age groups is warranted. We sought to describe outcomes after pediatric Ross procedure across different pediatric age groups at time of Ross procedure and also assess the influence of root-reinforced Ross procedure on outcomes in pediatric patients.

**Methods:** Ross procedure is performed since 1991 at our center. All patients aged < 18 years who have undergone a Ross or Ross Konno procedure between April 1991 and April 2020 were included. Parameters were obtained and measured as described in the Guidelines for Reporting Mortality and Morbidity after Cardiac Valve Interventions [1]. Early mortality was defined as death occurring within 30 days of surgery or prior to hospital discharge after Ross procedure. Mortality cross check via the national health insurance and was available for 97.1% of the included patients. Patients who were transferred from foreign centers for surgery could not be cross checked and were censored at the time of the last available follow-up data at the center. Kaplan-Meier analysis was used to asses time-related outcome events. Outcomes were compared between groups according to age at time of Ross

procedure: patients aged 0–11 months, patients aged 1–5 years, patients aged 6–13 years and patients aged 14–17 years. Additionally, autograft reoperation rate was analyzed for patients, who underwent root-reinforced Ross procedure.

**Results:** From April 1991 until April 2020 102 pediatric patients underwent a Ross ($n=88$) respectively Ross Konno procedure ($n=14$). The patients (70.6% male) had a median age of 10.1 (IQR 5.7–14.4) years and 66.8% of the patients had undergone a least one previous aortic valve intervention (percutaneous and surgical). All early deaths ($n=3$) occurred in patients aged 0–11 months ($p<0.001$). Overall survival did not differ ($p=0.263$) between the age groups with 83.3 ± 10.8% at 15 years in patients aged 0–11 months, 92.9 ± 6.9% at 15 years in patients aged 1–5 years, 94.8 ± 3.6% at 15 years in patients aged 6–13 years and 96 ± 3.9% at 15 years in patients aged 14–17 years. Freedom from RV-PA conduit reoperation differed ($p<0.001$)between age groups with 0% at 9 years in patients aged 0–11 months, 66.7 ± 19.2% at 20 years in patients aged 1–5 years, 75.8 ± 7.7% at 20 years in patients aged 6–13 years and 95.2 ± 4.6% at 20 years in patients aged 14–17 years. Freedom from autograft reoperation was 100% at 10 years in patients aged 0–11 months, 100% at 15 years in patients aged 1–5 years, 94.1 ± 4.1% at 15 years in patients aged 6–13 years and 82.8 ± 9.3% at 15 years in patients aged 14–17 years ($p=0.467$). In the age groups 6–13 years and 14–17 years, freedom from autograft reoperation was 100% at 8 years in patients, who underwent root-reinforced Ross procedure compared to 92 ± 3.8% at 10 years in patients without root-reinforcement ($p=0.577$).

**Conclusion:** Survival rates after pediatric Ross procedure are good. Early mortality occurred only in infancy. Unavoidably, somatic outgrowth leading to patient-prosthesis-mismatch limits the durability of RV-PA conduits in younger children. In the infancy cohort of patients aged 0–11 months the freedom from RV-PA reoperation was 0% at 9 years. No autograft reoperation occurred in patients aged 0–11 months and patients aged 1–5 years at 10 and 20 years respectively. Infants and young children have good long-term autograft durability regarding autograft dilatation and consecutive aortic valve regurgitation. In older children, who completed somatic growth the option of root-reinforcement might hinder autograft dilatation and prolong durability. In our cohort no autograft reoperation was observed at 8 years in patients, who underwent root-reinforced Ross procedure. The Ross-PEARS (Personalized External Aortic Root Support) procedure provides a more recent surgical approach to potentially reduce the risk of autograft dilatation and subsequent aortic regurgitation. It was only introduced after the study period at our center. The outcomes in the adult patient population are promising [2], and short- to mid-term outcomes in the pediatric population are to be awaited.

## References


1. Akins CW, Miller DC, Turina MI, Kouchoukos NT, Blackstone EH, Grunkemeier GL, et al. Guidelines for Reporting Mortality and Morbidity After Cardiac Valve Interventions. Ann Thorac Surg. 2008;85(4):1490–5.
2. Redondo A, Austin C. Our 7-Year Experience Supporting the Ross Autograft with the Novel Technique of Personalized External Aortic Root Support. Jtcvs Tech. 2024;24:121–7.


## 27-5

## Tunnelling from Suspected Fetal Cardiomyopathy to the Correct Diagnosis: A Neonatal Aortico-Ventricular Tunnel


**Narancsik Z.[1], Öffl N.[2], Köstenberger M.[1], Laufer G.[3], Sallmon H.[1], Kurath-Koller S.[1]**

[1]Klinische Abteilung für pädiatrische Kardiologie, Medizinische Universität Graz, Graz, Austria
[2]Klinische Abteilung für pädiatrische Kardiologie, LKH Graz, Graz, Austria
[3]Klinische Abteilung für Herzchirurgie, Medizinische Universität Graz, Graz, Austria


**Introduction:** Aortico-ventricular tunnel is a rare congenital extracardiac defect characterized by a channel connecting the ascending aorta above the sinotubular junction to a heart ventricle, bypassing the semilunar valves (1). The presence of the aortic orifice and absence of intramural course differentiate it from a ruptured sinus of Valsalva aneurysm and a coronary-cameral fistula, respectively (2). Usually, the left ventricle (LV) is involved with possible semilunar valve abnormalities. Timely surgical correction enables normalisation of the ventricle size and function (3).

**Methods:** We present a case of a term female newborn in whom fetal echocardiography revealed a dilated, functionally impaired LV and aortic dilation. Unfortunately the aortico-ventricular tunnel failed to be detected. Postnatally, no cardiac decompensation occurred and a diastolic murmur was detected. Echocardigraphy revealed a 4–5 mm tunnel connecting the aorta above the right sinus of Valsalva to the LV. The right coronary artery originated from the tunnel. Color Doppler demonstrated a large diastolic flow to the LV and a small flow into the right ventricle. The aortic valve was structurally normal and competent; the pulmonary valve showed mild dysplasia without significant stenosis.

**Results:** At 17 days of life, surgical closure of both tunnel orifices with tunnel resection and reimplantation of the right coronary artery were performed. Follow-up demonstrated a gradual normalisation of the LV size and function.

**Conclusion:** Although extremely rare, the case highlights the importance of detailed imaging for accurate anatomical delineation and prompt surgical correction, enabling a favourable outcome.

## References


1. Sun et al., ‚Characteristics and Long-Term Outcomes of Aortico-Left Ventricular Tunnel'.
2. McKay et al., ‚The Aorto-Ventricular Tunnels'.
3. Horváth et al., ‚Surgical Treatment of Aortico-Left Ventricular Tunnel'.

# POSTERSITZUNG 28 – KORONARE HERZKRANKHEIT & AKUTES KORONARSYNDROM 2

## 28-1

### Diabetes-specific Features in Machine Learning Prediction of Coronary Stenosis

**Schnetzer L.[1], Bermeitinger B.[2], Muendlein A.[1], Drexel H.[1,3,4,5], Saely C.[3,1,6], Leiherer A.[3,1,7]**

[1]Vorarlberg Institute for Vascular Investigation & Treatment (VIVIT), Feldkirch, Austria
[2]Institute of Computer Science in Vorarlberg, University of St.Gallen (HSG), Dornbirn, Austria
[3]Private University of the Principality of Liechtenstein, Triesen, Liechtenstein
[4]Drexel University College of Medicine, Philadelphia, Philadelphia, United States
[5]Vorarlberger Landeskrankenhausbetriebsgesellschaft, Feldkirch, Austria
[6]Department of Medicine I, Academic Teaching Hospital Feldkirch, Feldkirch, Austria
[7]Central Medical Laboratories Feldkirch, Feldkirch, Austria

**Introduction:** Coronary angiography is the gold standard for diagnosing coronary artery disease (CAD) but carries procedural risks. Predicting angiographic outcomes with machine learning (ML) can help avoiding unnecessary procedures, yet risk profiles may differ between persons with and without type 2 diabetes. We developed a ML model to predict angiographic findings, focusing on diabetes-specific differences in feature importance.

**Methods:** Clinical and laboratory data of 1472 patients was analyzed. Angiographic outcomes were classified as no (X0), non-significant (X1), or significant stenosis (X2). Multiple ML algorithms were compared, with gradient boosting machines achieving the best performance. SHAP-based feature importance ranks were assessed separately in persons with and without diabetes.

**Results:** The model demonstrated a sensitivity of 98% and a precision of 61% for X2 and for X0 28% and 76% respectively. Features showing the largest diabetes-specific rank differences in importance for X2 were urinary albumin, BMI and waist circumference (higher in persons with diabetes), and waist to hip ratio, Lp(a) and LDL-C/ApoB-ratio (higher in persons without diabetes).

**Conclusion:** The gbm-based model has the potential to reduce unnecessary invasive procedures in clinical practice. Diabetes-specific differences in predictive features are highlighted and suggest that tailored prediction models may improve the pre-angiographic assessment of CAD.

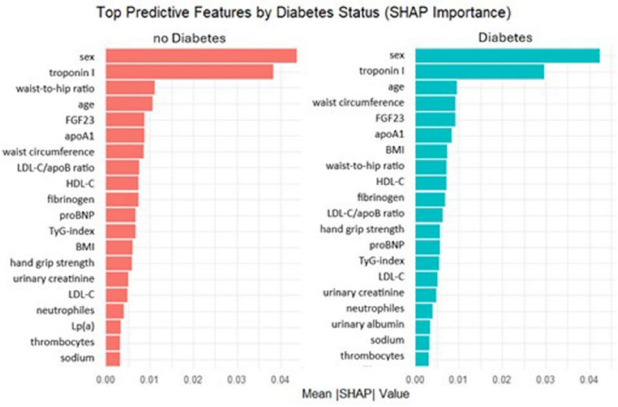


Fig. 1 | 28-1

## 28-2

### Sex-specific Features in Machine Learning Prediction of Coronary Stenosis

**Schnetzer L.[1], Bermeitinger B.[2], Muendlein A.[1], Drexel H.[1,3,4,5], Saely C.[3,1,6], Leiherer A.[3,1,7]**

[1]Vorarlberg Institute for Vascular Investigation & Treatment (VIVIT), Feldkirch, Austria
[2]Institute of Computer Science in Vorarlberg, University of St.Gallen (HSG), Dornbirn, Austria
[3]Private University of the Principality of Liechtenstein, Triesen, Liechtenstein
[4]Drexel University College of Medicine, Philadelphia, Philadelphia, United States
[5]Vorarlberger Landeskrankenhausbetriebsgesellschaft, Feldkirch, Austria
[6]Department of Medicine I, Academic Teaching Hospital Feldkirch, Feldkirch, Austria
[7]Central Medical Laboratories Feldkirch, Feldkirch, Austria

**Introduction:** Coronary angiography is the gold standard for diagnosing coronary artery disease (CAD) but carries procedural risks especially for patients with diabetes. Predicting angiographic outcomes with machine learning (ML) can help avoiding unnecessary procedures, yet risk profiles differ between women and men. We developed a ML model to predict angiographic findings, focusing on sex-specific differences in feature importance.

**Methods:** Clinical and laboratory data of 1472 patients was analyzed. Angiographic outcomes were classified as no (X0), non-significant (X1), or significant stenosis (X2). Multiple ML algorithms were compared, with gradient boosting machines achieving the best performance. SHAP-based feature importance ranks were assessed separately in women and men.

**Results:** The model achieved a sensitivity of 98% and a precision of 61% for X2 and 28% and 76% for X0 respectively. Features showing the largest sex-specific rank differences in importance for X2 were Cer(d18:1/24:0), HbA1c, waist-to-hip ratio, hand-grip strength, BMI, and LDL-C (higher in women), and fibrinogen, TyG index, proBNP, thrombocytes, and sodium (higher in men).

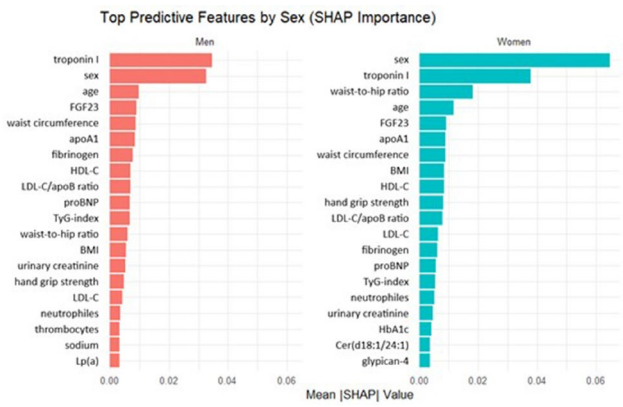


Fig. 1 | 28-2

**Conclusion:** The gbm-based model has the potential to reduce unnecessary invasive procedures in clinical practice. Sex-specific differences in predictive features are highlighted and suggest that tailored, sex-aware prediction models may improve the pre-angiographic assessment of CAD.

## 28-3

### Heterogeneity in definitions of acute coronary occlusion and possible implications: insights from a retrospective analysis

**Gallob F.[1,2], Barnaba M.[1], Strohhofer C.[3], Toth G.[3], Bugger H.[3], Verheyen N.[3], Mantawy S.[3], Sourij H.[4], von Lewinski D.[3], Markus W.[3]**

[1]Medizinische Universität Graz, Graz, Austria
[2]Zentrum für Akutmedzin, Universitätsklinikum Graz, Graz, Austria
[3]Universitätsklinik für Innere Medizin, Abteilung Kardiologie, Medizinische Universität Graz, Graz, Austria
[4]Universitätsklinik für Innere Medizin, Abteilung Endokrinologie und Diabetologie, Medizinische Universität Graz, Graz, Austria

**Introduction:** Acute coronary syndrome (ACS) has been categorized into the distinct entities of ST-segment elevation myocardial infarction (STEMI), Non-ST-segment elevation myocardial infarction (NSTEMI) and unstable angina pectoris (UAP). In this concept the presence of ST-elevation criteria entails immediate reperfusion, whereas patients without ST-elevation have varying delays to angiography and reperfusion.[1] Importantly, the severity of the underlying pathology (reduced or absent blood flow through a coronary artery) does not in itself define the distinction of ACS entities, yet ST-elevation criteria have been adopted as a surrogate marker of ongoing coronary occlusion.[2] However, in a review of 40,777 patients with NSTEMI a total coronary occlusion was observed in 25%, despite the absence of ST-elevation. This total occlusion was associated with significantly worse outcomes.[3] Therefore, new modalities including new ECG patterns, risk modifiers, echocardiography or utilisation of artificial intelligence have been proposed to identify acute coronary occlusion in patients without ST-eleva-

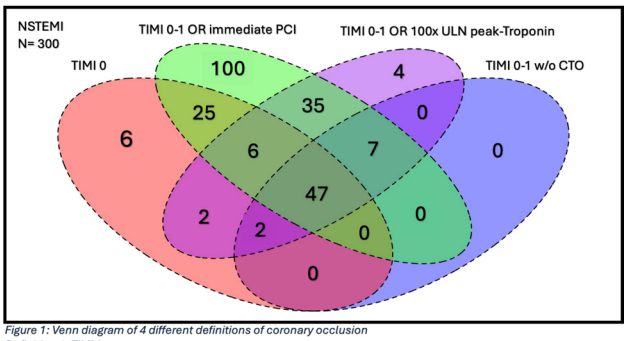


*Figure 1: Venn diagram of 4 different definitions of coronary occlusion*
*Definition 1: TIMI 0*
*Definition 2: TIMI 0-1 of the infarct-related artery without evidence of a chronic occlusion*
*Definition 3: TIMI 0-1 of the infarct-related artery OR immediate percutaneous coronary intervention on angiography*
*Definition 4: TIMI 0-1 of the infarct-related artery OR TIMI 2-3 of the infarct-related vessel AND peak Troponin measurement higher than 100 times the upper limit of normal*

**Fig. 1 | 28-3** Venn diagram of 4 different definitions of coronary occlusion

**Table 1 | 28-3** Definitions of acute coronary occlusion

| Definition | Modality of identification under investigation | Positivity rate in 300 NSTEMI patients |
|---|---|---|
| TIMI 0 | Risk factors for total coronary occlusion | 28,7 % |
| TIMI 0 without evidence of a chronic occlusion | ST-elevation in lead aVR | 15,7 % |
| TIMI 0–1 without evidence of a chronic occlusion | • Strain echocardiography<br>• ECG criteria for subtle anterior infarction (4 variable-formula) | 18,0 % |
| • TIMI 0–1 of the infarct-related artery OR<br>• angiographic evidence of coronary thrombosis and peak cardiac troponin I ≥ 10.0 ng/mL or T ≥ 1.0 ng/mL | Modified Sgarbossa criteria for paced rhythms or for left bundle branch block | 33,7 % |
| • TIMI 0–2 of the infarct related artery OR<br>• TIMI 3 flow culprit with peak troponin T ≥ 1.0 ng/mL or I ≥ 10.0 ng/mL | • Expert ECG interpretation for occlusion myocardial infarction<br>• Ischemic ST-Segment Depression Maximal in V1-V4 | 40,0 % |
| • TIMI 0–2 of the infarct related artery OR peak Troponin I > 10 ng/mL OR<br>• new wall motion abnormalities AND peak Troponin I > 10 ng/mL IF no angiography is available | • Posterior leads V7-V9 | NA |
| • TIMI 0–1 of the infarct related artery OR<br>• TIMI 2 AND >70 % stenosis AND peak 4th generation troponin of 5-10 ng/ml | • Artificial intelligence-based ECG analysis with generation of both a dichotomized analysis and a risk score | NA |
| • TIMI 0 of the infarct related artery OR<br>• acute coronary lesion with TIMI 1–3 and troponin rise and fall above the 99th percentile upper reference limit | • Barcelona criteria for left bundle branch block | 90,3 % |
| • TIMI 0–1 of the infarct related artery OR<br>• acute coronary lesion with TIMI 2–3 with emergent or urgent percutaneous revascularization | • Artificial intelligence-based ECG analysis | 73,3 % |
| Adjudication of the outcome by blinded reviewers | • Artificial intelligence-based ECG analysis<br>• Aslanger pattern | NA |

NA: not available (for these definitions no calculation could be performed in the NSTEMI sample, since at least one item of the definition was not captured in the available data) NSTEMI: Non-ST elevation myocardial infarction TIMI: Thrombolysis in myocardial infarction

tion and hence facilitate timely reperfusion. Yet definitions of specific entities that should be detected by these new modalities are inconsistent. The aim of this study is to assess various definitions of acute coronary occlusion and to investigate the differences and overlap between these definitions, when they are applied to a sample of 300 patients with NSTEMI.

**Methods:** An informal literature search was conducted for contemporary publications on the rapid identification of acute coronary occlusion. Identified publications were screened for their definition of acute coronary occlusion. These definitions were used in a sample of 300 subsequent NSTEMI patients that have been treated in the catheter laboratory in the university hospital Graz from January 2022 onwards. The positivity rate is presented for each definition. The overlap and differences between 4 selected distinct definitions are presented as Venn diagram. These data were part of a prior study that received approval of the ethics committee of the medical university of Graz (36–161 ex 23/24).

**Results:** First, we identified an inconsistency in the labelling of the outcome under investigation. Commonly used terms are acute coronary occlusion, total coronary occlusion, occlusion myocardial infarction or acute myocardial infarction needing revascularisation. For these various terms 10 different definitions were identified and are summarised in table 1. The publications offered limited justification for the definitions used. All definitions include angiographic features with usage of the "Thrombolysis in Myocardial Infarction" (TIMI) score. To account for the possibility of a spontaneous or medically induced reperfusion of an occluded artery prior to angiography, many definitions include peak troponin levels as markers for the extent of myocardial damage. In some publications, a standardized definition was omitted due to the aforementioned issue of reperfusion before angiography; instead, blinded expert adjudication was applied that was based on all available relevant clinical information. The positivity rates of the definitions varied between 15.7% and 90.3% in the sample of 300 NSTEMI patients. Only 47 patients were classified as acute coronary occlusions by all definitions. In comparison to this overlap, the difference between the most restricted and the most liberal definition were 224 patients. The overlap and differences of 4 distinct and commonly used definitions are presented in Fig. 1.

**Conclusion:** We found considerable inconsistency in the medical literature regarding what constitutes an acute coronary occlusion and how it is labelled. These inconsistencies in terminology and definitions lead to heterogeneous study results and consequently limit the generalizability of clinical implications. However, this may also reflect the persistent uncertainty concerning the extent of myocardial ischemia that benefits from immediate reperfusion versus deferred angiography. Ultimately, the optimal timing of reperfusion across the spectrum of patients with ACS will remain uncertain until adequately powered randomized trials provide robust evidence across various patient subgroups. Importantly, due to the retrospective design of most studies on the identification of acute coronary occlusion, the definition of acute coronary occlusion must be determined prior to the analysis to avoid overfitting of diagnostic performance through post-hoc selection of convenient outcome definitions.

## References


1. Byrne RA, Ireland C, Rossello X, Coughlan JJ, Ireland TFC, Barbato E, et al. ESC Guidelines for the management of acute coronary syndromes. Eur Heart J. 2023;2023(00):1–107.
2. Avdikos G, Michas G, Smith SW. From Q/Non-Q Myocardial Infarction to STEMI/NSTEMI: Why It's Time to Consider Another Simplified Dichotomy; a Narrative Literature Review. Arch. Acad Emerg Med. 2022;10:1–12. https://doi.org/10.22037/aaem.v10i1.1783.
3. Khan AR, Golwala H, Tripathi A, Bin Abdulhak AA, Bavishi C, Riaz H, et al. Impact of total occlusion of culprit artery in acute non-ST elevation myocardial infarction: A systematic review and meta-Analysis. Eur Heart J. 2017;38:3082–9. https://doi.org/10.1093/eurheartj/ehx418.


## 28-4

## The oral microbiome in patients with different stages of coronary artery disease


**Glantschnig T.[1], Pöttler M.[1], Horvath A.[2], Krois A.[1], Trummer-Herbst V.[1], Stadlbauer-Köllner V.[2], Zirlik A.[1], Kirnbauer B.[3], Kargl J.[4], Rainer P.[1]**

[1]Medizinische Universität Graz, Abteilung für Kardiologie, Graz, Austria
[2]Medizinische Universität Graz, Abteilung für Gastroenterologie und Hepatologie, Graz, Austria
[3]Medizinische Universität Graz, Univ.– Klinik für Zahnmedizin und Mundgesundheit, Graz, Austria
[4]Medizinische Universität Graz, Lehrstuhl für Pharmakologie, Graz, Austria


**Introduction:** The human gut and oral microbiome impacts atherosclerosis.(1,2) We hypothesize that microbiome dysbiosis drives systemic inflammatory responses and thereby plaque stability. Here, we assessed oral and gut microbiota composition in stable vs unstable coronary artery disease.

**Methods:** We recruited 110 patients in 3 different groups: Group A, patients with acute myocardial infarction with ST-elevation. Group B, chronic coronary syndrome (CCS), Group C included patients without known atherosclerotic disease, but with pre-existing CV risk factors. Baseline characteristics as age, sex, BMI, pre-existing treated or not treated CV risk factors, and pre-medication were noted. We further collected blood, stool and deep gingival samples in 98 of the participants. 16S sequencing was used to analyze microbiota patterns.

**Results:** In oral samples, several genera were identified to be differentially abundant between the groups. The genera Streptococcus and Rothia were more abundant in healthy oral samples compared to the CAD groups. Gingival microbiomes of patients with CCS were associated with the genera Anaeroglobus, Oribacterium and Bifidobacterium. Patients with STEMI showed higher levels of F0058, Desulfobulbus, Catonella, Blautia and Peptococcus (Fig. 1). Streptococcus shows a gradual

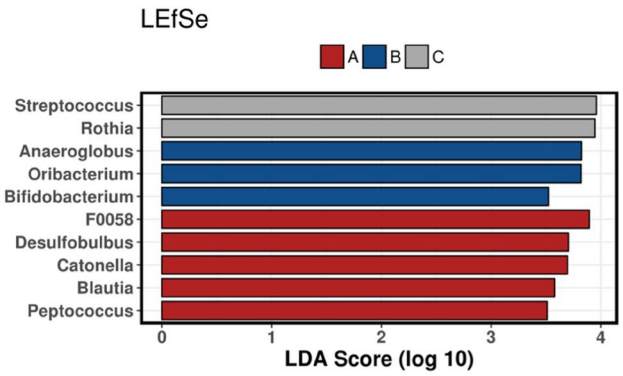


**Fig. 1 | 28-4** LEfSe results for gingival samples analyzed according to the group affiliation

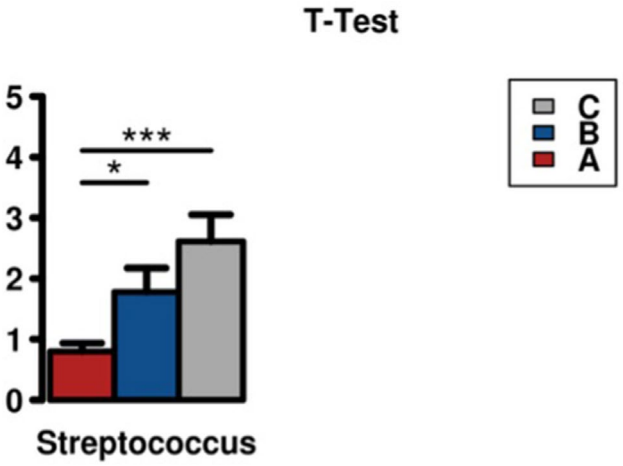


**Fig. 2 | 28-4** ANCOM selected Streptococcus to be differentially abundant in gingival samples from patients with STEMI compared to stable patients and healthy controls

decrease from healthy controls over CCS patients to patients with STEMI (Fig. 2).

**Conclusion:** In our study, oral microbiota were differentially expressed according to CAD disease status. Streptococcus are known commensals of a healthy oral microbiome (3) and where more abundant in healthy controls. We speculate that oral microbiota dysbiosis drives atherosclerosis progression and plaque stability.

## References

1. Tang WHW, Kitai T, Hazen SL. Gut Microbiota in Cardiovascular Health and Disease. Circ Res. 2017;31;120(7):1183. Mar.
2. Fusco W, Adolph T, Cammarota G, Gasbarrini A, Ianiro G, Tilg H. Gut microbiota and atherosclerosis. Gut. 2025;11;63(12):1209–15. Jul.
3. Baty JJ, Stoner SN, Commensal Streptococci SJAO. Gatekeepers of the Oral Cavity. J Bacteriol. 2022;15;204(11):e25722. Nov.

# 28-5

## Admission C-Reactive Protein and Mortality After STEMI: A Retrospective Cohort Study Identifying Subgroup-Specific Risk Thresholds

**Kopp K.[1], Leitner M.[1], Clodi N.[1,2], Lichtenauer M.[1], Hammerer M.[1], Prinz E.[1], Wintersteller W.[1], Hoppe U.[1], Brandt M.[1], Boxhammer E.[1]**

[1]Universitätsklinik für Innere Medizin II, Kardiologie und internistische Intensivmedizin, Salzburg, Austria
[2]Universitätsklinik für Radiologie, Salzburg, Austria

**Introduction:** Inflammation plays a central role in myocardial injury and repair after ST-segment elevation myocardial infarction (STEMI). C-reactive protein (CRP) is an established biomarker of systemic inflammation; however, clinically relevant risk thresholds are commonly applied uniformly and may not reflect differences across patient subgroups.

**Methods:** In this retrospective cohort study, 958 consecutive STEMI patients admitted between 2018 and 2020 were analyzed. Admission CRP was measured prior to reperfusion and categorized into four groups (< 5.0, 5.0–9.9, 10.0–14.9, and ≥ 15.0 mg/dl). Mortality was assessed at 30, 90, and 180 days, as well as at 1, 3, and 5 years. Kaplan–Meier analyses and Cox regression models were used to evaluate associations between CRP and mortality. Receiver operating characteristic (ROC) analyses were performed to assess discrimination and identify optimal cut-offs across subgroups.

**Results:** Higher admission CRP levels were consistently associated with increased mortality across all time points, with the highest risk observed in patients with CRP ≥ 15 mg/dl compared with the reference group (< 5.0 mg/dl). For short-term mortality (30–180 days), CRP demonstrated moderate but significant discrimination (AUC 0.628–0.654; all $p < 0.001$). Importantly, CRP risk thresholds were not uniform but varied substantially across clinical subgroups. In diabetic patients, lower CRP levels (approximately 5–6 mg/dl) were already associated with increased mortality risk and showed the highest discriminatory performance (AUC up to 0.714). Similarly, younger patients

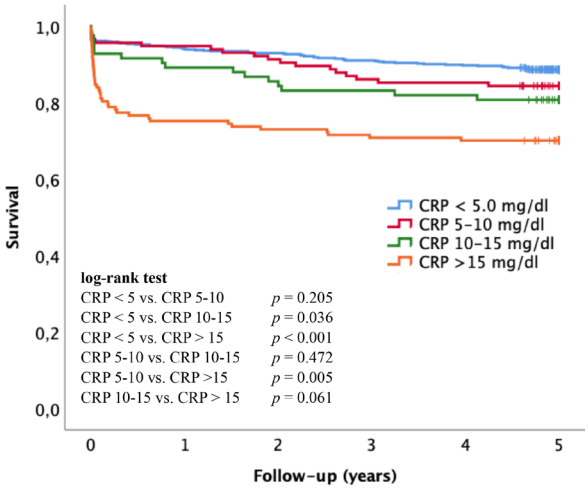


**No. at Risk**

| | | | | | | |
|---|---|---|---|---|---|---|
| CRP < 5 | 623 | 586 | 579 | 567 | 559 | 474 |
| CRP 5-10 | 115 | 109 | 105 | 99 | 98 | 83 |
| CRP 10-15 | 83 | 74 | 71 | 69 | 68 | 56 |
| CRP > 15 | 137 | 103 | 100 | 97 | 96 | 88 |
| Overall | 958 | 872 | 855 | 832 | 821 | 701 |

**Fig. 1 | 28-5** Kaplan-Meier Curve


**Fig. 2 | 28-5** Cox Regression Analysis (30d to 5y) according to Subgroups

and smokers exhibited lower risk thresholds compared with the overall cohort, whereas higher thresholds were observed in older patients. These findings indicate a context-dependent relationship between inflammatory burden and mortality risk.

**Conclusion:** Admission CRP is associated with short-term and long-term mortality after STEMI. However, CRP risk thresholds are context-dependent and differ across clinical subgroups. Lower CRP levels already confer increased risk in vulnerable populations such as patients with diabetes, younger age, and smoking, suggesting that individualized interpretation of inflammatory markers may improve risk stratification.

## 28-6

### Immunological Phenotypes and Cardiovascular Risk in Coronary Artery Disease

**Wüster D.[1], Anto Michel N.[1], Verheyen N.[1], Horstmann H.[2,3,4], Wolf D.[2,3], Binder C.[5], Zirlik A.[1], Peikert A.[1]**

[1]Department of Cardiology, University Heart Center Graz, Medical University of Graz, Graz, Austria
[2]Cardiology and Angiology, University Heart Center, University Medical Center, Freiburg, Germany
[3]Faculty of Medicine, University of Freiburg, Freiburg, Germany
[4]Department of Medicine, Division of Cardiology, NYU Grossman School of Medicine, New York, United States
[5]Department of Laboratory Medicine, Medical University of Vienna, Wien, Austria

**Introduction:** Coronary artery disease (CAD) is driven by chronic vascular inflammation mediated by traditional and non-traditional risk factors. While current cardiovascular risk assessment lacks precision on an individual level, distinct and potentially modifiable immunological phenotypes linked to specific risk factor profiles may improve risk stratification and prediction of adverse cardiovascular events beyond conventional measures.

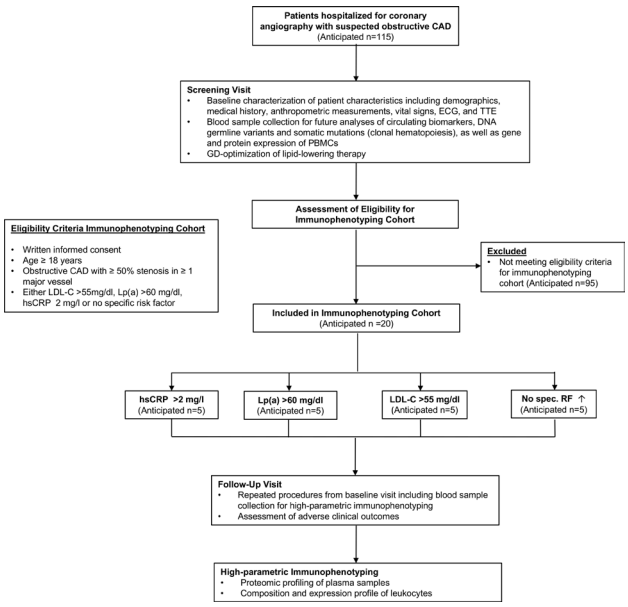


**Fig. 1 | 28-6**

**Methods:** This prospective cohort study aims to characterize participants hospitalized for coronary angiography with suspected obstructive CAD (Fig. 1). Patient characteristics and blood samples for future analyses of circulating biomarkers, genetics, and PBMCs will be collated at screening. A total of 20 patients with established diagnoses of obstructive CAD will be stratified into four groups of patients with either elevated levels of LDL-C, Lp(a), or hsCRP, and a control group comprising patients exhibiting either none or optimally controlled risk factors. In patients with elevated levels of LDL-C, lipid-lowering therapy will be optimized according to current guidelines. Circulating biomarkers (including markers of oxidative stress, inflammasome activation, and extracellular vesicle profiles), germline DNA variants and somatic mutations (clonal hematopoiesis), as well as gene and protein expression patterns of blood leukocytes (based on single-cell RNA sequencing), will be determined at baseline and after 12 months. High-parametric immunophenotyping readouts will be compared between groups at baseline, and associations between therapy-related changes in LDL-C and changes in high-parametric immunophenotyping readouts through 12 months will be analyzed. Exploratory analyses will further examine the associations between baseline immunophenotypes and adverse CV events.

**Results:** The study protocol has been finalized, and institutional review board and ethics committee review is currently in progress. Patient enrollment is projected to commence in mid-2026.

**Conclusion:** This study will determine immunological phenotypes of CAD patients according to individual risk factor profiles, evaluate the impact of risk factor modification on these phenotypes, and explore their association with adverse cardiovascular outcomes, potentially enhancing personalized cardiovascular risk stratification.

# POSTERSITZUNG 29 – RISIKOFAKTOREN, PRÄVENTION, STOFFWECHSEL & LIPIDOLOGIE 2

## 29-1

### PCSK9 inhibition reduces LDL-C/ApoB discordance at guideline LDL-C targets: patient-level and within-patient analyses

**Bernhard J., Wollmann F., Hengstenberg C., Speidl W., Krychtiuk K.**

Medizinische Universität Wien, AKH, Universitätsklinik für Innere Medizin II, Klinische Abteilung für Kardiologie, Wien, Austria

**Introduction:** Introduction: LDL cholesterol (LDL-C) target attainment may not reflect residual atherogenic particle burden when apolipoprotein B (ApoB) remains elevated [1–3]. The prevalence of LDL–ApoB discordance at very low LDL-C and its modification by PCSK9 inhibition in routine care are incompletely characterized. Our aim was therefore to quantify LDL–ApoB discordance across lipid-lowering therapy intensities at recommended LDL-C targets and to assess within-patient changes after addition of a PCSK9 inhibitor.

**Methods:** We analyzed a tertiary lipid clinic cohort using a patient-level design (latest visit per patient). Discordance was defined as LDL-C < 40 mg/dL with ApoB ≥ 65 mg/dL and LDL-C < 55 mg/dL with ApoB ≥ 80 mg/dL. Lipid lowering ther-

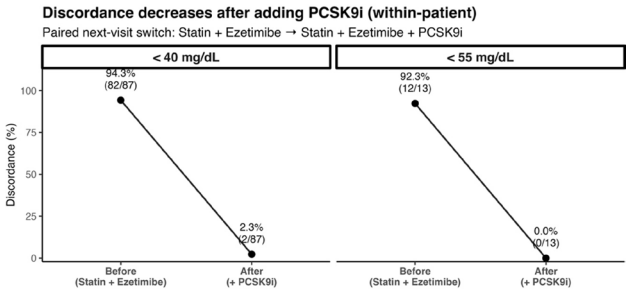


**Fig. 1 | 29-1** Discordance decreases after adding PCSK9i

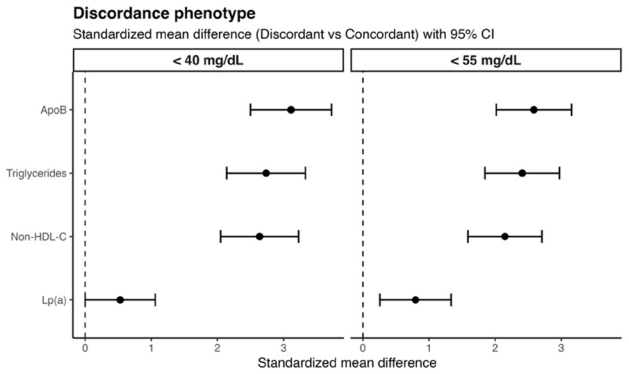


**Fig. 2 | 29-1** Discordance phenotype

apy was categorized as statin mono-therapy, statin + ezetimibe, or statin + ezetimibe + PCSK9 inhibitor. A pooled comparison combined non-PCSK9i therapies (statin ± ezetimibe) versus triple therapy including PCSK9i. Group differences were tested with Fisher's exact test.

**Results:** At LDL-C < 40 mg/dL, discordance was present in 17.6% (13/74) with statin ± ezetimibe versus 1.7% (2/119) with triple lipid-lowering therapy ($p < 0.001$). At LDL-C < 55 mg/dL, discordance occurred in 6.9% (14/204) with statin ± ezetimibe versus 0.0% (0/141) with triple therapy ($p < 0.001$). Phenotype profiling showed that discordant patients had a consistent atherogenic signature: triglycerides and non-HDL-C were higher in discordant versus concordant individuals across both LDL targets, whereas Lp(a) was only modestly higher, indicating that discordance at target LDL-C is predominantly associated with a remnant/metabolic profile with a smaller genetically mediated contribution.

**Conclusion:** In patients who achieve ESC LDL-C targets, ApoB frequently remains above guideline-aligned thresholds under statins ± ezetimibe, indicating residual atherogenic particle burden despite "on-target" LDL-C. PCSK9i-based intensification is associated with near-elimination of discordance at both < 55 and < 40 mg/dL thresholds. These data suggest that, among LDL-C target achievers, discordance is enriched in patients with higher triglycerides and non-HDL-C, consistent with cholesterol-depleted but ApoB-rich particles (remnant/VLDL-related burden) despite low LDL-C. Lp(a) may contribute in a subset, but the stronger TG/non-HDL-C signal supports a pragmatic approach in which ApoB assessment is prioritized when triglycerides or non-HDL-C remain elevated and LDL-C is already at guideline target.

## References

1. Johannesen CDL, Mortensen MB, Nordestgaard BG, Langsted A. Discordance analyses comparing LDL cholesterol, Non-HDL cholesterol, and apolipoprotein B for cardiovascular risk estimation. Atherosclerosis. 2025 Apr;403:119139. https://doi.org/10.1016/j.atherosclerosis.2025.119139. Epub 2025 Feb 17. PMID: 40073776.
2. Glavinovic T, Thanassoulis G, de Graaf J, Couture P, Hegele RA, Sniderman AD. Physiological Bases for the Superiority of Apolipoprotein B Over Low-Density Lipoprotein Cholesterol and Non-High-Density Lipoprotein Cholesterol as a Marker of Cardiovascular Risk. J Am Heart Assoc. 2022 Oct 18;11(20):e025858. https://doi.org/10.1161/JAHA.122.025858. Epub 2022 Oct 10. PMID: 36216435; PMCID: PMC9673669.
3. Peng AW, Gianos E, Shapiro MD, Navar AM, Zahid S, Marvel FA, Blaha MJ, Rodriguez F, Soffer DE, Morris PB, Blumenthal RS, Martin SS. Prevalence of Apolipoprotein B and LDL Cholesterol Discordance: Insights From the VLDbL and NHANES. Circulation. 2026 Jan 27;153(4):290–293. https://doi.org/10.1161/CIRCULATIONAHA.125.077998. Epub 2025 Nov 9. PMID: 41206821.

# 29-2

## The Triglyceride–Glucose Index Predicts the Development of Type 2 Diabetes Mellitus in Patients Without Lipid-Lowering Therapy

**Plattner T.[1,2,3], Vonbank A.[3,2,1], Larcher B.[3,1], Mader A.[3,1], Schnetzer L.[1], Neyer M.[1], Vogel J.[1], Elsner P.[2], Muendlein A.[1], Leiherer A.[2,1,4], Festa A.[1], Drexel H.[1,2,5,6], Saely C.[2,1,3]**

[1]Vorarlberg Institute for Vascular Investigation & Treatment (VIVIT), Feldkirch, Austria
[2]Private University of the Principality of Liechtenstein, Triesen, Liechtenstein
[3]Department of Medicine I, Academic Teaching Hospital Feldkirch, Feldkirch, Austria
[4]Central Medical Laboratories Feldkirch, Feldkirch, Austria
[5]Drexel University College of Medicine, Philadelphia, Philadelphia, United States
[6]Vorarlberger Landeskrankenhausbetriebsgesellschaft, Feldkirch, Austria

**Introduction:** The triglyceride–glucose (TyG) index is a reliable biomarker of insulin resistance and is associated with metabolic syndrome and type 2 diabetes mellitus (T2 DM), but prospective data on its power to predict the incidence of T2 DM are sparse. Lipid-lowering drugs reduce the TyG index and are therefore important confounders in studies addressing its impact on clinical outcomes.

**Methods:** We therefore prospectively recorded incident diabetes over 4 years in 704 consecutive non-diabetic Caucasian patients who were not taking lipid-lowering medications at baseline. Diabetes was diagnosed according to American Diabetes Association (ADA) criteria.

**Results:** At baseline, 34.9% of participants met the diagnostic criteria for the metabolic syndrome (MetS). The TyG index was significantly higher in patients with the MetS compared with those without the MetS (8.43 [8.15–8.69] vs. 9.03 [8.79–9.29]; $p < 0.001$). During follow-up, 101 individuals developed diabetes, corresponding to 10.8% of the study population. The TyG index was strongly predictive for incident diabetes both in univariate analysis (OR 1.79 [1.44–2.21]; $p < 0.001$) and after multivariable adjustment for age, sex, smoking, BMI and MetS (OR 1.47 [1.11–1.94]; $p = 0.007$).

**Conclusion:** In conclusion, the TyG index strongly and independently predicts the development of T2 DM in individuals not receiving lipid-lowering therapy.

## 29-3

### Adherence to lipid-lowering therapy measured by proportion of days covered in patients with and in subjects without type 2 diabetes following coronary angiography

**Neyer M.[1], Vogel J.[1], Elsner P.[2], Vonbank A.[3,2,1], Mader A.[3,1], Larcher B.[3,1], Muendlein A.[1], Schnetzer L.[1], Festa A.[1], Leiherer A.[2,1,4], Drexel H.[1,2,5,6], Saely C.[2,1,3]**

[1]Vorarlberg Institute for Vascular Investigation & Treatment (VIVIT), Feldkirch, Austria
[2]Private University of the Principality of Liechtenstein, Triesen, Liechtenstein
[3]Department of Medicine I, Academic Teaching Hospital Feldkirch, Feldkirch, Austria
[4]Central Medical Laboratories Feldkirch, Feldkirch, Austria
[5]Drexel University College of Medicine, Philadelphia, Philadelphia, United States
[6]Vorarlberger Landeskrankenhausbetriebsgesellschaft, Feldkirch, Austria

**Introduction:** Medication adherence in chronic cardiovascular disease is reported to be low, particularly regarding lipid-lowering therapy. To date, no gold-standard for adherence measurement has been established. To estimate adherence, we calculated proportions of days covered (PDC) from filled prescriptions in cardiovascular high-risk patients with and without type 2 diabetes (T2 DM).

**Methods:** The filled prescriptions of 220 patients within a year following elective coronary angiography for the evaluation of suspected or established coronary artery disease were analyzed using the ATC classification. Lipid-lowering therapy was defined as medication with code C10 and PDC ≥ 80% as probable adherence.

**Results:** In total, 89.1% ($n = 196$) of patients had at least one lipid-lowering drug in their discharge medication, and 33.2% ($n = 65$) had T2 DM according to ADA criteria. Of these, 16.9% patients with ($n = 11$) and 10.7% of subjects without T2 DM ($n = 14$) never filled a prescription for a lipid-lowering drug during the one-year observation period ($p = 0.218$). Based on PDC, adherence was significantly higher in patients with T2 DM than in those who did not have diabetes (67.6% vs. 45.9%; $p = 0.027$). This result was confirmed after adjustment for potential confounders in logistic regression analysis (OR = 2.14; 95% CI, 1.05–5.54).

**Conclusion:** In conclusion, adherence to lipid-lowering therapy measured by proportion of days covered is higher in patients with T2 DM than in subjects who do not have diabetes over one year following coronary angiography.

## 29-4

### Prognostic Value of the Endothelial Activation and Stress Index (EASIX) in Patients Undergoing TAVI: Results of a Real World Cohort

**Haidbauer V.[1], Clodi N.[1,2], Lichtenauer M.[1], Hoppe U.[1], Hammerer M.[1], Boxhammer E.[1]**

[1]Universitätsklinik für Innere Medizin II, Kardiologie und internistische Intensivmedizin, Salzburg, Austria
[2]Universitätsklinik für Radiologie, Salzburg, Austria

**Introduction:** The Endothelial Activation and Stress Index (EASIX) has emerged as a biomarker reflecting endothelial dysfunction, inflammation, and systemic vulnerability. Data on its long-term prognostic relevance in transcatheter aortic valve implantation (TAVI) remain limited. The aim of this study was to evaluate the prognostic value of EASIX for long-term mortality after TAVI and to examine its performance across clinical phenotypes.

**Methods:** In this retrospective real-world cohort, consecutive patients undergoing transfemoral TAVI between 2016 and 2022 were analyzed. Baseline EASIX was calculated, and receiver

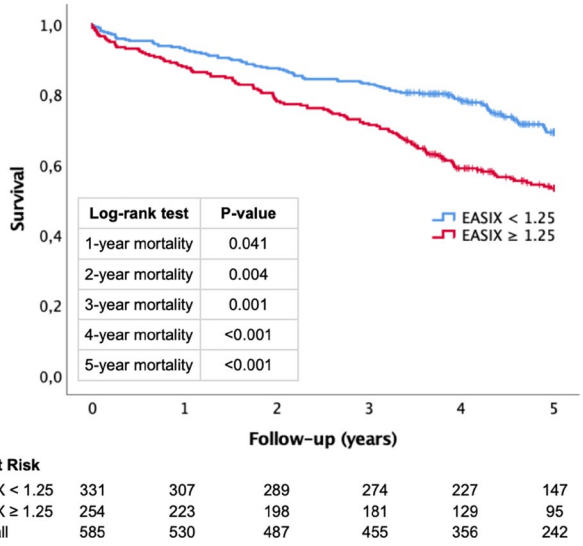


**Fig. 1 | 29-4** Kaplan–Meier survival curves stratified by ROC-derived EASIX threshold

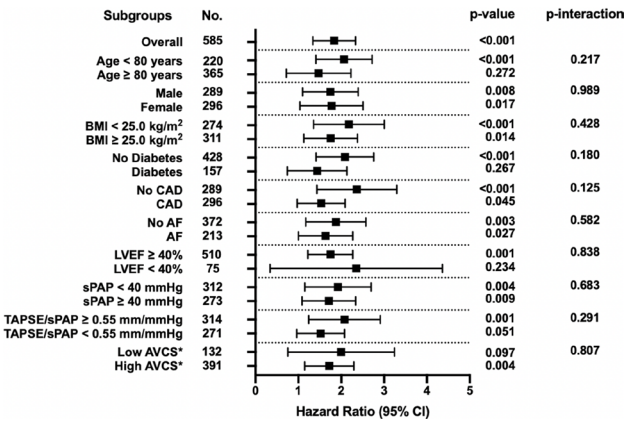


**Fig. 2 | 29-4** Subgroup-specific hazard ratios for long-term mortality according to EASIX category

operating characteristic (ROC) analyses for 1- to 5-year mortality were performed. Cox proportional hazards models assessed the association between EASIX and all-cause mortality. Restricted cubic splines were used to explore potential non-linear associations of continuous log-transformed EASIX. Prespecified subgroup analyses with formal interaction testing were performed.

**Results:** Among 585 patients (mean age 82.1 ± 5.1 years; 49.4% male), the optimal ROC-derived EASIX threshold was 1.25 across all time horizons, with moderate discrimination (AUC 0.56–0.60). EASIX ≥ 1.25 was associated with higher long-term mortality (log-rank $p < 0.001$) and remained independently associated with mortality in multivariable Cox regression (HR 1.52, 95% CI 1.14–2.03; $p = 0.003$), alongside age, male sex, and atrial fibrillation. Spline analyses of continuous log(EASIX) showed no significant overall association ($p = 0.24$) and no evidence of non-linearity ($p$ for non-linearity = 0.22). Subgroup analyses demonstrated broadly consistent associations without statistically significant interaction.

**Conclusion:** EASIX ≥ 1.25 is an independent predictor of long-term mortality after TAVI. Continuous spline analyses did not indicate a strong dose–response relationship, supporting a pragmatic threshold-based use of EASIX as a simple adjunct for pre-procedural risk stratification.

## 29-5

### Parenteral antilipid therapy prescription management in very high risk cardiovascular patients: a low threshold remote online program

**Theurl M.[1], Gomes D.[1], Bode E.[2], Moll C.[3], Mussner-Seeber C.[4], Hoschek S.[5], Priakhina A.[1], Friedrich G.[1]**

[1]Univ. Klinik Innere Medizin III Kardiologie, Innsbruck, Austria
[2]Praxis, Wörgl, Austria
[3]Praxis, Kufstein, Austria
[4]Praxis, Innsbruck, Austria
[5]Praxis, Zirl, Austria

**Introduction:** Predefined low target LDL cholesterol (LDL-C) values in very high risk cardiovascular patients are warranted. Particularly in secondary prevention settings antilipid therapy should be adapted in order to reach very low LDL-C. Medical options for lipid lowering including parenteral agents having significantly improved over the last years, focus should be laid on effective, low-threshold but guideline adherent prescription pathways. Following recently updated ESC guidelines, patients diagnosed with significant plaques (> 50 stenosis) by invasive coronary angiography (CA) or Coronary Computed Tomography (CCT) are classified as very high risk cardiovascular individuals. Furthermore,very high-risk status is established in patients with Acute Coronary Syndrome (ACS) as well as patients with prior Coronary Artery Bypass Grafting (CABG) or PCI. We sought to investigate the need for parenteral antilipid therapy in this very high risk patient cohort presenting with inadequate or inefficient oral antilipid management in regard to predefined LDL-C target values.

**Methods:** In cooperation with resident physicians, we included patients with documented hyperlipidaemia and at least one or more of the following criteria: baseline high coronary calcium or significant CCT plaque imaging, stenotic CA findings, history of ACS or/and PCI/CABG procedure. Patients were treated with stepwise escalation of oral antilipid therapy to reach target LDL-C levels and reevaluated for potential parenteral management. Using a remote online data exchange program a low threshold online prescription pathway was evaluated concerning guideline adherent indications and subsequent implementation.

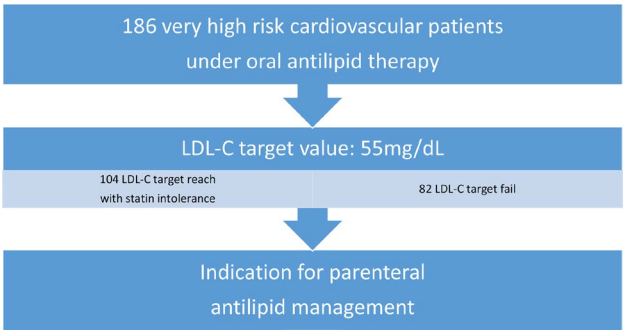


**Fig. 1 | 29-5**

**Results:** We included 186 patients with one or more of the previously stated criteria. After oral antilipid therapy 104 presented with statin intolerance, 82 did not reach LDL-C target values (< 55 mg/dl) despite highest tolerated statin dosage in addition to ezetimibe and/or bempedoic acid therapy. CCT, CA reports, ACS events, CABG and PCI procedures, LDL-C values as well as actual oral medication were recorded. Parenteral antilipid therapy indications including documented correct risk group allocation and failure of oral antilipid management could be confirmed in all 186 patients.

**Conclusion:** The data could demonstrate a high quality diagnostic level concerning the allocation of patients to their correct cardiovascular risk group as well as insufficient oral antilipid treatment in all patients included. Our remote online program thus allowing a low threshold fast and effective prescription procedure of parenteral antilipid therapy to reach predefined low LDL-C values.

## 29-6

### Identification of potentially heat-vulnerability increasing drugs

**Lehmann D.[1], Abou El-Atta H.[1], Quinton T.[2], Stöllberger C.[2]**

[1]Klinik Landstrasse, Wien, Austria
[2]Institut Gesünder Leben, Wien, Austria

**Introduction:** Introduction and Purpose: Vulnerability to heat-related illnesses may be increased by certain drugs due to various mechanisms. Whereas in articles only rough classifications of heat-vulnerability increasing drugs (HVID) are mentioned, a detailed compilation of suspected HVID is still missing. Aim of the study was to identify HVID.

**Methods:** Using data from the literature, potential HVID were searched. The evidence for increasing heat-vulnerability, based on PubMed research, was rated as “high”, “possible” or “unlikely” by 3 investigators, independently and blinded to the others’ results.

**Results:** The initial search retrieved 572 potential HVID. After analyzing 27 trials in healthy subjects, 25 cohort-studies, 19 case-reports, 14 reviews, 7 prospective trials in patients and 4 pharmacovigilance-studies, the evidence to increase heat-vulnerability was assessed as “high” for 110, “possible” for 390 and “unlikely” for 72 drugs. Drugs for the nervous-system, cardiovascular-system and alimentary-tract were most frequent (Table). Hypohidrosis ($n = 127$), disturbed thermoregulation ($n = 35$) or skin-circulation ($n = 15$) and dehydration ($n = 10$) were frequent mechanisms. Outcome events in cohort-studies

**Table 1 | 29–6** Heat-vulnerability increasing drugs (HVID): Anatomic therapeutic classification and assessed evidence, sorted according the number of "high evidence" HVID

| ATC Code | Description | HVID ($n=500$) | Evidence assessed as „high" ($n=110$) | Evidence assessed as „possible" ($n=390$) |
|---|---|---|---|---|
| N05 | Psycholeptics | 69 | 26 | 43 |
| N06 | Psychoanaleptics | 66 | 16 | 50 |
| N03 | Antiepileptics | 34 | 9 | 25 |
| A03 | Drugs for functional gastrointestinal disorders | 34 | 6 | 28 |
| Patches | | 6 | 6 | 0 |
| C07 | Beta blocking agents | 22 | 5 | 17 |
| M01 | Antiinflammatory and antirheumatic products | 43 | 5 | 38 |
| N04 | Anti Parkinson drugs | 13 | 5 | 8 |
| C03 | Diuretics | 24 | 4 | 20 |
| N02 | Analgesics | 7 | 4 | 3 |
| R06 | Antihistamines for systemic use | 49 | 4 | 45 |
| A04 | Antiemetics and antinauseants | 10 | 3 | 7 |
| A10 | Drugs used in diabetes | 6 | 3 | 3 |
| C09 | Agents acting on the renin-angiotensin system | 27 | 3 | 24 |
| B01 | Antithrombotic agents | 2 | 2 | 0 |
| G04 | Urologicals | 14 | 2 | 12 |
| H03 | Thyroid therapy | 4 | 2 | 2 |
| A07 | Antidiarrheals | 1 | 1 | 0 |
| C02 | Antihypertensives | 1 | 1 | 0 |
| C08 | Calcium channel blockers | 18 | 1 | 17 |
| N07 | Other nervous system drugs | 12 | 1 | 11 |
| C01 | Cardiac therapy | 1 | 0 | 1 |
| M03 | Muscle relaxants | 5 | 0 | 5 |
| R01-R05 | Cough and cold preparations | 4 | 0 | 4 |
| A06 | Drugs for constipation | 25 | 0 | 25 |

ATC = Anatomic therapeutic classification, HVID = Heat-vulnerability increasing drugs

were heat-illness/dehydration ($n=10$), causes of death ($n=5$), heat-related hospital admissions ($n=4$), heat-stroke ($n=4$), drug-overdose in heat-periods ($n=1$) and hypohidrosis ($n=1$). Comedication, when reported, disclosed additional HVID in all patients. Conflicting results about heat-vulnerability properties were found for 10 HVID.

**Conclusion:** Knowledge about HVID and their clinical relevance is limited. The quality of data is poor and derives mainly from young and healthy subjects. The outcome events are heterogeneous. Interdisciplinary research involving pharmacologists, physicians of different disciplines, pharmacists and health-care workers is needed to create and evaluate plans about modification of drug-therapy during heatwaves.

## 29-7

## Erectile Dysfunction and Chronic Kidney Disease Among Patients With Type 2 Diabetes Undergoing Coronary Angiography

**Elsner P.[1], Schnetzer L.[2], Neyer M.[2], Vogel J.[2], Plattner T.[2,1,3], Saely C.[1,2,3], Drexel H.[2,1,4,5], Leiherer A.[1,2,6], Festa A.[2]**

[1]Private University of the Principality of Liechtenstein, Triesen, Liechtenstein
[2]Vorarlberg Institute for Vascular Investigation & Treatment (VIVIT), Feldkirch, Austria
[3]Department of Medicine I, Academic Teaching Hospital Feldkirch, Feldkirch, Austria
[4]Drexel University College of Medicine, Philadelphia, Philadelphia, United States
[5]Vorarlberger Landeskrankenhausbetriebsgesellschaft, Feldkirch, Austria
[6]Central Medical Laboratories Feldkirch, Feldkirch, Austria

**Introduction:** Erectile dysfunction (ED) and type 2 diabetes mellitus (T2 DM) frequently co-occur and share a broad

range of risk factors. Their individual associations with coronary artery disease (CAD) are well established. In patients with T2 DM, microvascular damage is a major complication and a leading contributor to chronic kidney disease (CKD). The prevalence of ED is also notably high among individuals with CKD. However, the relation between ED and CKD in patients with (T2 DM+) or without (T2 DM-) T2 DM is not well understood. This study aimed to address this gap in a cohort of male patients undergoing elective coronary angiography.

**Methods:** A total of 419 male patients completed a questionnaire assessing the presence or absence of ED. T2 DM was defined by the definition of the American Diabetes Association (ADA) and CKD was determined as an estimated glomerular filtration rate (eGFR) of < 60 mL/min/1.73 $m^2$. Participants were categorized into four groups: ED-/T2 DM- ($n$ = 167), ED+/T2 DM- ($n$ = 110), ED-/T2 DM+ ($n$ = 71), and ED+/T2 DM+ ($n$ = 71).

**Results:** ED was significantly associated with CKD in the overall study population. In univariate logistic regression, ED was linked to more than a twofold increased odds of CKD (OR = 2.08, 95% CI:1.19–3.66, $p$ < 0.001). This association remained statistically significant after adjusting for age, hypertension, BMI, HbA1c, lipid parameters, and smoking (OR = 2.14, 95% CI:1.21–3.77, $p$ = 0.009), confirming ED as an independent predictor of CKD. Compared to the reference group (ED-/T2 DM-), both ED+/T2 DM- (OR = 2.63, 95% CI:1.33–5.23, $p$ = 0.006) and ED-/T2 DM+ (OR = 2.38, 95% CI:1.18–4.80, $p$ = 0.016) were significantly associated with higher CKD risk. Patients with both ED and T2 DM (ED+/T2 DM+) exhibited the same odds ratio for CKD as those with T2 DM but without ED (ED-/T2 DM+) (OR = 2.38, 95% CI:1.18–4.80, $p$ = 0.016).

**Conclusion:** These findings highlight the clinical relevance of ED, assessed using a simple questionnaire, as a strong and independent predictor of CKD in high-risk male patients with and without T2 DM.

## A



## B



## C

## D



## E



## F



## G

Gierlinger, Gregor
Gindlhuber, Jürgen
Glantschnig, Theresa
Gloser, Anja
Gökler, Johannes
Gold, Thomas
Goliasch, Georg
Gollmann-Tepeköylü, Can
Gollmer, Johannes
Gölly, Katharina
Gomes, Daniel
Gorlitzer, Michael
Gössinger, Bea
Gottardi, Roman
Gottsberger, Jessica
Götzinger, Felix
Grabenwöger, Martin
Graber, Michael
Grall, Andreas
Gräni, Christoph
Granitz, Christina
Granner, Matthias
Gregshammer, Bernhard
Gremmel, Thomas
Grill, Maria
Grimm, Michael
Groche, Max
Gruber, Nadja
Grübler, Martin
Grubmüller, Anna
Grund, Michael
Grundmann, Sebastian
Güler, Ali
Gundendorfer, Michael
Günter, Schreier
Gutwenger, Theresa
Gygax, Erich
Gyöngyösi, Mariann

## H

Haase, Bianca
Haase-Fielitz, Anja
Haberl, Thomas
Hacker, Marcus
Hafner-Gießauf, Hildegard
Hagenauer, Julia
Hagleitner, Georg
Hagn, Gerhard
Haidbauer, Viktoria
Haider, Patrick
Halavina, Kseniya
Haller, Paul
Hammer, Andreas
Hammerer, Matthias
Hammerer-Lercher, Angelika
Hamzaraj, Kevin
Häner, Jonas
Hangler, Herbert
Hannover, Albert
Hanser, Anja
Harakaly-Bottka, Eva
Harbich, Paul
Harrer, Marieluise
Haschka, David
Haslacher, Helmuth
Haslinger, Maximilian
Häßner, Jonathan
Hasun, Matthias
Hatzl, Stefan
Hau, Dominik
Hauptmann, Laurenz
Hauptvogel, Karolin
Hausleiter, Jörg
Hecht, Stefan
Hecke, Gretha
Hecking, Manfred
Heg, Dik
Heger, Lukas
Heim, Vanessa
Heinz, Gottfried
Heitzinger, Gregor
Hemetsberger, Rayyan
Hengstenberg, Christian
Hergan, Klaus
Herkner, Harald
Heuböck, Elisabeth
Hildebrandt, Tom
Hilgendorf, Ingo
Hinterbuchner, Karin
Hintringer, Florian
Hirsch, Jakob
Hirtenlehner, Felix
Hlodakova, Viera
Hödlmoser, Sebastian
Hofbauer, Thomas
Höfer, Daniel
Hofer, Felix
Hofer, Florian
Hoffmann, Michael
Hohensinner, Philipp
Holfeld, Johannes
Höller, Viktoria
Holzapfel, Gerhard
Holzer, Michael
Holzhey, David
Holzknecht, Magdalena
Hölzl, Matthias
Hopfer, Anja
Hoppe, Uta
Horstmann, Hauke

Kullnig, Peter

Kurath – Koller, Stefan

Kurath-Koller, Stefan

Kushwah, Chandrabhan

## L

Lacaita, Pietro

Lacher, Justin

Lambert, Thomas

Lamm, Gudrun

Lamm, Leonhard

Lang, Irene

Langbein, Anke

Langsenlehner, Tanja

Langthaler, Patrick

Langthaler-Kabicher, Gudrun

Lanser, Lukas

Lanzerstorfer, Johannes

Larcher, Barbara

Laufer, Günther

Lazarevic, Aleksa

Lechner, Christopher

Lechner, Ivan

Lehmann, David

Lehmann, Ronja

Leibetseder, Sarah

Leiherer, Andreas

Leitner, Magdalena

Lemes, Christine

Lemeš, Christine

Lemesch, Simone

Lenz, Max

Lenz, Verena

Leonhardt, Martin

Li, Xiaowei

Lichtblau, Leonhard

Lichtenauer, Michael

Likar, Rudolf

Linni, Klaus

Linz, Dominik

Lipp, Anna

List, Luca

Ljubojevic-Holzer, Senka

Loewe, Christian

Lohmann, Ronja

Lorenz, Matthias

Losdat, Sylvain

Lucka, Julia

Ludvik, Bernhard

Lugmayr, Sara

Lukas, Julia

Lukosch, Mona

Lukovic, Dominika

Lunelli, Riccardo

Lunzer, Laura

Lustig, Paul

## M

Mach, Markus

Mächler, Heinrich

Mader, Arthur

Madl-Liebenberger, Lisa

Mahfoud, Felix

Mahmoudi, Mahdi

Mahr, Stephane

Maier, Julian

Mair, Roland

Mair, Rudolf

Mairhofer, Hannah

Maleiner, Babette

Mamunchak, Olga

Mandl, Markus

Manka, Robert

Mann, Christopher

Manninger-Wünscher, Martin

Manojlovic, Verina

Mantawy, Sayed

Manville, Emely

Manzanilla Romero, Hector

Marchini, Timoteo

Markus, Wallner

Marschang, Peter

Martinek, Martin

März, Winfried

Mascherbauer, Julia

Mascherbauer, Katharina

Mason, Christopher

Masood, Shehroz

Massberg, Steffen

Masser, Sarah

Matejka, Matthias

Matzer, Ingrid

Mauerhofer, Elisabeth

Maurer, Thomas

Mayr, Agnes

McIntyre, William

McMurray, John

Medeiros-Domingo, Argelia

Meinhart, Johann

Meissner, Markus

Meledeth, Christy

Merkely, Béla

Merl, Lion

Merlo, Marco

Merz, Andreas

Messner, Moritz

Metzler, Bernhard

Meyer, Tim

Michael, Nadia

## N



## O



## P

## Q



## R



## S

## T

## U



## V



## W



## Y

## Z